ZYGOTIC AND NON-ZYGOTIC EMBRYOGENESIS: EVOLUTIONARY, DEVELOPMENTAL AND PRACTICAL ASPECTS

EDITED BY: Jorge M. Canhoto, Paloma Moncaleán, Sandra Isabel Correia, Víctor M. Loyola-Vargas and Jonny E. Scherwinski-Pereira

PUBLISHED IN: Frontiers in Plant Science

frontiers Research Topics

ISSN 1664-8714
ISBN 978-2-88976-696-3
DOI 10.3389/978-2-88976-696-3

About Frontiers

Frontiers is more than just an open-access publisher of scholarly articles: it is a pioneering approach to the world of academia, radically improving the way scholarly research is managed. The grand vision of Frontiers is a world where all people have an equal opportunity to seek, share and generate knowledge. Frontiers provides immediate and permanent online open access to all its publications, but this alone is not enough to realize our grand goals.

Frontiers Journal Series

The Frontiers Journal Series is a multi-tier and interdisciplinary set of open-access, online journals, promising a paradigm shift from the current review, selection and dissemination processes in academic publishing. All Frontiers journals are driven by researchers for researchers; therefore, they constitute a service to the scholarly community. At the same time, the Frontiers Journal Series operates on a revolutionary invention, the tiered publishing system, initially addressing specific communities of scholars, and gradually climbing up to broader public understanding, thus serving the interests of the lay society, too.

Dedication to Quality

Each Frontiers article is a landmark of the highest quality, thanks to genuinely collaborative interactions between authors and review editors, who include some of the world's best academicians. Research must be certified by peers before entering a stream of knowledge that may eventually reach the public - and shape society; therefore, Frontiers only applies the most rigorous and unbiased reviews.
Frontiers revolutionizes research publishing by freely delivering the most outstanding research, evaluated with no bias from both the academic and social point of view. By applying the most advanced information technologies, Frontiers is catapulting scholarly publishing into a new generation.

What are Frontiers Research Topics?

Frontiers Research Topics are very popular trademarks of the Frontiers Journals Series: they are collections of at least ten articles, all centered on a particular subject. With their unique mix of varied contributions from Original Research to Review Articles, Frontiers Research Topics unify the most influential researchers, the latest key findings and historical advances in a hot research area! Find out more on how to host your own Frontiers Research Topic or contribute to one as an author by contacting the Frontiers Editorial Office: frontiersin.org/about/contact

ZYGOTIC AND NON-ZYGOTIC EMBRYOGENESIS: EVOLUTIONARY, DEVELOPMENTAL AND PRACTICAL ASPECTS

Topic Editors:
Jorge M. Canhoto, University of Coimbra, Portugal
Paloma Moncaleán, Neiker Tecnalia, Spain
Sandra Isabel Correia, University of Coimbra, Portugal
Víctor M. Loyola-Vargas, Scientific Research Center of Yucatán (CICY), Mexico
Jonny E. Scherwinski-Pereira, Brazilian Agricultural Research Corporation (EMBRAPA), Brazil

Citation: Canhoto, J. M., Moncaleán, P., Correia, S. I., Loyola-Vargas, V. M., Scherwinski-Pereira, J. E., eds. (2023). Zygotic and Non-Zygotic Embryogenesis: Evolutionary, Developmental and Practical Aspects. Lausanne: Frontiers Media SA. doi: 10.3389/978-2-88976-696-3

Table of Contents

frontiers in Plant Science

ORIGINAL RESEARCH
published: 12 April 2021
doi: 10.3389/fpls.2021.631239

Proteome-Wide Analysis of Heat-Stress in *Pinus radiata* Somatic Embryos Reveals a Combined Response of Sugar Metabolism and Translational Regulation Mechanisms

Ander Castander-Olarieta[1], Cátia Pereira[1,2], Itziar A. Montalbán[1†], Vera M. Mendes[3], Sandra Correia[2], Sonia Suárez-Álvarez[1], Bruno Manadas[3], Jorge Canhoto[2] and Paloma Moncaleán[1†]*

[1] Department of Forestry Science, NEIKER, Arkaute, Spain, [2] Center for Functional Ecology, Department of Life Sciences, University of Coimbra, Coimbra, Portugal, [3] CNC - Center for Neuroscience and Cell Biology, University of Coimbra, Coimbra, Portugal

OPEN ACCESS

Edited by:
Jesus V. Jorrin Novo,
University of Cordoba, Spain

Reviewed by:
Monica Escandon,
University of Cordoba, Spain
Jesús Pascual,
University of Turku, Finland

***Correspondence:**
Paloma Moncaleán
pmoncalean@neiker.eus

[†] These authors have contributed equally to this work

Specialty section:
This article was submitted to Plant Proteomics and Protein Structural Biology, a section of the journal Frontiers in Plant Science

Received: 08 January 2021
Accepted: 22 March 2021
Published: 12 April 2021

Citation:
Castander-Olarieta A, Pereira C, Montalbán IA, Mendes VM, Correia S, Suárez-Álvarez S, Manadas B, Canhoto J and Moncaleán P (2021) Proteome-Wide Analysis of Heat-Stress in Pinus radiata Somatic Embryos Reveals a Combined Response of Sugar Metabolism and Translational Regulation Mechanisms. Front. Plant Sci. 12:631239. doi: 10.3389/fpls.2021.631239

Somatic embryogenesis is the process by which bipolar structures with no vascular connection with the surrounding tissue are formed from a single or a group of vegetative cells, and in conifers it can be divided into five different steps: initiation, proliferation, maturation, germination and acclimatization. Somatic embryogenesis has long been used as a model to study the mechanisms regulating stress response in plants, and recent research carried out in our laboratory has demonstrated that high temperatures during initial stages of conifer somatic embryogenesis modify subsequent phases of the process, as well as the behavior of the resulting plants *ex vitro*. The development of high-throughput techniques has facilitated the study of the molecular response of plants to numerous stress factors. Proteomics offers a reliable image of the cell status and is known to be extremely susceptible to environmental changes. In this study, the proteome of radiata pine somatic embryos was analyzed by LC-MS after the application of high temperatures during initiation of embryonal masses [(23°C, control; 40°C (4 h); 60°C (5 min)]. At the same time, the content of specific soluble sugars and sugar alcohols was analyzed by HPLC. Results confirmed a significant decrease in the initiation rate of embryonal masses under 40°C treatments (from 44 to 30.5%) and an increasing tendency in the production of somatic embryos (from 121.87 to 170.83 somatic embryos per gram of embryogenic tissue). Besides, heat provoked a long-term readjustment of the protein synthesis machinery: a great number of structural constituents of ribosomes were increased under high temperatures, together with the down-regulation of the enzyme methionine-tRNA ligase. Heat led to higher contents of heat shock proteins and chaperones, transmembrane transport proteins, proteins

related with post-transcriptional regulation (ARGONAUTE 1D) and enzymes involved in the synthesis of fatty acids, specific compatible sugars (myo-inositol) and cell-wall carbohydrates. On the other hand, the protein adenosylhomocysteinase and enzymes linked with the glycolytic pathway, nitrogen assimilation and oxidative stress response were found at lower levels.

Keywords: carbohydrates, compatible solutes, heat shock proteins, high temperatures, methylation, proteomics, radiata pine, somatic embryogenesis

INTRODUCTION

As sessile organisms, plants are continuously exposed to a great number of external stimuli and fluctuating stress factors, which are becoming progressively more common due to the on-going climate change situation. Derived from the current global warming trend, heat and drought are becoming a growing concern, as they provoke adverse effects on plant growth and development, significantly determining the productivity and viability of both natural ecosystems and planted forests (Allen et al., 2010; Shen et al., 2015).

Somatic embryogenesis (SE) has long been used as a model to study the different physiological, developmental and biochemical mechanisms underpinning stress response in plants, and it is clear that it can also be used as an interesting tool to modulate the behavior of somatic embryo-derived plants, as postulated by several authors (Kvaalen and Johnsen, 2008; García-Mendiguren et al., 2017).

In previous studies we have reported that high temperatures can determine the success of the different stages of SE, provoking negative effects during initiation but increasing the production of somatic embryos during maturation (García-Mendiguren et al., 2016b; Castander-Olarieta et al., 2019). Those treatments can alter the morphology of embryonal masses (EMs) and Se's in *Pinus radiata* and *Pinus halepensis*, as well as their hormonal and metabolic profiles (Moncaleán et al., 2018; Castander-Olarieta et al., 2019, 2020a,b; Pereira et al., 2020). Besides, the initial culture conditions can have long-lasting effects, modulating the development and drought stress resilience of somatic plants years later (Castander-Olarieta et al., 2020b), presumably by changes in the expression of stress-related genes and epigenetic marks (Castander-Olarieta et al., 2020c). However, very few proteomic studies have been carried out in pine species addressing heat-stress, and, as far as we know, this is the first report carried out along SE applying such high temperatures.

Heat is responsible for alterations in membrane structures, DNA/RNA stability and cytoskeleton dynamics (Hasanuzzaman et al., 2013; Niu and Xiang, 2018); heat disturbs primary metabolic pathways, leading to internal metabolic imbalances, which in turn can cause the accumulation of toxic reactive oxygen species (ROS). Changes in the redox homeostasis can result in protein denaturation and aggregation, altering the activity of essential enzymes (Paciolla et al., 2016).

In this regard, plants have evolved to rapidly detect and respond to all those factors by modifications and readjustments of a complex molecular machinery. The molecules forming this sophisticated network involve a great variety of metabolites, such as hormones, enzymes and other types of proteins (de Diego et al., 2012, 2013a,b, 2015; Taïbi et al., 2015; Escandón et al., 2017). Besides, recent research has demonstrated that plants can store information from stressful conditions and respond in a more efficient way to future environmental constraints (Turgut-Kara et al., 2020).

Proteomics, which provides the missing link between the genome/transcriptome and the metabolome, allows the identification and quantification of stress-tolerance associated proteins and can be applied as a very useful tool to study stress tolerance in plants (Pinheiro et al., 2014). In the same way, the identification of stress-related proteins gives the possibility to use protein markers to improve selection of elite genotypes with high levels of tolerance to stress, conferring fitness advantages in a climate change scenario (Lippert et al., 2005).

Despite the fact that the diversity of proteins present in a cell is considerably smaller than the number of transcripts, this approach presents numerous advantages if compared to transcriptomics. Proteomics gives a more connected understanding of the phenotype because most biological functions in a cell are executed by proteins rather than by mRNAs, and changes in transcriptome are not always correlated with changes in the abundance of the corresponding protein species (Correia et al., 2016). Proteomics provides important information regarding post-transcriptional and post-translational regulation mechanisms and other factors such as mRNA localization and transport, translation rates, transcript and protein stability, and intercellular protein trafficking (Wang et al., 2013; Passamani et al., 2017). Besides, proteomic studies are very useful when working with non-model plant species because protein sequences are more conserved and allow their identification by comparison with orthologous proteins (García-Mendiguren et al., 2016a).

As a result, proteomics has become a necessary and complementary approach in the post-genomic era, and in recent years, high-throughput techniques have facilitated the study of proteomic responses in several plant species to many different abiotic stresses including cold (Yuan et al., 2019), heat (Escandón et al., 2017), drought (Taïbi et al., 2015), salinity (Passamani et al., 2017), or UV light (Pascual et al., 2017). Several studies in different plant species have identified some protein groups related to heat-stress responses, which include antioxidative enzymes, heat shock proteins (HSPs), proteins related to energy and carbohydrate metabolism, redox homeostasis, protein synthesis and degradation, signal transduction, and transcription

factors (Escandón et al., 2017; Parankusam et al., 2017). The latest reports have also highlighted the importance of some nuclear proteins such as histones, methyl cycle enzymes or spliceosome elements during thermopriming and epigenetic-driven regulatory mechanisms (Lamelas et al., 2020).

In this work we are interested in corroborating the hypothesis that the application of heat-stress during initiation of SE in radiata pine (*P. radiata* D.Don) could determine the different stages of the SE process, as well as the protein profile of somatic embryos (Se's) 7 months later. This approach could give us useful information about the molecular mechanism underpinning stress responses during embryo formation, and shed light on how stress tolerance is built and maintained during the embryogenic process.

To this aim, we have applied a short-gel liquid chromatography coupled to mass spectrometry (Short-GeLC-MS/MS) approach in combination with both data dependent acquisition (DDA) and data independent acquisition (DIA) methods, which is, somehow, novel in the plant scenario. Moreover, we have used the sequential window acquisition of all theoretical fragment ion spectra (SWATH) method (Anjo et al., 2015) which, when compared with the classically employed two-dimensional electrophoresis systems (2-DE), substantially reduces the amount of sample handling and lightens the data analysis process without compromising the protein identification efficiency. Furthermore, this strategy enables the detection of challenging insoluble transmembrane proteins and has great potential when working with non-sequenced species (Heringer et al., 2018).

Finally, in order to have a broader perspective and confirm our results, a high-performance liquid chromatography (HPLC) analysis has been carried out to find whether specific changes in the proteome could have resulted in modifications of several metabolic pathways, i.e., sugar metabolism, which is known to have a key role in stress-response mechanisms (de Diego et al., 2013b).

MATERIALS AND METHODS

Plant Material and Heat Stress Treatments

Green female cones of *Pinus radiata* from five genetically different mother trees in a seed orchard established by Neiker in Deba (Spain, latitude: 43°16′59″N, longitude: 2°17′59″W, altitude: 50 m), were collected in June 2018 and processed according to Montalbán et al. (2012) (**Figure 1A**). Seeds were sterilized following the aforementioned protocol and megagametophytes enclosing immature zygotic embryos were carefully extracted and placed horizontally onto Petri dishes containing Embryo Development Medium (EDM, Walter et al., 2005), supplemented with 3.5 g L^{-1} gellan gum (Gelrite®, Duchefa, Haarlem, Netherlands). Intact megagametophytes were subjected to different incubation conditions (Cond1 = 23°C; Cond2 = 40°C, 4 h; Cond3 = 60°C, 5 min) (**Figure 1B**). In all cases, the Petri dishes were prewarmed to the desirable temperature prior to the cultivation of the megagametophytes. Eight megagametophytes were used per Petri dish, ten Petri dishes per treatment, and 400 megagametophytes were cultured per incubation condition, comprising a total of 1,200 megagametophytes, including all treatments and mother trees. After the treatments, all the samples were kept at 23°C in darkness and the following steps of SE (proliferation and maturation) were carried out at standard conditions as reported in Montalbán and Moncaleán (2018).

After 8 weeks on initiation medium, initiation rates were calculated as the percentage of megagametophytes that had extruded embryonal masses in a sufficient size (7–10 mm of diameter) to be proliferated out of the total number of megagametophytes cultured (**Figure 1C**). Growing EMs were separated from the megagametophytes and subcultured to a fresh EDM initiation medium. After 14 days, EMs were subcultured onto the same medium but 4.5 gL^{-1} gellan gum every 2 weeks until they reached a sufficient amount of tissue for maturation (2–3 months) (**Figure 1D**). At that moment, actively growing EMs were recorded as established embryogenic cell lines (ECL), and the percentage of proliferating lines respect to the EMs initiated was calculated following Castander-Olarieta et al. (2019).

Maturation of ECLs was performed as described by Montalbán and Moncaleán (2018), using six replicates (Petri dishes) per ECL and 10 ECLs per treatment. After 13 weeks, maturation success was evaluated, the number of mature and well-formed Se's per gram of embryogenic tissue was calculated and 100 mg of Se's (20 to 40 Se's, depending on their size) per ECL were frozen in liquid nitrogen for both protein and soluble sugar analyses (**Figure 1E**). Five ECLs were used from 23 and 40°C treatments and 4 ECLs for 60°C treatment, comprising a total of 14 ECLs analyzed.

Protein and Metabolite Extraction and Protein Mass Spectrometry

Protein and metabolite extractions from mature Se's were performed following the combined protocol described by Valledor et al. (2014) using 100 mg of liquid nitrogen grinded Se's. After extraction, metabolites from the polar fraction were saved to new tubes and stored at −80°C until HPLC analysis (explained in section "Soluble Sugar Analysis") and protein pellets were air dried and re-suspended in 100 μL of solubilisation buffer [7 M urea, 2 M thiourea, 2% (w/v) CHAPS, 1% (w/v) DTT].

As a preparatory step prior to LC-MS analysis, protein extracts (50 μL) were re-precipitated with 4 volumes of cold acetone (250 μL) for 30 min at −80°C. Samples were centrifuged at 20,000 *g*, refrigerated at 4 °C for about 20 min and the pellet was re-suspended in 50 μL of 1 × Laemmli Sample Buffer. The total protein concentration was measured for each sample using the Pierce 660 nm Protein Assay kit (Thermo Scientific™, Waltham, MA, United States). For DDA experiments, samples from each condition (Cond1 = 23°C, control; Cond2 = 40°C, 4 h; Cond3 = 60°C, 5 min) were pooled to create the library of each condition before sample processing and for DIA each sample was processed individually for quantification purposes, as described by Anjo et al. (2015). Protein content from each sample (adjusted based on the protein quantification values obtained previously) was separated by SDS-PAGE for about 17 min at

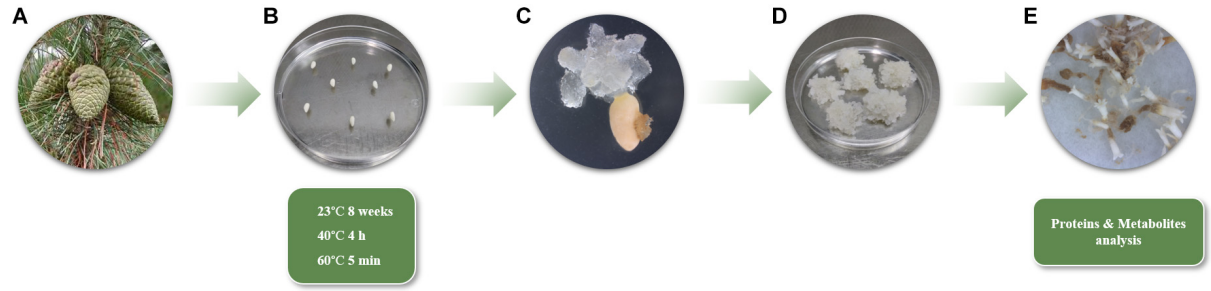

FIGURE 1 | (A) Radiata pine green female cones enclosing immature zygotic embryos from five different mother trees. **(B)** Culture of megagametophytes in EDM medium under three different temperature conditions (Cond1 = 23°C, control; Cond2 = 40°C, 4 h; Cond3 = 60°C, 5 min). **(C)** Extrusion of embryogenic tissue from megagametophytes (8 weeks). **(D)** Proliferating EMs (10 weeks). **(E)** Mature Se's collected for proteins and metabolites analyses (13 weeks).

110 V (Short-GeLC Approach, Anjo et al., 2015) and stained with Coomassie Brilliant Blue G-250. For DDA experiments, each lane was divided into 5 gel pieces (to increase the depth of the analysis and to acquire more fragmentation spectra to correlate with the database) and for DIA experiments into 3 gel pieces for further individual processing. After destaining with a 50 mM ammonium bicarbonate and 30% acetonitrile solution, gel bands were incubated overnight with trypsin for protein digestion and peptides were extracted from the gel using 3 solutions containing different percentages of acetonitrile (30, 50, and 98%) with 1% formic acid. The organic solvent was evaporated using a vacuum-concentrator and peptides were re-suspended in 30 μL of a solution containing 2% acetonitrile and 0.1% formic acid. Each sample was sonicated using a cup-horn (Ultrasonic processor, 750 W) for about 2 min, 40% amplitude, and pulses of 1 s ON/OFF. Ten μL of each sample were analyzed by LC-MS/MS, either for DIA or DDA experiments.

Protein samples were analyzed on a NanoLC^{TM} 425 System coupled to a Triple TOF^{TM} 6600 mass spectrometer (Sciex, Framingham, MA, United States). The ionization source was the OptiFlow® Turbo V Ion Source equipped with the SteadySpray^{TM} Low Micro Electrode (1–10 μL). The chromatographic separation was performed on a Triart C18 Capillary Column 1/32″ (12 nm, S-3 μm, 150 mm × 0.3 mm, YMC) and using a Triart C18 Capillary Guard Column (0.5 μm × 5 mm, 3 μm, 12 nm, YMC) at 50°C. The flow rate was set to 5 μL min-1 and mobile phases A and B were 5% DMSO plus 0.1% formic acid in water and 5% DMSO plus 0.1% formic acid in acetonitrile, respectively. The LC program was performed as followed: 5–35% of B (0–40 min), 35–90% of B (40–41 min), 90% of B (41–45 min), 90–5% of B (45–46 min), and 5% of B (46–50 min). The ionization source was operated in the positive mode set to an ion spray voltage of 4,500 V, 10 psi for nebulizer gas 1 (GS1), 15 psi for nebulizer gas 2 (GS2), 25 psi for the curtain gas (CUR), and source temperature (TEM) at 100°C. For DDA experiments, the mass spectrometer was set to scanning full spectra (m/z 350-1250) for 250 ms, followed by up to 100 MS/MS scans (m/z 100–1500). Candidate ions with a charge state between +1 and +5 and counts above a minimum threshold of 10 counts per second were isolated for fragmentation and one MS/MS spectrum was collected before adding those ions to the exclusion list for 15 s (mass spectrometer operated by Analyst® TF 1.7, Sciex). The rolling collision was used with a collision energy spread of 5. For SWATH experiments, the mass spectrometer was operated in a looped product ion mode and specifically tuned to a set of 90 overlapping windows, covering the precursor mass range of 350–1,250 m/z. A 50 ms survey scan (350–1,250 m/z) was acquired at the beginning of each cycle, and SWATH-MS/MS spectra were collected from 100 to 1,800 m/z for 35 ms resulting in a cycle time of 3.2 s.

Soluble Sugar Analysis

For soluble sugar quantification, 200 μL of metabolite samples obtained in Section "Protein and Metabolite Extraction and Protein Mass Spectrometry" were totally dried on a Speedvac to remove the methanol from the extraction buffer and re-suspended in 100 μL distilled water. Soluble sugar and sugar alcohol analysis was performed by HPLC using an Agilent 1260 Infinity II coupled to refractive index detector (RID) (Agilent Technologies, Santa Clara, CA, United States). A Hi-Plex Ca column (7.7 mm × 300 mm, 8 μm) was used for separation of fructose, glucose, sucrose, mannitol and sorbitol. The mobile phase was pure water and the samples were injected in the column at a flow rate of 0.2 mL min^{-1} at 80°C for 40 min. Sugar concentrations were determined from internal calibration curves constructed with the corresponding commercial standards. The concentrations obtained from the HPLC analysis were conveniently adjusted taking into account the initial concentration step (2 times), and results were expressed as μmol g FW^{-1}. The mass spectrometry proteomics data have been deposited to the ProteomeXchange Consortium via the PRIDE (Perez-Riverol et al., 2019) partner repository with the data set identifier PXD022711.

Data Analysis

Ion-Library Construction (DDA Information)

A specific ion-library of the precursor masses and fragment ions was created by combining all files from the DDA experiments in one protein identification search using the ProteinPilot^{TM} software (v5.0, Sciex®). The paragon method parameters were the following: searched against the reviewed Viridiplantae database

(Swissprot) downloaded on 1st April from UniProtKB[1] (The UniProt Consortium, 2019), cysteine alkylation by acrylamide, digestion by trypsin, and gel-based ID. An independent False Discovery Rate (FDR) analysis, using the target-decoy approach provided by Protein Pilot™, was used to assess the quality of identifications.

Relative Quantification of Proteins (SWATH-MS)

SWATH data processing was performed using SWATH™ processing plug-in for PeakView™ (v2.0.01, Sciex®). Protein relative quantification was performed in all samples using the information from the protein identification search. Quantification results were obtained for peptides with less than 1% of FDR and by the sum of up to 5 fragments/peptide. Each peptide was normalized for the total sum of areas for the respective sample. Protein relative quantities were obtained by the sum of the normalized values for up to 15 peptides/protein. A correlation analysis between samples was performed using the Spearman Rank Correlation method and considering the relative quantification values determined for all the samples to assure that those from the same condition showed the same behavior.

Statistical Analysis

The effect of each treatment on the initiation and proliferation rates was evaluated performing a logistic regression and the corresponding analysis of deviance. The mother tree was introduced into the model as a block variable to reduce variability and the Tukey's *post hoc* test ($\alpha = 0.05$) was used for multiple comparisons. In the case of the number of Se's per gram of embryogenic tissue, the usual analysis of variance (ANOVA) did not fulfill the normality hypothesis, and thus, a linear mixed effects model was considered, including the ECL as a random effect with different variance parameters for each treatment level to correct for heteroscedasticity.

For the analysis of the protein results, two different approaches were employed, combining multivariate and univariate analyses. First, we performed a partial least square-discriminant analysis (PLS-DA) using the MetaboAnalyst web-based platform[2] (Pang et al., 2020) to find out the separation between the three conditions and simultaneously identify the most significant top protein features able to classify the three groups based on variable influence on projections (VIP) values. Those proteins were then clustered based on their biological function according to the FunRich software and the Plants database from UniProtdatabase[3]. In parallel, as cross-validation, a Kruskal–Wallis test was performed to select the proteins which were statistically different between the 3 conditions. The Dunn's test of Multiple Comparisons, with Benjamini–Hochberg *p*-value adjustment, was performed to determine in which comparisons statistical differences were observed. Finally, proteins overlapping between the Kruskal–Wallis test significant proteins and PLS-DA VIP list were selected and a cluster analysis was performed to them using the MetaboAnalyst web-based platform in order to investigate their relation and relative abundance by generating heatmap and correlation matrix plots. For the heatmap hierarchical clustering the Euclidean distance and the Complete algorithm were used and for the correlation matrix the Pearson's correlation test was applied.

To assess the effect of the treatments on the levels of each sugar, an ANOVA was conducted followed by multiple comparisons based on Tukey's *post hoc* test ($\alpha = 0.05$). When the ANOVA did not fulfill the normality hypothesis the Kruskal–Wallis test was performed.

[1] www.uniprot.org

[2] www.metaboanalyst.ca

[3] https://www.uniprot.org/help/plants

RESULTS

Effect of Temperature Treatments on Somatic Embryogenesis

Analyzing the effect of each treatment on the different steps of SE (initiation, proliferation, and maturation), statistically significant differences were only observed during initiation ($p < 0.05$). Initiation rates were significantly lower at 40°C for 4 h, whereas control and 60°C for 5 min treatments presented similar values (**Table 1**). Regarding proliferation, no differences could be observed among treatments. The three treatments showed similar proliferation rates, being the ones obtained at 60°C for 5 min slightly higher than the other two (**Table 1**). Maturation rates were beyond 90% for the three treatments, so temperature did not reduce the maturation capacity of EMs. Although not significant, the number of Se's produced per gram of embryogenic tissue was higher in samples originating from high temperature culture conditions, especially in those from 40°C for 4 h treatment (**Table 1**).

Relative Quantification of Proteins

Proteomic analysis allowed the identification of 1,020 proteins from the reviewed Viridiplantae database. After data processing 758 proteins were used for quantitative analyses (**Supplementary Table 1**). The correlation analysis performed demonstrated that samples were highly correlated between all them, with correlation values above 0.72 (data not shown). In the case of samples from the same temperature treatment correlation values were even higher (>0.78).

For visualization of sample groups and to reduce the complexity of the results, a PLS-DA analysis was performed, a supervised model that uses multivariate techniques to extract via linear combinations of original variables that can predict

TABLE 1 | Embryonal mass initiation (%) and proliferation rates (%), and number of somatic embryos per gram of embryogenic tissue from *P. radiata* megagametophytes cultured under different temperature conditions.

Treatment	Initiation %	Proliferation %	Se's g^{-1} ET
23°C, control	44 ± 2.95^{a}	31.82 ± 2.09^{a}	121.87 ± 45.72^{a}
40°C, 4 h	30.5 ± 3.08^{b}	30.33 ± 3.01^{a}	170.83 ± 53.86^{a}
60°C, 5 min	43.5 ± 2.99^{a}	36.21 ± 2.54^{a}	129.4 ± 41.71^{a}

Data are presented as mean values ± SE. Significant differences at $p < 0.05$ are indicated by different letters.

class membership giving the largest predicted indicator variable. The three conditions employed in this experiment were clearly distinguished and separated by the loading plots of the first and second components of PLS-DA pairwise comparison models (**Figure 2**). These two components accounted for almost the 33% of the total variance. The first component potentially gathered variability related to heat-stress responses, while the biological function of the second component remained unclear due to an excess of variability.

The proteins presenting VIP values greater than 1 were considered the best classifiers, the ones contributing the most to the separation of the three conditions and thus, the ones involved in heat-stress responses. This selection included 262 proteins (**Supplementary Figure 1**), which were subjected to a gene ontology enrichment analysis to extract information about their mayor biological function. This analysis revealed that the selected proteins belonged to numerous pathways, covering a great number of cellular processes, from primary to secondary metabolism (**Figure 3**). However, three biological functions were considerably more represented than the other ones, which included proteins involved in direct stress response and adaptation processes, proteins constituents of the translation machinery, translation regulation and proteome reorganization, and proteins involved in carbohydrate metabolism. Other pathways such as amino acid or lipid metabolisms were also represented, although to a lesser extent, and a great proportion

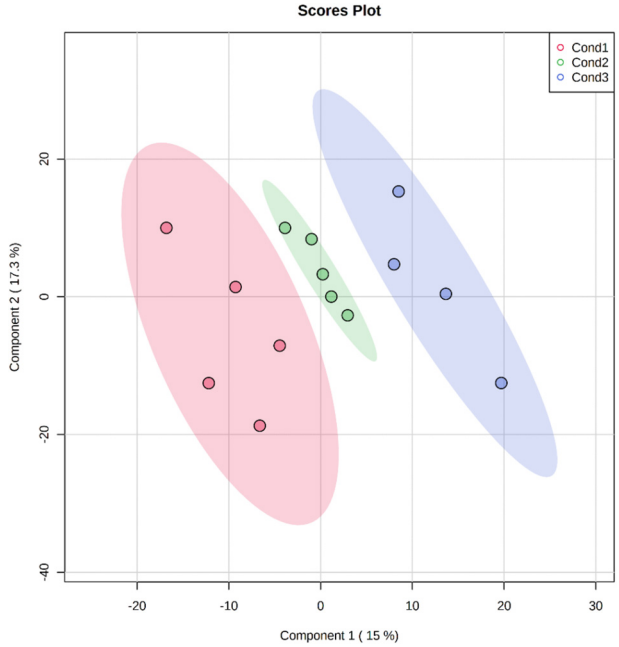

FIGURE 2 | Bi-dimensional representation of the scores for the PLS-DA analysis using the 758 quantified proteins extracted from somatic embryos originating from embryonal masses initiated under three different conditions (Cond1 = 23°C, control: Cond2 = 40°C, 4 h; Cond3 = 60°C, 5 min). Data normalization was performed using the AutoScale method and the scores of the two first components are represented showing the ovals at 95% confidence interval.

of functions related to the life cycle of proteins were detected (folding, catalysis, and transport), accounting for almost the 20% of the total enrichment analysis. At the transcriptome level, some proteins involved in gene expression regulation and RNA processing/metabolism also seemed to be involved in the response to heat, together with signal receptors and proteins constituents of signaling cascades. Finally, a small group of proteins taking part in cell division, response to abscisic acid and methylation processes were also selected by the PLS-DA analysis.

The univariate statistical analysis revealed that 64 proteins were differentially accumulated ($p < 0.05$) between the three conditions (**Supplementary Table 2**). Comparing these proteins with the 262 proteins selected from the PLS-DA analysis we observed that 54 proteins were common between both statistical approaches and were considered the top significant proteins after heat-stress response in our samples (**Supplementary Figure 2**). The complete list of these proteins, their accession number, the fold-change between conditions, and the results from both statistical analyses are shown in **Tables 2**, **3**.

In order to better visualize the relation between proteins, a cluster analysis was performed with the selected 54 top significant proteins by generating a heatmap (**Figure 4**) and a correlation matrix (**Supplementary Figure 3**). These analyses showed two clearly differenced groups of proteins based on their relative abundance between conditions. One of the groups presented an abundance increasing tendency from the control condition of 23°C (Cond1) to the highest temperature condition of 60°C (Cond3). The condition of 40°C for 4 h (Cond2) showed an intermediate behavior. As observed in the correlation matrix, all the proteins from this group were closely interrelated, presenting high positive correlation coefficients. This protein group included a great variety of proteins, among which some of them were specific of the group: HSPs and chaperones (small heat shock protein, DnaJ protein homolog ANJ1, DnaJ protein homolog) and proteins involved in ion and small molecules transport (outer plastidial membrane protein porin, mitochondrial outer membrane protein porin 2, mitochondrial outer membrane protein porin 5, sugar transporter ESL1). Some proteins related to the synthesis of specific sugars and sugar alcohols were also over-accumulated under high temperatures, such as UDP-glucuronic acid decarboxylase 4 and inositol 3-phosphate synthase isozyme 3. Following the same pattern, a great number of structural constituents of ribosomes and translation regulation factors were detected (40S ribosomal protein S1, 60S ribosomal protein L23, 60S ribosomal protein L17, 40S ribosomal protein S2-1, 60S ribosomal protein L4-1, 60S ribosomal protein L26-2, protein translation factor SUI1 homolog, polyadenylate-binding protein 8, eukaryotic translation initiation factor 3 subunit D). Finally, it is also remarkable the observed higher amount of proteins involved in the post-transcriptional regulation of RNA metabolism at high temperatures, such as RNA-binding protein ARP1 and protein ARGONAUTE 1D, and of one protein that takes part in the fatty acid biosynthetic process (acetyl-coenzyme A carboxylase carboxyl transferase subunit alpha). Besides, some of these proteins presented high fold changes between control (Cond1) and treatments (Cond2 and

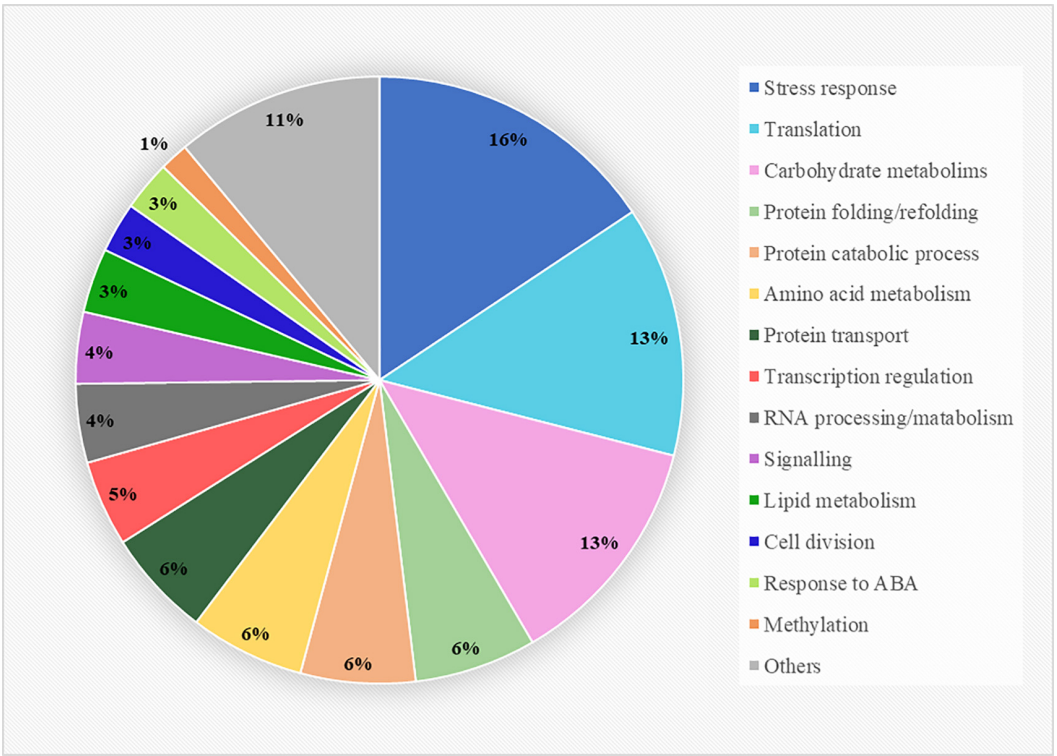

FIGURE 3 | Gene ontology enrichment analysis of the 262 proteins selected from the PLS-DA analysis presenting VIP values greater than 1. The biological function clustering was performed using the FunRich software and the Plants database from UniProtdatabase.

Cond3), such as small heat shock protein, 60 S ribosomal protein L4-1 and inositol 3-phosphate synthase isozyme 3 (**Tables 2**, **3**).

On the contrary, the other subgroup of proteins showed reduced abundance levels under high temperature conditions, especially at 60°C for 5 min (**Figure 4**), and was negatively correlated with the first group of proteins (**Supplementary Figure 3**). This cluster was composed to a vast extent by central metabolism enzymes, covering diverse pathways such as, glycolysis, citric acid cycle, fatty acid beta-oxidation or Calvin cycle (pyruvate dehydrogenase E1 component subunit beta-1, enolase, ribulose bisphosphate carboxylase/oxygenase activase A, ribulose bisphosphate carboxylase/oxygenase activase, 3-ketoacyl-CoA thiolase 1), and some proteins involved in the synthesis of specific sugars such as fructokinase-6, sucrose-phosphate synthase 2, UDP-arabinopyranose mutase 1 and phosphomannomutase. Proteins involved in oxidative-stress defense were clearly down-expressed (thiamine biosynthetic bifunctional enzyme BTH1, 4-coumarate–CoA ligase-like 5, phospholipid hydroperoxide glutathione peroxidase, EXPORTIN 1A), together with those implicated in amino acid synthesis and protein catalysis (threonine synthase, ketol-acid reductoisomerase, proteasome subunit alpha type-6, proteasome subunit alpha type-7-A, aminopeptidase M1). Other proteins found at lower concentrations at high temperatures included structural constituents of the cytoskeleton (actin-2, translationally-controlled tumor protein homolog), some proteins related with translation (60S ribosomal protein L3-2, 60S ribosomal protein L30-3, and methionine–tRNA ligase), post-transcriptional gene regulation and epigenetic mechanisms (ribonuclease TUDOR 2, adenosylhomocysteinase), nitrogen metabolism (ferredoxin–nitrite reductase), cellular receptors for nuclear import (importin subunit alpha-2) or electron transport proteins (cytochrome c oxidase subunit 6b-3). It is noticeable that some of them presented high fold changes: enolase, methionine–tRNA ligase, adenosylhomocysteinase, and 4-coumarate–CoA ligase-like 5 (**Tables 2**, **3**).

Soluble Sugar Content Quantification

The HPLC approach revealed the presence of three (fructose, glucose, and sucrose) of the five sugar and sugar alcohols analyzed. Sorbitol and mannitol could not be detected in Se's using this technique. All sugars presented similar concentrations, although the levels of sucrose and fructose were slightly higher than those of glucose (**Table 4**). Taking into account the effect of the treatments, no significant differences were observed. However, the levels of sucrose were on the verge of statistical significance (p = 0.078), showing a decreasing tendency at high temperatures, especially at 60°C for 5 min treatment (%23 decrease with respect to control treatment of 23°C). This pattern was not appreciable for the rest of sugars detected, although the lowest levels were also observed at 60°C for 5 min treatment (**Table 4**).

TABLE 2 | Top significant proteins selected from the combination of univariate statistical analysis (Kruskal–Wallis test) and multivariate PLS-DA analysis ($p < 0.05$ and VIP > 1) in somatic embryos of *P. radiata* originating from embryonal masses induced under high temperature conditions (Cond1 = 23°C, control; Cond2 = 40°C, 4 h; Cond3 = 60°C, 5 min).

		Fold change			Kruskal–Wallis	PLS-DA
Description	**Accession**	**Cond2/Cond1**	**Cond3/Cond1**	**Cond3/Cond2**	***p*-value**	**VIP**
60S ribosomal protein L3-2	P22738	0.84	0.55	0.65	0.005	2.43
Small heat shock protein, chloroplastic	Q95661	2.68	1.94	0.72	0.007	1.38
Methionine–tRNA ligase, cytoplasmic	Q9SVN5	0.35	0.12	0.34	0.009	2.22
Outer plastidial membrane protein porin	P42054	1.1	1.58	1.43	0.01	2.25
Mitochondrial outer membrane protein porin 2	Q6L5I5	0.91	1.38	1.51	0.011	1.9
DnaJ protein homolog	Q04960	1.42	1.51	1.06	0.013	2.17
Unknown protein 3 (Fragment)	P85487	0.66	0.47	0.71	0.013	2.12
40S ribosomal protein S12	Q9XHS0	1.39	1.76	1.27	0.015	2.28
Thiamine biosynthetic bifunctional enzyme BTH1, chloroplastic	O48881	1.03	0.71	0.69	0.016	1.86
Translationally-controlled tumor protein homolog	Q9ZRX0	0.85	0.68	0.8	0.017	2.21
Ketol-acid reductoisomerase, chloroplastic	Q65XK0	0.74	0.4	0.53	0.017	2.22
Ribulose bisphosphate carboxylase/oxygenase activase, chloroplastic	P93431	0.71	0.58	0.82	0.018	2.42
Actin-2	P0C539	1.3	0.4	0.31	0.018	1.51
Probable fructokinase-6, chloroplastic	Q9C524	0.7	0.65	0.93	0.018	2.08
Ferredoxin–nitrite reductase, chloroplastic	Q39161	0.59	0.64	1.09	0.018	1.51
60S ribosomal protein L23	Q9XEK8	0.98	1.37	1.4	0.018	2.11
Adenosylhomocysteinase	P68173	0.93	0.22	0.24	0.018	1.98
Pyruvate dehydrogenase E1 component subunit beta-1	Q6Z1G7	0.89	0.69	0.78	0.02	2.27
Ribulose bisphosphate carboxylase/oxygenase activase A	Q40073	0.68	0.52	0.77	0.02	2.35
Sugar transporter ESL1	Q94KE0	1.19	1.77	1.49	0.021	1.85
Casein kinase II subunit alpha-2	Q9AR27	0.63	0.71	1.13	0.021	1.67
Protein translation factor SUI1 homolog	Q9SM41	1.02	1.23	1.21	0.021	1.96
Probable RNA-binding protein ARP1	Q9M1S3	1.36	1.74	1.28	0.022	2.38
Polyadenylate-binding protein 8	Q9FXA2	1.24	1.57	1.27	0.022	2.37
Aminopeptidase M1	Q8VZH2	0.56	0.5	0.89	0.025	1.97
Phosphomannomutase	Q1W374	0.95	0.65	0.68	0.026	2.23

Fold changes are presented as the ratio between one condition and the other.

DISCUSSION

In this work, we have tried to study the proteome of Se's to obtain insights about the effect of heat-stress at early stages of radiata pine SE and elucidate how that effect can modulate the success of different stages of the process.

Following the same tendency observed in previous studies (Castander-Olarieta et al., 2019), in this work the combination of high temperatures and long exposure time-periods (40°C, 4 h) provoked a considerable decrease of around 13% in the initiation success of EMs. This could be attributed to oxidative damage and structural imbalances at cellular and tissue level, as reported in Castander-Olarieta et al. (2019). On the other hand, no differences were observed at the proliferation stage. Castander-Olarieta et al. (2019) reported that the detrimental effects of the application of high temperatures during initiation could also be observed after four subculture periods (2 months) during proliferation. Results obtained at this stage seem quite ambiguous, as other authors reported higher proliferation rates when EMs were induced under stressful conditions (Fehér, 2015; García-Mendiguren et al., 2016b). This fact could be attributed to the type and dose of the applied stress and the capacity of EMs to overcome the consequences of stress.

Although not significant, the number of Se's increased under high temperatures, a long-observed trend in our laboratory for both *P. radiata* and *P. halepensis* EMs initiated under high temperatures (García-Mendiguren et al., 2016b; Castander-Olarieta et al., 2019; Pereira et al., 2020). The same pattern was detected in similar temperature-based experiments during initiation of *Pinus pinaster* SE (Arrillaga et al., 2019), confirming the role of temperature as an activator of embryo development. On top of that, Castander-Olarieta et al. (2019) reported altered morphologies in both EMs and Se's originating from different temperature treatments, and despite not observing germination and acclimatization differences, the resulting somatic plants showed changes at phenotypic level in terms of growth and stress-resilience (Castander-Olarieta et al., 2020a). To shed light on these phenomena, the proteome of Se's was analyzed.

TABLE 3 | Continuation of **Table 2**.

		Fold change			Kruskal–Wallis	PLS-DA
Description	**Accession**	**Cond2/Cond1**	**Cond3/Cond1**	**Cond3/Cond2**	***p*-value**	**VIP**
Probable UDP-arabinopyranose mutase 1	O04300	1.02	0.54	0.53	0.026	1.9
60S ribosomal protein L30-3	Q9LSA3	1.02	0.76	0.75	0.026	1.8
Inosine triphosphate pyrophosphatase	C5WZH0	0.84	0.8	0.95	0.026	2.11
4-coumarate–CoA ligase-like 5	Q7F1X5	0.38	0.14	0.37	0.026	1.76
60S ribosomal protein L17	O48557	0.94	1.4	1.49	0.027	1.83
Probable sucrose-phosphate synthase 2	O04933	0.96	0.53	0.56	0.027	2.05
40S ribosomal protein S2-1	Q8L8Y0	1.15	1.36	1.18	0.028	2.21
60S ribosomal protein L4-1	Q9SF40	2.93	3.55	1.21	0.03	1.85
Eukaryotic translation initiation factor 3 subunit D	P56820	1.2	1.46	1.22	0.032	1.97
Proteasome subunit alpha type-6	Q9XG77	0.88	0.81	0.91	0.032	1.98
Protein argonaute 1D	Q5Z5B2	1.67	1.66	0.99	0.032	1.48
Threonine synthase, chloroplastic	Q9MT28	0.87	0.77	0.89	0.033	2.1
Probable inositol 3-phosphate synthase isozyme 3	Q9LX12	1.97	3.2	1.62	0.034	2.29
Proteasome subunit alpha type-7-A	Q6YT00	0.81	0.64	0.79	0.034	2.01
Protein EXPORTIN 1A	Q9SMV6	1.09	0.43	0.39	0.035	1.25
Ras-related protein RIC1	P40392	0.59	0.36	0.6	0.037	1.82
V-type proton ATPase subunit E	Q9SWE7	1.02	1.25	1.22	0.038	1.71
3-ketoacyl-CoA thiolase 1, peroxisomal	Q8LF48	0.98	0.72	0.74	0.038	1.87
Importin subunit alpha-2	F4JL11	1.05	0.76	0.72	0.039	1.66
Acetyl-coenzyme A carboxylase carboxyl transferase subunit alpha, chloroplastic	Q41008	1.06	1.46	1.37	0.039	1.83
Enolase	Q43321	0.93	0.04	0.05	0.039	2.1
Probable phospholipid hydroperoxide glutathione peroxidase	O23814	0.69	0.62	0.89	0.04	2.07
Mitochondrial outer membrane protein porin 5	Q84P97	1.09	1.28	1.17	0.042	1.94
DnaJ protein homolog ANJ1	P43644	1.29	1.34	1.04	0.046	1.87
60S ribosomal protein L26-2	Q9FJX2	1.02	1.36	1.33	0.046	1.86
Ribonuclease TUDOR 2	Q9FLT0	0.67	0.69	1.03	0.047	1.76
Cytochrome c oxidase subunit 6b-3	Q9SUD3	1.19	1.47	1.24	0.048	2.04
UDP-glucuronic acid decarboxylase 4	Q8S8T4	1.1	1.31	1.19	0.048	2.02

Top significant proteins selected from the combination of univariate statistical analysis (Kruskal–Wallis test) and multivariate PLS-DA analysis ($p < 0.05$ and VIP > 1) in somatic embryos of P. radiata originating from embryonal masses induced under high temperature conditions (Cond1 = 23°C, control; Cond2 = 40°C, 4 h; Cond3 = 60°C, 5 min). Fold changes are presented as the ratio between one condition and the other.

The proteomic analysis enabled the identification of 1,020 proteins; similar values to the ones obtained at plant level in radiata pine (Escandón et al., 2017) and in somatic embryos of other pine species (Morel et al., 2014b). Multivariate statistical analysis of the proteomic results revealed a large amount of proteins differentially responding to the three temperature conditions even several months later at Se's stage. This fact could explain the altered behaviors described during the different stages of SE in this study and previous ones. These proteins covered a broad spectrum of biological and molecular functions, but three groups were clearly more represented, including proteins involved in stress responses, proteome readjustment and carbohydrate metabolism. In spite of being at lower levels, proteins taking part in other interesting metabolic pathways were also detected, such as amino acid and lipid synthesis, transcription regulation, RNA metabolism and methylation. These results are in agreement with other studies carried out in radiata pine plantlets subjected to different stress conditions (Escandón et al., 2017; Pascual et al., 2017; Lamelas et al., 2020).

Further statistical analyses combining multivariate with univariate approaches highlighted the importance of 54 proteins as the top significant ones contributing to the separation between the three conditions. Among these proteins, it is noticeable the higher presence of HSPs and molecular chaperones in Se's originating from EMs induced at high temperatures. HSPs are up-regulated under supra-optimal high temperatures (Yuan et al., 2019; Jiang et al., 2020) and prevent proteins from being denatured by assisting in protein folding and processing. In that way, proteins can maintain a proper stability and function under unfavorable conditions (Hasanuzzaman et al., 2013; Krishnan et al., 2020).

Many studies have observed that these types of molecules are essential for heat-tolerance (Meiri and Breiman, 2009; Perez et al., 2009). In fact, while other stress responsive proteins such as ROS detoxifying enzymes have been described as important mediators in basal thermo-tolerance and early response processes, HSPs and chaperones appear to be required for both basal and acquired thermo-tolerance (Bokszczanin and Fragkostefanakis, 2013),

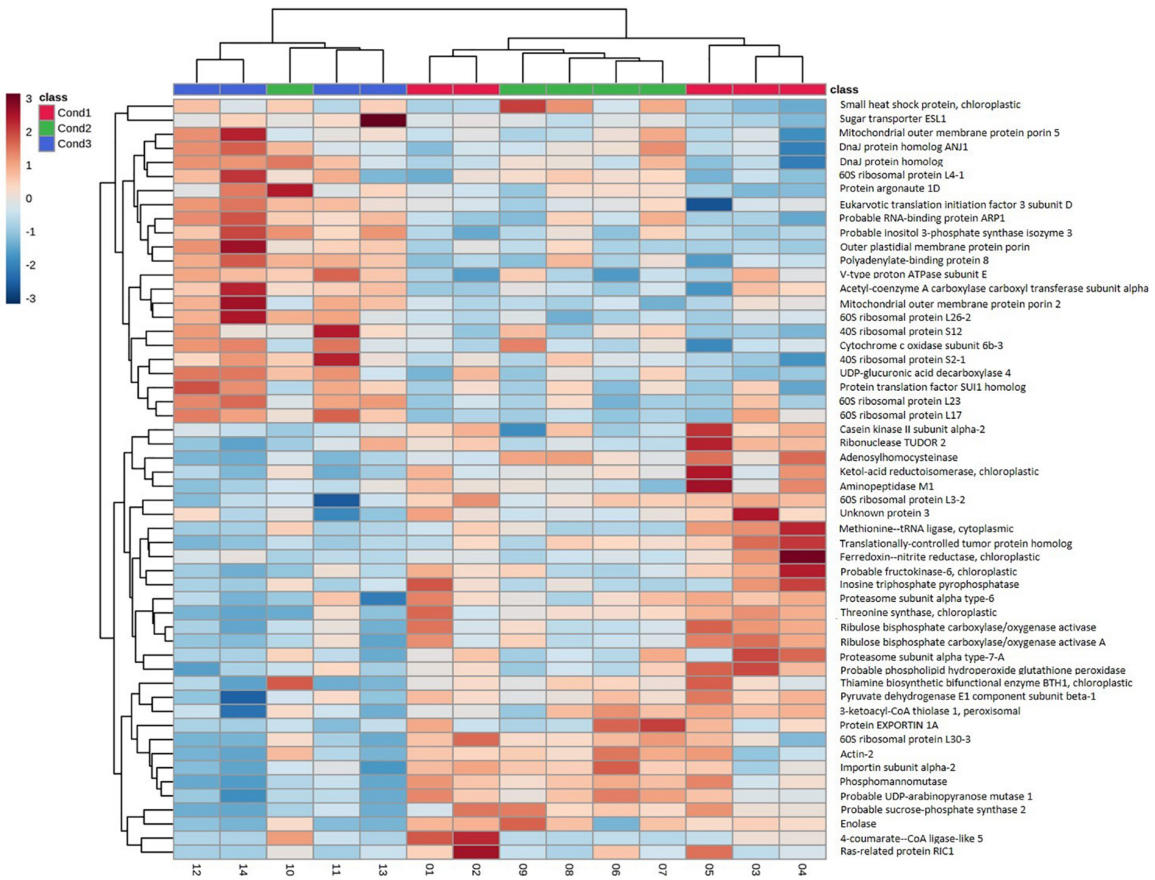

FIGURE 4 | Hierarchical clustering heatmap using the 54 proteins selected from the combination of Kruskal–wallis test and the PLS-DA analysis in somatic embryos of *P. radiata* originating from high temperature conditions (Con1 = 23°C, control; Cond2 = 40°C, 4 h; Cond3 = 60°C, 5 min). Hierarchical clustering was performed at the protein (rows) using Euclidean distance and Complete for the clustering algorithm.

even contributing to plant acclimation (Escandón et al., 2017). Reinforcing this idea, there are several examples of transgenic plants constitutively expressing HSPs that without a previous heat treatment exhibit an enhanced thermo-tolerance (Lee et al., 1995; Malik et al., 1999). As a result, it would be interesting to confirm if this protein profile is maintained throughout the SE process, influencing the *ex vitro* performance of the generated plants, as observed at the physiological level under control and drought stress conditions in Castander-Olarieta et al. (2020b). Besides, the accumulation of HSPs has also been observed under other abiotic stress conditions, including drought (Kosová et al., 2011; Taïbi et al., 2015), which could provide simultaneous protection against more than one environmental constraint.

Chaperones and HSPs seem to be closely related with many other proteins in cells, such as post-transcriptional regulation elements. This is the case of protein ARGONAUTE 1D (Q5Z5B2), which was found at higher concentrations under high temperature conditions, positively correlating with HSPs. Similar responses have also been observed in other plant model systems (Zhang et al., 2012). These types of proteins bind to short RNAs such as microRNAs (miRNAs) or short interfering RNAs (siRNAs), and repress the translation of mRNAs which are complementary to them. These gene expression regulatory mechanisms have been reported to be key players during the formation of temperature-dependent epigenetic memory in Norway spruce (Yakovlev and Fossdal, 2017). However, other proteins related with post-transcriptional regulation, such as the ribonuclease TUDOR 2, were down-regulated under high temperatures, contradicting the studies that remark the interplay between HSPs, stress granules and processing bodies (Miroshnichenko et al., 2005). In this sense, TUDOR 2 is essential for the integrity and function of stress

TABLE 4 | Effect of temperature treatment (23°C, control; 40°C, 4 h; 60°C, 5 min) on the levels of the following sugars and sugar alcohols in somatic embryos of *P. radiata*: fructose, glucose and sucrose (μmol g FW^{-1}).

Treatment	Fructose	Glucose	Sucrose
23°C, control	70.88 ± 1.95^{a}	46.77 ± 5.03^{a}	72.98 ± 5.34^{a}
40°C, 4 h	74.57 ± 3.31^{a}	46.75 ± 5.64^{a}	67.41 ± 5.88^{a}
60°C, 5 min	66.12 ± 6.55^{a}	40.76 ± 6.26^{a}	56.19 ± 3.52^{a}

Data are presented as mean values ± SE. Significant differences among treatments at $p < 0.05$ are indicated by letters.

granules and processing bodies, which apart from protecting RNAs from harmful conditions (Jang et al., 2020), seem to be important sites of post-transcriptional gene regulation (Gutierrez-Beltran et al., 2015).

Adenosylhomocysteinase, another protein related to epigenetic regulation, showed a decreasing pattern in Se's from high temperatures, especially at 60°C for 5 min. It controls methylation through regulation of the intracellular concentration of adenosylhomocysteine, a competitive inhibitor of *S*-adenosyl-L-methionine-dependent methyl transferase reactions. These data suggest that heat-stress might have derived in hypomethylation of Se's, as observed in embryonal masses and somatic plants originating from the same temperature treatments in previous studies (Castander-Olarieta et al., 2020c). Similar results were obtained by Lamelas et al. (2020), indicating that DNA methylation, together with post-transcriptional regulation mechanisms may be involved in the maintenance of acquired thermotolerance and in the establishment of an epigenetic memory. It would be interesting to perform further analyses to confirm this hypothesis and study its evolution along the whole SE process to see if the altered behavior of the resulting somatic plants in Castander-Olarieta et al. (2020b) could be attributed to this fact.

In the same way, the proteome analysis revealed that the translasome machinery, including ribosomal proteins and translation regulation factors, together with proteins involved in protein catalysis and homeostasis such as different proteasome subunits, had a relevant role during heat-stress response, as already described in other studies (Wang et al., 2018; Li et al., 2019). Although varying patterns were observed under the different temperature conditions, most of the ribosomal proteins and all the translation regulation factors followed an accumulation tendency when heat was applied, while all the proteins involved in protein degradation were down-represented. In fact, one of the proteins presenting the highest fold-changes was the 60S ribosomal protein L4-1, which was detected at higher concentrations at both 40 and 60°C treatments. This protein has been found to be temperature sensitive, increasing considerably its expression under cold (Schlaen et al., 2015). As a result, we can state that heat provokes a deep reorganization of the proteome, by a strict regulation of translation and an altered ribosome composition that could result in a selective mRNA translation to better cope with adverse conditions.

Besides, the relative abundance and differential expression of the aforementioned proteins seem to have further implications in different plant developmental processes via interconnections with phytohormones and other signaling molecules. For example, the function of some ribosomal proteins is linked with cytokinin molecular circuits (Černý et al., 2013). Interestingly, the application of the same high temperature conditions at initiation of *P. radiata* and *P. halepensis* SE provoked changes in the cytokinin profile of EMs (Castander-Olarieta et al., 2020a,b; Pereira et al., 2020). It would be of special interest for future studies to confirm if those changes are maintained in Se's and study their relationship with the translasome machinery.

Apart from that, protein homeostasis seems to have special relevance during conifer SE, as indicated by the differential expression of specific proteasome subunits and translation elongation factors during EM proliferation and Se's development in numerous conifer species (Trontin et al., 2016). Specifically, at maturation stage the synthesis of major storage proteins of the globulin and albumin families and proteins involved in acquisition of desiccation tolerance (late embryogenesis abundant proteins) appear to be of great relevance, even determining the germination capacity of Se's (Klimaszewska et al., 2004; Businge et al., 2013). Furthermore, Lippert et al. (2005) proposed the proteasome complex as a molecular marker of embryo development. Consequently, the different proteasome and translation regulation factors profiles observed in this study could be associated with the enhanced capacity of EMs subjected to heat-stress to produce Se's and with the different morphologies observed in Castander-Olarieta et al. (2019) among Se's originating from different temperature treatments.

Heat also induced changes in the metabolism of Se's. The levels of acetyl-coenzyme A carboxylase carboxyl transferase subunit alpha, an enzyme that takes part in a sub-pathway of the fatty acid biosynthetic process, was clearly accumulated at high temperatures. Heat-stress increases membrane fluidity and as a result plants need to alter fatty acid composition of lipids to compensate for those changes (Escandón et al., 2017).

On the other hand, the glycolytic pathway, as well as the citric acid cycle and β-oxidation of fatty acids appeared to be less active in samples originating from high temperatures, as the proteins pyruvate dehydrogenase E1 component subunit beta-1, enolase and 3-ketoacyl-CoA thiolase 1 were found at lower levels. Parankusam et al. (2017) and Wang et al. (2018) also observed the same pattern when applying heat to chickpea and radish plants, respectively. A decrease in carbon catabolism has also been detected under favorable maturation conditions in *P. pinaster* EMs, leading to high quality embryos (Morel et al., 2014a). However, other reports in *Picea glauca* and some broad-leaf woody plants highlight the importance of high enolase activity as a marker of embryogenic character and normal embryo development (Lippert et al., 2005; Correia et al., 2012).

In the same way, the levels of enzymes involved in the synthesis of starch and sucrose (fructokinase-6 and sucrose-phosphate synthase 2) were reduced under high temperatures, as confirmed by the HPLC analysis for sucrose. Despite this fact, the levels of sucrose were considerably higher in all samples if compared with those from EMs in previous studies (Castander-Olarieta et al., 2019). The increase of sucrose during the formation of Se's has long been documented as a symbol of acquisition of desiccation tolerance (Businge et al., 2013).

The simultaneous decrease of the glycolytic activity and of the synthesis of disaccharides and polysaccharides would result in the accumulation of free soluble monosaccharides like glucose or fructose. However, this was not observed at the HPLC analysis, and thus, we could assume that these molecules might be serving as precursors for the synthesis of other specific compounds. In fact, inositol 3-phosphate synthase isozyme 3, the key enzyme for the synthesis of myo-inositol from glucose, was notably accumulated under high temperatures, as already observed in other plant species (Khurana et al., 2012). This molecule acts as a compatible solute, maintaining plant cell

turgor and stabilizing membranes and proteins (Bokszczanin and Fragkostefanakis, 2013). Nonetheless, the levels of mannitol and sorbitol, molecules previously identified as important osmolytes under heat and drought (Alhaithloul, 2019; Ivanov et al., 2019), were not detectable in radiata pine Se's using HPLC.

Likewise, the differential expression of phosphomannomutase, UDP-arabinopyranose mutase and UDP-glucuronic acid decarboxylase 4 also suggests a drift from glycolysis and starch accumulation toward the synthesis of cell-wall non-cellulosic polysaccharides. Specifically, UDP-glucuronic acid takes part in the synthesis of D-xylose, a constituent component of cell-wall polymers whose concentration has been demonstrated to change under heat-stress (Lima et al., 2013).

In correlation with these enzymes we found a huge amount of proteins involved in oxidative stress response processes and in the synthesis of certain amino acids. All of them showed a decreasing tendency in Se's originating from high temperature conditions, probably conditioned by the decreased in central metabolism activity, the reduced availability of carbon skeletons and a simultaneous reduction of nitrogen assimilation (lower levels of ferredoxin–nitrite reductase). These proteins included an enzyme responsible of the synthesis of thiamine (thiamine biosynthetic bifunctional enzyme BTH1), which provides oxidative stress resistance via regulation of glucose metabolism (Kartal and Palabiyik, 2019), and 4-coumarate–CoA ligase-like 5, involved in the flavonoid and phenylpropanoid biosynthesis pathway, whose accumulation is essential for the prevention of oxidative damage (Eliášová et al., 2017). Phospholipid hydroperoxide glutathione peroxidase, which protects cells and enzymes from oxidative damage (Yant et al., 2003) was also included in this group. Similar results were obtained for EXPORTIN 1A, a protein involved in heat-induced oxidative stress basal resistance (Wu et al., 2010), and threonine synthase, whose product, threonine, is the precursor of isoleucine (Joshi et al., 2010), other amino acid whose enzyme was down-expressed (ketol-acid reductoisomerase). Previous studies carried out in our laboratory (Castander-Olarieta et al., 2019) reported the accumulation of phenolic compounds and branched chain amino acids (isoleucine) in EMs at first subculture after heat application, in opposition to the results from this study in Se's months later. As a result, we can assume that the response to oxidative stress is more relevant during short-term heat exposures, as observed by Escandón et al. (2017), rather than during acclimatization or acquired tolerance.

Finally, it is noticeable that several transmembrane transport proteins (porins) and sugar transporters were found at higher levels under high temperatures. Several authors have remarked the importance of these proteins during osmotic stress adaptation and thermal sensing (Brumós et al., 2009; Yakovlev et al., 2016). Based on the positive correlation of these proteins and the increased levels of specific compatible solutes such as myo-inositol, we can hypothesize that a synergistic response is taking place for an enhanced and controlled transport of osmolytes in Se's originating from heat stress conditions.

This study provides novel information about the long-term effect of heat-stress on radiata pine SE at the proteome level. Results indicated a complex and selective reorganization of the proteome, combined with the possible activation of certain epigenetic and post-transcriptional regulation mechanisms, as well as the accumulation of HSPs and chaperones and a drift in the carbohydrate metabolism toward the synthesis of fatty acids, specific compatible solutes and cell-wall remodeling carbohydrates. These results suggest that the application of stress during initial steps of the SE process could provoke delayed effects in embryogenic cells leading to changes in the subsequent stages up to plant level. This has great potential as the starting point of further research and toward practical applications such as modulating the characteristics of plants using somatic embryogenesis.

DATA AVAILABILITY STATEMENT

The data has been uploaded to the PRIDE repository with the dataset identifier PXD022711.

AUTHOR CONTRIBUTIONS

PM, IM, JC, SC, CP, and AC-O conceived and planned the experiments. AC-O prepared all the plant material and executed the heat stress experiments. AC-O, CP, VM, and SC carried out the protein analysis. AC-O, CP, and SS-Á performed the soluble sugar content quantification. AC-O, VM, SC, and BM carried out the data curation and statistical analysis. AC-O and VM wrote the manuscript. All authors provided critical feedback and helped to shape the research, analyses, and manuscript.

FUNDING

This research was funded by MINECO project (AGL2016-76143-C4-3R), CYTED (P117RT0522), DECO (Basque government) and MULTIFOREVER project, supported under the umbrella of ERA-NET Cofund ForestValue by ANR (FR), FNR (DE), MINCyT (AR), MINECO-AEI (ES), MMM (FI), and VINNOVA (SE). ForestValue has received funding from the European Union's Horizon 2020 Research and Innovation Programme under grant agreement no. 773324. This work was also supported by Renature: Projecto ReNature (Centro-01-0145-FEDER-000007)—Valorização dos Recursos Naturais Endógenos da Região Centro; and Portuguese Foundation for Science and Technology (FCT) (SFRH/BD/123702/2016), Fundo Social Europeu (FSE), and Programa Operacional Regional do Centro – Centro 2020 (UE), POCI-01-0145-FEDER-031999, POCI-01-0145-FEDER-007440 (strategic project UIDB/04539/2020), and by The National Mass Spectrometry Network (RNEM) under the contract POCI-01-0145-FEDER-402-022125 (ROTEIRO/0028/2013).

SUPPLEMENTARY MATERIAL

The Supplementary Material for this article can be found online at: https://www.frontiersin.org/articles/10.3389/fpls.2021.631239/full#supplementary-material

REFERENCES

Alhaithloul, H. A. S. (2019). Impact of combined heat and drought stress on the potential growth responses of the desert grass *Artemisia sieberi alba*: relation to biochemical and molecular adaptation. *Plants* 8:416. doi: 10.3390/plants8100416

Allen, C. D., Macalady, A. K., Chenchouni, H., Bachelet, D., McDowell, N., Vennetier, M., et al. (2010). A global overview of drought and heat-induced tree mortality reveals emerging climate change risks for forests. *For. Ecol. Manag.* 259, 660–684. doi: 10.1016/j.foreco.2009.09.001

Anjo, S. I., Santa, C., and Manadas, B. (2015). Short GeLC-SWATH: a fast and reliable quantitative approach for proteomic screenings. *Proteomics* 15, 757–762. doi: 10.1002/pmic.201400221

Arrillaga, I., Morcillo, M., Zanón, I., Lario, F., Segura, J., and Sales, E. (2019). New approaches to optimize somatic embryogenesis in maritime pine. *Front. Plant Sci.* 10:138. doi: 10.3389/fpls.2019.00138

Bokszczanin, K. L., and Fragkostefanakis, S. (2013). Perspectives on deciphering mechanisms underlying plant heat stress response and thermotolerance. *Front. Plant Sci.* 4:315. doi: 10.3389/fpls.2013.00315

Brumós, J., Colmenero-Flores, J. M., Conesa, A., Izquierdo, P., Sánchez, G., Iglesias, D. J., et al. (2009). Membrane transporters and carbon metabolism implicated in chloride homeostasis differentiate salt stress responses in tolerant and sensitive citrus rootstocks. *Funct. Integr. Genomics* 9:293. doi: 10.1007/s10142-008-0107-6

Businge, E., Bygdell, J., Wingsle, G., Moritz, T., and Egertsdotter, U. (2013). The effect of carbohydrates and osmoticum on storage reserve accumulation and germination of Norway spruce somatic embryos. *Physiol. Plant.* 149, 273–285. doi: 10.1111/ppl.12039

Castander-Olarieta, A., Moncaleán, P., Pereira, C., Pěnčík, A., Petřík, I., Pavloviæ, I., et al. (2020a). Cytokinins are involved in drought tolerance of *Pinus radiata* plants originating from embryonal masses induced at high temperatures. *Tree Physiol.* taa055 (in press). doi: 10.1093/treephys/tpaa055

Castander-Olarieta, A., Montalbán, I. A., de Medeiros Oliveira, E., Dell'Aversana, E., D'Amelia, L., Carillo, P., et al. (2019). Effect of thermal stress on tissue ultrastructure and metabolite profiles during initiation of radiata pine somatic embryogenesis. *Front. Plant Sci.* 9:2004. doi: 10.3389/fpls.2018.02004

Castander-Olarieta, A., Pereira, C., Montalbán, I. A., Pěnčík, A., Petřík, I., Pavlović, I., et al. (2020b). Quantification of endogenous aromatic cytokinins in *Pinus radiata* embryonal masses after application of heat stress during initiation of somatic embryogenesis. *Trees* (in press). doi: 10.1007/s00468-020-02047-x

Castander-Olarieta, A., Pereira, C., Sales, E., Meijón, M., Arrillaga, I., Cañal, M. J., et al. (2020c). Induction of radiata pine somatic embryogenesis at high temperatures provokes a long-term decrease in DNA methylation/hydroxymethylation and differential expression of stress-related genes. *Plants* 9:1762. doi: 10.3390/plants9121762

Černý, M., Kuklová, A., Hoehenwarter, W., Fragner, L., Novák, O., Rotková, G., et al. (2013). Proteome and metabolome profiling of cytokinin action in *Arabidopsis* identifying both distinct and similar responses to cytokinin down- and up-regulation. *J. Exp. Bot.* 64, 4193–4206. doi: 10.1093/jxb/ert227

Correia, S., Vinhas, R., Manadas, B., Lourenço, A. S., Veríssimo, P., and Canhoto, J. M. (2012). Comparative proteomic analysis of auxin-induced embryogenic and nonembryogenic tissues of the solanaceous tree *Cyphomandra betacea* (tamarillo). *J. Proteome Res.* 11, 1666–1675. doi: 10.1021/pr200856w

Correia, S. I., Alves, A. C., Veríssimo, P., and Canhoto, J. M. (2016). "Somatic embryogenesis in broad-leaf woody plants: what we can learn from proteomics," in *In Vitro Embryogenesis in Higher Plants*, eds M. Germana and M. Lambardi (Totowa, NJ: Humana Press), 117–129. doi: 10.1007/978-1-4939-3061-6_6

de Diego, N., Pérez-Alfocea, F., Cantero, E., Lacuesta, M., and Moncaleán, P. (2012). Physiological response to drought in radiata pine: phytohormone implication at leaf level. *Tree Physiol.* 32, 435–449. doi: 10.1093/treephys/tps029

de Diego, N., Rodríguez, J. L., Dodd, I. C., Pérez-Alfocea, F., Moncaleán, P., and Lacuesta, M. (2013a). Immunolocalization of IAA and ABA in roots and needles of radiata pine (*Pinus radiata*) during drought and rewatering. *Tree Physiol.* 33, 537–549. doi: 10.1093/treephys/tpt033

de Diego, N., Saiz-Fernández, I., Rodríguez, J. L., Pérez-Alfocea, P., Sampedro, M. C., Barrio, R. J., et al. (2015). Metabolites and hormones are involved in the intraspecific variability of drought hardening in radiata pine. *J. Plant Physiol.* 188, 64–71. doi: 10.1016/j.jplph.2015.08.006

de Diego, N., Sampedro, M. C., Barrio, R. J., Saiz-Fernández, I., Moncaleán, P., and Lacuesta, M. (2013b). Solute accumulation and elastic modulus changes in six radiata pine breeds exposed to drought. *Tree Physiol.* 33, 69–80. doi: 10.1093/treephys/tps125

Eliášová, K., Vondráková, Z., Malbeck, J., Trávníčková, A., Pešek, B., Vágner, M., et al. (2017). Histological and biochemical response of Norway spruce somatic embryos to UV-B irradiation. *Trees Struct. Funct.* 31, 1279–1293. doi: 10.1007/s00468-017-1547-1

Escandón, M., Valledor, L., Pascual, J., Pinto, G., Cañal, M. J., and Meijón, M. (2017). System-wide analysis of short-term response to high temperature in Pinus radiata. *J. Exp. Bot.* 68, 3629–3641. doi: 10.1093/jxb/erx198

Fehér, A. (2015). Somatic embryogenesis - stress-induced remodeling of plant cell fate. *Biochim. Biophys. Acta Gene Regul. Mech.* 1849, 385–402. doi: 10.1016/j.bbagrm.2014.07.005

García-Mendiguren, O., Montalbán, I. A., Correia, S., Canhoto, J., and Moncaleán, P. (2016a). Different environmental conditions at initiation of radiata pine somatic embryogenesis determine the protein profile of somatic embryos. *Plant Biotechnol.* 33, 143–152. doi: 10.5511/plantbiotechnology.16.0520a

García-Mendiguren, O., Montalbán, I. A., Goicoa, T., Ugarte, M. D., and Moncaleán, P. (2016b). Environmental conditions at the initial stages of *Pinus radiata* somatic embryogenesis affect the production of somatic embryos. *Trees Struct. Funct.* 30, 949–958. doi: 10.1007/s00468-015-1336-7

García-Mendiguren, O., Montalbán, I. A., Goicoa, T., Ugarte, M. D., and Moncaleán, P. (2017). Are we able to modulate the response of somatic embryos of pines to drought stress? *Act. Hortic.* 1155, 77–84. doi: 10.17660/ActaHortic.2017.1155.10

Gutierrez-Beltran, E., Moschou, P. N., Smertenko, A. P., and Bozhkov, P. V. (2015). Tudor staphylococcal nuclease links formation of stress granules and processing bodies with mRNA catabolism in *Arabidopsis*. *Plant Cell* 27, 926–943. doi: 10.1105/tpc.114.134494

Hasanuzzaman, M., Nahar, K., Alam, M. M., Roychowdhury, R., and Fujita, M. (2013). Physiological, biochemical, and molecular mechanisms of heat stress tolerance in plants. *Int. J. Mol. Sci.* 14, 9643–9684. doi: 10.3390/ijms14059643

Heringer, A. S., Santa-Catarina, C., and Silveira, V. (2018). Insights from proteomic studies into plant somatic embryogenesis. *Proteomics* 18:e1700265. doi: 10.1002/pmic.201700265

Ivanov, Y. V., Kartashov, A. V., Zlobin, I. E., Sarvin, B., Stavrianidi, A. N., and Kuznetsov, V. V. (2019). Water deficit-dependent changes in non-structural carbohydrate profiles, growth and mortality of pine and spruce seedlings in hydroculture. *Environ. Exp. Bot.* 157, 151–160. doi: 10.1016/j.envexpbot.2018.10.016

Jang, G. J., Jang, J. C., and Wu, S. H. (2020). Dynamics and functions of stress granules and processing bodies in plants. *Plants* 9:1122. doi: 10.3390/plants9091122

Jiang, C., Bi, Y., Mo, J., Zhang, R., Qu, M., Feng, S., et al. (2020). Proteome and transcriptome reveal the involvement of heat shock proteins and antioxidant system in thermotolerance of *Clematis florida*. *Sci. Rep.* 10:8883. doi: 10.1038/s41598-020-65699-2

Joshi, V., Joung J. G., Fei Z., and Jander G. (2010) Interdependence of threonine, methionine and isoleucine metabolism in plants: accumulation and transcriptional regulation under abiotic stress. *Amino Acids* 39, 933–947. doi: 10.1007/s00726-010-0505-7

Kartal, B., and Palabiyik, B. (2019). Thiamine leads to oxidative stress resistance via regulation of the glucose metabolism. *Cell Mol. Biol.* 65, 73–77. doi: 10.14715/cmb/2019.65.1.13

Khurana, N., Chauhan, H., and Khurana, P. (2012). Expression analysis of a heat-inducible, Myo-inositol-1-phosphate synthase (MIPS) gene from wheat and the alternatively spliced variants of rice and *Arabidopsis*. *Plant. Cell Rep.* 31, 237–251. doi: 10.1007/s00299-011-1160-5

Klimaszewska, K., Morency, F., Jones-Overton, C., and Cookeb, J. (2004). Accumulation pattern and identification of seed storage proteins in zygotic embryos of *Pinus strobus* and in somatic embryos from different maturation treatments. *Physiol. Plant.* 121, 682–690. doi: 10.1111/j.1399-3054.2004.00370.x

Kosová, K., Vítámvás, P., Prášil, I. T., and Renaut, J. (2011). Plant proteome changes under abiotic stress - contribution of proteomics studies to understanding plant stress response. *J. Proteomics* 74, 1301–1322. doi: 10.1016/j.jprot.2011.02.006

Krishnan, H. B., Kim, W. S., Oehrle, N. W., Smith, J. R., and Gillman, J. D. (2020). Effect of heat stress on seed protein composition and ultrastructure of protein storage vacuoles in the cotyledonary parenchyma cells of soybean genotypes that are either tolerant or sensitive to elevated temperatures. *Int. J. Mol. Sci.* 21:4775. doi: 10.3390/ijms21134775

Kvaalen, H., and Johnsen, Ø (2008). Timing of bud set in *Picea abies* is regulated by a memory of temperature during zygotic and somatic embryogenesis. *New Phytol.* 177, 49–59. doi: 10.1111/j.1469-8137.2007.02222.x

Lamelas, L., Valledor, L., Escandón, M., Pinto, G., Cañal, M. J., and Meijón, M. (2020). Integrative analysis of the nuclear proteome in *Pinus radiata* reveals thermopriming coupled to epigenetic regulation. *J. Exp. Bot.* 71, 2040–2057. doi: 10.1093/jxb/erz524

Lee, J. H., Hubel, A., and Schoffl, F. (1995). Derepression of the activity of genetically engineered heat shock factor causes constitutive synthesis of heat shock proteins and increased thermotolerance in transgenic *Arabidopsis*. *Plant J.* 8, 603–612. doi: 10.1046/j.1365-313x.1995.8040603.x

Li, S., Yu, J., Li, Y., Zhang, H., Bao, X., Bian, J., et al. (2019). Heat-responsive proteomics of a heat-sensitive spinach variety. *Int. J. Mol. Sci.* 20:3872. doi: 10.3390/ijms20163872

Lima, R. B., Dos Santos, T. B., Vieira, L. G. E., Ferrarese, M. D. L. L., Ferrarese-Filho, O., Donatti, L., et al. (2013). Heat stress causes alterations in the cell-wall polymers and anatomy of coffee leaves (*Coffea arabica* L.). *Carbohydr. Polym.* 93, 135–143. doi: 10.1016/j.carbpol.2012.05.015

Lippert, D., Jun, Z., Ralph, S., Ellis, D. E., Gilbert, M., Olafson, R., et al. (2005). Proteome analysis of early somatic embryogenesis in *Picea glauca*. *Proteomics* 5, 461–473. doi: 10.1002/pmic.200400986

Malik, M. K., Slovin, J. P., Hwang, C. H., and Zimmerman, J. L. (1999). Modified expression of a carrot small heat shock protein gene, Hsp17.7, results in increased or decreased thermotolerance. *Plant J.* 20, 89–99. doi: 10.1046/j.1365-313x.1999.00581.x

Meiri, D., and Breiman, A. (2009). *Arabidopsis* ROF1 (FKBP62) modulates thermotolerance by interacting with HSP90.1 and affecting the accumulation of HsfA2-regulated sHSPs. *Plant J.* 59, 387–399. doi: 10.1111/j.1365-313X.2009.03878.x

Miroshnichenko, S., Tripp, J., Zur Nieden, U., Neumann, D., Conrad, U., and Manteuffel, R. (2005). Immunomodulation of function of small heat shock proteins prevents their assembly into heat stress granules and results in cell death at sublethal temperatures. *Plant J.* 41, 269–281. doi: 10.1111/j.1365-313X.2004.02290.x

Moncaleán, P., García-Mendiguren, O., Novák, O., Strnad, M., Goicoa, T., Ugarte, M. D., et al. (2018). Temperature and water availability during maturation affect the cytokinins and auxins profile of radiata rine somatic embryos. *Front. Plant Sci.* 9:1898. doi: 10.3389/fpls.2018.01898

Montalbán, I. A., de Diego, N., and Moncaleán, P. (2012). Enhancing initiation and proliferation in radiata pine (*Pinus radiata* D. Don) somatic embryogenesis through seed family screening, zygotic embryo staging and media adjustments. *Acta Physiol. Plant.* 34, 451–460. doi: 10.1007/s11738-011-0841-6

Montalbán, I. A., and Moncaleán, P. (2018). "*Pinus radiata* (D. Don) somatic embryogenesis," in *Step Wise Protocols for Somatic Embryogenesis of Important Woody Plants*, eds S. Jain, and P. Gupta (Cham: Springer International Publishing), 1–11. doi: 10.1007/978-3-319-89483-6_1

Morel, A., Teyssier, C., Trontin, J. F., Pešek, B., Eliášová, K., Beaufour, M., et al. (2014a). Early molecular events involved in *Pinus pinaster* Ait. Somatic embryo development under reduced water availability: transcriptomic and proteomic analysis. *Physiol. Plant.* 152, 184–201. doi: 10.1111/ppl.12158

Morel, A., Trontin, J. F., Corbineau, F., Lomenech, A. M., Beaufour, M., Reymond, I., et al. (2014b). Cotyledonary somatic embryos of *Pinus pinaster* Ait. Most closely resemble fresh, maturing cotyledonary zygotic embryos: biological, carbohydrate and proteomic analyses. *Planta* 240, 1075–1095. doi: 10.1007/s00425-014-2125-z

Niu, Y., and Xiang, Y. (2018). An overview of biomembrane functions in plant responses to high-temperature stress. *Front. Plant Sci.* 9:915. doi: 10.3389/fpls.2018.00915

Paciolla, C., Paradiso, A., and de Pinto, M. C. (2016). "Cellular redox homeostasis as central modulator in plant stress response," in *Redox State as a Central Regulator of Plant-Cell Stress Responses*, eds D. Gupta, J. Palma, and F. Corpas (Cham: Springer International Publishing), 1–23. doi: 10.1007/978-3-319-44081-1_1

Pang, Z., Chong, J., Li, S., and Xia, J. (2020). MetaboAnalystR 3.0: toward an optimized workflow for global metabolomics. *Metabolites* 10:186. doi: 10.3390/metabo10050186

Parankusam, S., Bhatnagar-Mathur, P., and Sharma, K. K. (2017). Heat responsive proteome changes reveal molecular mechanisms underlying heat tolerance in chickpea. *Environ. Exp. Bot.* 141, 132–144. doi: 10.1016/j.envexpbot.2017.07.007

Pascual, J., Canal, M. J., Escandon, M., Meijon, M., Weckwerth, W., and Valledor, L. (2017). Integrated physiological, proteomic, and metabolomic analysis of ultra violet (UV) stress responses and adaptation mechanisms in Pinus radiata. *Mol. Cell. Proteomics* 16, 485–501. doi: 10.1074/mcp.M116.059436

Passamani, L. Z., Barbosa, R. R., Reis, R. S., Heringer, A. S., Rangel, P. L., Santa-Catarina, C., et al. (2017). Salt stress induces changes in the proteomic profile of micropropagated sugarcane shoots. *PLoS One* 12:e0176076. doi: 10.1371/journal.pone.0176076

Pereira, C., Castander-Olarieta, A., Montalbán, I. A., Pěnčík, A., Petřík, I., Pavlović, I., et al. (2020). Embryonal masses induced at high temperatures in *Aleppo pine*: cytokinin profile and cytological characterization. *Forests* 11:807. doi: 10.3390/f11080807

Perez, D. E., Hoyer, J. S., Johnson, A. I., Moody, Z. R., Lopez, J., and Kaplinsky, N. J. (2009). BOBBER1 is a noncanonical Arabidopsis small heat shock protein required for both development and thermotolerance. *Plant Physiol.* 151, 241–252. doi: 10.1104/pp.109.142125

Perez-Riverol, Y., Csordas, A., Bai, J., Bernal-Llinares, M., Hewapathirana, S., Kundu, D. J., et al. (2019). The PRIDE database and related tools and resources in 2019: improving support for quantification data. *Nucleic Acids Res.* 47, 442–450.

Pinheiro, C., Guerra-Guimarães, L., David, T. S., and Vieira, A. (2014). Proteomics: state of the art to study Mediterranean woody species under stress. *Environ. Exp. Bot.* 103, 117–127. doi: 10.1016/j.envexpbot.2014.01.010

Schlaen, R. G., Mancini, E., Sanchez, S. E., Perez-Santángelo, S., Rugnone, M. L., Simpson, C. G., et al. (2015). The spliceosome assembly factor GEMIN2 attenuates the effects of temperature on alternative splicing and circadian rhythms. *Proc. Natl. Acad. Sci. U.S.A.* 112, 9382–9387. doi: 10.1073/pnas.1504541112

Shen, H., Zhong, X., Zhao, F., Wang, Y., Yan, B., Li, Q., et al. (2015). Overexpression of receptor-like kinase ERECTA improves thermotolerance in rice and tomato. *Nat. Biotechnol.* 33, 996–1003. doi: 10.1038/nbt.3321

Taïbi, K., del Campo, A. D., Aguado, A., and Mulet, J. M. (2015). The effect of genotype by environment interaction, phenotypic plasticity and adaptation on *Pinus halepensis* reforestation establishment under expected climate drifts. *Ecol. Eng.* 84, 218–228. doi: 10.1016/j.ecoleng.2015.09.005

The UniProt Consortium (2019). UniProt: a worldwide hub of protein knowledge. *Nucleic Acids Res.* 47, 506–515. doi: 10.1093/nar/gky1049

Trontin, J. F., Klimaszewska, K., Morel, A., Hargreaves, C., and Lelu-Walter, M. A. (2016). "Molecular aspects of conifer zygotic and somatic embryo development: a review of genome-wide approaches and recent insights," in *In Vitro Embryogenesis in Higher Plants*, eds M. Germana, and M. Lambardi (Totowa, NJ: Humana Press), 167–207. doi: 10.1007/978-1-4939-3061-6_8

Turgut-Kara, N., Arikan, B., and Celik, H. (2020). Epigenetic memory and priming in plants. *Genetica* 148, 47–54. doi: 10.1007/s10709-020-00093-4

Valledor, L., Escandón, M., Meijón, M., Nukarinen, E., Cañal, M. J., and Weckwerth, W. (2014). A universal protocol for the combined isolation of metabolites, DNA, long RNAs, small RNAs, and proteins from plants and microorganisms. *Plant J.* 79, 173–180. doi: 10.1111/tpj.12546

Walter, C., Find, J. I., and Grace, L. J. (2005). "Somatic embryogenesis and genetic transformation in *Pinus radiata*," in *Protocol for Somatic Embryogenesis in Woody Plants*, eds S. M. Jain, and P. K. Gupta (Dordrecht: Springer International Publishing), 11–24.

Wang, R., Mei, Y., Xu, L., Zhu, X., Wang, Y., Guo, J., et al. (2018). Differential proteomic analysis reveals sequential heat stress-responsive regulatory network in radish (*Raphanus sativus* L.) taproot. *Planta* 247, 1109–1122. doi: 10.1007/s00425-018-2846-5

Wang, X., Liu, Z., Niu, L., and Fu, B. (2013). Long-term effects of simulated acid rain stress on a staple forest plant, *Pinus massoniana* lamb: a proteomic analysis. *Trees* 27, 297–309. doi: 10.1007/s00468-012-0799-z

Wu, S. J., Wang, L. C., Yeh, C. H., Lu, C. A., and Wu, S. J. (2010). Isolation and characterization of the *Arabidopsis* heat-intolerant 2 (hit2) mutant reveal

the essential role of the nuclear export receptor EXPORTIN1A (XPO1A) in plant heat tolerance. *New Phytol.* 186, 833–842. doi: 10.1111/j.1469-8137.2010.03225.x

Yakovlev, I. A., Carneros, E., Lee, Y., Olsen, J. E., and Fossdal, C. G. (2016). Transcriptional profiling of epigenetic regulators in somatic embryos during temperature induced formation of an epigenetic memory in Norway spruce. *Planta* 5, 1237–1249. doi: 10.1007/s00425-016-2484-8

Yakovlev, I. A., and Fossdal, C. G. (2017). In silico analysis of small RNAs suggest roles for novel and conserved miRNAs in the formation of epigenetic memory in somatic embryos of Norway spruce. *Front. Physiol.* 8:674. doi: 10.3389/fphys.2017.00674

Yant, L. J., Ran, Q., Rao, L., Van Remmen, H., Shibatani, T., Belter, J. G., et al. (2003). The selenoprotein GPX4 is essential for mouse development and protects from radiation and oxidative damage insults. *Free Radic Biol Med.* 34, 496–502. doi: 10.1016/s0891-5849(02)01360-6

Yuan, L., Wang, J., Xie, S., Zhao, M., Nie, L., Zheng, Y., et al. (2019). Comparative proteomics indicates that redox homeostasis is involved in high-and low-temperature stress tolerance in a novel wucai (*Brassica campestris* L.) genotype. *Int. J. Mol. Sci.* 20:3760. doi: 10.3390/ijms20153760

Zhang, T., Zhao, X., Wang, W., Pan, Y., Huang, L., Liu, X., et al. (2012). Comparative transcriptome profiling of chilling stress responsiveness in two contrasting rice genotypes. *PLoS One* 7:e43274. doi: 10.1371/journal.pone.0043274

Conflict of Interest: The authors declare that the research was conducted in the absence of any commercial or financial relationships that could be construed as a potential conflict of interest.

frontiers in Plant Science

ORIGINAL RESEARCH
published: 12 October 2021
doi: 10.3389/fpls.2021.748110

Marker-Assisted Selection for Pollen-Free Somatic Plants of Sugi (Japanese Cedar, *Cryptomeria japonica*): A Simple and Effective Methodology for Selecting Male-Sterile Mutants With *ms1-1* and *ms1-2*

Momi Tsuruta[1], Tsuyoshi E. Maruyama[1], Saneyoshi Ueno[1], Yoichi Hasegawa[1] and Yoshinari Moriguchi[2]*

[1]*Department of Forest Molecular Genetics and Biotechnology, Forestry and Forest Products Research Institute, Tsukuba, Japan,* [2]*Graduate School of Science and Technology, Niigata University, Niigata, Japan*

OPEN ACCESS

Edited by:
Paloma Moncaleán, Neiker Tecnalia, Spain

Reviewed by:
Kaoru Tonosaki, Iwate University, Japan
Véronique Jorge, Institut National de recherche pour l'agriculture, l'alimentation et l'environnement (INRAE), France

***Correspondence:**
Tsuyoshi E. Maruyama
tsumaruy@ffpri.affrc.go.jp

Specialty section:
This article was submitted to Plant Development and EvoDevo, a section of the journal Frontiers in Plant Science

Received: *27 July 2021*
Accepted: *13 September 2021*
Published: *12 October 2021*

Citation:
Tsuruta M, Maruyama TE, Ueno S, Hasegawa Y and Moriguchi Y (2021) Marker-Assisted Selection for Pollen-Free Somatic Plants of Sugi (Japanese Cedar, Cryptomeria japonica): A Simple and Effective Methodology for Selecting Male-Sterile Mutants With ms1-1 and ms1-2. Front. Plant Sci. 12:748110. doi: 10.3389/fpls.2021.748110

Pollen allergy caused by sugi (Japanese cedar, *Cryptomeria japonica*) is a serious problem in Japan. One of the measures against pollinosis is the use of male-sterile plants (MSPs; pollen-free plants). In this context, the development of a novel technique for the efficient production of sugi MSPs, which combines marker-assisted selection (MAS) with somatic embryogenesis (SE), was recently reported by our research group. To improve the efficiency of MSP production, in this paper we report improved MAS for male-sterile individuals from embryogenic cells, cotyledonary embryos, and somatic plants of sugi using a newly developed marker in the form of the causative mutation of *MS1* itself, selecting individuals with *ms1-1* and *ms1-2* male-sterile mutations. We also describe simplified methods for extracting DNA from different plant materials and for MAS using LAMP diagnostics. Finally, we show that MAS can be efficiently performed using the one-step indel genotyping (ING) marker developed in this study and using InstaGene for DNA extraction. The combination of SE and 100% accurate marker selection during the embryogenic cell stage enables the mass production of *MS1* male-sterile sugi seedlings.

Keywords: clonal propagation, Cupressaceae, gibberellin-induced flowering, loop-mediated isothermal amplification diagnosis, male-sterile plant, *MS1* gene, PCR marker, somatic embryogenesis

INTRODUCTION

Tree pollen-induced allergy has been reported in many countries around the world, and currently almost 40% of people living in Japan suffer from pollinosis caused by sugi [Japanese cedar, *Cryptomeria japonica* (Thunb. ex L.f.) D.Don, Cupressaceae] pollen (Matsubara et al., 2020). As a countermeasure against this, there is an urgent need to spread sugi cultivars with low pollen production or male sterility. Sugi is the most commercially important forestry conifer in Japan, where it covers approximately 4.4 million ha (44% of the total artificial forest; Forestry Agency, 2020). Replacing these trees planted on a vast scale with low-pollen-producing

or male-sterile plants (MSPs; pollen-free plants) would require many seedlings, but is also associated with other problems.

First, to date, 23 strains of male-sterile sugi have been found (Saito, 2010), but the materials that can be used for breeding are still limited. *MALE STERILITY* (*MS*)*1* to *MS4* are known as the causative genes of male sterility in sugi, named after the different abnormalities in pollen development with which they are associated (Taira et al., 1999; Yoshii and Taira, 2007; Miyajima et al., 2010; Saito, 2010). Of these, the major gene for male sterility is *MS1*, associated with a developmental abnormality in the pollen tetrad period, caused by one recessive allele (*ms1*; Taira et al., 1999; Miura et al., 2011). Recently, Hasegawa et al. (2021) identified the *MS1* gene itself, determining that the causative mutation was a 4- or 30-bp deletion in the coding region of the CJt020762 gene, designated as *ms1-1* and *ms1-2*, respectively. Using the mutations as genetic markers, it is now possible to accurately identify male-sterile (homozygous for *ms1*) and potentially sterile trees (heterozygous for *ms1*), as well as male-fertile trees (wild-type), making it easier to search for material that can be used for sugi breeding (Hasegawa et al., 2020, 2021; Moriguchi et al., 2020). Of these trees with *ms1* alleles, *ms1-1* (i.e., 4-bp deletion) is the major causative mutation, whereas only seven trees with an *ms1-2* mutation (30-bp deletion) allele were found in previous screenings (Moriguchi et al., 2020; Hasegawa et al., 2021).

Another major problem is the mass propagation of seedlings. Currently, male-sterile sugi seedlings are eventually obtained after the artificial crossing of a sterile tree (*ms1*/*ms1*) as a seed parent and a pollen donor with heterozygous sterile alleles (*Ms1*/*ms1*), growing seedlings from the seeds, inducing male flowering by the application of gibberellin (GA), and then selecting MSPs. Therefore, about half of the obtained plants are unusable fertile individuals and maintaining those strains until male-sterile and -fertile plants can be selected is extremely resource-intensive in terms of labor and space. Thus, our goal is to establish protocols for efficiently propagating male-sterile sugi seedlings by combining early selection of pollen-free lines using genetic markers (marker-assisted selection or marker aided selection, MAS) and a clonal mass propagation method. Among the available clonal propagation methods, somatic embryogenesis (SE) is the most attractive technique for the large-scale propagation and long-term conservation of different embryogenic cell lines (ECLs) without changing their initial characteristics (Park et al., 1998). However, for many coniferous species, *in vitro* clonal propagation is still difficult or inefficient (Bonga et al., 2010). Currently, the most well-established source of SE propagation in sugi is immature zygotic embryos, for which protocols have been established up to the stage of plant regeneration (Maruyama et al., 2020, 2021a, 2021b). Selecting a male-sterile strain as early as possible in this process will improve the efficiency of MSP production. In a study by Maruyama et al. (2020), a marker closely linked to *MS1* was used to identify male-sterile ECLs.

In the present study, we aimed to further improve the efficiency of MAS for a system for effectively propagating sugi by focusing on the following three points. (1) Examination of genetic markers to be used: The linked marker used in the previous study was not the *MS1* gene itself, but closely linked to *MS1* (0.58 cM; Ueno et al., 2019). This genetic distance means that recombination can occur in 1 out of 200 individuals, and they can be misclassified (Ueno et al., 2019). Additionally, linked markers need to be carefully evaluated in terms of whether they can be adapted to different families from the one in which the marker was developed. Therefore, in this study, we used direct genetic markers that are markers of the causative mutation of the *MS1* gene itself for MAS. Allele-specific PCR (ASP) markers, which detect each wild-type (*Ms1*) or mutated allele (*ms1-1*), were developed on the causative CJt020762 gene (Hasegawa et al., 2020). We also developed a new genetic marker, named the single-tube indel genotyping (ING) marker, which can immediately determine the genotype of the causative gene, which can improve the accuracy of selection. The detection of male sterility by loop-mediated isothermal amplification (LAMP, Notomi et al., 2000), in which the reaction is completed faster than for PCR (typically within 1 h) and there is no need for electrophoresis, is expected to lead to further time savings. LAMP applicability for MAS of MSP was also investigated.

(2) We also investigated DNA extraction methods to save labor. Currently, a variety of DNA preparation methods and commercial kits are available. Of these, freeze-grinding under liquid nitrogen (LN_2) and extraction with hexadecyltrimethylammonium bromide (CTAB) buffer are commonly used for sugi, but they are time- and labor-intensive (e.g., Maruyama et al., 2020; Moriguchi et al., 2020; Hasegawa et al., 2021). Simple DNA extraction methods that do not require grinding with LN_2 and toxic chemicals like phenol and chloroform, such as using Chelex resin and filter paper, have been reported in not only model plants and grasses but also some woody plant species (Berthold et al., 1993; Lange et al., 1998; Lin et al., 2000; HwangBo et al., 2010; Siegel et al., 2017). For MAS of a large number of samples, these simple DNA extraction methods will be effective (Mbogori et al., 2006). The applicability of these methods was verified at each stage of SE. Finally, (3) by combining these methods, we investigated which culture stages and methods were suitable for *MS1* diagnosis. From the above, we provide an effective MAS protocol on male-sterile sugi SE propagation that will be applicable to conifer SE breeding.

MATERIALS AND METHODS

Plant Material and Culture Conditions for SE Initiation

Embryogenic cells (ECs), somatic embryos, and plants derived from five full-sib seed families of *C. japonica* carrying the male-sterile allele in *MS1*, namely, *ms1*, were used as the main experimental materials for this study ($N = 93$, **Table 1**). Additionally, plant materials of four lines derived from seed families without any male-sterility alleles (T2-14-1, T2-14-149, T4-4-1, and T4-11-51) were used as an experimental control. For SE initiation, the entire megagametophyte (~3–4 mm long) including zygotic embryo was used as the initial explant.

TABLE 1 | Sugi seed families carrying the male-sterility gene *MS1* used as main experimental plant material.

Seed family	Male sterility genotype	Collection year	Reference[1]	Abbreviation name	Sample number
('Toyama-funen 1' × 'Ohara 2') × 'Suzu 2'	*Ms1/ms1-1* × *Ms1/ms1-1*	2014	[1]	TOS	3
'Shindai 3' × 'Suzu 2'	*ms1-1/ms1-1* × *Ms1/ms1-1*	2016	[2],[3]	S3S2	39
		2017	[2],[3]	SS	47
'Fukushima-funen 1' × ('Shindai 3' × 'Kamikiri 2')	*ms1-1/ms1-1* × *Ms1/ms1-1*	2017	[2],[3]	FSKam	10
'Fukushima-funen 1' × 'Ōi 7'	*ms1-1/ms1-1* × *Ms1/ms1-2*	2017	[2],[3]	FO7	8
'Fukushima-funen 1' × ('Shindai 3' × 'Kashiwazaki-shi 3')	*ms1-1/ms1-1* × *Ms1/ms1-1*	2017	[2],[3]	FSKas	6

[1]*Reference; [1] Maruyama et al. (2014), [2] Maruyama et al. (2020), [3] Maruyama et al. (2021a).*

The collected seeds were surface-sterilized with 1% (w/v) antiformin solution (Sodium Hypochlorite Solution; Wako Pure Chemical, Osaka, Japan) for 15 min and then rinsed three times with sterile distilled water for 5 min each, before isolation of megagametophyte explants. For the induction of ECs, explants were placed horizontally onto initiation medium contained in 90 × 15-mm quad-plates (3 explants per well, 12 per plate) sealed with Parafilm® and cultured in the dark at 25°C. Initiation medium containing basal salts reduced by half the concentration from the standard EM medium (Maruyama et al., 2000) was supplemented with 10 g L^{-1} sucrose, 10 μM 2,4-dichlorophenoxyacetic acid (2,4-D), 5 μM 6-benzylaminopurine (BA), 0.5 g L^{-1} casein acid hydrolysate, and 1 g L^{-1} glutamine, and solidified with 3 g L^{-1} gellan gum. The pH was adjusted to 5.8 prior to autoclaving the medium for 15 min at 121°C.

Mature seeds were also collected from the 'Shindai 3' × 'Suzu 2' family and seedlings were cultivated ($N = 20$).

Maintenance and Proliferation of ECLs

Tissues of established ECLs were regularly subcultured every 2–3 weeks on maintenance/proliferation medium containing basal salts reduced to half the concentration from the standard EM medium (Maruyama et al., 2000) supplemented with 3 μM 2,4-D, 1 μM BA, 30 g L^{-1} sucrose, 1.5 g L^{-1} glutamine, and 3 g L^{-1} gellan gum. Clumps of ECs (12 per plate) on plates sealed with Parafilm® were cultured in the dark at 25°C.

Maturation of Somatic Embryos

For the maturation of somatic embryos, 2-week-old proliferated ECLs were cultured in clumps (5 masses per 90 × 20-mm plate, 100 mg each) on maturation medium for 8 weeks. Maturation medium containing the basal salt concentration of the standard EM medium (Maruyama et al., 2000) was supplemented with 30 g L^{-1} maltose, 100 μM abscisic acid, 2 g L^{-1} activated charcoal, amino acids (in g L^{-1}: glutamine 2, asparagine 1, arginine 0.5, citrulline 0.079, ornithine 0.076, lysine 0.055, alanine 0.04, and proline 0.035), 175 g L^{-1} polyethylene glycol (Av. Mol. Wt.: 7,300–9,300; Wako Pure Chemical), and 3.3 g L^{-1} gellan gum. The plates were sealed with Parafilm® and kept in the dark at 25°C.

Germination, Plantlet Conversion, and Acclimation of Somatic Plants

Cotyledonary embryos picked up from maturation medium were laid horizontally onto germination medium (maintenance/proliferation medium containing 20 g L^{-1} sucrose, 2 g L^{-1} activated charcoal, and 10 g L^{-1} agar, but without plant growth regulators) and cultured at 25°C under a photon flux density of 45–65 μmol m^{-2} s^{-1} for 16 h per day. The emergence of roots as "germination" and the emergence of both roots and epicotyl as "plant conversion" were recorded after 8 weeks of culture. To promote the growth of converted plantlets, they were transferred to culture flasks containing growth medium (germination medium supplemented with 30 g L^{-1} sucrose and 5 g L^{-1} activated charcoal) and cultured under the same conditions as described above for about 10–12 weeks before *ex vitro* acclimatization. Developed somatic plants removed from the culture flasks were gently washed with tap water to remove traces of agar from their roots and then transplanted into plant containers filled with Spagmoss (*Sphagnum subnitens*; Besgrow, Christchurch, New Zealand), and kept inside plastic boxes with transparent covers (Assist No. 2; Shinki Gosei Co., Ltd., Tokyo, Japan). Plant containers were irrigated with tap water as needed during the first 2 weeks. After this initial 2-week period, the covers were gradually opened and the plant containers were fertilized with Nagao's nutrient solution (Nagao, 1983). The covers were completely removed about 4 weeks after transplanting. Subsequently, acclimated somatic plants were transplanted into individual Wagner's pots (ICW-2; ICM Co., Ltd., Tsukuba, Japan) containing vermiculite and grown in a greenhouse for about 3 months until an approximate height of 30 cm was attained, after which they were treated with GA to induce male flowering.

Induction of Male Flowering by GA

To induce male flowering in regenerated somatic plants of sugi, two spraying applications of GA were carried out during July and August. The first application was performed in late July (when the rainy season ends) and the second in early August (about 10 days later). The treatment solution containing 100 mg L^{-1} GA_3 (Gibberellin A3; Wako Pure Chemical) was sprayed onto the somatic plants until dripping of the solution from the branches was evident. Treated somatic plants were

fertilized twice a week with Nagao's nutrient solution. To determine the presence or absence of normal pollen inside the flowers induced after treatment with GA_3, the respective observations were performed on samples collected at the end of January. Randomly collected male flowers (about three to five per tested plant) were dissected longitudinally with a razor blade, after which they were observed under a stereomicroscope. The experiment was repeated in two consecutive years using at least three plants per tested line.

DNA Extraction From ECLs, Cotyledonary Embryos, and Somatic Plants

From the ECLs (**Figure 1C**), cotyledonary embryos (**Figure 1D**), and shoots of developed plants (**Figures 1G,H**) and seedlings of 117 somatic plant lines consisting of five crossing families carrying the *ms1* allele (**Table 1**) and 4 non-*ms1* individuals (control), DNA was extracted using the simplified CTAB method and/or non-LN_2 grinded extraction method described below. These samples had previously been genotyped for *MS1* using the *MS1*-linked marker (Maruyama et al., 2020).

From the shoot tips of *ex vitro*- or *in vitro*-cultured plants, crude genomic DNA was extracted using the simplified CTAB method. The pre-chilled sample with LN_2 was powdered using TissueLyser II (Qiagen, Hilden, Germany), suspended in CTAB buffer (2% CTAB, 0.1 M Tris–HCl, 20 mM EDTA, 2 M NaCl, 0.4% 2-mercaptoethanol, and 0.5% RNase A), and incubated at 65°C for 10 min. An equal volume of chloroform/isoamyl alcohol (CIA) was added and mixed gently, and the supernatant was collected by centrifugation (11,000 rpm, room temperature, 10 min). This CIA isolation procedure was repeated twice. After adding a 3/4 volume of isopropanol and mixing gently, the nuclear precipitate was collected by centrifugation (15,000 rpm, 4°C, 15 min). After rinsing with 70% ethanol and drying, the DNA was dissolved in 200 µl of nuclease-free water.

Thirty-one ECLs, 29 cotyledonary embryos, and 28 developed plant samples were used to investigate the applicability of the simple extraction method using InstaGene matrix (Bio-Rad, Hercules, CA, USA). The extraction procedure of InstaGene followed the method described by HwangBo et al. (2010). Briefly, 5 mg of ECs, cotyledonary embryos, or a shoot tip of the developed plants was added to 200 µl of InstaGene matrix without homogenization and vortexed for 10 s. Following 8 min of incubation at 100°C and vortexing for 10 s, centrifugation was performed at 13,000 rpm for 1 min. The obtained supernatant was used as a DNA template. Some of these samples were also used for DNA extraction with a Whatman FTA MicroCard (GE Healthcare, Chicago, IL, USA). EC and cotyledonary embryo samples were applied to FTA Card by pressing the cells with a spatula. The shoot tip was applied by spotting 20 µl of the homogenate ground in a mortar with 50 µl of TE (10 mM Tris-HCl, 0.1 mM EDTA, pH 8.0). Then, each FTA Card was dried for at least 1–2 h at room temperature. Subsequent DNA preparation, including disk sampling, washing with FTA Purification Reagent and TE buffer, and drying were performed in accordance with the enclosed manual.

Development of One-Step Indel Genotyping Marker and 30-bp Deletion Diagnostic LAMP

Based on the strategy described by Lin et al. (2020), we developed a new *MS1* genotyping marker detecting the 4-bp deletion of *MS1* by single-tube PCR and agarose gel electrophoresis. Using the CJt020762 gene sequence of male-sterile and -fertile trees, 'Fukushima-funen 1' (*ms1-1*/*ms1-1*, GenBank ID: LC536580), 'Ajigasawa 20' (*Ms1*/*Ms1*, LC538204), and 'Ōi 7' (*Ms1*/*ms1-2*, LC538205), primer sequences were designed by Primer3 (Rozen and Skaletsky, 2000) and were selected to minimize the formation of self- and cross-dimers based on PrimerPooler (Brown et al., 2017). 'Ōi 7' was previously written as "Ooi-7," but has been

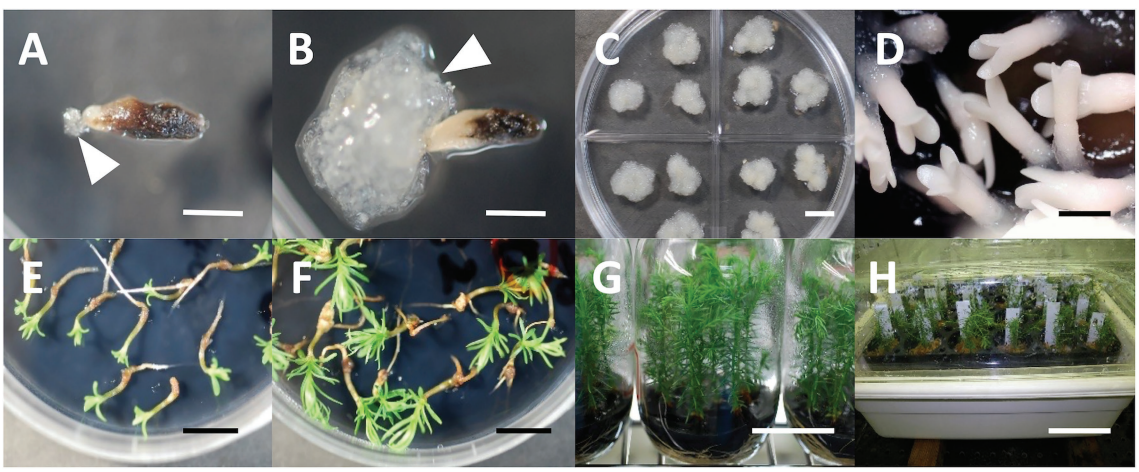

FIGURE 1 | SE and plant regeneration in sugi (Japanese cedar, *Cryptomeria japonica*), **(A)** extrusion of ECs (arrow) from megagametophyte explant, **(B)** established ECL (arrow represent ECs), **(C)** maintenance/proliferation of ECs, **(D)** cotyledonary embryo formation from ECs, **(E)** embryo germination, **(F)** plantlet conversion, **(G)** *in vitro* growth of plantlets, **(H)** acclimation of somatic plants. *Bars*: 5 mm **(A,B,D)**, 1 cm **(C,E,F)**, 5 cm **(G)**, and 10 cm **(H)**.

changed to follow the International Code of Nomenclature of Cultivated Plants (Brickell et al. 2016). The marker genotyping was verified using the male-fertile trees with different *MS1* genotypes, 'Ōi 7' (*Ms1/ms1-2*), 'Suzu 2' (*Ms1/ms1-1*), 'Shimowada 29' (*Ms1/Ms1*), and Ishinomaki 7 (*Ms1/ms1-2*), all of which had already been genotyped at *MS1* (Hasegawa et al., 2021). Ten microliters of PCR reaction mixture contained 1 µl of DNA extract, 3 µl of 2× QIAGEN Multiplex PCR Master Mix (Qiagen), and 0.2 µM each primer. PCR cycling comprised denaturation at 94°C for 15 min, followed by 35 cycles of 94°C for 15 s, 60°C for 30 s, and 72°C for 30 s, with final extension for 5 min at 72°C. PCR products were then separated by 1–1.5% agarose gel (Agarose L03; Takara, Kusatsu, Japan) electrophoresis, stained with Midori Green Xtra (Nippon Genetics, Tokyo, Japan), and genotyped.

We also developed a rapid diagnostic primer set for the LAMP reaction to detect the 30-bp deletion of the *ms1-2* allele. Based on the allele sequences of *MS1* ('Fukushima-funen 1') and *ms1-2* ('Ōi 7'), six primers (FIP, BIP, F3, B3, LF, and LB) were designed manually with reference to PrimerExplorer V5 software (Eiken Chemical, https://primerexplorer.jp/index.html). In some LAMP reactions, clamping primer of peptide nucleic acid (PNA) was used to suppress non-specific alternative allele amplification (e.g., Minnucci et al. 2012; Itonaga et al. 2016). We designed two PNA primers for the wild-type sequences corresponding to both ends of the 30-bp deletion. LAMP diagnosis was verified using 'Ōi 7' and 'Suzu 2' DNA. A total of 12.5 µl of LAMP reaction mixture consisting of 1 µl of template DNA, 6.25 µl of WarmStart Colorimetric LAMP 2× Master Mix (New England Biolabs, Ipswich, MA, USA), 1.6 µM each FIP and BIP primer, 0.2 µM F3 and B3, 0.4 µM LF and LB, and 1.6 µM each PNA primer was incubated at 65°C for 90 min. The color of the reaction solution was observed every 10 min to determine the appropriate reaction time for the diagnosis of *ms1-2*.

MAS for Male-Sterility Lines by PCR and LAMP Diagnostics

DNA extracted from each culture stage was used as a template to genotype *MS1* with genetic markers. The ASP marker detection for the presence of either wild-type or mutant allele *ms1-1* followed the procedure described by Hasegawa et al. (2020). For the ING marker, the reaction conditions were as described above, except that for the extracts of cotyledonary embryo and developed plant shoot by InstaGene and FTA Card, the reaction conditions were changed to 5 µl of Multiplex PCR Master Mix and extension at 72°C for 45 s. Hasegawa et al. (2021) showed that the male-fertile tree 'Ōi 7,' a heterozygous for *MS1*, had the *ms1-2* allele. In the offspring that had 'Ōi 7' as a pollen parent (FO7), we added amplified length polymorphism (ALP) marker genotyping (Hasegawa et al., 2020) to determine the presence of the *ms1-2* allele and the accurate *MS1* genotype. In addition, these FO7 samples and control individuals without *ms1-2* alleles were used to test the applicability of LAMP. The LAMP reaction was performed as described above, and the presence of an *ms1-2* allele was determined by the change in color (red to yellow) of the solution. In the case of FTA Card samples, the disk rinsed with nuclease-free water following TE washing steps was used as a template.

Finally, to choose the optimal genotyping method, the *MS1* phenotype, namely, male-sterile or -fertile, was compared among the previous *MS1*-linked marker results (Maruyama et al., 2020), observations of male flower dissections, and the genetic marker diagnoses of the present study. The genotyping results of ING marker and LAMP reaction were also compared between the templates of different cultured stages extracted by InstaGene and FTA Card.

RESULTS

SE and Plant Regeneration

SE and plant regeneration of *C. japonica* were described in our previous reports (Maruyama et al., 2020, 2021a, 2021b). The extrusion of ECs from the explants could begin about 2 weeks after the start of culture (**Figure 1A**) and the establishment of stable lines with evident EC proliferation was most frequently observed 4 weeks after it (**Figure 1B**). Established ECLs can be maintained and proliferated by continuous routine subculture at 2–3-week intervals on maintenance/proliferation medium (**Figure 1C**). Embryo maturation was induced by culturing ECs on maturation medium (**Figure 1D**). Subsequently, germination (**Figure 1E**) and plantlet conversion (**Figure 1F**) from cotyledonary embryos were achieved about 1–2 weeks and 3–6 weeks after culture on plant growth regulator-free medium, respectively. Developed plantlets (**Figure 1G**) were successfully acclimated in plant containers (**Figure 1H**).

Induction of Male Flowering

Male flowers were successfully induced after the application of GA_3. The beginning of the formation of male flowers in the branches of the treated plants was observed approximately 1 month after the second application of GA_3 solution, showing evident development 2 months after the treatment (**Figure 2A**). Subsequently, the flowers continued their development, reaching a size close to the maturity stage 3 months after the GA_3 treatment (**Figure 2B**). Then, when the flowers had fully matured (around late January), they were collected and dissected to confirm the presence or absence of pollen inside.

Male Flower Collection and Dissection

Mutations in the *MS1* gene lead to the collapse of microspores after the separation of pollen tetrads (Saito et al. 1998). Therefore, we can observe full of pollen grains in anther locules in male-fertile trees, whereas yellow mass without pollen grains in male-sterile trees (Igarashi et al. 2006; Futamura et al. 2019). From the observation of dissected male flowers, we determined the male-fertile line or male-sterile line. The results from two consecutive years of observation are presented in **Supplementary Table S1**. Some representative types of male flowers in male-fertile and -sterile (pollen-free) lines are shown in **Figure 3**.

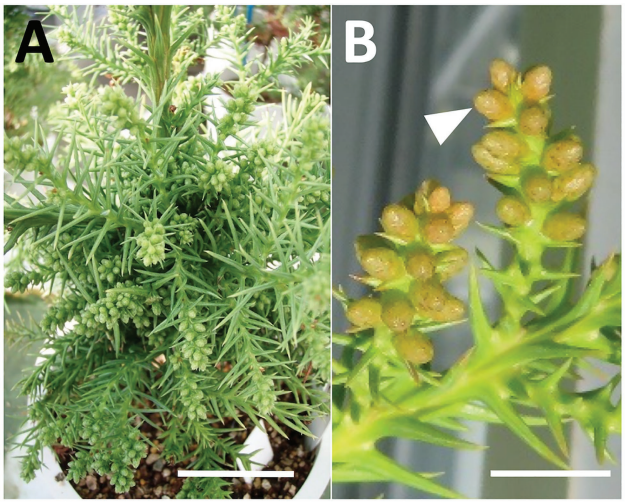

FIGURE 2 | Induction of male flowering in sugi (Japanese cedar, *Cryptomeria japonica*) by GA application, **(A)** male flowering induction 2 months after treatment, **(B)** male flower development 3 months after treatment (arrow). *Bars*: 5 cm **(A)** and 1 cm **(B)**.

Development of a Simple and Robust Indel Genotyping Marker

Here, we have developed a simple genetic marker for determining the *MS1* genotype based on one of the causative mutations of male sterility, a 4-bp deletion in the CJt020762 gene (ING marker). The marker consists of two primer pairs specific for wild-type and mutant alleles (**Table 2**; **Supplementary Figure S1**). Two or three bands, namely, a common band (385 bp and/or 381 bp) and wild-type (233 bp) and/or mutant-specific bands (183 bp), were amplified by one-step PCR, and the genotype could be easily identified by agarose gel electrophoresis (**Table 2**; **Figure 4**). The genotype detection results corresponded with those of the previous *MS1* genotyping (Hasegawa et al., 2021).

Identification of Male-Sterile Lines Using Genetic Markers

Using the ASP and new ING markers, we determined the *MS1* genotype in the 117 somatic plant lines, including 31 ECLs, 24 cotyledonary embryos, and 108 converted seedling samples (91 for ASP marker and 80 for ING marker, **Supplementary Table S1**). Of these, 45 lines were male-fertile and 72 were male-sterile. The detection results based on the ASP marker, ING marker, and male flower dissection for the 117 samples completely matched (**Supplementary Table S1**). The *MS1* genotyping results obtained in this study were almost entirely consistent with the previous results. Only the S-55 sample had different diagnostic results (**Supplementary Table S1**), which may have been due to an error in judgment resulting from recombination of the linked marker and the *MS1* locus. The *MS1* genotyping also required attention regarding the offspring of 'Fukushima-funen 1' and 'Ōi 7' (FO7). Here, by adding the genotyping of *ms1-2* using the ALP marker, the genotype of *MS1* could be accurately determined and corresponded with the male flower dissection results (**Supplementary Table S1**; **Supplementary Figure S2A**).

PCR and LAMP Reaction With DNA Template From Different Extraction Methods

Both the InstaGene and FTA Card extraction templates from the ECs enabled PCR amplification with the ING marker (**Figure 5A**), and the genotyping of *MS1* was the same as the results using DNA extracted from the seedlings as a template. In cotyledonary embryos, PCR amplification was also possible from InstaGene extracts. However, PCR amplification failed in some samples, and was never observed from FTA Card templates (**Figure 5B**; **Supplementary Table S1**). The extracted template of InstaGene and FTA Card from the shoots of developed plantlets could be applied to the MAS using the ING marker (**Figure 5C**). However, the amplified bands of the seedling samples tended to be somewhat weak in intensity.

A LAMP reaction system was constructed to detect alleles of *ms1-2* with the 30-bp deletion, including six primers and PNAs (**Table 3**; **Supplementary Figure S1**). After 30–40 min of isothermal incubation at 65°C, the *ms1-2* allele was detected with a change in the color of the reaction solution (**Supplementary Figure S2B**). After 90 min of incubation, the color change was also observed in control samples. Therefore, we chose the color change at 30–60 min as an indicator of the presence of *ms1-2*.

To test the adaptability of the LAMP reaction, DNA templates extracted by CTAB, InstaGene, and FTA Card in FO7 offspring were further used. For InstaGene extracts, the lines carrying the mutant *ms1-2* allele showed positive results after about 30 min of isothermal reaction, while lines without *ms1-2* did not show any color change even after 60 min of reaction (**Figure 6A**). LAMP diagnoses on both ECLs and developed plants were consistent with the *ms1-2* genotyping results of the ALP marker. However, shoot samples were often observed with a delayed reaction (taking 50 min for color change, as shown in **Figure 6A**). FTA Card extracts of plant shoots also showed delayed responses and often false negatives (**Figure 6B**). Such false negatives were sometimes observed in the diagnosis with crude DNA of shoots extracted by the simplified CTAB method (**Supplementary Figure S2B**). In contrast, some FTA Card-extracted samples of plantlet shoots showed false positives (**Figure 6B**).

DISCUSSION

Discrimination of Male-Fertile and -Sterile Lines Using Pollen Production After GA Treatment

The observations of male flowers for the discrimination of male-fertile and -sterile lines based on pollen production after GA treatment matched perfectly with our results of MAS using the mutation itself as a direct marker (**Supplementary Table S1**). This suggests that the discrimination of male-fertile and -sterile

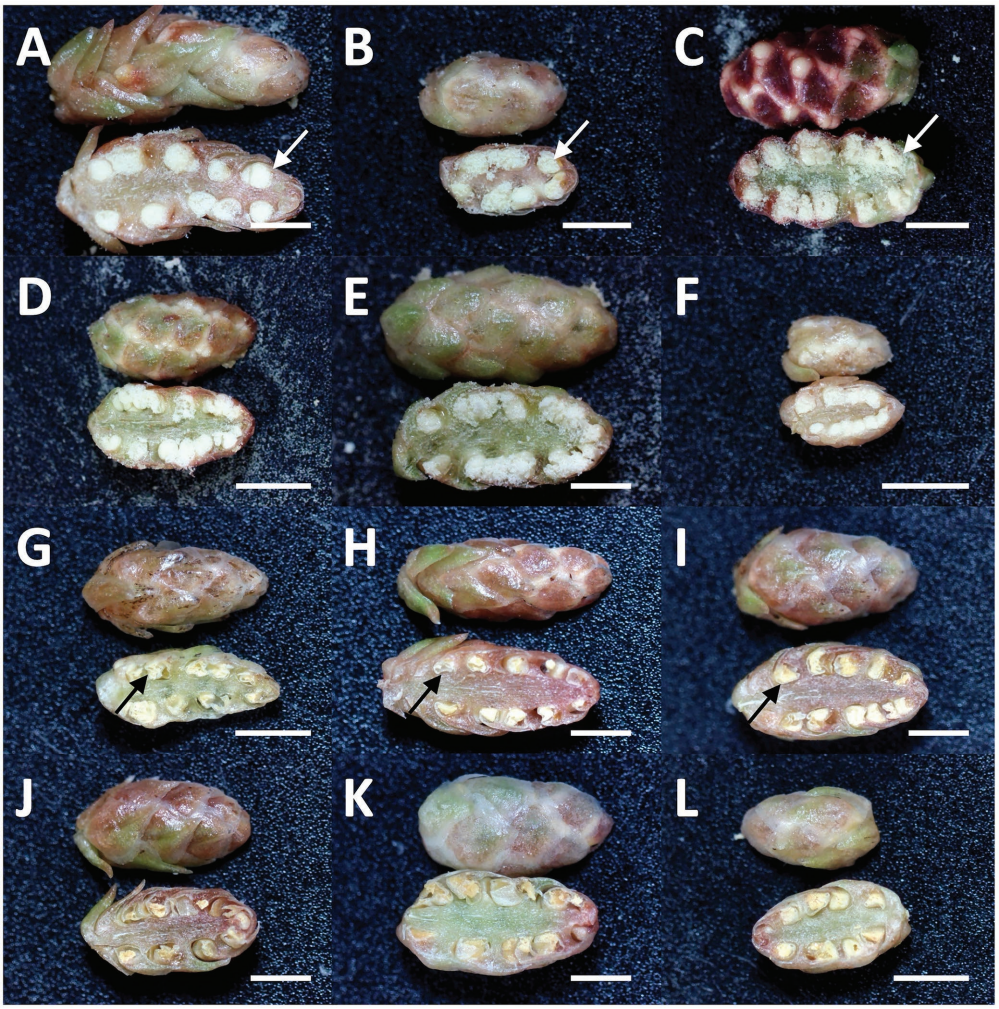

FIGURE 3 | Representative types of dissected male flowers in sugi (Japanese cedar, *Cryptomeria japonica*) about 6 months after GA application, **(A–F)** male flowers of male-fertile lines with normal pollen grains in the anthers (white arrow), **(G–L)** male flowers of male-sterile (pollen-free) lines without pollen grain (black arrow). *Bars*: 2 mm.

TABLE 2 | Primer sequences and products of one-step indel genotyping marker.

	Primer name	Sequence (5′ to 3′)	Amplified products	
A	Mt + rightPrimer_2_F	CTCACTGGCCACAGTCACAC	A + B: mutant allele specific band (183 bp)	B + C: common band (385 bp + 381 bp)
B	Mt + rightPrimer_2_R	TGCAGGCAACTTATAATTAAGCAC		
C	WT + leftPrimer_2_F	GACGTCTTCTGCAACAACAATGG	C + D: wild-type specific band (233 bp)	
D	WT + leftPrimer_2_R	ACCCTGCGTGGGTGTTGATG		

individuals based on the mutation itself as a direct marker is practically reliable and applicable for the early selection at the undifferentiated cell stage (EC) to produce MSPs at a rate of 100%. This implies that the GA-induced judgment method, which requires a lot of space and is labor- and time-intensive, can be replaced by the MAS methodology described in this paper. This would directly increase the efficiency of production of pollen-free plants and result in a low cost of seedlings (**Table 4**).

MAS for Male-Sterile Lines Using Genetic Markers

Using the previously developed ASP marker and the newly developed ING marker, we were able to determine the genotype of *MS1* at three culture stages: ECs, cotyledonary embryos, and developed plants. In the allele-specific PCR including ASP (Hasegawa et al., 2020) and *MS1*-linked marker (Ueno et al., 2019), PCR amplifications were performed in separate tubes using each primer pair specific for the wild-type allele and

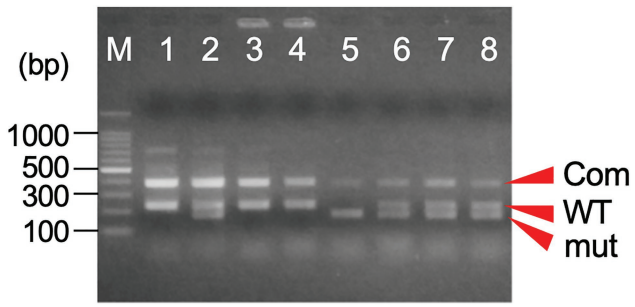

FIGURE 4 | An example of the agarose gel electrophoresis of one-step indel genotyping marker for *MS1* diagnosis. The amplified PCR product consists of a common band (Com: 385 bp + 381 bp) and the allele-specific band for wild-type (WT: 233 bp) and/or mutant allele (mut: 183 bp). M: 100 bp ladder marker, 1: 'O++i 7' (*Ms1/ms1-2*), 2: 'Suzu 2' (*Ms1/ms1-1*), 3: 'Shimowada 29' (*Ms1/Ms1*), 4: Ishinomaki 7 (*Ms1/ms1-2*), and 5–8: somatic embryogenic lines.

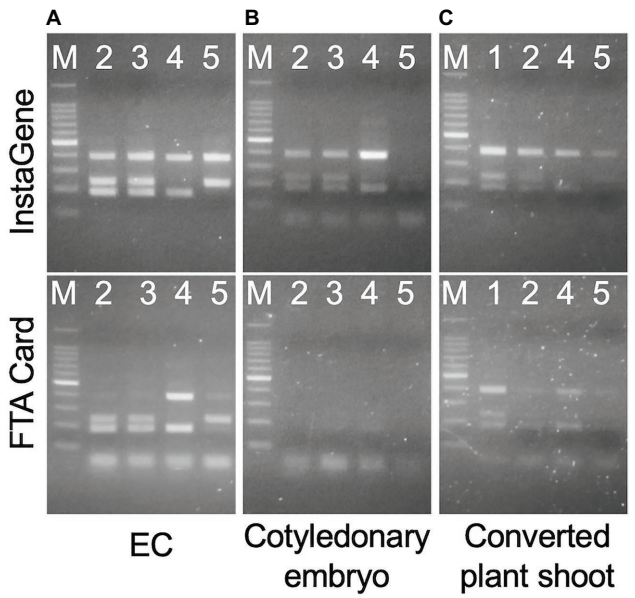

FIGURE 5 | Amplification of one-step indel genotyping (ING) marker from EC **(A)**, cotyledonary embryo **(B)**, and developed plant shoot **(C)** extracted by InstaGene (top) and FTA Card (bottom). M: 100 bp ladder marker, 1: FO7-97, 2: FO7-141, 3: FO7-144, 4: SSD-18, 5: T4-11-51.

TABLE 3 | LAMP primers and PNA sequences for detecting alleles of *ms1-2* with the 30-bp deletion.

Primer name	Sequence (5′ to 3′)
FIP	ATGCAGTGATCCCCAAAATAGCCG-CGGATGATTCGCCCTTTCC
BIP	ACTGCATTGAAGTTTGATACACCG-TTGAACTCTGTTTCCATGGCA
F3	ATGGAGAGCGTTCCCGATC
B3	CGGAATACAGACAACAGCAAT
LF	GGCTCCAGCAATGCTAAC
LB	GAGGTTTAAAACTTTAACATATTTCTTC
PNA_WT1	GATCACTGCTAACCG
PNA_WT2	TTCAATGCAAATAAC

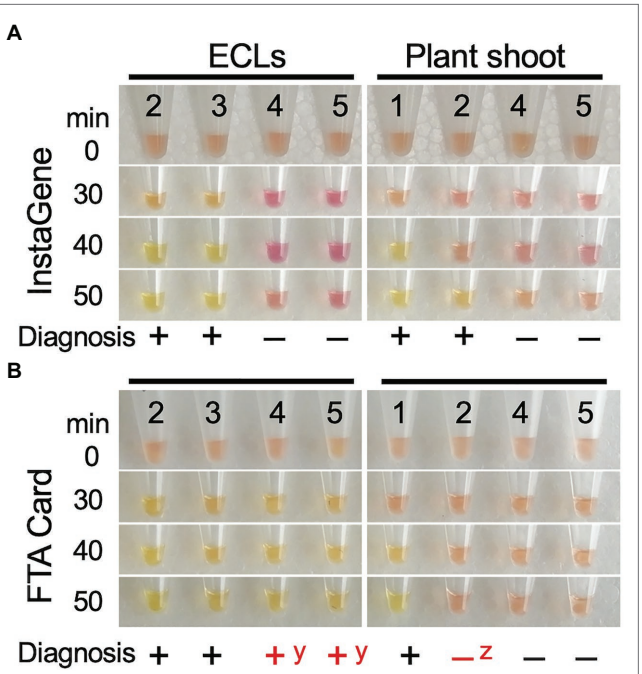

FIGURE 6 | LAMP diagnosis of the presence of mutant allele *ms1-2* on the ECs and shoot tip of the developed plants using DNA template extracted by InstaGene **(A)** and FTA Card **(B)**. 1–3: *ms1-2*-positive samples (1: FO7-97, 2: FO7-141, 3: FO7-144), 4, 5: negative (without *ms1-2*) samples (4, SSD-18, 5: T4-11-51). [y]false positive, [z]false negative.

the *ms1-1* mutant allele, and the genotypes were determined by the presence or absence of the specific band. If we are only interested in the presence or absence of one of the alleles, one reaction is sufficient, but to determine the genotype, it takes double the effort (**Table 4**). With the newly developed ING marker, the genotype of *MS1-1* could be easily determined with a single PCR and electrophoresis. In addition, the previous marker diagnosis was accompanied by difficulties in judgment with unclear PCR products (denoted as "doubted lines" by Maruyama et al., 2020), probably due to the instability of the band during PCR amplification. During our ASP marker detection, doubted non-specific amplification was also observed (data not shown). In addition, the previous decision was an erroneous judgment in one sample (S-55). This may have been due to so-called linked markers. Our newly developed ING marker was able to stably determine the *MS1-1* genotype and solved this problem. From the diagnosis using the mutation itself as a direct marker showing perfect agreement with the results of the male flower dissection, we would like to emphasize the importance of identifying the mutant gene itself for MAS in the breeding of *C. japonica*. This may now be referred to as "gene-assisted selection" or "molecular diagnosis."

We also showed that determination of the *MS1* genotype requires attention on the family having different causative mutation sites on *MS1*. 'Fukushima-funen 1' is homozygous for the *ms1* allele caused by the *ms1-1* mutant allele

TABLE 4 | MSP diagnosis methods used in this study and applicable SE materials.

Diagnostic methods	Detectable *MS1* allele (genotype)	Duration or reaction required for diagnosis	DNA extraction methods	Applicable SE materials[1]			References
				EC	Cotyledonary embryo	Developed plant	
Gibberellin-induced flowering + microscope	Fertile or male-sterile	3–4 years	--	--	--	○	This study
MS1 linked marker	*Ms1* and *ms1-1*	2 PCRs + electrophoresis	CTAB	○	n.d.	○	Ueno et al. 2019; Maruyama et al. 2020
ASP (allele-specific PCR) marker	*Ms1* and *ms1-1*	2 PCRs + electrophoresis	CTAB	n.d.	n.d.	○	Hasegawa et al. 2020; This study
ALP (amplified length polymorphism) marker	*Ms1* and *ms1-2*	One PCR + electrophoresis	CTAB	n.d.	n.d.	○	Hasegawa et al. 2020; This study
ING (one-step indel genotyping) marker	*Ms1* and *ms1-1*	One PCR + electrophoresis	CTAB	n.d.	n.d.	○	This study
			InstaGene	○	▲	○	
			FTA Card	○	×	○	
LAMP (loop-mediated isothermal amplification)	*ms1-2*	An isothermal reaction (less than 1 h)	CTAB	n.d.	n.d.	×	This study
			InstaGene	○	n.d.	▲	
			FTA Card	×	n.d.	×	

[1]*○: applicable, ▲: conditionally applicable, ×: unsuitable, n.d.: not done.*

(*ms1-1*/*ms1-1*), while 'Ōi 7' is heterozygous for the *ms1* allele derived from the *ms1-2* mutation (*Ms1*/*ms1-2*; Hasegawa et al., 2021). Therefore, the genotype of the offspring of FO7 would be *MS1*/*ms1-1* or *ms1-1*/*ms1-2*. Here, if only the genetic marker for the *ms1-1* mutation is used for discrimination, the genotype that is actually *ms1-1*/*ms1-2* would be mistyped as *Ms1*/*ms1-1*. The additional *ms1-2* determination would finally achieve a diagnosis that is consistent with the results of male flower dissection (**Supplementary Table S1**). Because heterozygous offspring of the two mutations in the coding region (*ms1-1*/*ms1-2*) became male-sterile, there is no doubt that the CJt020762 gene is *MS1* itself.

Applicability of LAMP Reaction for Diagnosing *ms1-2*

We examined the applicability of the LAMP reaction for the diagnosis of *ms1-2* in the FO7 family. The lines carrying the mutant *ms1-2* allele showed positive results after about 30–40 min of isothermal reaction. This is a significant time saving compared with PCR. Although the diagnosis results using the DNA template extracted from ECs by InstaGene were in complete agreement with those of the ALP marker, the reaction was delayed in some samples, potentially resulting in false-negative results, when shoot tips of the developed plants were used as the template. The same misjudgment was also observed when using crude DNA extracted from the seedlings, suggesting that the reason for this is not the yield of DNA, but rather the contaminants of secondary metabolites in the adult leaves as inhibitors of the enzymatic reaction. LAMP should be applicable to ECLs, which may contain fewer of these inhibitors, and FTA Card extraction could not be applied to the LAMP reaction (**Table 4**). Another limitation of LAMP is that it is necessary to add a wild-type diagnostic reaction in order to determine the genotype because LAMP is a dominant marker.

Simple and Effective Combination of DNA Extraction and Marker Analysis for Achieving MAS of *MS1* in Somatic Plants

As recently reported, two mutations in the same *MS1* gene have been found to cause male sterility (Hasegawa et al., 2021). Therefore, in some crossing families, for example, FO7, it is necessary to determine both *ms1-1* and *ms1-2* mutation alleles in order to detect male sterility. To identify both *ms1-1* and *ms1-2* genotypes simultaneously, the method of ALP_ms1 reported by Hasegawa et al. (2020) can be used. This method is accurate and cost-effective (Moriguchi et al., 2020), but requires expensive laboratory equipment such as capillary sequencers. PCR and electrophoresis-based methods, such as ASP and our ING markers, do not require capillary sequencers and can be used for rapid determination. If in a less well-equipped laboratory, LAMP can also be used for *MS1* MAS, but it is limited for ECLs with the CTAB or InstaGene extraction methods (**Table 4**).

To increase the effectiveness of MAS, it is best to perform the diagnosis at an early stage of culture. In other words, it is expected to be applied to the initial ECLs. In this case, DNA extraction methods of both InstaGene and FTA Card were applicable for PCR markers. These methods yielded a DNA template with simple laboratory equipment from ECLs. Of these, FTA Card takes about half a day, including a few hours of drying, while InstaGene takes only 15 min per sample. On the other hand, in later SE samples, cotyledonary embryos and shoot tips of developed plantlets, PCR amplification, and LAMP reactions become increasingly difficult. Sugi leaves contain high levels of complex organic compounds such as polysaccharides and polyphenols. Because the presence of polysaccharides has been shown to inhibit enzyme activity (Fang et al., 1992; Pandey et al., 1996), it is necessary to control the contamination of these substances, which is often a cumbersome procedure.

Our recommended method for MAS of *MS1* is to extract DNA with InstaGene at the EC stage, perform one-step PCR amplification with a newly developed ING marker, and carry out genotyping by agarose gel electrophoresis. For the families with mutations of *ms1-2*, additional genotyping of the ALP marker, which can also be genotyped in a single PCR and gel electrophoresis, has been required. In any case, this combination of methods should greatly reduce the labor-intensiveness of subsequent culturing, as the results can be obtained within a few hours from a small callus sample.

CONCLUDING REMARKS

A simple and effective method for selecting MSPs of *C. japonica* carrying the male-sterility gene *MS1*, the principal causative gene of male sterility within the mutant trees discovered to date, is described for the first time. This method uses the mutation itself as a direct marker to determine male sterility in somatic plants. This implies that male-fertile and -sterile individuals can be discriminated based on this new direct marker without the possibility of incorrectly identifying individuals. This represents a major improvement in MAS efficiency compared with the approach applied in our previous study (Maruyama et al., 2020). Furthermore, the simple methods of DNA extraction from different plant materials described here could further simplify the methodology for MAS in sugi. We believe that the methodology improved in this study will serve not only to accelerate the production of pollen-free plants but also to improve molecular breeding technology for MSPs of Japanese cedar.

DATA AVAILABILITY STATEMENT

The original contributions presented in the study are included in the article/**Supplementary Materials**, further inquiries can be directed to the corresponding author.

AUTHOR CONTRIBUTIONS

MT, TM, SU, and YM: conceptualization and methodology. YM: funding acquisition and project administration. TM: plant material preparation. MT, TM, YH, and SU: data curation and experiments and data analysis. MT and TM: writing – original draft. MT, TM, YH, SU, and YM: writing – review and editing. All authors contributed to the article and approved the submitted version.

FUNDING

This research was supported by grants from the Ministry of Agriculture, Forestry and Fisheries of Japan (MAFF) and Bio-oriented Technology Research Advancement Institution (BRAIN). The Science and Technology Research Promotion Program for Agriculture, Forestry, Fisheries and Food Industry (No. 28013B) and grants from Bio-oriented Technology Research Advancement Institution (BRAIN) Research Program on Development of Innovative Technology (No. 28013BC).

ACKNOWLEDGMENTS

The authors would like to thank Niigata Prefectural Forest Research Institute and Forestry Research Institute of Toyama Prefectural Agricultural, Forestry & Fisheries Research Center for the logistic support in the preparation of seed materials.

SUPPLEMENTARY MATERIAL

The Supplementary Material for this article can be found online at: https://www.frontiersin.org/articles/10.3389/fpls.2021.748110/full#supplementary-material

REFERENCES

Berthold, D. A., Best, B. A., and Malkin, R. (1993). A rapid DNA preparation for PCR from *Chlamydomonas reinhardtii* and *Arabidopsis thaliana*. *Plant Mol. Biol. Report.* 11, 338–344. doi: 10.1007/BF02905336

Bonga, J. M., Klimaszewska, K., and von Aderkas, P. (2010). Recalcitrance in clonal propagation, in particular of conifers. *Plant Cell Tissue Organ Cult.* 100, 241–254. doi: 10.1007/s11240-009-9647-2

Brickell, C. D., Alexander, C., Cubey, J. J., David, J. C., Hoffman, M. H. A., Leslie, A. C., et al. (2016). "International code of nomenclature for cultivated plants, ninth edition," in *Scripta Hort.* Leuven: International Society for Horticultural Science, 18.

Brown, S. S., Chen, Y. W., Wang, M., Clipson, A., Ochoa, E., and Du, M. Q. (2017). PrimerPooler: automated primer pooling to prepare library for targeted sequencing. *Biol. Methods Protoc.* 2:bpx006. doi: 10.1093/biomethods/bpx006

Fang, G., Hammar, S., and Grumet, R. (1992). A quick and inexpensive method for removing polysaccharides from plant genomic DNA. *BioTechniques* 13, 52–56

Forestry Agency (2020). Statistical Handbook of Forest and Forestry 2020. Tokyo, Forestry Agency, Ministry of Agriculture, Forestry and Fisheries.

Futamura, N., Igasaki, T., Saito, M., Taira, H., and Shinohara, K. (2019). Comparison of fertile and sterile male gametogenesis in *Cryptomeria japonica* D. Don. *Tree Genet. Genomes* 15:30. doi: 10.1007/s11295-019-1335-8

Hasegawa, Y., Ueno, S., Wei, F. J., Matsumoto, A., Uchiyama, K., Ujino-Ihara, T., et al. (2021). Identification and genetic diversity analysis of a male-sterile gene (*MS1*) in Japanese cedar (*Cryptomeria japonica* D. Don). *Sci. Rep.* 11:1496. doi: 10.1038/s41598-020-80688-1

Hasegawa, Y., Ueno, S., Wei, F. J., Matsumoto, A., Ujino-Ihara, T., Uchiyama, K., et al. (2020). Development of diagnostic PCR and LAMP markers for *MALE STERILITY 1* (MS1) in *Cryptomeria japonica* D. Don. *BMC Res. Notes* 13:457. doi: 10.1186/s13104-020-05296-8

HwangBo, K., Son, S. H., Lee, J. S., Min, S. R., Ko, S. M., Liu, J. R., et al. (2010). Rapid and simple method for DNA extraction from plant and algal species suitable for PCR amplification using a chelating resin Chelex 100. *Plant Biotechnol. Rep.* 4, 49–52. doi: 10.1007/s11816-009-0117-4

Igarashi, M., Watanabe, J., Saito, H., Ozawa, H., Saito, N., Furukawa, S., et al. (2006). Breeding of *Cryptomeria japonica* for the countermeasure of pollinosis. *Bull. Fukushima Prefect. For. Res. Cent.* 39, 1–9.

Itonaga, M., Matsuzaki, I., Warigaya, K., Tamura, T., Shimizu, Y., Fujimoto, M., et al. (2016). Novel methodology for rapid detection of *KRAS* mutation using PNA-LNA mediated loop-mediated isothermal amplification. *PLoS One* 11:e0151654. doi: 10.1371/journal.pone.0151654

Lange, D. A., Penuela, S., Denny, L. R., Mudge, J., Concidido, V. C., Orf, H. J., et al. (1998). A plant isolation protocol suitable for polymerase chain reaction based marker-assisted breeding. *Crop Sci.* 138, 217–220.

Lin, J. J., Fleming, R., Kuo, J. M. B. F., Matthews, B. F., and Saunders, J. A. (2000). Detection of plant genes using a rapid, nonorganic DNA purification method. *BioTechniques* 28, 346–350. doi: 10.2144/00282pf01

Lin, B., Sun, J., and Fraser, I. D. (2020). Single-tube genotyping for small insertion/deletion mutations: simultaneous identification of wild type, mutant and heterozygous alleles. *Biol. Methods Protoc.* 5:bpaa007. doi: 10.1093/biomethods/bpaa007

Maruyama, E. T., Hosoi, Y., Futamura, N., and Saito, M. (2014). Initiation of embryogenic cultures from immature seeds of pollen-free sugi (*Cryptomeria japonica*). *Kanto Shinrin Kenkyu* 65, 107–110.

Maruyama, E., Tanaka, T., Hosoi, Y., Ishii, K., and Morohoshi, N. (2000). Embryogenic cell culture, protoplast regeneration, cryopreservation, biolistic gene transfer and plant regeneration in Japanese cedar (*Cryptomeria japonica* D. Don). *Plant Biotechnol.* 17, 281–296. doi: 10.5511/plantbiotechnology.17.281

Maruyama, E. T., Ueno, S., Hirayama, S., Kaneeda, T., and Moriguchi, Y. (2020). Somatic embryogenesis and plant regeneration from sugi (Japanese cedar, *Cryptomeria japonica* D. Don, Cupressaceae) seed families by marker assisted selection for the male sterility allele *ms1*. *Plan. Theory* 9:1029. doi: 10.3390/plants9081029

Maruyama, E. T., Ueno, S., Hosoi, Y., Miyazawa, S.-I., Mori, H., Kaneeda, T., et al. (2021a). Somatic embryogenesis initiation in sugi (Japanese cedar, *Cryptomeria japonica* D. Don): responses from male-fertile, male-sterile, and polycoss-pollinated-derived seed explants. *Plan. Theory* 10:398. doi: 10.3390/plants10020398

Maruyama, E. T., Ueno, S., Mori, H., Kaneeda, T., and Moriguchi, Y. (2021b). Factors influencing somatic embryo maturation in sugi (Japanese cedar, *Cryptomeria japonica* (Thunb. ex L.f.) D. Don). *Plan. Theory* 10:874. doi: 10.3390/plants10050874

Matsubara, A., Sakashita, M., Gotoh, M., Kawashima, K., Matsuoka, T., Kondo, S., et al. (2020). Epidemiological survey of allergic rhinitis in Japan 2019. *Nippon Jibiinkoka Gakkai Kaiho* 123, 485–490. doi: 10.3950/jibiinkoka.123.485

Mbogori, M. N., Kimani, M., Kuria, A., Lagat, M., and Danson, J. W. (2006). Optimization of FTA technology for large scale plant DNA isolation for use in marker assisted selection. *Afr. J. Biotechnol.* 5, 693–696.

Minnucci, G., Amicarelli, G., Salmoiraghi, S., Spinelli, O., Montalvo, M. L. G., Giussani, U., et al. (2012). A novel, highly sensitive and rapid allele-specific loop-mediated amplification assay for the detection of the *JAK2V617F* mutation in chronic myeloproliferative neoplasms. *Haematologica* 97, 1394–1400. doi: 10.3324/haematol.2011.056184

Miura, S., Nameta, M., Yamamoto, T., Igarashi, M., and Taira, H. (2011). Mechanisms of male sterility in four *Cryptomeria japonica* individuals with obvious visible abnormality at the tetrad stage. *J. Jpn. For. Soc.* 93, 1–7. doi: 10.4005/jjfs.93.1

Miyajima, D., Yoshii, E., Hosoo, Y., and Taira, H. (2010). Cytological and genetic studies on male sterility in *Cryptomeria japonica* D. Don (Shindai 8). *J. Jpn. For. Soc.* 92, 106–109. doi: 10.4005/jjfs.92.106

Moriguchi, Y., Ueno, S., Hasegawa, Y., Tadama, T., Watanabe, M., Saito, R., et al. (2020). Marker-assisted selection of trees with *MALE STERILITY 1* in *Cryptomeria japonica* D. Don. *Forests* 11:734. doi: 10.3390/f11070734

Nagao, A. (1983). Differences of flower initiation of *Cryptomeria japonica* under various alternating temperatures. *J. Jap. For. Soc.* 65, 335–338.

Notomi, T., Okayama, H., Masubuchi, H., Yonekawa, T., Watanabe, K., Amino, N., et al. (2000). Loop-mediated isothermal amplification of DNA. *Nucleic Acids Res.* 28:e63. doi: 10.1093/nar/28.12.e63

Pandey, R. N., Adams, R. P., and Flournoy, L. E. (1996). Inhibition of random amplified polymorphic DNAs (RAPDs) by plant polysaccharides. *Plant Mol. Biol. Report.* 14, 17–22. doi: 10.1007/BF02671898

Park, J. S., Barret, J. D., and Bonga, J. M. (1998). Application of somatic embryogenesis in high-value clonal forestry: deployment, genetic control, and stability of cryopreserves clones. *Cell. Dev. Biol. Plant* 34, 231–239. doi: 10.1007/BF02822713

Rozen, S., and Skaletsky, H. (2000). "Primer3 on the WWW for general users and for biologist programmers," in *Bioinformatics Methods and Protocols* eds. S. Misener and S. A. Krawetz (Totowa, NJ: Humana Press), 365–386.

Saito, M. (2010). Breeding strategy for the pollinosis preventive cultivars of *Cryptomeria japonica* D. Don. *J. Jpn. For. Soc.* 92, 316–323. doi: 10.4005/jjfs.92.316

Saito, M., Taira, H., and Furuta, Y. (1998). Cytological and genetical studies on male sterility in *Cryptomeria japonica* D. Don. *J. For. Res.* 3, 167–173.

Siegel, C. S., Stevenson, F. O., and Zimmer, E. A. (2017). Evaluation and comparison of FTA card and CTAB DNA extraction methods for non-agricultural taxa. *Appl. Plant Sci.* 5:1600109. doi: 10.3732/apps.1600109

Taira, H., Saito, M., and Furuta, Y. (1999). Inheritance of the trait of male sterility in *Cryptomeria japonica*. *J. For. Res.* 4, 271–273.

Ueno, S., Uchiyama, K., Moriguchi, Y., Ujino-Ihara, T., Matsumoto, A., Wei, F. J., et al. (2019). Scanning RNA-Seq and RAD-Seq approach to develop SNP markers closely linked to *MALE STERILITY 1* (*MS1*) in *Cryptomeria japonica* D. Don. *Breed. Sci.* 69, 19–29. doi: 10.1270/jsbbs.17149

Yoshii, E., and Taira, H. (2007). Cytological and genetical studies on male sterile Sugi (*Cryptomeria japonica* D. Don), Shindai 1 and Shindai 5. *J. Jpn. For. Soc.* 89, 26–30. doi: 10.4005/jjfs.89.26

Conflict of Interest: The authors declare that the research was conducted in the absence of any commercial or financial relationships that could be construed as a potential conflict of interest.

Publisher's Note: All claims expressed in this article are solely those of the authors and do not necessarily represent those of their affiliated organizations, or those of the publisher, the editors and the reviewers. Any product that may be evaluated in this article, or claim that may be made by its manufacturer, is not guaranteed or endorsed by the publisher.

frontiers in Plant Science

REVIEW
published: 29 October 2021
doi: 10.3389/fpls.2021.764999

Taking the Wheel – *de novo* DNA Methylation as a Driving Force of Plant Embryonic Development

*Lucija Markulin†, Andreja Škiljaica†, Mirta Tokić†, Mateja Jagić, Tamara Vuk, Nataša Bauer and Dunja Leljak Levanić**

Division of Molecular Biology, Department of Biology, Faculty of Science, University of Zagreb, Zagreb, Croatia

During plant embryogenesis, regardless of whether it begins with a fertilized egg cell (zygotic embryogenesis) or an induced somatic cell (somatic embryogenesis), significant epigenetic reprogramming occurs with the purpose of parental or vegetative transcript silencing and establishment of a next-generation epigenetic patterning. To ensure genome stability of a developing embryo, large-scale transposon silencing occurs by an RNA-directed DNA methylation (RdDM) pathway, which introduces methylation patterns *de novo* and as such potentially serves as a global mechanism of transcription control during developmental transitions. RdDM is controlled by a two-armed mechanism based around the activity of two RNA polymerases. While PolIV produces siRNAs accompanied by protein complexes comprising the methylation machinery, PolV produces lncRNA which guides the methylation machinery toward specific genomic locations. Recently, RdDM has been proposed as a dominant methylation mechanism during gamete formation and early embryo development in *Arabidopsis thaliana*, overshadowing all other methylation mechanisms. Here, we bring an overview of current knowledge about different roles of DNA methylation with emphasis on RdDM during plant zygotic and somatic embryogenesis. Based on published chromatin immunoprecipitation data on PolV binding sites within the *A. thaliana* genome, we uncover groups of auxin metabolism, reproductive development and embryogenesis-related genes, and discuss possible roles of RdDM at the onset of early embryonic development via targeted methylation at sites involved in different embryogenesis-related developmental mechanisms.

Keywords: DNA methylation, RdDM, plant embryogenesis, zygotic embryogenesis, somatic embryogenesis, RNA polymerase V, *Arabidopsis thaliana*

OPEN ACCESS

Edited by:
Paloma Moncaleán, Neiker-Tecnalia, Spain

Reviewed by:
Markus Kuhlmann, Leibniz Institute of Plant Genetics and Crop Plant Research (IPK), Germany
Célia M. Miguel, University of Lisbon, Portugal
Joseph Colasanti, University of Guelph, Canada

****Correspondence:***
Dunja Leljak Levanić
dunja@zg.biol.pmf.hr

† These authors have contributed equally to this work and share first authorship

Specialty section:
This article was submitted to Plant Development and EvoDevo, a section of the journal Frontiers in Plant Science

Received: *26 August 2021*
Accepted: *13 October 2021*
Published: *29 October 2021*

Citation:
Markulin L, Škiljaica A, Tokić M, Jagić M, Vuk T, Bauer N and Leljak Levanić D (2021) Taking the Wheel – de novo DNA Methylation as a Driving Force of Plant Embryonic Development. Front. Plant Sci. 12:764999. doi: 10.3389/fpls.2021.764999

INTRODUCTION

In vascular plants, embryogenesis begins by establishing cell embryogenic competence, which is followed by formation of distinct embryonic stages. Besides the dominant form of embryogenesis which involves a fertilized egg cell or a zygote (zygotic embryogenesis, ZE), flowering plants have evolved alternative fertilization-independent mechanisms of embryo formation (classified under the umbrella term asexual embryogenesis; AE). The general characteristic of AE mechanisms is the variability of cells that can develop competency for embryogenesis. Common forms of AE

that occur *in vivo* are parthenogenesis, where a reduced egg cell develops the embryo, gametic embryogenesis, where an unreduced egg cell or sperm cell develops the embryo and adventitious embryony, where embryo is formed from cells of nucellus or integument (Hand et al., 2016). The rarest naturally occurring AE process is somatic embryogenesis (SE), characterized by the possibility of embryo formation from virtually any somatic cell. This process is independent not only of fertilization but also of existence of gametes, gametophyte, ovules or reproductive tissues, and is the strongest evidence of plant cell totipotency. It is thought that a plant cell in any developmental stage or form has the potential to, under suitable environmental conditions, initiate regulatory mechanisms which will lead to cell dedifferentiation to a state of competency followed by re-differentiation and consequently embryonic development (Fehér, 2005).

Although ZE and SE differ in the initiation stage of embryogenesis, evidence shows overall similarity between the two processes on the level of both morphology and genetics. For instance, a somatic cell undergoing embryogenesis mimics the zygotic pattern of cell division – in other words, just like its zygotic counterpart, it divides asymmetrically (Dodeman et al., 1997; Vasilenko et al., 2000) and forms a suspensor-like structure and a somatic embryo (Leljak-Levanić et al., 2015). Furthermore, similar to zygotic embryogenesis which is marked by existence of embryo and non-embryonic endosperm, different cell types were found in SE cultures, such as embryonic and non-embryonic cell clusters identified in maize microspore cultures (Massonneau et al., 2005). Analyses of cellular types and secreted molecules of *in vitro* cultures suggest endosperm-like functions of these non-embryonic cell clusters, which are thought to communicate with embryonic cells via signaling molecules to direct embryo development, much like the mutually dependent development of embryo and endosperm within the female gametophyte (reviewed in Matthys-Rochon, 2005). In Arabidopsis and other dicots, cultured somatic embryos go through all the major stages of development described for zygotic embryos, namely the globular, heart, torpedo and cotyledonary stage (Kurczyńska et al., 2007). Additionally, similar sets of transcription factors are active during SE and ZE, indicating similar transcriptional regulatory mechanisms between the two processes (Gliwicka et al., 2013; Jin et al., 2014; Leljak-Levanić et al., 2015). With this in mind, a recent RNAseq study of an Arabidopsis embryonic culture reveals surprising results – remarkably, the SE transcriptome has more similarities with transcriptome of germinating seeds than early zygotic embryos (Hofmann et al., 2019). Contrary to previous indications, this finding suggests there might be no general regulatory mechanisms mediating ZE and SE, but does not exclude a subset of specific mechanisms common for both ZE and SE. Identification of these specific yet common mechanisms presents both a challenge and an opportunity for implementing novel approaches to DNA methylation research. Comparative analysis of ZE and SE transcriptome during the initiation stage still holds potential for identification of a specific set of common regulators and regulatory mechanisms between the two types of embryogenesis. If we consider the vast array of possibilities that might lead to SE (different cell types, different environmental conditions etc.), it seems even more likely that some of the mechanisms and molecules involved in SE will overlap with initiation of ZE.

Embryogenesis implies a state of intensive developmental transitions. The role of epigenetic mechanisms during the initiation and maturation stages of embryogenesis was shown in analyses of mostly SE in species such as barley, soybean, common bean, cotton, Norway spruce (for a review, see Nic-Can and De la Peña, 2014), Arabidopsis (Grzybkowska et al., 2018), carrot (LoSchiavo et al., 1989; Yamamoto et al., 2005), pumpkin (Leljak-Levanić et al., 2004) and others. In Arabidopsis, DNA methylation mechanisms have been shown to underlie both ZE (Xiao et al., 2006; Pillot et al., 2010; Ingouff et al., 2017; Forgione et al., 2019) and SE (Grzybkowska et al., 2018; Osorio-Montalvo et al., 2018). Here, we review recent findings on DNA methylation during plant ZE and SE, and propose a central role of RdDM in gene expression regulation during these processes. Assuming that RdDM activity is determined by PolV targeting, we analyze recently published chromatin-immunoprecipitation data based on the Arabidopsis genome (Liu et al., 2018) and list genes related to reproductive development, embryogenesis and auxin dynamics as possible targets of RdDM.

EPIGENETIC REPROGRAMMING AND DNA METHYLATION IN EARLY PLANT DEVELOPMENT

DNA methylation is an epigenetic mechanism commonly found in mammals, plants, filamentous fungi, fish and insect species, among others (Martienssen and Colot, 2001; Li, 2002; Chan et al., 2005; Zhong, 2016; Bewick et al., 2017; Anastasiadi et al., 2018). While many aspects of DNA methylation show striking levels of evolutionary conservation, different organisms have also evolved unique mechanisms. For instance, despite a high structural similarity between mammal and plant methyltransferases, the exact mechanisms by which they establish DNA methylation and the regulatory factors they associate with during this process are often different (Zhong, 2016). In contrast to mammals that primarily methylate CG dinucleotides, plants methylate their DNA in all sequence contexts: symmetric CG, CHG, and asymmetric CHH (H = A, C, or T) by different classes of DNA methyltransferases (Elhamamsy, 2016).

Pioneer work in the field has associated DNA methylation with a range of cellular functions, including transposable element silencing, maintenance of genome integrity, genomic imprinting and X-chromosome inactivation (for a review, see Zhang et al., 2018). In recent years, the focus of attention has become the elucidation of DNA methylation mechanisms in regulation of gene expression, which has also been implicated during plant growth and development (Finnegan et al., 1996; Jacobsen et al., 2000; Xiao et al., 2006; Bartels et al., 2018; Zhang et al., 2018).

In plants, global methylation levels are dynamic and variable throughout development. On the one hand, DNA methylation can be conservatively inherited through cell divisions, ensuring epigenetic memory of their cellular predecessors and can be

heritable across generations (Schmitz et al., 2013; Iwasaki and Paszkowski, 2014). On the other hand, differences in methylation profiles can be found even between cells of the same origin separated by only a few divisions, such as different cells of a plant gametophyte, as shown for Arabidopsis and rice (Ibarra et al., 2012; Park et al., 2016; Han et al., 2019; Borg et al., 2021). Perhaps the most dramatic feature of epigenetics is 'epigenetic reprogramming,' a term used to describe a process in which epigenetic marks of a previous developmental stage or cellular form are erased and a novel epigenetic pattern is established *de novo*. Plants are remarkable in this aspect because they seem to possess a dual ability to both stably inherit epialleles across generations, and to undergo significant epigenetic reprogramming during male and female gametophyte development and embryogenesis (reviewed in Kawashima and Berger, 2014; Gehring, 2019). In recent years, several papers demonstrated the occurrence of epigenetic reprogramming during developmental transitions in different species of the plant kingdom. In the liverwort *Marchantia polymorpha*, a species with a dominant gametophyte generation, epigenetic reprogramming occurs at least twice, once in the gametophytic and once in the sporophytic generation (Schmid et al., 2018). Because the morphology and transcriptional profiles of flowering plants markedly shift between the haploid gametophyte and diploid sporophyte, it is safe to assume that epigenetic reprogramming occurs here as well, once at the diploid-to-haploid transition and a second time during haploid-to-diplod transition. In Arabidopsis, the loss of histone H3 methylation (H3K9me2) and DNA demethylation of transposon-associated *cis*-regulatory elements guides the diploid-to-haploid transition, which later in the vegetative nucleus of pollen grain unlocks genes involved in sperm cell transport and delivery. Conversely, the loss of another methylation mark (H3K27me3) underlies the haploid-to-diploid transition in sperm cells, unlocking the set of developmental genes required to initiate development of the new generation upon fertilization (Borg et al., 2020, 2021). Similar epigenetic reprogramming might regulate egg and central cell fates and transitions between haploid and diploid generations in the female gametophyte. Furthermore, it seems plausible that embryonic epigenetic reprogramming is involved in control of post-embryogenic development, as specifically shown for a seed-specific transcription factor in Arabidopsis (Tao et al., 2017), and that epigenetically based communication pathways exist between distinct embryonic stages to finely tune development of a new organism.

DNA Demethylases in Plants

In plants, as in mammals, the loss of DNA methylation marks can be achieved passively during cell division when DNA methyltransferases are inactive, but it can also be an active, site-specific process (Furner and Matzke, 2011; Elhamamsy, 2016). In mammals, active demethylation occurs by oxidation or deamination. First, ten–eleven translocation enzymes (TET) hydroxylate 5-methylcytosine to 5-hydroxymethylcytosine. Further oxidation by TET produces 5-formylcytosine, which can be either further oxidized or cleaved by thymine-DNA glycosylase (TDG) (Elhamamsy, 2016). In plants, DEMETER DNA GLYCOSYLASES (DME) and REPRESSOR OF SILENCING 1 (ROS1) are multifunctional enzymes that function as DNA gylcosylases that specifically excise 5-methylcytosine through cleavage of the *N*-glycosylic bond (Penterman et al., 2007).

ROS1 is the dominant DNA demethylase in vegetative tissues (Gong et al., 2002), where it presumably targets specific TEs and prevents spreading of their methylation patterns onto nearby protein-coding genes (Tang et al., 2016). In reproductive tissues, DME is the major DNA demethylase specifically expressed in the central cell of the female gametophyte, i.e., the future endosperm (Choi et al., 2002) and the vegetative cell of the bicellular male gametophyte (Schoft et al., 2011). In the endosperm, DME is involved in establishing gene imprinting, or the preferential expression of either the maternal or paternal allele of the same gene. For instance, DME demethylates Polycomb-group protein genes *MEDEA* (*MEA*) and *FERTILIZATION INDEPENDENT SEED 2* (*FIS2*) (Gehring et al., 2006; Jullien et al., 2012) and a transcription factor gene *FLOWERING WAGENINGEN* (*FWA*) (Kinoshita et al., 2004), all of which are maternally expressed. The exact mechanism of gene imprinting regulation is still unclear, with indications of several additional factors other than DME affecting endosperm imprinting, such as the antagonistic effect of DNA methylation (Xiao et al., 2003), histone methylation (Gehring et al., 2006), and parental genome dosage imbalance (Jullien and Berger, 2010). Nevertheless, the importance of DME during Arabidopsis reproductive development is illustrated by evidence that DME accounts for all demethylation in the central cell (Choi et al., 2002), and that central cell demethylation also reinforces transposon methylation in the egg cell (Park et al., 2020). The same scenario occurs in the male gametophyte, all of which probably contributes to stable silencing of transposable elements across generations (Ibarra et al., 2012). Functionally related to DME and ROS1 demethylases, proteins known as Effector of transcription (ET) were recently proposed as epigenetic regulators during reproductive development. Lack of ETs expression is manifested during gametophyte and endosperm development (Tedeschi et al., 2019), suggesting them as novel plant-specific regulators of DNA methylation during reproduction.

Maintenance and *de novo* Methyltransferases in Plants

DNA methylation can be either maintained or established *de novo*. In plants, two DNA methyltransferases work to maintain DNA methylation, DNA METHYLTRANSFERASE 1 (MET1), an ortholog of mammalian DNMT1 which maintains CG methylation, and the plant-specific CHROMOMETHYLASE 3 (CMT3) which maintains CHG methylation (H = A, C, or T) (Finnegan and Kovac, 2000; Chan et al., 2005). A related methyltrasferase, CMT2, maintains CHG and CHH methylation in a process guided by methylation of histone H3 (Stroud et al., 2014). A different pathway, RNA-directed DNA methylation (RdDM) is responsible for *de novo* DNA methylation in all three sequence contexts and is mediated by activity of two methyltransferases, DOMAINS REARRANGED METHYLTRANSFERASE 1 and 2 (DRM1 and DRM2)

(Cao and Jacobsen, 2002; Zhang and Jacobsen, 2006). RdDM is controlled by a two-armed mechanism based around the activity of two RNA polymerases. PolIV transcribes siRNA precursors (P4-RNAs), which are processed in two steps: first, RNA-DEPENDENT RNA POLYMERASE 2 (RDR2) transcribes them into double-stranded RNAs (Haag et al., 2012) and then the DICER-LIKE 3 (DCL3) protein cleaves them into 24 nt-long siRNAs (Qi et al., 2005). The ARGONAUTE 4 (AGO4) protein binds the siRNAs, forming AGO4-siRNA complexes (Qi et al., 2006; Kuo et al., 2017). The second polymerase, PolV, produces long non-coding RNAs (lncRNAs) using specific genomic loci as templates (Wierzbicki et al., 2008; Böhmdorfer et al., 2016). Genomic positioning of PolV is reinforced through binding of previously methylated DNA sites by the SU(VAR)3–9 homolog proteins SUVH2 and SUVH9 (Liu et al., 2014) and interaction with the DDR complex consisting of DEFECTIVE IN MERISTEM SILENCING 3 (DMS3), DEFECTIVE IN RNA-DIRECTED DNA METHYLATION 1 (DRD1), and RNA-DIRECTED DNA METHYLATION 1 (RDM1) (Zhong et al., 2012). It is thought that PolV-produced lncRNAs act as scaffolds for base-pairing with siRNA and associated AGO4 (Wierzbicki et al., 2009) which brings the main components of the two arms of RdDM – one led by PolIV and the other by PolV – into contact with the DRM2-mediated methylation machinery, recruiting it onto specific sites on the genome (Zhong et al., 2014). The mechanism described is the so-called canonical RdDM pathway and according to its current model, the genomic position destined for methylation is determined primarily by the activity of PolV and its suite of supporting proteins (Zhong et al., 2012; Böhmdorfer et al., 2016). Novel findings constantly challenge the current model of RdDM. For instance, although the model assumes that the slicing activity of AGO4 is not required for siRNA biogenesis, recent evidence shows that a subset of 24 nt-siRNAs is indeed sliced by AGO4, which possibly occurs in a self-reinforced loop dependent on PolV and DRM2 (Wang and Axtell, 2017). Not only that, AGO4 can also slice PolV nascent transcripts, suggesting a dual mechanism by which AGO4 recruits DRM2 through both protein-protein interaction (current model) and Pol V transcript slicing (Liu et al., 2018). The importance of AGO4 and related AGO6 and AGO9 was highlighted in a study by Gallego-Bartolomé et al. (2019) who analyzed the order of action within the RdDM pathway and the ability of different components to induce methylation when others are mutated. Their results show an essential role of AGO proteins in methylation targeting and, to make matters even more complex, show that an AGO protein can successfully bridge PolV and DRM2 to induce *de novo* DNA methylation even in the absence of siRNAs produced by PolIV (Gallego-Bartolomé et al., 2019). There is still a long way to go in understanding the mechanisms and roles of RdDM in plants. Indeed, canonical RdDM further extends into several non-canonical pathways which, like canonical RdDM, utilize siRNA-AGO-PolV complexes, but in which siRNAs are produced by Pol II. Non-canonical RdDM pathways are largely unexplored, possibly due to their minor role in transcription silencing. They are limited in their dependence on Pol II production of mRNA and are mostly targeting the same loci as canonical RdDM, seemingly acting as a means to produce alternatively sourced siRNAs to feed into the more predominant canonical form (for a review, see Cuerda-Gil and Slotkin, 2016). Canonical or not, there seems to be a consensus about the crucial role of PolV in determining the genomic site to be methylated via RdDM. This is particularly interesting in the context of land plant evolution – unlike the PolIV arm of RdDM, which is commonly found in land plant species, the PolV arm has reached its most complex level in flowering plants, involving several plant-specific members, and characterized by rapid evolution of its main polymerase (for a review, see Matzke et al., 2015).

In the following chapters, we discuss the role of DNA methylation during plant reproductive development and embryogenesis. **Figure 1** illustrates the changes in activity of maintenance methyltransferases (CMT3 and MET1), the RdDM pathway and demethylase DME during specific developmental stages of zygotic and somatic embryogenesis in *Arabidopsis thaliana*, providing an overview of latest findings and a comparison of the two processes.

DNA METHYLATION AT THE ONSET OF ZYGOTIC EMBRYOGENESIS

Zygotic embryogenesis in flowering plants begins with the process of double fertilization. Of the two identical sperm cells, one fuses with the egg cell and the other with the central cell, which leads to simultaneous formation of the embryo and the endosperm, respectively. In other words, within the female gametophyte, in the mutually close proximity begins the rise of two distinct kinds of progeny, the embryo as the progenitor of the next generation and the triploid endosperm with a temporary and supporting role. The majority of findings on the subject of angiosperm embryogenesis was built on evidence gained from *A. thaliana*, a species with highly predictable patterns of cell division and cell fate determination during embryogenesis (Mayer et al., 1993; Möller and Weijers, 2009).

Arabidopsis embryogenesis begins with a two-fold to three-fold elongation of the zygote, followed by the first asymmetric cell division which gives rise to a two-celled proembryo. The apical cell gives rise to most of the embryo, while the basal cell forms the extraembryonic suspensor which gradually disintegrates through programmed cell death. Only the topmost cell of the suspensor, the hypophysis, comprises the embryo and later forms a root meristem (Willemsen and Scheres, 2004). From the very onset of embryogenesis, asymmetricity plays the lead role, as eventually evident by establishment of the apical-basal axis which will guide the development of shoot and root tissues later on. Elongation and asymmetric division of the zygote is coordinated by two leading factors: a paternally activated MAPKK Kinase YODA (YDA) and a patterning gene *WOX8* (Lukowitz et al., 2004; Ueda et al., 2011). The YDA signaling pathway regulates zygote elongation and induces phosphorylation of transcription factor WRKY2, which then directly activates WOX8 and leads to a polarized positioning of organelles and eventually an asymmetric zygote division (Ueda et al., 2011, 2017). The YDA-WRKY2-WOX8 signaling cascade is the first major regulatory point at

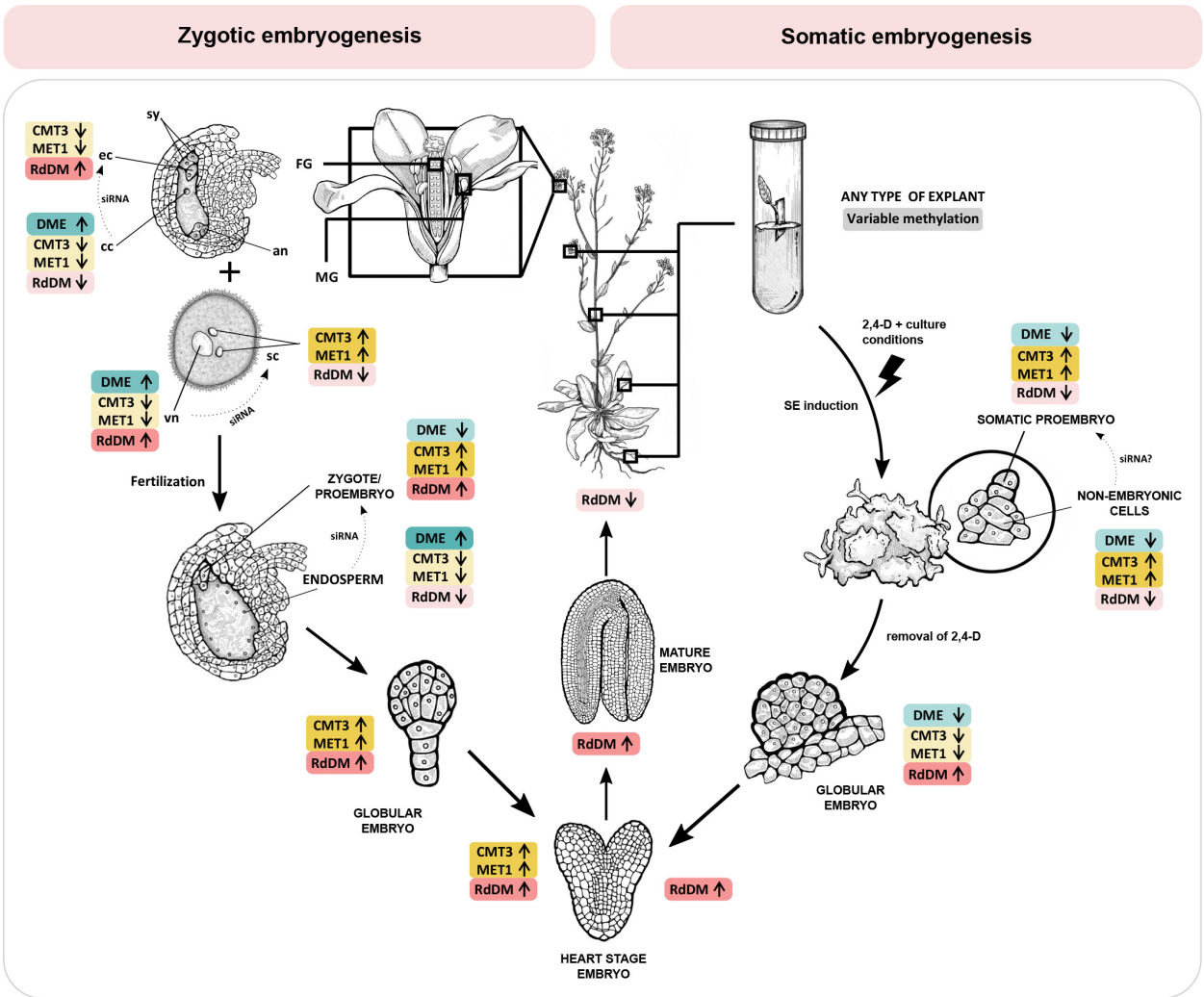

FIGURE 1 | DNA methylation mechanisms change activity during specific stages of zygotic and somatic embryogenesis in *Arabidopsis thaliana*. CMT3 and MET1 (yellow) maintain DNA methylation in CHG and CG context, respectively. The RdDM pathway (red) methylates DNA *de novo* in all contexts, and DME (blue) actively demethylates DNA regardless of context. Zygotic embryogenesis **(left)**. Before fertilization, RdDM is the dominant DNA methylation mechanism in the egg cell. Conversely, in the central cell, CMT3, MET1 and RdDM activity is low and DME activity is high, resulting in DNA hypomethylation. In the two spermal cells, CMT3 and MET1 are the dominant methyltransferases. Conversely, in the vegetative cell CMT3 and MET1 activity is low and DME activity is high, resulting in DNA hypomethylation. RdDM activity in the vegetative nucleus progressively increases. Embryogenesis begins when two spermal cells fertilize the egg and central cell of the female gametophyte, respectively. After fertilization, DNA methylation in the zygote and proembryo increases due to inherited activity of RdDM and increased expression of MET1 and CMT3. In the endosperm, all three methylation mechanisms reduce their activity, and DME remains active, resulting in DNA hypomethylation. RdDM activity progressively increases during embryo maturation, and drops after germination. Somatic embryogenesis **(right)**. Upon induction of somatic embryogenesis by 2,4-D and specific culture conditions, CMT3 and MET1 become the dominant methyltransferases in both the somatic embryo and the surrounding non-embryonic cell clusters. DME activity is low. RdDM activity is initially low but progressively increases during embryo maturation, following a course similar to zygotic embryogenesis. The DNA of the central cell, vegetative nucleus and the endosperm is hypomethylated, resulting in expression of transposons and eventually biogenesis of siRNA which are transferred into the egg cell, spermal cells and the embryo, respectively (dotted arrows), to ensure genome stability. As of yet, there is no evidence of siRNA-mediated communication between somatic proembryo and non-embryonic cells in culture. Information presented in the figure is based on findings published in Jullien et al. (2012); Grzybkowska et al. (2018), and Gehring (2019). 2,4-D, 2,4-dichlorophenoxyacetic acid; an, antipodal cells; cc, central cell; CMT3, CHROMOMETHYLASE 3; DME, DEMETER DNA GLYCOSYLASE; ec, egg cell; FG, female gametophyte; MET1, DNA METHYLTRANSFERASE 1; MG, male gametophyte; RdDM, RNA-directed DNA methylation; sc, sperm cell; siRNA, small interfering RNA; sy, synergide; vn, vegetative nucleus. Enzyme activity is indicated by arrows and color intensity (up/dark – high activity, down/bright – low activity).

which DNA methylation could affect early embryo development, and there has been indication that MET1 might play a role in this process (**Figure 1**). Namely, mutations of the *MET1* gene significantly impact DNA methylation, *YDA*, *WOX2* and *WOX8* gene expression, and embryo development (Xiao et al., 2006; **Table 1**).

The plant hormone auxin is the second major component guiding the establishment of the apical-basal axis. Specifically,

TABLE 1 | Changes in DNA methylation and/or gene expression detected in embryos and young seedlings of Arabidopsis mutants with non-functional DNA methylation mechanisms.

Mutant	Developmental stage or tissue type	Gene(s) or sequences	Methylation status	Expression status	References
met1	Embryo at 4 DAP	*YDA*	Not tested	UP	Xiao et al., 2006
	10 days old seedlings	*YDA*	↓ CG	Not tested	
	Embryo at 4 DAP	*WOX2, WOX8*	Not tested	DOWN	
	10 days old seedlings	*PIN1*	No mCG detected	Not tested	
drm1	Embryo	*MEA* (methylation marker)	= CHH	Not tested	Jullien et al., 2012
drm2	Embryo	*MEA* (methylation marker)	↓ CHH	Not tested	Jullien et al., 2012
	Egg cell	Globally	*↓ CHH	Not tested	Ingouff et al., 2017
drm1 drm2	Embryo	*MEA* (methylation marker)	*↓ CHH	Not tested	Jullien et al., 2012
	5–15 days old somatic embryo	*LEC1, LEC2, BBM*	Not tested	UP	Grzybkowska et al., 2018
	Meiocyte	*RPS16B*	↓ CG, CHG, CHH	UP	Walker et al., 2017
		AT5G67280, AT2G23430	↓ mC	UP	
		MPS1 (PRD2)	↓ CG, CHG, CHH	UP, mis-spliced	
	Closed flower	*SPL/NZZ*	Not tested	UP	Mendes et al., 2020
drm1 drm2 cmt3	13 days old leaves	*YUCCA2*	↓ mC	UP	Forgione et al., 2019
		TAA1, ARF7	↓/ = mC	UP	
		SAUR76, PIN1, PIN3, PIN4	Not tested	DOWN	
	6 days old roots	*PIN1*, *PIN7*	Not tested	DOWN	
	5–15 days old somatic embryo	*LEC1, LEC2, BBM*	Not tested	UP	Grzybkowska et al., 2018
nrpd1b	Embryo	*MEA* (methylation marker)	*↓ CHH	Not tested	Jullien et al., 2012
nrpd1a	Egg cell	Globally	↓/ = CHH	Not tested	Ingouff et al., 2017
nrpd1 nrpe1	Egg cell	Globally	↓ CHH	Not tested	Ingouff et al., 2017
nrpd2a nrpd2b	Embryo	*MEA* (methylation marker)	*↓ CHH	Not tested	Jullien et al., 2012

DAP, days after pollination; (↓), decreased; (↓), significantly decreased; (↓/=), slightly decreased; (=), no significant change; mC, changes in cytosine methylation with no differentiation between sequence contexts; UP, upregulated; DOWN, downregulated.*

what drives axis development is the sum effect of auxin biosynthesis, canalization and global distribution. In Arabidopsis, the bulk of indole-3-acetic acid, a predominant form of auxin, is synthesized from tryptophan in two steps. The first step is catalyzed by TRYPTOPHANE AMINOTRANSFERASE OF ARABIDOPSIS 1 (TAA1) and the TAA1-related enzymes TAR1/TAR2, and the second step is under control of YUCCA monooxygenases (YUC1–11). Expression of these genes has been interpreted as a proxy for auxin production (Zhao, 2012.) Interestingly, transcription of *YUCCA* was also shown to be methylation-dependent (Forgione et al., 2019). During embryogenesis, auxin is distributed into developmentally relevant auxin maximums via activity of embryogenic efflux carriers of the PINFORMED (PIN) family (Friml et al., 2003). Their expression is also regulated by methylation, which can be induced by different classes of methyltransferases (Xiao et al., 2006; Forgione et al., 2019). The first PIN protein expressed in the early embryo is PIN7, whose activity is limited to the basal cell after the first division of the zygote, and later the suspensor. The protein localizes in the apical domain of the plasma membrane, which results in a bottom-to-top efflux of auxin and creates an auxin maximum in the apical cell. Lack of PIN7-derived auxin maximum causes an abnormal division of the apical cell, which highlights the importance of directed auxin efflux at the 2-celled proembryo stage. In *pin7* mutant embryos, the auxin maximum shifts basally into the suspensor (Friml et al., 2003; Robert et al., 2013). A similar pattern emerges in the triple methylation mutant *drm1 drm2 cmt3,* also termed *ddc* (Forgione et al., 2019).

Different Methyltransferases Are Dominant Before and After Fertilization

To clarify the role of DNA methylation during embryogenesis, Jullien et al. (2012) analyzed the activity of specific DNA methyltransferases in different embryonic stages of *Arabidopsis thaliana*. This study shows a dramatic shift in availability of methyltransferases between the egg cell and the zygote (**Figure 1**). In the egg cell, DNA methylation relies predominantly on *de novo* DNA methyltransferases DRM1 and DRM2. Expression of all three methyltranferases of the DRM class (DRM1, DRM2, and DRM3) is high, while expression of methylation-maintaining enzymes MET1 and CMT3 is low. Genes encoding other

components of the RdDM pathway (AGOs, PolIV, PolV, DMS3) are also highly expressed, pointing toward an important role of RdDM during this reproductive stage (Jullien et al., 2012). Following fertilization and the first division of the zygote, *DRM1* expression dramatically decreases and DRM2 becomes the main *de novo* methyltransferase during embryogenesis (Jullien et al., 2012). This could be the cause of a significant increase in CHH methylation during embryogenesis in Arabidopsis (Bouyer et al., 2017), an effect which was also shown in soybean (Lin et al., 2017), chickpea (Rajkumar et al., 2020), and *Brassica rapa* (Chakraborty et al., 2021). Additionally, all three major DNA methyltransferases (MET1, CMT3, and DRM2) become strongly expressed in both the embryo proper and the suspensor (Jullien et al., 2012; **Figure 1**). The authors suggest that the fertilization event is the trigger which leads to a rise in methyltransferase activity to levels higher than those in vegetative tissues. If so, the same trend of methylation changes would be expected in both fertilized gametes, the egg and the central cell, regardless of the different levels of methylation established in them before fertilization (Gehring et al., 2009). However, fertilization of the central cell does not lead to a similar rise in DNA methyltransferase activity but actually leads to a wholly different effect – a decrease in global methylation and quantity of methyltranferases (Ibarra et al., 2012; Park et al., 2016, 2020), despite both spermal cells possessing identical regulatory potential (Ingouff et al., 2017). Therefore, strong activation of DNA methyltranferases could occur independently of fertilization and a similar rise in activity might be occurring during both ZE and SE, or any other type of asexual embryogenesis. This implies that a set of signals beyond the fertilization event marks the beginning of embryogenesis and thus shapes the methylation patterns of the early embryo, regardless of its origin.

DNA METHYLATION AT THE ONSET OF SOMATIC EMBRYOGENESIS

Somatic embryogenesis is a process during which somatic cells gain embryogenic competence to develop morphologically distinct embryonic stages which will give rise to a new plant organism. Virtually any plant cell at any given moment has the capacity to acquire developmental characteristics of a fertilized egg cell, which is followed by intensive developmental reprogramming (Nishiwaki et al., 2000; Fehér et al., 2003; Fehér, 2005). Although SE can occur naturally, as found in the genus Kalanchoë, it is much more common in plant *in vitro* culture, where it can be induced in numerous plant species and from different types of explants if granted adequate conditions (Loyola-Vargas and Ochoa-Alejo, 2016). Acquiring embryogenic competence relies on morphological, genetic and most likely epigenetic plasticity. The first effect is dedifferentiation to a state of totipotency which can then lead to a broad spectrum of possible redifferentiation outcomes, including embryogenesis (Verdeil et al., 2007). Specific plant growth regulators or application of stressful conditions can be used to stimulate embryogenic competence in somatic cells. Auxins, and especially synthetic auxin 2,4-dichlorophenoxyacetic acid (2,4-D), are the most effective inductors of SE, while their removal from growth medium stimulates embryo maturation. Exogenous auxin helps establish the auxin gradient within the explant. The auxin maximum builds at the site of contact between medium and tissue and, following auxin uptake by the tissue, the auxin level progressively decreases depending on the direction of auxin transport within the explant. At specific sites, the optimal auxin level and hormone balance is reached, which ensures favorable conditions for acquiring embryogenic competence (Fehér, 2005). In Arabidopsis SE, much like in ZE, PIN-mediated polar transport of auxin is essential for establishing auxin gradients and subsequent induction of embryogenesis (Su et al., 2009). Similar auxin dynamics in ZE and SE are backed by similar transcription patterns of genes involved in auxin distribution and transport, as well as genes involved in regulation of specific auxin responses, such as genes encoding AUXIN RESPONSE FACTORS (ARFs) and AUXIN/IAA inhibitors (Aux/IAAs) (Gliwicka et al., 2013). In general, there are many similarities between ZE and SE at the level of gene expression. In cotton, the processes of ZE and SE share more than 50% of highly expressed genes involved in methylation, stress response, hormone response, embryonic fate regulation, polarity and pattern formation (Jin et al., 2014). A similar overlap exists in Arabidopsis, where most abundant transcription factors during SE are those involved in developmental processes, phytohormone and stress responses (Gliwicka et al., 2013) and many of these genes were also found during ZE (Leljak-Levanić et al., 2015). However, a recent global transcriptome analysis in Arabidopsis revealed a higher level of similarity between transcriptomes of SE and germinating seeds, rather than ZE, indicating more complex dynamics than suggested by previous research (Hofmann et al., 2019).

Auxin Treatment Regulates DNA Methyltransferase Activity and Expression of Somatic Embryogenesis-Marker Genes

Reports on *Daucus carota* and Arabidopsis indicate that auxin-related conditions which promote embryogenesis are associated with DNA hypermethylation (LoSchiavo et al., 1989; Yamamoto et al., 2005; Jiang et al., 2015). Exogenous auxin increases cytosine methylation during somatic embryo induction in carrot, while auxin removal rapidly decreases it (LoSchiavo et al., 1989). This is probably a consequence of auxin-mediated increase of DNA methyltransferase gene expression and downregulation of demethylases (**Figure 1**), as described for Arabidopsis (Grzybkowska et al., 2018). Leljak-Levanić et al. (2004) show that in pumpkin (*Cucurbita pepo*) not only auxin treatment but other SE-inducing stress treatments, like nitrogen-starvation, cause hypermethylation of DNA during SE induction. However, in the majority of reports an inverse relationship between embryogenic competence and DNA methylation was observed. In *Eleutherococcus senticosus* (Chakrabarty et al., 2003), *Pinus nigra* (Noceda et al., 2009), and *Picea abies* (Ausin et al., 2016) DNA hypomethylation seems to be associated with early stages and embryo induction. Moreover, DNA

hypomethylation provoked by demethylation agents 5-azacitide has been recommended for improving the embryogenic capacity of poorly responding plant species or for aged cultures of *Theobroma cacao* (Pila Quinga et al., 2017). Due to the diversity of results, it is clear that the global level of DNA methylation is not specifically related to the embryogenesis process but more likely reflects the epigenetic status of explants caused by tissue culture conditions.

A recent gene expression analysis of four major methyltranferases during SE in Arabidopsis shows that *MET1* and *CMT3* transcripts highly accumulate during early SE and that expression of *DRM1* and *DRM2* decreases, but is followed by a striking increase in *DRM2* expression in later stages (Grzybkowska et al., 2018). Similarly, addition of 2,4-D to carrot culture positively correlates with expression of *MET1* during induction of SE and before the formation of embryonic cell clumps (Yamamoto et al., 2005). It appears that MET1 and CMT3 are the dominant methyltransferases during induction of SE (**Figure 1**), and in Arabidopsis this interplay is nicely illustrated by the presence of an Auxin Response Element (AuxRE) in the *CMT3* promoter, signifying a mode through which auxin can directly control CMT3 activity (Grzybkowska et al., 2018). It is interesting to note that during Arabidopsis SE, an increase in methyltransferase gene expression is combined with a decrease in expression of demethylase genes but that overall, surprisingly, global methylation level decreases (Grzybkowska et al., 2018). When it comes to global methylation, it remains difficult to clarify the highly complex regulation of DNA methylation mechanisms during SE. However, the authors show that in SE cultures of a mutant with non-functional DRMs (*drm1 drm2*) and a triple mutant with non-functional DRMs and CMT3 (*drm1 drm2 cmt3*) SE-related genes of the *LEAFY COTYLEDON* (*LEC*) transcription factor family, *LEC1*, *LEC2* (Lotan et al., 1998; Harada, 2001; Gaj et al., 2005; Stone et al., 2008; Wójcikowska et al., 2013) and *BABYBOOM (BBM;* Boutilier et al., 2002; Casson et al., 2005) are significantly upregulated (Grzybkowska et al., 2018), which indicates that these same genes could be differentially methylated genes during SE, a hypothesis which remains to be tested in the future. In embryogenic culture of *Daucus carota*, promoters of *LEC1* and *WUSCHEL (WUS)* are hypomethylated (Shibukawa et al., 2009). Similarly, promoters of *SOMATIC EMBRYOGENESIS RECEPTOR KINASE* (*SERK*; Schmidt et al., 1997; Hecht et al., 2001), *LEC2*, and *WUS* are hypomethylated in embryogenic tissue of *Boesenbergia rotunda* (Karim et al., 2018). In addition, a recent epigenome-wide study of nine different developmental stages of SE in soybean revealed an early wave of hypermethylation, especially in the CHH context. This was linked to auxin treatment and increased RdDM activity during induction and early SE (Ji et al., 2019).

DEFECTS IN REPRODUCTIVE DEVELOPMENT OF DNA METHYLATION MUTANTS

DNA methylation mutants of *Arabidopsis thaliana* have been invaluable for exploration of mechanisms which underlie the activity of specific DNA methylation pathways during ZE and SE. First, DNA methylation mechanisms involve numerous proteins and different combinations of their mutations lead to different phenotypic characteristics, from those evident during haploid reproductive stages to those which manifest during embryogenesis. For a comprehensive list of mutations and the associated phenotypes, see **Supplementary Table 1**. Abolition of different DNA methylation mechanisms by loss-of-function mutations causes temporally specific phenotypes, affecting different stages of reproductive development. For instance, the loss of function of both RdDM methyltransferases, DRM1 and DRM2 (*drm1 drm2*), causes an aberrant female gametophyte, while loss of function of MET1 and CMT3 results in aberrant embryos (Jullien et al., 2012).

Phenotypic changes related to premeiotic development can be observed during cell fate specification of the megaspore mother cell (MMC). In wild type Arabidopsis, one cell of the hypodermal ovule layer is specified as the MMC. In the double *drm1 drm2* mutant, multiple cells become specified as the MMC, resulting in multiple precursors of the female gametophyte (Mendes et al., 2020; **Figure 2**). Here, loss of DRM function causes upregulation of the *SPOROCYTELESS/NOZZLE* (*SPL/NZZ*) transcript encoding a protein involved in balancing the reproductive cell fate establishment in the premeiotic ovule (Mendes et al., 2020). A similar phenotype develops in mutants of the *AGO4*, *AGO6*, *AGO8* and *AGO9* genes (shown for *AGO4* in **Figure 2**), and depending on the mutated gene, the number of MMCs varies, from two to four (Hernández-Lagana et al., 2016). Multiple MMC-like cells are also caused by loss-of-function mutations of genes encoding proteins involved in the PolIV arm of RdDM, such as the aforementioned polymerase RDR2 (*rdr2*) which produces double-stranded siRNAs, its ortholog RDR6 (*rdr6*) which acts in non-canonical RdDM, an RNA-binding protein called SUPPRESSOR OF GENE SILENCING 3 (*sgs3*) and the siRNA-processing protein DCL3 (*dcl3*) (Olmedo-Monfil et al., 2010). A similar phenotype is also found in a double mutant in which both NRPD1a and NRPD1b (also known as NRPE1), the respective largest subunits of PolIV and PolV are mutated (*nrpd1a nrpd1b*) and both polymerases are non-functional (Olmedo-Monfil et al., 2010). It should be noted here that loss of function of newly discovered ET demethylases decreases the *SPL/NZZ* expression (Tedeschi et al., 2019) suggesting the possible balancing effects of RdDM methylation and ET-specific demethylation during plant reproduction.

Besides exhibiting a premeiotic phenotype, *ago9, rdr2*, *dcl3* and the *nrpd1a nrpd1b* double mutant are additionally affected in postmeiotic development, with noted formation of multiple female gametophytes (shown for *nrpd1a nrpd1b* and *ago9* in **Figure 2**). In some cases, two developing gametophytes are separated by several somatic cells, indicating that they originated from non-sister cells, of which one had to be of somatic origin (Olmedo-Monfil et al., 2010). This phenomenon could serve as an illustration of the potency of epigenetic mechanisms in regulating development and even establishing a novel trajectory of development from unlikely origins, as described for SE. In the aforementioned mutants with non-functional RdDM, methyltransferase MET1

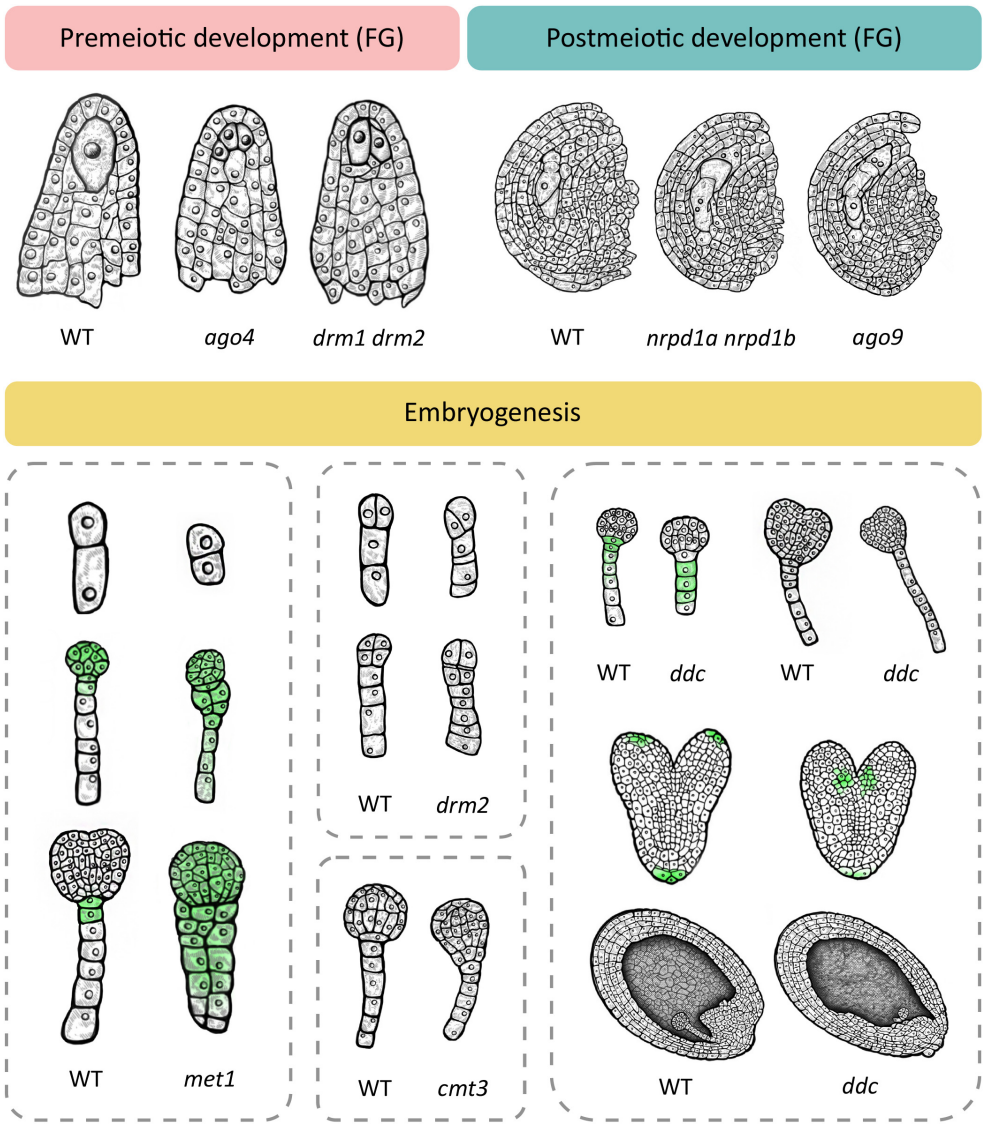

FIGURE 2 | Loss of function of different methylation mechanisms leads to several dominant phenotypes at the premeiotic and postmeiotic stage and during embryogenesis. Premeiotic development. In wild type, one cell of the ovule is specified as the megaspore mother cell (MMC) which divides meiotically to give rise to the female gametophyte (FG). Several mutants with non-functional RdDM develop multiple MMC-like cells in premeiotic ovules, exemplified here in *ago4* and *drm1 drm2*. Postmeiotic development. The wild type megaspore divides mitotically to produce a female gametophyte. RdDM mutants such as *ago9* and the double *nrpd1 nrpd2* mutant exhibit two female gametophytes in postmeiotic ovules. Embryogenesis. Wild type embryogenesis begins with zygote elongation, asymmetrical division and subsequent formation of embryo and suspensor. In the *met1* mutant with non-functional MET1, the zygote remains short and divides symmetrically **(top)** and longitudinal divisions in the suspensor lead to unclear demarcation of the embryo-suspensor border **(middle and bottom)**. Additionally, auxin transport is disturbed which leads to even distribution of auxin throughout the embryo (green). The *cmt3* mutant with non-functional CMT3 also shows unclear demarcation of the embryo-suspensor border in early globular stage. Loss of function of RdDM leads to similar aberrations. The *drm2* mutant shows disturbed patterns of cell divisions in the early embryo in both the suspensor **(top and bottom)** and the embryo proper **(bottom)**. The triple *drm1 drm2 cmt3* mutant (*ddc*) exhibits a reduced number of suspensor cells at the globular stage with a hypophysis devoid of auxin signal **(top left)** and a longer suspensor at early heart stage **(top right)**. At the heart stage, auxin maximums appear basally from cotyledons **(middle)**. Wild type embryos are positioned in parallel with the top–bottom axis of the ovule. In a portion of *ddc* mutant plants, embryos are positioned perpendicular to the axis, and the endosperm is histologically disorganized **(bottom)**. This schematic image was created based on phenotypes described in relevant scientific articles. For details and references, see **Supplementary Table 1**.

is functional but it does not compensate for the lack of RdDM, possibly due to low expression of *MET1* (Jullien et al., 2012) or the functional limitations of MET1 activity, i.e., its dependence on previous methylation and specificity for the CG context.

Deficiencies in RdDM and other DNA methylation mechanisms also cause aberrations during embryonic development. Interestingly, the loss-of-function MET1 mutant (*met1*), displays a wide array of successive phenotypes (Xiao et al., 2006; **Figure 2**) which first manifest during the elongation

and asymmetric division of the zygote and continue later with abnormalities in numbers and planes of cell division throughout embryogenesis as well as delays in embryo development. According to Xiao et al. (2006), loss of MET1 directly or indirectly affects transcription of genes that regulate cell identity during early embryogenesis. Specifically, it causes downregulation of *WOX2* and *WOX8*, upregulation of *YDA* and altered expression pattern of *PIN1*, which becomes evenly distributed throughout the entire embryo, in stark contrast to its usual accumulation in the apical cell-derived regions. Concurrently, auxin becomes evenly distributed in both the apical and basal cell-derived regions, which hinders the establishment of the auxin maximum, possibly accounting for the lack of demarcation between embryo and suspensor (**Figure 2**). The authors postulate that hypomethylation is the most probable cause of phenotypic defects in the *met1* mutant. They also suggest the possibility of compensation for loss of CG-specific MET1 through induced activation of other methylation mechanisms which could then cause ectopic hypermethylation on specific positions and result in further developmental aberrations (Xiao et al., 2006).

Loss of function of the non-CG-specific methyltransferase CMT3 (*cmt3*) leads to aberrations in later stages of embryogenesis, with a lack of clear demarcation between the embryo and suspensor due to longitudinal cell divisions in the suspensor (**Figure 2**). The double *met1 cmt3* mutant embryos display similar aberrations but with more dramatic effects on embryo development, seed viability and plant development (Xiao et al., 2006).

Unlike MET1 and CMT3, *de novo* methyltransferase DRM2 can induce DNA methylation in all three sequence contexts (Chan et al., 2005). Ingouff et al. (2017) show that the *drm2* mutant suffers a global loss of maternally provided CHH methylome in the egg cell, causing abnormal patterning and division plane defects in the early embryo (**Figure 2**). Furthermore, the triple *ddc* mutant, in which DRM1, DRM2 and CMT3 are non-functional, shows various phenotypic aberrations during embryogenesis, which has been linked to an impaired auxin pathway (Forgione et al., 2019; **Figure 2**). In the early embryo stage, the *ddc* mutant exhibits a reduced number of suspensor cells and a delayed suspensor development. In the globular stage, suspensor cell proliferation is arrested, resulting in a shorter suspensor with a hypophysis devoid of auxin signal, while increased proliferation and a more elongated suspensor marks the young heart embryo stage. When the embryo reaches heart stage, auxin maximums appear basally from cotyledons, contrary to the usual accumulation of auxin in the apical regions of the cotyledons (**Figure 2**). Finally, aberrations in the embryo are combined with disordered histological organization of the endosperm (**Figure 2**). Interestingly, this aberration reminds of a phenotype described for the *yda* mutant, where embryos are positioned perpendicular to the top-bottom axis of the ovule, as if lying on their sides (Lukowitz et al., 2004). The leaf of the *ddc* mutant is marked by increased expression of genes involved in the auxin biosynthesis pathway, namely *YUC2* and *TAA1*, and while *TAA1* was not differentially methylated, the authors report significant demethylation in the promoter region of *YUC2* (Forgione et al., 2019). Although gene expression and methylation levels of auxin-related genes have not been examined in *ddc* embryos (Forgione et al., 2019), the results obtained in leaf tissues combined with described auxin-related embryo aberrations serve as a novel link between *de novo* DNA methylation and the role of auxin pathways in embryonic development, which remains to be further explored in the future.

In mammals, loss-of-function mutation of DNA methyltransferase Dnmt1 causes an embryo lethal phenotype (Li et al., 1992), a dramatic effect which does not occur in plants, including Arabidopsis, when either of their three major methyltransferases is mutated. On the other hand, a number of methylation mutants of investigated plant species were shown to be either lethal at some point during development, hypomorphic, or depleted in multiple methylation contexts (Domb et al., 2020). To date, an Arabidopsis mutant with a complete loss of all DNA methylation has not been described, as zero-methylation state is most likely lethal. The existence of single mutants, however, suggests redundancy between mechanisms, additionally supported by the fact that mutations affecting more than one methylation mechanism lead to more pronounced developmental aberrations (Xiao et al., 2006). Interestingly, single-mechanism mutations lead to temporally specific phenotypes, indicating activity shaped by developmental needs. RdDM is particularly interesting in this aspect as it could naturally serve as a potent mechanism in not only substituting for missing methylation marks, but also in establishing novel methylation patterns in response to various internal and external cues. The RdDM pathway is comprised of numerous components, not all of which are indispensable for DNA methylation to occur. The highest level of functional promiscuity has been ascribed to DMS3, a protein which recruits PolV to the genome, and which seems to perform this role even when most other RdDM components have been mutated (Gallego-Bartolomé et al., 2019). The research of RdDM seems to be marked by exceptions, rather than rules, which could point to the pathway's highly versatile roles, at least some of which could be linked to embryogenesis, including a specific role of auxin dynamics in regulating embryonic development. Clarification of the role of RdDM in these processes could be aided by identification of genes directly regulated by RdDM-mediated DNA methylation during embryogenesis. In the following section, we bring an overview of genomic regions which are potential targets of the PolV polymerase, a component of RdDM which determines the future methylation site, and analysis of loci specifically linked to auxin dynamics, reproductive development and embryogenesis.

DETERMINATION OF GENOMIC LOCI TARGETED BY RNA-DIRECTED DNA METHYLATION

The chromatin association profile of NRPE1 (the largest subunit of PolV) in *Arabidopsis thaliana* Col-0 flowers is published by Liu et al. (2018). To determine specific genes potentially regulated by RdDM, read filtering, mapping, peak calling and peak annotation was performed to retain only the peaks associated with 1142

TABLE 2 | Potential PolV binding sites.

Gene	Locus	Position relative to TSS/gene	Protein function	Development/phenotype	References
RIE1	AT2G01735	0/overlap with start	E3 ubiquitin ligase	Seed development/Arrest at globular stage	Xu and Li, 2003
ADA2B	AT4G16420	0/overlap with start	Transcriptional adapter	Pleiotropic/Auxin overproducing mutant-like phenotype	Vlachonasios et al., 2003
ZAR1	AT2G01210	0/overlap with start	Receptor protein kinase-like	Zygote asymmetric division and daughter cell fate	Yu et al., 2016
AGL23	AT1G65360	0/overlap with start	Agamous-like MADS-box	Female gametophyte and chloroplast development in embryo/developmental arrest at the megaspore stage	Colombo et al., 2008
SIR3	AT1G16540	0/overlap with start	Molybdenum cofactor sulfurase (LOS5) (ABA3)	Conversion of ABA-aldehyde to ABA/Modulates cold and osmotic stress responsive genes	Xiong et al., 2001
ECA1 gametogenesis related family	AT2G24205	0/overlap with entire gene	ECA1 gametogenesis related family protein	Flowering plant reproduction/not tested	Sprunck et al., 2014
EXPB2	AT1G65680	0/overlap with start	Putative expansin-B2	Unidimensional cell growth, expressed in reproductive tissues of maize/Drought resistance	Wu et al., 2001; Ezquer et al., 2020
ECA1 gametogenesis related family	AT5G44495	0/overlap with entire gene	Small signaling CRP	Flowering plant reproduction/not tested	Sprunck et al., 2014
ECA1 gametogenesis related family	AT5G60964	0/overlap with entire gene	Small signaling CRP	Flowering plant reproduction/not tested	Sprunck et al., 2014
SAUR-like auxin responsive family	AT5G42410	0/overlap with start	SAUR43	Substrate of RDR1/Not expressed in rdr1 mutants	Hua et al., 2021
EMB1691	AT4G09980	0/overlap with start	Methyltransferase B	N6-adenosine methylation of mRNA/mRNA modification, splicing, metabolism	Muñoz-Nortes et al., 2017; Meinke, 2019
ECA1 gametogenesis related family	AT5G60945	0/overlap with entire gene	Small signaling CRP	Flowering plant reproduction/not tested	Sprunck et al., 2014
ECA1 gametogenesis related family	AT5G42895	0/overlap with entire gene	Small signaling CRP	Flowering plant reproduction/not tested	Sprunck et al., 2014
PIN4	AT2G01420	0/overlap with start	Auxin efflux carrier component	Maintenance of embryonic auxin gradients/Root pattering	Friml et al., 2002
SEN1	AT3G45590	2/upstream	DNA helicase	tRNA splicing in the initiation of zygote division/zygote-lethal	Yang et al., 2017
LIS	AT2G41500	24/upstream	a protein with seven WD40 repeats	Prevents accessory cells from adopting gametic cell fate/supernumerary egg cells	Groß-Hardt et al., 2007
ECA1 gametogenesis related family	AT2G27315	28/overlap with end	Small signaling CRP	Flowering plant reproduction/not tested	Sprunck et al., 2014
EMB1796	AT3G49240	35/upstream	Pentatricopeptide repeat-containing protein	Posttranscriptional RNA editing/Embryo lethality	Guillaumot et al., 2017
NAC081	AT5G08790	37/upstream	NAC family transcription factor	Regulates *NIT2* gene involved in auxin biosynthesis/Reduced sensitivity to indole-3-acetonitrile	Huh et al., 2012
CYP75B1/TT7	AT5G07990	40/upstream	Flavonoid-30-hydroxylase	Flavonoid biosynthetic pathway/Modulated auxin transport	Peer and Murphy, 2007
ABCI7 (SufD)	AT1G32500	48/upstream	ATP-binding cassette (ABC) proteins	Fe-S cluster biogenesis, housekeeping functions in embryogenesis/Globular stage lethality	Xu and Møller, 2011
PIN7	AT1G23080	50/inside gene	Auxin efflux carrier component 7	Setting up the apical-basal axis in the embryo/Failed to establish the apical–basal auxin gradient	Friml et al., 2003; Robert et al., 2013

ChIP-seq data obtained with anti-NRPE1 antibody in Col-0 flower tissues published in Liu et al. (2018) were reanalyzed with a focus on targets involved in reproductive development, embryogenesis and auxin metabolism. Genes with associated peaks positioned up to 50 bp upstream from the TSS were selected from the 224 peaks listed in ***Supplementary Table 3****.*

genes categorized into 79 gene ontologies (GO) related to auxin metabolism, reproductive development, and zygotic and somatic embryogenesis (for a complete list of GOs, refer to **Supplementary Table 2**). Finally, of the 441 remaining peaks, we retained peaks with fold change greater than 2.0, *p*-value less than 10^-12 and which were positioned up to 3000 bp upstream from the associated gene, resulting in 224 peaks in total (**Supplementary Table 3**). Following selection, most of the auxin metabolism genes with known roles in SE or ZE mentioned earlier were found as targets of PolV. Namely, the list contained genes involved in the biosynthesis of auxin (*TAA1, TAR1, TAR2, YUC2, YUC5, YUC10, YUC1, LEC2*), in the regulation of directed auxin transport (*PIN3, PIN4, PIN7*) and genes encoding auxin response factors (*ARF1, ARF2, ARF8*) and AUX/IAA inhibitors (*IAA6, IAA8, IAA14, IAA18, IAA27*). It was previously shown that *YUC2* is hypomethylated in the *dcc* mutant, indicating a role of RdDM, possibly in combination with CMT3, while *PIN1*, *PIN3*, *PIN4,* and *PIN7* have been suggested as potential targets due to their variable expression in the *ddc* mutant (Forgione et al., 2019). In addition, the *WOX8* gene encoding a protein involved in establishment of apical-basal axis in the young embryo was also identified as a potential PolV target. Although it was previously shown that regulation of the *WOX2*/*WOX8* pair depends on MET1 (Xiao et al., 2006), the connection with RdDM indicates the redundancy of this pathway in the *WOX2*/*WOX8* gene expression regulation.

One of our additional criteria for gene selection was position of the peak up to 3000 bp upstream from the TSS of an associated gene. Zhong et al. (2012) show that PolV binds to promoters and that the loss of its largest subunit (NRPE1) leads to an increase in expression of genes located near the PolV binding site. Specifically, when PolV is non-functional, the effect of its loss on gene expression, i.e., upregulation, is higher for genes which have the PolV binding site closer to the TSS (Zhong et al., 2012). Therefore, we selected genes with up to 50 bp distance between the peak and the TSS to generate a list of genes most likely to be regulated by RdDM. This selection resulted in a list of 22 genes (**Table 2**), among which only *SIR3* is functionally related to stress response. The remaining 21 genes are directly or indirectly related to reproductive development and their loss of function leads to aberrations in megaspore development, formation of supernumerary egg cells, zygotes or embryos and disturbances in auxin metabolism, transport or effects (for references see **Table 2**). Additionally, some of these genes affect embryogenesis through regulation of transcription, posttranscriptional regulation, proteasomal degradation, cell-to-cell signalization, t-RNA splicing, flavonoid biosynthesis, and biogenesis of multifunctional iron–sulfur clusters (for references see **Table 2**). Interestingly, out of 22 genes on the list, six belong to Early Culture Abundant 1 (ECA1) gametogenesis-related family, which is one of the three largest families encoding small cysteine-rich proteins, many of which are expressed during reproductive development (reviewed in Sprunck et al., 2014). Members of this family were first described in barley, where HvECA1 is responsible for stress-induced switch from gametophytic pathway to embryogenic route (Vrinten et al., 1999). Functional characterization of HvECA1 resulted in discovery of a significant number of similar CRPs in egg cell transcriptomes of different flowering plants. In Arabidopsis, there are 124 genes of ECA1 gametogenesis-related family (Sprunck et al., 2014). The best described protein candidate, EGG CELL 1 (EC1), is secreted from the egg cell and responsible for sperm cell activation to gain competence for gamete fusion, which indicates that it is essential for the reproductive phase of development (Sprunck et al., 2012). Besides egg cell-specific genes, a significant number of ECAs are expressed in synergids under control of the synergide-specific MYB98 transcription factor (Jones-Rhoades et al., 2007). Sprunck et al. (2014) argue that members of this family potentially partake in different processes related to reproductive development, including androgenesis, as occurs in barley (Sprunck et al., 2014). Our overview of PolV-bound genomic loci indicates ECA1 gametogenesis-related proteins as interesting targets for further research of RdDM roles in reproductive development. Interestingly, genes encoding ECA1 gametogenesis-related proteins have an unusual transposon-like pattern of methylation, in which RdDM mediates gene body methylation in CG, CHG and CHH contexts. This type of methylation is generally linked to expression downregulation in vegetative tissues and is usually low in synergids, in which many CRP genes are expressed (You et al., 2012). Therefore, ECA1 gametogenesis-related family could be additionally used to study the role of RdDM in transition between the reproductive and vegetative stage.

CONCLUDING REMARKS AND PERSPECTIVES

There are still many aspects of plant embryogenesis that are not fully understood, especially at its onset. How is the reprogramming of the transcriptome and DNA methylome at the onset of embryogenesis controlled and what are the signals that direct or redirect the zygote or a somatic cell into a state of embryogenic competence? There is substantial evidence linking RdDM to gametophyte development and embryogenesis, but the exact mechanisms through which RdDM could regulate gene expression prior to and at the onset of plant embryogenesis remains to be elucidated. Here, we propose a list of genes presumably targeted by PolV, which could serve as a pool of gene candidates for future research of the roles of RdDM in reproductive development and embryogenesis, as well as the mechanisms by which auxin dynamic might shape these processes. Different components of the RdDM pathway certainly play their own distinct roles in this process. For instance, members of the AGO4 clade, consisting of AGO4, AGO6, and AGO9, all participate in the RdDM pathway but functionally diverge in terms of their ability to promote short RNA accumulation and DNA methylation, and this distinction is present even when different AGOs bind the same short RNAs (Havecker et al., 2010). At least in part, the difference in AGO function could be attributed to their distinct expression profiles (Havecker et al., 2010), with AGO9 primarily expressed in female gametes, where it has a role in TE silencing (Olmedo-Monfil et al., 2010). The specificity of individual components of

RdDM for distinct tissues and even cell types could indicate the existence of specialized branches of RdDM, assembled according to different biological requirements and possibly consisting of undiscovered and highly specialized associated factors. In the future, it would be interesting to compare the siRNA profile of AGO9 with the PolV-bound genome sites, and potentially retrieve a set of genes presumably regulated by RdDM in a tissue-specific manner, with functions related to female gametophyte development. Clarification of the RdDM mechanism at the onset of embryogenesis is also of practical value, as it could open the door to an applicative function combining DNA methylation-based techniques with SE- mediated propagation. Treatment with epigenetic regulators that induce global demethylation, such as 5-azacytidine, was shown to be beneficial in plant breeding (Kondo et al., 2006), showing that loss of methylation can be a significant source of variation, with potentially favorable effects. On the other hand, the application of CRISPR/Cas technology to edit epigenetic marks at specific loci (McDonald et al., 2016; Papikian et al., 2019) and to consequently modulate gene expression, may lead to more precise and predictable breeding (Mercé et al., 2020), especially if we take into account that epigenetic marks are heritable through at least a few generations (Papikian et al., 2019).

AUTHOR CONTRIBUTIONS

DLL developed the idea. LM carried out the bioinformatics and determination of RdDM genomic loci. MT and AŠ performed the mutant manuscript analysis and prepared the illustrations. DLL and AŠ drafted and wrote most of the manuscript while MT, NB, MJ, and TV participated in writing. All the authors contributed to the article and approved the submitted version.

FUNDING

This work was supported by grants from the Croatian Science Foundation (project PHYTOMETHDEV; IP 2016-06-6229 to DLL).

SUPPLEMENTARY MATERIAL

The Supplementary Material for this article can be found online at: https://www.frontiersin.org/articles/10.3389/fpls.2021.764999/full#supplementary-material

REFERENCES

Anastasiadi, D., Esteve-Codina, A., and Piferrer, F. (2018). Consistent inverse correlation between DNA methylation of the first intron and gene expression across tissues and species. *Epigenetics Chromatin* 11:37. doi: 10.1186/s13072-018-0205-1

Ausin, I., Feng, S., Yu, C., Liu, W., Kuo, H. Y., Jacobsen, E. L., et al. (2016). DNA methylome of the 20-gigabase Norway spruce genome. *Proc. Natl. Acad. Sci. U.S.A.* 113, E8106–E8113. doi: 10.1073/pnas.1618019113

Bartels, A., Han, Q., Nair, P., Stacey, L., Gaynier, H., Mosley, M., et al. (2018). Dynamic DNA methylation in plant growth and development. *Int. J. Mol. Sci.* 19:2144. doi: 10.3390/ijms19072144

Bewick, A. J., Vogel, K. J., Moore, A. J., and Schmitz, R. J. (2017). Evolution of DNA methylation across insects. *Mol. Biol. Evol.* 34, 654–665. doi: 10.1093/molbev/msw264

Böhmdorfer, G., Sethuraman, S., Rowley, M. J., Krzyszton, M., Rothi, M. H., Bouzit, L., et al. (2016). Long non-coding RNA produced by RNA polymerase V determines boundaries of heterochromatin. *Elife* 5:e19092. doi: 10.7554/eLife.19092

Borg, M., Jacob, Y., Susaki, D., LeBlanc, C., Buendía, D., Axelsson, E., et al. (2020). Targeted reprogramming of H3K27me3 resets epigenetic memory in plant paternal chromatin. *Nat. Cell Biol.* 22, 621–629. doi: 10.1038/s41556-020-0515-y

Borg, M., Papareddy, R. K., Dombey, R., Axelsson, E., Nodine, M. D., Twell, D., et al. (2021). Epigenetic reprogramming rewires transcription during the alternation of generations in *Arabidopsis*. *Elife* 10:e61894. doi: 10.7554/eLife.61894

Boutilier, K., Offringa, R., Sharma, V. K., Kieft, H., Ouellet, T., Zhang, L., et al. (2002). Ectopic expression of BABY BOOM triggers a conversion from vegetative to embryonic growth. *Plant Cell* 14, 1737–1749. doi: 10.1105/tpc.001941

Bouyer, D., Kramdi, A., Kassam, M., Heese, M., Schnittger, A., Roudier, F., et al. (2017). DNA methylation dynamics during early plant life. *Genome Biol.* 18:179. doi: 10.1186/s13059-017-1313-0

Cao, X., and Jacobsen, S. E. (2002). Locus-specific control of asymmetric and CpNpG methylation by the DRM and CMT3 methyltransferase genes. *Proc. Natl. Acad. Sci. U.S.A.* 99(Suppl. 4), 16491–16498. doi: 10.1073/pnas.162371599

Casson, S., Spencer, M., Walker, K., and Lindsey, K. (2005). Laser capture microdissection for the analysis of gene expression during embryogenesis of *Arabidopsis*. *Plant J.* 42, 111–123. doi: 10.1111/j.1365-313X.2005.02355.x

Chakrabarty, D., Yu, K. W., and Paek, K. Y. (2003). Detection of DNA methylation changes during somatic embryogenesis of Siberian ginseng (*Eleuterococcus senticosus*). *Plant Sci.* 165, 61–68. doi: 10.1016/S0168-9452(03)00127-4

Chakraborty, T., Kendall, T., Grover, J. W., and Mosher, R. A. (2021). Embryo CHH hypermethylation is mediated by RdDM and is autonomously directed in *Brassica rapa*. *Genome Biol.* 22:140. doi: 10.1186/s13059-021-02358-3

Chan, S. W., Henderson, I. R., and Jacobsen, S. E. (2005). Gardening the genome: DNA methylation in *Arabidopsis thaliana*. *Nat. Rev. Genet.* 6, 351–360. doi: 10.1038/nrg1601

Choi, Y., Gehring, M., Johnson, L., Hannon, M., Harada, J. J., Goldberg, R. B., et al. (2002). DEMETER, a DNA glycosylase domain protein, is required for endosperm gene imprinting and seed viability in *Arabidopsis*. *Cell* 110, 33–42. doi: 10.1016/S0092-8674(02)00807-3

Colombo, M., Masiero, S., Vanzulli, S., Lardelli, P., Kater, M. M., and Colombo, L. (2008). AGL23, a type I MADS-box gene that controls female gametophyte and embryo development in *Arabidopsis*. *Plant J.* 54, 1037–1048. doi: 10.1111/j.1365-313X.2008.03485.x

Cuerda-Gil, D., and Slotkin, R. K. (2016). Non-canonical RNA-directed DNA methylation. *Nat. Plants* 2:16163. doi: 10.1038/nplants.2016.163

Dodeman, V. L., Ducreux, G., and Kreis, M. (1997). Zygotic embryogenesis versus somatic embryogenesis. *J. Exp. Bot.* 48, 1493–1509. doi: 10.1093/jxb/48.8.1493

Domb, K., Katz, A., Harris, K. D., Yaari, R., Kaisler, E., Nguyen, V. H., et al. (2020). DNA methylation mutants in *Physcomitrella patens* elucidate individual roles of CG and non-CG methylation in genome regulation. *Proc. Natl. Acad. Sci. U.S.A.* 117, 33700–33710. doi: 10.1073/pnas.2011361117

Elhamamsy, A. R. (2016). DNA methylation dynamics in plants and mammals: overview of regulation and dysregulation. *Cell Biochem. Funct.* 34, 289–298. doi: 10.1002/cbf.3183

Ezquer, I., Salameh, I., Colombo, L., and Kalaitzis, P. (2020). Plant cell walls tackling climate change: biotechnological strategies to improve crop adaptations and photosynthesis in response to global warming. *Plants* 9:212. doi: 10.3390/plants9020212

Fehér, A. (2005). Why somatic plant cells start to form embryos? *Plant Cell Monogr.* 2, 85–101. doi: 10.1007/7089_019

Fehér, A., Pasternak, T. P., and Dudits, D. (2003). Transition of somatic plant cells to an embryogenic state. *Plant Cell Tissue Organ Cult.* 74, 201–228. doi: 10.1023/A:1024033216561

Finnegan, E. J., and Kovac, K. A. (2000). Plant DNA methyltransferases. *Plant Mol. Biol.* 43, 189–201. doi: 10.1023/A:1006427226972

Finnegan, E. J., Peacock, W. J., and Dennis, E. S. (1996). Reduced DNA methylation in *Arabidopsis thaliana* results in abnormal plant development. *Proc. Natl. Acad. Sci. U.S.A.* 93, 8449–8454. doi: 10.1073/pnas.93.16.8449

Forgione, I., Wołoszyńska, M., Pacenza, M., Chiappetta, A., Greco, M., Araniti, F., et al. (2019). Hypomethylated drm1 drm2 cmt3 mutant phenotype of *Arabidopsis thaliana* is related to auxin pathway impairment. *Plant Sci.* 280, 383–396. doi: 10.1016/j.plantsci.2018.12.029

Friml, J., Benková, E., Blilou, I., Wisniewska, J., Hamann, T., Ljung, K., et al. (2002). AtPIN4 mediates sink-driven auxin gradients and root patterning in *Arabidopsis*. *Cell* 108, 661–673. doi: 10.1016/S0092-8674(02)00656-6

Friml, J., Vieten, A., Sauer, M., Weijers, D., Schwarz, H., Hamann, T., et al. (2003). Efflux-dependent auxin gradients establish the apical–basal axis of *Arabidopsis*. *Nature* 426, 147–153. doi: 10.1038/nature02085

Furner, I. J., and Matzke, M. (2011). Methylation and demethylation of the *Arabidopsis* genome. *Curr. Opin. Plant Biol.* 14, 137–141. doi: 10.1016/j.pbi.2010.11.004

Gaj, M. D., Zhang, S., Harada, J. J., and Lemaux, P. G. (2005). Leafy cotyledon genes are essential for induction of somatic embryogenesis of *Arabidopsis*. *Planta* 222, 977–988. doi: 10.1007/s00425-005-0041-y

Gallego-Bartolomé, J., Liu, W., Kuo, P. H., Feng, S., Ghoshal, B., Gardiner, J., et al. (2019). Co-targeting RNA polymerases IV and V promotes efficient de novo dna methylation in *Arabidopsis*. *Cell* 176, 1068.e–1082.e. doi: 10.1016/j.cell.2019.01.029

Gehring, M. (2019). Epigenetic dynamics during flowering plant reproduction: evidence for reprogramming? *New Phytol.* 1, 91–96. doi: 10.1111/nph.15856

Gehring, M., Bubb, K. L., and Henikoff, S. (2009). Extensive demethylation of repetitive elements during seed development underlies gene imprinting. *Science* 324, 1447–1451. doi: 10.1126/science.1171609

Gehring, M., Huh, J. H., Hsieh, T.-F., Penterman, J., Choi, Y., Harada, J. J., et al. (2006). DEMETER DNA glycosylase establishes MEDEA polycomb gene self-imprinting by allele-specific demethylation. *Cell* 124, 495–506. doi: 10.1016/j.cell.2005.12.034

Gliwicka, M., Nowak, K., Balazadeh, S., Mueller-Roeber, B., and Gaj, M. D. (2013). Extensive modulation of the transcription factor transcriptome during somatic embryogenesis in *Arabidopsis thaliana*. *PLoS One* 8:e69261. doi: 10.1371/journal.pone.0069261

Gong, Z., Morales-Ruiz, T., Ariza, R. R., Roldán-Arjona, T., David, L., and Zhu, J.-K. (2002). ROS1, a repressor of transcriptional gene silencing in *Arabidopsis*, encodes a DNA glycosylase/lyase. *Cell* 111, 803–814. doi: 10.1016/S0092-8674(02)01133-9

Groß-Hardt, R., Kägi, C., Baumann, N., Moore, J. M., Baskar, R., Gagliano, W. B., et al. (2007). LACHESIS restricts gametic cell fate in the female gametophyte of *Arabidopsis*. *PLoS Biol.* 5:e47. doi: 10.1371/journal.pbio.0050047

Grzybkowska, D., Morończyk, J., Wójcikowska, B., and Gaj, M. D. (2018). Azacitidine (5-AzaC)-treatment and mutations in DNA methylase genes affect embryogenic response and expression of the genes that are involved in somatic embryogenesis in *Arabidopsis*. *Plant Growth Regul.* 85, 243–256. doi: 10.1007/s10725-018-0389-1

Guillaumot, D., Lopez-Obando, M., Baudry, K., Avon, A., Rigaill, G., Falcon de Longevialle, A., et al. (2017). Two interacting PPR proteins are major *Arabidopsis* editing factors in plastid and mitochondria. *Proc. Natl. Acad. Sci. U.S.A.* 114, 8877–8882. doi: 10.1073/pnas.1705780114

Haag, J. R., Ream, T. S., Marasco, M., Nicora, C. D., Norbeck, A. D., Pasa-Tolic, L., et al. (2012). *In vitro* transcription activities of Pol IV. Pol V, and RDR2 reveal coupling of Pol IV and RDR2 for dsRNA synthesis in plant RNA silencing. *Mol. Cell* 48, 811–818. doi: 10.1016/j.molcel.2012.09.027

Han, Q., Bartels, A., Cheng, X., Meyer, A., An, Y. C., Hsieh, T.-F., et al. (2019). Epigenetics regulates reproductive development in plants. *Plants* 8:564. doi: 10.3390/plants8120564

Hand, M. L., de Vries, S., and Koltunow, A. M. (2016). A comparison of *in vitro* and *in vivo* asexual embryogenesis. *Methods Mol. Biol.* 1359, 3–23. doi: 10.1007/978-1-4939-3061-6_1

Harada, J. J. (2001). Role of *Arabidopsis* LEAFY COTYLEDON genes in seed development. *J. Plant Physiol.* 158, 405–409. doi: 10.1078/0176-1617-00351

Havecker, E. R., Wallbridge, L. M., Hardcastle, T. J., Bush, M. S., Kelly, K. A., Dunn, R. M., et al. (2010). The *Arabidopsis* RNA-Directed DNA methylation argonautes functionally diverge based on their expression and interaction with target loci. *Plant Cell* 22, 321–334. doi: 10.1105/tpc.109.072199

Hecht, V., Vielle-Calzada, J.-P., Hartog, M. V., Schmidt, E. D., Boutilier, K., Grossniklaus, U., et al. (2001). The *Arabidopsis* SOMATIC EMBRYOGENESIS RECEPTOR KINASE 1 gene is expressed in developing ovules and embryos and enhances embryogenic competence in culture. *Plant Physiol.* 127, 803–816. doi: 10.1104/pp.127.3.803

Hernández-Lagana, E., Rodríguez-Leal, D., Lúa, J., and Vielle-Calzada, J.-P. (2016). A multigenic network of ARGONAUTE4 clade members controls early megaspore formation in *Arabidopsis*. *Genetics* 204, 1045–1056. doi: 10.1534/genetics.116.188151

Hofmann, F., Schon, M. A., and Nodine, M. D. (2019). The embryonic transcriptome of *Arabidopsis thaliana*. *Plant Reprod.* 32, 77–91. doi: 10.1007/s00497-018-00357-2

Hua, X., Berkowitz, N. D., Willmann, M. R., Yu, X., Lyons, E., and Gregory, B. D. (2021). Global analysis of RNA-dependent RNA polymerase-dependent small RNAs reveals new substrates and functions for these proteins and SGS3 in *Arabidopsis*. *Non Coding RNA* 7:28. doi: 10.3390/ncrna7020028

Huh, S. U., Lee, S.-B., Kim, H. H., and Paek, K.-H. (2012). ATAF2, a NAC transcription factor, binds to the promoter and regulates NIT2 gene expression involved in auxin biosynthesis. *Mol. Cells* 34, 305–313. doi: 10.1007/s10059-012-0122-2

Ibarra, C. A., Feng, X., Schoft, V. K., Hsieh, T.-F., Uzawa, R., Rodrigues, J. A., et al. (2012). Active DNA demethylation in plant companion cells reinforces transposon methylation in gametes. *Science* 337, 1360–1364. doi: 10.1126/science.1224839

Ingouff, M., Selles, B., Michaud, C., Vu, T. M., Berger, F., Schorn, A. J., et al. (2017). Live-cell analysis of DNA methylation during sexual reproduction in *Arabidopsis* reveals context and sex-specific dynamics controlled by noncanonical RdDM. *Genes Dev.* 31, 72–83. doi: 10.1101/gad.289397.116

Iwasaki, M., and Paszkowski, J. (2014). Epigenetic memory in plants. *EMBO J.* 33, 1987–1998. doi: 10.15252/embj.201488883

Jacobsen, S. E., Sakai, H., Finnegan, E. J., Cao, X., and Meyerowitz, E. M. (2000). Ectopic hypermethylation of flower-specific genes in *Arabidopsis*. *Curr. Biol.* 10, 179–186. doi: 10.1016/S0960-9822(00)00324-9

Ji, L., Mathioni, S. M., Johnson, S., Tucker, D., Bewick, A. J., Do Kim, K., et al. (2019). Genome-wide reinforcement of DNA methylation occurs during somatic embryogenesis in soybean. *Plant Cell* 31, 2315–2331. doi: 10.1105/tpc.19.00255

Jiang, F., Xu, X., Liu, H., and Zhu, J. (2015). *DRM1* and *DRM2* are involved in *Arabidopsis* callus formation. *Plant Cell. Tissue Organ Cult.* 123, 221–228. doi: 10.1007/s11240-015-0812-5

Jin, F., Hu, L., Yuan, D., Xu, J., Gao, W., He, L., et al. (2014). Comparative transcriptome analysis between somatic embryos (SEs) and zygotic embryos in cotton: evidence for stress response functions in SE development. *Plant Biotechnol. J.* 12, 161–173. doi: 10.1111/pbi.12123

Jones-Rhoades, M. W., Borevitz, J. O., and Preuss, D. (2007). Genome-wide expression profiling of the *Arabidopsis* female gametophyte identifies families of small, secreted proteins. *PLoS Genet.* 3, 1848–1861. doi: 10.1371/journal.pgen.0030171

Jullien, P. E., and Berger, F. (2010). Parental genome dosage imbalance deregulates imprinting in *Arabidopsis*. *PLoS Genet.* 6:e1000885. doi: 10.1371/journal.pgen.1000885

Jullien, P. E., Susaki, D., Yelagandula, R., Higashiyama, T., and Berger, F. (2012). DNA methylation dynamics during sexual reproduction in *Arabidopsis thaliana*. *Curr. Biol.* 22, 1825–1830. doi: 10.1016/j.cub.2012.07.061

Karim, R., Tan, Y. S., Singh, P., Khalid, N., and Harikrishna, J. A. (2018). Expression and DNA methylation of SERK. BBM, LEC2 and WUS genes in *in vitro* cultures of *Boesenbergia rotunda* (L.) Mansf. *Physiol. Mol. Biol. Plants* 24, 741–751. doi: 10.1007/s12298-018-0566-8

Kawashima, T., and Berger, F. (2014). Epigenetic reprogramming in plant sexual reproduction. *Nat. Rev. Genet.* 15, 613–624. doi: 10.1038/nrg3685

Kinoshita, T., Miura, A., Choi, Y., Kinoshita, Y., Cao, X., Jacobsen, S. E., et al. (2004). One-way control of FWA imprinting in *Arabidopsis* endosperm by DNA methylation. *Science* 303, 521–523. doi: 10.1126/science.1089835

Kondo, H., Ozaki, H., Itoh, K., Kato, A., and Takeno, K. (2006). Flowering induced by 5-azacytidine, a DNA demethylating reagent in a short-day plant, *Perilla frutescens var. crispa*. *Physiol. Plant.* 127, 130–137. doi: 10.1111/j.1399-3054.2005.00635.x

Kuo, H. Y., Jacobsen, E. L., Long, Y., Chen, X., and Zhai, J. (2017). Characteristics and processing of Pol IV-dependent transcripts in *Arabidopsis*. *J. Genet. Genomics* 44, 3–6. doi: 10.1016/j.jgg.2016.10.009

Kurczyńska, E. U., Gaj, M. D., Ujczak, A., and Mazur, E. (2007). Histological analysis of direct somatic embryogenesis in *Arabidopsis thaliana* (L.) Heynh. *Planta* 226, 619–628. doi: 10.1007/s00425-007-0510-6

Leljak-Levanić, D., Bauer, N., Mihaljević, S., and Jelaska, S. (2004). Somatic embryogenesis in pumpkin (*Cucurbita pepo* L.): control of somatic embryo development by nitrogen compounds. *J. Plant Physiol.* 161, 229–236. doi: 10.1078/0176-1617-01055

Leljak-Levanić, D., Mihaljević, S., and Bauer, N. (2015). Somatic and zygotic embryos share common developmental features at the onset of plant embryogenesis. *Acta Physiol. Plant.* 37, 1–14. doi: 10.1007/s11738-015-1875-y

Li, E. (2002). Chromatin modification and epigenetic reprogramming in mammalian development. *Nat. Rev. Genet.* 3, 662–673. doi: 10.1038/nrg887

Li, E., Bestor, T. H., and Jaenisch, R. (1992). Targeted mutation of the DNA methyltransferase gene results in embryonic lethality. *Cell* 69, 915–926. doi: 10.1016/0092-8674(92)90611-F

Lin, J.-Y., Le, B. H., Chen, M., Henry, K. F., Hur, J., Hsieh, T. F., et al. (2017). Similarity between soybean and and *Arabidopsis* seed methylomes and loss of non-CG methylation does not affect seed development. *Proc. Natl. Acad. Sci* 114, E9730–E9739. doi: 10.1073/pnas.1716758114

Liu, W., Duttke, S. H., Hetzel, J., Groth, M., Feng, S., Gallego-Bartolomé, J., et al. (2018). RNA-directed DNA methylation involves co-transcriptional small-RNA-guided slicing of polymerase V transcripts in *Arabidopsis*. *Nat. Plants* 4, 181–188. doi: 10.1038/s41477-017-0100-y

Liu, Z.-W., Shao, C.-R., Zhang, C.-J., Zhou, J.-X., Zhang, S.-W., Li, L., et al. (2014). The SET domain proteins SUVH2 and SUVH9 are required for Pol V occupancy at RNA-directed DNA methylation loci. *PLoS Genet.* 10:e1003948. doi: 10.1371/journal.pgen.1003948

LoSchiavo, F., Pitto, L., Giuliano, G., Torti, G., Nuti-Ronchi, V., Marazziti, D., et al. (1989). DNA methylation of embryogenic carrot cell cultures and its variations as caused by mutation, differentiation, hormones and hypomethylating drugs. *Theor. Appl. Genet.* 77, 325–331. doi: 10.1007/BF00305823

Lotan, T., Ohto, M., Yee, K. M., West, M. A., Lo, R., Kwong, R. W., et al. (1998). Arabidopsis LEAFY COTYLEDON1 is sufficient to induce embryo development in vegetative cells. *Cell* 93, 1195–1205. doi: 10.1016/S0092-8674(00)81463-4

Loyola-Vargas, V. M., and Ochoa-Alejo, N. (2016). "Somatic embryogenesis. An overview," in *Somatic Embryogenesis: Fundamental Aspects and Applications*, eds V. Loyola-Vargas and N. Ochoa-Alejo (Cham: Springer), 1–8. doi: 10.1007/978-3-319-33705-0_1

Lukowitz, W., Roeder, A., Parmenter, D., and Somerville, C. (2004). A MAPKK kinase gene regulates extra-embryonic cell fate in *Arabidopsis*. *Cell* 116, 109–119. doi: 10.1016/S0092-8674(03)01067-5

Martienssen, R. A., and Colot, V. (2001). DNA methylation and epigenetic inheritance in plants and filamentous fungi. *Science* 293, 1070–1074. doi: 10.1126/science.293.5532.1070

Massonneau, A., Coronado, M.-J., Audran, A., Bagniewska, A., Mòl, R., Testillano, P. S., et al. (2005). Multicellular structures developing during maize microspore culture express endosperm and embryo-specific genes and show different embryogenic potentialities. *Eur. J. Cell Biol.* 84, 663–675. doi: 10.1016/j.ejcb.2005.02.002

Matthys-Rochon, E. (2005). Secreted molecules and their role in embryo formation in plants: a min-review. *Acta Biol. Cracoviensia* 47, 23–29.

Matzke, M. A., Kanno, T., and Matzke, A. J. (2015). RNA-Directed DNA methylation: the evolution of a complex epigenetic pathway in flowering plants. *Annu. Rev. Plant Biol.* 66, 243–267. doi: 10.1146/annurev-arplant-043014-114633

Mayer, U., Buttner, G., and Jurgens, G. (1993). Apical-basal pattern formation in the *Arabidopsis* embryo: studies on the role of the gnom gene. *Development* 117, 149–162. doi: 10.1242/dev.117.1.149

McDonald, J. I., Celik, H., Rois, L. E., Fishberger, G., Fowler, T., Rees, R., et al. (2016). Reprogrammable CRISPR/Cas9-based system for inducing site-specific DNA methylation. *Biol. Open.* 5, 866–874. doi: 10.1242/bio.019067

Meinke, D. W. (2019). Genome-wide identification of EMBRYO-DEFECTIVE (EMB) genes required for growth and development in *Arabidopsis*. *New Phytol.* 226, 306–325. doi: 10.1111/nph.16071

Mendes, M. A., Petrella, R., Cucinotta, M., Vignati, E., Gatti, S., Pinto, S. C., et al. (2020). The RNA-dependent DNA methylation pathway is required to restrict SPOROCYTELESS/NOZZLE expression to specify a single female germ cell precursor in *Arabidopsis*. *Development* 147:dev194274. doi: 10.1242/dev.194274

Mercé, C., Bayer, P. E., Tay Fernandez, C., Batley, J., and Edwards, D. (2020). Induced methylation in plants as a crop improvement tool: progress and perspectives. *Agronomy* 10:1484. doi: 10.3390/agronomy10101484

Möller, B., and Weijers, D. (2009). Auxin control of embryo patterning. *Cold Spring Harb. Perspect. Biol.* 1:a001545. doi: 10.1101/cshperspect.a001545

Muñoz-Nortes, T., Candela, H., and Micol, J. L. (2017). Suitability of two distinct approaches for the high-throughput study of the post-embryonic effects of embryo-lethal mutations in *Arabidopsis*. *Sci. Rep.* 7:17010. doi: 10.1038/s41598-017-17218-z

Nic-Can, G. I., and De la Peña, C. (2014). *Epigenetic Advances on Somatic Embryogenesis of Agronomical and Important Crops. In: Epigenetics in Plants of Agronomic Importance: Fundamentals and Applications*. Cham: Springer. doi: 10.1007/978-3-319-07971-4_6

Nishiwaki, M., Fujino, K., Koda, Y., Masuda, K., and Kikuta, Y. (2000). Somatic embryogenesis induced by the simple application of abscisic acid to carrot (*Daucus carota* L.) seedlings in culture. *Planta* 211, 756–759. doi: 10.1007/s004250000387

Noceda, C., Salaj, T., Pérez, M., Viejo, M., Cañal, M. J., Salaj, J., et al. (2009). DNA demethylation and decrease on free polyamines is associated with the embryogenic capacity of *Pinus nigra* Arn. cell culture. *Trees* 23, 1285–1293. doi: 10.1007/s00468-009-0370-8

Olmedo-Monfil, V., Durán-Figueroa, N., Arteaga-Vázquez, M., Demesa-Arévalo, E., Autran, D., Grimanelli, D., et al. (2010). Control of female gamete formation by a small RNA pathway in *Arabidopsis*. *Nature* 464, 628–632. doi: 10.1038/nature08828

Osorio-Montalvo, P., Sáenz-Carbonell, L., and De-la-Peña, C. (2018). 5-Azacytidine: a promoter of epigenetic changes in the quest to improve plant somatic embryogenesis. *Int. J. Mol. Sci.* 19:3182. doi: 10.3390/ijms19103182

Papikian, A., Liu, W., Gallego-Bartolomé, J., and Jacobsen, S. E. (2019). Site-specific manipulation of *Arabidopsis* loci using CRISPR-Cas9 SunTag systems. *Nat. Commun.* 10:729. doi: 10.1038/s41467-019-08736-7

Park, K., Kim, M. Y., Vickers, M., Park, J.-S., Hyun, Y., Okamoto, T., et al. (2016). DNA demethylation is initiated in the central cells of *Arabidopsis* and rice. *Proc. Natl. Acad. Sci. U.S.A.* 113, 15138–15143. doi: 10.1073/pnas.1619047114

Park, K., Lee, S., Yoo, H., and Choi, Y. (2020). DEMETER-mediated DNA demethylation in gamete companion cells and the endosperm, and its possible role in embryo development in *Arabidopsis*. *J. Plant Biol.* 63, 321–329. doi: 10.1007/s12374-020-09258-2

Peer, W. A., and Murphy, A. S. (2007). Flavonoids and auxin transport: modulators or regulators? *Trends Plant Sci.* 12, 556–563. doi: 10.1016/j.tplants.2007.10.003

Penterman, J., Zilberman, D., Huh, J. H., Ballinger, T., Henikoff, S., and Fischer, R. L. (2007). DNA demethylation in the *Arabidopsis* genome. *Proc. Natl. Acad. Sci. U.S.A.* 104, 6752–6757. doi: 10.1073/pnas.0701861104

Pila Quinga, L. A., Pacheco de Freitas Fraga, H., do Nascimento Vieira, L., and Guerra, M. P. (2017). DNA methylation and recovery of embryogenic potential. *Plant Cell. Tissue Organ Cult.* 131, 295–305. doi: 10.1007/s11240-017-1284-6

Pillot, M., Baroux, C., Vazquez, M. A., Autran, D., Leblanc, O., Vielle-Calzada, J. P., et al. (2010). Embryo and endosperm inherit distinct chromatin and transcriptional states from the female gametes in *Arabidopsis*. *Plant Cell* 22, 307–320. doi: 10.1105/tpc.109.071647

Qi, Y., Denli, A. M., and Hannon, G. J. (2005). Biochemical specialization within *Arabidopsis* RNA silencing pathways. *Mol. Cell* 19, 421–428.

Qi, Y., He, X., Wang, X.-J., Kohany, O., Jurka, J., and Hannon, G. J. (2006). Distinct catalytic and non-catalytic roles of ARGONAUTE4 in RNA-directed DNA methylation. *Nature* 443, 1008–1012. doi: 10.1038/nature05198

Rajkumar, M. S., Gupta, K., Khemka, N. K., Garg, R., and Jain, M. (2020). DNA methylation reprogramming during seed development and its functional relevance in seed size/weight determination in chickpea. *Commun. Biol.* 3:340. doi: 10.1038/s42003-020-1059-1

Robert, H. S., Grones, P., Stepanova, A. N., Robles, L. M., Lokerse, A. S., Alonso, J. M., et al. (2013). Local auxin sources orient the apical-basal axis in *Arabidopsis* embryos. *Curr. Biol.* 23, 2506–2512. doi: 10.1016/j.cub.2013.09.039

Schmid, M. W., Giraldo-Fonseca, A., Rövekamp, M., Smetanin, D., Bowman, J. L., and Grossniklaus, U. (2018). Extensive epigenetic reprogramming during the life cycle of *Marchantia polymorpha*. *Genome Biol.* 19:9. doi: 10.1186/s13059-017-1383-z

Schmidt, E. D., Guzzo, F., Toonen, M. A., and de Vries, S. C. (1997). A leucine-rich repeat containing receptor-like kinase marks somatic plant cells competent to form embryos. *Development* 124, 2049–2062. doi: 10.1242/dev.124.10.2049

Schmitz, R. J., He, Y., Valdés-López, O., Khan, S. M., Joshi, T., Urich, M. A., et al. (2013). Epigenome-wide inheritance of cytosine methylation variants in a recombinant inbred population. *Genome Res.* 23, 1663–1674. doi: 10.1101/gr.152538.112

Schoft, V. K., Chumak, N., Choi, Y., Hannon, M., Garcia-Aguilar, M., Machlicova, A., et al. (2011). Function of the DEMETER DNA glycosylase in the *Arabidopsis thaliana* male gametophyte. *Proc. Natl. Acad. Sci. U.S.A.* 108, 8042–8047. doi: 10.1073/pnas.1105117108

Shibukawa, T., Yazawa, K., Kikuchi, A., and Kamada, H. (2009). Possible involvement of DNA methylation on expression regulation of carrot LEC1 gene in its 5'-upstream region. *Gene* 437, 22–31. doi: 10.1016/j.gene.2009.02.011

Sprunck, S., Hackenberg, T., Englhart, M., and Vogler, F. (2014). Same same but different: sperm-activating EC1 and ECA1 gametogenesis-related family proteins. *Biochem. Soc. Trans.* 42, 401–407. doi: 10.1042/BST20140039

Sprunck, S., Rademacher, S., Vogler, F., Gheyselinck, J., Grossniklaus, U., and Dresselhaus, T. (2012). Egg cell–secreted EC1 triggers sperm cell activation during double fertilization. *Science* 338, 1093–1097. doi: 10.1126/science.1223944

Stone, S. L., Braybrook, S. A., Paula, S. L., Kwong, L. W., Meuser, J., Pelletier, J., et al. (2008). Arabidopsis LEAFY COTYLEDON2 induces maturation traits and auxin activity: implications for somatic embryogenesis. *Proc. Natl. Acad. Sci. U.S.A.* 105, 3151–3156. doi: 10.1073/pnas.0712364105

Stroud, H., Do, T., Du, J., Zhong, X., Feng, S., Johnson, L., et al. (2014). Non-CG methylation patterns shape the epigenetic landscape in *Arabidopsis*. *Nat. Struct. Mol. Biol.* 21, 64–72. doi: 10.1038/nsmb.2735

Su, Y. H., Zhao, X. Y., Liu, Y. B., Zhang, C. L., O'Neill, S. D., and Zhang, X. S. (2009). Auxin-induced WUS expression is essential for embryonic stem cell renewal during somatic embryogenesis in *Arabidopsis*. *Plant J.* 59, 448–460. doi: 10.1111/j.1365-313X.2009.03880.x

Tang, K., Lang, Z., Zhang, H., and Zhu, J.-K. (2016). The DNA demethylase ROS1 targets genomic regions with distinct chromatin modifications. *Nat. Plants* 2:16169. doi: 10.1038/nplants.2016.169

Tao, Z., Shen, L., Gu, X., Wang, J., Yu, H., He, Y., et al. (2017). Embryonic epigenetic reprogramming by a pioneer transcription factor in plants. *Nature* 551, 124–128. doi: 10.1038/nature24300

Tedeschi, F., Rizzo, P., Huong, B. T. M., Czihal, A., Rutten, T., Altschmied, L., et al. (2019). EFFECTOR OF TRANSCRIPTION factors are novel plant-specific regulators associated with genomic DNA methylation in *Arabidopsis*. *New Phytol* 221, 261–278. doi: 10.1111/nph.15439

Ueda, M., Aichinger, E., Gong, W., Groot, E., Verstraeten, I., Vu, L. D., et al. (2017). Transcriptional integration of paternal and maternal factors in the *Arabidopsis* zygote. *Genes Dev.* 31, 617–627. doi: 10.1101/gad.292409.116

Ueda, M., Zhang, Z., and Laux, T. (2011). Transcriptional activation of *Arabidopsis* axis patterning genes WOX8/9 links zygote polarity to embryo development. *Dev. Cell* 20, 264–270. doi: 10.1016/j.devcel.2011.01.009

Vasilenko, A., McDaniel, J. K., and Conger, B. V. (2000). Ultrastructural analyses of somatic embryo initiation, development and polarity establishment from mesophyll cells of *Dactylis glomerata*. *Vitr. Cell. Dev. Biol. Plant* 36, 51–56. doi: 10.1007/s11627-000-0012-8

Verdeil, J.-L., Alemanno, L., Niemenak, N., and Tranbarger, T. J. (2007). Pluripotent versus totipotent plant stem cells: dependence versus autonomy? *Trends Plant Sci.* 12, 245–252. doi: 10.1016/j.tplants.2007.04.002

Vlachonasios, K. E., Thomashow, M. F., and Triezenberg, S. J. (2003). Disruption mutations of ADA2b and GCN5 transcriptional adaptor genes dramatically affect *Arabidopsis* growth, development, and gene expression. *Plant Cell* 15, 626–638. doi: 10.1105/tpc.007922

Vrinten, P. L., Nakamura, T., and Kasha, K. J. (1999). Characterization of cDNAs expressed in the early stages of microspore embryogenesis in barley (*Hordeum vulgare*) L. *Plant Mol. Biol.* 41, 455–463. doi: 10.1023/A:1006383724443

Walker, J., Gao, H., Zhang, J., Aldridge, B., Vickers, M., Higgins, J. D., et al. (2017). Sexual-lineage-specific DNA methylation regulates meiosis in *Arabidopsis*. *Nat. Genet.* 50, 130–137. doi: 10.1038/s41588-017-0008-5

Wang, F., and Axtell, M. J. (2017). AGO4 is specifically required for heterochromatic siRNA accumulation at Pol V-dependent loci in *Arabidopsis thaliana*. *Plant J.* 90, 37–47. doi: 10.1111/tpj.13463

Wierzbicki, A. T., Haag, J. R., and Pikaard, C. S. (2008). Noncoding transcription by RNA polymerase Pol IVb/Pol V mediates transcriptional silencing of overlapping and adjacent genes. *Cell* 135, 635–648. doi: 10.1016/j.cell.2008.09.035

Wierzbicki, A. T., Ream, T. S., Haag, J. R., and Pikaard, C. S. (2009). RNA polymerase V transcription guides ARGONAUTE4 to chromatin. *Nat. Genet.* 41, 630–634. doi: 10.1038/ng.365

Willemsen, V., and Scheres, B. (2004). Mechanisms of pattern formation in plant embryogenesis. *Annu. Rev. Genet.* 587–614. doi: 10.1146/annurev.genet.38.072902.092231

Wójcikowska, B., Jaskóła, K., Gąsiorek, P., Meus, M., Nowak, K., and Gaj, M. D. (2013). LEAFY COTYLEDON2 (LEC2) promotes embryogenic induction in somatic tissues of *Arabidopsis*, via YUCCA-mediated auxin biosynthesis. *Planta* 238, 425–440. doi: 10.1007/s00425-013-1892-2

Wu, Y., Meeley, R. B., and Cosgrove, D. J. (2001). Analysis and expression of the α-expansin and β-expansin gene families in maize. *Plant Physiol.* 126, 222–232. doi: 10.1104/pp.126.1.222

Xiao, W., Custard, K. D., Brown, R. C., Lemmon, B. E., Harada, J. J., Goldberg, R. B., et al. (2006). DNA methylation is critical for *Arabidopsis* embryogenesis and seed viability. *Plant Cell* 18, 805–814. doi: 10.1105/tpc.105.038836

Xiao, W., Gehring, M., Choi, Y., Margossian, L., Pu, H., Harada, J. J., et al. (2003). Imprinting of the MEA Polycomb gene is controlled by antagonism between MET1 methyltransferase and DME glycosylase. *Dev. Cell* 5, 891–901. doi: 10.1016/S1534-5807(03)00361-7

Xiong, L., Ishitani, M., Lee, H., and Zhu, J.-K. (2001). The *Arabidopsis* LOS5/ABA3 locus encodes a molybdenum cofactor sulfurase and modulates cold stress– and osmotic stress–responsive gene expression. *Plant Cell* 13, 2063–2083. doi: 10.1105/TPC.010101

Xu, R., and Li, Q. Q. (2003). A RING-H2 zinc-finger protein gene RIE1 is essential for seed development in *Arabidopsis*. *Plant Mol. Biol.* 53, 37–50. doi: 10.1023/B:PLAN.0000009256.01620.a6

Xu, X. M., and Møller, S. G. (2011). Iron-sulfur clusters: biogenesis, molecular mechanisms, and their functional significance. *Antioxid. Redox Signal.* 15, 271–307. doi: 10.1089/ars.2010.3259

Yamamoto, N., Kobayashi, H., Togashi, T., Mori, Y., Kikuchi, K., Kuriyama, K., et al. (2005). Formation of embryogenic cell clumps from carrot epidermal cells is suppressed by 5-azacytidine, a DNA methylation inhibitor. *J. Plant Physiol.* 162, 47–54. doi: 10.1016/j.jplph.2004.05.013

Yang, K.-J., Guo, L., Hou, X.-L., Gong, H.-Q., and Liu, C.-M. (2017). ZYGOTE-ARREST 3 that encodes the tRNA ligase is essential for zygote division in *Arabidopsis*. *J. Integr. Plant Biol.* 59, 680–692. doi: 10.1111/jipb.12561

You, W., Tyczewska, A., Spencer, M., Daxinger, L., Schmid, M. W., Grossniklaus, U., et al. (2012). Atypical DNA methylation of genes encoding cysteine-rich peptides in *Arabidopsis thaliana*. *BMC Plant Biol.* 12:51. doi: 10.1186/1471-2229-12-51

Yu, T.-Y., Shi, D.-Q., Jia, P.-F., Tang, J., Li, H.-J., Liu, J., et al. (2016). The *Arabidopsis* receptor kinase ZAR1 is required for zygote asymmetric division and its daughter cell fate. *PLoS Genet.* 12:e1005933. doi: 10.1371/journal.pgen.1005933

Zhang, H., Lang, Z., and Zhu, J.-K. (2018). Dynamics and function of DNA methylation in plants. *Nat. Rev. Mol. Cell Biol.* 19, 489–506. doi: 10.1038/s41580-018-0016-z

Zhang, X., and Jacobsen, S. E. (2006). Genetic analyses of DNA methyltransferases in *Arabidopsis thaliana*. *Cold Spring Harb. Symp. Quant. Biol.* 71, 439–447. doi: 10.1101/sqb.2006.71.047

Zhao, Y. (2012). Auxin biosynthesis: a simple two-step pathway converts tryptophan to indole-3-acetic acid in plants. *Mol. Plant* 5, 334–338. doi: 10.1093/mp/ssr104

Zhong, X. (2016). Comparative epigenomics: a powerful tool to understand the evolution of DNA methylation. *New Phytol.* 210, 76–80. doi: 10.1111/nph.13540

Zhong, X., Du, J., Hale, C. J., Gallego-Bartolomé, J., Feng, S., Vashisht, A. A., et al. (2014). Molecular mechanism of action of plant DRM de novo DNA methyltransferases. *Cell* 157, 1050–1060. doi: 10.1016/j.cell.2014.03.056

Zhong, X., Hale, C. J., Law, J. A., Johnson, L. M., Feng, S., Tu, A., et al. (2012). DDR complex facilitates global association of RNA polymerase V to promoters and evolutionarily young transposons. *Nat. Struct. Mol. Biol.* 19, 870–875. doi: 10.1038/nsmb.2354

Conflict of Interest: The authors declare that the research was conducted in the absence of any commercial or financial relationships that could be construed as a potential conflict of interest.

frontiers in Plant Science

ORIGINAL RESEARCH
published: 12 November 2021
doi: 10.3389/fpls.2021.718932

Sexual and Apogamous Species of Woodferns Show Different Protein and Phytohormone Profiles

Helena Fernández[1], Jonas Grossmann[2,3], Valeria Gagliardini[4], Isabel Feito[5], Alejandro Rivera[1], Lucía Rodríguez[5], Luis G. Quintanilla[6], Víctor Quesada[7], Mª Jesús Cañal[1] and Ueli Grossniklaus[4]*

[1] Area of Plant Physiology, Department of Organisms and Systems Biology, Oviedo University, Oviedo, Spain, [2] Functional Genomics Center, Zurich, Switzerland, [3] Swiss Institute of Bioinformatics, Lausanne, Switzerland, [4] Department of Plant and Microbial Biology & Zurich and Basel Plant Science Center, University of Zurich, Zurich, Switzerland, [5] Servicio Regional de Investigación y Desarrollo Agroalimentario (SERIDA), Finca Experimental La Mata, Grado, Spain, [6] Department of Biology and Geology, Physics and Inorganic Chemistry, Rey Juan Carlos University, Móstoles, Spain, [7] Department of Biochemistry and Molecular Biology, Institute of Oncology of the Principality of Asturias, Oviedo University, Móstoles, Spain

OPEN ACCESS

Edited by:
Paloma Moncaleán, Neiker Tecnalia, Spain

Reviewed by:
Danuše Tarkowská, Academy of Sciences of the Czech Republic, Czechia
Fulvio Pupilli, National Research Council (CNR), Italy

***Correspondence:**
Helena Fernández
fernandezelena@uniovi.es

Specialty section:
This article was submitted to Plant Proteomics and Protein Structural Biology, a section of the journal Frontiers in Plant Science

Received: *01 June 2021*
Accepted: *23 September 2021*
Published: *12 November 2021*

Citation:
Fernández H, Grossmann J, Gagliardini V, Feito I, Rivera A, Rodríguez L, Quintanilla LG, Quesada V, Cañal MJ and Grossniklaus U (2021) Sexual and Apogamous Species of Woodferns Show Different Protein and Phytohormone Profiles. Front. Plant Sci. 12:718932. doi: 10.3389/fpls.2021.718932

The gametophyte of ferns reproduces either by sexual or asexual means. In the latter, apogamy represents a peculiar case of apomixis, in which an embryo is formed from somatic cells. A proteomic and physiological approach was applied to the apogamous fern *Dryopteris affinis* ssp. *affinis* and its sexual relative *D. oreades.* The proteomic analysis compared apogamous vs. female gametophytes, whereas the phytohormone study included, in addition to females, three apogamous stages (filamentous, spatulate, and cordate). The proteomic profiles revealed a total of 879 proteins and, after annotation, different regulation was found in 206 proteins of *D. affinis* and 166 of its sexual counterpart. The proteins upregulated in *D. affinis* are mostly associated to protein metabolism (including folding, transport, and proteolysis), ribosome biogenesis, gene expression and translation, while in the sexual counterpart, they account largely for starch and sucrose metabolism, generation of energy and photosynthesis. Likewise, ultra-performance liquid chromatography-tandem spectrometry (UHPLC-MS/MS) was used to assess the levels of indol-3-acetic acid (IAA); the cytokinins: 6-benzylaminopurine (BA), trans-Zeatine (Z), trans-Zeatin riboside (ZR), dyhidrozeatine (DHZ), dyhidrozeatin riboside (DHZR), isopentenyl adenine (iP), isopentenyl adenosine (iPR), abscisic acid (ABA), the gibberellins GA_3 and GA_4, salicylic acid (SA), and the brassinosteroids: brassinolide (BL) and castasterone (CS). IAA, the cytokinins Z, ZR, iPR, the gibberellin GA_4, the brassinosteoids castasterone, and ABA accumulated more in the sexual gametophyte than in the apogamous one. When comparing the three apogamous stages, BA and SA peaked in filamentous, GA_3 and BL in spatulate and DHRZ in cordate gametophytes. The results point to the existence of large metabolic differences between apogamous and sexual gametophytes, and invite to consider the fern gametophyte as a good experimental system to deepen our understanding of plant reproduction.

Keywords: apogamy, apomixis, *Dryopteris affinis* ssp. *affinis*, *Dryopteris oreades*, fern, gametophyte, plant growth regulator, proteomic

INTRODUCTION

Understanding the factors underlying plant reproduction represents a challenge to which many research groups contribute given its enormous repercussions. In contrast to animals, in which the germ line differentiates early in development, flowering plants have no distinct germ line (Poethig et al., 1986). Instead, totipotent meristematic cells proceed through a long period of vegetative development before they eventually form complex sexual organs, the flowers (Vyskot and Hobza, 2004). Most angiosperms reproduce sexually through seeds, but the formation of seeds by asexual means is also possible, a process called apomixis. The production of seeds without sexual union is considered the holy grail of agriculture (Grossniklaus et al., 1998, 2001; Hofmann, 2010), but the molecular mechanisms operating behind apomixis remain unclear. Although plants with apomictic reproductive ability exceed 400 species (Grimanelli et al., 2003; Koltunow and Grossniklaus, 2003), no major seed crops are apomictic. Likewise, the distribution of apomictic taxa across plant lineages is uneven, with estimations of 0.1% in angiosperms, up to 10% in ferns, and with little or no evidence of its existence in gymnosperms, mosses, liverworts or hornworts (Lovis, 1978; Asker and Jerling, 1992; Dyer et al., 2012). Apomixis is especially frequent in the Dryopteridaceae family, which, together with Pteridaceae, comprises around 70% of the reported apomictic fern species (Liu et al., 2012).

Ferns represent a major vascular plant group, in which haploid and diploid generations are completely separated, and the gametophyte is an appealing experimental system to deal with reproduction. Moreover, in ferns, apomixis is an important mode of asexual reproduction, which has evolved several times independently within the group (Ekrt and Koutecký, 2016). Apomixis in ferns includes "apogamy," the formation of sporophytes from somatic cells of the prothallium, and "agamospory" (or diplospory), which represents the production of unreduced (diplo) spores in the fronds. In contrast, in gametophytes reproducing sexually, there are two organogenic events, producing antheridia and archegonia, bearing the male and female gametes, respectively. Performing molecular analyses in ferns has been elusive, as they exhibit higher chromosome numbers and larger genomes than mosses and seed plants (Barker and Wolf, 2010), which made it difficult to obtain genomic data. However, the advent of next-generation sequencing (NGS) technologies, by which it is possible to characterize the transcriptome in plants, represents a small but information reach-target compared to complete genome characterization (Ward et al., 2012). The variation in gene expression, induced by whatever environmental or endogenous conditions, can be examined in non-model organisms because these techniques have become more feasible as automation and efficiency have reduced costs. Until present, some transcriptome and proteome data sets have been published for ferns, which include the species *Pteridium aquilinum* (Der et al., 2011), *Ceratopteris richardii* (Salmi et al., 2010; Cordle et al., 2012), *Blechnum spicant* (Valledor et al., 2014), *Lygodium japonicum* (Aya et al., 2015), and *D. affinis* ssp. *affinis* (Grossmann et al., 2017; Wyder et al., 2020). Over the last case, both transcriptomic and proteomic analyses were performed by using next-generation sequencing (NGS) and shotgun proteomics by tandem mass spectrometry (MS/MS).

Several papers have been published to deepen on sexual and asexual reproduction in ferns. Two of them were driven in the model fern species *C. richardii*, looking for genes associated with female expression, and also male expression mediated by the pheromone antheridiogen in gametophytes (Atallah et al., 2018; Chen et al., 2019). Also, a comparative transcriptome analyses was done by Fu and Chen (2019) between apogamous and sexual gametophytes in *Adiantum reniforme* var. *sinense*. Previously, Bui et al. (2017) in *C. richardii* reported an AINTEGUMENTA-LIKE unigene, inducing the sporophyte formation without fertilization. It mirrors *BABY BOOM* (*BBM*) gene, a transcription factor of AP2/ERF family, which in angiosperms are known to promote somatic embryogenesis. Likewise, Domzalska et al. (2017) found proteins differently regulated during somatic embryogenesis in the tree fern *Cyathea delgadii*. Freshly, in the apogamous species, we have done a RNA-Seq approach to compare gene expression profiles of one- and two-dimensional gametophytes, finding several thousands of genes differentially expressed, and related to different aspect of either vegetative or reproductive behavior of the gametophyte (Wyder et al., 2020). In summary, with the increasing availability of genomic data from non-model species, better approaches will improve the sensitivity in protein identification for species distantly related to models.

On the other hand, phytohormones take part in the regulation of almost all phases of plant development, and also mediate the responses to various environmental stresses (Hicks, 1894; Rademacher, 2000; Dobrev et al., 2002). In ferns, growth and development of gametophyte and sporophyte are controlled by plant growth regulators, receiving especial attention their applications on morphogenesis, and its great repercussion on the sporophyte multiplication of ornamental ferns (Amaki and Higuchi, 1992; Fernández and Revilla, 2003; Somer et al., 2010; Rybczynski et al., 2018; Singh and Johari, 2018). The impact of phytohormones on gametophyte reproduction has been scrutinized in several species, some of them governed by an antheridiogen system, such as *B. spicant*, being these compounds devoted to promote genetic exchange, and linked chemically to gibberellin-related diterpenoids (Yamane, 1998; Menéndez et al., 2006a,b; Kazmierczak, 2010; Tanaka et al., 2014; Valledor et al., 2014). In *B. spicant*, Menéndez et al. (2006b) found similar levels of the gibberellins GA_4, GA_7, and GA_{20} in male and female gametophytes, while ABA has been reported to act as an antheridiogen antagonist in *C. richardii* (Warne

Abbreviations: ABA, abscisic acid; BA, 6-benzylaminopurine; BL, brassinolide; CS, castasterone; DA, *Dryopteris affinis*; DO, *Dryopteris oreades*; DHZ, dihydrozeatin; DHZR, dihydrozeatin riboside; GA_3, gibberellic acid; GA_4, gibberellin GA4; IAA, indole-3-acetic acid; iP, isopentenyl adenine; iPR, isopentenyl adenosine; JA, jasmonic acid; MS/MS, mass spectrometry; MS, Murashige and Skood mineral medium (1962); SA, salicylic acid; ZR, trans-zeatin riboside; Z, trans-zeatin.

and Hickok, 1989). In the sexual fern *Asplenium nidus*, which lacks antheridiogens, a significant increase in the content of the cytokinins iP and iPR was found in female gametophytes, and also qualitative differences in the content of gibberellins between the gametophyte and sporophyte generations were reported (Menéndez et al., 2011). In the gametophytes of *Polystichum aculeatum* and *Dryopteris filix-mas*, qualitative and quantitative changes of phytohormone content associated with the regulation of growth and gametangia formation, were recently documented (Kosakivska et al., 2019, 2020). On the other hand, variations in the content of phytohormones have been noted in *D. affinis* ssp. *affinis* (Menéndez et al., 2006c), associated to apogamy process. Yet, little attention has been paid so far to other phytohormones such as SA or brassinosteroids in basal branching vascular plants (i.e., lycophytes and ferns) (Sun et al., 2010; Choudhary et al., 2012). The former was traditionally associated with pathogen defense, together with jasmonic acid (de Vries et al., 2018), and the latter, in junction with auxins and gibberellins, is part of a key subset of plant hormones considered major determinants of plant growth and development (Ross and Reid, 2010; Gómez-Garay et al., 2018).

For a better understanding of the functions of the phytohormones and even possible interactions between them, exhaustive determination of their contents is of great importance (Bai et al., 2010). Analyses of phytohormones have focused on auxins, gibberellins, cytokinins, abscisic acid, or ethylene, while others like jasmonates or brassinosteroids were recently added, as standards and protocols became available. In the last few years, the advent of rapid, sensitive, accurate and efficient methods, even when small amounts of sample are available, has made possible to broaden the number of compounds analyzed (Du F. et al., 2012; Porfírio et al., 2016; Delatorre et al., 2017). HPLC-MS is the most accurate method to perform quantitative analysis of endogenous phytohormones or plant regulators (Pan et al., 2008, 2010; Delatorre et al., 2017), and at present day, a step forward is the use of UHPLC to detect those small amounts of phytohormones in fresh tissue, giving even better results on a wide spectrum of plant hormones.

In this work, a physiological and proteomic study was carried out in the fern *D. oreades* and its close relative *D. affinis* ssp. *affinis* (hereafter referred to as *D. affinis*). *D. oreades* is a sexual diploid and thus its gametophytes are haploid. *D. affinis* is also diploid but has two distinct genomes, one from *D. oreades* and one from an unknown "pure" *D. affinis* ancestor (Fraser-Jenkins, 1980). *D. affinis* is obligately apogamous and its gametophytes are diploid with the same genome constitution as that of sporophytes (Sheffield et al., 1983). Thus, this species pair provides an experimental system for investigating the gene expression an phytohormonal changes linked to sexual or apogamous reproduction. Specifically, our analyses involved (1) a proteomic comparison between sexual and apogamous gametophytes, and (2) the assessment of the endogenous content of fourteen phytohormones in sexual gametophytes and in three developmental stages of apogamous gametophytes: one-dimensional or filamentous; and two-dimensional or spatulate, and heart-shaped or cordate.

MATERIALS AND METHODS

Plant Material and Growth Conditions

Spores of *D. affinis* were obtained from sporophytes growing in Turón valley (Asturias, Spain), 477 m a.s.l., 43°12′10″N−5°43′43″W. In the case of *D. oreades*, spores were collected from sporophytes growing in Burgos, Neila lagoons, 1920 m a.s.l., 42°02′48″N−3°03′44″W. Spores were released from sporangia, soaked in water for 2 h, and then washed for 10 min with a solution of NaClO (0.5%) and Tween 20 (0.1%). Then, they were rinsed three times with sterile, distilled water. Spores were centrifuged at 1,300 *g* for 3 min between rinses, and then cultured in 500-mL Erlenmeyer flasks containing 100 mL of liquid Murashige and Skoog (MS) medium (Murashige and Skoog, 1962). Unless otherwise noted, media were supplemented with 2% sucrose (w/v), and the pH adjusted to 5.7 with 1 or 0.1 M NaOH. The cultures were kept at 25°C under cool-white fluorescent light (70 μmol $m^{-2}s^{-1}$) with a 16:8 h light: dark photoperiod, and put on an orbital shaker (75 rpm).

Following spore germination, gametophytes of both species go through three sequential growth stages, as in most ferns (Nayar and Kaur, 1971): filamentous, because of one-dimensional growth; spatulate, when growth becomes two-dimensional; and cordate (heath-shaped), when a notch meristem is formed in the middle of the upper margin. Gametophytes of *D. affinis* were collected at these three stages (**Figures 1A–C**), and, in the case of cordate ones, with visible signs (under a light microscope) of an evolving apogamic center (**Figure 1D**), composed of smaller and darker isodiametric cells. Filamentous gametophytes were collected 30 days after the start of spore culture. Spatulate and cordate gametophytes were obtained by transferring 30-day old filamentous gametophytes to 200 mL flask containing 25 mL of MS medium supplemented with 2% sucrose (w/v) and 0.7% agar, and being collected after 20 or 30 additional days, respectively. Gametophytes of *D. oreades* needed around 6 months to become cordate and reach sexual maturity (**Figures 1E,F**). They were then picked up and, in all cases, only female reproductive organs (i.e., archegonia) were observed under a light microscope. Samples of the three types of apogamous gametophytes (filamentous, spatulate and cordate) and sexual cordate, were weighted before and after being lyophilized for 48 h (Telstar-Cryodos) and stored in *Eppendorf* tubes on a freezer at −80°C until required.

Protein Extraction

From the cordate apogamous and cordate sexual gametophytes (three samples each), an amount of 20 mg dry weight of gametophytes were homogenized using a Silamat S5 shaker (Ivoclar Vivadent, Schaan, Liechtenstein). Homogenized samples were solubilized in 800 μL of buffer A [0.5 M Tris-HCL pH 8.0, 5 mM EDTA, 0.1 M Hepes-KOH, 4 mM DTT, 15 mM EGTA,

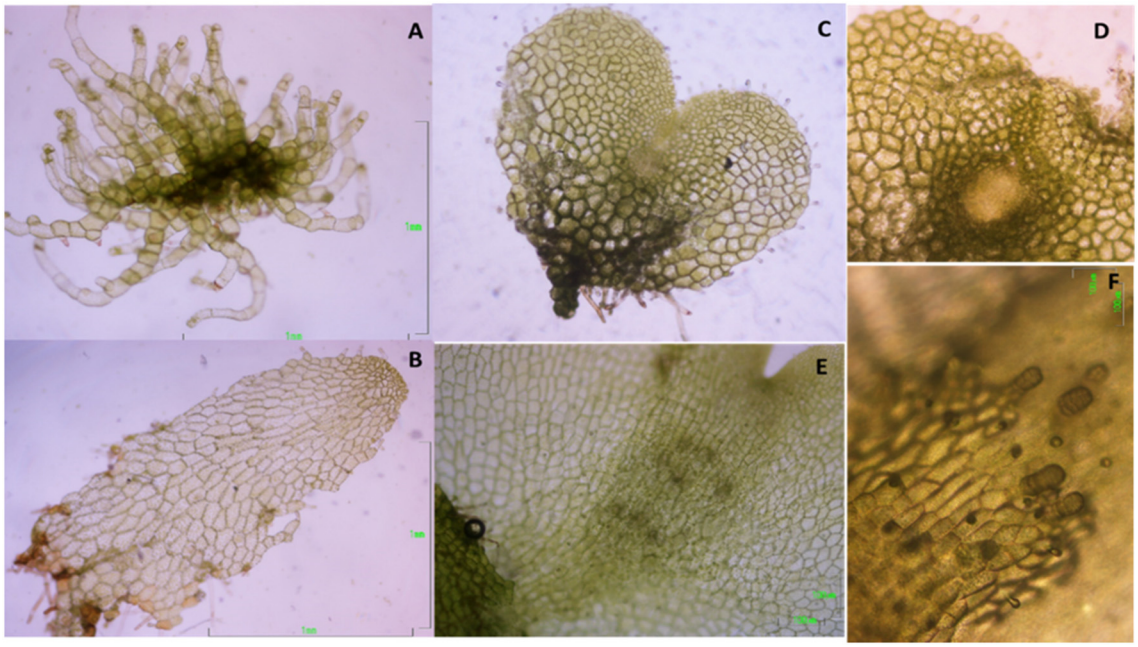

FIGURE 1 | Morphological features in the growth stages of the apogamous fern *Dryopteris affinis*: **(A)** filamentous; **(B)** spatulate; **(C)** cordate or heart-shaped; **(D)** detail of first steps in the embryo development; and its sexual relative *D. oreades*: **(E)** archegonium cushion in the middle of gametophyte; **(F)** archegonia.

1 mM PMSF, 0.5% PVP and 1 × protease inhibitor cocktail (Roche, Rotkreuz, Switzerland)] using a Potter homogenizer (Thermo Fisher Scientific, Bremen, Germany).

Proteins were extracted in two steps: first, the homogenate was subjected to centrifugation at 16,200 *g* for 10 min at 4°C on a table top centrifuge and, second, the supernatant was subjected to ultracentrifugation at 117–124 kPa (∼100,000 *g*) for 45 min at 4°C. Post-ultracentrifugation the supernatant contained the soluble protein fraction. The pellet from the first ultracentrifugation was re-dissolved in 200 μL of buffer B (40 mM Tris base, 40 mM DTT, 4% SDS, 1 × protease inhibitor cocktail (Roche, Rotkreuz, Switzerland) to extract membrane proteins using ultracentrifugation as described before. The supernatant after the second ultracentrifugation step contained the membrane protein fraction. Ultracentrifugation was performed using an Airfuge (Beckman Coulter, Pasadena, CA).

Protein concentrations were determined using a Qubit Fluorometer (Invitrogen, Carlsbad, CA). For 1 D gel electrophoresis, ∼1 mg protein per each soluble and membrane fraction was loaded separately onto a 0.75 mm tick, 12% SDS-PAGE mini-gel. Samples were treated with sample loading buffer and 2 M DTT, heated at 99°C for 5 min, followed by a short cooling period on ice, and loaded onto the gel. 1D gel electrophoresis was performed at 150 V and 250 mA for 1 h in 1X Running Buffer.

Protein Separation and In-gel Digestion

After 1D SDS-PAGE each gel lane was cut into six 0.4 cm wide sections using a custom-made gel cutter, resulting in 48 slices. These slices were further fragmented into smaller pieces and subjected to 10 mM DTT (in 25 mM AmBic pH8) for 45 min at 56°C and 50 mM Iodoacetamide for 1 h at room temperature in the dark, prior to trypsin digestion at 37°C overnight (Baerenfaller et al., 2008). The small pieces were washed twice with 100 μL of 100 mM NH_4HCO_3/50% acetonitrile, and washed once with 50 μL acetonitrile. All three supernatants were discarded and peptides digested with 20 μL trypsin (5 ng/μL in 10 mM Tris/2 mM $CaCl_2$, pH 8.2) and 50 μL buffer (10 mM Tris/2 mM $CaCl_2$, pH 8.2). After microwave-heating for 30 min at 60°C, the supernatant was removed and gel pieces extracted once with 150 μL 0.1% TFA/50% acetonitrile. All supernatants were combined and dried, and samples were then dissolved in 15 μL 0.1% formic acid/3% acetonitrile and transferred to auto-sampler vials for liquid chromatography (LC)-MS/MS where 5 μL were injected.

Protein Identification, Verification, and Bioinformatic Downstream Analyses

MS/MS and peptide identification (Orbitrap XL) were performed accordingly (Grossmann et al., 2017). Scaffold software (version Scaffold 4.2.1, Proteome Software Inc., Portland, OR) was used to validate MS/MS-based peptide and protein identifications. Mascot results were analyzed together using the MudPIT option. Peptide identifications were accepted if they scored better than 95.0% probability as specified by the Peptide Prophet algorithm with delta mass correction, and protein identifications were accepted if the Protein Prophet probability was above 95%. Proteins that contained same peptides and could not be differentiated based on MS/MS alone were grouped to satisfy the principles of parsimony using scaffolds cluster analysis option.

Only proteins that met the above criteria were considered positively identified for further analysis. The amount of random matches was evaluated by performing the Mascot searches against a database containing decoy entries and checking how many decoy entries (proteins or peptides) passed the applied quality filters. The peptide FDR and protein FDR was estimated at 2 and 1%, respectively, indicating the stringency of the analyses.

A semi-quantitative spectrum counting analysis was conducted. The "total spectrum count" for each protein and each sample was reported, and these spectrum counts were averaged for each species, *D. affinis* (DA) and *D. oreades* (DO). Then, one "1" was added to each average (DA and DO) in order to prevent division by zero and then a log2-ratio of the averaged spectral counts from DA vs. DO was calculated. Proteins were considered to be differentially expressed if this log2Ratio is above 0.99. This refers to at least twice as much peptide spectrum match (PSM) assignments in one group compared to the other. Also, in order to have a functional understanding of the identified proteins, we blasted the whole protein sequences of all identified proteins against *Sellginella moellendorfii* and *Arabidopsis thaliana* Uniprot sequences and retrieved the best matching identifier from each of them, along with the corresponding e-value, accepting blast-hits which evaluate below 1E-7. These better described ortholog identifiers are then used in further downstream analysis.

Protein Analysis Using STRING-DB Platform

The identifiers of the genes from the apogamous and sexual gametophyte samples were used as input for String version 11.0 analysis and networks were built based on high confidence in the ranking (0.7).

Endogenous Phytohormone Analyses

The extraction of phytohomones was done from 0.2 g fresh weight of each of the four gametophyte samples (filamentous, spatulate and cordate apogamous; and cordate sexual), according to the protocol of Pan et al. (2008) with modifications from Delatorre et al. (2017), which avoid derivatization and purification of the samples, and six replicates were considered for sample. The phytohormones analyzed were: ABA, IAA, the cytokinins iP, iPR, Z, ZR, DHZ, DHZR, the gibberellins GA_3 and GA_4, SA, and the brassinosteroids BL and CS (Sigma-Aldrich, St. Louis, MO, USA). The following deuterated standards were employed: IAA-d_5, SA-d_6, DHZ-d_3, and ABA-d_6 (20 ng); GA_9-d_2 and CS-d_5 (40 ng) and BA-d_7 (10 ng). All of them were supplied by Olchemim Ltd. (Czech Republic) except d6-SA obtained from Sigma Aldrich (St. Louis, MO, USA). Starting from these internal standards, known samples homogenized in liquid N_2, were extracted with 1 ml of extraction buffer (2-propanol/Mili Q water/Hydrochloric acid; 2:1:0.002; v/v/v) in 2 mL propylene Eppendorf tubes (Eppendorf Safe Lock England), and agitated by repeated inversion (60 rpm) for 20 min, at 4°C, in the dark. The resulting homogenate was transferred to a teflon tube (Oak Rifge Centrifuge Tube, Thermo Scientific, England) with 1.8 ml dichloromethane and reextracted by repeated and inverted agitation for 30 min, at 4°C in the dark. After 30 min standing, three phases were obtained, an aqueous, a material debris and an organic phase. The organic bottom phase was recovered and the intermediate debris phase was also re-extracted again. The propanol of combined extracts was evaporated under N_2 flow. Resulting dried extracts were resuspended in 150 μL of 100% methanol and filtered through a 0.2 μm regenerated cellulose Captiva Premium Syringe filter (Agilent Technologies, California, USA). The chromatographic separation takes place on a reverse phase chromatographic column (*Zorbax* SB-C18 2.1 × 50 mm) coupled to a *Zorbax* plus eclipse pre-column (C18 2.1 × 5 mm) at 40°C. Two solvents are used as mobile phases with a flow rate of 0.45 mL / min: MeOH acidified with 0.1% formic acid (solvent A) and ammonium formate 10 mM, pH 4 (solvent B).

Samples were injected into UHPLC System (1290 Infinity binary LC system, Agilent Technologies, Madrid Spain). The UHPLC was coupled to a Triple Quadrupole (6460 Triple Quad, LC/MS equipped with ESI-Ion Source). All compounds were separated and quantified following the protocol described by Delatorre et al. (2017).

Statistical Analyses of Phytohormone Content

Deviation from normality and homogeneity of variance were tested respectively with Shapiro-Wilk and Levene tests. One-way ANOVA was carried out with a Tukey-HSD test to group samples. From the obtained means squares estimates, values were used to identify the role played by each kind of gametophyte in overall variability through the Principal Component Analysis (PCA). This PCA was performed on the mean values recorded for 14 phytohormones assessed from four kind of gametophytes. From this PCA, a bioplot graph was drawn in an attempt to classify the endogenous content of phytohormones into similarity groups. All statistical analyses were completed in R environment with R Studio (Team, 2016) or the free software from *Past.uio 3.26* (Hammer, 2001).

RESULTS

Identification of Differentially Expressed Genes by LC-MS/MS

The proteomic analyses generated a total of 879 quantifiable proteins (**Supplementary Table 1**), rejecting those proteins not having a homolog and those having two DA/DO proteins the same homolog and repetitions. The "differential" protein regulation between the apogamous species and its sexual relative took into account proteins that were not "borderline," exhibiting a total of three assigned spectra, and rejecting those with less counts. According to this criterium, from the total number of annotated proteins, 206 and 166 were upregulated in 2 month-old apogamictic and sexual gametophytes, respectively (**Figure 2**). One-third of total annotated proteins (35.7%) had BLAST hits to proteins from *A. thaliana*, followed by *Oryza sativa* (4.7%). The remain matches of proteins are distributed among several species such as the seed plants *Nicotiana tabacum, Zea mays, Glycine max, Solanum tuberosum*, etc., animals like *Bos taurus*, *Mus musculus*, *Caenorhabditis elegans,* seedless plants like the moss

Physcomitrella patens or the lycophyte *Sellaginella moellemdorfii*, and microorganisms such as *Saccharomyces cerevisiae*, *Bacillus* sp., etc. (**Figure 3**).

Over-represented Categories for Differentially Regulated Proteins in Apogamous and Its Sexual Relative Gametophyte

The collections of differentially regulated proteins were analyzed by using the STRING database (http://String-db.org). Regarding those of the apogamous species, the results show 206 nodes and 1,047 edges, and a PPI enrichment p-value $= 1.0\ e^{-16}$; in the sexual relative, 166 nodes and 259 edges were scored, with a PPI enrichment p-value $= 5.55\ e^{-16}$. In both of cases, data reflected that our proteins have more interactions among themselves than what would be expected for a random set of proteins of similar size, drawn from the genome. Thus, the proteins are at least partially biologically connected, as a group.

In order to obtain a better knowledge about the function of both collections of proteins, Gene Ontology (GO), and KEGG enrichment analyses provided by the String platform were obtained. In total, 206 and 166 proteins differentially regulated were clustered to a number of GO and KEGG pathways significantly enriched (FDR's). Regarding the GO databank, proteins were checked according to standard categories of biological function, molecular function and cellular components (**Figure 4**). In both species, more than half of differentially regulated proteins (60–70%) counted for general metabolic and cellular processes (**Figure 4A**). The apogamous species, totals more proteins involved in the primary metabolism like amino acids, peptides and proteins (including folding, transport and proteolysis), nucleic acids and cofactors, nitrogen and sulfur metabolism, ribosome biogenesis, gene expression and translation. Instead, the sexual counterpart accumulated more proteins involved in generation of precursor metabolites and energy, and photosynthesis. In addition, it was found more proteins involved in response to hormones in this species. There are also biological functions such as response to stimulus or metabolism linked to carbohydrates, in which both species show a similar increase in the number of proteins scored but different profiles when detailing each kind of processes.

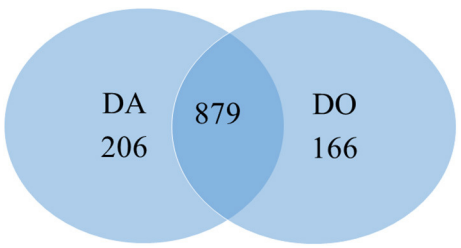

FIGURE 2 | Venn diagram totaling the number of proteins similarly and differently regulated in heart-shaped gametophytes from the apomictic fern *Dryopteris affinis* (DA), and its sexual relative *D. oreades* (DO).

Under "molecular function" category, the list of proteins differentially regulated was headed by binding activity in both species, being a ten percent higher in the apogamous gametophyte (**Figure 4B**). This activity is dominated by organic cyclic compounds and ion binding, in both gametophytes, respectively, followed by oxidoreductase activity, higher in the sexual gametophyte. The apogamous gametophytes expressed more proteins related to structural molecule activity, protein folding chaperone and translation initiation factor.

Additionally, under "cellular components" most part of the proteins was linked to cytoplasm and intracellular organelles, especially plastids and chroloplasts (**Figure 4C**). Both species upregulated proteins involved in cell wall, plasma membrane, and mitochondrion. In the apogamous gametophytes, it was significant the presence of proteins linked to nucleus, ribosome and peroxisome. On the other hand, in the sexual relative, increased the content of proteins associated to the photosynthetic machinery such as tylakoids, plastoglobule, and photosystems.

KEGG clustering showed an important expression of proteins associated to ribosome, aminoacid metabolism and proteasome in both species, being higher in the apogamous gametophyte (**Figure 5**). In this species, proteins drop in protein processing in endoplasmic reticulum, porphyrin and chlorophyll metabolism, spliceosome, RNA degradation, arginine biosynthesis, etc. In the sexual counterpart, proteins are involved in starch and sucrose metabolism, amino sugar and nucleotide sugar metabolism, photosynthesis, oxidative phosphorylation, lipid metabolism, etc. A selection of those proteins differentially regulated is reported in **Tables 1**, **2**.

Quantification of Endogenous Phytohormones

The endogenous levels of the plant growth regulators analyzed are shown in **Table 3**. The auxin IAA was found in a greater quantity in *D. oreades* gametophytes than in any growth stage of *D. affinis*, and in spatulate compared to filamentous and cordate gametophytes. Regarding cytokinins, BA peaked in the filamentous gametophytes of *D. affinis,* and Z and ZR showed low levels in *D. affinis* (<0.1 ng/g FW) and markedly higher in the sexual counterpart.

No differences were found in the content of DHZ, while the levels of its riboside, DHZR, significantly shrank in spatulate gametophytes of *D. affinis* compared to cordate gametophytes, dropping considerably in the sexual parent. Finally, no differences were found regarding the isoprenoid cytokinin iP, while the levels of its riboside, iPR, was lower in the spatulate and cordate than in the filamentous apogamous gametophytes, and also than in the sexual gametophytes.

The levels of plant growth inhibitor ABA increased in the sexual gametophytes and no differences were observed among the three developmental stages of apogamous gametophytes. Salicylic acid showed substantial differences among the four gametophyte samples. Levels up to 35 ng/g FW were detected in filamentous apogamous gametophytes, falling significantly in sexual ones. In relation to the tested gibberellins, high levels of GA_4 were noticed in sexual gametophytes, being also significant

in apogamous ones. In addition, GA_3 reached a maximum in spatulate apogamous gametophytes. Finally, on one hand, the brassinosteroid CS was undetected from filamentous and spatulate apogamous samples, and low in cordate apogamous gametophytes. On the other hand, this phytohormone was 10 times more abundant in sexual than in apogamous gametophytes. BL is 25 times more abundant in sexual than in apogamous gametophytes (but only one sample was achieved). In addition, significant differences were found between spatulate and the other apogamous stages.

Principal Component Analyses (PCA) revealed that one component (PC1) included the most part of the variance (90%), splitting sexual and apogamous gametophytes (**Figure 6**). Biplot shows the phytohormones grouping into the four gametophyte samples. DHZ and DHZR are common to filamentous and spatulate *D. affinis* gametophytes, and GA_3 is the hormone which differentiates both groups of samples. Apogamous filamentous samples showed variation with a great dispersion, and they shared differences with both spatulate and cordate stages by the cytokinin BA and salicylic acid.

DISCUSSION

Our results revealed substantial differences in the protein content between apogamous and sexual gametophytes of two closely related woodfern species. Specifically, *D. affinis* and *D. oreades* showed differences in terms of the expression of proteins involved in some biological, molecular and cellular aspects of plant development. Part of these differences can be explained by the distinct reproductive systems. Furthermore, although both species share the *D. oreades* genome, *D. affinis* has an additional genome (Fraser-Jenkins, 1980) whose expression also contributes to the divergent proteomic profiles.

Apogamous Gametophytes Upregulate Proteins Related to Protein Folding, Transport, Targeting, Proteolysis, Ribosome Biogenesis, Gene Expression and Translation

It has been reported an important role of protein metabolism on apomixis in angiosperms (Schmidt, 2020). Certainly, cellular processes related to proteins, such as in transport, folding, targeting or proteolysis are upregulated in the gametophyte of our apogamous species. For instance, we found RAN3, a small GTP-binding nuclear protein, required for the import of protein into the nucleus, RNA export, chromatin condensation and the control of cell cycle (Yano et al., 2006); and a puromycin-sensitive aminopeptidase, which plays an essential role during prophase I of meiosis for correct meiotic recombination in both male and female gametophytes (Sánchez-Morán et al., 2004). In addition, protein folding chaperones such as HSP60, HSP60-2, and the translation initiation factors FUG1, IF3-4 or ELF 3C, were found. Then, two signal chloroplastic recognition particles: cpSRP43 (CAO) and cpSRP54, involved in protein heterotrimerization, deserve to be mentioned. They act as a highly specific chaperones for LHCPs, preventing aggregation and being able to dissolve aggregates (Falk and Sinning, 2010; Falk et al., 2010). G-protein signaling is an integral part of the G-protein network important in many agronomic traits, including architecture and grain yield, and which is lost in many monocots (Bhatnagar and Pandey, 2020). In *D. affinis*, another interesting annotation is the chaperone protein htpG family protein or SHD, which encodes an ortholog of GRP94, an ER-resident HSP90-like protein involved in regulation of meristem size and organization. This protein is suggested to be required for the correct folding and/or complex formation of CLV proteins (Ishiguro et al.,

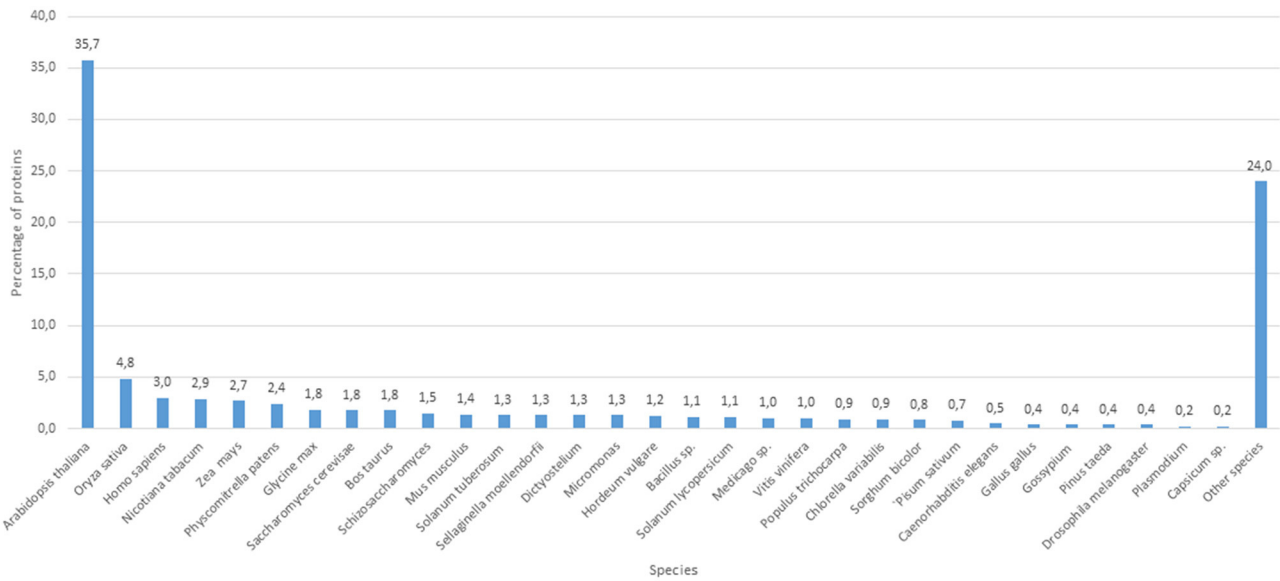

FIGURE 3 | Number of protein clusters obtained from the apogamous gametophytes of *Dryopteris affinis* and its sexual relative *D. oreades*, with the best hits to species belonging to the phylogenetic groups specified.

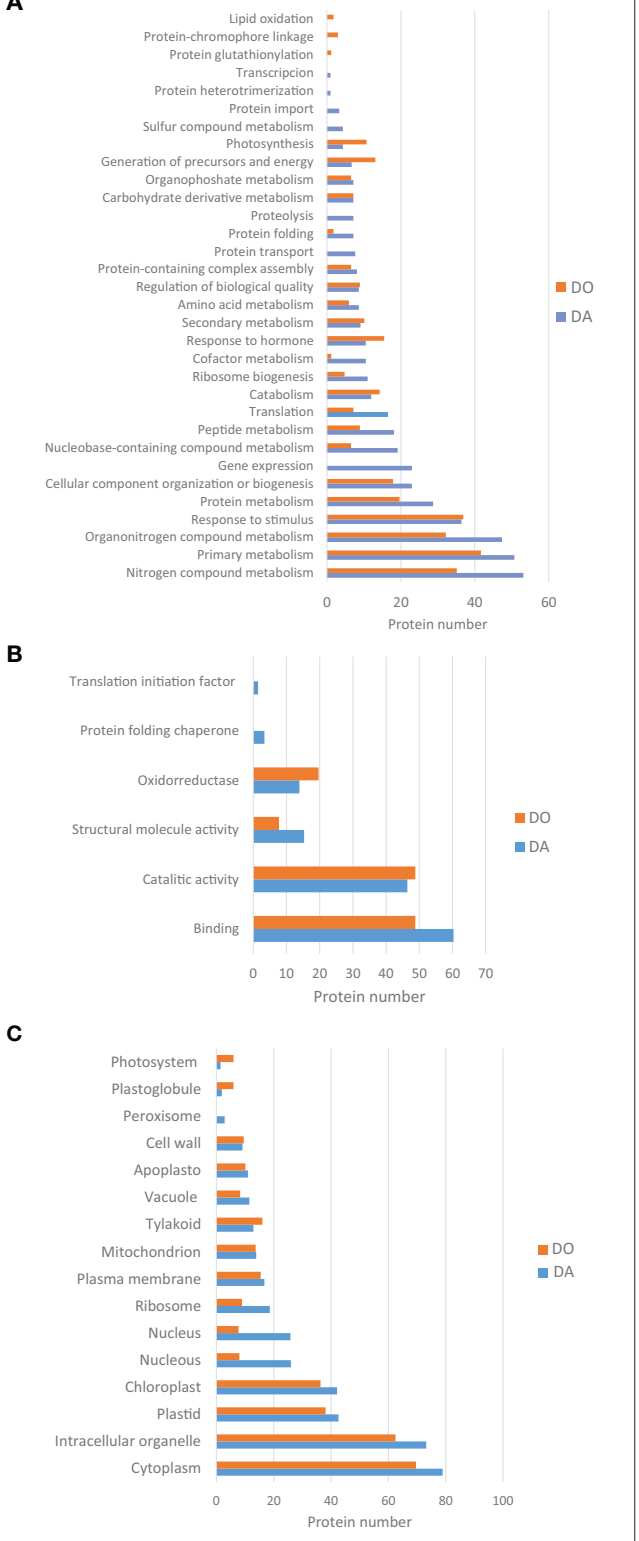

FIGURE 4 | GO classification of proteins differentially upregulated in the apogamous fern *Dryopteris affinis* and its sexual relative *D. oreades*, in the three main categories: **(A)** biological function; **(B)** molecular function; and **(C)** cellular component.

2002), and it is also involved in resistance to tunicamycin- or high calcium-induced ER stress (Chong et al., 2015). Indeed, Hsp70s are key components that facilitate folding of *de novo* synthesized proteins, assist translocation of precursor proteins into organelles, and are responsible for degradation of damaged proteins under stress conditions (Lee et al., 2009).

In apogamous gametopytes, we also found proteins related to the ribosome organelle, including a wide number of processes such as ribosome biogenesis, processing, gene expression, translation and cell cycle control. As an example, the protein CPR, member of metallopeptidase M24 family, is involved in the regulation of rRNA processing and ribosome assembly, and is required for expression of cell cycle genes such as CYCD3-1, RNR2A, and CDKB1-1, playing a role in the entry into mitosis. Besides, it promotes, in a dose- and auxin-dependent manner, organ growth by stimulating both cell proliferation and expansion, via the regulation of RBR1 levels (Horváth et al., 2006). The list also included an emb3010 or 40S ribosomal protein S6-2, which may play an important role in controlling cell growth and proliferation through the selective translation of particular classes of mRNAs (Zhou et al., 2015).

Ribosome assembly and function are correlated with the activity of RNA binding proteins, often associated to ribonucleoprotein complexes of RNA as well as helicases (Schmidt, 2020). The former includes proteins like the phosphoprotein AtLa1, required for normal ribosome biogenesis and embryogenesis (Fleurdépine et al., 2007), and the latter, a 50S ribosomal protein L13 or embryo defective 1473, involved in translation and biological processes such as embryo development ending in seed dormancy or stress tolerance (Moin et al., 2016).

RNA helicases are considered of crucial importance for gene regulation of developmental processes, exerting an epigenetic control. In the apogamous species, two helicases, to unwind nucleic acids, were reported: the emb1138, member of the DEAD-box ATP–dependent RNA helicase 3, and At3G62310, a probable pre-mRNA-splicing factor ATP-dependent RNA helicase DEAH2, which might be involved in pre-mRNA splicing. The DEAD-box helicases are involved in various aspects of RNA metabolism, including nuclear transcription, pre-mRNA splicing, ribosome biogenesis, nucleocytoplasmic transport, translation, RNA decay and organellar gene expression. Different studies provided evidence of RNA helicases to be likely involved in regulating apomictic development (Schmidt, 2020). In *A. thaliana*, mutants for the RNA helicase MNEME form unreduced gametophytes, resembling apospory (Schmidt et al., 2011). Also, in apomictic *Brachiaria brizantha* and in *Hypericum perforatum*, BrizHELIC and a of MATERNAL EFFECT EMBYO ARREST29, are differentially expressed in tissues of apomictic plants (Silveira et al., 2012; Barcaccia and Albertini, 2013). In our work, a homologue of MATERNAL EFFECT EMBRYO ARREST 59 (MEE59) is up regulated in the apogamous gametophyte, but its biological function is unknown. Furthermore, we found TFL2, a chromo domain-containing protein LHP1, structural component of heterochromatin, and the transducin/WD40 repeat-like superfamily protein, which is a component of the

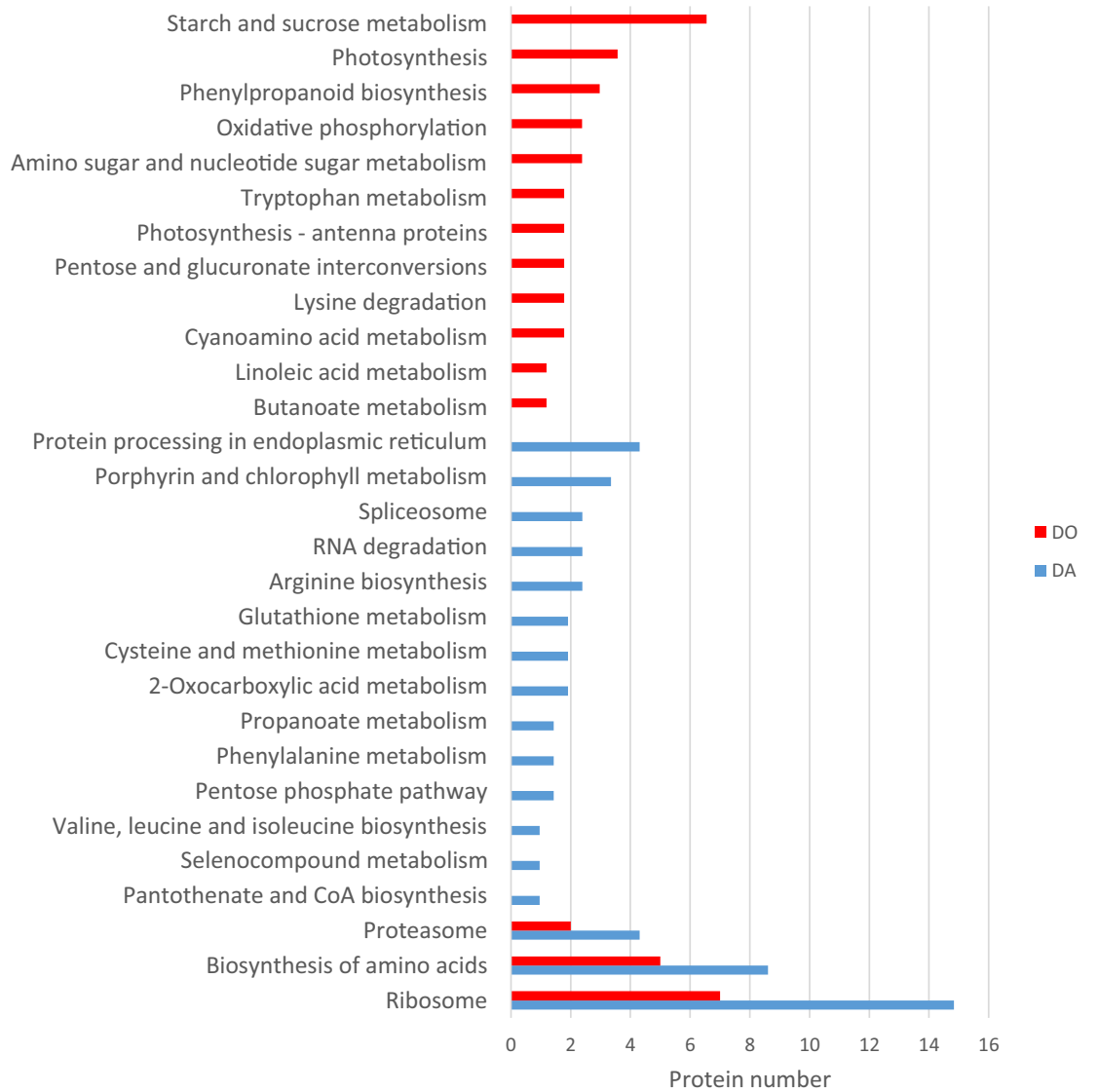

FIGURE 5 | KEGG classification of proteins differentially upregulated in the apogamous fern *Dryopteris affinis* and its sexual relative *D. oreades*.

PAF1 complex (PAF1C), involved in epigenetic gene repression of several floral homeotic genes, such as FLT, that regulates flowering time, and is required for maintenance of vernalization-induced repression of FLC (Kotake et al., 2003; Zhang et al., 2003; Xu and Shen, 2008). An interesting finding is the ortologue of the transcriptional regulation protein Methyl-CpG-binding domain-containing protein 10, required for nucleolar dominance that leads to the silencing of rRNA genes inherited from one progenitor in interspecific hybrids (Preuss et al., 2008). It must be noted that *D. affinis* ssp. *affinis* is actually a fertile hybrid in which both sporophyte and gametophyte have two genomes from two different species (Fraser-Jenkins, 1980). Finally, it is reported the mitochondrial pentatricopeptide repeat-containing protein At1g63130, a trans-acting siRNA (ta-siRNA) generating locus (Yoshikawa et al., 2005).

Some annotated proteins may be involved on reproduction, such as D-3-phosphoglycerate dehydrogenase 1, which apart from participating in the plastidial phosphorylated pathway of serine biosynthesis (PPSB) (Benstein et al., 2013), might act on pollen development, megagametogenesis or seed dormancy (Toujani et al., 2013). Also, a DC1 domain-containing protein, associated to the generation of lipid signaling molecules in pistil (Qin et al., 2009), a dihydrolipoyl dehydrogenase 1, highly expressed in developing seeds, and the translation

TABLE 1 | Selected proteins upregulated in the apogamous fern *Dryopteris affinis* ssp. *affinis*.

Description	Idex in Supp table	Accession number	MW kD	Uniprot accessions	e-Evalue	log2Ratio _DAvsDO	% Coverage	Total unique peptide count
GTP-binding nuclear protein Ran-3	325	43286-387_3_ORF1 (+68)	29	Q8H156	1.8912E-157	1.00	14	6
Puromycin-sensitive aminopeptidase	1,071	166554-171_3_ORF1 [7]	115	F4I3R1	0	2.32	2.5	6
Metallopeptidase M24 family protein	589	207675-131_6_ORF2	43	Q96327	0	1.32	4.9	4
40S ribosomal protein S6-2	332	7438-849_3_ORF2	29	P51430	1.1336E-150	1.50	24	9
DEAD-box ATP-dependent RNA helicase 3	987	133309-212_3_ORF2 [8]	84	Q8L7S8	0	2.13	13	13
Maternal effect embryo arrest 59 (MEE59)	304	102286-246_3_ORF2	28	O23157	4.92172E-18	2.32	7.5	2
Chromo domain-containing protein LHP1	828	152641-192_2_ORF2 (+1)	59	Q946J8	1.00311E-43	3.17	10	5
Transducin/WD40 repeat-like superfamily protein	182	362879-38_5_ORF2 (+2)	22	Q9SZQ5	1.5458E-164	1.42	2	3
AtLa1	720	278034-81_6_ORF2	50	Q93ZV7	1.05674E-96	1.74	12	5
Embryo defective 1473 (emb1473)	336	188230-148_1_ORF2 (+1)	30	Q9SYL9	4.9526E-104	1.42	10	4
Methyl-CpG-binding domain-containing protein 10	435	254886-96_1_ORF2 (+1)	34	Q9XI36	1.22143E-24	2.32	8.9	2
Pentatricopeptide repeat-containing protein At1g63130	1,010	62277-321_4_ORF2	90	Q9CAN0	3.09193E-32	2.00	5.1	7
D-3-phosphoglycerate dehydrogenase 1	918	229414-114_3_ORF1	68	O49485	0	1.00	23	14
DC1 domain-containing protein	919	167954-169_4_ORF1	68	O80763	8.1609E-154	1.58	5.4	3
Dihydrolipoyl dehydrogenase 1	867	143453-204_6_ORF2 [2]	63	A8MS68	0	1.58	13	9
Membrane-associated progesterone binding protein 2	65	142203-205_1_ORF1	15	Q9SK39	1.60057E-42	1.58	19	3
Magnesium-chelatase subunit ChlD	985	3146-1200_2_ORF1	84	Q9SJE1	1.5299E-178	1.32	4.5	3
Magnesium-chelatase subunit ChlH	1,103	102670-246_5_ORF2 (+4)	159	Q9FNB0	0	1.00	1.9	2
P-loop containing nucleoside triphosphate hydrolases superfamily protein	718	237628-108_3_ORF2 (+2)	50	P16127	0	1.58	14	7
Coproporphyrinogen-III oxidase 1	639	263607-90_6_ORF2 (+1)	46	Q9LR75	0	3.00	11	3
Carbamoyl-phosphate synthase large chain	1,088	39629-404_3_ORF2 [3]	133	Q42601	0	1.32	2.6	3
Argininosuccinate synthase	740	1466-1535_4_ORF1 [4]	52	Q9SZX3	0	1.00	7.1	3
Prohibitin-3	372	25450-498_6_ORF2 [5]	31	O04331	1.6594E-147	1.00	15	5
Acetyl-CoA carboxylase 1	1,122	1892-1420_1_ORF2 [3]	265	Q38970	0	1.22	12	28
Nucleoid-associated protein At2g24020	145	16884-601_6_ORF1	20	O82230	7.88432E-68	1.00	11	2
Winged-helix DNA-binding transcription factor family protein	646	275958-82_2_ORF1	46	F4INW2	4.61845E-21	2.58	16	8
60S acidic ribosomal protein family	12	63281-318_4_ORF1	9	Q9FLV1	2.36329E-27	3.00	51	2
Eukaryotic translation initiation factor 3 subunit C	1,068	205951-132_1_ORF2 (+3)	113	O49160	0	2.32	6.5	7
Triosephosphate isomerase	441	151710-194_2_ORF2 [4]	34	Q9SKP6	1.3778E-154	2.22	6.9	8
Lactate/malate dehydrogenase family protein	717	130359-215_1_ORF1	50	Q8H1E2	0	1.87	16	7
Homolog of human CAND1	1,090	112593-234_6_ORF2	137	Q8L5Y6	0	2.32	2.6	3

elongation factor emb2726, member of the broad mutant family found in *Arabidopsis*, EMBRYO DEFECTIVE (Meinke, 2020).

Our results give support to a role of the metabolism of arginin, precursor of polyamines, on gametophyte reproduction, due to the increase of the protein argininosuccinate synthase and carbamoyl-phosphate synthase. A possible role of polyamines on gametophyte development is a recurring data in our previous analyses in these fern species (Grossmann et al., 2017; Wyder et al., 2020). Finally, the metabolism of cell wall pectins acquires some importance with the protein UGD2, which is involved in the biosynthesis of UDP-glucuronic acid (UDP-GlcA), providing

TABLE 2 | Selected proteins upregulated in the sexual fern *Dryopteris oreades*.

Description	Idx in spp table	Accession number	MW (kD)	Uniprot accessions	Evalue	log2Ratio _DAvsDO	% Coverage	Total unique peptide count
Alpha-amylase-like	827	266991-88_5_ORF2	59	Q8VZ56	7.9347E-154	−1	7.1	3
Beta-amylase 2	857	190175-146_3_ORF2 (+1)	62	O65258	0	−2.81	6	4
pfkB-like carbohydrate kinase family protein	621	222710-119_2_ORF2 [5]	45	Q9C524	2.947E-180	−1.66	19	9
Phosphoglucan, water dikinases	1,089	316777-59_1_ORF2	135	Q6ZY51	0	−2.08	18	17
Probable sucrose-phosphate synthase 3	1,081	165303-173_5_ORF1 [19]	123	Q8RY24	0	−2.81	7.3	9
Glucose-1-phosphate adenylyltransferase small subunit	809	tr|A9SGH8|A9SGH8_PHYPA	57	P55228	0	−1.22	14	6
Glucose-6-phosphate isomerase 1	933	373594-34_6_ORF1 [7]	70	Q8H103	0	−1	13	6
Fructose-1,6-bisphosphatasa	491	tr|D8RRD1|D8RRD1_SELML	37	Q9MA79	0	−2.32	12	6
Linoleate 9S-lipoxygenase 1	1,041	38467-410_3_ORF2	102	Q06327	0	−1.58	3.8	3
Lipoxygenase 3	1,027	61725-322_6_ORF3	95	Q9LNR3	0	−3	8.5	8
Peroxisomal fatty acid beta-oxidation multifunctional protein MFP2	977	46601-373_3_ORF2	80	Q9ZPI5	0	−1.32	3.2	3
Monocopper oxidase-like protein SKU5	895	149426-198_2_ORF2	65	Q9SU40	0	−1.42	13	6
Late embryogenesis abundant protein (LEA) family protein	184	415079-17_4_ORF2 (+1)	22	Q9SUB2	0.000692152	−1.07	31	7
Late embryogenesis abundant protein 31	376	43963-384_3_ORF2 [2]	31	Q9LJ97	4.74152E-40	−1.15	30	8
Late embryogenesis abundant protein, group 1 protein	108	281637-79_2_ORF2 (+1)	17	Q39138	2.65719E-05	−2.52	20	5
Embryo defective 1579 (emb1579)	1,082	27243-483_2_ORF1 (+1)	123	F4IS91	9.02076E-73	−1.77	20	14
Late embryogenesis abundant (LEA) protein in group 3	61	253001-98_1_ORF1	14	Q9SKP0	1.43925E-11	−1.55	49	9
Villin-2; Ca(2+)-regulated actin-binding protein	1,014	80596-281_5_ORF2	92	O81644	0	−2.58	3.2	3
NAP1-related protein 2	410	354891-42_3_ORF1 (+1)	33	Q8LC68	4.8665E-99	−1	7.8	2
Persulfide dioxygenase ETHE1 homolog	399	249504-100_3_ORF2	32	Q9C8L4	9.9249E-145	−2.32	12	3
ATP-dependent zinc metalloprotease FTSH 2	956	64641-315_3_ORF2	75	A0A1P8AXC1	0	−1.32	5	4
UPF0603 protein	396	128797-216_2_ORF2	32	Q9ZVL6	4.7595E-112	−1	13	3
Arginase/deacetylase superfamily protein	584	1738-1468_5_ORF1 [4]	43	Q9ZPF5	6.0531E-168	−4.46	33	10
NAD(P)-binding Rossmann-fold superfamily protein	296	66706-309_6_ORF2	28	Q94EG6	7.7668E-135	−1.13	25	6
GroES-like zinc-binding dehydrogenase family protein	583	70975-299_4_ORF2	42	Q96533	0	−1.32	9.4	3
Nudix hydrolase homolog 8	428	416362-16_5_ORF3 (+3)	34	Q8L7W2	2.86086E-92	−2.32	8.9	3
Flavone 3'-O-methyltransferase 1	528	1607-1505_6_ORF1	39	Q9FK25	1.09086E-60	−2.58	8.7	4
Glutamate decarboxylase 1	797	tr|B9H3K1|B9H3K1_POPTR	56	Q42521	0	−1.58	5.7	5
Glutathione S-transferase TAU 20	50	423746-11_3_ORF1 [2]	14	Q8L7C9	2.22255E-16	−1	23	4
AMP-dependent synthetase and ligase family protein	814	681-1862_1_ORF2	58	Q9SMT7	0	−1	4.3	2
Phosphoserine aminotransferase 1, chloroplastic	647	350227-43_2_ORF2	46	Q96255	0	−1.74	12	4
Embryo defective 2171 (emb2171)	76	18818-572_2_ORF2 (+3)	16	P49690	1.51032E-96	−1.32	17	3
RNA-binding (RRM/RBD/RNP motifs) family protein (LIF2)	873	71037-299_5_ORF2	63	Q9ASP6	1.00527E-36	−1.32	7.2	4
Sec14p-like phosphatidylinositol transfer family protein	922	420882-13_1_ORF2	68	Q94C59	5.0715E-123	−2.66	15	10

(Continued)

TABLE 2 | Continued

Description	Idx in spp table	Accession number	MW (kD)	Uniprot accessions	Evalue	log2Ratio _DAvsDO	% Coverage	Total unique peptide count
Rubber elongation factor protein (REF)	194	sp|O82803|SRPP_HEVBR	22	Q9MA63	1.01539E-67	−3.17	15	3
Encodes a dual-targeted protein believed to act as a pyruvate, orthophosphate dikinase	1042	418542-15_2_ORF1 [22]	102	O23404	0	−1.64	12	10
Peroxidase family protein	476	167942-169_1_ORF2	36	Q9LSP0	8.46546E-91	−2.58	14	4
Mediator of RNA polymerase II transcription subunit 36a	324	6971-870_2_ORF2 [4]	29	Q94AH9	2.3256E-162	−1.91	24	6
Pollen Ole e 1 allergen and extensin family protein	471	133239-212_4_ORF2 (+1)	36	Q8RWG5	6.10012E-29	−1.74	11	4
Pectin lyase-like superfamily protein	555	18361-579_1_ORF2 (+2)	41	Q8VYZ3	3.1298E-116	−1	11	3

TABLE 3 | Endogenous content of phytohormones in three growth stages of apogamous fern *Dryopteris affinis* and one stage of its relative *D. oreades*.

	Dryopteris affinis* ssp. *affinis						***D. oreades***
	Filamentous		**Spatulate**		**Heart**		**Heart**
ng/gFW	**Mean**	**SE**	**Mean**	**SE**	**Mean**	**SE**	**Mean**
IAA	0.33	0.02	0.16	0.03	0.29	0.05	0.88
BA	0.31	0.03	0.18	0.02	0.18	0.02	0.19
Z	0.02	0.00	0.03	0.00	0.02	0.00	0.16
ZR	0.98	0.08	0.94	0.07	1.00	0.10	3.13
DHZ	0.03	0.00	0.03	0.00	0.02	0.00	0.02
DHZR	0.16	0.02	0.11	0.01	0.22	0.04	0.08
iP	0.23	0.01	0.24	0.01	0.25	0.01	0.25
iPR	1.19	0.09	0.70	0.09	0.83	0.06	2.29
GA3	0.74	nd	3.61	0.81	1.33	0.13	2.33
GA4	141.56	35.14	135.60	19.48	164.57	21.26	278.73
ABA	2.89	0.20	2.21	0.06	2.17	0.13	3.48
SA	35.53	5.77	20.27	0.85	14.70	0.18	8.42
CS	nd	nd	nd	nd	10.13	1.75	369.92
BL	2.55	0.67	4.53	0.54	1.58	0.58	58.64

Data are mean ± standard error. IAA,indol-3-acetic acid, BA, 6-benzylaminopurine; Z, trans-Zeatin; ZR, Zeatin riboside; DHZ, dihydrozeatin; DHZR, dihydrozeatin riboside; iP, isopentenyl adenine; iPR, isopentenyl adenosine; ABA,abscisic acid; SA, salicylic acid; GA_3, gibberellic acid; GA_4, gibberellin 4; BL, brassinolide; CS, castasterone; nd, below detection limit.

nucleotide sugars for cell-wall polymers. A possible connection to the apogamy will need further research.

Sexual Gametophytes Upregulate Proteins Related to Starch and Sucrose Metabolism, Generation of Precursor Metabolites and Energy, and Photosynthesis

Starch and sucrose metabolism appear to be relevant processes in the sexual gametophytes. Specifically, among other proteins upregulated in the studied female gametophytes, we found alpha and beta amylase, pfkB-like carbohydrate kinase family protein, phosphoglucan, water dikinase (PWD), cytosolic fructose 1-6-bisphosphatase, a probable sucrose-phosphate synthase 3, glucose-1-phosphate adenylyltransferase, chloroplastic glucose-6-phosphate isomerase 1, etc. In *Ceratopteris thalictroides*, proteins linked to photosynthesis were over-represented in hermaphrodite gametophytes compared to male ones induced by antheridiogens, which had smaller size (Chen et al., 2019).

Regarding the generation of precursor metabolites and energy annotations, several proteins of both aerobic or anaerobic paths, such as the citrate cycle (TCA cycle), oxidative phosporilation or glucolysis/gluconeogenesis, significantly increased in sexual gametophytes. Moreover, in these gametophytes the number of proteins upregulated in photosynthesis and antenna proteins was double that of the apogamous one, and they act on chromophore-linkage and assembly and repair of the photosystetic apparatus (PSBB, PSAB, LHCB5, LHCB3, LHCA3, VAR2, PSB27, TLP18.3, PORA, PORC). PORA, for instance, may function as a photoprotectant during the transitory stage from dark to light, and also in photomorphogenesis and throughout the plant life under specific light conditions (Paddock et al., 2012). There are also proteins associated with pigment biosynthetic processes, such as the magnesium-chelatases ALB1 and GUN5, which can

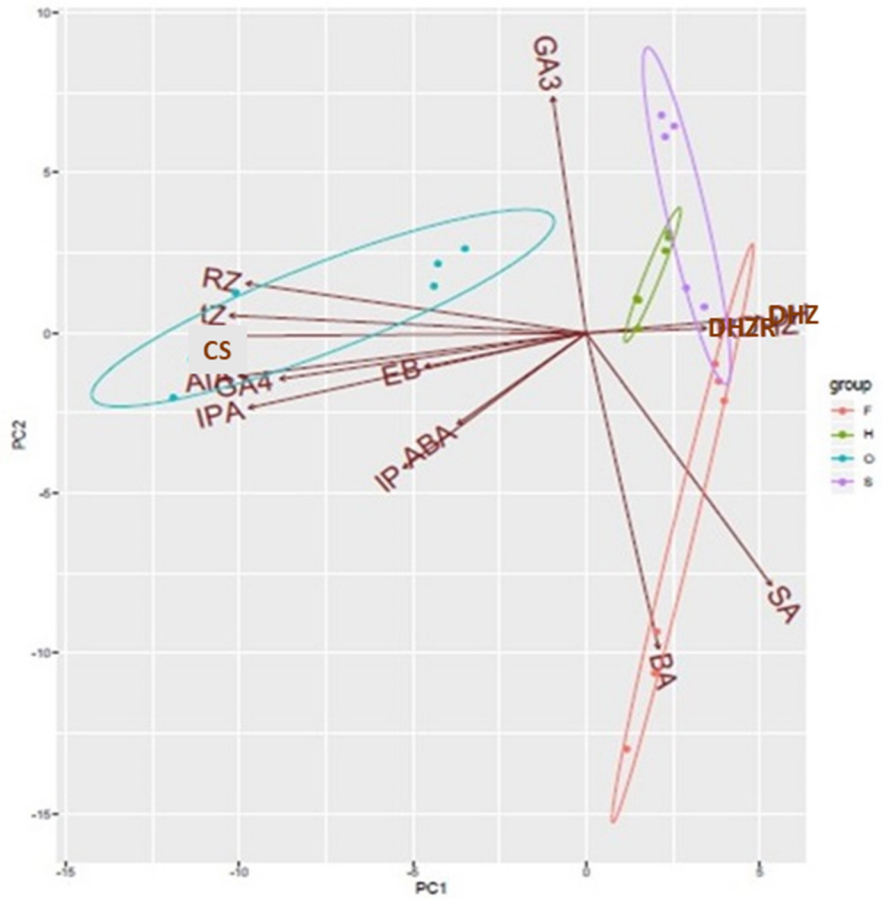

FIGURE 6 | PCA biplot showing the contribution of all variables to the variation in the endogenous content of phytohormones in filamentous (F), spatulate (S), and heart-shaped (H) gametophytes of the apogamous species *Dryopteris affinis,* and heart-shaped gametophytes (O) of its sexual relative *D. oreades*. Ellipses encircle group samples from the same origin. IAA, indol-3-acetic acid; BA, 6-benzylaminopurine; Z, trans-Zeatin; Zr, Zeatin riboside; DHZ, dihydrozeatin; DHZR, dihydrozeatin riboside; iP, isopentenyl adenine; iPR, isopentenyl adenosine; ABA, abscisic acid; SA, salicylic acid; GA_3, gibberellic acid; GA_4, gibberellin 4; BL, brassinolide; CS, castasterone.

have other functions as GUN5 acting in ABA signaling (Du S. Y. et al., 2012).

In our experiments, both sexual and apogamous gametophytes were cultured under similar conditions of light, photoperiod, humidity, nutrients, or pH. Although it was not scored, the growth rate of gametophytes was clearly slower in *D. oreades* than in *D. affinis*. However, final size of the sexual gametophyte was bigger than that of the apogamous one. In the gametophytes, although scarce, there are some data supporting differences in photochemical efficiency linked to sex gender, increasing in female individuals, which thus could provide more energy for the development of archegonia, fertilization and the further growth of sporophytes (Valledor et al., 2014; Slate et al., 2017; Chen et al., 2019). Our data suggest that the sexual gametophytes are more energy-demanding than the apogamous counterparts. We propose that the gametophyte of *D. affinis* devotes all resources to quickly grow and differentiate an embryo, while the female gametophytes have to attain a more complex organization level, building a decisive central area, the archegonium cushion, a several cell layers thick which is the place where the archegonia and future embryo will develop. At first glance, the larger and more complex sexual gametophyte could thus demand more energy than the smaller and fast-growing apogamous gametophytes.

The lipid metabolism seems especially important in the sexual gametophytes, upregulating proteins involved in linoleic acid metabolism such as the lipoxygenases LOX1 and LOX 3, as well as the peroxisomal fatty acid beta-oxidation multifunctional protein MFP2. These proteins are linked to functions such as growth and development, pest resistance, senescence or responses to wounding (Vellosillo et al., 2007), and in the tree fern *C. delgadii*, key enzymes in fatty acid biosynthesis were told to have an important role during embryogenesis (Domzalska et al., 2017).

Other proteins found in the sexual gametophyte are related to different aspects of reproduction, such as embryo

defective 1579, involved in embryo development ending in seed dormancy, several LEA proteins such as LEA4-1 or ECP63, which may be linked to the BHLH109-mediated regulation of somatic embryogenesis (Nowak and Gaj, 2016), and Villin-2, a Ca(2+)-a regulated actin-binding protein, required for the construction of actin collars in pollen tubes (van der Honing et al., 2012; Qu et al., 2013). In addition, NAP1-related protein 2 acts as histone H2A/H2B chaperone in nucleosome assembly, being essential, together NRP1, for the maintenance of cell proliferation and differentiation in postembryonic root growth, and for intramolecular and intermolecular somatic homologous recombination (Zhu et al., 2006). Furthermore, we annotated two interesting proteins: an ADP-ribosylation factor-like protein, member of ARF GTPase family partaking in cell division, expansion, and cellulose production; and the monocopper oxidase-like protein SKU5, a GPI-anchor protein involved in directed root tip growth (Sedbrook et al., 2002).

Other interesting protein is a flavone 3'-Omethyltransferase, involved in melatonin biosynthesis (Byeon et al., 2014), and the protein glutamate decarboxylase 1, which catalysis the production of GABA (Bouché et al., 2004). Finally, it deserves to mention the protein FIB2, a S-adenosyl-L-methionine-dependent methyltransferase, which has been speculated to be involved on methylation of RNAs and proteins, including histones, having an important role on defense against bacterial pathogens (Seo et al., 2019).

Phytohormones: Hormonal Content and Protein Regulation

Information acquired so far about the physiology and molecular events operating inside this free-leaving fern generation is scarce. As far as we know, the present study represents the first assessment of a large number of phytohormones in fern gametophytes, and shows changes in phytohormone profiles related to reproductive systems in non-model species.

The presence of SA at higher levels in the filamentous apogamous gametophytes could be related to a stressful environment as could be *in vitro* culture itself, especially at the beginning of gametophyte development (Kosakivska et al., 2019; Wyder et al., 2020). SA influences a wide range of processes, including seedling establishment and responses to abiotic and biotic stresses (Vlot et al., 2009), being one of the first features in plant-microbe interactions that is present in basal-branching algae (Pieterse et al., 2012; Hori et al., 2014). Although this phytohormone showed higher levels at the filamentous stage, the proteomic data point out an important presence of its metabolic pathways along the whole gametophyte development, as shown later.

Although very simple morphologically, gametophytes go through successive developmental changes until sexual maturity. An early crucial event in the formation of the two-dimensional gametophyte involves the re-orientation of cell plate, from a transverse to a longitudinal alignment (Nayar and Kaur, 1971; Banks, 1999; Racusen, 2002). Our results suggest a possible connection between the cytokinin BA and the filamentous morphology, and between GA_3 and the spatulate shape. Cytokinins might affect the rate and pattern of cell division, cell elongation and cell differentiation in ferns (Romanov, 2009). Although gametophytes of *B. spicant* and *Osmunda regalis* became shorter, widened and lacking meristem in response to cytokinins (Menéndez et al., 2006a; Greer et al., 2012), these phytohormones induced transition from one- to two-dimensional growth in *C. richardii* (Spiro et al., 2004). The increase of GA_3 in our spatulate gametophytes is consistent with previous data with other sexual and apogamous fern species such as *B. spicant*, *Anemia phillitidis*, and *Polystichum aculeatum* (Kazmierczak, 2003; Menéndez et al., 2006b,c, 2009; Kosakivska et al., 2020).

The levels of IAA, Z, ZR, iPR, the gibberellin GA_4, the brassinosteoid castasterone and ABA were higher in sexual cordate gametophytes than in the apogamous cordate ones. The primary role of zeatin riboside in reproductive processes has been stated in ferns (Abul et al., 2010; Vedenecheva and Sytnik, 2013; Vedenicheva and Kosakivska, 2016, 2018). In the last case, zeatin and seatin riboside levels increased in the sporophyte of the fern *D. filix-mas* when sporulation happens, while zeatin and zeatin riboside content became higher during intensive vegetative growth in *P. acculeatum*. Recently, an increase of IAA, ZR, iP, iPR, GA_3 and ABA in the cordate gametophyte of *P. aculeatum* has been documented by the same authors (Kosakivska et al., 2020), pointing out a key role of these phytohormones in the regulation of growth and development of the cushion. The iP bases cytokinins are characteristic of mosses and ferns, being more difficult to be detected zeatin derivatives (Johri, 2008). Additionally, in cordate gametophytes of *D. filix-mas* an increase in the IAA and Z, at the formation of both sexual organs, archegonia and antheridia, has been reported (Kosakivska et al., 2019). These authors concluded also that GA_3 was dominant at all stages of gametophyte development, reaching the highest content during the development of the sexual organs. The gibberellin GA_4 prevails over GA_3 either in apogamic or sexual development, being especially high in the latter. Previously, high levels of GA_4 and GA_7 were assessed in *D. affinis*, as an apogamous embryo evolved (Menéndez et al., 2006c), and in gametophytes governed by an antheridiogen system, GA_4 has been associated with the induction of antheridia, and also with contributing to the genetic exchange (Tanaka et al., 2014). The accumulation of GA_4 in the cordate sexual gametophytes of *D. oreades* suggests a wider role on gametophyte development not yet dilucidated by the gibberellins.

The sexual gametophytes also had a noticeable increase in ABA. It has recently been reported that the origin of the core ABA signaling pathway in seed plants might lie in the sexual differentiation of ferns (McAdam et al., 2016). In female gametophytes of *D. oreades*, a possible connection of ABA with their antheridiogen-release capacity could be to protect themselves against the activity of these pheromone, preserving the female condition (Hickok, 1983; Banks et al., 1993). Regarding the active brassinosteroids analyzed, both BL and CS were detected. Many processes have been linked with brassinosteroids function such as

cell elongation, cell division, reproductive and vascular development, stress responses, or senescence, but information about their role on ferns is scarce (Gómez-Garay et al., 2018). Interestingly, the amount of CS was high, pointing at some possible role of brassinosteroids on sexual development of gametophytes in *D. oreades*. Moreover, CS was identified in most of the ferns studied by Yokota et al. (2017) but not BL.

As noted above, our proteomic analysis revealed a myriad of proteins related to the biosynthesis and/or function of the analyzed phytohormones, giving strong support to the important role of these regulators on gametophyte development. In the apogamous gametophyte, the histidine phosphotransfer protein AHP1, linked to cytokinin signaling was annotated (Hwang et al., 2002), and the protein, emb22 (also named Gurke or Pasticcino3), which is an acetyl-CoA carboxylase 1, related to cell proliferation and tissue patterning (Baud et al., 2003), embryo morphogenesis (Torres-Ruiz et al., 1996); or supressing cytokinin activity (Faure et al., 1998). Also the protein Cand1, required for SCF^{TIR} activity, participating in several resposes such as response to auxin (Cheng et al., 2004). In addition, there are proteins on defense or stress, such as prohibitin-3, required to regulate ethylene-mediated signaling, and nitric oxide (NO)-mediated responses (Van Aken et al., 2007; Wang et al., 2010).

On the other hand, sexual gametophytes overexpressed the plasma membrane-type ATPase 1, which has been suggested to be involved in brassinosteroid signaling (Ladwig et al., 2015); tryptophan synthase beta type 2 (TSBtype2), acting on the auxin biosynthesis (Zhao, 2014); proteins linked to the ABA response, such as those of NAD(P)-binding Rossmann-fold superfamily proteins (Ghelis et al., 2008); to polyamines or proline as arginase/deacetylase (Patel et al., 2017), whose over-expression decreases susceptibility to the fungal pathogen *Botrytis cinerea* (Brauc et al., 2012). We also found Nudix hydrolase homolog 8, which may act on SA signaling (Fonseca and Dong, 2014).

Another interesting protein is a transcriptional activator belonging to RNA-binding (RRM/RBD/RNP motifs) family protein, antagonist and promoter of polycomb LHP1 gene regulation activity, to regulate the transcription of stress-responsive and flowering genes (Latrasse et al., 2011). Besides, it may function as a suppressor of cell-autonomous immune responses involving glucosinolates, SA, and JA pathways toward pathogenic bacteria and fungi (Le Roux et al., 2014). Finally, glutathione S-transferase TAU 20 is another protein upregulated in the sexual gametophyte, involved in the regulation of far-red light influence on development as a regulator of the interplay between light and JA signaling (Chen et al., 2007, 2017) and playing a role in gravitropic signal transduction (Schenck et al., 2013).

Conclusions

Qualitative and quantitative differences in protein and phytohormone profiles between apogamous and sexual gametophytes are reported. Our results indicate that phytohormone contents vary either between cordate apogamous gametophytes and their sexual counterpart. Our main conclusions were: (1) Seven out of fourteen phytohormones accumulated more in the sexual (female) gametophyte, especially auxin IAA, the cytokinins Z, ZR, iPR, the active gibberellin GA_4, and the active brassinosteoids CS. (2) The proteins upregulated in the apogamous species are associated with the primary metabolism of aminoacids, peptides and proteins (including folding, transport and proteolysis), nucleic acids and cofactors, nitrogen metabolism, ribosome biogenesis, translation and gene expression and stress response. (3) The sexual counterpart accumulated more proteins coping with starch and sucrose metabolism, generation of energy and photosynthesis, lipid oxidation and response to hormones. Asexual vs. sexual gametophyte involves two different metabolic scenarios, with apogamous reproduction more connected to stress responses while sexual reproduction is more resource demanding.

DATA AVAILABILITY STATEMENT

The datasets presented in this study can be found in online repositories. The names of the repository/repositories and accession number(s) can be found in the article/**Supplementary Material**.

AUTHOR CONTRIBUTIONS

HF and UG: conceive the project. HF, AR, and MC: *in vitro* culture of ferns and sampling. LQ: supplied plant material. AR and VQ: statistical analyses. JG: performed bioinformatics. VG: protein extraction and purification. IF and LR: phytohormones analyses. All authors discussed the results and contributed to the final manuscript.

FUNDING

This work was supported by the University of Zurich and Project PRIME-XS-0002520 funded by the European Union's 7th Framework Program.

ACKNOWLEDGMENTS

We thank the University of Oviedo for a grant from International Mobility of Research Staff, accordingly to the collaboration agreement CESSTT1819 and the Functional Genomics Center Zurich for access to its infrastructure.

SUPPLEMENTARY MATERIAL

The Supplementary Material for this article can be found online at: https://www.frontiersin.org/articles/10.3389/fpls.2021.718932/full#supplementary-material

REFERENCES

Abul, Y., Menéndez, V., Gómez-Campo, C., Revilla, M. A., Lafont, F., et al. (2010). Occurence of plant growth regulators in Psilotum nudum. *J. Plant Physiol.* 167, 1211–1213. doi: 10.1016/j.jplph.2010.03.015

Amaki, W., and Higuchi, H. (1992). A possible propagation system of Nephrolepis, Asplenium, Pteris, Adiantum and Rumohra (Arachniodes) through tissue culture. *Acta Hortic.* 300, 237–244. doi: 10.17660/ActaHortic.1992.300.33

Asker, S. E., and Jerling, L. (1992). *Apomixis in Plants*. Boca Ratón,FL : CRC Press.

Atallah, N. M., Vitek, O., Gaiti, F., Tanurdzic, M., and Banks, J. A. (2018). Sex determination in Ceratopteris richardii is accompanied by transcriptome changes that drive epigenetic reprogramming of the young gametophyte. *Genes Genomes Genetics* 8, 2205–2214. doi: 10.1534/g3.118.200292

Aya, K., Kobayashi, M., Tanaka, J., Ohyanagi, H., Suzuki, T., et al. (2015). De novo transcriptome assembly of a fern, Lygodium japonicum, and a web resource database, Ljtrans DB. *Plant Cell Physiol.* 56:e5. doi: 10.1093/pcp/pcu184

Baerenfaller, K., Grossmann, J., Grobei, M. A., Hull, R., Hirsch-Hoffmann, M., et al. (2008). Genome-scale proteomics reveals *Arabidopsis thaliana* gene models and proteome dynamics. *Science* 320, 938–941. doi: 10.1126/science.1157956

Bai, Y., Du, F., and Liu, H. (2010). Determination strategies of phytohormones: recent advances. *Anal. Methods* 2, 1867–1873. doi: 10.1039/c0ay00471e

Banks, J. A. (1999). Gametophyte development in ferns. *Annu. Rev. Plant Physiol. Plant Mol. Biol.* 50, 163–183. doi: 10.1146/annurev.arplant.50.1.163

Banks, J. A., Hickok, L. G., and Webb, M. A. (1993). The programming of sexual phenotype in the homosporous fern Ceratopteris richardii. *Int. J. Plant Sci.* 154, 522–534. doi: 10.1086/297135

Barcaccia, G., and Albertini, E. (2013). Apomixis in plant reproduction: a novel perspective on an old dilemma. *Plant Reprod.* 26, 159–179. doi: 10.1007/s00497-013-0222-y

Barker, M. S., and Wolf, P. G. (2010). Unfurling fern biology in the genomics age. *Bioscience* 60, 177–185. doi: 10.1525/bio.2010.60.3.4

Baud, S., Guyon, V., Kronenberger, J., Wuillème, S., Miquel, M., et al. (2003). Multifunctional acetyl-CoA carboxylase 1 is essential for very long chain fatty acid elongation and embryo development in Arabidopsis. *Plant J. Cell Mol. Biol.* 33, 75–86. doi: 10.1046/j.1365-313X.2003.016010.x

Benstein, R. M., Ludewig, K., Wulfert, S., Wittek, S., Gigolashvili, T., et al. (2013). Arabidopsis phosphoglycerate dehydrogenase1 of the phosphoserine pathway is essential for development and required for ammonium assimilation and tryptophan biosynthesis. *Plant Cell* 25, 5011–5029. doi: 10.1105/tpc.113.118992

Bhatnagar, N., and Pandey, S. (2020). Heterotrimeric G-protein interactions are conserved despite regulatory element loss in some plants. *Plant Physiol.* 22:01309. doi: 10.1104/pp.20.01309

Bouché, N., Fait, A., Zik, M., and Fromm, H. (2004). The root-specific glutamate decarboxylase (GAD1) is essential for sustaining GABA levels in Arabidopsis. *Plant Mol. Biol.* 55, 315–325. doi: 10.1007/s11103-004-0650-z

Brauc, S., De Vooght, E., Claeys, M., Geuns, J. M. C., Höfte, M., and Angenon, G. (2012). Overexpression of arginase in Arabidopsis thaliana influences defence responses against Botrytis cinerea. *Plant Biol.* 14, 39–45. doi: 10.1111/j.1438-8677.2011.00520.x

Bui, L. T., Pandzic, D., Youngstrom, C. E., Wallace, S., Irish, E. E., Szövényi, P., et al. (2017). A fern AINTEGUMENTA gene mirrors BABY BOOM in promoting apogamy in Ceratopteris richardii. *Plant J.* 90, 122–132. doi: 10.1111/tpj.13479

Byeon, Y., Lee, H. Y., Lee, K., and Back, K. (2014). Caffeic acid *O* -methyltransferase is involved in the synthesis of melatonin by methylating *N* -acetylserotonin in *Arabidopsis*. *J. Pineal Res.* 57, 219–227. doi: 10.1111/jpi.12160

Chen, C. Y., Ho, S. S., Kuo, T. Y., Hsieh, H. L., and Cheng, Y. S. (2017). Structural basis of jasmonate-amido synthetase FIN219 in complex with glutathione S-transferase FIP1 during the JA signal regulation. *Proc. Natl. Acad. Sci. U.S.A.* 114, E1815–E1824. doi: 10.1073/pnas.1609980114

Chen, I. C., Huang, I. C., Liu, M. J., Wang, Z. G., Chung, S. S., and Hsieh, H. L. (2007). Glutathione S-transferase interacting with far-red insensitive 219 is involved in phytochrome A-mediated signaling in arabidopsis. *Plant Physiol.* 143, 1189–1202. doi: 10.1104/pp.106.094185

Chen, X., Chen, Z., Huang, W., Fu, H., Wang, Q., Wang, Y., et al. (2019). Proteomic analysis of gametophytic sex expression in the fern Ceratopteris thalictroides. *PLoS ONE* 14:e0221470. doi: 10.1371/journal.pone.0221470

Cheng, Y., Dai, X., and Zhao, Y. (2004). AtCAND1, a Heat-repeat protein that participates in auxin signaling in Arabidopsis. *Plant Physiol.* 135, 1020–1026. doi: 10.1104/pp.104.044495

Chong, L. P., Wang, Y., Gad, N., Anderson, N., Shah, B., and Zhao, R. (2015). A highly charged region in the middle domain of plant endoplasmic reticulum (ER)-localized heat-shock protein 90 is required for resistance to tunicamycin or high calcium-induced ER stresses. *J. Exp. Bot.* 66, 113–124. doi: 10.1093/jxb/eru403

Choudhary, S. P., Yu, J. Q., Yamaguchi-Shinozaki, K., Shinozaki, K., and Tran, L. S. P. (2012). Benefits of brassinosteroid crosstalk. *Trends Plant Sci.* 17, 594–605. doi: 10.1016/j.tplants.2012.05.012

Cordle, A., Irish, E., and Cheng, C.l., L. (2012). Gene expression associated with apogamy commitment in Ceratopteris richardii. *Sex. Plant Reprod.* 25, 293–304. doi: 10.1007/s00497-012-0198-z

de Vries, S., de Vries, J., Teschke, H., von Dahlen, J. K., Rose, L. E., and Gould, S. B. (2018). Jasmonic and salicylic acid response in the fern Azolla filiculoides and its cyanobiont. *Plant Cell Environ.* 41, 2530–2548. doi: 10.1111/pce.13131

Delatorre, C., Rodríguez, A., Rodríguez, L., Majada, J. P., Ordás, R. J., and Feito, I. (2017). Hormonal profiling: Development of a simple method to extract and quantify phytohormones in complex matrices by UHPLC–MS/MS. *J. Chromatogr. B Analyt. Technol. Biomed. Life Sci.* 1040, 239–249. doi: 10.1016/j.jchromb.2016.11.007

Der, J. P., Barker, M. S., Wickett, N. J., dePamphilis, C. W., and Wolf, P. G. (2011). *De novo* characterization of the gametophyte transcriptome in bracken fern, Pteridium aquilinum. *BMC Genomics* 12:99. doi: 10.1186/1471-2164-12-99

Dobrev, P., Kamínek, M., Ivanov Dobrev, P., Kamínek, M., Dobrev, P., and Kamínek, M. (2002). Fast and efficient separation of cytokinins from auxin and abscisic acid and their purification using mixed-mode solid-phase extraction. *J. Chromatogr. A* 950, 21–29. doi: 10.1016/S0021-9673(02)00024-9

Domzalska, L., Kedracka-Krok, S., Jankowska, U., Grzyb, M., Sobczak, M., Rybczyński, J. J., et al. (2017). Proteomic analysis of stipe explants reveals differentially expressed proteins involved in early direct somatic embryogenesis of the tree fern Cyathea delgadii Sternb. *Plant Sci.* 258, 61–76. doi: 10.1016/j.plantsci.2017.01.017

Du, F., Ruan, G., and Liu, H. (2012). Analytical methods for tracing plant hormones. *Anal. Bioanal. Chem.* 403, 55–74. doi: 10.1007/s00216-011-5623-x

Du, S. Y., Zhang, X. F., Lu, Z., Xin, Q., Wu, Z., et al. (2012). Roles of the different components of magnesium chelatase in abscisic acid signal transduction. *Plant Mol. Biol.* 80, 519–537. doi: 10.1007/s11103-012-9965-3

Dyer, R. J., Savolainen, V., and Schneider, H. (2012). Apomixis and reticulate evolution in the Asplenium monanthes fern complex. *Ann. Bot.* 110, 1515–1529. doi: 10.1093/aob/mcs202

Ekrt, L., and Koutecký, P. (2016). Between sexual and apomictic: Unexpectedly variable sporogenesis and production of viable polyhaploids in the pentaploid fern of the Dryopteris affinis agg. (Dryopteridaceae). *Ann. Bot.* 117, 97–106. doi: 10.1093/aob/mcv152

Falk, S., Ravaud, S., Koch, J., and Sinning, I. (2010). The C terminus of the Alb3 membrane insertase recruits cpSRP43 to the thylakoid membrane. *J. Biol. Chem.* 285, 5954–5962. doi: 10.1074/jbc.M109.084996

Falk, S., and Sinning, I. (2010). cpSRP43 is a novel chaperone specific for light-harvesting chlorophyll a,b-binding proteins. *J. Biol. Chem.* 285, 21655–21661. doi: 10.1074/jbc.C110.132746

Faure, J. D., Vittorioso, P., Santoni, V., Fraisier, V., Prinsen, E., et al. (1998). The PASTICCINO genes of Arabidopsis thaliana are involved in the control of cell division and differentiation. *Development* 125, 909–918. doi: 10.1242/dev.125.5.909

Fernández, H., and Revilla, M. A. (2003). *In vitro* culture of ornamental ferns. *Plant Cell Tissue Organ Cult.* 73, 1–13. doi: 10.1023/A:1022650701341

Fleurdépine, S., Deragon, J. M., Devic, M., Guilleminot, J., and Bousquet-Antonelli, C. (2007). A bona fide La protein is required for embryogenesis in *Arabidopsis thaliana*. *Nucleic Acids Res.* 35, 3306–3321. doi: 10.1093/nar/gkm200

Fonseca, J. P., and Dong, X. (2014). Functional characterization of a Nudix Hydrolase AtNUDX8 upon pathogen attack indicates a positive role in plant immune responses. *PLoS ONE* 9:e114119. doi: 10.1371/journal.pone.0114119

Fraser-Jenkins, C. R. (1980). *Dryopteris Affinis: A New Treatment for a Complex Species in the European Pteridophyte Flora (Vol. 10)*. Berlin: Botanischer Garten und Botanisches Museum.

Fu, Q., and Chen, L. Q. (2019). Comparative transcriptome analysis of two reproductive modes in Adiantum reniforme var. sinense targeted to explore possible mechanism of apogamy. *BMC Genet.* 20:55. doi: 10.1186/s12863-019-0762-8

Ghelis, T., Bolbach, G., Clodic, G., Habricot, Y., Miginiac, E., Sotta, B., et al. (2008). Protein tyrosine kinases and protein tyrosine phosphatases are involved in

abscisic acid-dependent processes in Arabidopsis seeds and suspension cells. *Plant Physiol.* 148, 1668–1680. doi: 10.1104/pp.108.124594

Gómez-Garay, A., Gabriel y Galán, J. M., Cabezuelo, A., Pintos, B., Prada, C., and Martín, L. (2018). "Ecological significance of brassinosteroids in three temperate ferns," in *Current Advances in Fern Research*, ed H. Fernández (New York, NY: Springer International Publishing), 1–544.

Greer, G. K., Dietrich, M. A., Devol, J. A., Rebert, A., American, S., et al. (2012). The effects of exogenous cytokinin on the morphology and gender expression of Osmunda regalis gametophytes. *Amer. Fern J.* 102, 32–46. doi: 10.1640/0002-8444-102.1.32

Grimanelli, D., García, M., Kaszas, E., Perotti, E., and Leblanc, O. (2003). Heterochronic expression of sexual reproductive programs during apomictic development in Tripsacum. *Genetics* 165, 1521–1531. doi: 10.1093/genetics/165.3.1521

Grossmann, J., Fernández, H., Chaubey, P. M., Valdés, A. E., Gagliardini, V., et al. (2017). Proteogenomic analysis greatly expands the identification of proteins related to reproduction in the apogamous fern *Dryopteris affinis* ssp. affinis. *Front. Plant Sci.* 8:336. doi: 10.3389/fpls.2017.00336

Grossniklaus, U., Koltunow, A. M., and van Lookeren Campagne, M. (1998). A bright future for apomixis. *Trends Plant Sci.* 3, 415–416. doi: 10.1016/S1360-1385(98)01338-7

Grossniklaus, U., Nogler, G. A., and van Dijk, P. J., (2001). How to avoid sex: the genetic control of developmental aspects. *Plant Cell (July)* 13, 1491–1497. doi: 10.2307/3871381

Hammer, Ø. (2001). PAST: Paleontological statistics software package for education and data analysis. *Palaeontol. Electron.* 4:9. Available online at: http://palaeo-electronica.org/2001_1/past/issue1_01.htm

Hickok, L. G. (1983). Abscisic acid blocks antheridiogen-induced antheridium formation in gametophytes of the fern *Ceratopteris*. *Can. J. Bot.* 61, 888–892. doi: 10.1139/b83-098

Hicks, G. H. (1894). Nourishment of the Embryo and importance of the endosperm in viviparous mangrove plants. *Bot. Gazette* 19, 327–330. doi: 10.1086/327078

Hofmann, N. R. (2010). Apomixis and gene expression in Boechera. *Plant Cell* 22:539. doi: 10.1105/tpc.110.220312

Hori, K., Maruyama, F., Fujisawa, T., Togashi, T., Yamamoto, N., et al. (2014). Klebsormidium flaccidum genome reveals primary factors for plant terrestrial adaptation. *Nat. Commun.* 5, 2–6. doi: 10.1038/ncomms4978

Horváth, B. M., Magyar, Z., Zhang, Y., Hamburger, A. W., Bakó, L., et al. (2006). EBP1 regulates organ size through cell growth and proliferation in plants. *EMBO J.* 25, 4909–4920. doi: 10.1038/sj.emboj.7601362

Hwang, I., Chen, H. C., and Sheen, J. (2002). Two-component signal transduction pathways in Arabidopsis. *Plant Physiol.* 129, 500–515. doi: 10.1104/pp.005504

Ishiguro, S., Watanabe, Y., Ito, N., Nonaka, H., Takeda, N., et al. (2002). SHEPHERD is the Arabidopsis GRP94 responsible for the formation of functional CLAVATA proteins. *EMBO J.* 21, 898–908. doi: 10.1093/emboj/21.5.898

Johri, M. (2008). Hormonal regulation in green plant lineage families. *Physiol. Mol. Biol. Plants Int. J. Funct. Plant Biol.* 14, 23–38. doi: 10.1007/s12298-008-0003-5

Kazmierczak, A. (2003). Induction of cell division and cell expansion at the beginning of gibberellin A3-induced precocious antheridia formation in Anemia phyllitidis gametophytes. *Plant Sci.* 165, 933–939. doi: 10.1016/S0168-9452(03)00217-6

Kazmierczak, A. (2010). "Gibberellic acid and ethylene control male sex determination and development of anemia phyllititdis gametophytes," in *Working With Ferns. Issues and Applications*, eds H. Fernández, A. Kumar, and A Revilla (New York, NY: Springer), 49–65.

Koltunow, A. M., and Grossniklaus, U. (2003). Apomixis: a developmental perspective. *Annu. Rev. Plant Biol.* 54, 547–574. doi: 10.1146/annurev.arplant.54.110901.160842

Kosakivska, I. V., Romanenko, K., Voytenko, L., Vasyuk, V., Schcherbatiuk, M., and Babenko, L. (2019). Hormonal complex of gametophytes of Dryopteris filix-mass (Dryopteridaceae) *in vitro* culture. *Plant Physiol. Biochem. Cell Mol. Biol.* 76, 260–269. doi: 10.15407/ukrbotj76.03.260

Kosakivska, I. V., Vasyuk, V. A., Voytenko, L. V., Shcherbatiuk, M. M., Romanenko, K. O., and Babenko, L. M. (2020). Endogenous phytohormones of fern *Polystichum aculeatum* (L.) Roth gametophytes at different stages of morphogenesis *in vitro* culture. *Cytol. Genet.* 54, 23–30. doi: 10.3103/S0095452720010089

Kotake, T., Takada, S., Nakahigashi, K., Ohto, M., and Goto, K. (2003). Arabidopsis terminal Flower 2 gene encodes a heterochromatin protein 1 homolog and represses both FLOWERING LOCUS T to regulate flowering time and several floral homeotic genes. *Plant Cell Physiol.* 44, 555–564. doi: 10.1093/pcp/pcg091

Ladwig, F., Dahlke, R. I., Stührwohldt, N., Hartmann, J., Harter, K., and Sauter, M. (2015). Phytosulfokine regulates growth in arabidopsis through a response module at the plasma membrane that includes cyclic nucleotide-gated channel17, H+-ATPase, and BAK1. *Plant Cell* 27, 1718–1729. doi: 10.1105/tpc.15.00306

Latrasse, D., Germann, S., Houba-Hérin, N., Dubois, E., Bui-Prodhomme, D., et al. (2011). Control of flowering and cell fate by LIF2, an RNA binding partner of the polycomb complex component LHP1. *PLoS ONE* 6:e16592. doi: 10.1371/journal.pone.0016592

Le Roux, C., Del Prete, S., Boutet-Mercey, S., Perreau, F., Balagué, C., et al. (2014). The hnRNP-Q Protein LIF2 participates in the plant immune response. *PLoS ONE* 9:e99343. doi: 10.1371/journal.pone.0099343

Lee, S., Lee, D. W., Lee, Y., Mayer, U., Stierhof, Y. D., et al. (2009). Heat shock protein cognate 70-4 and an E3 ubiquitin ligase, CHIP, mediate plastid-destined precursor degradation through the ubiquitin-26S proteasome system in *Arabidopsis*. *Plant Cell* 21, 3984–4001. doi: 10.1105/tpc.109.071548

Liu, H.-M., Dyer, R. J. R. J., Guo, Z.-Y., Meng, Z., Li, J.-H., and Schneider, H. (2012). The evolutionary dynamics of apomixis in ferns: a case study from Polystichoid ferns. *J. Bot.* 2012, 1–11. doi: 10.1155/2012/510478

Lovis, J. D. (1978). Evolutionary patterns and processes in ferns. *Adv. Bot. Res.* 4, 229–415. doi: 10.1016/S0065-2296(08)60371-7

McAdam, S. A. M., Brodribb, T. J., Banks, J. A., Hedrich, R., Atallah, N. M., et al. (2016). Abscisic acid controlled sex before transpiration in vascular plants. *Proc. Natl. Acad. Sci. U.S.A.* 113, 12862–12867. doi: 10.1073/pnas.1606614113

Meinke, D. W. (2020). Genome-wide identification of EMBRYO-DEFECTIVE (EMB) genes required for growth and development in Arabidopsis. *New Phytol.* 226, 306–325. doi: 10.1111/nph.16071

Menéndez, V., Abul, Y., Bohanec, B., Lafont, F., and Fernández, H. (2011). The effect of exogenous and endogenous phytohormones on the in vitro development of gametophyte and sporophyte in Asplenium nidus L. *Acta Physiol. Plant.* 33, 2493–2500. doi: 10.1007/s11738-011-0794-9

Menéndez, V., Revilla, M. A., Bernard, P., Gotor, V., and Fernández, H. (2006a). Gibberellins and antheridiogen on sex in Blechnum spicant L. *Plant Cell Rep.* 25:1104. doi: 10.1007/s00299-006-0149-y

Menéndez, V., Revilla, M. A., Fal, M. A., and Fernández, H. (2009). The effect of cytokinins on growth and sexual organ development in the gametophyte of Blechnum spicant L. *Plant Cell Tissue Organ Cult.* 96, 245–250. doi: 10.1007/s11240-008-9481-y

Menéndez, V., Revilla, M. A., and Fernández, H. (2006b). Growth and gender in the gametophyte of Blechnum spicant L. *Plant Cell Tissue Organ Cult.* 86, 47–53. doi: 10.1007/s11240-006-9095-1

Menéndez, V., Villacorta, N. F., Revilla, M. A., Gotor, V., Bernard, P., and Fernández, H. (2006c). Exogenous and endogenous growth regulators on apogamy in *Dryopteris affinis* (Lowe) Fraser-Jenkins sp. affinis. *Plant Cell Rep.* 25, 85–91. doi: 10.1007/s00299-005-0041-1

Moin, M., Bakshi, A., Saha, A., Dutta, M., Madhav, S. M., and Kirti, P. B. (2016). Rice ribosomal protein large subunit genes and their spatio-temporal and tress regulation. *Front. Plant Sci.* 7:1284. doi: 10.3389/fpls.2016.01284

Murashige, T., and Skoog, F. (1962). A revised medium for rapid growth and bioassays with tobacco tissue cultures. *Plant Physiol.* 15, 473–497. doi: 10.1111/j.1399-3054.1962.tb08052.x

Nayar, B. K., and Kaur, S. (1971). Gametophytes of homosporous ferns. *Bot. Rev.* 37, 295–396. doi: 10.1007/BF02859157

Nowak, K., and Gaj, M. D. (2016). Stress-related function of bHLH109 in somatic embryo induction in Arabidopsis. *J. Plant Physiol.* 193, 119–126. doi: 10.1016/j.jplph.2016.02.012

Paddock, T., Lima, D., Mason, M. E., Apel, K., and Armstrong, G. A. (2012). Arabidopsis light-dependent protochlorophyllide oxidoreductase A (PORA) is essential for normal plant growth and development. *Plant Mol. Biol.* 78, 447–460. doi: 10.1007/s11103-012-9873-6

Pan, X., Welti, R., and Wang, X. (2008). Simultaneous quantification of major phytohormones and related compounds in crude plant extracts by liquid chromatography-electrospray tandem mass spectrometry. *Phytochemistry* 69, 1773–1781. doi: 10.1016/j.phytochem.2008.02.008

Pan, X., Welti, R., and Wang, X. (2010). Quantitative analysis of major plant hormones in crude plant extracts by high-performance liquid chromatography-mass spectrometry. *Nat. Protoc.* 5, 986–992. doi: 10.1038/nprot.2010.37

Patel, J., Ariyaratne, M., Ahmed, S., Ge, L., Phuntumart, V., Kalinoski, A., et al. (2017). Dual functioning of plant arginases provides a third route for putrescine synthesis. *Plant Sci.* 262, 62–73. doi: 10.1016/j.plantsci.2017.05.011

Pieterse, C. M. J., Van der Does, D., Zamioudis, C., Leon-Reyes, A., and Van Wees, S. C. M. (2012). Hormonal modulation of plant immunity. *Annu. Rev. Cell Dev. Biol.* 28, 489–521. doi: 10.1146/annurev-cellbio-092910-154055

Poethig, R. S., Coe, E. H., and Johri, M. M. (1986). Cell lineage patterns in maize embryogenesis: a clonal analysis. *Dev. Biol.* 117, 392–404. doi: 10.1016/0012-1606(86)90308-8

Porfírio, S., Gomes da Silva, M. D. R., Peixe, A., Cabrita, M. J., and Azadi, P. (2016). Current analytical methods for plant auxin quantification–a review. *Anal. Chim. Acta* 902, 8–21. doi: 10.1016/j.aca.2015.10.035

Preuss, S. B., Costa-Nunes, P., Tucker, S., Pontes, O., Lawrence, R. J., et al. (2008). Multimegabase silencing in nucleolar dominance involves siRNA-directed DNA methylation and specific methylcytosine-binding proteins. *Mol. Cell* 32, 673–684. doi: 10.1016/j.molcel.2008.11.009

Qin, Y., Leydon, A. R., Manziello, A., Pandey, R., Mount, D., et al. (2009). Penetration of the stigma and style elicits a novel transcriptome in pollen tubes, pointing to genes critical for growth in a pistil. *PLoS Genet.* 5:e1000621. doi: 10.1371/journal.pgen.1000621

Qu, X., Zhang, H., Xie, Y., Wang, J., Chen, N., and Huang, S. (2013). Arabidopsis villins promote actin turnover at pollen tube tips and facilitate the construction of actin collars. *Plant Cell* 25, 1803–1817. doi: 10.1105/tpc.113.110940

Racusen, R. H. (2002). Early development in fern gametophytes: Interpreting the transition to prothallial architecture in terms of coordinated photosynthate production and osmotic ion uptake. *Ann. Bot.* 89, 227–240. doi: 10.1093/aob/mcf032

Rademacher, W. (2000). Growth retardants: effects on gibberellin biosynthesis and other metabolic pathways. *Annu. Rev. Plant Physiol. Plant Mol. Biol.* 51, 501–531. doi: 10.1146/annurev.arplant.51.1.501

Romanov, G. A. (2009). How do cytokinins affect the cell? *Russian J. Plant Physiol.* 56, 268–290. doi: 10.1134/S1021443709020174

Ross, J. J., and Reid, J. B. (2010). Evolution of growth-promoting plant hormones. *Funct. Plant Biol.* 37, 795–805. doi: 10.1071/FP10063

Rybczynski, J. J., Tomiczak, K., Grzyb, M., and Mikula, A. (2018). "Morphogenic events in ferns: single and multicellular explants *in vitro*," in *Current Advances in Fern Research*, ed H. Fernández (New York, NY: Springer International Publishing), 99–120.

Salmi, M. L., and Bushart, T. J., R. S. (2010). "Cellular, molecular, and genetic changes during the development of ceratopteris richardii gametophytes," in *Working With Ferns. Issues and Applications*, eds H. Fernández, A. Kumar, and A. Revilla (New York, NY: Springer), 11–24.

Sánchez-Morán, E., Jones, G. H., Franklin, F. C. H., and Santos, J. L. (2004). A puromycin-sensitive aminopeptidase is essential for meiosis in *Arabidopsis thaliana*. *Plant Cell* 16, 2895–2909. doi: 10.1105/tpc.104.024992

Schenck, C. A., Nadella, V., Clay, S. L., Lindner, J., Abrams, Z., and Wyatt, S. E. (2013). A proteomics approach identifies novel proteins involved in gravitropic signal transduction. *Am. J. Bot.* 100, 194–202. doi: 10.3732/ajb.1200339

Schmidt, A. (2020). Controlling apomixis: shared features and distinct characteristics of gene regulation. *Genes* 11:329. doi: 10.3390/genes11030329

Schmidt, A., Wuest, S. E., Vijverberg, K., Baroux, C., Kleen, D., and Grossniklaus, U. (2011). Transcriptome analysis of the arabidopsis megaspore mother cell uncovers the importance of RNA helicases for plant germline development. *PLoS Biol.* 9:1001155. doi: 10.1371/journal.pbio.1001155

Sedbrook, J. C., Carroll, K. L., Hung, K. F., Masson, P. H., and Somerville, C. R. (2002). The Arabidopsis SKU5 gene encodes an extracellular glycosyl phosphatidylinositol-anchored glycoprotein involved in directional root growth. *Plant Cell* 14, 1635–1648. doi: 10.1105/tpc.002360

Seo, J. S., Diloknawarit, P., Park, B. S., and Chua, N. H. (2019). Elf18-induced long noncoding RNA 1 evicts fibrillarin from mediator subunit to enhance PATHOGENESIS-RELATED GENE 1 (PR1) expression. *New Phytol.* 221, 2067–2079. doi: 10.1111/nph.15530

Sheffield, E., Laird, S., and Bell, P. (1983). Ultrastructural aspects of sporogenesis in the apogamous fern Dryopteris borreri. *J. Cell Sci.* 63, 125–134. doi: 10.1242/jcs.63.1.125

Silveira, É. D., Guimarães, L. A., de Dusi, D. M. A., da Silva, F. R., Martins, N. F., et al. (2012). Expressed sequence-tag analysis of ovaries of Brachiaria brizantha reveals genes associated with the early steps of embryo sac differentiation of apomictic plants. *Plant Cell Rep.* 31, 403–416. doi: 10.1007/s00299-011-1175-y

Singh, A. P., and Johari, D. (2018). "Scope of ferns in horticulture and economic development," in *Current Advances in Fern Research*, ed H. Fernández (New York, NY: Springer International Publishing), 153–175.

Slate, M. L., Rosenstiel, T. N., and Eppley, S. M. (2017). Sex-specific morphological and physiological differences in the moss Ceratodon purpureus (Dicranales). *Ann. Bot.* 120, 845–854. doi: 10.1093/aob/mcx071

Somer, M., Arbes,ú, R., Menéndez, V., Revilla, M. A., and Fernández, H. (2010). Sporophyte induction studies in ferns in vitro. *Euphytica* 171, 203–210. doi: 10.1007/s10681-009-0018-1

Spiro, M. D., Torabi, B., and Cornell, C. N. (2004). Cytokinins induce photomorphogenic development in dark-grown gametophytes of Ceratopteris richardii. *Plant Cell Physiol.* 45, 1252–1260. doi: 10.1093/pcp/pch146

Sun, Y., Fan, X. Y., Cao, D. M., Tang, W., He, K., Zhu, J. Y., et al. (2010). Integration of brassinosteroid signal transduction with the transcription network for plant growth regulation in Arabidopsis. *Dev. Cell* 19, 765–777. doi: 10.1016/j.devcel.2010.10.010

Tanaka, J., Yano, K., Aya, K., Hirano, K., Takehara, S., et al. (2014). Antheridiogen determines sex in ferns via a spatiotemporally split gibberellin synthesis pathway. *Science* 346, 469–473. doi: 10.1126/science.1259923

Team, Rs (2016). *RStudio: Integrated Development for R*. Boston, MA: RStudio.

Torres-Ruiz, R. A., Lohner, A., and Jurgens, G. (1996). The GURKE gene is required for normal organization of the apical region in the Arabidopsis embryo. *Plant J.* 10, 1005–1016. doi: 10.1046/j.1365-313X.1996.10061005.x

Toujani, W., Muñoz-Bertomeu, J., Flores-Tornero, M., Rosa-Téllez, S., Anoman, A. D., et al. (2013). Functional characterization of the plastidial 3-phosphoglycerate dehydrogenase family in Arabidopsis. *Plant Physiol.* 163, 1164–1178. doi: 10.1104/pp.113.226720

Valledor, L., Menéndez, V., Canal, M. J., Revilla, M. A., and Fernández, H. (2014). Proteomic approaches to sexual development mediated by antheridiogen in the fern Blechnum spicant L. *Proteomics* 14, 1–11. doi: 10.1002/pmic.201300166

Van Aken, O., Pečenkov,á, T., van de Cotte, B., De Rycke, R., Eeckhout, D., et al. (2007). Mitochondrial type-I prohibitins of *Arabidopsis thaliana* are required for supporting proficient meristem development. *Plant J.* 52, 850–864. doi: 10.1111/j.1365-313X.2007.03276.x

van der Honing, H. S., Kieft, H., Emons, A. M. C., and Ketelaar, T. (2012). Arabidopsis VILLIN2 and VILLIN3 are required for the generation of thick actin filament bundles and for directional organ growth. *Plant Physiol.* 158, 1426–1438. doi: 10.1104/pp.111.192385

Vedenecheva, N. P., and Sytnik, K. M. (2013). Cytokinins localization and dynamics in different parts of Equisetum arvense L. *Dop. Nac. akad. nauk Ukr.* 11, 150–156.

Vedenicheva, N. P., and Kosakivska, I. V. (2016). Endogenous cytokinins of water fern Salvinia natans (Salviniaceae), Ukr. *Bot. J.* 72, 277–282. doi: 10.15407/ukrbotj73.03.277

Vedenicheva, N. P., and Kosakivska, I. V. (2018). Endogenous cytokinins dynamics during development of perennial fern *Dryopteris filix-mas* and *Polystichum aculeatum*. *Ukr. Bot. J.* 75, 384–391. doi: 10.15407/ukrbotj75.04.384

Vellosillo, T., Martínez, M., López, M. A., Vicente, J., Cascón, T., et al. (2007). Oxylipins produced by the 9-lipoxygenase pathway in Arabidopsis regulate lateral root development and defense responses through a specific signaling cascade. *Plant Cell* 19, 831–846. doi: 10.1105/tpc.106.046052

Vlot, A. C., Dempsey, D. A., and Klessig, D. F. (2009). Salicylic acid, a multifaceted hormone to combat disease. *Annu. Rev. Phytopathol.* 47, 177–206. doi: 10.1146/annurev.phyto.050908.135202

Vyskot, B., and Hobza, R. (2004). Gender in plants: sex chromosomes are emerging from the fog. *Trends Genet. Elsevier Curr. Trends* 20, 432–438. doi: 10.1016/j.tig.2004.06.006

Wang, Y., Ries, A., Wu, K., Yang, A., and Crawford, N. M. (2010). The Arabidopsis prohibitin gene phb3 functions in nitric oxide-mediated responses and in

hydrogenperoxide-induced nitric oxide accumulation. *Plant Cell* 22, 249–259. doi: 10.1105/tpc.109.072066

Ward, J., Ponnala, L., and Weber, C. (2012). Strategies for transcriptome analysis in nonmodel plants. *Am. J. Bot.* 99, 267–276. doi: 10.3732/ajb.1100334

Warne, T. R., and Hickok, L. G. (1989). Evidence for a gibberellin biosynthetic origin of Ceratopteris antheridiogen. *Plant Physiol.* 89, 535–538. doi: 10.1104/pp.89.2.535

Wyder, S., Rivera, A., Valdés, A. E., Jesús, M., Gagliardini, V., Fernández, H., et al. (2020). Plant physiology and biochemistry differential gene expression profiling of one- and two-dimensional apogamous gametophytes of the fern Dryopteris affinis ssp. affinis. *Plant Physiol. Biochem.* 148, 302–311. doi: 10.1016/j.plaphy.2020.01.021

Xu, L., and Shen, W. H. (2008). Polycomb silencing of KNOX genes confines shoot stem cell niches in Arabidopsis. *Curr. Biol.* 18, 1966–1971. doi: 10.1016/j.cub.2008.11.019

Yamane, H. (1998). Fern antheridiogens. *Int. Rev. Cytol.* 184, 1–6. doi: 10.1016/S0074-7696(08)62177-4

Yano, A., Kodama, Y., Koike, A., Shinya, T., Kim, H. J., et al. (2006). Interaction between methyl CpG-binding protein and Ran GTPase during cell division in tobacco cultured cells. *Ann. Bot.* 98, 1179–1187. doi: 10.1093/aob/mcl211

Yokota, T., Ohnishi, T., Shibata, K., Asahina, M., Nomura, T., et al. (2017). Occurrence of brassinosteroids in non-flowering land plants, liverwort, moss, lycophyte and fern. *Phytochemistry* 136, 46–55. doi: 10.1016/j.phytochem.2016.12.020

Yoshikawa, M., Peragine, A., Park, M. Y., and Poethig, R. S. (2005). A pathway for the biogenesis of trans-acting siRNAs in Arabidopsis. *Genes Dev.* 19, 2164–2175. doi: 10.1101/gad.1352605

Zhang, H., Ransom, C., Ludwig, P., and van Nocker, S. (2003). Genetic analysis of early flowering mutants in Arabidopsis defines a class of pleiotropic developmental regulator required for expression of the flowering-time switch flowering Locus C. *Genetics* 164, 347–358. doi: 10.1093/genetics/164.1.347

Zhao, Y. (2014). Auxin Biosynthesis. *Arabidopsis Book* 12:e0173. doi: 10.1199/tab.0173

Zhou, X., Liao, W.-J., Liao, J.-M., Liao, P., and Lu, H. (2015). Ribosomal proteins: functions beyond the ribosome. *J. Mol. Cell Biol.* 7, 92–104. doi: 10.1093/jmcb/mjv014

Zhu, Y., Dong, A., Meyer, D., Pichon, O., Renou, J. P., Cao, K., et al. (2006). Arabidopsis NRP1 and NRP2 encode histone chaperones and are required for maintaining postembryonic root growth. *Plant Cell* 18, 2879–2892. doi: 10.1105/tpc.106.046490

Conflict of Interest: The authors declare that the research was conducted in the absence of any commercial or financial relationships that could be construed as a potential conflict of interest.

Publisher's Note: All claims expressed in this article are solely those of the authors and do not necessarily represent those of their affiliated organizations, or those of the publisher, the editors and the reviewers. Any product that may be evaluated in this article, or claim that may be made by its manufacturer, is not guaranteed or endorsed by the publisher.

frontiers in Plant Science

ORIGINAL RESEARCH
published: 22 November 2021
doi: 10.3389/fpls.2021.751866

Global Transcriptome and Coexpression Network Analyses Reveal New Insights Into Somatic Embryogenesis in Hybrid Sweetgum (*Liquidambar styraciflua* × *Liquidambar formosana*)

Shuaizheng Qi[1†], Ruirui Zhao[1†], Jichen Yan[1], Yingming Fan[1], Chao Huang[1], Hongxuan Li[1], Siyuan Chen[1], Ting Zhang[1], Lisheng Kong[1,2], Jian Zhao[1] and Jinfeng Zhang[1*]*

[1] College of Biological Science and Biotechnology, Beijing Forestry University, Beijing, China, [2] Department of Biology, Centre for Forest Biology, University of Victoria, Victoria, BC, Canada

OPEN ACCESS

Edited by:
Víctor M. Loyola-Vargas, Scientific Research Center of Yucatán (CICY), Mexico

Reviewed by:
Tzvetanka D. Dinkova, National Autonomous University of Mexico, Mexico
Geovanny I. Nic-Can, Universidad Autónoma de Yucatán, Mexico

***Correspondence:**
Jian Zhao
zhaojian0703@bjfu.edu.cn
Jinfeng Zhang
zjf@bjfu.edu.cn

[†] These authors have contributed equally to this work and share first authorship

Specialty section:
This article was submitted to Plant Development and EvoDevo, a section of the journal Frontiers in Plant Science

Received: 02 August 2021
Accepted: 22 October 2021
Published: 22 November 2021

Citation:
Qi S, Zhao R, Yan J, Fan Y, Huang C, Li H, Chen S, Zhang T, Kong L, Zhao J and Zhang J (2021) Global Transcriptome and Coexpression Network Analyses Reveal New Insights Into Somatic Embryogenesis in Hybrid Sweetgum (Liquidambar styraciflua × Liquidambar formosana). Front. Plant Sci. 12:751866. doi: 10.3389/fpls.2021.751866

Somatic embryogenesis (SE) is a process of somatic cells that dedifferentiate to totipotent embryonic stem cells and generate embryos *in vitro*. Despite recent scientific headway in deciphering the difficulties of somatic embryogenesis, the overall picture of key genes, pathways, and co-expression networks regulating SE is still fragmented. Therefore, deciphering the molecular basis of somatic embryogenesis of hybrid sweetgum remains pertinent. In the present study, we analyzed the transcriptome profiles and gene expression regulation changes via RNA sequencing from three distinct developmental stages of hybrid sweetgum: non-embryogenic callus (NEC), embryogenic callus (EC), and redifferentiation. Comparative transcriptome analysis showed that 19,957 genes were differentially expressed in ten pairwise comparisons of SE. Among these, plant hormone signaling-related genes, especially the auxin and cytokinin signaling components, were significantly enriched in NEC and EC early. The K-means method was used to identify multiple transcription factors, including *HB-WOX*, *B3-ARF*, *AP2/ERF*, and *GRFs* (growth regulating factors). These transcription factors showed distinct stage- or tissue-specific expression patterns mirroring each of the 12 superclusters to which they belonged. For example, the *WOX* transcription factor family was expressed only at NEC and EC stages, *ARF* transcription factor was expressed in EC early, and *GRFs* was expressed in late SE. It was noteworthy that the *AP2/ERF* transcription factor family was expressed during the whole SE process, but almost not in roots, stems and leaves. A weighted gene co-expression network analysis (WGCNA) was used in conjunction with the gene expression profiles to recognize the genes and modules that may associate with specific tissues and stages. We constructed co-expression networks and revealed 22 gene modules. Four of these modules with properties relating to embryonic potential, early somatic embryogenesis, and somatic embryo development, as well as some hub genes, were identified for further functional studied. Through a combination analysis of WGCNA and K-means, SE-related genes including *AUX22*, *ABI3*, *ARF3*, *ARF5*, *AIL1*, *AIL5*, *AGL15*,

WOX11, *WOX9*, *IAA29*, *BBM1*, *MYB36*, *LEA6*, *SMR4* and others were obtained, indicating that these genes play an important role in the processes underlying the progression from EC to somatic embryos (SEs) morphogenesis. The transcriptome information provided here will form the foundation for future research on genetic transformation and epigenetic control of plant embryogenesis at a molecular level. In follow-up studies, these data could be used to construct a regulatory network for SE; Key genes obtained from coexpression network analysis at each critical stage of somatic embryo can be considered as potential candidate genes to verify these networks.

Keywords: hybrid sweetgum, somatic embryogenesis, transcriptome, coexpression network, qRT-PCR

INTRODUCTION

Chinese sweetgum (*Liquidambar formosana* Hance) is distributed in most temperate and subtropical regions of China and is used mainly for medicinal and ornamental purposes (Sun et al., 2016). American sweetgum (*Liquidambar styraciflua* L.) is a common southern American hardwood that has become an important feedstock for the timber and paper industries. These two species are interfertile even after 10 million years of separation (Vendrame et al., 2001). Some clones of hybrid sweetgum (*L. styraciflua* × *L. formosana*) have biomass productivity that is superior that of either parent species due to faster growth rates and higher wood density, demonstrating obvious heterosis (Merkle, 2018). Thus, the breeding of hybrid sweetgum is expected to have great potential value for the wood industry. Furthermore, potentially scalable SE-based propagation systems have been reported for both *L. styraciflua* (Merkle et al., 1998) and hybrid sweetgum (*L. styraciflua* × *L. formosana*) (Vendrame et al., 2001; Merkle et al., 2010). We successfully developed a SE system for hybrid sweetgum from hybrid immature seed explants. This system will be the foundation for breeding research and large-scale propagation of hybrid sweetgum. However, the mechanism of its SE remains unclear, which strongly hampers the advancement of breeding research and efficient propagation.

Somatic embryogenesis is one of the biotechnological tools which makes somatic embryos (SEs), similar in morphology to zygotic embryo without fertilization. Somatic embryos is bipolar structure which has both shoot apex and root apex (Dodeman et al., 1997; Ikeda et al., 2006). Also, SE is a multi-step regeneration process that includes three stages: embryonic induction, embryonic development, and somatic embryo development (Elhiti et al., 2013). First, a individual somatic cell or group of somatic cells under suitable *in vitro* conditions generates embryogenic or non-embryogenic cells. Some of these non-embryogenic callus (NEC) cells can differentiate further into embryogenic callus (EC) cells (Wen et al., 2020). The formation of callus is usually considered as a manifestation of the dedifferentiated cellular state. Second, the callus/proembryogenic cell mass (PEM) undergoes a series of biochemical and morphological changes to form SEs through redifferentiation or eventually to form a whole plant (Jiménez, 2005; Quiroz-Figueroa et al., 2006). The stages of somatic embryos include globular embryos (GE), heart-shaped embryos (HE), torpedo-shaped embryos (TE), and cotyledonary embryos (CE), all of which closely resemble those of zygotic embryos, both morphologically and temporally (Dodeman et al., 1997); hence, molecular information generated by studying the SE pathway can be used to explain the dynamic molecular interactions that occur during SE (Zimmerman, 1993; Quiroz-Figueroa et al., 2006). Somatic embryos has been reported in many plant species, including woody plants (more than 180 species of angiosperms and more than 35 species of gymnosperms) such as *Theobroma cacao* (Alemanno et al., 1996) and *Hevea brasiliensis* (Michaux-Ferrière and Carron, 1989), and has become an attractive regeneration method for *in vitro* mass propagation, germplasm preservation, and genetic improvement (Karami and Saidi, 2010).

Many studies have examined the biochemical and physiological changes of SE in varieties of plant species with the goal of understanding the mechanisms and functions of regulation of gene expression related to SE. These studies have identified genes that are differentially expressed in SE, highlighted pathways that may be involved in SE, and revealed molecular or protein markers for SE (Mantiri et al., 2008; Chen et al., 2020). Many studies have reported that some genes and proteins play a key role in SE. The identification of key genes in model plants could help us understand the mechanism underlying SE. The expression of several key regulators, including *Somatic Embryogenesis Receptor-Like Kinase 1 (SERK1)* gene, which was overexpression increases the efficiency of somatic cell initiation in Arabidopsis (Hecht et al., 2001). *LEAFY COTYLEDON2* (*LEC2*) (Gaj et al., 2005; Rupps et al., 2016), *ABSCISIC ACID INSENSITIVE3* (*ABI3*), *FUSCA3* (*FUS3*), which encode B3 domain transcription factors that are key regulators of embryogenesis (Freitas et al., 2019), were identified and verified as direct target genes of *AGAMOUS-LIKE15* (*AGL15*). Genes identified as targets of the B3 genes are also targets of *AGL15* (Zheng et al., 2009). The homologous domain transcription factor *WUS*, which can regulate the formation and maintenance of stem cells, was an early marker gene for *SAM* initiation in embryos (Weigel and Jürgens, 2002; Elhiti et al., 2010). *BABY BOOM* (*BBM*) encodes an *APETALA2* (*AP2*) domain transcription factor that is preferentially expressed in developing embryos and seeds. Overexpression of *BBM* can trigger spontaneous formation of somatic embryo (Maulidiya et al., 2020). In addition to these genes, *WUSCHEL homeobox 2* (*WOX2*) (Tvorogova et al., 2015),

AUXIN RESPONSE FACTOR 19 (*ARF19*) (Xiao et al., 2020), and LATE EMBRYOGENESIS ABUNDANT (LEA) protein (Wickramasuriya and Dunwell, 2015; Jamaluddin et al., 2017) also play key roles in SE. However, the gene changes and regulations in the SE of hybrid sweetgum remain unknown.

In the present research, we analyzed the transcriptome profiles and gene regulation changes in the SE process of hybrid sweetgum using a combination of K-means and WGCNA methods. Some genes were identified as being related to the NEC, EC, and redifferentiation of SE. These included genes related to hormones, embryogenesis, and various transcription factors (TFs). This is the first report of SE transcriptomes in hybrid sweetgum, and the results improve our understandings of the molecular mechanisms in the SE of hybrid sweetgum. Some new molecular marker genes were identified, which enriched the molecular regulatory network during SE and provided a new perspective for improving the efficiency of SE through genetic transformation. Furthermore, the results of this research will be provide a valuable resource for future studies and will be helpful to the research in this field, especially hybrid sweetgum breeding programs.

MATERIALS AND METHODS

Plant Material and RNA Extraction

To obtain hybrid seeds, we performed controlled pollinations between *L. formosana* and *L. styraciflua* trees. Developing fruits (multiples of capsules) were collected from the *L. styraciflua* trees. Whole fruits were surface-disinfested using the following sequence: rinse with water for 30 min, soaked in 75% ethanol for 1min and sodium hypochlorite for 4 min on the ultra-clean table, and cleaned with sterile distilled water for 5–6 times. The fruits were then dissected aseptically with a scalpel to remove the immature seeds. Each seed was nicked with a scalpel and cultured, ten seeds per plate, on induction medium: A modified Blaydes medium (Merkle et al., 1998) with 1.0 mg/L 2,4-dichlorophenoxyacetic acid (2,4-D), 0.5 mg/L 6-benzylaminopurine (6-BA), and 1.0 g/L casein hydrolysate (CH). The medium was Explants were transferred to fresh media of the same composition monthly until NEC (callus that were completely NEC or had both NEC and EC) started to form. Callus were transferred to fresh medium every 3 weeks. EC were transferred to embryo development medium –modified Blaydes basal medium without plant growth regulators (PGRs) – and incubated in the dark for 3–4 weeks, until embryos began to emerge from the PEMs. Individual somatic embryos were selected and cultured (16 per 90-mm plastic petri plate) on fresh medium of the same composition, also in the dark. When the embryos had enlarged to 2–3 mm in length, they were transferred to medium lacking PGRs and CH and incubated under cool white fluorescent light (140 μmol m^{-2} s^{-1}) for germination. The cultures at different developmental stages, including NEC, friable EC, PEM after maturation cultured for 20 days (PEM1), PEM after maturation cultured for 45 days (PEM2), GE, HE, TE, CE, roots (R), stems (S), and leaves (L) were sampled, as shown schematically in **Figures 1**, **2**. We collected the NEC, EC, PEM1, PEM2, GE, HE, TE, CE, and vegetative organs of plantlet samples (roots, stems, and leaves) from tissues in each of the three replicates and stored these at –80°C for RNA extraction.

Illumina Sequencing and Data Analysis

A total of 1 μg of RNA per sample was used as the input material for the RNA sample preparations. Three experimental replicates per sample were used for RNA library construction. RNA-Seq libraries were generated using the NEBNext Ultra RNA Library Prep Kit for Illumina (New England Biolabs, United States) following the manufacturer's recommendations, and index codes were added to attribute sequences to each sample. After sequencing, the raw data were filtered to remove adaptor contamination and low-quality reads. All clean reads were then mapped to the hybrid sweetgum genome using the HISAT2 program. The mapped reads of each gene were extracted using HISAT2 (Kim et al., 2015). We filtered the significantly differentially expressed genes (DEGs) using $|\log_2(\text{fold change})| \geq 1.5$ and P-value < 0.01 between seven pairwise comparisons: NEC_vs_EC, EC_vs_PEM1, PEM1_vs_PEM2, PEM2_vs_GE, GE_vs_HE, HE_vs_TE, TE_vs_CE, CE_vs_R, CE_vs_L, and CE_vs_S. Gene expression levels were normalized using the [fragments per kilobase of transcript per million fragments mapped (FPKM)] (Florea et al., 2013) method. All samples had more genes expressed at the level of 10 to 100 FPKM, and only 1196 to 1426 genes were identified at levels higher than 100 FPKM (**Supplementary Table 1**).

K-Means Clustering Analysis

K-means clustering with Euclidean distance in MeV 4.9 software yielded 50 clusters based on inputs of $\log_2$ relative FPKM values. In total, 13,574 genes residing in clusters with even more obvious tissue- or stage-specific expression trends were selected to make the final 35 K-means clusters. Only 18 of the 35 clusters are shown in **Figure 5**. TFs were extracted from the respective clusters. The $\log_2$ relative FPKM value of each TF was used to produce heat maps in TBtools (Chen et al., 2018) (**Figure 5B**).

Co-expression Network Construction and Hub Gene Search

For co-expression network analysis, the WGCNA (Zhang and Horvath, 2005; Langfelder and Horvath, 2008) package was used. Based on the $\log_2$ (1 + FPKM) values, a matrix of pairwise (spearman correlation coefficient) SCCs between all pairs of genes was generated and transformed into an adjacency matrix (a matrix of connection strengths) using the following formula: connection strength (adjacency value) = $|(1 + \text{correlation})/2|^{\beta}$. Here, β represents the soft threshold for the correlation matrix, which gives greater weight to the strongest correlations while maintaining gene–gene connectivity. Based on the scale-free topology criterion, the β value was selected as 13 (**Supplementary Figure 1A**). The adjacent matrix was transformed into topological overlap (TO) matrix by TOM similarity algorithm, and the hierarchical clustering of genes was carried out based on TO similarity. The dynamic tree-cutting algorithm was used to cut the

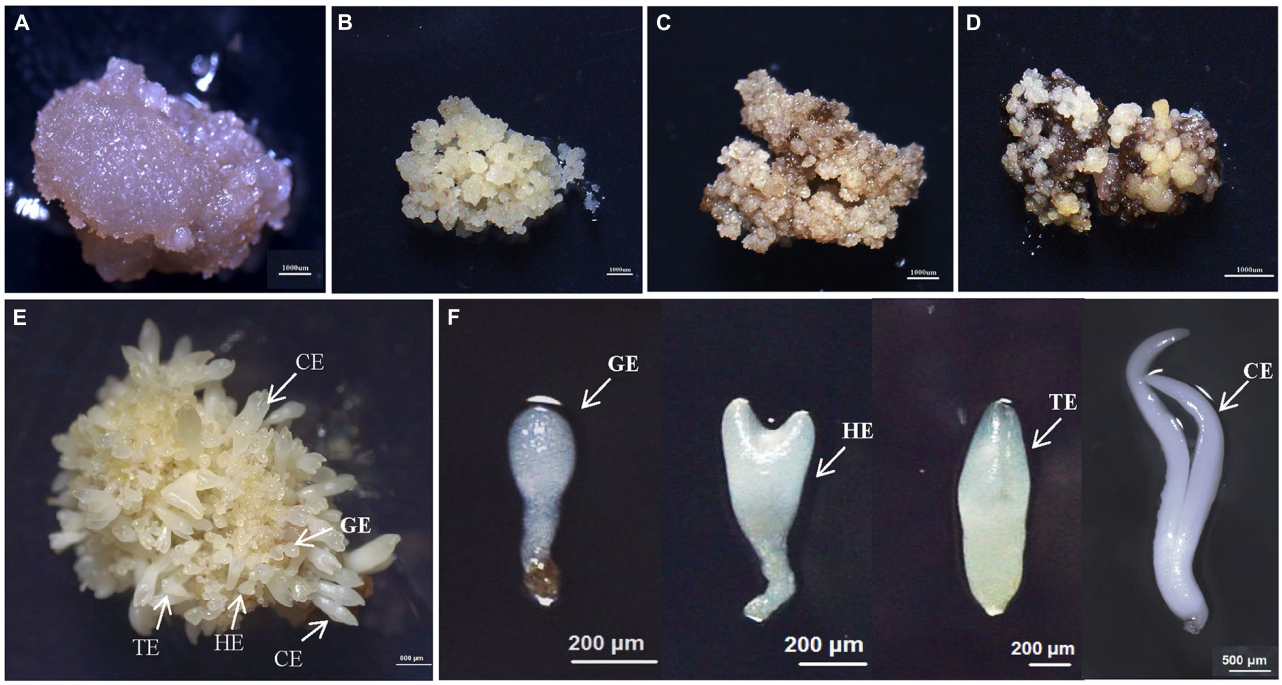

FIGURE 1 | The synchronized cultures during hybrid sweetgum SE. **(A)** NEC: non-embryogenic callus; **(B)** EC: friable-embryogenic callus; **(C)** PEM1: 20 days of pro-embryogenic mass; **(D)** PEM2: 45 days of pro-embryogenic mass; **(E)** embryogenic callus with somatic embryos; **(F)** Somatic embryos at different developmental stages (globular embryo, heart-shaped embryo, torpedo-shaped embryo, cotyledonal embryo). A–D Bars = 1000 μm; E Bars = 800 μm; F Bars = 200 μm, 500 μm.

hierarchal clustering dendrogram, decomposed/merged branches and defined modules to achieve a stable number of clusters (**Supplementary Figure 1B**) (Langfelder and Horvath, 2008). For each module, a summary profile (module eigengene) was calculated via principal component analysis. Further, the modules with higher TO values (average TO for all genes in a given module) than those of modules comprised of randomly selected genes were retained. Finally, the gene interactions in key modules were visualized using Cytoscape software, and a gene co-expression network based on the hit number was constructed. Cytoscape software (Shannon et al., 2003) was used to visualize the gene interactions of key modules and constructed the gene co-expression network based on hit number. Considering the expression information, we marked these genes and confirmed the top 20 hub unigenes per group. The Cytoscape working data are available in **Supplementary Table 2**.

Gene Ontology and Pathway Enrichment Analysis

Gene Ontology (GO) enrichment analysis for DEG sets was performed using Cytoscape (BiNGO plug-in) (Maere et al., 2005). The P-value for enrichment was calculated for each represented GO term and corrected using the Benjamini–Hochberg error correction method. The GO terms exhibiting a corrected (after adjusting with the false discovery rate) P-value ≤ 0.05 were considered to be significantly enriched. Furthermore, pathway enrichment analysis of different sets of genes was performed using MapMan (v 3.6.0RC1) categories (significance value ≤ 0.05). MapMan bins of supercluster genes were assigned using the Mercator pipeline for automated sequence annotation (Thimm et al., 2004)[1].

Quantitative Real-Time PCR Analysis

Quantitative real-time polymerase chain reaction (qRT-PCR) was conducted on 33 RNA samples that were used in the preparation of sequencing libraries using a CFX Connect® Real-Time PCR Detection System (CFX Connect, Bio-Rad, Munich, Germany). Each sample included three biological replicates. Nine genes that specifically highly expressed in non-embryogenic callus, embryogenic callus and somatic embryo development stage, respectively, were selected for qRT-PCR to verify the RNA-seq results, and then reverse transcribed of 1 μg total RNA into cDNA using a *TransScript* One-Step DNA Removal and cDNA Synthesis SuperMix Kit (Beijing Transgen Biotech Co. Ltd., Beijing, China). Each PCR reaction mixture contained 10 μl of Trans Start Top Green qPCR SuperMix (Beijing Transgen Biotech Co. Ltd., Beijing, China), 1 μl of template cDNA, 0.4 μl of forwarding primer, 0.4 μl of reverse primer (**Supplementary Table 3**), and 8.2 μl ddH_2O to a final volume of 20 μl with three technical replicates of each gene. The amplification condition for qRT-PCR was under the following program: denaturation at 94°C for 30 s, 40 cycles at 94°C for 5 s, 60°C for 15 s, 72°C for 15 s, with a melt cycle from 65 to 95°C. The apple EF1-α gene (Zheng et al., 2017)

[1]https://www.plabipd.de/portal/web/guest/mercator4

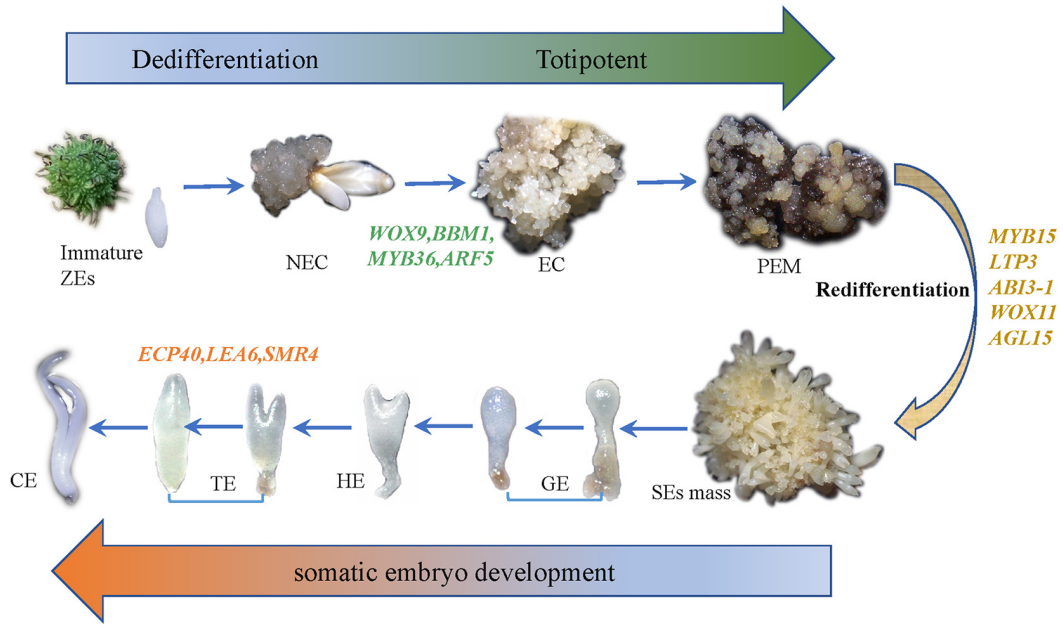

FIGURE 2 | The whole experimental diagram and hypothesized molecular mechanisms of SE.

served as the internal standard. The relative gene expression in each sample was normalized to EF1 Ct value and calculated using the $2^{-\Delta\Delta Ct}$ method.

RESULTS

Morphological Characterization of Somatic Callus

To study the SE of hybrid sweetgum, immature seeds of hybrid sweetgum (*L. styraciflua* × *L. formosana*) were tissue culture-induced to NEC. The NEC cells could be differentiated from the EC cells by visual discrimination. The NECs were dense and watery, white to brown in color, and had disorganized growth (**Figure 1A**). The ECs were friable, light yellow in color, and had organized globular structures that gave rise to SEs (**Figure 1B**). Once embryogenic cells have formed, they continue to proliferate and form PEMs. Browning takes place in PEMs when they are cultured on maturation medium for 20 days (**Figure 1C**), and the browning callus can regrow a new globular structure callus that continues to culture for 25 days (**Figure 1D**). Finally, globular, heart, torpedo, and cotyledon stage somatic embryos appear after 60 days (**Figures 1E,F**, **2**).

Transcriptome Sequencing and Gene Expression Profiles

To provide a clear understanding of hybrid sweetgum at the transcription level, we sequenced the 33 cDNA libraries constructed from 11 developmental stages: NEC, EC, PEM1, PEM2, GE, HE, TE, CE, roots (R), stems (S), and leaves (L) (**Figure 1**). In total, 998,501,629 clean reads (containing about 299.46 G of nucleotides) were obtained with quality checking. After alignment with the hybrid sweetgum reference genome, the clean data were mapped to the reference genome with a mapping ratio varying from 48,451,523 (76.36%) to 38,189,210 (81.49%). Among these, the unique mapping ratio varied from 47,112,326 (74.25%) to 37,112,232 (79.19%). In each sample, more than 91.08% had a base score of Q30 or higher. In our transcriptome, alternative splicing (AS) events were predicted by ASprofile. In total, 1,528,934 AS events, including alternative 5' splicing, alternative 3' splicing, exon skipping, intron retention, and the other 12 types of AS, were checked across the 33 samples. HE2 has the largest number of AS events (51,015), and the smallest was detected in L2 (37,151). A summary of the mapping statistics obtained for each sample is given in **Supplementary Table 4**.

The aim of this study was to reveal the potential key genetic factors related in the SE of hybrid sweetgum. Among these seven comparisons (**Figure 3A**), 3737, 5726, 7984, 6371, 136, 403, and 72 DEGs were identified, respectively. In comparison with NEC, EC had 1866 upregulated and 1871 downregulated genes. In comparison with EC, PEM1 had 3009 upregulated and 2717 downregulated genes. In comparison with PEM1, PEM2 had 3367 upregulated and 4307 downregulated genes. In comparison with PEM1, GE had 3433 upregulated and 2938 downregulated genes. In comparison with GE, HE had 49 upregulated and 87 downregulated genes. In comparison with HE, TE had 192 upregulated and 211 downregulated genes. In comparison with TE, CE had 36 upregulated and 36 downregulated genes. The Upset plot was also created to find the overlapped genes in the comparisons of eleven pairwise comparisons of hybrid sweetgum SE (**Figure 3B**). As shown in **Figure 3B**, 853 genes were exclusive to PEM1_vs_PEM2. 618 genes were exclusive to PEM2_vs_GE. Moreover, 598 genes were found in NEC_vs_EC.

DEG analysis showed that the hybrid sweetgum transcriptome changed significant dynamically during SE, especially during the transition period from PEM1 to PEM2.

Functional Classification of Differentially Expressed Genes Based on Gene Ontology and Kyoto Encyclopedia of Genes and Genomes Analyses

To evaluate the potential functions of the DEGs, we used GO term assignment to classify the functions of the DEGs in pairwise comparisons under three main GO categories: biological process, cellular component, and molecular function (**Supplementary Figure 2**). In all pairwise comparisons, the term with the largest proportion in biological process was metabolic process, followed by cellular process, single-organism process, biological regulation, respond to stimulus and localization, the term with the largest proportion in cellular component were cell and cell part, followed by membrane and organelle, the term with the largest proportion in molecular function was catalytic activity, followed by binding, transporter activity, structural molecular activity and nucleic acid binding transcription factor activity. In all pairwise comparisons among the functional groups, "metabolic process," "cell," "catalytic activity" terms were dominant. To investigate the biological pathways of the DEGs, we used the Kyoto Encyclopedia of Genes and Genomes (KEGG) database to classify the functions of the DEGs with emphasis on biological pathways (**Supplementary Figure 3**). According to the KEGG annotations, 701 DEGs (NEC_vs_EC) were assigned to 120 pathways, 1308 DEGs (EC_vs_PEM1) were assigned to 125 pathways, 1403 DEGs (PEM1_vs_PEM2) were assigned to 123 pathways, 1389 DEGs (PEM2_vs_GE) were annotated to 123 pathways, 18 DEGs (GE_vs_HE) were annotated to 21 pathways, 100 DEGs (HE_vs_TE) were assigned to 63 pathways, and 17 DEGs (TE_vs_CE) were annotated to 18 pathways. The pathway enrichment analysis showed that the annotated changes in NEC_vs_EC were mainly related to plant hormone signal transduction and fatty acid elongation. Among them, the genes annotated to fatty acid metabolism were up-regulated. The annotated changes in EC_vs_PEM1 were primarily involved in ribosomes and oxidative phosphorylation. The annotated changes in PEM1_vs_PEM2 were primarily involved in glutathione metabolism and phenylpropanoid biosynthesis. The annotated changes in PEM2_vs_GE were primarily involved in ribosomes and fatty acid elongation. Among them, the genes annotated to ribosome biogenesis in eukaryotes were up-regulated. The annotated changes in GE_vs_HE were mostly involved in brassinosteroid biosynthesis and starch and sucrose metabolism. Among them, the genes annotated to brassinosteroid biosynthesis pathway were significantly up-regulated, while the genes with alpha-linolenic acid metabolism were significantly down-regulated. The annotated changes in HE_vs_TE were primarily involved in phenylpropanoid biosynthesis and biosynthesis of amino acids. Among them, the genes annotated to phenylalanine metabolism were down-regulated. The annotated changes in TE_vs_CE were primarily involved in linoleic acid metabolism and alpha-linoleic acid metabolism. Among them, the genes annotated to alpha-linolenic acid metabolism and linolenic acid metabolism were down-regulated.

Differential Expression Analysis of Plant Hormone Signaling Pathway-Related Genes During Hybrid Sweetgum Somatic Embryos

Based on the KEGG and GO annotations, plant hormone signal transduction, zeatin biosynthesis, and IAA biosynthesis were the representative pathways in our study. A large number of genes involved in auxin (95 DEGs) and cytokinin (40 DEGs) biosynthesis and signal transduction pathways were differentially expressed when comparing EC with NEC and different SE stages.

For example, the expression levels of *PIN1-like*, *PIN2*, *AUX1*, *ARFs* (*ARF5*, *ARF17*, *ARF18*, *ARF19*), *GH3* (*GH3.6*, *GH3.1*, *GH3.17*), and five *SAUR* genes—all involved in auxin signal transduction—were significantly upregulated from NEC to EC. Nevertheless, *AUX1*, *GNOM*, *GNOM-like*, *DRM1*, *PIN*, *PIN2*, *AUX4-like*, *TIR1*, *IAA9*, *ARFs* (*ARF4*, *ARF6*, *ARF19-like*), *GH3* (*GH3.9*, *GH3.1*, *GH3*, *GH3.17-like*), and *SAUR* (*SAUR50*, *SAUR72*) were mainly expressed in the NEC stage and downregulated in EC. From the EC to PEM and GE stages, *GNOM*, *AFB2*, *GH3.6*, *IAA33*, *ARFs* (*ARF1*, *ARF1-like*, *ARF6*, *ARF18*, *ARF19*, *ARF19-like*), and two *SAUR32-like* genes showed noteworthy upregulated expression (**Figure 4A**). In indole-3-acetic acid (IAA) biosynthesis, *NIT* and *TSB* were upregulated in EC. *CYP714A1*, *CYP90A1*, *CYP1A1*, *CYP724B1*, and three *NIT* genes showed an NEC-specific expression pattern. One *YUCCA3*, three *CYP1A1*, and one *PAI* gene were upregulated in PEM, and *CYP724B1*, *CYP714A1*, *CYP90A1*, *ASA*, and *NIT* remained upregulated during the development stage of SEs (**Figure 4B**).

As shown in **Figure 4C**, Three *CKS*, one *IPT*, and one *Cis-ZOG* family genes involved in *cis*-zeatin O-glycosylation were highly expressed in NEC and significantly downregulated from NEC to EC and stages of somatic embryo development. Two *TPIT1* and one *CKS* gene were notably downregulated from NEC to EC and PEM and interestingly decreased during somatic embryogenesis, and the expression trends of these genes were consistent in studies on somatic embryogenesis of Longan (Chen et al., 2020). One *CYP735A was* upregulated in somatic embryo development. For the cytokinin signaling pathway, four *A_ARR*, two *AHP*, three *B_ARR*, and *CRE1* genes were mainly expressed in NEC but downregulated in EC. Two *A_ARR*, one *B_ARR*, and three *AHP* genes were upregulated in EC. One *A_ARR*, four *B_ARR*, and three *AHP* genes were upregulated in PEM, and one *CRE1*, one *B_ARR*, and three *A_ARR* genes showed upregulated expression during the development stage of SEs (**Figure 4D**). Analysis of differential gene expression patterns indicated that genes related to cytokinin signal transduction and synthesis were differentially expressed during somatic embryogenesis, which may be involved in the regulation of somatic embryogenesis in hybrid sweetgum. Multiple sequences of the same hormone-related genes were compared, and the highest alignment rate was 97.21%, while the lowest was 17.58%. Most of the gene sequences

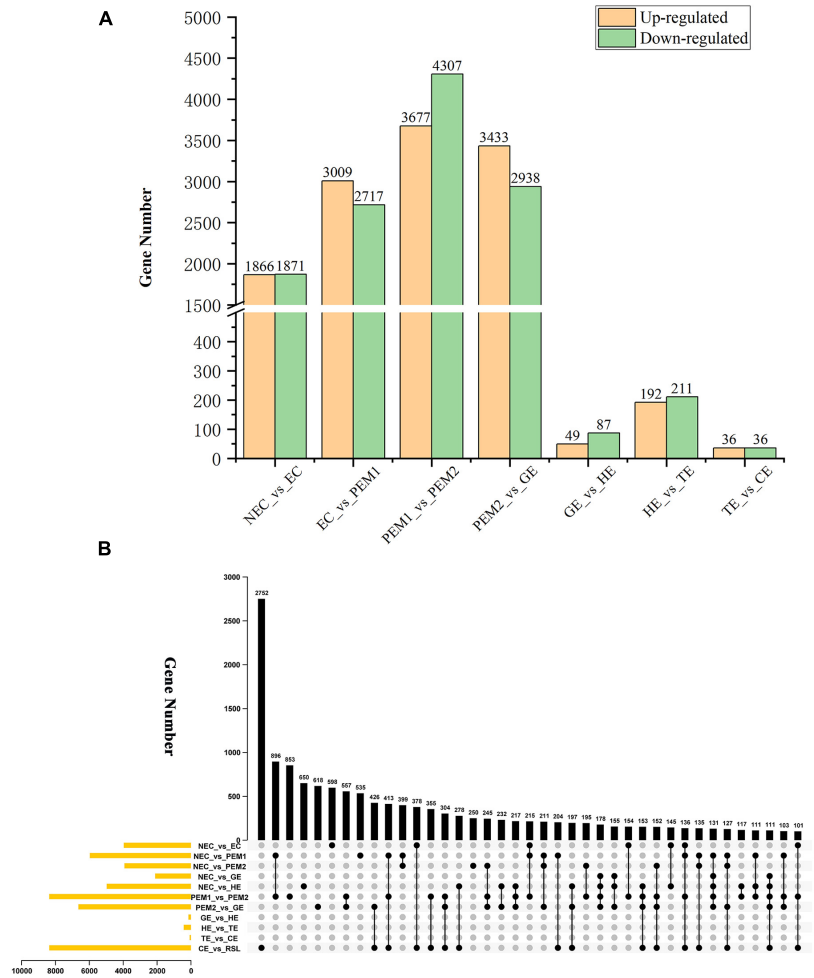

FIGURE 3 | Statistical analysis of differentially expressed unigenes in NEC, PEMs and different SE stages. **(A)** Statistic of Up/Down regulated genes in pairwise comparisons of NEC_vs_EC, EC_vs_PEM1, PEM1_vs_PEM2, PEM2_vs_GE, GE_vs_HE, HE_vs_TE and TE_vs_CE. **(B)** The Upset plot of expressed genes in eleven pairwise comparisons.

were different, indicating that these genes were different isoforms (**Supplementary Figure 4**).

Identification of Spatiotemporal Expression Trends Across Hybrid Sweetgum Transcriptomes

Thirty-five K-means clusters (containing 19,957 genes) with the most obvious tissue- and stage-specific expression trends were selected. Among these, 18 clusters representing 6815 genes are shown in **Figure 5A** and **Supplementary Table 5**. The 18 clusters can be divided into four large clusters, which are NEC, early SE (EC, PEM1, PEM2, GE), somatic embryo development (GE, HE, TE, CE) and vegetative organ (L, R, S). Early SE-specific gene clusters (C23, C20, C26, and C19) and embryo development-specific gene clusters (C17, C19, C34, and C35) were identified (**Figure 5A**). The NEC and vegetative organ categories had highly unique transcriptomes; almost 60% of the genes with tissue-specific expression were found in the NEC (C2 and C14) and vegetative organ (C1, C4, C5, C7, C8, C12, C13, C16, and C32) groups. However, a unique transcriptome was also found during the somatic embryo development stage; almost 10% of the genes with stage-specific expression were in embryo development.

Clusters with similar expression trends were combined into 12 superclusters (**Figure 5A**), and specific genes or pathway enriched in specific superclusters were identified by MapMan Bins (**Figure 5C** and **Supplementary Table 5**). The top abundant MapMan bin for the NEC-specific supercluster (supercluster 1) was polyamine metabolism, protein homeostasis, and secondary metabolism. As shown in **Figure 5C**, the biological functions associated with early somatic embryogenesis, nutrient uptake, enzyme classification, multi-process regulation, protein modification, and RNA processing were enriched in EC, PEM, and GE. Genes that participated in major vesicle trafficking, redox homeostasis, and regulation of proteins, including biosynthesis, homeostasis, and translocation, were particularly enriched in the somatic embryo development stage.

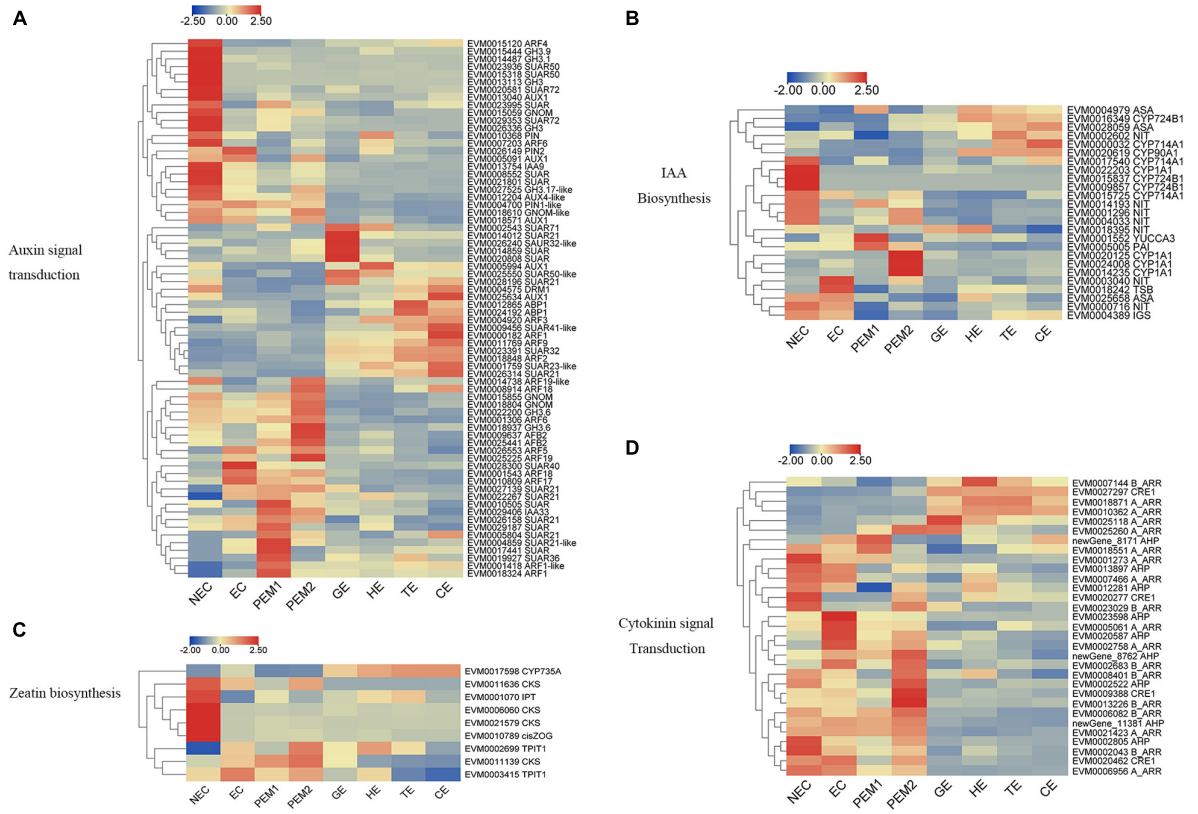

FIGURE 4 | Heatmap of the differentially expressed genes in auxin and cytokinin signaling pathway during hybrid sweetgum SE. **(A)** Auxin signal transduction; **(B)** IAA biosynthesis; **(C)** Zeatin biosynthesis; **(D)** Cytokinin signal transduction. The heatmap was clustered by pearson method of TBtools software. Heatmap indicate the gene expression level by Log2[FPKM] with a color scale, each row represents a single gene, the IDs and names of selected DEGs are indicated to the right of the histograms, and each column represents a sample.

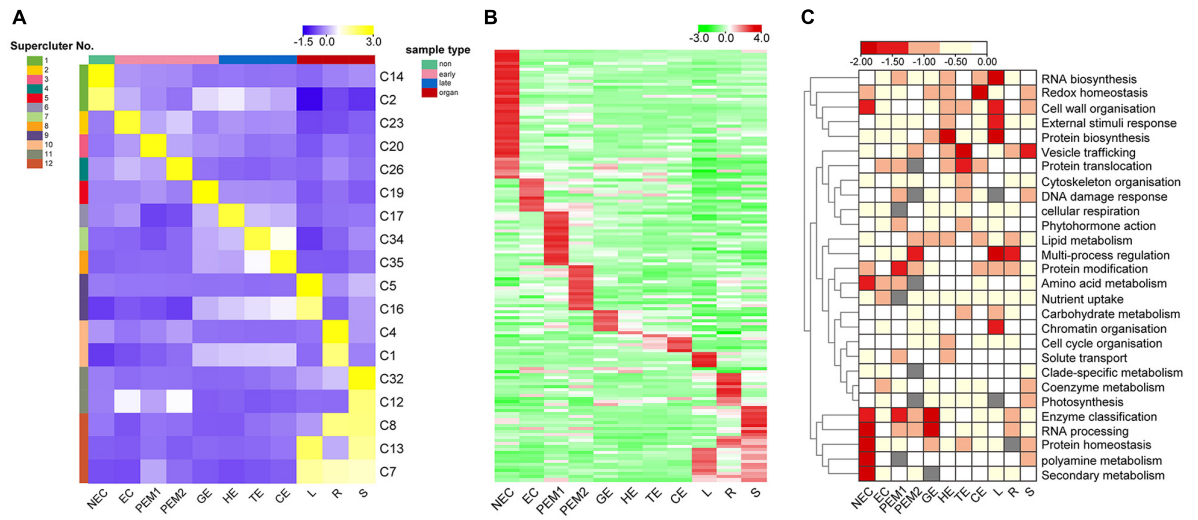

FIGURE 5 | K-means clustering reveals unique tissue- and/or stage-specific expression trends. **(A)** Eighteen clusters representing 6,815 genes are shown with distinct stage- and tissue-specific expression patterns. Averaged Normalized FPKM of all the genes in each cluster was used to generate the heat map. These clusters are further grouped into 12 superclusters shown to the right. Heat map indicate the gene expression level by gradient color scale in which yellow indicates high expression. **(B)** Clustering based on Normalized FPKM of 142 transcription factors. Red scale indicates high expression. **(C)** Enriched MapMan bins shown to the right for each of the 12 superclusters. Significant enrichment is indicated by low P values.

Among the 6815 genes that make up the aforementioned 12 superclusters (**Figure 5A**), 142 are TFs belonging to 60 families (**Figure 5B** and **Supplementary Table 5**). These TFs exhibit different stage- or tissue-specific expression patterns, and the dynamic and stage- or tissue-specific expression patterns of these TFs may reflect the pivotal roles that they play. For instance, the EC-specific (supercluster 2) cluster has four *RLK/Pelle* family kinases, one *C2C2* gene, and one ethylene response factor gene with potential roles in embryogenic competence. Interestingly, the embryo development-specific (superclusters 5–8) cluster has one *GRF* gene, indicating that this gene plays a key role in the morphogenesis of SEs.

Co-expression Network Analysis With Weighted Gene Co-expression Network Analysis

As an alternative analysis tool, weighted gene coexpression network analysis (WGCNA), was adopted. WGCNA is a systems biology approach that aims to understand entire gene networks rather than single genes. In this study, we constructed a co-expression network based on the pairable correlation of gene co-expression trends in all sample tissues. Modules were defined as clusters of genes that were highly interrelated; The correlation coefficient between genes in the same cluster was high. This analysis resulted in 22 different modules, color-coded in the dendrogram (**Figure 6A** and **Supplementary Figure 1B**), where each branch constitutes a module and each branch is a gene (**Figure 6A** and **Supplementary Table 2**). The first principal component of a given module was the module eigengene, which represented the gene expression profile of the module. Due to the tissue-specific expression profile of the eigengene, 22 characteristic genes of 22 different modules were associated with different tissue types. In comparison with other co-expression modules, for instance, the module with the highest correlation with NEC was the lightcyan module ($p = 8 \times 10^{-22}$, $r = 0.99$), whereas genes in the green module had a higher correlation with EC ($p = 3 \times 10^{-2}$, $r = 0.42$) than NEC, except for PEM2. Genes in the blue module were comparatively highly correlated with early SE (EC, PEM1, PEM2). Interestingly, three co-expression modules, the pink, salmon, and purple modules, showed relatively high correlation ($r \geq 0.15$) with somatic embryo development stages (GE, HE, TE, CE) (**Figure 6B**). Many of the modules were correlated with more than one vegetative organ of the plantlet; however, a few were correlated with only a specific vegetative organ of the plantlet. For example, the yellow module was specifically correlated ($p = 7 \times 10^{-14}$, $r = 0.95$) with leaf tissue, whereas the midnight-blue and red modules were specifically correlated with root ($p = 2 \times 10^{-20}$, $r = 0.98$) and stem ($p = 5 \times 10^{-13}$, $r = 0.94$) tissues, respectively (**Figure 6B**).

Figures 7A,C,E,G show the eigengene expressions for the lightcyan (NEC), thistle (EC) modules, blue (EC, PEM1, PEM2) and pink (GE, HE, TE, CE) modules. The heatmap shows the expression profiles of all co-expressed genes from the blue, pink, lightcyan, and thistle modules. WGCNA can also be used to drawn gene networks, where each node represents a gene and the edges are the connecting lines between nodes, represent co-expression-related genes. The node gene with the highest connectivity, as the hub gene, may play a key role in different modules. The lightcyan, thistle, blue and pink module networks are shown in **Figures 7B,D,F,H**. Some of the more interconnected node genes are those of TFs. Only the top 20 genes with high connectivity were selected, and 10 TFs representing different families were obtained, including the *WRKY*, *RLK-Pelle*, *MYB*, and *STE_STE11* TFs. Another nine hub genes were also identified as key proteins or enzymes that play a key role in early SE (blue module) (**Figure 7F** and **Supplementary Table 2**). In the pink module network, 77 of the 965 genes encode TFs. Selecting only the top 23 genes showing high connectivity weight resulted in 11 TFs representing distinct families, including the *AP2/ERF-ERF*, *C2C2*, *C3H*, *bHLH*, *GRF*, and *bZIP* TFs. Another 12 hub genes, namely *cyclin-dependent protein kinase inhibitor* (*SMR4*), *seed biotin-containing protein* (*SBP65*), and *late embryogenesis abundant protein 6* (*LEA6*), are involved in regulation of the cell cycle, seed germination capacity, and embryo development ending in seed dormancy (**Figure 7H** and **Supplementary Table 2**). In the lightcyan module network (**Figure 7B**), 37 of the 416 genes encode TFs. Selecting only the top 19 genes showing high connectivity weight indicated 11 TFs representing distinct families, including the *AUX/IAA* (EVM0009101; EVM0009101), *C2C2-Dof*, *GNAT*, *bHLH*, *AP2/ERF-ERF*, and *NAC* TFs (**Supplementary Table 2**). Another eight hub genes, namely *protein NRT1/PTR FAMILY 4.3* (*NPF4.3*), *cytokinin dehydrogenase 1* (*CKX1*), and *brassinosteroid-related acyltransferase 1* (*BAT1*), are involved in regulation of transmembrane transporter activity, cytokinin metabolic processes, and response to brassinosteroids. Interestingly, after we performed the co-expression analysis of the data again, we observed that one module displayed opposite expression patterns between the two types of calluses (NEC and EC) having different embryogenic potentials. For example, the thistle module showed low transcript abundance in NEC but high abundance in EC. In this module, 38 of the 212 genes encode TFs. Selecting only the top 15 genes showing high connectivity weight revealed 10 TFs representing distinct families, including the *HB-WOX*, *AP2/ERF-AP2*, *MYB*, *B3-ARF*, *AP2/ERF-ERF*, *FAR1*, and *C2H2* TFs. Another five hub genes, namely, *peptidyl-prolyl cis-trans isomerase* (*FKBP43*), *CASP-like protein 1E1*, *beta-fructofuranosidase*, *insoluble isoenzyme 1* (*INV1*), *GDSL esterase/lipase* (*At5g45910*), and *WAT1-related protein* (*At1g25270*) were involved in regulation of peptidyl-prolyl cis-trans isomerase activity, protein histidine kinase binding, carbohydrate storage, lipid catabolic processes, and transmembrane transporter activity (**Figure 7D**). Interestingly, the *FKBP43* gene is a fundamental protein that regulates cell division, adhesion and elongation throughout the plant development and embryogenesis and required for the spatial organization of apical meristems. These results suggest that the *FKBP43* gene may play a key role in the proliferation and maintenance of embryogenic ability of embryogenic callus.

Gene Ontology (GO) enrichment analysis was performed for each module using Cytoscape (BiNGO plug-in) (Maere et al., 2005) highlighted important biological processes represented

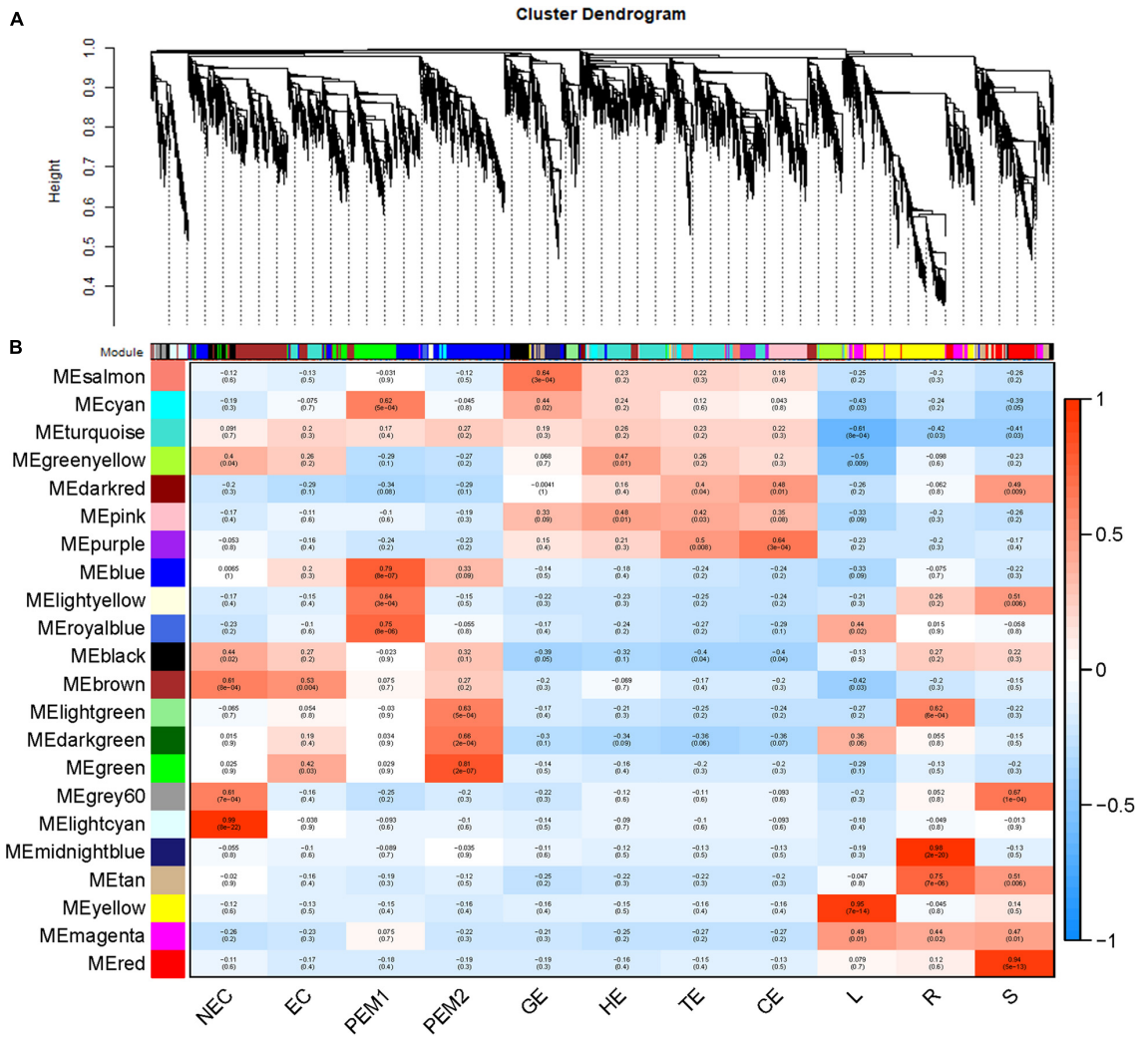

FIGURE 6 | WGCNA of genes in eleven tissues. **(A)** Hierarchical cluster tree showing coexpression modules identified by WGCNA. Each leaf in the tree is one gene. The major tree branches constitute 22 modules labeled by different colors. **(B)** Module-tissue association. Each row corresponds to a module. The number of genes in each module is indicated on the left. Each column corresponds to a specific tissue. The color of each cell at the row-column intersection indicates the correlation coefficient between the module and the tissue type. A high degree of correlation between a specific module and the tissue type is indicated by red.

by a range of co-expressed genes. The blue module formed a cluster of 2632 DEGs enriched in functions related to phosphorus metabolic processes (phosphate metabolic process, phosphorylation, and protein amino acid phosphorylation) and amine metabolic processes (aminoglycan catabolic process, chitin metabolic process, and aminoglycan catabolic process) (**Supplementary Figure 5C**). The pink module formed a cluster of 965 DEGs enriched in functions related to RNA metabolic processes (RNA processing, rRNA metabolic process, rRNA processing, and ncRNA processing) and responses to stress (response to cold, response to temperature stimulus, and response to abiotic stimuli) (**Supplementary Figure 5D**). The lightcyan module formed a cluster of 416 DEGs enriched in functions related to the catabolic process, carbohydrate catabolic process, polysaccharide catabolic process, pectin catabolic process, and cotyledon vascular tissue pattern formation (**Supplementary Figure 5A**). The thistle module obtained from the other WGCNA analysis formed a cluster of 211 DEGs enriched in functions related to regulation of metabolic processes (transcription, macromolecule metabolic process, RNA metabolic process, and nucleic acid metabolic process) and developmental processes (reproductive developmental process, anatomical structure development, and multicellular organismal development) (**Supplementary Figure 5B**).

Quantification of the Level of Relative Expression

To verify the reliability of transcriptome data, twenty genes related to SE were selected.

The *GLP1-13* (EVM0020840), *ARF5* (EVM0026553), *ABI3-1* (EVM0020968), *LTP3* (EVM0021586), *WOX9* (EVM0013624), *LEA6* (EVM0000925), *SMR4* (EVM0007351),

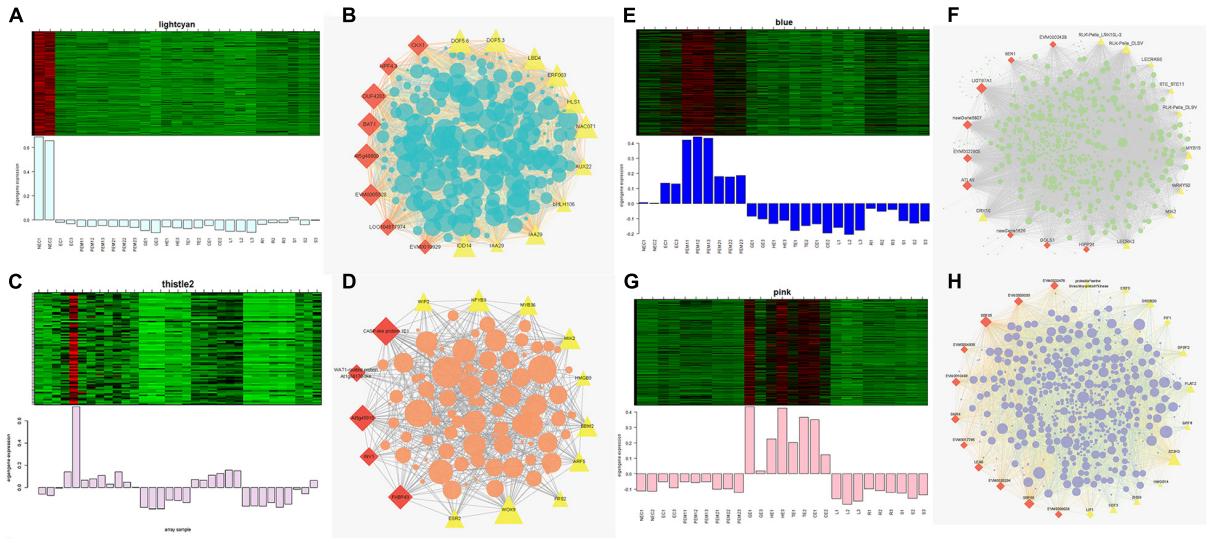

FIGURE 7 | Expression profile and transcriptional regulatory network associated with the tissue-specific modules. Heatmaps of **(A)** lightcyan module (NEC), **(C)** thistle modules (EC), **(E)** blue module (early SE), **(G)** pink module (somatic embryo development stages) show the expression profile of all the coexpressed genes in the modules (labeled on top). The color scale represents Z-score. Bar graphs (below the heat maps) show the consensus expression pattern of the coexpressed genes in each module. **(B)** Correlation network of genes in lightcyan module (NEC). **(D)** Correlation network of genes in thistle module (EC). **(F)** Correlation network of genes in blue module (early SE). **(H)** Correlation network of genes in pink module (somatic embryo development stages). Red diamonds indicate hub genes, and yellow triangles indicate transcription factors.

ECP40 (EVM0003818), and *MYB36* (EVM0015487) genes with high specific expression in various stages of hybrid sweetgum transcriptome were selected as marker genes to measure expression by qRT-PCR (**Supplementary Table 3**). The qRT-PCR analysis showed that expression levels during different SE phases changed between the genes (**Figure 8**). *WOX9* and *MYB36*, as selected molecular marker genes, were almost not expressed in NEC, while they mainly expressed during early SE, with the highest expression at EC stage and then decreased in the mature somatic embryos of SE. This showed that those molecular markers played a key role in the maintenance and acquisition of embryogenic ability. Meanwhile, *ECP40*, *ABI3-1*, and *LEA6* were highly expressed or up-regulated during somatic embryo development processes, and minimally or undetected in NEC. Which suggested that those marker genes may promote the hybrid sweetgum somatic embryo development. *LTP3*, *SMR4*, and *ARF5* were highly expressed or up-regulated during the whole SE processes, and low expression in NEC and vegetative organ (R, L, S), indicated that those molecular markers played a key role in SE. In addition, the transcription level of *GLP1-13* was highly and specific expressed in NEC, and this gene may inhibit the transition from non-embryonic to embryonic cells. qRT-PCR verification of SE-related genes also demonstrated a high correlation between RNA-seq and qRT-PCR data.

DISCUSSION

Because hybrid sweetgum (*L. styraciflua* × *L. formosana*) is a tree species that grows faster and has higher wood density than its parents, its SE is becoming increasingly important. We successfully developed an SE system for hybrid sweetgum from hybrid seed explants. However, the mechanism of its SE remained unknown. In this study, we performed transcriptomic analyses of 11 types of tissues and stages of SE. The RNA sequencing (RNA-seq) data were analyzed using two different bioinformatics methods, K-means and WGCNA. This analysis yielded several new insights, including the identification of some time-specific modules, hub genes, and transcription factors.

Important Roles of Auxin and Cytokinin in Hybrid Sweetgum Somatic Embryos

As we all known that auxin and cytokinin are important factors in plant cell division, differentiation, and SE induction. In this study, auxin and cytokinin signal transduction and biosynthesis related genes were significantly expressed during somatic embryogenesis, among which there were many auxin signal transduction genes, such as *SUAR* (small auxin up RNA) family genes had the largest number. However, the levels of endogenous auxin and cytokinin are influenced by their exogenous application (Vondráková et al., 2011; Xu et al., 2013). Auxin is considered to be the central regulator of SE, which may be due to the establishment of an auxin gradient during SE induction (Yang et al., 2012). To date, the effect of exogenous auxin during SE has been reported in several studies (Yang et al., 2012; Chu et al., 2017). In accordance with these results, we found a mass of auxin-responsive genes differentially expressed between tissues with contrasting embryogenic potential and at particular stages in hybrid sweetgum SE.

In samples of EC, contents of many auxin related genes, such as *ARF17*, *ARF18* and *AUX1*, were significantly higher than those

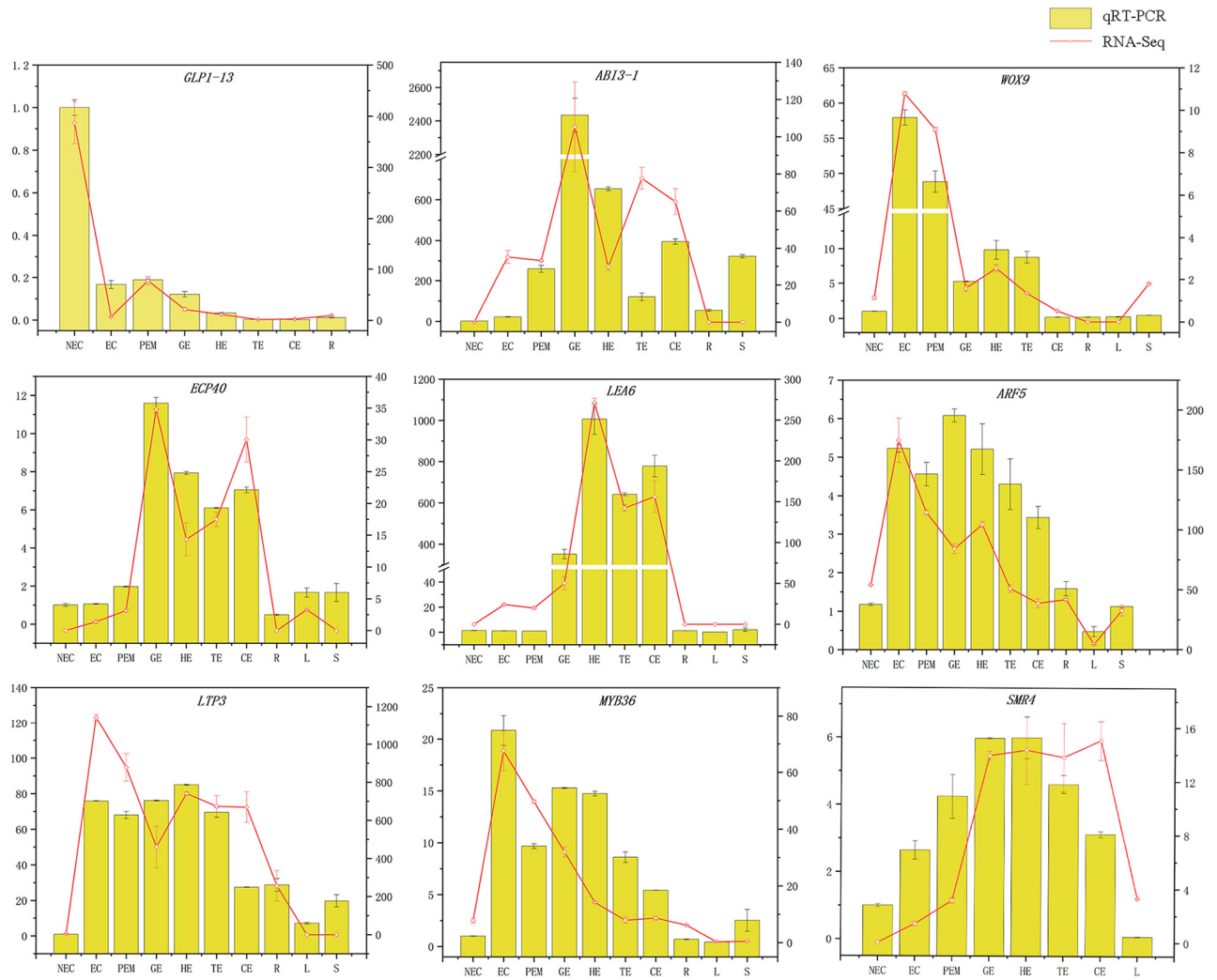

FIGURE 8 | Comparison of expression profiles of ten representative genes as measured by RNA-seq and qRT-PCR. Columns represent expression determined by qRT-PCR (left y-axis), while lines represent expression by RNA-seq in FPKM values (right y-axis). The x-axis in each chart represents the ten stages (NEC-S). For qRT-PCR assay, the mean was calculated from three biological replicates each with three technical replicates (n = 9). For RNA-seq, each point is the mean of three biological replicates.

of NEC. The expression levels of *ARF9* and *ARF2* were significant during somatic embryo development, and increased gradually with somatic embryo development, and reached the highest in cotyledon embryo maturation. It is well-known that members of the *ARF* and *AUX/IAA* transcription regulator/signaling families act in concert to regulate the expression of responsive genes (Vanneste and Friml, 2009; Kieffer et al., 2010). The level of endogenous IAA has been correlated with PEM formation and high-frequency SE competency (Zhou et al., 2017). The balance of free IAA and IAA conjugates during SE induction of *Coffea canephora* was critical for embryogenic potential (Ayil-Gutierrez et al., 2013). The conjugation of auxin is synthesized by the *GH3* family (Chen et al., 2010), and *PIN1* plays a fundamental role in maintaining the embryonic auxin gradients (Feher, 2019). To summarize, we found that some of these family genes (*PIN1-like*, *PIN2*, *AUX1*, *ARFs*, *GH3*, and *SAUR*) had lower expression in NEC. Most of them were dramatically upregulated in EC and downregulated during SE, indicating that the auxin-responsive genes played an important role in hybrid sweetgum SE. Tryptophan (Trp)-dependent IAA biosynthesis is an important pathway in higher plants, and exogenous application of doses of Trp and IAA produced similar enhancements during rice SE (Siriwardana and Nabors, 1983). In our study, the expression levels of *TSB* genes, key genes in Trp synthesis, were drastically upregulated in EC and downregulated during SE. No Trp synthesis gene showed NEC specificity with high FPKM, suggesting that the level of Trp was higher during SE than during NEC.

Aside from auxin being a main inducer of SE, the use of exogenously supplied cytokinin to induce SE has been well established in many species (Sagare et al., 2000; Cabrera-Ponce et al., 2018). Large numbers of transcripts involved in

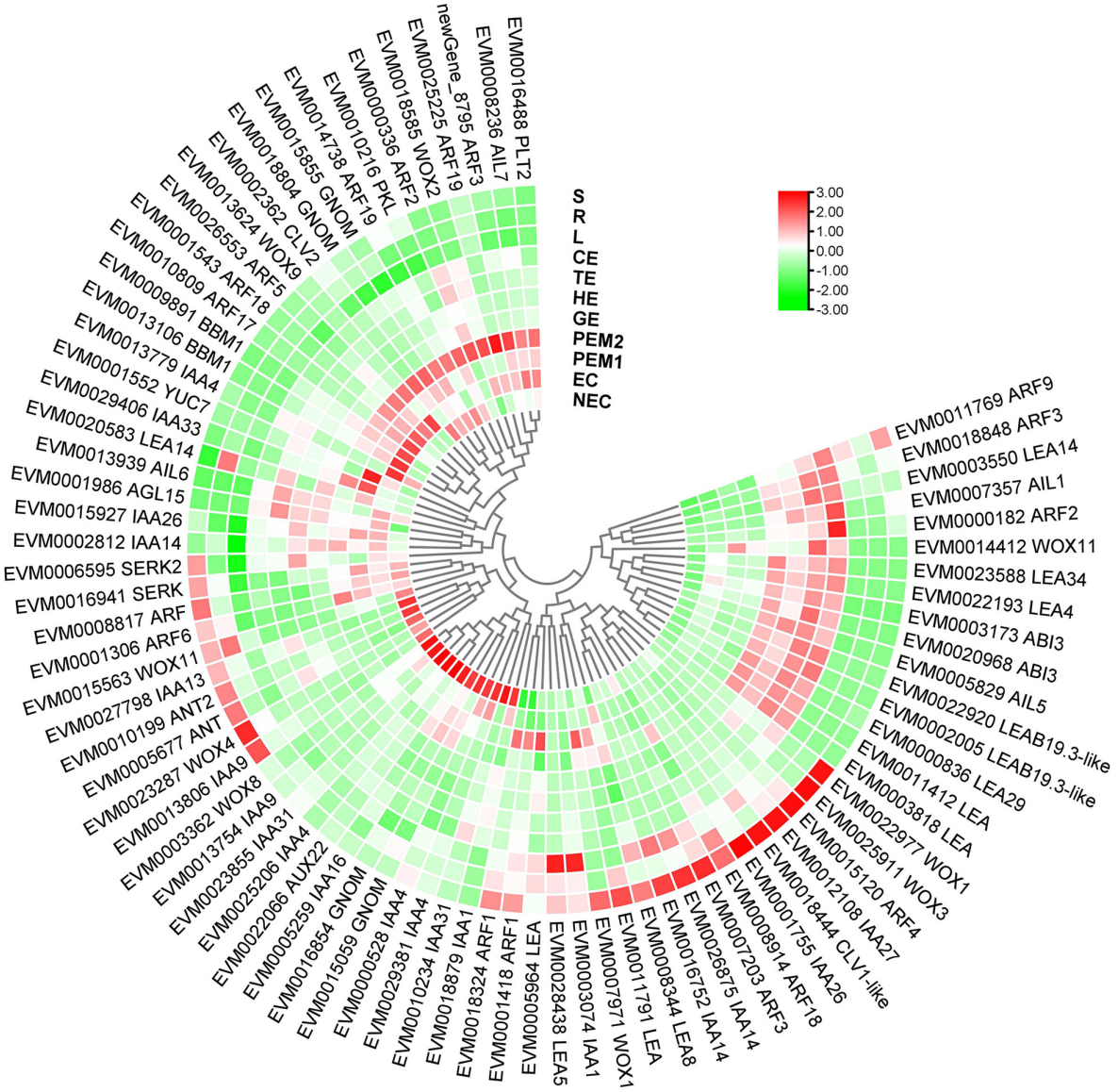

FIGURE 9 | Heatmap of the differentially expressed SE-related genes during hybrid sweetgum SE. The heatmap was clustered by pearson method of TBtools software. Heatmap indicate the gene expression level by Log2[FPKM] with a color scale, each row represents a single gene, the IDs and names of selected DEGs are indicated to the outside of fan, and each circle represents a sample.

zeatin biosynthesis and signal transduction are differentially expressed during cotton SE (Xu et al., 2013). Furthermore, endogenous cytokinin levels have been shown to be higher in SE than in NEC (Lai and Chen, 2002). In our study, from NEC to EC, a total of 31 DEGs were implicated in cytokinin signal transduction, including four *CRE1* (two upregulated and one downregulated), seven *B-ARR* (two upregulated and five downregulated), and 11 *A-ARR* (two upregulated and four downregulated) genes. In the zeatin synthesis pathway, *TRIT1* was upregulated from NEC to EC, and most of the *CisZOG*, *IPT*, and *CKS* were downregulated in EC and remained low during SE. However, IAA and zeatin biosynthesis- and signal transduction-related genes regulate SE in a complex and comprehensive way. Additional study of these genes in hybrid sweetgum SE is required.

Key Role of Somatic Embryos-Related Genes During Hybrid Sweetgum Somatic Embryos

Many genes and TFs have been reported as key factors in SE induction. Some TFs, including *LEC1*, *LEC2*, *FUS3*, *ABI3*, *WOX9*, *WOX2*, and *BBM*, were identified as molecular marker genes for early microspore embryogenesis of *Brassica napus* (Malik et al., 2007). In our study, 11 molecular markers were TFs (*AUX22*, *ABI3*, *ARF3*, *ARF5*, *AIL1*, *AIL5*, *AGL15*, *WOX11*,

WOX9, *IAA29*, *BBM1*, and *MYB36*), and some of these gene functions on embryogenesis have been well characterized in various plants (**Figure 9** and **Supplementary Table 6**). *LEC2*, *ABI3*, and *FUS3* are B3 domain-containing transcription factors; *ABI3* is highly expressed in embryogenic masses of *Coffea arabica*, and it has been speculated that its activity is related to embryogenic potential (Freitas et al., 2019). The *AP2/ERF* family has two very important members, namely *BBM* and *PLT2*, which have been reported to play important roles in microspore, somatic, and zygotic embryogenesis (Tsuwamoto et al., 2007). Overexpression of *BBM* can trigger spontaneous formation of SEs in *Arabidopsis thaliana* and *B. napus*. Therefore, *BBM1* can serve as a marker gene for embryogenic callus cells in *B. napus* (Boutilier et al., 2002). In this assay, *BBM* and *ABI3* were highly expressed during the SE processes. However, *BBM1* was more highly expressed during the embryonic processes, and it can be used as a remarkable marker for maintenance of totipotent potential in hybrid sweetgum. To date, The *MADS-box* gene of *AGL15* is expressed preferentially during embryonic development, and the protein accumulation reaches the highest level; it is expressed at lower levels at the later stage of germination (Fernandez et al., 2000; Yang and Zhang, 2010). Notably, *AGL15* was shown to be beneficial to somatic embryo development and promoted the production of secondary embryonic callus from cultured zygotic embryos (Harding et al., 2003). The homologous domain transcription factor *WUS*, which can regulate the formation and maintenance of stem cells, was an early marker gene for *SAM* initiation in embryos (Weigel and Jürgens, 2002). *STIMPY/WOX9* played an key role in increasing the proliferation rate and preventing premature differentiation in emerging seedlings (Wu et al., 2005). *WOX2* and *WOX9* were highly expressed at the early stage of SE in *Picea abies*, and may play a role together in conifer embryo model (Palovaara et al., 2010). *WOX11* and *WOX12* genes promoted the division of procambium cells and played a key role in callus and adventitious root formation (Liu et al., 2014). In this assay, *WOX9* was specifically expressed in EC and downregulated during SE. *WOX11* was highly expressed throughout SE and almost not expressed in NEC or vegetative organs. Hence, these genes might play an important role in hybrid sweetgum SE.

Identification of Weighted Gene Co-expression Network Analysis Module Genes Highly Associated With Hybrid Sweetgum Somatic Embryos

As an effective data mining method, WGCNA can screen genes related to specific traits and conduct modular classification on large samples to obtain co-expression modules with high biological significance (Zhao et al., 2010). Weighted gene co-expression network analysis has been used widely for plants in recent years (Zhao et al., 2020; Liu et al., 2021; Panahi and Hejazi, 2021). Therefore, we constructed a hybrid sweetgum gene co-expression network using a WGCNA approach and identified co-expression modules using transcriptome data. In total, according to the gene expression pattern, 22 modules were identified, several of which showed functional specificity at different stages (**Figure 6**). Then, to investigate the functional biological roles of these DEGs, BiNGO (Maere et al., 2005) software was used (**Supplementary Table 2**).

Our analysis identified many genes that were differentially expressed in the thistle module (EC). Of those with annotations, we found that the expression of many TFs, such as the *HB-WOX*, *AP2/ERF-AP2*, *MYB*, *B3-ARF*, *AP2/ERF-ERF*, *FAR1*, and *C2H2* TFs, increased in EC. TFs played an important role in regulating plant differentiation and development. For instance, *MYB* TFs may regulate cell proliferation and elongation (Wen et al., 2020). Several *R2R3-MYB* TFs are barely expressed in NEC, significantly upregulated from NEC to EC, and maintained at high levels during early SE in longan (Chen et al., 2020). *WUSCHEL-related homeobox* (*WOX*) genes encoding plant-specific homeobox TFs play key roles in plant development and growth (Li et al., 2019), can regulate stem cell maintenance and formation, and are an early molecular marker for shoot apical meristem (SAM) initiation in embryos (Weigel and Jürgens, 2002). *AP2/ERF* TFs function in the response to phytohormones and/or biotic or abiotic stresses. *BBM* and *ESR2*, which are known to be associated with cellular pluripotency in *Arabidopsis* (Matsuo et al., 2011; Kulinska-Lukaszek et al., 2012), are also involved in pluripotency acquisition in hybrid sweetgum callus. Therefore, these genes may play a key role in the acquisition and maintenance of embryogenic ability during somatic embryogenesis.

In the pink module (somatic embryo development), 23 hub genes that showed high connectivity weight included 11 TFs representing distinct families, such as the *AP2/ERF-ERF*, *C2C2*, *C3H*, *bHLH*, *GRF*, and *bZIP* TFs (**Supplementary Table 2**). Another 12 hub genes included *SMR4*, *SBP65*, *LEA6*, *LIP1*, and others. Based on their BiNGO annotations, some genes associated with SEs development are involved in stress signaling pathways and RNA processes, revealing the relationship between SE development and stress signaling. The rRNA gene are an important part of protein synthesis and ribosome production, and the change of rRNA can cause the change of nucleolus volume (Koukalova et al., 2005). Gaudino and Pikaard (1997) reported that exogenous application of cytokinin stimulated polymerase I transcription of rRNA genes in *Arabidopsis* (Gaudino and Pikaard, 1997). LEA proteins were first identified in cotton seeds more than 30 years ago (Danyluk et al., 1998) and were later found to be abundantly expressed in late zygotic embryogenesis in many plant species, including cotton, barley, rice, oilseed rape, and wheat (Dure et al., 1989). *LEA* gene was highly expressed in carrot callus and somatic embryo stage (Kiyosue et al., 1992). We speculated these genes may regulate the synthesis and accumulation of cellular proteins and small RNA through some stress signals, thus affecting somatic embryo development and promoting somatic embryo maturation.

CONCLUSION

According to our main findings of the hybrid sweetgum SE DEGs and their related networks (K-mean, WGCNA), in combination with the relevant literature, we herein propose a possible

molecular model for hybrid sweetgum SE, as shown in **Figure 2**. During totipotency acquisition, the molecular pathways of the cell undergo drastic changes. There are 4 candidate genes that seem to affect the maintain of totipotency, like the homeotic transcription factor *WOX9*, an important regulator of plant stem cell fate in the shoot meristem, which also may regulate the stem cell fate in the callus; the *BBM1* transcription factor involved in the growth regulation of organ primordia; the *R2R3-MYB* transcription factors are involved in cell proliferation and elongation, which may promote callus proliferation. ARF proteins are believed to activate or repress the target genes and in the transient and heterologous assays, individual *ARFs* are classified as activators/repressors of the gene transcription. *ARF5* is a activator, which encodes the MONOPTEROS (MP) protein, to be the most highly expressed member of the *ARF* gene family in the embryogenic culture of Arabidopsis. About the early embryo development stage, there are interesting interactions between *MYB15*, *AGL15*, *LTP3*, *WOX11,* and *ABI3*. *MYB15* was involved in drought and salt tolerance and may enhance expression levels of genes involved in abscisic acid (ABA) biosynthesis and signaling, as well as those encoding stress-protective proteins. Therefore, *MYB15* may promote somatic embryogenesis by regulating the dryness stress in early SE. *AGL15* is known to enhance the embryogenic response in somatic cells if ectopically overexpressed. *AGL15* can stimulates *ABI3* expression and also represses the auxin response and interacts with GA metabolism to promotes the generation of somatic embryos. The *LTP* homologous gene has been implicated as a well-known early marker of somatic embryogenesis induction in different systems, being that it is linked to the protoderm layer formation, which exerts a regulatory role in controlling cell expansion during embryo development in developing somatic. The *WOX11* genes participate in the early stages of the formation of callus and adventitious roots, initiating the division of the procambium cells. With the further development of somatic embryos, the need for energy stimulates the high expression of *SMR4*, *ECP40* and *LEA6*, which are involved in the stress signaling pathway, RNA process and protein synthesis, resulting in the accumulation of proteins and ribosomes in proper embryo cells and promoting the maturation of somatic embryos. Our study is the first to use an integrated approach to study SE in hybrid sweetgum. The results of our study are an important starting point for future analyses and provide new insights useful for exploring alternative strategies and possibilities.

DATA AVAILABILITY STATEMENT

The data presented in the study are deposited in the NCBI repository, accession number PRJNA762421.

AUTHOR CONTRIBUTIONS

JFZ, LK, and JZ designed the study. SQ and RZ conducted the experiments, analyzed the data, and drafted the manuscript. CH, HL, JY, TZ, YF, and SC critically reviewed and improved the manuscript. All authors have read and approved the final version of the manuscript.

FUNDING

This work was supported by National Forestry and Grassland Administration Promotion Project of China (2020133102), the project fund (Somatic embryogenesis and efficient propagation technology in trees) provided by Beijing Advanced Innovation Center for Tree Breeding by Molecular Design, Forestry Science and Technology Innovation Special Project of Jiangxi Province (2019-16), the Fundamental Research Funds for the Central Universities (2019ZY39), the Fundamental Research Funds for the Central Universities (2015ZCQ-SW-02), Major Science and Technology Special Project of Xuchang, Henan province, China (20170112006).

ACKNOWLEDGMENTS

We would like to show our special thanks to Shenzhou Lvpeng Agricultural Technology Co., Ltd. for all of its supports to this study.

SUPPLEMENTARY MATERIAL

The Supplementary Material for this article can be found online at: https://www.frontiersin.org/articles/10.3389/fpls.2021.751866/full#supplementary-material

REFERENCES

Alemanno, L., Berthouly, M., and Michaux-Ferrière, N. (1996). Histology of somatic embryogenesis from floral tissues cocoa. *Plant Cell Tissue Organ Cult.* 46, 187–194. doi: 10.1007/BF02307094

Ayil-Gutierrez, B., Galaz-Avalos, R., Pena-Cabrera, E., and Loyola-Vargas, V. (2013). Dynamics of the concentration of IAA and some of its conjugates during the induction of somatic embryogenesis in Coffea canephora. *Plant Signal. Behav.* 8:e26998. doi: 10.4161/psb.26998

Boutilier, K., Offringa, R., Sharma, V. K., Kieft, H., Ouellet, T., Zhang, L., et al. (2002). Ectopic expression of BABY BOOM triggers a conversion from vegetative to embryonic growth. *Plant Cell* 14, 1737–1749. doi: 10.1105/tpc.001941

Cabrera-Ponce, J. L., González-Gómez, I. A., León-Ramírez, C. G., Sánchez-Arreguín, J. A., and Jofre Y Garfias, A. E. (2018). Somatic Embryogenesis in Common BeanPhaseolus vulgaris L. *Methods Mol. Biol.* 1815, 189–206. doi: 10.1007/978-1-4939-8594-4_12

Chen, C., Chen, H., He, Y., and Xia, R. J. B. (2018). TBtools, a toolkit for biologists integrating various biological data handling tools with a user-friendly interface. *bioRxiv* [Preprint]. doi: 10.1101/289660

Chen, Q., Westfall, C. S., Hicks, L. M., Wang, S., and Jez, J. M. (2010). Kinetic basis for the conjugation of auxin by a GH3 family indole-acetic acid-amido synthetase. *J. Biol. Chem.* 285, 29780–29786. doi: 10.1074/jbc.M110.146431

Chen, Y., Xu, X., Liu, Z., Zhang, Z., XuHan, X., Lin, Y., et al. (2020). Global scale transcriptome analysis reveals differentially expressed genes involve in

early somatic embryogenesis in Dimocarpus longan Lour. *BMC Genomics* 21:4. doi: 10.1186/s12864-019-6393-7

Chu, Z., Chen, J., Sun, J., Dong, Z., Yang, X., Wang, Y., et al. (2017). De novo assembly and comparative analysis of the transcriptome of embryogenic callus formation in bread wheat (Triticum aestivum L.). *BMC Plant Biol.* 17:244. doi: 10.1186/s12870-017-1204-2

Danyluk, J., Perron, A., Houde, M., Limin, A., Fowler, B., Benhamou, N., et al. (1998). Accumulation of an acidic dehydrin in the vicinity of the plasma membrane during cold acclimation of wheat. *Plant Cell* 10, 623–638. doi: 10.1105/tpc.10.4.623

Dodeman, V. L., Ducreux, G., and Kreis, M. (1997). REVIEW ARTICLE: zygotic embryogenesis versus somatic embryogenesis. *J. Exp. Bot.* 48, 1493–1509. doi: 10.1093/jxb/48.8.1493

Dure, L. III, Crouch, M., Harada, J., Ho, T. H., Mundy, J., Quatrano, R., et al. (1989). Common amino acid sequence domains among the LEA proteins of higher plants. *Plant Mol. Biol.* 12, 475–486. doi: 10.1007/bf00036962

Elhiti, M., Stasolla, C., and Wang, A. (2013). Molecular regulation of plant somatic embryogenesis. *In Vitro Cell. Dev. Biol. Plant* 49, 631–642. doi: 10.1007/s11627-013-9547-3

Elhiti, M., Tahir, M., Gulden, R. H., Khamiss, K., and Stasolla, C. (2010). Modulation of embryo-forming capacity in culture through the expression of Brassica genes involved in the regulation of the shoot apical meristem. *J. Exp. Bot.* 61, 4069–4085. doi: 10.1093/jxb/erq222

Feher, A. (2019). Callus, Dedifferentiation, Totipotency, Somatic Embryogenesis: what These Terms Mean in the Era of Molecular Plant Biology?. *Front. Plant Sci.* 10:536. doi: 10.3389/fpls.2019.00536

Fernandez, D. E., Heck, G. R., Perry, S. E., Patterson, S. E., Bleecker, A. B., and Fang, S.-C. J. T. P. C. (2000). The embryo MADS domain factor AGL15 acts postembryonically: inhibition of perianth senescence and abscission via constitutive expression. *Plant Cell* 12, 183–197. doi: 10.1105/tpc.12.2.183

Florea, L., Song, L., and Salzberg, S. L. (2013). Thousands of exon skipping events differentiate among splicing patterns in sixteen human tissues. *F1000Res.* 2:188. doi: 10.12688/f1000research.2-188.v2

Freitas, N. C., Barreto, H. G., Torres, L. F., Freire, L. L., Rodrigues, L. A. Z., Diniz, L. E. C., et al. (2019). In silico and in vivo analysis of ABI3 and VAL2 genes during somatic embryogenesis of Coffea arabica: competence acquisition and developmental marker genes. *Plant Cell Tissue Organ Cult.* 137, 599–611. doi: 10.1007/s11240-019-01594-7

Gaj, M. D., Zhang, S., Harada, J. J., and Lemaux, P. G. (2005). Leafy cotyledon genes are essential for induction of somatic embryogenesis of Arabidopsis. *Planta* 222, 977–988. doi: 10.1007/s00425-005-0041-y

Gaudino, R. J., and Pikaard, C. S. (1997). Cytokinin induction of RNA polymerase I transcription in Arabidopsis thaliana. *J. Biol. Chem.* 272, 6799–6804. doi: 10.1074/jbc.272.10.6799

Harding, E. W., Tang, W., Nichols, K. W., Fernandez, D. E., and Perry, S. E. (2003). Expression and maintenance of embryogenic potential is enhanced through constitutive expression of AGAMOUS-Like 15. *Plant Physiol.* 133, 653–663. doi: 10.1104/pp.103.023499

Hecht, V., Vielle-Calzada, J.-P., Hartog, M. V., Schmidt, E. D. L., Boutilier, K., Grossniklaus, U., et al. (2001). The Arabidopsis Somatic Embryogenesis Receptor Kinase 1 Gene Is Expressed in Developing Ovules and Embryos and Enhances Embryogenic Competence in Culture. *Plant Physiol.* 127, 803–816. doi: 10.1104/pp.010324

Ikeda, M., Umehara, M., and Kamada, H. (2006). Embryogenesis-related genes; its expression and roles during somatic and zygotic embryogenesis in carrot and Arabidopsis. *Plant Biotechnol.* 23, 153–161. doi: 10.5511/plantbiotechnology.23.153

Jamaluddin, N. D., Mohd Noor, N., and Goh, H. H. (2017). Genome-wide transcriptome profiling of Carica papaya L. embryogenic callus. *Physiol. Mol. Biol. Plants* 23, 357–368. doi: 10.1007/s12298-017-0429-8

Jiménez, V. M. (2005). Involvement of Plant Hormones and Plant Growth Regulators on in vitro Somatic Embryogenesis. *Plant Growth Regul.* 47, 91–110. doi: 10.1007/s10725-005-3478-x

Karami, O., and Saidi, A. (2010). The molecular basis for stress-induced acquisition of somatic embryogenesis. *Mol. Biol. Rep.* 37, 2493–2507. doi: 10.1007/s11033-009-9764-3

Kieffer, M., Neve, J., and Kepinski, S. (2010). Defining auxin response contexts in plant development. *Curr. Opin. Plant Biol.* 13, 12–20. doi: 10.1016/j.pbi.2009.10.006

Kim, D., Langmead, B., and Salzberg, S. L. (2015). HISAT: a fast spliced aligner with low memory requirements. *Nat. Methods* 12, 357–360. doi: 10.1038/nmeth.3317

Kiyosue, T., Yamaguchi-Shinozaki, K., Shinozaki, K., Higashi, K., Satoh, S., Kamada, H., et al. (1992). Isolation and characterization of a cDNA that encodes ECP31, an embryogenic-cell protein from carrot. *Plant Mol. Biol.* 19, 239–249. doi: 10.1007/BF00027345

Koukalova, B., Fojtova, M., Lim, K. Y., Fulnecek, J., Leitch, A. R., and Kovarik, A. (2005). Dedifferentiation of tobacco cells is associated with ribosomal RNA gene hypomethylation, increased transcription, and chromatin alterations. *Plant Physiol.* 139, 275–286. doi: 10.1104/pp.105.061788

Kulinska-Lukaszek, K., Tobojka, M., Adamiok, A., and Kurczynska, E. J. B. (2012). Expression of the BBM gene during somatic embryogenesis of Arabidopsis thaliana. *Biol. Plant.* 56, 389–394. doi: 10.1007/s10535-012-0105-3

Lai, Z., and Chen, C. (2002). Changes of Endogenous Phytohormones in the Process of Somatic Embryogenesis in Longan (Dimocarpus longan Lour.). *Chin. J. Trop. Crops* 23, 41–47.

Langfelder, P., and Horvath, S. (2008). WGCNA: an R package for weighted correlation network analysis. *BMC Bioinformatics* 9:559. doi: 10.1186/1471-2105-9-559

Li, M., Wang, R., Liu, Z., Wu, X., and Wang, J. (2019). Genome-wide identification and analysis of the WUSCHEL-related homeobox (WOX) gene family in allotetraploid Brassica napus reveals changes in WOX genes during polyploidization. *BMC Genomics* 20:317. doi: 10.1186/s12864-019-5684-3

Liu, J., Sheng, L., Xu, Y., Li, J., Yang, Z., Huang, H., et al. (2014). WOX11 and 12 are involved in the first-step cell fate transition during de novo root organogenesis in Arabidopsis. *Plant Cell* 26, 1081–1093. doi: 10.1105/tpc.114.122887

Liu, S., Zenda, T., Dong, A., Yang, Y., Wang, N., and Duan, H. (2021). Global Transcriptome and Weighted Gene Co-expression Network Analyses of Growth-Stage-Specific Drought Stress Responses in Maize. *Front. Genet.* 12:645443. doi: 10.3389/fgene.2021.645443

Maere, S., Heymans, K., and Kuiper, M. J. B. (2005). BiNGO: a Cytoscape plugin to assess overrepresentation of gene ontology categories in biological networks. *Bioinformatics* 21, 3448–3449. doi: 10.1093/bioinformatics/bti551

Malik, M. R., Wang, F., Dirpaul, J. M., Zhou, N., Polowick, P. L., Ferrie, A. M., et al. (2007). Transcript profiling and identification of molecular markers for early microspore embryogenesis in Brassica napus. *Plant Physiol.* 144, 134–154. doi: 10.1104/pp.106.092932

Mantiri, F. R., Kurdyukov, S., Lohar, D. P., Sharopova, N., Saeed, N. A., Wang, X. D., et al. (2008). The transcription factor MtSERF1 of the ERF subfamily identified by transcriptional profiling is required for somatic embryogenesis induced by auxin plus cytokinin in Medicago truncatula. *Plant Physiol.* 146, 1622–1636. doi: 10.1104/pp.107.110379

Matsuo, N., Makino, M., and Banno, H. (2011). Arabidopsis ENHANCER OF SHOOT REGENERATION (ESR)1 and ESR2 regulate in vitro shoot regeneration and their expressions are differentially regulated. *Plant Sci.* 181, 39–46. doi: 10.1016/j.plantsci.2011.03.007

Maulidiya, A. U. K., Sugiharto, B., Dewanti, P., and Handoyo, T. (2020). Expression of somatic embryogenesis-related genes in sugarcane (Saccharum officinarum L.). *J. Crop Sci. Biotechnol.* 23, 207–214. doi: 10.1007/s12892-020-00024-x

Merkle, S. (2018). The ups and downs of developing hybrid sweetgum varieties for the US bioenergy and pulp and paper industries: a 20-year case study. *Clonal Trees in the Bioeconomy Age: opportunities and Challenges*. Vienna, Austria: International Union of Forest Research Organizations (IUFRO).

Merkle, S., Montello, P., Kormanik, T., and Le, H. (2010). Propagation of novel hybrid sweetgum phenotypes for ornamental use via somatic embryogenesis. *Propag. Ornam. Plants* 10, 220–226.

Merkle, S. A., Neu, K. A., Battle, P. J., and Bailey, R. L. J. P. S. (1998). Somatic embryogenesis and plantlet regeneration from immature and mature tissues of sweetgum (*Liquidambar styraciflua*). *Plant Sci.* 132, 169–178. doi: 10.1016/S0168-9452(98)00007-7

Michaux-Ferrière, N., and Carron, M.-P. (1989). Histology of early somatic embryogenesis in Hevea brasiliensis: the importance of the timing of subculturing. *Plant Cell Tissue Organ Cult.* 19, 243–256. doi: 10.1007/BF00043351

Palovaara, J., Hallberg, H., Stasolla, C., and Hakman, I. (2010). Comparative expression pattern analysis of WUSCHEL-related homeobox 2 (WOX2) and WOX8/9 in developing seeds and somatic embryos of the gymnosperm Picea abies. *New Phytol.* 188, 122–135. doi: 10.1111/j.1469-8137.2010.03336.x

Panahi, B., and Hejazi, M. A. (2021). Weighted gene co-expression network analysis of the salt-responsive transcriptomes reveals novel hub genes in green halophytic microalgae Dunaliella salina. *Sci. Rep.* 11:1607. doi: 10.1038/s41598-020-80945-3

Quiroz-Figueroa, F. R., Rojas-Herrera, R., Galaz-Avalos, R. M., and Loyola-Vargas, V. M. (2006). Embryo production through somatic embryogenesis can be used to study cell differentiation in plants. *Plant Cell Tissue Organ Cult.* 86, 285–301. doi: 10.1007/s11240-006-9139-6

Rupps, A., Raschke, J., Rummler, M., Linke, B., and Zoglauer, K. (2016). Identification of putative homologs of Larix decidua to BABYBOOM (BBM), LEAFY COTYLEDON1 (LEC1), WUSCHEL-related HOMEOBOX2 (WOX2) and SOMATIC EMBRYOGENESIS RECEPTOR-like KINASE (SERK) during somatic embryogenesis. *Planta* 243, 473–488. doi: 10.1007/s00425-015-2409-y

Sagare, A., Lee, Y., Lin, T., Chen, C., and Tsay, H. J. P. S. (2000). Cytokinin-induced somatic embryogenesis and plant regeneration in Corydalis yanhusuo (Fumariaceae)—a medicinal plant. *Plant Sci.* 160, 139–147. doi: 10.1016/S0168-9452(00)00377-0

Shannon, P., Markiel, A., Ozier, O., Baliga, N. S., Wang, J. T., Ramage, D., et al. (2003). Cytoscape: a software environment for integrated models of biomolecular interaction networks. *Genome Res.* 13, 2498–2504. doi: 10.1101/gr.1239303

Siriwardana, S., and Nabors, M. W. (1983). Tryptophan enhancement of somatic embryogenesis in rice. *Plant Physiol.* 73, 142–146. doi: 10.1104/pp.73.1.142

Sun, R., Lin, F., Huang, P., and Zheng, Y. (2016). Moderate Genetic Diversity and Genetic Differentiation in the Relict Tree Liquidambar formosana Hance Revealed by Genic Simple Sequence Repeat Markers. *Front. Plant Sci.* 7:1411. doi: 10.3389/fpls.2016.01411

Thimm, O., Bläsing, O., Gibon, Y., Nagel, A., Meyer, S., Krüger, P., et al. (2004). MAPMAN: a user-driven tool to display genomics data sets onto diagrams of metabolic pathways and other biological processes. *Plant J.* 37, 914–939.

Tsuwamoto, R., Fukuoka, H., and Takahata, Y. (2007). Identification and characterization of genes expressed in early embryogenesis from microspores of Brassica napus. *Planta* 225, 641–652. doi: 10.1007/s00425-006-0388-8

Tvorogova, V. E., Lebedeva, M. A., and Lutova, L. A. (2015). Expression of WOX and PIN genes during somatic and zygotic embryogenesis in Medicago truncatula. *Russ. J. Genet.* 51, 1189–1198. doi: 10.1134/s1022795415120121

Vanneste, S., and Friml, J. (2009). Auxin: a trigger for change in plant development. *Cell* 136, 1005–1016. doi: 10.1016/j.cell.2009.03.001

Vendrame, W., Holliday, C., and Merkle, S. (2001). Clonal propagation of hybrid sweetgum (*Liquidambar styraciflua* × L. formosana) by somatic embryogenesis. *Plant Cell Rep.* 20, 691–695. doi: 10.1007/s00299-001-0394-z

Vondráková, Z., Eliášová, K., Fischerová, L., and Vágner, M. (2011). The role of auxins in somatic embryogenesis of Abies alba. *Cent. Eur. J. Biol.* 6, 587–596. doi: 10.2478/s11535-011-0035-7

Weigel, D., and Jürgens, G. J. N. (2002). Stem cells that make stems. *Nature* 415, 751–754. doi: 10.1038/415751a

Wen, L., Li, W., Parris, S., West, M., Lawson, J., Smathers, M., et al. (2020). Transcriptomic profiles of non-embryogenic and embryogenic callus cells in a highly regenerative upland cotton line (Gossypium hirsutum L.). *BMC Dev. Biol.* 20:25. doi: 10.1186/s12861-020-00230-4

Wickramasuriya, A. M., and Dunwell, J. M. (2015). Global scale transcriptome analysis of Arabidopsis embryogenesis in vitro. *BMC Genomics* 16:301. doi: 10.1186/s12864-015-1504-6

Wu, X., Dabi, T., and Weigel, D. (2005). Requirement of homeobox gene STIMPY/WOX9 for Arabidopsis meristem growth and maintenance. *Curr. Biol.* 15, 436–440. doi: 10.1016/j.cub.2004.12.079

Xiao, Y., Li, J., Zhang, Y., Zhang, X., Liu, H., Qin, Z., et al. (2020). Transcriptome analysis identifies genes involved in the somatic embryogenesis of Eucalyptus. *BMC Genomics* 21:803. doi: 10.1186/s12864-020-07214-5

Xu, Z., Zhang, C., Zhang, X., Liu, C., Wu, Z., Yang, Z., et al. (2013). Transcriptome profiling reveals auxin and cytokinin regulating somatic embryogenesis in different sister lines of cotton cultivar CCRI24. *J. Integr. Plant Biol.* 55, 631–642. doi: 10.1111/jipb.12073

Yang, X., and Zhang, X. (2010). Regulation of Somatic Embryogenesis in Higher Plants. *Crit. Rev. Plant Sci.* 29, 36–57. doi: 10.1080/07352680903436291

Yang, X., Zhang, X., Yuan, D., Jin, F., Zhang, Y., and Xu, J. (2012). Transcript profiling reveals complex auxin signalling pathway and transcription regulation involved in dedifferentiation and redifferentiation during somatic embryogenesis in cotton. *BMC Plant Biol.* 12:110. doi: 10.1186/1471-2229-12-110

Zhang, B., and Horvath, S. (2005). A general framework for weighted gene co-expression network analysis. *Stat. Appl. Genet. Mol. Biol.* 4:17. doi: 10.2202/1544-6115.1128

Zhao, M. L., Chen, M. S., Ni, J., Xu, C. J., Yang, Q., and Xu, Z. F. (2020). Comparative transcriptome analysis of gynoecious and monoecious inflorescences reveals regulators involved in male flower development in the woody perennial plant Jatropha curcas. *Plant Reprod.* 33, 191–204. doi: 10.1007/s00497-020-00396-8

Zhao, W., Langfelder, P., Fuller, T., Dong, J., Li, A., and Hovarth, S. (2010). Weighted gene coexpression network analysis: state of the art. *J. Biopharm. Stat.* 20, 281–300. doi: 10.1080/10543400903572753

Zheng, L., Ma, J., Song, C., An, N., Zhang, D., Zhao, C., et al. (2017). Genome-wide identification and expression profiling analysis of brassinolide signal transduction genes regulating apple tree architecture. *Acta Physiol. Plant.* 39:177. doi: 10.1007/s11738-017-2479-5

Zheng, Y., Ren, N., Wang, H., Stromberg, A. J., and Perry, S. E. (2009). Global identification of targets of the Arabidopsis MADS domain protein AGAMOUS-Like15. *Plant Cell* 21, 2563–2577. doi: 10.1105/tpc.109.068890

Zhou, X., Zheng, R., Liu, G., Xu, Y., Zhou, Y., Laux, T., et al. (2017). Desiccation Treatment and Endogenous IAA Levels Are Key Factors Influencing High Frequency Somatic Embryogenesis in Cunninghamia lanceolata (Lamb.) Hook. *Front. Plant Sci.* 8:2054. doi: 10.3389/fpls.2017.02054

Zimmerman, J. L. (1993). Somatic embryogenesis: a model for early development in higher plants. *Plant Cell* 5:1411. doi: 10.1105/tpc.5.10.1411

Conflict of Interest: The authors declare that the research was conducted in the absence of any commercial or financial relationships that could be construed as a potential conflict of interest.

frontiers in Plant Science

ORIGINAL RESEARCH
published: 26 November 2021
doi: 10.3389/fpls.2021.771464

The Chemical Environment at Maturation Stage in *Pinus* spp. Somatic Embryogenesis: Implications in the Polyamine Profile of Somatic Embryos and Morphological Characteristics of the Developed Plantlets

Antonia Maiara Marques do Nascimento[1], Luiza Giacomolli Polesi[2], Franklin Panato Back[2], Neusa Steiner[3], Miguel Pedro Guerra[2], Ander Castander-Olarieta[1], Paloma Moncaleán[1†] and Itziar Aurora Montalbán[1*†]*

[1] Neiker-BRTA, Centro de Arkaute, Campus Agroalimentario de Arkaute, Arkaute, Spain, [2] Laboratório de Fisiologia do Desenvolvimento e Genética Vegetal, Universidade Federal de Santa Catarina, Florianópolis, Brazil, [3] Departamento de Botânica, Universidade Federal de Santa Catarina, Florianópolis, Brazil

Changes in the chemical environment at the maturation stage in *Pinus* spp. somatic embryogenesis will be a determinant factor in the conversion of somatic embryos to plantlets. Furthermore, the study of biochemical and morphological aspects of the somatic embryos could enable the improvement of somatic embryogenesis in *Pinus* spp. In the present work, the influence of different amino acid combinations, carbohydrate sources, and concentrations at the maturation stage of *Pinus radiata* D. Don and *Pinus halepensis* Mill. was analyzed. In *P. radiata*, the maturation medium supplemented with 175 mM of sucrose and an increase in the amino acid mixture (1,100 mgL^{-1} of L-glutamine, 1,050 mgL^{-1} of L-asparagine, 350 mgL^{-1} of L-arginine, and 35 mgL^{-1} of L-proline) promoted bigger embryos, with a larger stem diameter and an increase in the number of roots in the germinated somatic embryos, improving the acclimatization success of this species. In *P. halepensis*, the maturation medium supplemented with 175 mM of maltose improved the germination of somatic embryos. The increase in the amount of amino acids in the maturation medium increased the levels of putrescine in the germinated somatic embryos of *P. halepensis*. We detected significant differences in the amounts of polyamines between somatic plantlets of *P. radiata* and *P. halepensis*; putrescine was less abundant in both species. For the first time, in *P. radiata* and *P. halepensis* somatic embryogenesis, we detected the presence of cadaverine, and its concentration changed according to the species.

Keywords: ***Pinus halepensis, Pinus radiata*, sugars, amino acids, osmolality**

OPEN ACCESS

Edited by:
Jonny E. Scherwinski-Pereira, Brazilian Agricultural Research Corporation (EMBRAPA), Brazil

Reviewed by:
Rodrigo J. Hasbun, University of Concepción, Chile
Pedro Alfonso Sansberro, Instituto de Botánica del Nordeste (IBONE), Consejo Nacional de Investigaciones Científicas y Técnicas (CONICET), Argentina

***Correspondence:**
Paloma Moncaleán
pmoncalean@neiker.eus
Itziar Aurora Montalbán
imontalban@neiker.eus

† These authors have contributed equally to this work

Specialty section:
This article was submitted to Plant Development and EvoDevo, a section of the journal Frontiers in Plant Science

Received: *06 September 2021*
Accepted: *28 October 2021*
Published: *26 November 2021*

Citation:
do Nascimento AMM, Polesi LG, Back FP, Steiner N, Guerra MP, Castander-Olarieta A, Moncaleán P and Montalbán IA (2021) The Chemical Environment at Maturation Stage in Pinus spp. Somatic Embryogenesis: Implications in the Polyamine Profile of Somatic Embryos and Morphological Characteristics of the Developed Plantlets. Front. Plant Sci. 12:771464. doi: 10.3389/fpls.2021.771464

INTRODUCTION

Somatic embryogenesis has been suggested as the most promising method for vegetative propagation for a large number of conifers (Gupta et al., 1993), and it can help to capture the greatest benefits from traditional breeding programs by multiplying trees with desirable characteristics for plantation forestry (Pullman and Bucalo, 2014).

Pinus radiata D. Don is one of the most planted pine species in the world, and it is widely used to produce quality wood (Escandon et al., 2017; Fuentes-Sepulveda et al., 2020). Alternatively, *Pinus halepensis* Mill. is a species with high forest importance for reforestation because it can survive under low precipitation levels, and it has higher tolerance to thermal and drought stress (Gazol et al., 2017; Manrique-Alba et al., 2020; Quinto et al., 2021).

Previous studies carried out in our laboratory have demonstrated that *P. radiata* and *P. halepensis* showed different responses to abiotic stress such as drought and high temperature (do Nascimento et al., 2020). Also, in previous experiments, we have focused on the optimization of somatic embryogenesis (SE) processes. In this sense, the optimization of initiation and proliferation stages of SE in *P. radiata* (Montalbán et al., 2010, 2012) and *P. halepensis* (Montalbán et al., 2013) has been our objective in recent years. Recently, some studies focused on promoting and improving the embryogenic process in terms of quality and quantity of somatic embryos (ses) obtained by reduction of water availability in *P. radiata* (Garcia-Mendiguren et al., 2016; Castander-Olarieta et al., 2020) and *P. halepensis* (Pereira et al., 2016, 2017; do Nascimento et al., 2020) have been carried out. However, the rate of germination (%) and the subsequent conversion into plantlets is sometimes low (do Nascimento et al., 2020), and additional research is needed to increase somatic plantlet regeneration (Montalbán and Moncaleán, 2019).

The source of organic nitrogen is an important component of the culture media for the success of the SE process, and in this sense, amino acids are commonly used to improve the maturation of ses, modifying its type and concentration (Gerdakaneh et al., 2011; Satish et al., 2016; Dahrendorf et al., 2018). As Maruyama et al. (2021) reported, the presence of organic nitrogen improved the production of ses. Casein and glutamine are usually used in the SE of conifers (Afele and Saxena, 1995; Pullman and Bucalo, 2014; Dahrendorf et al., 2018), but, in some species, such as *Pinus patula* Schiede ex Schltdl. and Cham. or *P. radiata,* it has been seen that mixtures of amino acids can be more beneficial for the process (Malabadi and Van Staden, 2005; Montalbán et al., 2010).

The beneficial effect of chemical environment modification in a certain stage of the process can be witnessed not only in that stage but also in the following ones (Dahrendorf et al., 2018; Castander-Olarieta et al., 2019; do Nascimento et al., 2020). In this case, the presence of a carbon source in the culture medium is necessary due to the heterotrophy conditions in which the cells grow (Yaseen et al., 2013). In addition, the carbohydrates used in the SE increase the osmolality of the culture medium (Smeekens et al., 2010; Kube et al., 2014). The most common source of carbohydrates in the culture medium is sucrose, but other carbohydrates such us maltose have been used in other *Pinus* species such as *Pinus nigra* Arn. (Salaj et al., 2019). Therefore, due to the different responses observed in the SE of various species, it is necessary to carry out a study about the effect of different carbohydrates and concentrations (Yang et al., 2020).

Polyamines are considered to be a class of compounds related to cellular proliferation (Bais and Ravishankar, 2002; Jimenez, 2005) and play an important role in the regulation of SE (Silveira et al., 2004; Jin et al., 2020; Sundararajan et al., 2021). Moreover, polyamines (PAs) could be associated with the stress caused in plant cells, protecting them and upregulating stress-related genes (Alcazar et al., 2020; Kielkowska and Adamus, 2021). PAs levels vary according to each stage of SE, for example, during the intense cell division observed in the proliferation phase; higher diamine putrescine (Put) contents were reported (Minocha et al., 2004), whereas, in the maturation stage, where intense cell differentiation occurs, higher levels of triamine spermidine (Spd) and tetraamine spermine (Spm) were observed (Minocha et al., 2004; Gemperlova et al., 2009). In conifers, the accumulation of high levels of PAs was correlated also with the conversion of ses in plants (Gemperlova et al., 2009). Moreover, PAs have been considered as markers of SE competence in several species, such as *Oryza sativa* L. (Shoeb et al., 2001), *Medicago sativa* L. (Huang et al., 2001), and *Panax ginseng* C.A. Meyer (Monteiro et al., 2002).

In plants, the three most common PAs are Put, Spd, Spm (Bouchereau et al., 1999; Minocha et al., 2014), and cadaverine (Cad), which are rarely reported (Jancewicz et al., 2016). Additionally, as the amino acids are precursors of PAs biosynthesis, the exogenous addition of amino acids in the medium culture can directly influence PA profiles (Bagni and Tassoni, 2001; Pullman and Bucalo, 2014). The biosynthesis of Put, Spd, and Spm is directly related to arginine and ornithine (de Oliveira et al., 2018), while the biosynthesis of Cad is associated with lysine and ornithine (Liu et al., 2014). In *Araucaria angustifolia* Bert. O. Ktze., the ratio of PAs determined the transition from embryonal masses (EMs) to ses (Farias-Soares et al., 2014).

The aim of this work was to evaluate the influence of the different amino acid mixtures and carbohydrate sources, applied during the maturation stage of the SE, on the number and morphology of the ses obtained, their PAs profile, and the morphological characteristics of the *P. radiata* and *P. halepensis* plantlets developed.

MATERIALS AND METHODS

Plant Material

Embryonal masses (Ems) were obtained from immature cones of *P. radiata*, collected from four mother trees in a seed orchard set-up by Neiker-BRTA in Deba (Spain; latitude: 43°16′59″N, longitude: 2°17′59″W, elevation: 50 m) and of *P. halepensis*, collected from five mother trees in Berantevilla (Spain; latitude: 42°40′57.14″N, longitude: 2°51′29.95″W, elevation: 473 m). The immature seeds of both species were extracted and surface sterilized, following Montalbán et al. (2010, 2012). Seed coats

were removed, and intact megagametophytes were excised out aseptically and cultured on initiation media for both species; for *P. radiata*, the basal medium was Embryo Development Medium (EDM; Walter et al., 2005), and for *P. halepensis*, the basal medium used was the DCR medium (Gupta and Durzan, 1985). Initiation and proliferation were carried out following the protocols described by Montalbán et al. (2012, 2013) for *P. radiata* and *P. halepensis,* respectively. Five established cell lines (ECLs) were used for each experiment and species.

Amino Acid Supplementation Experiment

The maturation of *P. halepensis* and *P. radiata* EMs was carried out following the method described in Montalbán et al. (2010, 2013), respectively. Briefly, the EMs were suspended in a liquid basal medium without plant growth regulators and then filtered on a filter paper in a Büchner funnel. Aliquots containing 0.08 g of EMs on the filter papers were placed on each maturation media. The basal media (DCR for *P. halepensis* and EDM for *P. radiata*) were supplemented with 175 mM of sucrose, 9 gL^{-1} of Gelrite®, and 75 μM of abscisic acid (ABA) for *P. halepensis* or 60 μM of ABA for *P. radiata*; these maturation media were supplemented after autoclaving with different amino acid mixtures as described in **Table 1**: MIX I (Control) (Walter et al., 2005), MIX II – two times the concentration in the MIX I of the L-glutamine (Gln), L-asparagine (Asn), L-arginine (Arg), and L-proline (Pro); and MIX III – 4-fold the concentration in the MIX I of the Gln (**Table 1**).

Both, *P. radiata* and *P. halepensis* cultures were kept at 23°C and in darkness for 16 weeks on maturation media.

The germination of cotyledonary ses and the acclimatization of plantlets were performed according to Montalbán and Moncaleán (2019). Briefly, the ses were germinated for 8 weeks on half macronutrients LP [Quoirin and Lepoivre (1977), modified by Aitken-Christie et al. (1988)], supplemented with 2 gL^{-1} of activated charcoal and 9 gL^{-1} of Difco Agar granulated (Becton and Dickinson). First, petri dishes (90 mm × 15 mm) were used as containers, with the root caps of the ses pointing downward at an angle of approximately 60°. After this, the germinated plantlets were subcultured in the same medium for another month, but, in EcoBox® (Eco2Box/green filter: a polypropylene vessel with a "breathing" hermetic cover, 125 mm × 65 mm × 80 mm, Duchefa). The cultures were kept at 23°C under 16-h photoperiod at 120 $\mu molm^{-2}\ s^{-1}$ provided by cool white fluorescent tubes (TFL 58 W/33; Philips, France) (Montalbán and Moncaleán, 2019).

After the germination, the plantlets were acclimatized in 43-cm^3 pots, containing blond peat moss (Pindstrup, Ryomgård, Denmark): vermiculite (8:2, v/v) in the greenhouse under controlled conditions.

TABLE 1 | Different combinations of amino acids used in the maturation media (EDM and DCR) for *Pinus radiata* D. Don and *Pinus halepensis* Mill.

Amino acids	Treatments (mgL^{-1})		
	MIX I (Control)	MIX II	MIX III
L-glutamine	550	1100	2200
L-asparagine	525	1050	525
L-arginine	175	350	175
L-proline	17.5	35	17.5
L-citrulline	19.75	19.75	19.75
L-ornithine	19	19	19
L-lysine	13.75	13.75	13.75
L-alanine	10	10	10

Carbohydrate Supplementation Experiment

Pinus radiata and *P. halepensis* EMs obtained from the same materials and methods as in the amino acid supplementation experiment were used. The basal media described in amino acid supplementation experiment were supplemented with the MIX I (**Table 1**), and two different carbohydrate sources at two concentrations (four treatments) were assayed: 175 mM of sucrose (175 suc – control); 175 mM of maltose (175 mal); 350 mM of sucrose (350 suc), or 350 mM of maltose (350 mal). Cultures were kept at 23°C and in darkness for 16 weeks. Germination and acclimatization followed the same methodology described in the material and methods of the amino acid supplementation experiment.

Osmolality of the Maturation Media

The osmolality ($mosmkg^{-1}$) of all maturation media was measured at the onset of the experiment using a Micro-Osmometer Automatic (Löser Messtechnik, Berlin, Germany) according to the manufacturer's instructions. Aliquots containing 100 μl of each maturation medium without Gelrite® were measured, and the measurements were replicated three times (Montalbán et al., 2010).

Free Polyamine Content Determination

Germinated ses obtained after 2 weeks in germination media were analyzed for free PA content for *P. radiata* (amino acid supplementation experiment) and *P. halepensis* (amino acid supplementation experiment and carbohydrate supplementation experiment). Germinated ses of *P. radiata* were not analyzed for the carbohydrate supplementation experiment, because we only obtained viable germinated ses for the control treatment. PA quantification was carried out according to Silveira et al. (2004) with some modifications. Samples (200 mg of fresh weight) were briefly grounded in 1.4 ml of 5% perchloric acid (v/v) in a Precellys® shaker. After 1 h, the extraction solution was centrifuged for 20 min (15,000 *g*, 4°C), and supernatant was collected. The pellet was once again suspended in 0.2 ml of perchloric acid and centrifuged for 20 min (15,000 *g*, 4°C). Both extraction solutions were merged, homogenized, and frozen at −20°C for future analysis. Derivatization was performed according to Silveira et al. (2004), where 40 μl of each sample was mixed with 20 μl of diaminoheptane 0.05 mM, 50 μl of saturated sodium carbonate solution, and 100 μl of dansyl chloride in acetone 1.8 mM. After 50 min of incubation in the dark at 70°C, 25 μl of proline was added to the solution, followed by another 30-min incubation at room temperature.

After that, 200 μl of toluene was added, the solution was vigorously shaken, and 175 μl of the superior organic phase with PAs was taken to a SpeedVac freeze dryer for 40 min at 40°C. Finally, pellets were suspended in 175 μl of acetonitrile and were ready for high-performance liquid chromatography (HPLC) quantification. Mobile phases were composed of (A) 10% (v/v) acetonitrile/ultrapure water pH 3.5 adjusted with HCl and (B) 100% of acetonitrile. The gradient started at 65% of B and lasted for 11 min; it was raised to 100% B for up to 25 min, maintained in 100% B until 35.5 min and then returned to 65% B until the end at 44 min. The flow rate was constantly 1 ml min^{-1}, and oven temperature was maintained at 40°C. The stationary phase was a 5-μm Shim-pack CLC-ODS (M) 100 Å column with 250 mm × 4.6 mm equipped with a pre-column, both from Shimadzu®. The analyses were carried out in a Shimadzu Prominence HPLC equipped with a fluorescent detector configured to excitation of 340 nm and emission of 510-nm wavelengths. To determine PA concentration, peak areas of 20 μl samples were compared to triplicates of peak areas of correspondent standards of Put, Spd, Cad, and Spm, bought from Sigma-Merck®. The 1,7-diaminoheptane (DAH) (Sigma-Merck®) was used as an internal standard. Total free PAs were obtained by the sum of the individual PAs. Moreover, based on the fact that Put is a precursor to Spd and Spm (Mustafavi et al., 2018), the Put/(Spd + Spm) ratio was calculated. The final concentration of PAs was expressed in $mmol\mu g^{-1}$.

Data Collection and Statistical Analysis

For both species *P. radiata* and *P. halepensis*, the number of normal (NNE) (white to yellowish, non-germinating, with a distinct hypocotyl region, and at least three cotyledons) and abnormal mature ses (NAE) (germinating precociously, with fewer than three cotyledons or bearing abnormally shaped cotyledons) (Montalbán et al., 2010) per gram of embryogenic tissue was recorded. Also, the length (mm) (LE) and width (mm) (WE) of 240 (Amino acid supplementation experiment on each species) and 320 (Carbohydrate supplementation experiment on each species) NNE, and the LE/WE ratio of NNE were calculated. Embryos were obtained in three of the five maturated lines in both experiments and species. From the total of ses obtained, one half of them was germinated for the morphological analysis and the other half was germinated for the determination of free PA content. After 2 months in a germination medium, the germination rate for the NNE was calculated. Before *ex vitro* planting, the length of plantlets (mm), the length of aerial part (mm), the width of needles (mm), the stem diameter (mm), and the root length (mm) were measured with a digital caliber, and the number of secondary roots was counted in 10 plantlets per treatment. The percentage of acclimatization was calculated after 2 months in *ex vitro* conditions.

For Amino acid supplementation experiment, three different amino acid mixtures were tested in five ECLs for each species (R2, R9, R54, R82, and R137 for *P. radiata* and H48, H51, H149, H153, and H204 for *P. halepensis*) in a factorial with four repetitions (plates) per maturation condition and embryogenic cell line. In carbohydrate supplementation experiment, four different carbohydrates sources and concentrations were tested in five ECLs for *P. radiata* (R2, R9, R54, R82, and R137) and for *P. halepensis* (H48, H51, H149, H153, and H204) in a factorial with four repetitions.

For the effect of the ECLs on each of the variables of this study, an analysis of deviance was performed, followed by a Tukey *post hoc* test ($\alpha = 0.05$), adjusted for multiple comparisons. To obtain robust conclusions, ECL factors were introduced into all the models as a block variable to reduce variability and analyze the effect of the culture medium more accurately.

In Amino acid supplementation experiment, the width of needles and stem diameter, for *P. radiata*, and *P. halepensis*, respectively, were square root transformed, and an ANOVA was performed. Multiple comparisons were made using the Tukey *post hoc* tests ($\alpha = 0.05$). The same occurred in the carbohydrate supplementation experiment, for *P. halepensis*, in length of plantlets, width of needles, and the stem diameter.

In the amino acid supplementation experiment, for *P. radiata*, the NNE, length of plantlets, stem diameter, root part length, and number of secondary roots did not fulfill homoscedasticity and normality assumptions for ANOVA, and therefore, a Kruskal–Wallis was performed. The same occurred for the characteristics: *P. halepensis*—NNE, NAE, length of normal embryo, width of normal embryo, width of needles, and number of secondary roots in the amino acid supplementation experiment; *P. radiata*—length of normal embryo and the LE/WE ratio of ses in the carbohydrate supplementation experiment; and *P. halepensis*—NNE, NAE, length of normal

TABLE 2 | Analysis of deviance for the osmolality ($mosmkg^{-1}$ water) of the different maturation media (MM) for *Pinus radiata* D. Don (EDM medium) and *Pinus halepensis* Mill (DCR medium).

Treatment	df	EDM medium		DCR medium	
		***F*-value**	***P*-value**	***F*-value**	***P*-value**
MM	5	3751	≤0.05*	3388	≤0.05*

**Significant differences at $p \leq 0.05$; df, degrees of freedom. The values in the table correspond to the Kruskal–Wallis test.*

TABLE 3 | Osmolality ($mosmkg^{-1}$ water) of the maturation media (M ± *SE*) for *Pinus radiata* D. Don (EDM medium) and *Pinus halepensis* Mill. (DCR medium).

Treatment	EDM medium (± *SE*)	DCR medium (± *SE*)
Control (175 mM of sucrose + MIX I)	277 ± 0.00^{d}	260 ± 0.67^{d}
175 mM of maltose	240 ± 0.58^{e}	226 ± 0.88^{e}
350 mM of sucrose	484 ± 3.18^{a}	499 ± 1.00^{a}
350 mM of maltose	428 ± 2.08^{b}	411 ± 2.65^{b}
MIX II	294 ± 1.00^{c}	278 ± 2.96^{c}
MIX III	293 ± 0.88^{c}	272 ± 0.33^{c}

Different letters within a column show significant differences in the means observed by a Kruskal–Wallis test. MIX I (Control) – 550 mgL^{-1} of L-glutamine (Gln), 525 mgL^{-1} of L-asparagine (Asn), 175 mgL^{-1} of L-arginine (Arg), 17.5 mgL^{-1} of L-proline (Pro), 19.75 mgL^{-1} of L-citrulline, 19 mgL^{-1} of L-ornithine, 13.75 mgL^{-1} of L-lysine, and 10 mgL^{-1} of L-alanine; MIX II – two times the concentration in the MIX I of the Gln, Asn, Arg, and Pro; and MIX III – 4-fold the concentration in the MIX I of the Gln. SE, standard error.

TABLE 4 | Analysis of deviance for the effect of the different mixes of amino acids (MA) in the maturation stage in: the number of normal and abnormal somatic embryos per 0.08 g of embryonal masses, the morphological characteristics of normal embryos, the germination of somatic embryos, the morphological characteristics, and the acclimatization of plantlets of *Pinus radiata* D. Don and *Pinus halepensis* Mill., respectively.

Characteristics	Source	df	*Pinus radiata*		*Pinus halepensis*	
			F-value	*P*-value	*F*-value	*P*-value
Number of normal embryos	MA	2	3.85	$>0.05^{ns}$	0.37[1]	$>0.05^{ns}$
Number of abnormal embryos	MA	2	6.06	$\leq 0.01^{**}$	0.98[1]	$>0.05^{ns}$
Length of normal embryos	MA	2	6.29	$\leq 0.01^{**}$	52.48[1]	$\leq 0.05^{*}$
Width of normal embryos	MA	2	13.24	$\leq 0.05^{*}$	51.21[1]	$\leq 0.05^{*}$
Length/Width ratio (mm)	MA	2	18.40	$>0.05^{ns}$	21.45	$>0.05^{ns}$
Germination of somatic embryos	MA	2	16.61	$\leq 0.001^{***}$	22.59	$\leq 0.01^{**}$
Length of plantlets (mm)	MA	2	4.47	$>0.05^{ns}$	0.58	$>0.05^{ns}$
Length of aerial part (mm)	MA	2	0.59	$>0.05^{ns}$	0.13	$>0.05^{ns}$
Width of needles (mm)	MA	2	1.78	$>0.05^{ns}$	5.48[1]	$>0.05^{ns}$
Stem diameter (mm)	MA	2	10.12	$\leq 0.05^{*}$	1.16	$>0.05^{ns}$
Root part length (mm)	MA	2	2.73	$>0.05^{ns}$	1.44	$>0.05^{ns}$
Number of secondary roots	MA	2	7.11	$\leq 0.05^{*}$	0.18[1]	$>0.05^{ns}$
Acclimatization of plantlets	MA	2	56.85	$\leq 0.001^{***}$	19.33	$>0.05^{ns}$

; **; * Significant differences at $p \leq 0.05$, $p \leq 0.01$, or $p \leq 0.001$, respectively; ^{ns}, non-significant at $p \leq 0.05$; MA, mixes of amino acids; df, degrees of freedom. [1]The values in the table correspond to the Kruskal–Wallis test.*

embryo, width of normal embryo, the LE/WE ratio of ses, root part length, and number of secondary roots in the carbohydrate supplementation experiment.

For free PA content determination, the data obtained were *log* transformed, and an ANOVA was performed, followed by Tukey *post hoc* tests ($\alpha = 0.05$), adjusted for multiple comparisons.

The data were analyzed using R software®, version 3.6.1. (R Core Team, 2017).

RESULTS

Osmolality of the Maturation Medium

Statistically significant differences in the osmolality were observed between all the culture media with different compositions of amino acids and carbohydrates (**Table 2**). The osmolalities of the maturation media (EDM and DCR) were significantly higher when they contained 350 mM of sucrose compared with other carbohydrate and amino acid treatments (**Table 3**). Both of the maturation media supplemented with 175 mM of maltose showed the lowest values of osmolality (**Table 3**). Statistically significant differences were observed when comparing the osmolality of MIX I (control) with the media supplemented with MIX II and MIX III (**Table 3**).

Amino Acid Supplementation Experiment

Regarding the amino acid mixture used in the maturation media, statistically significant differences were found for all the parameters evaluated in *P. radiata* (NAE, LE, WE, germination of ses, and acclimatization of plantlets) except for the NNE and LE/WE ratio (**Table 4**).

In the case of *P. halepensis*, the different mixtures of amino acids produced statistically significant differences for the LE, WE, and germination rate of NNE (**Table 4**). However, the mixture of different amino acids did not show statistically significant differences for the NNE, NAE, the LE/WE ratio, and acclimatization of plantlets (**Table 4**).

Figures 1A,B show normal and aberrant morphologies of ses of *P. radiata*, respectively. For *P. radiata*, although non-significant differences were found among the different combinations of amino acids when compared with the production of NNE (**Table 4**), an increase of the NNE in MIX II and MIX III (240 and 317 $sesg^{-1}$ fresh weight, respectively),

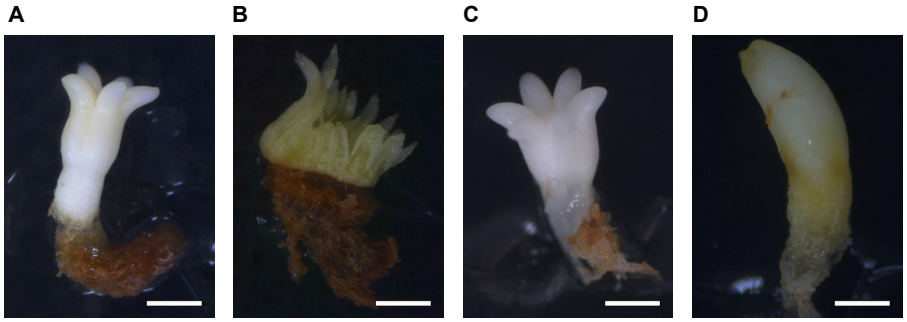

FIGURE 1 | Somatic embryos showing different morphologies: *Pinus radiata* D. Don normal somatic **(A)**, bar = 1.44 mm; *P. radiata* abnormal somatic embryo **(B)**, bar = 1.85 mm; *Pinus halepensis* Mill. normal somatic embryos **(C)**, bar = 0.84 mm; *P. halepensis* abnormal somatic embryos **(D)**, bar = 0.60 mm.

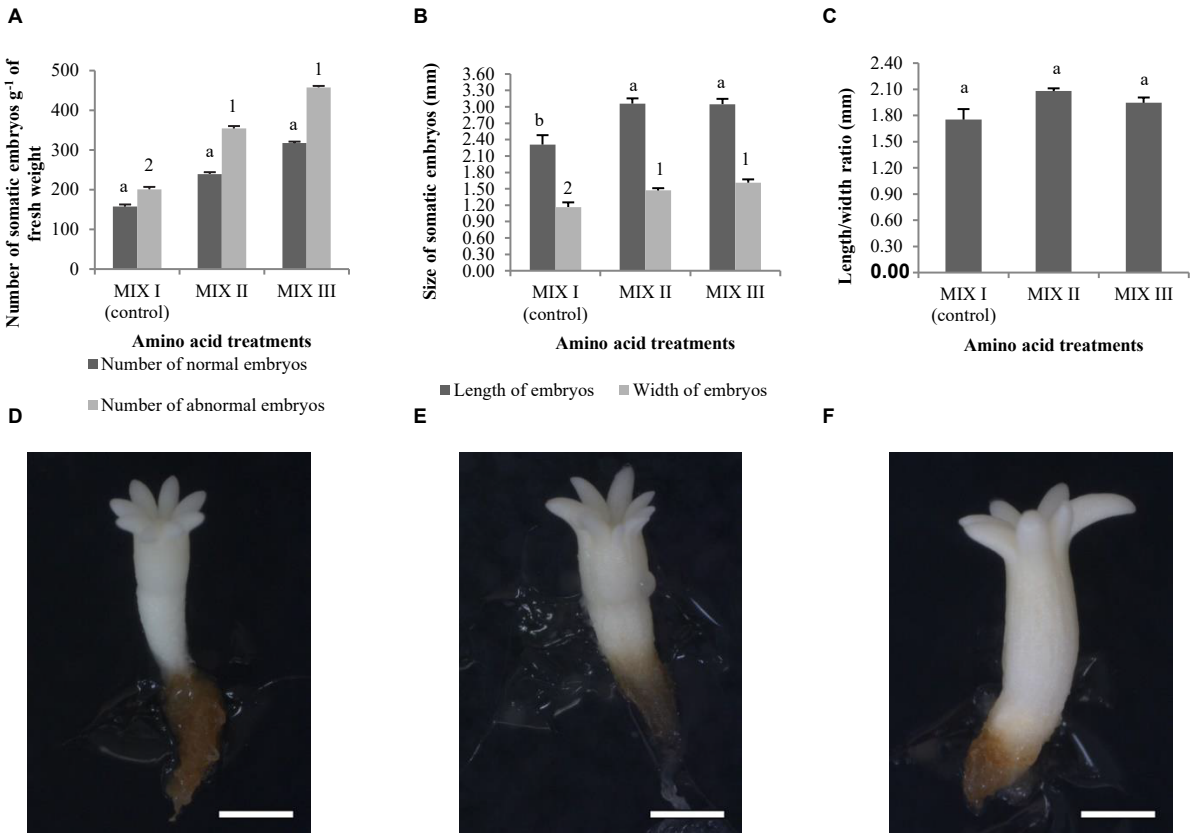

FIGURE 2 | *Pinus radiata* D. Don somatic embryos of maturation media supplemented with different mixes of amino acids. Number of normal and abnormal somatic embryos **(A)**; the length and width of normal embryos **(B)**; and the length/width ratio of normal embryos **(C)**. Bars indicate standard errors. Significant differences at $p \leq 0.05$ are indicated by different letters or numbers. *Pinus radiata* normal somatic obtained from maturation media supplemented with different mixes of amino acids. MIX I **(D),** bar = 1.85 mm; MIX II **(E)**, bar = 1.85 mm; and MIX III **(F)**, bar = 1.85 mm. MIX I (Control) – 550 mgL^{-1} of L-glutamine (Gln), 525 mgL^{-1} of L-asparagine (Asn), 175 mgL^{-1} of L-arginine (Arg), 17.5 mgL^{-1} of L-proline (Pro), 19.75 mgL^{-1} of L-citrulline, 19 mgL^{-1} of L-ornithine, 13.75 mgL^{-1} of L-lysine, and 10 mgL^{-1} of L-alanine; MIX II – two times the concentration in the MIX I of the Gln, Asn, Arg, and Pro; and MIX III – 4-fold the concentration in the MIX I of the Gln.

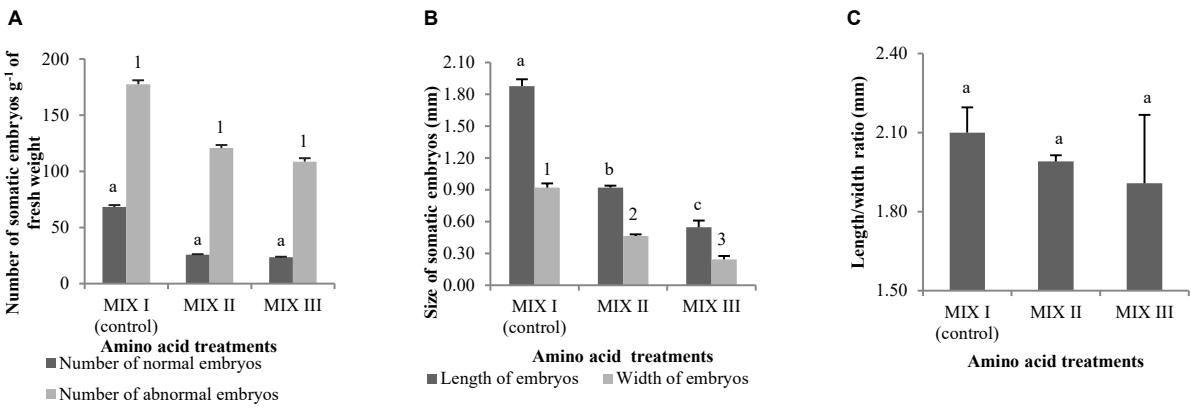

FIGURE 3 | *Pinus halepensis* Mill. somatic embryos obtained per gram of embryonal masses matured in different mixes of amino acids. Number of normal and abnormal somatic embryos **(A)**; the length and width of normal embryos **(B)**; the length/width ratio of normal embryos **(C)**. Bars indicate standard errors. Significant differences at $p \leq 0.05$ are indicated by different letters or numbers. MIX I (Control) – 550 mgL^{-1} of L-glutamine (Gln), 525 mgL^{-1} of L-asparagine (Asn), 175 mgL^{-1} of L-arginine (Arg), 17.5 mgL^{-1} of L-proline (Pro), 19.75 mgL^{-1} of L-citrulline, 19 mgL^{-1} of L-ornithine, 13.75 mgL^{-1} of L-lysine, and 10 mgL^{-1} of L-alanine; MIX II – two times the concentration in the MIX I of the Gln, Asn, Arg, and Pro; and MIX III – 4-fold the concentration in the MIX I of the Gln.

compared with the control (MIX I – 157 sesg^{-1} fresh weight), was observed (**Figure 2A**). The same tendency was found for the NAE, with a statistically significant increase for NAE in media supplemented with MIX II and MIX III when compared to MIX I (**Figure 2A**). Moreover, we observed that treatments MIX II and MIX III induced an increase in LE and WE when compared to control treatment (MIXI) (**Figures 2B,D,E,F**). With respect to the LE/WE ratio, non-significant differences were found between the different combinations of amino acids (**Figure 2C**).

Figures 1C,D show normal and aberrant morphologies of ses of *P. halepensis*, respectively. For *P. halepensis*, although non-significant differences were found among the different mixtures of amino acids for NNE and NAE (**Table 4**), the highest NNE and NAE were recorded in control conditions (68 sesg^{-1} fresh

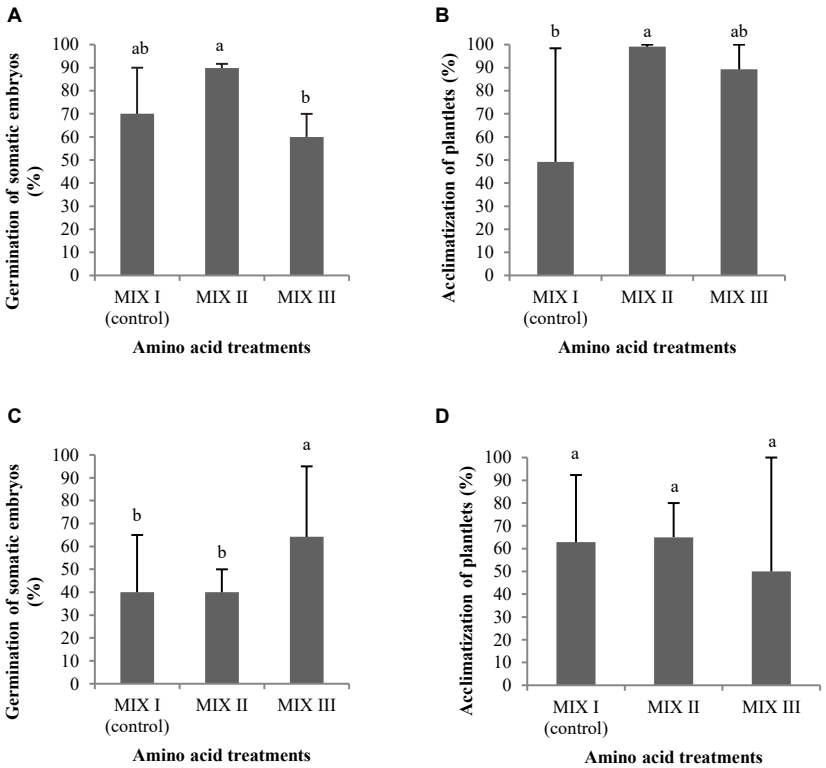

FIGURE 4 | *Pinus radiata* D. Don germination (%) of somatic embryos maturated in a medium supplemented with different mixes of amino acids **(A)**. Acclimatization (%) of plantlets of *P. radiata* obtained from somatic embryos maturated in a medium supplemented with different mixes of amino acids **(B)**. Germination (%) of somatic embryos of *Pinus halepensis* Mill. maturated in a medium supplemented with different mixes of amino acids **(C)**. Acclimatization (%) of plantlets of *P. halepensis* obtained from somatic embryos maturated in a medium supplemented with different mixes of amino acids **(D)**. Bars indicate standard errors. Significant differences at $p \leq 0.05$ are indicated by different letters. MIX I (Control) – 550 mgL^{-1} of L-glutamine (Gln), 525 mgL^{-1} of L-asparagine (Asn), 175 mgL^{-1} of L-arginine (Arg), 17.5 mgL^{-1} of L-proline (Pro), 19.75 mgL^{-1} of L-citrulline, 19 mgL^{-1} of L-ornithine, 13.75 mgL^{-1} of L-lysine, and 10 mgL^{-1} of L-alanine; MIX II – two times the concentration in the MIX I of the Gln, Asn, Arg, and Pro; and MIX III – 4-fold the concentration in the MIX I of the Gln.

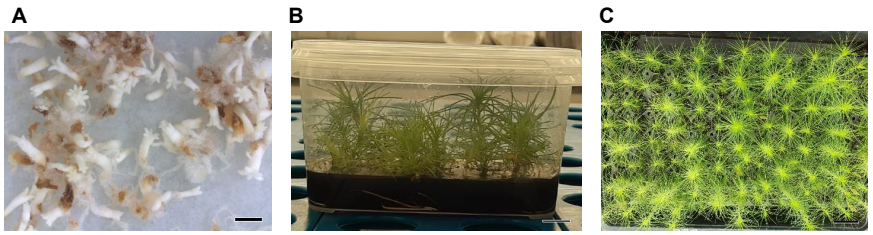

FIGURE 5 | Maturation, germination, and acclimatization of somatic embryos from *Pinus radiata* D. Don embryogenic cell lines. Somatic embryos after 4 months in a maturation medium **(A)**, bar = 3 mm; somatic plantlets after 3 months in a germination medium **(B)**, bar = 1.4 cm; plantlets derived from normal cotyledonary somatic embryos growing in the greenhouse **(C)**, bar = 2.35 cm. The maturation medium was supplemented with MIX I (Control) – 550 mgL^{-1} of L-glutamine (Gln), 525 mgL^{-1} of L-asparagine (Asn), 175 mgL^{-1} of L-arginine (Arg), 17.5 mgL^{-1} of L-proline (Pro), 19.75 mgL^{-1} of L-citrulline, 19 mgL^{-1} of L-ornithine, 13.75 mgL^{-1} of L-lysine, and 10 mgL^{-1} of L-alanine; MIX II – two times the concentration in the MIX I of the Gln, Asn, Arg, and Pro; and MIX III – 4-fold the concentration in the MIX I of the Gln.

TABLE 5 | Morphological characteristics of *P. radiata* D. Don somatic plantlets developed from ECLs maturated in a culture medium supplemented with different amino acid compositions (M ± SE).

Morphological characteristics	MIX I – control	MIX II	MIX III
Length of plantlets (mm)	38.13 ± 6.72	47.17 ± 5.83	47.66 ± 5.86
Length of aerial part (mm)	6.13 ± 0.59	6.91 ± 0.52	6.28 ± 0.48
Width of needles (mm)	0.28 ± 0.32	0.32 ± 0.02	0.27 ± 0.01
Root length (mm)	26.58 ± 4.04	20.68 ± 4.69	24.40 ± 4.66

MIX I (Control) – 550 mgL^{-1} of L-glutamine (Gln), 525 mgL^{-1} of L-asparagine (Asn), 175 mgL^{-1} of L-arginine (Arg), 17.5 mgL^{-1} of L-proline (Pro), 19.75 mgL^{-1} of L-citrulline, 19 mgL^{-1} of L-ornithine, 13.75 mgL^{-1} of L-lysine, and 10 mgL^{-1} of L-alanine; MIX II – two times the concentration in the MIX I of the Gln, Asn, Arg, and Pro; and MIX III – 4-fold the concentration in the MIX I of the Gln. SE, standard error.

weight for NNE and 178 sesg^{-1} fresh weight for NAE); MIX II showed intermediate values, and MIX III presented the lowest values (23 sesg^{-1} fresh weight for NNE and 109 sesg^{-1} fresh weight for NAE) (**Figure 3A**).

Pinus halepensis ses developed in control conditions (MIX I) were significantly wider and longer than those obtained in MIX II and MIX III. Significantly lower LE and WE values were obtained when the maturation medium was supplemented with a 4-fold concentration of Gln (MIX III) (**Figure 3B**), although the LE/WE ratio did not show significant differences (**Figure 3C**).

As observed in **Figure 4A**, the best germination percentage of *P. radiata* was obtained in those embryos coming from ECLs maturated on a medium supplemented with double the concentration of Gln, Asn, Arg, and Pro (MIX II), but not in relation to control treatment (MIX I). However, the treatment with 4-fold of Gln (MIX III) promoted a significant decrease of the ses germination with respect to MIX II (**Figure 4A**). Plantlets of *P. radiata* survived after acclimatization with significantly higher percentage of acclimatization when coming from ses maturated on a culture medium supplemented with MIX II (99%) and MIX III (89.29%) than compared with control (MIX I) (49.21%) (**Figures 4B**, **5**).

Pinus halepensis germination significantly increased in those embryos coming from ECLs maturated in the presence of 4-fold the concentration of Gln (MIX III) (64%) when compared to results obtained with other amino acid combinations (**Figure 4C**). Significant differences were not observed for the survival of plantlets in the greenhouse (62.82, 65, and 50% for MIX I, MIX II, and MIX III, respectively) (**Figure 4D**).

Statistically significant differences for the stem diameter and the number of secondary roots were observed in *P. radiata* (**Table 4**). The mean length of the plantlets ranged from 38.13 to 47.66 mm, and this value was divided into the aerial part and the root part (**Table 5**). In this sense, the width of the needle varied between 0.27 and 0.32 mm (**Table 5**). The MIX II and MIX III promoted a significant increase of the stem diameter when compared to the control (**Figure 6A**). The same tendency was observed with the number of secondary roots where the MIX II promoted a significant increase in the number of secondary roots (**Figures 6B,C**).

When evaluating the morphological characteristics of the germinated ses developed from ECLs of *P. halepensis* maturated in the presence of different combinations of amino acids, no statistically significant differences were observed (**Tables 4**, **6**).

Carbohydrate Supplementation Experiment

The carbohydrate sources significantly affected the NNE, the NAE, and the LE (**Table 7**). For NAE, WE, and the LE/WE ratio, a significant interaction between the carbohydrate sources and concentrations was observed (**Table 7**). Finally, the carbohydrate source and the carbohydrate concentration had a significant effect on the germination rates, but there was no interaction between the previously mentioned factors (**Table 7**).

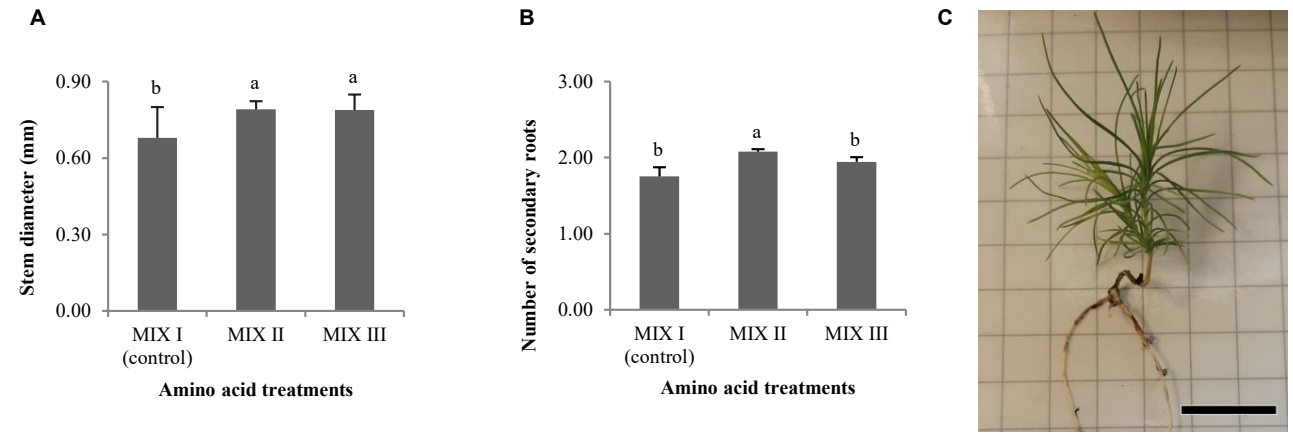

FIGURE 6 | Morphological characteristics of *Pinus radiata* D. Don plantlets, stem diameter (mm) **(A)**, and number of secondary roots **(B)**. Bars indicate standard errors. Significant differences at $p \leq 0.05$ are indicated by different letters or numbers. Plantlet obtained from somatic embryos maturated in EDM medium with MIX II **(C)**, bar = 2 cm. MIX I (Control) – 550 mgL^{-1} of L-glutamine (Gln), 525 mgL^{-1} of L-asparagine (Asn), 175 mgL^{-1} of L-arginine (Arg), 17.5 mgL^{-1} of L-proline (Pro), 19.75 mgL^{-1} of L-citrulline, 19 mgL^{-1} of L-ornithine, 13.75 mgL^{-1} of L-lysine and 10 mgL^{-1} of L-alanine; MIX II, twice the concentration in the MIX I of the Gln, Asn, Arg, and Pro; MIX III, fourfold the concentration in the MIX I of the Gln.

TABLE 6 | Morphological characteristics of *Pinus halepensis* Mill. somatic plantlets developed from ECLs maturated in a culture medium supplemented with different amino acid compositions (M ± SE).

Morphological characteristics	MIX I – control	MIX II	MIX III
Length of plantlets (mm)	77.96 ± 11.50	97.63 ± 15.37	92.98 ± 12.76
Length of aerial part (mm)	6.94 ± 1.24	7.58 ± 1.09	6.82 ± 1.05
Width of needles (mm)	0.31 ± 0.03	0.27 ± 0.03	0.23 ± 0.01
Stem diameter (mm)	0.68 ± 0.05	0.79 ± 0.06	0.79 ± 0.07
Root length (mm)	38.09 ± 10.23	64.64 ± 13.27	57.19 ± 10.47
Number of secondary roots	2 ± 0.36	2 ± 0.31	2 ± 0.29

MIX I (Control) – 550 mgL^{-1} of L-glutamine (Gln), 525 mgL^{-1} of L-asparagine (Asn), 175 mgL^{-1} of L-arginine (Arg), 17.5 mgL^{-1} of L-proline (Pro), 19.75 mgL^{-1} of L-citrulline, 19 mgL^{-1} of L-ornithine, 13.75 mgL^{-1} of L-lysine, and 10 mgL^{-1} of L-alanine; MIX II – two times the concentration in the MIX I of the Gln, Asn, Arg, and Pro; and MIX III – 4-fold the concentration in the MIX I of the Gln. SE, standard error.

Two types of carbohydrates in both concentrations produced normal and aberrant embryos in *P. radiata*. However, the use of sucrose in the maturation medium, regardless of the concentration, resulted in a significantly higher NNE (**Figure 7A**). In this regard, we also observed the highest NAE in the medium of maturation with sucrose but only at a concentration of 175 suc (control) in relation to maltose (**Figure 7A**). In addition, the same tendency was observed for LE and WE (**Figure 7B**), with the development of longer and wider ses in the maturation medium with sucrose, regardless of the concentration. The ses maturated in media with sucrose presented a significantly higher LE/WE ratio than those obtained from a medium with 350 mal (**Figure 7C**).

In *P. halepensis*, the NNE was not affected by the different carbohydrate treatments tested (**Table 7** and **Figure 7D**). However, NAE, LE, WE, and the LE/WE ratio were significantly affected by the interaction between the carbohydrate source and the concentration (**Table 7**). The medium with the highest maltose concentration produced a significantly higher number of NAE than the sucrose media (**Figure 7D**).

The LE and the WE of *P. halepensis* obtained in a maturation medium supplemented with 175 mal were significantly higher than the LE obtained after maturation with other carbohydrate sources or concentrations (**Figure 7E**). As noted in **Figure 7F**, a significantly higher LE/WE ratio was observed in ses maturated with the highest concentration of 350 suc when compared to results obtained in ses from media supplemented with maltose. Thus, higher concentrations of carbohydrates caused the formation of less developed embryos (**Figure 8**).

The use of 175 suc promoted a germination percentage of 70%, while the other treatments promoted a percentage lower than 15% for ses of *P. radiata* (**Figure 9A**). However, the ses maturated at a maturation medium with a high concentration of maltose did not promote the germination of ses (**Figure 9A**). Viable plantlets were only obtained in those embryos germinated in culture media with 175 suc where the acclimatization percentage was 49.21%.

The ses of *P. halepensis* maturated with 175 mal showed a germination percentage significantly (**Table 7**) higher than the rest of the treatments assayed (**Figure 9B**). However, the ses maturated with 350 suc did not germinate. The plantlets of *P. halepensis* from the maturation treatment with 175 mM of maltose survived after acclimatization in a significantly higher percentage (100%) than those that came from a treatment with 175 suc (control) (**Table 7** and **Figures 9C**, **10**). In contrast, the worst results were obtained in the treatment with a higher concentration of maltose (**Figure 9C**).

The length of aerial part and number of secondary roots were significantly affected by the different carbohydrate sources, and no differences were observed for the other morphological characteristics studied in *P. halepensis* (**Table 7**). It was observed that 175 mal promoted an increase in the aerial part and number

TABLE 7 | Analysis of deviance for the effect of the different carbohydrate sources (CS) and concentrations (CC) in the maturation stage in the number of normal and abnormal somatic embryos per 0.08 g of embryonal masses; the morphological characteristics of normal embryos; the germination of somatic embryos of *Pinus radiata* D. Don and *Pinus halepensis* Mill., respectively; and the effect of the different CS in the germination of somatic embryos, the morphological characteristics, and the acclimatization of plantlets *P. halepensis*.

Characteristics	Source	df	*Pinus radiata*		*Pinus halepensis*	
			F-value	*P*-value	*F*-value	*P*-value
Number of normal embryos	CS	1	5.15	≤0.05*	2.80[1]	>0.05^{ns}
	CC	1	0.67	>0.05^{ns}	0.90	>0.05^{ns}
	SC × CC	3	1.93	>0.05^{ns}	2.80	>0.05^{ns}
Number of abnormal embryos	CS	1	11.30	≤0.01**	16.89[1]	≤0.001***
	CC	1	1.45	>0.05^{ns}	0.27	>0.05^{ns}
	SC × CC	3	7.48	≤0.01**	16.90	≤0.001***
Length of normal embryos	CS	1	4.22[1]	≤0.05*	23.44[1]	≤0.05*
	CC	1	0.78	>0.05^{ns}	31.57	≤0.05*
	SC × CC	3	4.25	>0.05^{ns}	28.13	≤0.05*
Width of normal embryos	CS	1	0.44	>0.05^{ns}	32.10[1]	≤0.001***
	CC	1	0.65	>0.05^{ns}	20.19	≤0.001***
	SC × CC	3	20.17	≤0.01**	35.21	≤0.001***
Length/Width ratio (mm)	CS	1	5.86[1]	≤0.05*	12.88[1]	≤0.05*
	CC	1	1.08	>0.05^{ns}	3.16	>0.05^{ns}
	SC × CC	3	10.14	≤0.05*	17.21	≤0.05*
Germination of somatic embryos	CS	1	36.69	≤0.001***	82.11	≤0.001***
	CC	1	0.51	≤0.001***	–	–
	SC × CC	3	0.51	>0.05^{ns}	–	–
Length of plantlets (mm)	CS	1	–	–	1.21	>0.05^{ns}
Length of aerial part (mm)	CS	1	–	–	0.89	≤0.05*
Width of needles (mm)	CS	1	–	–	0.47	>0.05^{ns}
Stem diameter (mm)	CS	1	–	–	1.07	>0.05^{ns}
Root part length (mm)	CS	1	–	–	2.56[1]	>0.05^{ns}
Number of secondary roots	CS	1	–	–	4.76[1]	≤0.05*
Acclimatization of plantlets	CS	1	–	–	20.15	≤0.001***

; **; * Significant differences at p ≤ 0.05, p ≤ 0.01, or p ≤ 0.001, respectively; ^{ns}, non-significant at p ≤ 0.05; df, degrees of freedom. [1]The values in the table correspond to the Kruskal–Wallis test.*

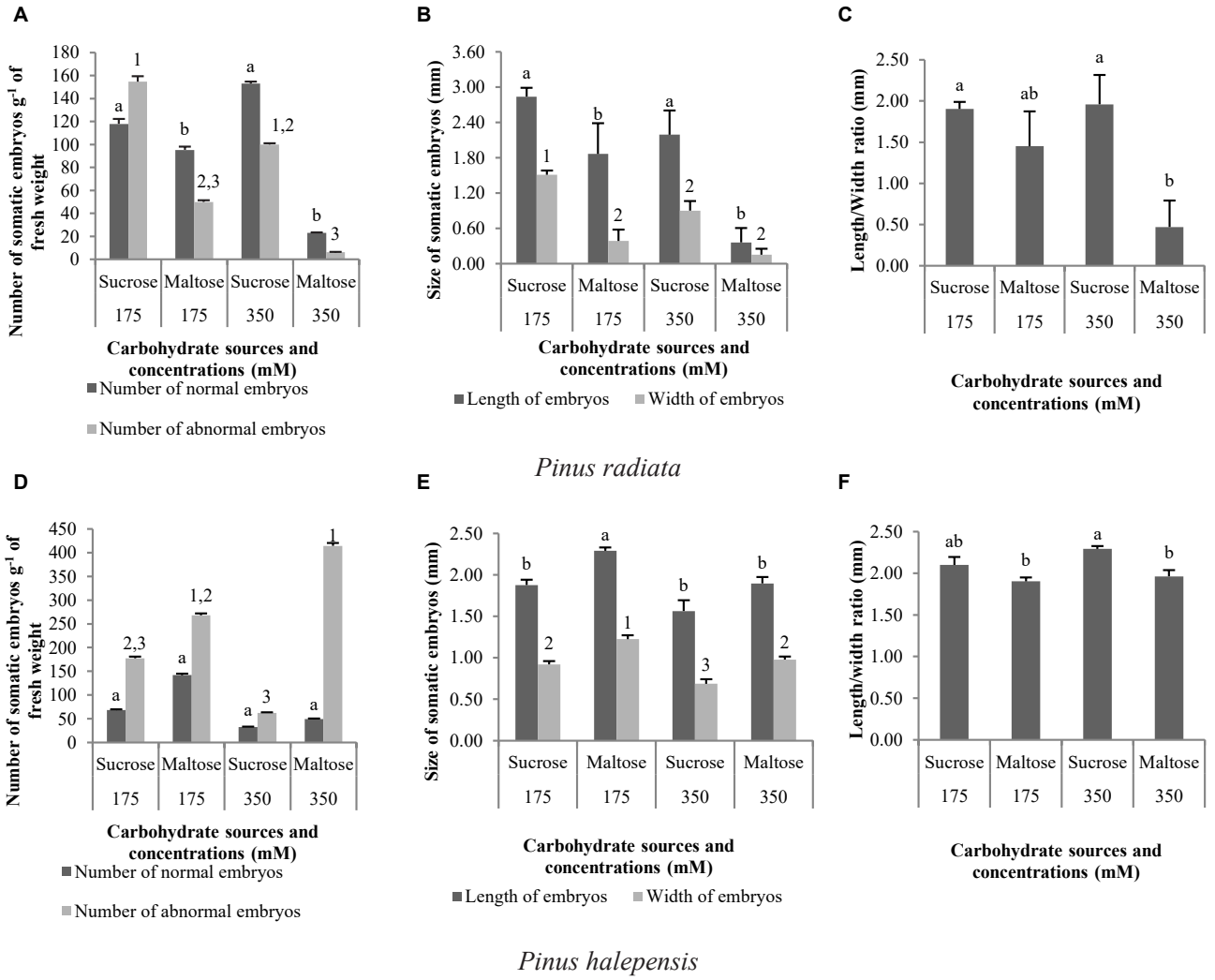

FIGURE 7 | *Pinus radiata* D. Don and *Pinus halepensis* Mill. somatic embryos obtained per gram of embryonal masses matured in different carbohydrate sources and concentrations. Number of normal and abnormal somatic embryos **(A,D)**; the length and width of normal embryos **(B,E)**; and the length/width ratio of normal embryos **(C,F)**. Bars indicate standard errors. Significant differences at $p \leq 0.05$ are indicated by different letters or numbers.

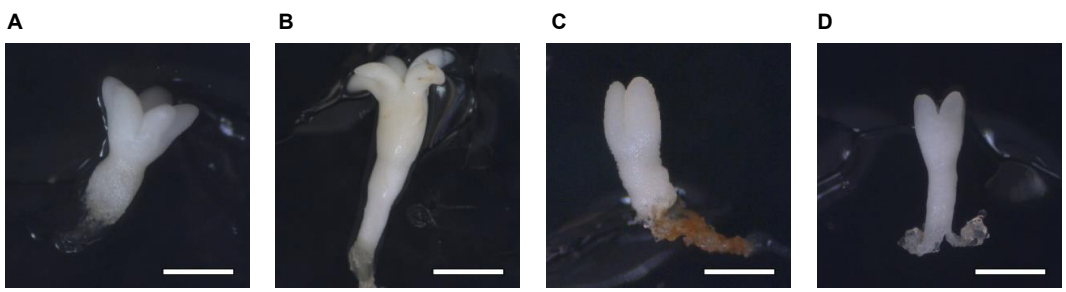

FIGURE 8 | Somatic embryos of *Pinus halepensis* Mill. maturated in the DCR medium supplemented with: 175 mM of sucrose **(A)**, bar = 1 mm; 175 mM of maltose **(B)**, bar = 1.57 mm; 350 mM of sucrose **(C)**, bar = 0.57 mm; and 350 mM of maltose **(D)**, bar = 1 mm.

of secondary roots in comparison with 175 suc (**Figures 11A,B**). Although significantly statistical differences were not found for the other morphological characteristics, an increase in the length of plantlets was observed in those obtained from the ses developed in a maturation medium supplemented with 175 mal (**Table 8** and **Figure 11C**). The same results were observed for a

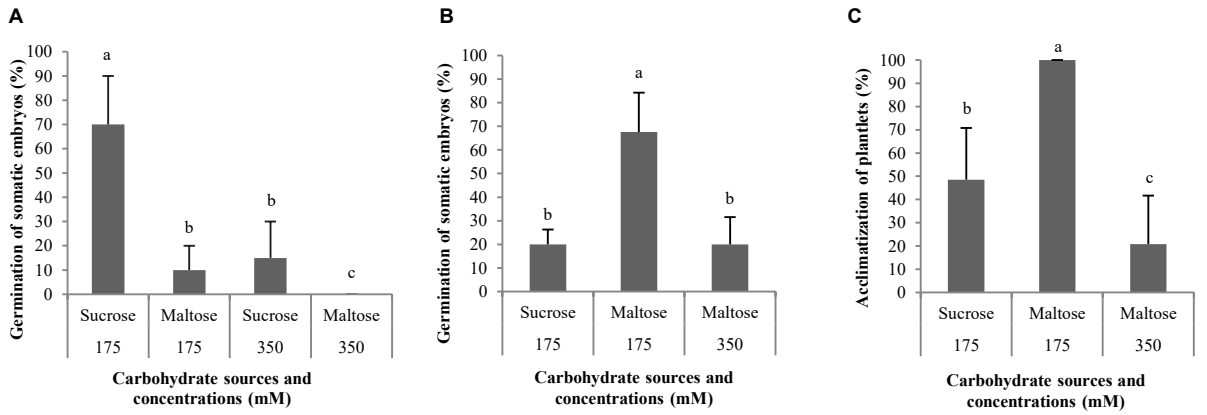

FIGURE 9 | Germination (%) of somatic embryos of *Pinus radiata* D. Don maturated in a medium supplemented with different carbohydrate sources and concentrations **(A)**. Germination (%) of somatic embryos of *Pinus halepensis* Mill. maturated in a medium supplemented with different carbohydrate sources and concentrations **(B)**. Acclimatization (%) of plantlets of *P. halepensis* obtained from somatic embryos maturated in a medium supplemented with different carbohydrate sources and concentrations **(C)**. Bars indicate standard errors. Significant differences at $p \leq 0.05$ are indicated by different letters.

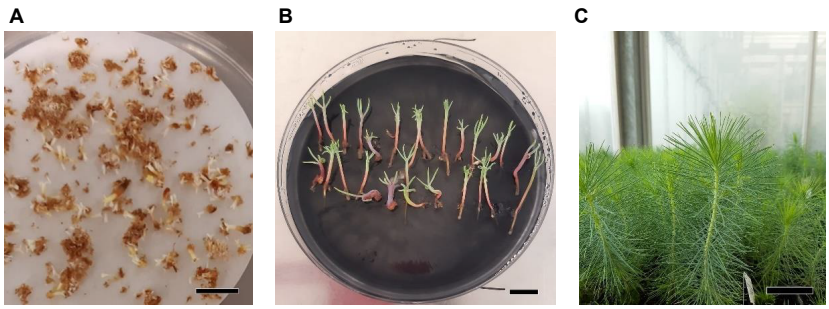

FIGURE 10 | Maturation, germination, and acclimatization of somatic embryos from *Pinus halepensis* Mill. embryogenic cell lines. Somatic embryos after 4 months in a maturation medium **(A)**, bar = 1 cm; somatic plantlets after 3 months cultivated in a germination medium **(B)**, bar = 1 cm; plantlets derived from normal cotyledonary somatic embryos growing in the greenhouse **(C)**, bar = 3 cm. The maturation medium was supplemented with MIX I (Control) – 550 mgL^{-1} of L-glutamine (Gln), 525 mgL^{-1} of L-asparagine (Asn), 175 mgL^{-1} of L-arginine (Arg), 17.5 mgL^{-1} of L-proline (Pro), 19.75 mgL^{-1} of L-citrulline, 19 mgL^{-1} of L-ornithine, 13.75 mgL^{-1} of L-lysine, and 10 mgL^{-1} of L-alanine; MIX II – two times the concentration in the MIX I of the Gln, Asn, Arg, and Pro; and MIX III – 4-fold the concentration in the MIX I of the Gln.

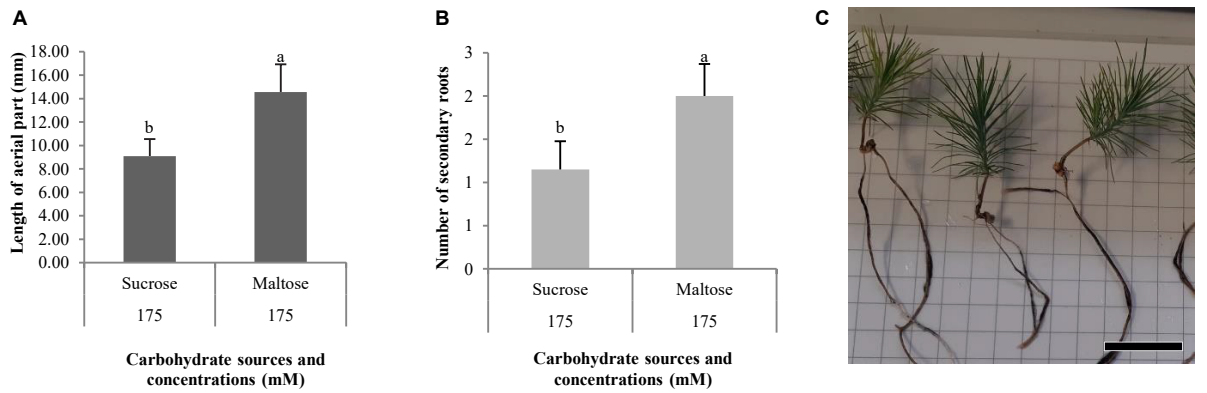

FIGURE 11 | Morphological characteristics of *Pinus halepensis* Mill. plantlets, length of aerial part (mm) **(A)**, and number of secondary roots **(B)**. Bars indicate standard errors. Significant differences at $p \leq 0.05$ are indicated by different letters or numbers. Plantlets of *Pinus halepensis* Mill. obtained from somatic embryos maturated in the EDM medium supplemented with 175 mM of maltose **(C)**, bar = 3 cm.

TABLE 8 | Morphological characteristics of *Pinus halepensis* Mill. somatic plantlets developed from ECLs maturated in a culture medium supplemented with different carbohydrate sources.

Morphological characteristics	175 mM of sucrose	175 mM of maltose
Length of plantlets (mm)	59.29 ± 10.57	74.19 ± 9.80
Width of needles (mm)	0.27 ± 0.03	0.25 ± 0.02
Stem diameter (mm)	0.66 ± 0.03	0.75 ± 0.06
Root length (mm)	28.24 ± 7.84	44.69 ± 8.25

SE, standard error.

stem diameter and the root length; but the largest width of the needle was observed in 175 suc (**Table 8**).

Free Polyamine Content Determination

The addition of different combinations of amino acids in the maturation medium did not provoke statistically significant differences in the ses germination of *P. radiata*, as well as no statistically significant differences were observed for the interaction between amino acid mixtures and the amounts of PAs (**Table 9**). However, the only statistically significant differences were found when the content of individual Put, Cad, Spd, and Spm was analyzed (**Table 9**). Conversely, total free PAs and the ratio Put/(Spd + Spm) did not show significant differences (**Table 9** and **Figures 12A,B**). A higher amount of total free PAs was observed, with means ranging from 300.09 to 368.80 mmolμg^{-1} (**Figure 12A**). Within the total Free PAs, Cad accounted for half the amount of the total quantity followed by Spd (**Figure 12C**). However, the ses germinated from *P. radiata* had three times less Spm when compared with the other PAs previously mentioned, while the amount of Put was the lowest free PAs detected (**Figure 12C**). Plantlets of *P. radiata* contained large amounts of Cad and Spd, intermediate amounts of Spm, and low amounts of Put (**Figure 12C**).

Statistically significant differences were observed in PAs and the interaction between the amino acid mixtures and free PAs in germinated ses of *P. halepensis* (**Table 9**). However, no statistically significant differences were observed for the total free PAs and the ratio Put/(Spd + Spm) (**Table 9** and **Figures 13A,B**). The highest concentrations of total free PAs were observed in ses from MIX II treatment (**Figure 13A**). The amounts of Cad, Spd, and Spm did not change during the germination of ses obtained from maturation media supplemented with different combinations of amino acids (**Figure 13C**). The level of these three PAs exhibited a slight increase in MIX I compared to the other treatments (**Figure 13C**). In this case, the amount of Spd increased slightly, followed by Cad (**Figure 13C**). In contrast, the Put concentration exhibited a considerable significant decrease in MIX I and MIX III (**Figure 13C**). Exogenous application of amino acids of MIX II in the maturation medium promoted similar amounts of four Pas analyzed in the germinated ses (**Figure 13C**).

For *P. halepensis*, statistically significant differences were observed for the different sources of carbohydrates, PAs, the interaction between carbohydrate sources, and carbohydrate concentrations and the triple interaction carbohydrate sources, carbohydrate concentrations, and PAs (**Table 10**).

TABLE 9 | Analysis of variance for the effect of the mixes of amino acids (MA) and the free individual polyamine levels (PAs); and for the effect of the mixes of MA on the total free Pas and the ratio Put/(Spd + Spm) in germinated somatic embryos of *Pinus radiata* D. Don and *Pinus halepensis* Mill.

PAs content	Source	df	*Pinus radiata*		*Pinus halepensis*	
			***F*-value**	***P*-value**	***F*-value**	***P*-value**
Free PAs (mmolμg^{-1})	MA	2	0.68	$>0.05^{ns}$	1.04	$>0.05^{ns}$
	PAs	3	190.99	$\leq 0.001^{***}$	54.04	$\leq 0.001^{***}$
	MA × PAs	6	0.44	$>0.05^{ns}$	3.21	$\leq 0.05^{*}$
Total free PAs (mmolμg^{-1})	MA	2	0.49	$>0.05^{ns}$	0.76	$>0.05^{ns}$
Ratio Put/(Spd + Spm) (mmolμg^{-1})	MA	2	0.28	$>0.05^{ns}$	3.23	$>0.05^{ns}$

; * Significant differences at $p \leq 0.05$ or $p \leq 0.001$, respectively; ^{ns}, non-significant at $p \leq 0.05$; df, degrees of freedom; Put, putrescine; Spd, spermidine; Spm, spermine. Mixes of amino acids: MIX I (Control) – 550 mgL^{-1} of L-glutamine (Gln), 525 mgL^{-1} of L-asparagine (Asn), 175 mgL^{-1} of L-arginine (Arg), 17.5 mgL^{-1} of L-proline (Pro), 19.75 mgL^{-1} of L-citrulline, 19 mgL^{-1} of L-ornithine, 13.75 mgL^{-1} of L-lysine, and 10 mgL^{-1} of L-alanine; MIX II – two times the concentration in the MIX I of the Gln, Asn, Arg, and Pro; and MIX III – 4-fold the concentration in the MIX I of the Gln.*

The total free PAs were not affected by the carbohydrate sources, carbohydrate concentrations, or the interaction between these factors (**Table 10** and **Figure 14A**). On the contrary, the ratio Put/(Spd + Spm) was affected by the interaction carbohydrate sources × carbohydrate concentration (**Table 10**). The *P. halepensis* germinated ses maturated in media with 350 suc or 175 mal showed significantly higher Put/(Spd + Spm) ratios than those obtained in a medium with the lowest maltose concentration (**Figure 14B**). Additionally, an intermediate value for Put/(Spd + Spm) ratios was observed in the germinated ses maturated in control conditions (175 suc) (**Figure 14B**). Germinated ses coming from maturation media with different carbohydrate sources and concentrations showed statistical higher values of all PAs, except Put (**Figure 14C**). In this case, levels of Put presented a marked decrease in germinated ses maturated in maturation media 350 mal when compared with the germinated ses maturated in maturation media 175 mal and 350 suc (**Figure 14C**). Cad, Spd, and Spm detected in germinated ses maturated in different carbohydrate sources and concentrations presented a similar behavior, but with an increase in the Cad amount in the germinated ses maturated in maturation media with 350 suc (**Figure 14C**).

DISCUSSION

Different amino acid or carbohydrate combinations significantly affected the osmolality of the maturation culture medium; it is common in the conifers SE process to restrict the water availability of the medium (increasing gellan gum concentration), modifying the osmolality in order to cause a shift in the developmental program of EMs and promote the formation of ses (Kvaalen and Johnsen, 2008; Garcia-Mendiguren et al., 2016). In our experiments, the best environment to achieve proper conversion of ses in plantlets was observed in maturation

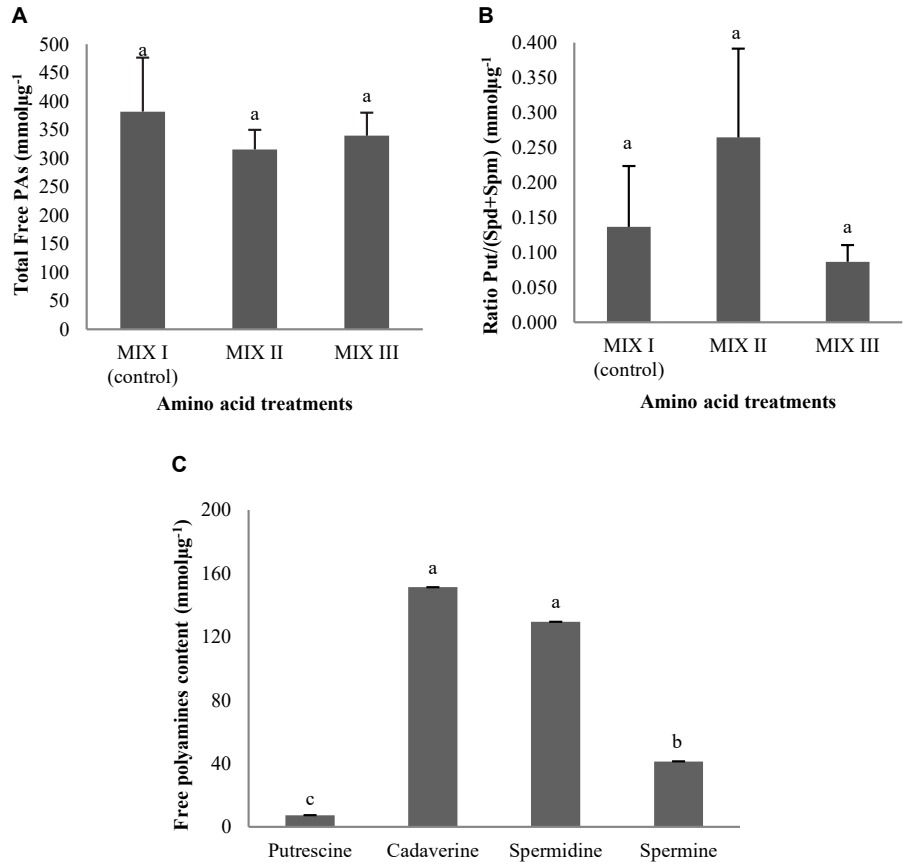

FIGURE 12 | Polyamine (PA) levels (mmolμg^{-1}) in germinated somatic embryos of *Pinus radiata* D. Don obtained from somatic embryos maturated in media supplemented with different mixes of amino acids. Total Free PAs **(A)**; the ratio Put/(Spd + Spm) **(B)**; and the individual free PAs **(C)**. Bars indicate standard errors. Significant differences at $p \leq 0.05$ are indicated by different letters. MIX I (Control) – 550 mgL^{-1} of L-glutamine (Gln), 525 mgL^{-1} of L-asparagine (Asn), 175 mgL^{-1} of L-arginine (Arg), 17.5 mgL^{-1} of L-proline (Pro), 19.75 mgL^{-1} of L-citrulline, 19 mgL^{-1} of L-ornithine, 13.75 mgL^{-1} of L-lysine, and 10 mgL^{-1} of L-alanine; MIX II – two times the concentration in the MIX I of the Gln, Asn, Arg, and Pro; and MIX III – 4-fold the concentration in the MIX I of the Gln.

media with osmolalities between 277 (175 mM of sucrose) and 294 $mosmkg^{-1}$ water (MIX II) for *P. radiata* and between 226 (175 mM of maltose) and 272 $mosmkg^{-1}$ water (MIX III) for *P. halepensis*. However, and in agreement with Montalbán et al. (2010), who obtained good results at osmolalities around 270 $mosmkg^{-1}$ water, the medium osmolality alone did not explain the results obtained because, in other media with similar osmolalities, such good results were not obtained in both species.

In our work, the highest osmolalities (above 400 $mosmkg^{-1}$ water) did not increase the maturation success; in contrast, in *Pseudotsuga menziesii* (Mirb.) Franco raising medium osmolality to 450 $mosmkg^{-1}$ water provoked an improvement in the vigor and morphology of ses developed (Gupta and Pullman, 1991). In this sense, the improvement in the number of ses in *P. radiata* and in *Cryptomeria japonica* D. Don was obtained in lower water availability in maturation media caused by 10 gL^{-1} of gellan gum and 17.5% of polyethylene glycol (PEG), respectively (Moncaleán et al., 2018; Maruyama et al., 2021). However, in *Pinus taeda* L., the maturation medium with 13% of PEG 8,000 and the osmolality ranging from 227 to 233 $mmolkg^{-1}$ allowed an increase in the number of ses (Pullman et al., 2003).

When the size of the *P. radiata* somatic embryos was analyzed, we found that the maturation with MIX I (550 mgL^{-1} of Gln, 525 mgL^{-1} of Asn, 175 mgL^{-1} of L-Arg, 17.5 mgL^{-1} of Pro, 19.75 mgL^{-1} of L-citrulline, 19 mgL^{-1} of L-ornithine, 13.75 mgL^{-1} of L-lysine, and 10 mgL^{-1} of L-alanine) promoted the formation of smaller ses, showing lower acclimatization success months later (**Figure 4B**). In contrast, germinated ses maturated on MIX II (1,100 mgL^{-1} of Gln, 1,050 mgL^{-1} of Asn, 350 mgL^{-1} of L-Arg, 35 mgL^{-1} of Pro, 19.75 mgL^{-1} of L-citrulline, 19 mgL^{-1} of L-ornithine, 13.75 mgL^{-1} of L-lysine, and 10 mgL^{-1} of L-alanine) promoted larger embryos, with a larger stem diameter and an increase in the number of roots in the germinated ses, improving the acclimatization to *ex vitro* conditions of this species (**Figure 4B**). Similar to our results with *P. radiata*, Afele and Saxena (1995) reported an increase in the size of the mature somatic embryos and plantlet development of *Picea pungens* Engelm. in the culture medium supplemented with Asn. The combination of several amino acids (Gln, Asn, Arg, L-citrulline, L-ornithine, L-lysine, L-alanine, and Pro) was also beneficial in *C. japonica* SE, and the increase of concentration of several amino acids (2 gL^{-1} of Gln, 1 gL^{-1} of Asn, and 0.5 gL^{-1}

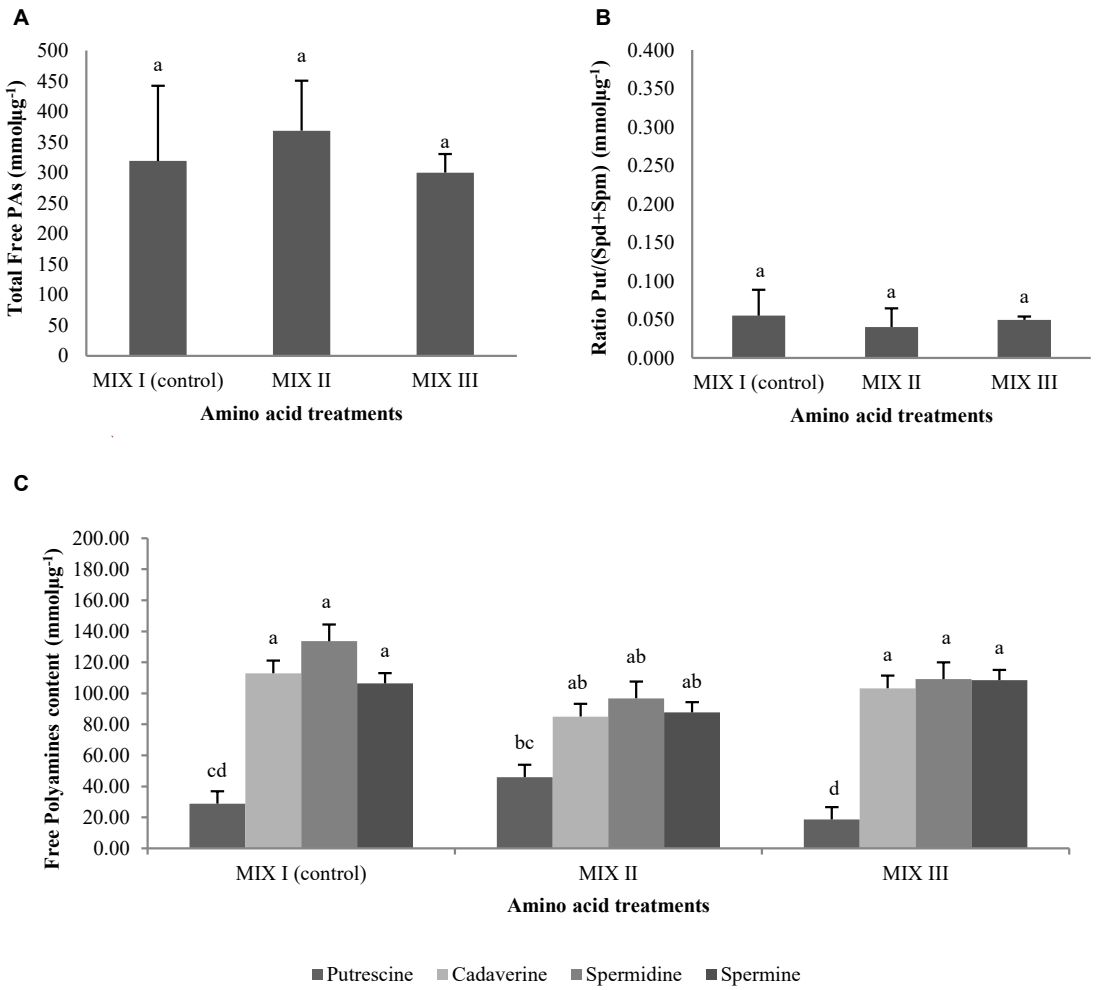

FIGURE 13 | Polyamine (PAs) levels (mmolμg^{-1}) in germinated somatic embryos of *Pinus halepensis* Mill. obtained from somatic embryos maturated in media supplemented with different mixes of amino acids. Total Free PAs **(A)**; the ratio Put/(Spd + Spm) **(B)**; and the individual free PAs **(C)**. Bars indicate standard errors. Significant differences at $p \leq 0.05$ are indicated by different letters. MIX I (Control) – 550 mgL^{-1} of L-glutamine (Gln), 525 mgL^{-1} of L-asparagine (Asn), 175 mgL^{-1} of L-arginine (Arg), 17.5 mgL^{-1} of L-proline (Pro), 19.75 mgL^{-1} of L-citrulline, 19 mgL^{-1} of L-ornithine, 13.75 mgL^{-1} of L-lysine, and 10 mgL^{-1} of L-alanine; MIX II – two times the concentration in the MIX I of the Gln, Asn, Arg, and Pro; and MIX III – 4-fold the concentration in the MIX I of the Gln.

of Arg) was essential to improve an efficient maturation of ses (>1,000 $sesg^{-1}$ fresh weight) (Maruyama et al., 2021). In addition, the inclusion of a mixture of amino acid solution with 17 amino acids (Gln, alanine, Pro, lysine, glycine, Arg, leucine, phenylalanine, serine, isoleucine, valine, histidine, threonine, tyrosine, Asn, tryptophan, and cysteine) in the maturation medium of *P. patula* tended to increase the production of ses and the later conversion of ses in plantlets (Malabadi and Van Staden, 2005). *P. halepensis* ses developed in culture media with MIX III (2,200 mgL^{-1} of Gln, 525 mgL^{-1} of Asn, 175 mgL^{-1} of L-Arg, 17.5 mgL^{-1} of Pro, 19.75 mgL^{-1} of L-citrulline, 19 mgL^{-1} of L-ornithine, 13.75 mgL^{-1} of L-lysine, and 10 mgL^{-1} of L-alanine) were smaller and showed better germination rates (**Figure 4C**). These results are in agreement with those found in *Pinus strobus* L. where an increase in the concentration of Gln in the maturation medium for an embryogenic line resulted in an increase in the number of ses (Garin et al., 2000). Our findings show the important role of Gln in the maturation of *P. halepensis*, enhancing the germination of ses obtained from the maturation medium with a 4-fold increase in this amino acid concentration. This result coincides with some authors who report the use of Gln as one of the main sources of organic nitrogen for SE in *Plinia peruviana* Poir. Govaerts, *Pinus koraiensis* Siebold, and Zucc. and *Viola canescens* Wall. Ex. Roxb. (Silveira et al., 2020; Gao et al., 2021; Khajuria et al., 2021). In agreement with the improvements observed in the germination of *P. halepensis* ses, it was reported that the Gln also influenced the growth of pro-embryogenic masses in *Picea abies* L. Karst. (Carlsson et al., 2017) and *P. peruviana* (Silveira et al., 2020), increasing production of ses and consequent conversion to viable plants in date palm (El-Dawayati et al., 2018), as well as induction of secondary ses in *Quercus suber* L. (Rahmouni et al., 2020).

In relation to the carbohydrate source in a maturation medium, our results showed a different response in *P. radiata*

TABLE 10 | Analysis of variance for the effect of the different carbohydrates sources (CS) and concentration (CC), and the free polyamine levels (PAs) (mmolμg^{-1}); and for the effect of the different carbohydrate sources (CS) and concentration (CC) in the total free polyamine (PAs) (mmolμg^{-1}) and the ratio Put/(Spd + Spm) in germinated somatic embryos of *Pinus halepensis* Mill.

PAs content	Source	df	*F*-value	*P*-value
Free PAs	CS	1	7.58	≤0.001***
	CC	1	0.88	>0.05^{ns}
	PAs	3	38.17	≤0.001***
	SC × CC	1	4.22	≤0.05*
	CS × PAs	3	2.21	>0.05^{ns}
	CC × PA	3	2.40	>0.05^{ns}
	CS × CC × PAs	3	10.28	≤0.001***
Total free PAs	CS	1	1.88	>0.05^{ns}
	CC	1	0.00	>0.05^{ns}
	SC × CC	1	0.10	>0.05^{ns}
Ratio Put/(Spd + Spm)	CS	1	0.00	>0.05^{ns}
	CC	1	1.85	>0.05^{ns}
	SC × CC	1	13.87	≤0.01**

; **; * Significant differences at p ≤ 0.05, p ≤ 0.01 or p ≤ 0.001, respectively; ^{ns}, non-significant at p ≤ 0.05; df, degrees of freedom; Put, putrescine; Spd, spermidine; Spm, spermine.*

and *P. halepensis*. In this sense, production, germination, and acclimatization of *P. radiata* ses were better in the presence of sucrose than in maltose in agreement with results obtained in *Pinus pinaster* Ait. (Ramarosandratana et al., 2001; Klimaszewska et al., 2007). Although, in our results, we did not see an improvement in the NNE at high carbohydrate concentrations in *P. radiata*, in *P. strobus*, the increase in its concentration (350 mM) produced a high amount of ses (Garin et al., 2000). Unlike *P. radiata*, the presence of 175 mM of maltose in *P. halepensis* maturation media promoted an increase in the size of ses, with a significant improvement in their germination rates. In this sense, plantlets obtained from *P. halepensis* ses developed in maturation media with 175 mM of maltose had an increase in the aerial part, and number of secondary roots and 100% of acclimatization was observed. Our results for *P. halepensis* are in agreement with those found in other *Pinus* species such as *P. patula* (Malabadi and Van Staden, 2005), *Pinus thunbergii* Parl. (Sun et al., 2021), and *Pinus elliottii* Engelm. (Yang et al., 2020).

Scott et al. (1995), studying the metabolism of maltose and sucrose in the embryogenesis of microspores isolated from *Hordeum vulgare* L., reported a higher assimilation of carbon in the culture medium, containing sucrose than in those containing maltose, probably because sucrose is well assimilated in both gymnosperms and angiosperms (Ameri et al., 2020; De Sousa et al., 2020; Peng et al., 2020; Shirin et al., 2020). However, different authors have shown controversial results; in this sense, Scott et al. (1995) associated the induction of embryogenesis with lower rates of substrate accumulation obtained from culture media containing maltose, and Carrion Pereira et al. (2019) described maltose as more efficient than sucrose to regenerate *Urochloa brizantha* cv. "Marandu" plants. Even when there are no reports describing morphological characteristics of ses with the concentration of maltose besides ours for *P. halepensis*, an increase in the production of the number of ses in *Pinus massoniana* Lamb. and *P. elliottii* has been reported (Yang et al., 2020; Xia et al., 2021). Similar to our results for *P. halepensis*, Salaj et al. (2019) reported that the presence of maltose in the maturation medium was essential for the formation ses with a consequent conversion of *P. nigra* plantlets.

In addition to morphological characteristics, the changes in the maturation medium also affected the PAs contents in germinated ses. PAs are extremely important for plants and are related to abiotic and biotic stress tolerance (Zou et al., 2021). Also, the Pas vary between species and the developmental stages of SE (Minocha et al., 1999; Silveira et al., 2004; Kuznetsov and Shevyakova, 2007; de Oliveira et al., 2020; Botini et al., 2021). In our work, the amount of PAs did not change with different treatments assayed in *P. radiata*. On the contrary, we observed that the amount of Put was more affected by the different treatments during the maturation stage than other Pas in *P. halepensis*. Moreover, this is the first report about the presence of endogenous Cad in *Pinus* spp. In this sense, concentrations of Cad were observed in the germinated ses obtained in both species and regardless of the treatments assayed. Cad is a lysine decomposition product, rare in plants, and associated with the accumulation of other Pas (Liu et al., 2014; Jancewicz et al., 2016). In our studies, the presence of Cad could not be associated with worse acclimatization, although, in *Pinus sylvestris* L., the root formation decreased in the presence of exogenous Cad (Niemi et al., 2002). In *Arabidopsis thaliana* L. Heynh., the presence of exogenous Cad was associated with the alterations in the morphological characteristics that modulate plant development, as well as environmental stress responses (Liu et al., 2014). In addition, in the same species, Cad inhibited primary root growth, and it was related to skewing, waving, and lateral root formation (Strohm et al., 2015). Moreover, it is possible to study the relationship of the Cad content with future stress experiments in *Pinus*, knowing that the Cad can improve the tolerance of abiotic stress in several species with an overexpression of the genes responsible for stress tolerance (Rajpal and Tomar, 2020).

Furthermore, differences between PAs contents were reported as important in SE. The reduction in Put content and the increase in other PAs (Spd, Spm, and Cad) during SE enabled the correct development of ses; for this reason, those differences have been used as important biochemical parameters for the selection of cell lines with embryogenic potential in *A. angustifolia* and *P. radiata* (Minocha et al., 1999; Jo et al., 2014; de Oliveira et al., 2015). In this work, regardless of the treatment of amino acids mixture, we observed an increase of Cad in relation to Put and Spm, but not in relation to Spd in the germinated *P. radiata* ses. Also, levels of Put were the lowest of all PAs detected in germinated ses; a similar profile was reported by Mikula et al. (2021) in *Cyathea delgadii* Sternb. SE process in which profiles of Cad and Spd increased in relation to other PAs. In agreement with these results and in opposition to ours, Minocha et al. (1999) reported that the most abundant PAs during the development of zygotic and ses in *P. radiata* was Spd in relation to Put and Spm. In contrast to our results, in the maturation of *Picea glauca* (Moench) Voss, the amount of Put was higher than Spd (Kong et al., 1998).

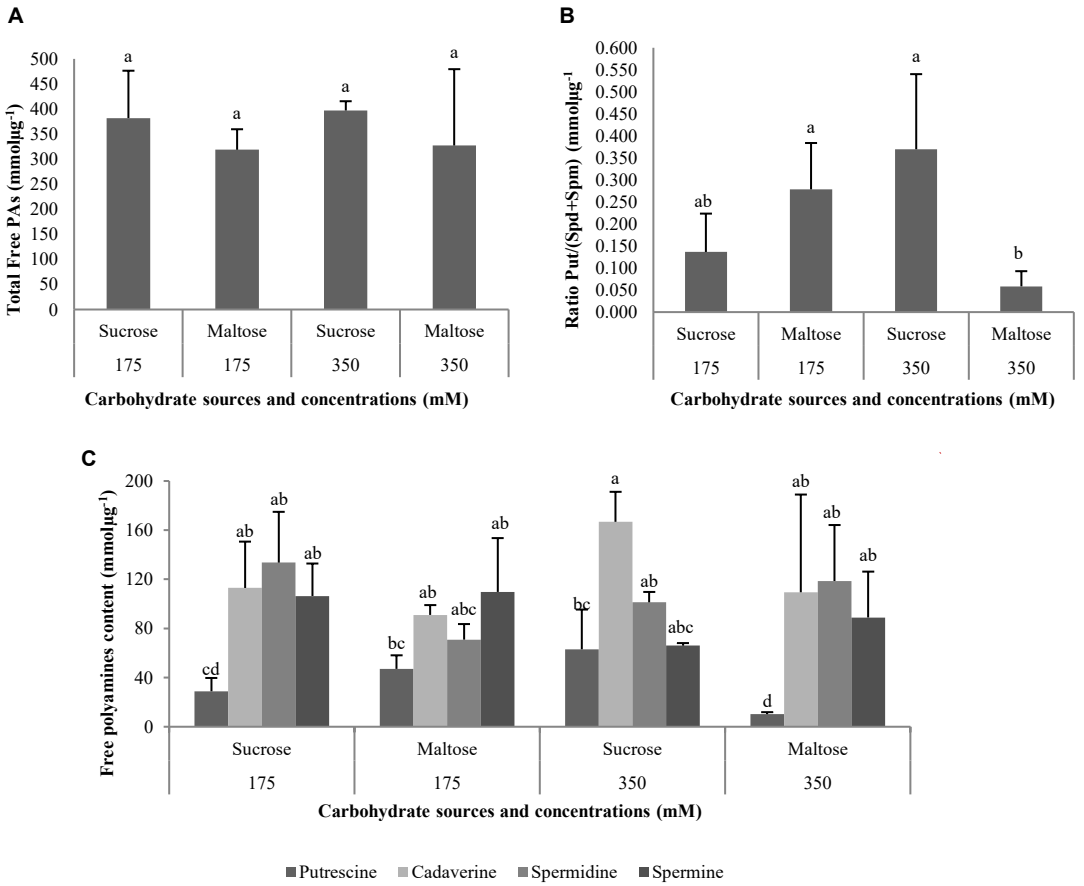

FIGURE 14 | Polyamine (PAs) levels (mmolμg^{-1}) in plantlets of *Pinus halepensis* Mill. obtained from germinated somatic embryos maturated in media supplemented with different carbohydrate sources and concentrations. Total Free Pas **(A)**; the ratio Put/(Spd + Spm) **(B)**; ant the Free Pas **(C)**. Bars indicate standard errors. Significant differences at $p \leq 0.05$ are indicated by different letters.

In *P. halepensis*, in MIX I, there were higher amounts of Cad, Spd, and Spm than in the remaining combinations, although there were no significant differences. In this sense, *Vicia faba* L. was reported that foliar application with different concentrations of amino acids mixture [Arg (5.2–6.2%), Pro (2.23–3.5%), Tiroanine (3.05–3.56%), Aspartic acid (3.2–3.45%), Serine (3.76–4.49%), Glutamic acid (7.24–9.12%), Lysine (1.87–2.45%), Alanine (2.16–2.20%), Cysteine (1.87–2.45%), Valine (2.8–3.1%), Methionine (0.23–0.3%), Isoleucine (1.26–1.7%), Leucine (1.98–2.8%), Tyrosine (0.48–1.02%), Phenylalanine (1.03–1.78%), lysine (1.39–2.3%), and Histidine (0.42–0.9%)] improved the PAs contents in the plants grown under seawater salinity stress (Sadak and Abdelhamid, 2015). Similar levels of Put and the other PAs were observed in germinated ses of *P. halepensis* from a maturation medium with an increase of 350 mgL^{-1} of L-Arg content (MIX II). However, with 2,200 mgL^{-1} of Gln (MIX III) in the maturation medium, a decrease in Put was observed in the germinated ses for *P. halepensis*. Our results are in agreement with those reported by Nieves et al. (2008), which showed that the addition of Arg in the culture medium of *Saccharum* spp. is related to the changes in the amount of PAs, especially Put. The observed levels of Put in our results can be explained due to PAs derived from amino acids through decarboxylation, and the Put can be synthesized from the arginine (Bagni and Tassoni, 2001; de Oliveira et al., 2015). Furthermore, the Put is a direct substrate for Spd and Spm (Mustafavi et al., 2018). For example, in embryogenic masses of *P. sylvestris*, the highest detected PA was Put compared to Spd and Spm (Salo et al., 2016). High amounts of Put appeared both in embryogenic lines that produced ses and in those that did not produce ses, while Spd was directly associated with the embryogenic lines and was able to produce ses in *P. sylvestris* (Salo et al., 2016). In *P. nigra*, the increase in the total amounts of free PAs was related with a lower embryogenic potential (Noceda et al., 2009). Meanwhile, the Spm was crucial to regulate the stress responses in *A. thaliana*, *Rosa damascene* Mill., and *Citrus reticulata* L., among others (Yamaguchi et al., 2007; Shi et al., 2010; Hassan et al., 2018; Hasan et al., 2021).

CONCLUSION

An improvement in the germination of ses, conversion of ses in plantlets, and the acclimatization of plantlets were obtained

in *P. radiata* and *P. halepensis* with alterations in the amino acid mixture or carbohydrate sources/concentrations in the maturation medium. Furthermore, changes in the maturation medium were not affected by the amount of PA levels in the ses of *P. radiata* but changed in *P. halepensis*. Cadaverine was detected in germinated ses of *P. radiata* and *P. halepensis*.

DATA AVAILABILITY STATEMENT

The raw data supporting the conclusions of this article will be made available by the authors, without undue reservation.

AUTHOR CONTRIBUTIONS

PM, IM, and AN conceived and planned the experiments. AN performed the experiments and wrote the manuscript. AC-O and AN carried out the statistical analyses for the amino acid supplementation experiment, and the carbohydrate supplementation experiment, and the characterization of the plantlets. AN, LP, FB, MG, and NS carried out the polyamines analysis. All authors provided critical feedback and helped shape the manuscript.

FUNDING

This research was funded by the MINECO (Spanish Government) project (AGL2016-76143-C4-3R), CYTED (P117RT0522), and MINECO (BES-2017-081249, "Ayudas para contratos predoctorales para la formación de doctores"). MULTIFOREVER [Project MULTIFOREVER is supported under the umbrella of ERA-NET co-founded through Forest Value *via* ANR (FR), FNR (DE), MINCyT (AR), MINECO-AEI (ES), MMM (FI), and VINNOVA (SE)]. Forest value has received funding from the European Union's Horizon 2020 research and innovation programmed under agreement No. 773324.

REFERENCES

Afele, J. C., and Saxena, P. K. (1995). "Somatic embryogenesis in blue spruce (*Picea pungens* Engelmann)," in *Somatic Embryogenesis in Woody Plants*, eds S. M. Jain, P. K. Gupta, and R. J. Newton (New York: Springer), 99–109.

Aitken-Christie, J., Singh, A. P., and Davies, H. (1988). "Multiplication of meristematic tissue: a new tissue culture system for radiata pine," in *Genetic Manipulation of Woody Plants*, eds J. W. Hanover and D. E. Keathley (New York: Springer), 413–432.

Alcazar, R., Bueno, M., and Tiburcio, A. (2020). Polyamines: small amines with large effects on plant abiotic stress tolerance. *Cells* 9:2373. doi: 10.3390/cells9112373

Ameri, A., Davarynejad, G., Moshtaghi, N., and Tehranifar, A. (2020). The Role of carbohydrates on the induction of somatic embryogenesis and the biochemical state of the embryogenic callus in*Pyrus communis* L. Cv. 'Dar Gazi'. *Erwerbs-Obstbau* 62, 411–419. doi: 10.1007/s10341-020-00518-6

Bagni, N., and Tassoni, A. (2001). Biosynthesis, oxidation and conjugation of aliphatic polyamines in higher plants. *Amino Acids* 20, 301–317. doi: 10.1007/s007260170046

Bais, H., and Ravishankar, G. (2002). Role of polyamines in the ontogeny of plants and their biotechnological applications. *Plant Cell Tissue Organ Cult.* 69, 1–34.

Botini, N., Almeida, F., Cruz, K., Reis, R., Vale, E., Garcia, A., et al. (2021). Stage-specific protein regulation during somatic embryo development of *Carica papaya* L. 'Golden'. *Biochim. Biophys. Acta Proteins Proteom.* 1869:140561. doi: 10.1016/j.bbapap.2020.140561

Bouchereau, A., Aziz, A., Larher, F., and Martin-Tanguy, J. (1999). Polyamines and environmental challenges: recent development. *Plant Sci.* 140, 103–125. doi: 10.1016/S0168-9452(98)00218-0

Carlsson, J., Svennerstam, H., Moritz, T., Egertsdotter, U., and Ganeteg, U. (2017). Nitrogen uptake and assimilation in proliferating embryogenic cultures of Norway spruce-Investigating the specific role of glutamine. *PLoS One* 12:e0181785. doi: 10.1371/journal.pone.0181785

Carrion Pereira, A. V., Midori Takamori, L., Harumi Yaguinuma, D., Mendonça de Oliveira, A., and Ferreira Ribas, A. (2019). Maltose in culture media improves the *in vitro* regeneration of *Urochloa brizantha* cv. Marandu plants. *Biotecnol. Veg.* 19, 205–213.

Castander-Olarieta, A., Montalban, I., Oliveira, E., Dell'Aversana, E., D'Amelia, L., Carillo, P., et al. (2019). Effect of thermal stress on tissue ultrastructure and metabolite profiles during initiation of radiata pine somatic embryogenesis. *Front. Plant Sci.* 9:2004. doi: 10.3389/fpls.2018.02004

Castander-Olarieta, A., Pereira, C., Sales, E., Meijon, M., Arrillaga, I., Canal, M., et al. (2020). Induction of Radiata Pine Somatic Embryogenesis at High Temperatures Provokes a Long-Term Decrease in DNA Methylation/Hydroxymethylation and Differential Expression of Stress-Related Genes. *Plants-Basel* 9:1762. doi: 10.3390/plants9121762

Dahrendorf, J., Clapham, D., and Egertsdotter, U. (2018). Analysis of nitrogen utilization capability during the proliferation and maturation phases of Norway spruce (*Picea abies* (L.) H.Karst.) Somatic Embryogenesis. *Forests* 9:288. doi: 10.3390/f9060288

de Oliveira, L., dos Santos, A., and Floh, E. (2020). Polyamine and amino acid profiles in immature *Araucaria angustifolia* seeds and their association with embryogenic culture establishment. *Trees Struct. Funct.* 34, 845–854. doi: 10.1007/s00468-019-01938-y

de Oliveira, L., Macedo, A., dos Santos, A., and Floh, E. (2015). "Polyamine levels, arginine and ornithine decarboxylase activity in embryogenic cultures of *Araucaria angustifolia* (Bert.) O. Kuntze," in *VIII International Symposium on In Vitro Culture and Horticultural Breeding 1083*), eds J. M. Canhoto and S. I. Correia (Leuven: International Society for Horticultural Science), 419–425.

de Oliveira, L., Navarro, B., Cerruti, G., Elbl, P., Minocha, R., Minocha, S., et al. (2018). Polyamine- and amino acid-related metabolism: the roles of arginine and ornithine are associated with the embryogenic potential. *Plant Cell Physiol.* 59, 1084–1098. doi: 10.1093/pcp/pcy049

De Sousa, P. C. A., Souza, S. S. S. E., Meira, F. S., Meira, R. D. O., Gomes, H. T., Silva-Cardoso, I. M. D. A., et al. (2020). Somatic embryogenesis and plant regeneration in *Piper aduncum* L. *In Vitro Cell. Dev. Biol. Plant* 56, 618–633. doi: 10.1007/s11627-020-10110-y

do Nascimento, A., Barroso, P., do Nascimento, N., Goicoa, T., Ugarte, M., Montalban, I., et al. (2020). *Pinus* spp. somatic embryo conversion under high temperature: effect on the morphological and physiological characteristics of plantlets. *Forests* 11:1181. doi: 10.3390/f11111181

El-Dawayati, M. M., Ghazzawy, H. S., and Munir, M. (2018). Somatic embryogenesis enhancement of date palm cultivar Sewi using different types of polyamines and glutamine amino acid concentration under *in-vitro* solid and liquid media conditions. *Int. J. Biosci.* 12, 149–159.

Escandon, M., Valledor, L., Pascual, J., Pinto, G., Canal, M., and Meijon, M. (2017). System-wide analysis of short-term response to high temperature in *Pinus radiata*. *J. Exp. Bot.* 68, 3629–3641. doi: 10.1093/jxb/erx198

Farias-Soares, F., Steiner, N., Schmidt, E., Pereira, M., Rogge-Renner, G., Bouzon, Z., et al. (2014). The transition of proembryogenic masses to somatic embryos in *Araucaria angustifolia* (Bertol.) Kuntze is related to the endogenous contents of IAA, ABA and polyamines. *Acta Physiol. Plant.* 36, 1853–1865. doi: 10.1007/s11738-014-1560-6

Fuentes-Sepulveda, R., Garcia-Herrera, C., Vasco, D., Salinas-Lira, C., and Ananias, R. (2020). Thermal characterization of *Pinus radiata* wood vacuum-impregnated with octadecane. *Energies* 13:942. doi: 10.3390/en13040942

Gao, F., Peng, C., Wang, H., Shen, H., and Yang, L. (2021). Selection of culture conditions for callus induction and proliferation by somatic embryogenesis of *Pinus koraiensis*. *J. For. Res.* 32, 483–491. doi: 10.1007/s11676-020-01147-1

Garcia-Mendiguren, O., Montalban, I., Correia, S., Canhoto, J., and Moncalean, P. (2016). Different environmental conditions at initiation of radiata pine somatic embryogenesis determine the protein profile of somatic embryos. *Plant Biotechnol.* 33, 143–152. doi: 10.5511/plantbiotechnology.16.0520a

Garin, É, Bernier-Cardou, M., Isabel, N., Klimaszewska, K., and Plourde, A. (2000). Effect of sugars, amino acids, and culture technique on maturation of somatic embryos of *Pinus strobus*on medium with two gellan gum concentrations. *Plant Cell Tissue Organ Cult.* 62, 27–37. doi: 10.1023/A:1006402215457

Gazol, A., Ribas, M., Gutierrez, E., and Camarero, J. (2017). Aleppo pine forests from across Spain show drought-induced growth decline and partial recovery. *Agric. For. Meteorol.* 232, 186–194. doi: 10.1016/j.agrformet.2016.08.014

Gemperlova, L., Fischerova, L., Cvikrova, M., Mala, J., Vondrakova, Z., Martincova, O., et al. (2009). Polyamine profiles and biosynthesis in somatic embryo development and comparison of germinating somatic and zygotic embryos of Norway spruce. *Tree Physiol.* 29, 1287–1298. doi: 10.1093/treephys/tpp063

Gerdakaneh, M., Mozafari, A., Sioseh-mardah, A., and Sarabi, B. (2011). Effects of different amino acids on somatic embryogenesis of strawberry (*Fragaria x ananassa* Duch.). *Acta Physiol. Plant.* 33, 1847–1852. doi: 10.1007/s11738-011-0725-9

Gupta, P., Pullman, G., Timmis, R., Kreitinger, M., Carlson, W., Grob, J., et al. (1993). Forestry in the 21st century. *Nat. Biotechnol.* 11, 454–459. doi: 10.1038/nbt0493-454

Gupta, P. K., and Durzan, D. J. (1985). Shoot multiplication from mature trees of Douglas-fir (*Pseudotsuga menziesii*) and sugar pine (*Pinus lambertiana*). *Plant Cell Rep.* 4, 177–179. doi: 10.1007/BF00269282

Gupta, P. K., and Pullman, G. S. (1991). *Method for Reproducing Coniferous Plants By Somatic Embryogenesis Using Abscisic Acid And Osmotic Potential Variation*. Alexandria: United States Patent and Trademark Office.

Hasan, M., Skalicky, M., Jahan, M., Hossain, M., Anwar, Z., Nie, Z., et al. (2021). Spermine: its emerging role in regulating drought stress responses in plants. *Cells* 10:261. doi: 10.3390/cells10020261

Hassan, F., Ali, E., and Alamer, K. (2018). Exogenous application of polyamines alleviates water stress-induced oxidative stress of *Rosa damascena* Miller var. *trigintipetala* Dieck. *S. Afr. J. Bot.* 116, 96–102. doi: 10.1016/j.sajb.2018.02.399

Huang, X., Li, X., Li, Y., and Huang, L. (2001). The effect of AOA on ethylene and polyamine metabolism during early phases of somatic embryogenesis in *Medicago sativa*. *Physiol. Plant.* 113, 424–429. doi: 10.1034/j.1399-3054.2001.1130317.x

Jancewicz, A., Gibbs, N., and Masson, P. (2016). Cadaverine's functional role in plant development and environmental response. *Front. Plant Sci.* 7:870. doi: 10.3389/fpls.2016.00870

Jimenez, V. (2005). Involvement of plant hormones and plant growth regulators on in vitro somatic embryogenesis. *Plant Growth Regul.* 47, 91–110. doi: 10.1007/s10725-005-3478-x

Jin, L., Yarra, R., Zhou, L., Zhao, Z., and Cao, H. (2020). miRNAs as key regulators via targeting the phytohormone signaling pathways during somatic embryogenesis of plants. *3 Biotech.* 10:495. doi: 10.1007/s13205-020-02487-9

Jo, L., Dos Santos, A., Bueno, C., Barbosa, H., and Floh, E. (2014). Proteomic analysis and polyamines, ethylene and reactive oxygen species levels of *Araucaria angustifolia* (Brazilian pine) embryogenic cultures with different embryogenic potential. *Tree Physiol.* 34, 94–104. doi: 10.1093/treephys/tpt102

Khajuria, A., Hano, C., and Bisht, N. (2021). Somatic embryogenesis and plant regeneration in *Viola canescens* Wall. Ex. Roxb.: an endangered himalayan herb. *Plants-Basel* 10:761. doi: 10.3390/plants10040761

Kielkowska, A., and Adamus, A. (2021). Exogenously applied polyamines reduce reactive oxygen species, enhancing cell division and the shoot regeneration from *Brassica oleracea* L. var. capitata protoplasts. *Agron. Basel* 11:735. doi: 10.3390/agronomy11040735

Klimaszewska, K., Trontin, J.-F., Becwar, M. R., Devillard, C., Park, Y.-S., and Lelu-Walter, M.-A. (2007). Recent progress in somatic embryogenesis of four *Pinus* spp. *Tree For. Sci. Biotechnol.* 1, 11–25.

Kong, L., Attree, S., and Fowke, L. (1998). Effects of polyethylene glycol and methylglyoxal bis(guanylhydrazone) on endogenous polyamine levels and somatic embryo maturation in white spruce (*Picea glauca*). *Plant Sci.* 133, 211–220. doi: 10.1016/S0168-9452(98)00040-5

Kube, M., Drazna, N., Konradova, H., and Lipavska, H. (2014). Robust carbohydrate dynamics based on sucrose resynthesis in developing Norway spruce somatic embryos at variable sugar supply. *In Vitro Cell. Dev. Biol. Plant* 50, 45–57. doi: 10.1007/s11627-013-9589-6

Kuznetsov, V. V., and Shevyakova, N. I. (2007). Polyamines and stress tolerance of plants. *Plant Stress* 1, 50–71.

Kvaalen, H., and Johnsen, O. (2008). Timing of bud set in *Picea abies* is regulated by a memory of temperature during zygotic and somatic embryogenesis. *New Phytologist* 177, 49–59. doi: 10.1111/j.1469-8137.2007.02222.x

Liu, T., Dobashi, H., Kim, D., Sagor, G., Niitsu, M., Berberich, T., et al. (2014). *Arabidopsis* mutant plants with diverse defects in polyamine metabolism show unequal sensitivity to exogenous cadaverine probably based on their spermine content. *Physiol. Mol. Biol. Plants* 20, 151–159. doi: 10.1007/s12298-014-0227-5

Malabadi, R., and Van Staden, J. (2005). Role of antioxidants and amino acids on somatic embryogenesis of *Pinus patula*. *In Vitro Cell. Dev. Biol. Plant* 41, 181–186. doi: 10.1079/IVP2004623

Manrique-Alba, A., Begueria, S., Molina, A., Gonzalez-Sanchis, M., Tomas-Burguera, M., del Campo, A., et al. (2020). Long-term thinning effects on tree growth, drought response and water use ef ficiency at two Aleppo pine plantations in Spain. *Sci. Total Environ.* 728:138536. doi: 10.1016/j.scitotenv.2020.138536

Maruyama, T. E., Ueno, S., Mori, H., Kaneeda, T., and Moriguchi, Y. (2021). Factors influencing somatic embryo maturation in Sugi (Japanese Cedar, *Cryptomeria japonica* (Thunb. ex Lf) D. Don). *Plants* 10:874.

Mikula, A., Tomaszewicz, W., Dziurka, M., Kazmierczak, A., Grzyb, M., Sobczak, M., et al. (2021). The Origin of the *Cyathea delgadii* Sternb. somatic embryos is determined by the developmental state of donor tissue and mutual balance of selected metabolites. *Cells* 10:1388. doi: 10.3390/cells10061388

Minocha, R., Majumdar, R., and Minocha, S. (2014). Polyamines and abiotic stress in plants: a complex relationship. *Front. Plant Sci.* 5:175. doi: 10.3389/fpls.2014.00175

Minocha, R., Minocha, S., and Long, S. (2004). Polyamines and their biosynthetic enzymes during somatic embryo development in red spruce (*Picea rubens* Sarg.). *In Vitro Cell. Dev. Biol. Plant* 40, 572–580. doi: 10.1079/IVP2004569

Minocha, R., Smith, D., Reeves, C., Steele, K., and Minocha, S. (1999). Polyamine levels during the development of zygotic and somatic embryos of *Pinus radiata*. *Physiol. Plant.* 105, 155–164. doi: 10.1034/j.1399-3054.1999.105123.x

Moncaleán, P., Garcia-Mendiguren, O., Novak, O., Strnad, M., Goicoa, T., Ugarte, M., et al. (2018). Temperature and water availability during maturation affect the cytokinins and auxins profile of radiata pine somatic embryos. *Front. Plant Sci.* 9:1898. doi: 10.3389/fpls.2018.01898

Montalbán, I. A., De Diego, N., and Moncaleán, P. (2010). Bottlenecks in *Pinus radiata* somatic embryogenesis: improving maturation and germination. *Trees* 24, 1061–1071. doi: 10.1007/s00468-010-0477-y

Montalbán, I. A., De Diego, N., and Moncaleán, P. (2012). Enhancing initiation and proliferation in radiata pine (*Pinus radiata* D. Don) somatic embryogenesis through seed family screening, zygotic embryo staging and media adjustments. *Acta Physiol. Plant.* 34, 451–460. doi: 10.1007/s11738-011-0841-6

Montalbán, I. A., and Moncaleán, P. (2019). Rooting of *Pinus radiata* somatic embryos: factors involved in the success of the process. *J. For. Res.* 30, 65–71. doi: 10.1007/s11676-018-0618-5

Montalbán, I. A., Setién-Olarra, A., Hargreaves, C. L., and Moncaleán, P. (2013). Somatic embryogenesis in *Pinus halepensis* Mill.: an important ecological species from the Mediterranean forest. *Trees* 27, 1339–1351. doi: 10.1007/s00468-013-0882-0

Monteiro, M., Kevers, C., Dommes, J., and Gaspar, T. (2002). A specific role for spermidine in the initiation phase of somatic embryogenesis in *Panax ginseng* CA Meyer. *Plant Cell Tissue Organ Cult.* 68, 225–232. doi: 10.1023/A:1013950729576

Mustafavi, S., Badi, H., Sekara, A., Mehrafarin, A., Janda, T., Ghorbanpour, M., et al. (2018). Polyamines and their possible mechanisms involved in plant physiological processes and elicitation of secondary metabolites. *Acta Physiol. Plant.* 40:102. doi: 10.1007/s11738-018-2671-2

Niemi, K., Haggman, H., and Sarjala, T. (2002). Effects of exogenous diamines on the interaction between ectomycorrhizal fungi and adventitious root formation in Scots pine *in vitro*. *Tree Physiol.* 22, 373–381. doi: 10.1093/treephys/22.6.373

Nieves, N., Sagarra, F., Gonzalez, R., Lezcano, Y., Cid, M., Blanco, M., et al. (2008). Effect of exogenous arginine on sugarcane (*Saccharum* sp.) somatic

embryogenesis, free polyamines and the contents of the soluble proteins and proline. *Plant Cell Tissue Organ Cult.* 95, 313–320. doi: 10.1007/s11240-008-9445-2

Noceda, C., Salaj, T., Perez, M., Viejo, M., Canal, M., Salaj, J., et al. (2009). DNA demethylation and decrease on free polyamines is associated with the embryogenic capacity of *Pinus nigra* Arn. cell culture. *Trees-Struct. Funct.* 23, 1285–1293. doi: 10.1007/s00468-009-0370-8

Peng, C., Gao, F., Wang, H., Shen, H., and Yang, L. (2020). Physiological and biochemical traits in Korean pine somatic embryogenesis. *Forests* 11:577. doi: 10.3390/f11050577

Pereira, C., Montalban, I., Garcia-Mendiguren, O., Goicoa, T., Ugarte, M., Correia, S., et al. (2016). *Pinus halepensis* somatic embryogenesis is affected by the physical and chemical conditions at the initial stages of the process. *J. For. Res.* 21, 143–150. doi: 10.1007/s10310-016-0524-7

Pereira, C., Montalban, I., Goicoa, T., Ugarte, M., Correia, S., Canhoto, J., et al. (2017). The effect of changing temperature and agar concentration at proliferation stage in the final success of Aleppo pine somatic embryogenesis. *Forest Syst.* 26:eSC05. doi: 10.5424/fs/2017263-11436

Pullman, G., and Bucalo, K. (2014). Pine somatic embryogenesis: analyses of seed tissue and medium to improve protocol development. *New Forests* 45, 353–377. doi: 10.1007/s11056-014-9407-y

Pullman, G., Johnson, S., Peter, G., Cairney, J., and Xu, N. (2003). Improving loblolly pine somatic embryo maturation: comparison of somatic and zygotic embryo morphology, germination, and gene expression. *Plant Cell Rep.* 21, 747–758. doi: 10.1007/s00299-003-0586-9

Quinto, L., Navarro-Cerrillo, R., Palacios-Rodriguez, G., Ruiz-Gomez, F., and Duque-Lazo, J. (2021). The current situation and future perspectives of *Quercus ilex* and *Pinus halepensis* afforestation on agricultural land in Spain under climate change scenarios. *New Forests* 52, 145–166. doi: 10.1007/s11056-020-09788-0

Quoirin, M., and Lepoivre, P. (1977). Etude de milieux adaptes aux cultures *in vitro* de *Prunus*. *Acta Hortic.* 78, 437–442.

R Core Team (2017). Changes in R From version 3.4.2 to version 3.4.3. *R. J.* 9, 568–570.

Rahmouni, S., El Ansari, Z. N., Badoc, A., Martin, P., El Kbiach, M. L. B., and Lamarti, A. (2020). Effect of amino acids on secondary somatic embryogenesis of moroccan cork oak (*Quercus suber* L.) Tree. *Am. J. Plant Sci.* 11, 626–641.

Rajpal, C., and Tomar, P. C. (2020). Cadaverine: a potent modulator of plants against abiotic stresses: cadaverine: a potent modulator. *J. Microbiol. Biotechnol. Food Sci.* 10, 205–210. doi: 10.15414/jmbfs.2020.10.2.205-210

Ramarosandratana, A., Harvengt, L., Bouvet, A., Calvayrac, R., and Pâques, M. (2001). Effects of carbohydrate source, polyethylene glycol and gellan gum concentration on embryonal-suspensor mass (ESM) proliferation and maturation of maritime pine somatic embryos. *In Vitro Cell. Dev. Biol. Plant* 37, 29–34.

Sadak, M., and Abdelhamid, M. (2015). Influence of amino acids mixture application on some biochemical aspects, antioxidant enzymes and endogenous polyamines of *Vicia faba* plant grown under seawater salinity stress. *Gesunde Pflanzen* 67, 119–129. doi: 10.1007/s10343-015-0344-2

Salaj, T., Klubicova, K., Matusova, R., and Salaj, J. (2019). Somatic embryogenesis in selected conifer trees *Pinus nigra* Arn. and *Abies* Hybrids. *Front. Plant Sci.* 10:13. doi: 10.3389/fpls.2019.00013

Salo, H., Sarjala, T., Jokela, A., Haggman, H., and Vuosku, J. (2016). Moderate stress responses and specific changes in polyamine metabolism characterize Scots pine somatic embryogenesis. *Tree Physiol.* 36, 392–402. doi: 10.1093/treephys/tpv136

Satish, L., Rathinapriya, P., Ceasar, S., Rency, A., Pandian, S., Rameshkumar, R., et al. (2016). Effects of cefotaxime, amino acids and carbon source on somatic embryogenesis and plant regeneration in four Indian genotypes of foxtail millet (*Setaria italica* L.). *In Vitro Cell. Dev. Biol. Plant* 52, 140–153. doi: 10.1007/s11627-015-9724-7

Scott, P., Lyne, R., and Aprees, T. (1995). Metabolism of maltose and sucrose by microspores isolated from barley (*Hordeum vulgare* L.). *Planta* 197, 435–441.

Shi, J., Fu, X.-Z., Peng, T., Huang, X.-S., Fan, Q.-J., and Liu, J.-H. (2010). Spermine pretreatment confers dehydration tolerance of *Citrusin vitro* plants via modulation of antioxidative capacity and stomatal response. *Tree Physiol.* 30, 914–922. doi: 10.1093/treephys/tpq030

Shirin, F., Bhadrawale, D., Mishra, J., Sonkar, M., and Maravi, S. (2020). Evaluation of biochemical changes during different stages of somatic embryogenesis in a vulnerable timber tree*Dalbergia latifolia*(Indian rosewood). *In Vitro Cell. Dev. Biol. Plant* 56, 894–902. doi: 10.1007/s11627-020-10099-4

Shoeb, F., Yadav, J., Bajaj, S., and Rajam, M. (2001). Polyamines as biomarkers for plant regeneration capacity: improvement of regeneration by modulation of polyamine metabolism in different genotypes of indica rice. *Plant Sci.* 160, 1229–1235. doi: 10.1016/S0168-9452(01)00375-2

Silveira, S. S., Sant Anna-Santos, B. F., Degenhardt-Goldbach, J., and Quoirin, M. (2020). Somatic embryogenesis from mature split seeds of jaboticaba (*Plinia peruviana* (Poir) Govaerts). *Acta Sci. Agron.* 42:e43798.

Silveira, V., Floh, E., Handro, W., and Guerra, M. (2004). Effect of plant growth regulators on the cellular growth and levels of intracellular protein, starch and polyamines in embryogenic suspension cultures of *Pinus taeda*. *Plant Cell Tissue Organ Cult.* 76, 53–60. doi: 10.1023/A:1025847515435

Smeekens, S., Ma, J., Hanson, J., and Rolland, F. (2010). Sugar signals and molecular networks controlling plant growth. *Curr. Opin. Plant Biol.* 13, 274–279. doi: 10.1016/j.pbi.2009.12.002

Strohm, A., Vaughn, L., and Masson, P. (2015). Natural variation in the expression of ORGANIC CATION TRANSPORTER 1 affects root length responses to cadaverine in *Arabidopsis*. *J. Exp. Bot.* 66, 853–862. doi: 10.1093/jxb/eru444

Sun, T., Wang, Y., Zhu, L., Liu, X., Wang, Q., and Ye, J. (2021). Evaluation of somatic embryo production during embryogenic tissue proliferation stage using morphology, maternal genotype, proliferation rate and tissue age of *Pinus thunbergii* Parl. *J. For. Res.* doi: 10.1007/s11676-021-01311-1 [Epub ahead of print].

Sundararajan, S., Sivakumar, H., Nayeem, S., Rajendran, V., Subiramani, S., and Ramalingam, S. (2021). Influence of exogenous polyamines on somatic embryogenesis and regeneration of fresh and long-term cultures of three elite indica rice cultivars. *Cereal Res. Commun.* 49, 245–253. doi: 10.1007/s42976-020-00098-x

Walter, C., Find, J. I., and Grace, L. J. (2005). "Somatic Embryogenesis and Genetic Transformation in *Pinus radiata*," in *Protocol for Somatic Embryogenesis in Woody Plants*, eds S. M. Jain and P. K. Gupta (Dordrecht: Springer), 11–24.

Xia, X., Yang, F., Ke, X., Chen, Y., Ye, J., and Zhu, L. (2021). Somatic embryogenesis of masson pine (*Pinus massoniana*): initiation, maturation and genetic stability analysis at SSR loci. *Plant Cell Tissue Organ Cult.* 145, 667–677. doi: 10.1007/s11240-021-02036-z

Yamaguchi, K., Takahashi, Y., Berberich, T., Imai, A., Takahashi, T., Michael, A., et al. (2007). A protective role for the polyamine spermine against drought stress in *Arabidopsis*. *Biochem. Biophys. Res. Commun.* 352, 486–490. doi: 10.1016/j.bbrc.2006.11.041

Yang, F., Xia, X.-R., Ke, X., Ye, J., and Zhu, L.-H. (2020). Somatic embryogenesis in slash pine (*Pinus elliottii* Engelm): improving initiation of embryogenic tissues and maturation of somatic embryos. *Plant Cell Tissue Organ Cult.* 143, 159–171. doi: 10.1007/s11240-020-01905-3

Yaseen, M., Ahmad, T., Sablok, G., Standardi, A., and Hafiz, I. (2013). Review: role of carbon sources for *in vitro* plant growth and development. *Mol. Biol. Rep.* 40, 2837–2849. doi: 10.1007/s11033-012-2299-z

Zou, C., Wang, Y., Wang, B., Liu, D., Liu, L., and Li, C. (2021). Effects of alkali stress on dry matter accumulation, root morphology, ion balance, free polyamines, and organic acids of sugar beet. *Acta Physiol. Plant.* 43:13. doi: 10.1007/s11738-020-03194-x

Conflict of Interest: The authors declare that the research was conducted in the absence of any commercial or financial relationships that could be construed as a potential conflict of interest.

Publisher's Note: All claims expressed in this article are solely those of the authors and do not necessarily represent those of their affiliated organizations, or those of the publisher, the editors and the reviewers. Any product that may be evaluated in this article, or claim that may be made by its manufacturer, is not guaranteed or endorsed by the publisher.

frontiers in Plant Science

ORIGINAL RESEARCH
published: 20 December 2021
doi: 10.3389/fpls.2021.791549

Somatic Embryo Yield and Quality From Norway Spruce Embryogenic Tissue Proliferated in Suspension Culture

Sakari Välimäki[1]*, *Teresa Hazubska-Przybył*[2], *Ewelina Ratajczak*[2], *Mikko Tikkinen*[1], *Saila Varis*[1] and *Tuija Aronen*[1]

[1] Natural Resources Institute Finland (Luke), Savonlinna, Finland, [2] Institute of Dendrology, Polish Academy of Sciences, Kórnik, Poland

OPEN ACCESS

Edited by:
Víctor M. Loyola-Vargas, Scientific Research Center of Yucatán (CICY), Mexico

Reviewed by:
Carolina Sánchez-Romero, University of Malaga, Spain
Elena Corredoira, Institute of Agrobiological Research of Galicia, Spanish National Research Council (CSIC), Spain

***Correspondence:**
Sakari Välimäki
sakari.valimaki@luke.fi

Specialty section:
This article was submitted to Plant Development and EvoDevo, a section of the journal Frontiers in Plant Science

Received: *08 October 2021*
Accepted: *23 November 2021*
Published: *20 December 2021*

Citation:
Välimäki S, Hazubska-Przybył T, Ratajczak E, Tikkinen M, Varis S and Aronen T (2021) Somatic Embryo Yield and Quality From Norway Spruce Embryogenic Tissue Proliferated in Suspension Culture. Front. Plant Sci. 12:791549. doi: 10.3389/fpls.2021.791549

Somatic embryogenesis is being piloted for the commercial production of genetically improved Norway spruce (*Picea abies* L. Karst) forest regeneration material in Finland. The main challenge to making the process commercially relevant is the dependence on time-consuming and highly skilled manual labor. Automation and scaling up are needed to improve cost-effectiveness. Moving from the proliferation of embryogenic tissue on semisolid media to suspension cultures could improve process scalability. In a series of four experiments (overall, with 20 cell lines, 4–9 per experiment), the suitability of proliferation in suspension culture for Norway spruce somatic embryogenesis was evaluated based on the growth rate, indicators of stress conditions, good-quality cotyledonary embryo yield, and embling survival in a greenhouse. The proliferation rate in suspension was found equal to on semisolid media, but with a remarkable genotypic variation. Embryogenic tissue matured directly without pre-treatments from suspension onto semisolid media produced lower numbers of good-quality embryos than tissue matured from semisolid media. Rinsing the suspension-grown tissue with hormone-free liquid media before maturation improved embryo yield, bringing it closer to that of semisolid-grown tissue. Decreasing 6-benzylaminopurine and 2,4-dichlorophenoxyacetic acid concentrations in suspension proliferation media to 0.5 or 0.1 times those in semisolid media did not affect tissue growth and did not improve embryo production. The hydrogen peroxide (H_2O_2) content and guaiacol peroxidase activity were elevated in suspension cultures compared with semisolid medium, which had the same plant growth regulator content. In one experiment out of four, the greenhouse survival of germinants was lower when proliferation was carried out in full strength suspension than on semisolid media; in other experiments the survival rates were equal.

Keywords: *Picea abies* (L.) Karst, vegetative propagation, maturation, plant growth regulator, H_2O_2–hydrogen peroxide, guaiacol peroxidase

INTRODUCTION

The demand for tree biomass and timber has increased due to the growing need for substitutes for fossil fuels (FAO, 2008; Lauri et al., 2014), for example. Using the best possible material, i.e., genetically improved stock in the forest regeneration of Norway spruce [*Picea abies* (L.) Karst]. more than 30% can be gained in stem volume growth (Haapanen, 2020). Increased efficacy in the use of managed forests could free up other forest areas for alternative use and conservation. To most efficiently implement the results achieved by tree breeding, materials derived *via* vegetative, i.e., asexual, propagation could be used to enable the production of plants of uniform quality and known selected characteristics (Bonga, 2016). Somatic embryogenesis has become the method of choice for the vegetative propagation of conifers due to its high multiplication rate and the maintenance of the juvenility of cell lines *via* cryopreservation (Park, 2002). However, the process is expensive due to the amount of skill-intensive manual labor required. Automation and increased production volume are needed to make somatic embryogenesis (SE) a commercially profitable way to produce forest regeneration material (Gupta and Timmis, 2005; Denchev and Grossnickle, 2019; Egertsdotter et al., 2019).

Before planting Norway spruce emblings, the SE cultures must be initiated, multiplied, i.e., proliferated, matured to cotyledonary embryos, germinated, acclimatized, and grown in the nursery (Högberg and Varis, 2016; Tikkinen et al., 2019). Currently, Norway spruce embryogenic tissue (ET) is grown on semisolid media and must be subcultured every other week by picking newly grown tissue onto new media with forceps (Varis, 2018). One option for scaling up embling production could be using liquid suspension cultures for the tissue's proliferation (Boulay et al., 1988; Denchev and Grossnickle, 2019). The cultures in liquid media are inherently more scalable, and their handling is easier to automate than semisolid cultures (Denchev and Grossnickle, 2019). The proliferation of Norway spruce ET is known to work in suspension, whereas the maturation phase has proven to be more difficult than in semisolid media, because somatic embryos appear to need physical support for proper development (Boulay et al., 1988; Filonova et al., 2000; Bozhkov et al., 2002; Sun et al., 2010). Proliferation rates are reported to be faster in suspension cultures than in semisolid media due to the lack of hindrance of adjacent tissues and increased dispersion of the tissues because of culture rotation (von Arnold et al., 2002; Mamun et al., 2018). Suspension cultures may also benefit from a more uniform growth environment than semisolid media, in which nutrient gradients may be formed because of reduced diffusion (Kubeš et al., 2014).

The maturation stage is likely to benefit more from the automation of the process than from scaling up, especially given the observed challenges of applying, e.g., bioreactors (Välimäki et al., 2020). Maturation on semisolid media also works reliably for Norway spruce, and there is no need for media changes or other manual labor during the seven- to eight-week maturation period (Tikkinen et al., 2018a, 2019). Therefore, after the plating of maturations from proliferation, no additional work is needed until germination is started. The ET from the suspension cultures can be matured on semisolid media without increasing the workload. After maturation, the plates can be moved to cold storage, and good-quality embryos can be selected for germination when required (Tikkinen et al., 2019).

Plant growth regulators (PGR) 6-benzylaminopurine (BA) and 2,4-dicholophenoxyacetic acid (2,4-D) are needed for a successful Norway spruce ET culture initiation and proliferation (Hakman et al., 1985; Varis, 2018). In suspension cultures, nutrients and PGRs are more accessible to cells and can be harmful in excess for development (Denchev and Grossnickle, 2019). The removal of 2,4-D and BA is necessary to start the maturation of early embryos into cotyledonary embryos, along with the addition of abscisic acid (von Arnold and Hakman, 1988). In particular, 2,4-D has negative effects on embryo development by disturbing the endogenous auxin gradient formation required for proper polarity development and maturation (Zhu et al., 2016; Garcia et al., 2019).

Several indicators have been used to characterize plant growth and development, the physiological state, and symptoms of stress. Important indicators of stress include hydrogen peroxide (H_2O_2) and various antioxidant enzymes, including peroxidases, e.g., guaiacol peroxidase (POX [EC 1.11.1.7]). Many studies have revealed that SE is sensitive to intracellular concentrations of H_2O_2 and antioxidant enzymes (Saeed and Shahzad, 2015; Zhou et al., 2016; Yang et al., 2021). H_2O_2 may act as a source of oxidative stress and as an important signaling molecule in many developmental and physiological processes in plants (Zhang et al., 2010; Cheng et al., 2015; Taiz et al., 2015). It participates in the regulation of all key processes such as growth, development, aging, programmed cell death, or responses to pathogen and abiotic stress (Slesak et al., 2007; Zhang et al., 2010; Baxter et al., 2014; Das and Roychoudhury, 2014; Cheng et al., 2015; Serrano et al., 2015; Mignolet-Spruyt et al., 2016; Singh et al., 2016; Liu et al., 2021). It is relatively persistent and can cross membranes by means of specialized aquaporins ("peroxyporins") that facilitate their transportation (Gechev et al., 2006). Increased H_2O_2 levels due to a variety of environmental stresses, including *in vitro* culture conditions, affect plant function by generating oxidative stress. On the other hand, H_2O_2 is involved as a secondary messenger in signal transduction, and it can regulate the gene expression and protein synthesis in plants (Kairong et al., 1999; Zhang et al., 2010; Smirnoff and Arnaud, 2018).

Guaiacol peroxidase (POX) participates in the processes of lignification, ethylene biosynthesis, and defense against pathogens, and exhibits antioxidant properties (Becana et al., 2000; Verma et al., 2012). Peroxidases are also involved in plant cell development, including somatic embryos of coniferous species (Kormuták et al., 2003; Zhang et al., 2010; Peng et al., 2020). POX activity has been detected by Hazubska-Przybył et al. (2013, 2020) during the SE induction phase in *Picea abies* and *P. omorika*. POX is active in explants (mature zygotic embryos), in 8-week-old embryogenic and nonembryogenic

Abbreviations: 2,4-D, 2,4-dichlorophenoxyacetic acid; BA, 6-Benzylaminopurine; ET, embryogenic tissue; FA, forced aeration; FW, fresh weight; H_2O_2, hydrogen peroxide; PGR, plant growth regulator; POX, guaiacol peroxidase; SE, somatic embryogenesis; TCA, trichloroacetic acid.

calluses, and induced ETs (Hazubska-Przybył et al., 2013). In both spruce species, the pattern of POX activity is similar, with the lowest activity found in explants and the highest in 8-week-old embryogenic and nonembryogenic calluses. In ETs, POX activity was moderate and independent of the type and concentrations of PGRs added to the induction and proliferation media. In *P. abies*, further studies have shown that 2,4-D and picloram stimulate POX activity during the proliferation of ETs (Hazubska-Przybył et al., 2020). Based on these results, POX is involved in the SE of both *Picea* spp., and may be an indicator of this process.

In this study, we tested the suitability of suspension cultures to increase the productivity of ET in the Norway spruce SE pilot pipeline compared with the current semisolid plate proliferation-based regime with refined maturation protocols. We also tested different suspension PGR concentrations, measured the level of selected indicators of stress conditions as H_2O_2 content and POX activity, and evaluated the quality of mature cotyledonary embryos and the survival of the emblings produced in both proliferation methods.

MATERIALS AND METHODS

Plant Material

The Norway spruce embryogenic cell lines (later referred to as lines) (**Table 1**) from full-sib families of progeny-tested plus trees were initiated in 2014 (11 lines, 8 families) from immature seed embryos according to Klimaszewska et al. (2001), and cryopreserved and thawed as described by Varis et al. (2017). The lines initiated in 2019 (9 lines, from 6 families) were subcultured every other week on semisolid media until used in the experiments.

Embryogenic Tissue Proliferation

The proliferation of ET prior to the experiments and as controls were done using Litvay's modified medium (mLM) (Litvay et al., 1985; Klimaszewska et al., 2001) according to Varis (2018) with 1% (w/v) sucrose, and half concentrations of macro-elements with pH adjusted to 5.8. The growth regulators were 2,4-D (Alfa Aesar, Kendel, Germany) and BA (Sigma Aldrich, Steinheim, Germany) at 10 and 5 μM, respectively. The semisolid proliferation medium was solidified with 4 g/l gellan gum (Phytagel, Sigma Aldrich, Steinheim, Germany), and 21 ml of medium was dosed in 92 × 16 mm sterile Petri dishes (Sarstedt, Nümbrecht, Germany). For all media, 500 mg/l L-glutamine was added after autoclaving by filter sterilization.

The suspension cultures in Experiments I–III were established by weighing 1,000 to 1,200 mg of ET grown on plates into a 50-ml sterilized centrifuge tube. Only fresh handpicked tissue was used as inoculum in Experiment III; in the other experiments, whole ET clumps were used without selection. In Experiment IV, a lower inoculum weight between 900 and 1,000 mg was used. Sterilized liquid mLM proliferation medium (45 ml) was added on top of the tissue, and the tube was shaken vigorously. The suspension was poured into a 500-ml laboratory bottle filled with 100 ml of medium (total suspension volume 145 ml). In Experiment IV, smaller 250-ml bottles with 125 ml of total media volume were used. The suspension cultures were grown in the dark at +21°C on a shaker (Infors AG CH4013, Bottmingen, Switzerland) at 120 rpm for 7 days. In Experiment I, the suspension culture was compared with the semisolid culture, with both having the same PGR concentrations. The ET mass on the semisolid plates was 800 to 1,050 mg (**Table 1**). In Experiments II and III, 0.5x PGR, and in Experiment IV, 0.1x PGR, concentrations were tested (**Table 1**). In Experiments I and II, each genotype were grown in each media in two bottles, in Experiment III, in one bottle, and Experiment IV in three bottles (**Table 1**). Forced aeration (FA) (10 min, every 3 h) implemented with peristaltic aquarium pumps and custom caps with tube passages was tested for the proliferation of four lines in Experiment IV.

The ET growth at the end of the culture in Experiments I, II, and IV was measured as fresh weight (FW) by pouring the suspension into a Büchner funnel with filter paper and sucking the liquid out. The tissue was weighed and divided by the inoculum weight to obtain the growth factor.

Analysis of Indicators of Stress Conditions

The samples were collected after 7 days from the previous subculture from each suspension bottle (three per treatment/line) and the control plates (two samples per treatment/line) in Experiment IV, and snap-frozen in liquid nitrogen. To determine the H_2O_2 content and POX activity, 80–100 mg (FW) of tissue per line per treatment was prepared and stored at −80°C until transportation with dry ice in the container.

Hydrogen Peroxide Content

The samples were finely ground in liquid nitrogen and homogenized with 5 ml of 5% (w/v) trichloroacetic acid (TCA) containing 10 mM ethylenediaminetetraacetic acid tetrasodium salt dihydrate (EDTA). The amount of H_2O_2 was determined following the procedure described by Sagisaka (1976). The reaction mixture consisted of 0.5 ml of supernatant, 1.5 ml of 50% TCA, 0.4 ml of 10 mM iron-ammonium sulfate, and 0.2 ml of 2.5 M potassium thiocyanate. The reaction mixture containing 0.5 ml of 5% TCA instead of supernatant was used as the control. Absorbance was measured at 480 nm with a (Shimadzu Corporation, Kyoto, Japan). The obtained analysis results were expressed as nmol g^{-1} FW.

Protein Extraction and Guaiacol Peroxidase Activity

Protein extraction was carried out at 4°C. The samples were ground in liquid nitrogen and homogenized in 50 mM sodium phosphate buffer, pH 7.0, containing 0.2 mM EDTA and 2% polyvinylpolypyrrolidone, and were incubated for 1 h. The homogenates were centrifuged at 4°C at 20,000 × g for 20 min.

The POX activity was measured spectrophotometrically from the same samples as H_2O_2 in line with the Chance and Maehly (1955) method. The guaiacol oxidation reaction was performed at 470 nm for 1 min at +20°C at an extinction coefficient of å = 26.6 mM/cm. The reaction mixture contained 1 ml of 0.1 M phosphate buffer, pH 7.0, 1 ml of 1% guaiacol, 1 ml of 0.2 M H_2O_2, and 12–25 μl of the enzyme extract. In the control assays, the enzyme extracts or substrates were replaced with a buffer. The reaction started after adding H_2O_2. The POX activity in the tested samples was presented as nkat min^{-1} mg^{-1} protein. The protein content

TABLE 1 | Information on lines and treatments used in each experiment.

	Experiment I	Experiment II	Experiment III	Experiment IV
Cell line	1,198	1,198	1,247	1,130
	2,816	4,089	1,266	1,375
	3,416	4,146	1,430	2,086
	4,611	5,115	1,810	2,816
	5,115		1,825	5,137
			2,020	
			2,064	
			3,129	
			4,312	
Inoculum	1,000–1,200 mg whole ET clumps	1,000–1,200 mg whole ET clumps	1,000–1,200 mg selected fresh ET	800 to 1,050 mg whole ET clumps
No. replicates in proliferation	2 in suspension, 2 in semisolid media	2	1	3
Treatments	1x PGR	1x PGR	1x PGR + Rinse	1x PGR + Rinse
	semisolid plates (proliferation and maturation)	0.5x PGR	0.5x PGR + Rinse	0.1x PGR + Rinse
		1x PGR + rinse		1x PGR + rinse + FA
		Semisolid plates (ET for maturation)	semisolid plates (ET for maturation)	semisolid plates (ET for maturation)
Inoculum in maturation	Suspension pipetted; tissue amount estimated visually	Suspension pipetted; tissue amount estimated visually	Suspension pipetted; tissue amount estimated visually	140–160 mg of tissue weighed from suspension
Replicates in maturation	6 from suspensions and 6 from semisolid media	6 from suspensions and 5 from semisolid plates	6 from suspension bottles and 6 from semisolid plates	9 from suspensions and 5 from semisolid plates
Embryos in cold storage (months)	10	9	4	7
Transplantation date	18th July 2020	18th July 2020	18th July 2020	1st July 2021

In Experiment I, proliferation in suspension was compared with proliferation on semisolid media. In Experiment II, rinsing ET before maturation or halved plant growth regulator (PGR) concentration in proliferation media was implemented to improve the maturation result. In Experiment III, embryogenic tissue (ET) was grown with halved PGR and rinsed. In Experiment IV, ultralow PGR concentration with rinsing the ET was tested. Increased gas exchange was also tried for a 1x PGR suspension (Forced aeration, FA). Semisolid grown ET was used as a control for maturations in all experiments. 1x PGR (10 μM 2,4-D and 5 μM BA) was the control treatment; experimental treatments with modified PGR rates (0.5x and 0.1x) were applied in Experiments II to IV. Additionally, ETs were rinsed (+ rinse) to reduce PGR residues during maturation. In Experiments I–III, ET was pipetted from suspension onto filter papers, and in Experiment IV, ET was matured as if from semisolid media by weighing 140 to 160 mg from suspension-grown ET dried with suction.

was estimated according to Bradford (1976) with bovine serum albumin (BSA) as a standard.

Maturation

Maturation on semisolid media was carried out according to Lelu-Walter et al. (2008) and optimized by Tikkinen et al. (2018a). Fresh tissue (140–200 mg) was picked from proliferation plates 5–7 days after the previous subculture and resuspended into 3 ml of liquid hormone-free maturation media in a 14 ml polypropylene (PP) tube. The tube was shaken and the contents poured onto a filter paper (Munktell no. 1, Ahlstrom-Munksjö, Falun, Sweden) placed inside a Büchner funnel and dried with a low-pressure pulse. Then the filter paper with ET was placed on an LM medium with 30 μM (±)-abscisic acid (Sigma Aldrich, Steinheim, Germany), 0.2 M sucrose, and 6 g/l gellan gum (Phytagel), and 140–200 mg of ET from semisolid plates or 2.5–3 ml from suspensions was added. Because of the heterogeneity of the suspensions, the amount of tissue in the pipette was visually estimated to be adequate before plating, and the maturation results for Experiments I–III are presented as embryos per plate. In Experiment IV, instead of pipetting the suspension, the ET from a culture bottle was first sucked dry on a filter paper in a Büchner funnel and weighed. After that, the maturation was done like previously described from semisolid plates. After maturation (7–8 weeks, in the dark, +21°C) good-quality cotyledonary embryos were counted using a stereomicroscope, plates resealed with parafilm and moved to cold storage (+2°C, in the dark) for four to ten months in closed boxes (Tikkinen et al., 2018b). In Experiments I, and III six and in Experiment II five, maturations were made from ET grown on semisolid media, and six from each suspension treatment for each line. In Experiment IV, five maturations from semisolid media and nine from each suspension treatment were made for each line.

Germination and Transplantation

From Experiments I, II, and III, up to 27 embryos from each treatment in each line (total 943) were germinated in intensity (photosynthetic photon flux density) of 190–210 μmol m^{-2} s^{-1} (Valoya L14 spectrum AP67 Milky LED, Valoya Oy, Helsinki, Finland), with an 18 h/6 h day/night photoperiod. After two weeks, they were transplanted into a peat-based substrate in a greenhouse in July 2020

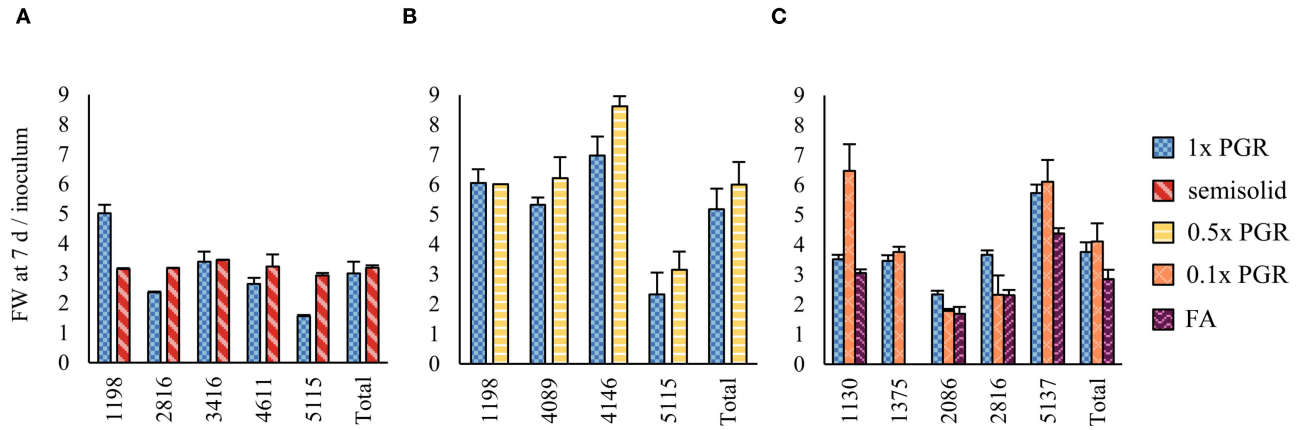

FIGURE 1 | Proliferation rates between different treatments in Experiments I **(A)**, II **(B)**, and IV **(C)**. 1x plant growth regulator (PGR), 0.5x PGR, and 0.1x PGR stand for the concentrations of plant growth regulators 2,4-dichlorophenoxyacetic acid (2,4-D) and 6-Benzylaminopurine (BA) in suspension cultures. Mean values of growth factors (fresh weight (FW) after 1 week/inoculum FW) are presented with the standard error of the mean (SEM). No significant differences were found between the treatments within each experiment.

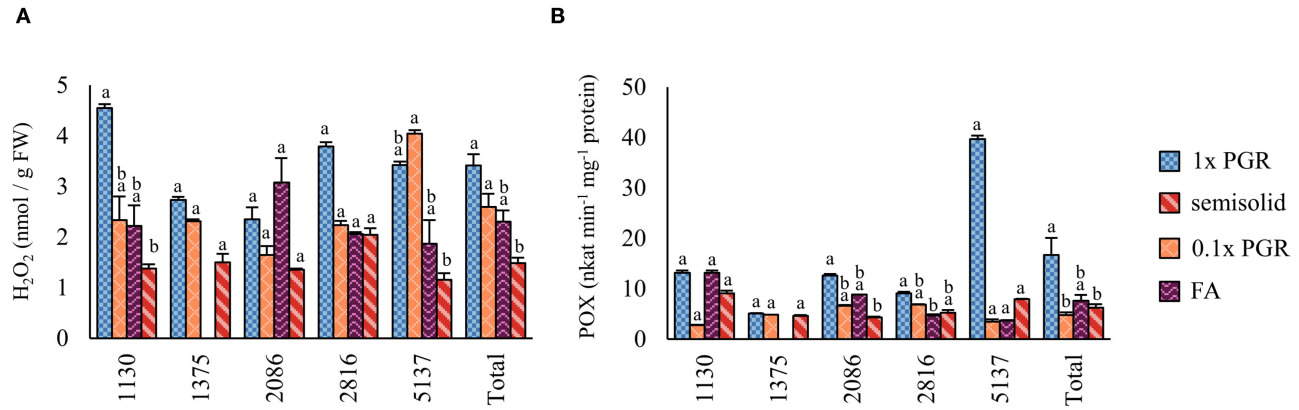

FIGURE 2 | Oxidative stress analysis results for Experiment IV as represented by **(A)** hydrogen peroxide (H_2O_2) content and **(B)** guaiacol peroxidase (POX) enzyme activity. Mean values are presented with error bars representing the SEM. Significant differences between treatments within lines or overall (Total) are marked with different letters.

(Tikkinen et al., 2018b). The survival (alive or dead) of each embling was evaluated after 41 days. In Experiment IV, all the available embryos (total 2,619) after cold storage were germinated as in the previous year and transplanted in July 2021. The survival of the embryos was evaluated after 42 days.

Statistical Analysis

Statistical analysis was carried out using IBM SPSS Version 27 software. The normality of the results was checked using the Shapiro-Wilk and Kolmogorov-Smirnov tests. As the data were not normally distributed, the non-parametric Mann-Whitney U test and the Kruskal-Wallis test were used to test for significant differences between the treatments, adjusted with the Bonferroni correction for multiple comparisons. $p < 0.05$ was considered significant. The differences between the treatments in greenhouse tests in Experiments I to III were analyzed with chi-square tests. In Experiment IV, greenhouse survival was analyzed with logistic regression with line, treatment and the location in the containers (row and column) as covariates.

RESULTS

Proliferation

Proliferation in suspension in Experiment I yielded similar amounts (FW) of ET after one week of culture to proliferation on semisolid plates in relation to inoculum mass (**Figure 1A**). The PGR concentrations were reduced in the subsequent Experiments II, III, and IV in an attempt to improve maturation results. Reducing both 2,4-D and BA concentrations to 0.5x (**Figure 1B**) or 0.1x (**Figure 1C**) did not significantly affect the proliferation in suspension cultures in Experiments II and IV. The mean growth in the 1x PGR suspension treatment in different experiments had variation that was probably due to different genotypes being used. Overall, there was less variation in the proliferation rate among genotypes on a semisolid

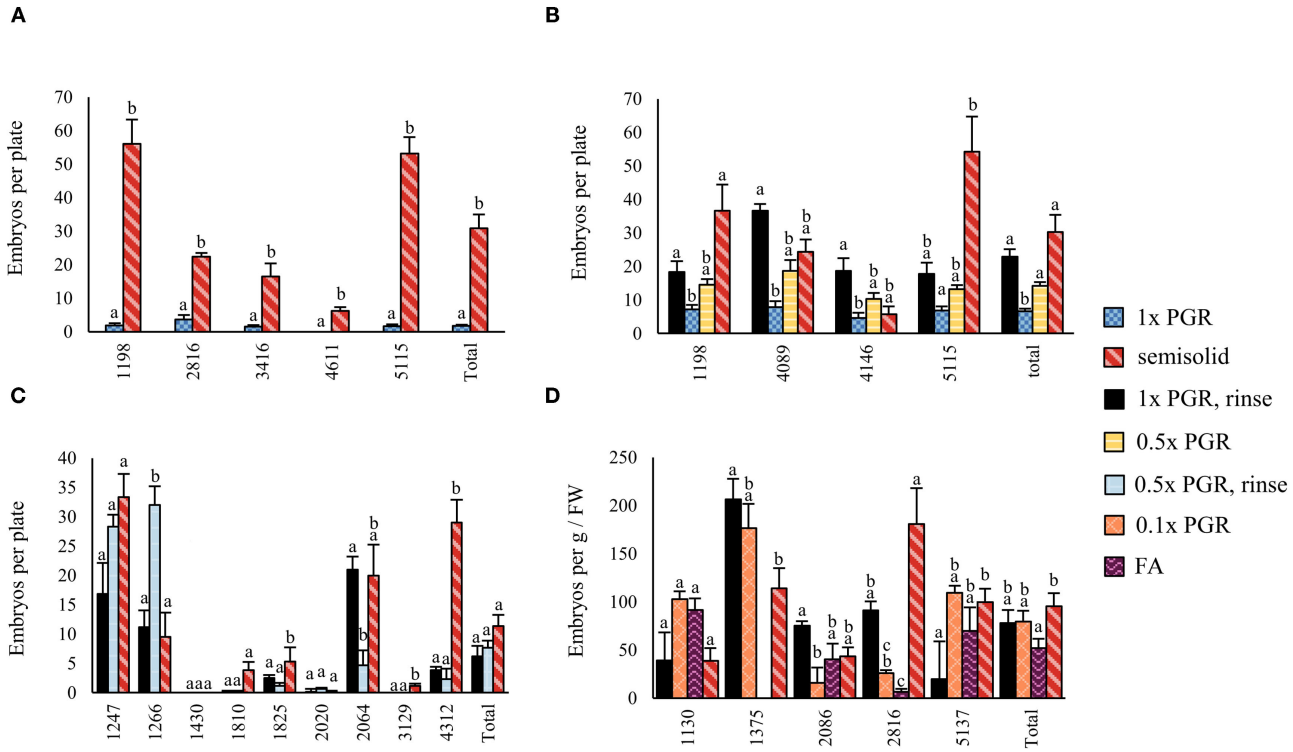

FIGURE 3 | Embryo production in Experiments I **(A)**, II **(B)**, III **(C)**, and IV **(D)**. 1x PGR, 0.5x PGR, and 0.1x PGR stand for the concentrations of plant growth regulators 2,4-D and BA in suspension cultures. In Experiments I–III, embryos per plate were counted, and in Experiment IV, it was standardized per g of ET put to maturation plates. Mean values are presented with the SEM. Significant differences between treatments within lines or overall (Total) are marked with different letters.

medium than in suspension treatments (**Figure 1**). The growth of ET was decreased by FA, but this can be at least partly attributed to agitation from aeration throwing tissue out of the medium onto the culture bottle walls, and the difference was not statistically significant.

Level of Indicators of Stress Conditions

In Experiment IV, the H_2O_2 concentration was lower in the ET samples grown on plates than in 1x PGR ($p < 0.01$) or 0.1x PGR ($p = 0.01$) suspensions (**Figure 2A**). The POX enzyme activity was lower in 0.1x PGR suspension ($p < 0.01$) and on plates ($p = 0.02$) than in 1x PGR suspensions (**Figure 2B**). No significant correlations were found between either POX activity or H_2O_2 concentration and embryo yield or ET growth in suspension.

Embryo Yield

In Experiment I, significantly fewer embryos were obtained from suspension-grown ET than from ET grown on semisolid medium ($p < 0.01$) (**Figure 3A**). Rinsing ET before maturation with hormone-free liquid maturation media increased cotyledonary embryo yield ($p < 0.01$), as did halving the PGR content in the liquid medium ($p < 0.01$) (**Figure 3B**). Semisolid media was not significantly better than a rinsed 1x PGR suspension ($p = 1.00$). A slightly lower embryo yield was obtained from a 1x PGR suspension in Experiment I than in Experiment II, but most of the lines used in the experiments differed. In Experiment III, the combination of halved PGRs and rinsing the tissue did not significantly improve embryo yield compared to just rinsing the tissue (**Figure 3C**). Again, no differences were found between a rinsed 1x PGR ($p = 0.10$) or rinsed 0.5x PGR ($p = 0.10$) suspension and semisolid medium.

In Experiment IV, maturations were conducted by drying suspension tissue and weighing the tissue for maturation instead of directly pipetting the suspension from culture bottles. In this way, results in relation to the FW of ET placed for maturation could be obtained (**Figure 3D**). As in previous experiments, no significant differences in embryo yield were found between ET grown on semisolid or rinsed from 1x PGR suspensions ($p = 1.00$) when all lines were tested together. Using ultralow 0.1x PGR concentrations did not improve embryo yield compared to 1x PGR ($p = 1.00$). FA decreased embryo yield significantly compared with semisolid-grown ET ($p = 0.03$). As in previous experiments, more significant differences were found between treatments within lines. For example, rinsed ET from a 1x PGR suspension produced more cotyledonary embryos than ET from plates in line 1,375 ($p = 0.04$), but the opposite was true for line 5,137 ($p = 0.04$). With line 1,130 0.1x PGR developed faster than 1x PGR, as exemplified by **Figure 4**, but this was not the case for all the lines.

Survival After Transplantation

No significant differences were found between the treatments regarding the survival of the embryos at 41 days after transplanting in Experiments I, II, and III (**Figure 5**). However,

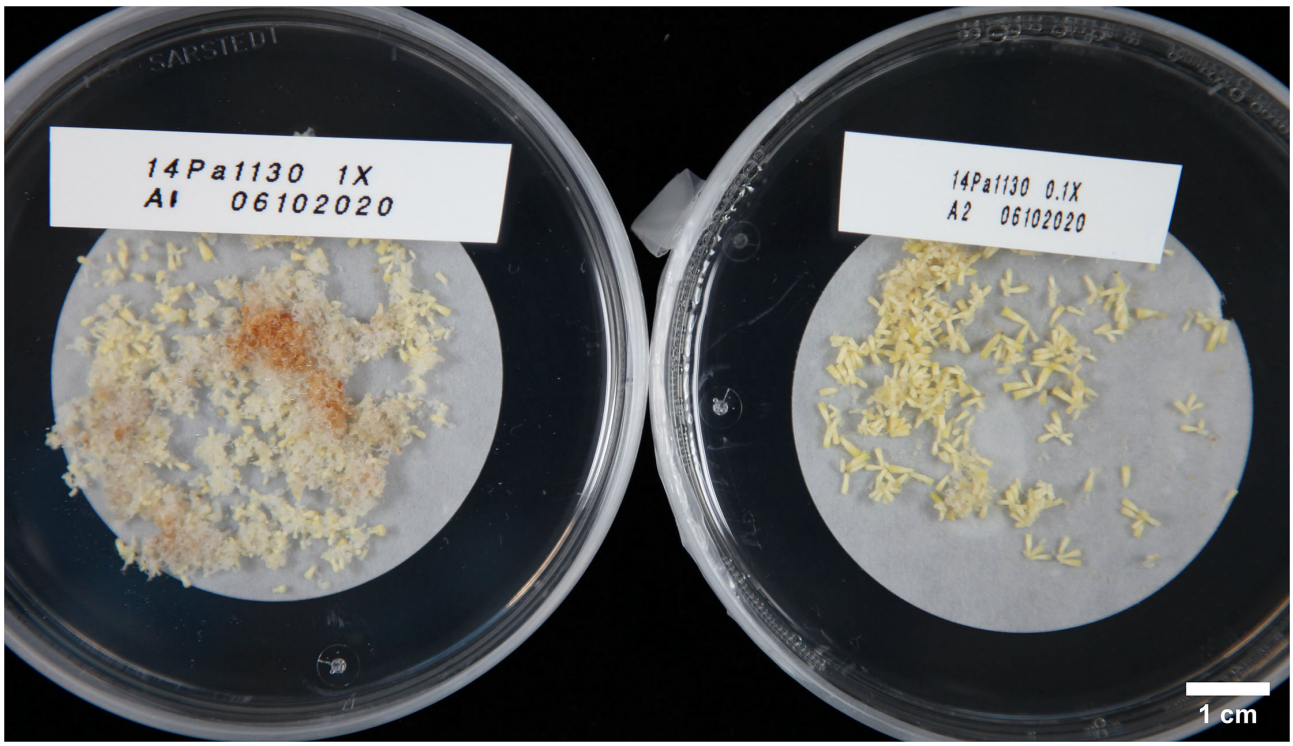

FIGURE 4 | Embryos from line 1,130 photographed 23 days after transfer from proliferation to maturation with rinsing in Experiment IV. The left plate has been matured from 1x PGR suspension and the right plate from 0.1x PGR suspension.

the embryo's overall survival was only 51%, probably because of the harsh summer conditions in July and the too heavy cover of woodchips applied to prevent the growth of algae and moss (Landis et al., 2010).

In Experiment IV, all the cotyledonary embryos on the plates after cold storage were transplanted. Due to the post-maturation of the slow-developing embryos, there were more cotyledonary embryos in the plates after cold storage than before it: 0.1x PGR had 1.5 times the embryos, 1x PGR 1.7 times, FA 1.8 times, and semisolid plates 1.5 times. Overall survival was higher than in the previous year, at 82%. Based on the binary logistic model (**Table 2**), a 1x PGR suspension with or without FA resulted in decreased survival compared to proliferation on semisolid media. However, a significant decrease in survival was not observed with 0.1x PGR suspension.

DISCUSSION

Suspension cultures are generally considered to have a higher multiplication rate than cultures on semisolid media (von Arnold et al., 2002; Gupta and Timmis, 2005). In the present study, In Experiment I, similar ET growth was achieved on semisolid media and in suspension cultures. Although the lack of semisolid controls and different lines hinders the comparison between experiments, better overall growth was achieved in suspension cultures in Experiments II and IV than in Experiment I, but the growth rate varied greatly among lines. A higher growth rate in suspension could be achieved by optimizing the inoculum, culture time, and medium composition (Denchev and Grossnickle, 2019). In our study, the same basal media composition was used for both semisolid and suspension cultures. The higher growth in suspension cultures is attributed to better nutrient availability and dispersion (von Arnold et al., 2002). The homogeneity of suspensions varied greatly among lines because some lines tended to form more tissue clusters than others. Higher rotation speeds, stirring mechanisms, or mechanical treatment of ET could be used to improve dispersion in the suspensions, and consequently growth (Mamun et al., 2018). This would also lead to a more even spread and more synchronized development on the maturation plates, which also show great variation for plate-grown ET. However, if rotation speeds are too high, it may lead to deficient suspensor development because of increased shear stress, which could impair embryo development later (Sun et al., 2010; González-Cabrero et al., 2018).

Scaling up the production unit's volume or area increases the risk of losing larger amounts of material if ET is contaminated. This is especially relevant for using liquid media where contaminated units cannot be rescued, which is sometimes possible for semisolid media with, e.g., a single bacterial colony. However, throughout these trials, no bottles were lost to contamination, which suggests that suspension cultures are safer than temporary immersion system bioreactors (Välimäki et al., 2020), for example. Yet no subcultures with liquid

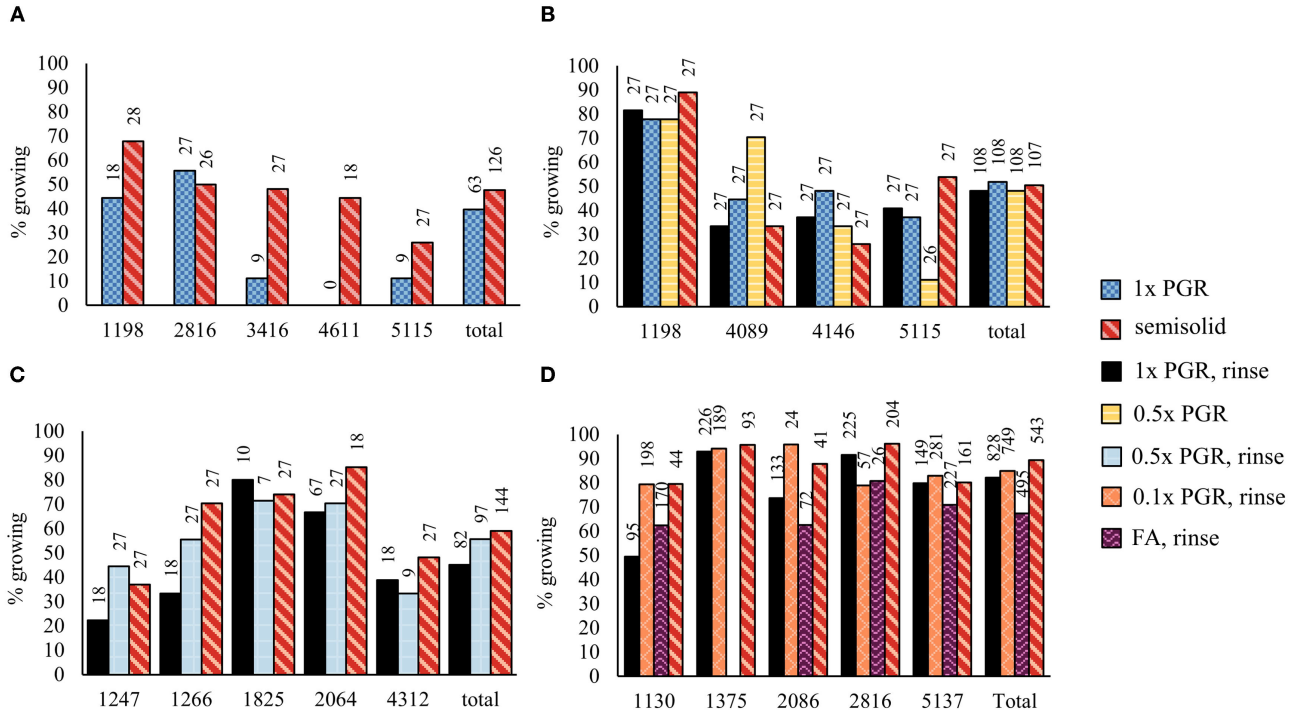

FIGURE 5 | Survival of emblings from Experiments I **(A)**, II **(B)**, and III **(C)** transplanted in July 2020 and Experiment IV **(D)** transplanted in July 2021. The survival in the greenhouse was evaluated 41 d and 42 d after transplantation in 2020 and 2021 respectively. 1x PGR, 0.5x PGR, and 0.1x PGR stand for the concentrations of plant growth regulators 2,4-D and BA in suspension cultures. The numbers at the end of the bars represent the number of embryos transplanted. The results of Experiment IV were analyzed with logistic regression presented in **Table 2**.

media were made which would predispose the cultures to handling, and therefore, potential contamination. Additionally, based on our results, there is greater genotypic variability in embryo production from suspension-grown ET, which may lead to a greater loss of lines from the production. The protocol's suitability for a large number of lines is important for maintaining sufficient genetic diversity and adaptability in the clonal forest regeneration material, especially in long-lived species such as Norway spruce (Park, 2002; Rosvall et al., 2019). The protocol's applicability to many lines also allows the selection of lines based on other characteristics than suitability for *in vitro* SE culture, and thus the effective implementation of the improvements from the tree-breeding program (Tikkinen et al., 2018b).

The PGRs needed for initiation and proliferation must be omitted for the maturation process to succeed. Interestingly, the reduction of PGRs in suspension cultures to 0.5x or even to 0.1x did not lead to reduced proliferation, which indicates that ET growth in suspension was not limited by PGR availability. Excessive PGR concentrations during proliferation can reduce embryo yield and lead to ET maturation into malformed embryos (Denchev and Grossnickle, 2019; Garcia et al., 2019). Furthermore, prolonged exposure to 2,4-D may lead to genetic or epigenetic variation (von Arnold et al., 2002; Garcia et al., 2019). Similar results are reported for *Pinus pinea* (L.), for which the use of ultra-low PGR concentrations does not compromise the growth of suspension cultures (González-Cabrero et al., 2018).

In Experiment I, maturations made from ET grown in suspension produced significantly fewer embryos than from ET grown on semisolid media. The pipetting of the suspension may have left residues of proliferation PGRs on maturation plates to interfere with maturation. Such a straightforward maturation design would be ideal for large-scale plant production purposes and automation. The measures taken in the subsequent Experiments II and III to reduce the 2,4-D and BA presence in maturation, rinsing or reducing PGR concentration, increased maturation yield. However, the combination of rinsing and reducing the PGR concentration did not lead to further improvement. Rinsing adds another step to the process, but it can be quite easily automated. In our current protocol, the semisolid-grown ET is inadvertently rinsed, because it is first suspended in a PGR-free medium before being spread onto filter papers on maturation media (Klimaszewska and Smith, 1997; Tikkinen et al., 2019). Synthetic PGRs like 2,4-D can have a lower turnover rate than their natural counterparts like indole-3-acetic acid (von Arnold et al., 2002; Grossmann, 2010). Therefore, pre-maturation treatments are often used in maturation protocols to reduce endogenous 2,4-D from ET and to increase the synchronization of the ET before exposure to abscisic acid treatment (Bozhkov et al., 2002; von Arnold et al., 2005; Mamun et al., 2018; Välimäki et al., 2020). The benefit of the

TABLE 2 | Logistic regression model used for analyzing the effect of proliferation and maturation treatments in Experiment IV on transplanted embryo survival.

Model, *log(p/1 – p)*	Variable	*P*-value	Odds ratio (95% CI)	Treatment or genotype	% of cases predicted correctly by model
$log(p/1-p) = 1.805 - 0.101p_1 - 0.616p_2 - 0.840p_3 - 0.496l_1 + 1.369l_2 - 0.062l_3 + 1.020l_4 + 0.000r_1 - 0.019c_4$					81.6
	Proliferation treatment	<0.001	1	Plate grown ET	
		0.579	0.904 (0.634–1.290)	0.1x PGR suspension, rinsed	
		<0.001	0.540 (0.386–0.757)	1x PGR suspension, rinsed	
		<0.001	0.432 (0.305–0.611)	1x PGR suspension, forced aeration, rinsed	
	Line	<0.001	1	5,137	
			0.609 (0.472–0.786)	1,130	
			3.933 (2.601–5.946)	1,375	
			0.940 (0.673–1.312)	2,086	
			2.774 (1.918–4.011)	2,816	
	Container location (row)	1.000	1.000 (0.961–1.041)		
	Container location (column)	0.350	0.981 (0.943–1.021)		

The binary response (alive or dead) was estimated from photographs 42 d after transplantation into nursery.

pre-maturation step in contrast to increased labor and material requirements, for suspension or semisolid culture, needs to be analyzed, and it is currently not used in our semisolid protocol.

Based on the results of Experiment IV, cold storage treatment according to Tikkinen et al. (2018b) improved the final cotyledonary embryo yield of 1x PGR suspension-grown ET somewhat more than plate-grown ET. This time, the comparison was possible, because all the embryos in Experiment IV were germinated and transplanted instead of being samples, as in Experiments I to III. Often due to precocious germination, 0.1x PGR maturations had a poor embryo yield, which could be ameliorated by shorter maturation treatment, as exemplified by the faster development of line 1,130 in **Figure 4**. However, with 1x PGR, this owed more to the large numbers of underdeveloped or aberrant embryos. It was hypothesized that this was related to the higher oxidative stress in 1x PGR suspensions. This could indicate that lower PGR concentrations may speed up the maturation, and higher concentrations, rather than impairing embryo development, may simply slow it down. Slow embryo development is not an issue with a sufficiently long cold storage period. There were many differences among the lines in post-maturation embryo development, even when all the lines used in experiments were known to perform well on a semisolid culture. However, treatments that had a greater increase in cotyledonary embryo numbers during the cold storage had a somewhat lower survival rate in the greenhouse.

The greenhouse survival of emblings in Experiments I–III showed no significant differences among treatments. When a larger number of embryos was transplanted in 2021, an increased number of plants revealed differences among the proliferation treatments. Embling survival was still highest on semisolid-grown ET, but again with high variation among lines. However, when the interaction between lines and treatments were considered in the model, no differences were found in embling survival between 0.1x PGR and semisolid plates. This suggests that the greenhouse survival of emblings was more affected by other factors than the amount of PGR during proliferation. The overall survival was better in 2021 (Exp. IV) than in 2020 (Exps. I–III), which was probably mainly due to the more suitable greenhouse conditions that year, but could be partly caused by different lines being used in different years.

The results' comparability suffers from a lack of standardization of the amount of starting tissue on maturation plates because the ET from suspension was pipetted and not weighed onto plates in Experiments I–III, therefore weighing was impossible. However, care was taken to visually produce samples with similar amounts of tissue. In Experiment IV suspension tissues were weighed onto plates like semisolid grown ET. This may have resulted in a more thorough rinsing and thus improved the result. However, the weighing of suspension for maturation is unfeasible in the large-scale application of SE, because no benefit in labor reduction is achieved. In our study, the time of proliferation in suspension was limited to one week. Improving the maturation became a priority because there was a dramatic difference in embryo yield observed in Experiment I already after 7 days of culture. Prolonged *in vitro* culture should be avoided to reduce the risk for somaclonal mutations, and reduced embryogenic potential that occurs over time (Breton et al., 2006; Egertsdotter, 2019). Mass-propagations are and will most likely be done using cryopreserved materials that are proliferated first on semisolid medium following thawing (Varis et al., 2017). Ideally, the suspension culture phase would only be a few rounds of bulking up the tissue before maturation, not the prolonged culture of multiple months.

An analysis of the H_2O_2 content in ET cultured in a semisolid medium and a suspension culture showed that it was lower in semisolid cultures. The results indicate that the culture's liquid environment is more conducive to H_2O_2 accumulation than the semisolid environment, probably because of higher nutrient availability in suspension cultures (Denchev and Grossnickle, 2019). As there was no correlation between H_2O_2 content or activity on the part of the antioxidant system and embryo performance from the ET growth in suspension, we cannot conclude that we are dealing here with pronounced oxidative

stress. Hence, we speculate that H_2O_2 plays a signaling role in this case instead of a stress factor role, as previously demonstrated by (Zhang et al., 2010) for *Larix leptolepis* and (Hazubska-Przybył et al., 2020) for *Picea* ssp. In *P. abies*, Hazubska-Przybył et al. (2020) have demonstrated that the production of H_2O_2 is linked to the auxin type applied during the proliferation of ETs. In the presence of 1-naphthaleneacetic acid, POX activity is reduced, and ET proliferation is increased. According to the authors, this may be related to the signaling role of H_2O_2, which is supported by the current results.

POX activity was significantly higher in a suspension culture with 1x PGRs than on a semisolid medium or in 0.1x PGR suspension cultures. This implies that supplementing the liquid medium with a higher concentration of PGRs resulted in a stronger response from the antioxidant system in the form of increased POX activity in the tissues, suggesting that in the liquid medium, higher PGR concentrations have a stronger effect on tissues in the semisolid medium. Previously, POX activity during induction of embryogenic *Picea* spp. has been shown by Hazubska-Przybył et al. (2013, 2020). Oulbi et al. (2021) obtained higher POX values for ET than for nonembryogenic callus, both induced from zygotic embryos of *Olea europaea*. In contrast, the POX activity in *P. koraiensins* is reduced in ET, and the antioxidant system controls the formation and development of the somatic embryos of this pine species (Peng et al., 2020). Previously, peroxidase activities have been reported in embryogenic and nonembryogenic tissues, as well as in *Eleutherococcus senticosus* somatic embryos, at different stages of development in a bioreactor (Shohael et al., 2007). This activity is lowest in the nonembryogenic callus and gradually increases, starting from the proembryogenic mass to the mature stage of the somatic embryo. In general, studies on the oxidative stress in trees during SE remain scarce and should be developed to better understand the mechanisms controlling this process *in vitro*, including suspension and bioreactor cultures.

Based on our results, suspension cultures can provide similar or better growth rates with better process scalability than semisolid cultures. Due to better PGR and nutrient availability, lower PGR concentrations can be used without decreasing proliferation rates. The differences in growth environment are exemplified by a higher H_2O_2 content and POX activity in ET grown in 1x PGR suspensions than on 1x PGR semisolid media. To achieve embryo yields comparable with yields from semisolid grown ET, rinsing before maturation is required. Using the full-strength PGR for suspension proliferation may lead to decreased embling survival after transplantation. The effects of long-term suspension culture need to be studied, and a comparison of the workload between semisolid and suspension cultures is needed to evaluate the potential of suspension SE cultures for commercial plant regeneration material production.

DATA AVAILABILITY STATEMENT

The raw data supporting the conclusions of this article will be made available by the authors, without undue reservation.

AUTHOR CONTRIBUTIONS

SakV had the main responsibility for designing and conducting the experiments, analyzing the data, and writing the manuscript. TH-P and ER planned and conducted the indicators of stress condition experiments and participated in writing the manuscript. MT, SaiV, and TA participated in planning the experiments, data analysis, and writing the manuscript. All the authors have read and agreed to the published version of the manuscript.

FUNDING

This research was funded by the European Regional Development Fund, South Savo Regional Council, and Savonlinna municipality (A76396) and work was supported by statutory research of the Institute of Dendrology of the Polish Academy of Sciences. The MULTIFOREVER project supported this research under the umbrella of the ERA-NET co-fund Forest Value by ANR (FR), FNR (DE), MINCyT (AR), MINECO-AEI (ES), MMM (FI), and VINNOVA (SE). Forest value has received funding from the European Union's Horizon 2020 research and innovation program, under agreement N° 773324.

ACKNOWLEDGMENTS

We wish to thank the technical staff at the Luke Savonlinna unit involved in laboratory and greenhouse work.

REFERENCES

Baxter, A., Mittler, R., and Suzuki, N. (2014). ROS as key players in plant stress signalling. *J. Exp. Bot*. 65, 1229–1240. doi: 10.1093/jxb/ert 375

Becana, M., Dalton, D. A., Moran, J. F., Iturbe-Ormaetxe, I., Matamoros, M. A., and Rubio, M. C. (2000). Reactive oxygen species and antioxidants in legume nodules. *Physiol. Plantarum*. 109, 372–381. doi: 10.1034/j.1399-3054.2000.100402.x

Bonga, J. M. (2016). "Conifer clonal propagation in tree improvement programs," in *Vegetative Propagation of Forest Trees*, eds. Y. S. Park, J. M. Bonga, and H.-K. Moon (Seoul, Korea: National Institute of Forest Science), 3–31.

Boulay, M. P., Gupta, P. K., Krogstrup, P., and Durzan, D. J. (1988). Development of somatic embryos from cell suspension cultures of Norway spruce (*Picea abies* Karst.). *Plant. Cell. Rep*. 7, 134–137. doi: 10.1007/BF00270123

Bozhkov, P. V., Filonova, L. H., and von Arnold, S. (2002). A key developmental switch during Norway spruce somatic embryogenesis is induced by withdrawal of growth regulators and is associated with cell death and extracellular acidification. *Biotechnol. Bioeng*. 77, 658–667. doi: 10.1002/bit.10228

Bradford, M. M. (1976). A rapid and sensitive method for the quantitation of microgram quantities of protein utilizing the principle of protein- dye binding. *Anal. Biochem*. 72, 248–254. doi: 10.1016/0003-2697(76)90527-3

Breton, D., Harvengt, L., Trontin, J. F., Bouvet, A., and Favre, J. M. (2006). Long-term subculture randomly affects morphology and subsequent maturation of

early somatic embryos in maritime pine. *Plant Cell Tiss. Org.* 87, 95–108. doi: 10.1007/s11240-006-9144-9

Chance, B., and Maehly, A. C. (1955). "Assay of catalases and peroxidases," in Methods in enzymology, eds. S. P. Collowick, N. O. Kapplan (New York, NY: Academic Press), 764–775. doi: 10.1016/S0076-6879(55)02300-8

Cheng, W. H., Wang, F. L., Cheng, X. Q., Zhu, Q. H., Sun, Y. Q., Zhu, H. G., et al. (2015). Polyamine and its metabolite H_2O_2 play a key role in the conversion of embryogenic callus into somatic embryos in upland cotton (*Gossypium hirsutum* L.). *Front. Plant Sci.* 6:1063. doi: 10.3389/fpls.2015.01063

Das, K., and Roychoudhury, A. (2014). Reactive oxygen species (ROS) and response of antioxidants as ROS-scavengers during environmental stress in plants. *Front. Environ. Sci.* 2:53. doi: 10.3389/fenvs.2014.00053

Denchev, P., and Grossnickle, S. C. (2019). Somatic embryogenesis for conifer seedling production: the biology of scaling. *Reforesta*. 7, 109–137. doi: 10.21750/REFOR.7.08.70

Egertsdotter, U. (2019). Plant physiological and genetical aspects of the somatic embryogenesis process in conifers. *Scand. J. Forest Res.* 34, 360–369. doi: 10.1080/02827581.2018.1441433

Egertsdotter, U., Ahmad, I., and Clapham, D. (2019). Automation and scale up of somatic embryogenesis for commercial plant production, with emphasis on conifers. *Front. Plant Sci.* 10:109. doi: 10.3389/fpls.2019.00109

FAO (2008). "Forests and energy: key issues," in *FAO Forestry Paper,* 154.

Filonova, L. H., Bozhkov, P. V., Brukhin, V. B., Daniel, G., Zhivotovsky, B., and von Arnold, S. (2000). Two waves of programmed cell death occur during formation and development of somatic embryos in the gymnosperm, Norway spruce. *J. Cell Sci.* 113, 4399–4411. doi: 10.1242/jcs.113.24.4399

Garcia, C., de Almeida, A. F., Costa, M., Britto, D., Valle, R., Royaert, S., et al. (2019). Abnormalities in somatic embryogenesis caused by 2,4-D: an overview. *Plant Cell Tiss. Org.* 137, 193–212. doi: 10.1007/s11240-019-01569-8

Gechev, T. S., van Breusegem, F., Stone, J. M., Denev, I., and Laloi, C. (2006). Reactive oxygen species as signals that modulate plant stress responses and programmed cell death. *Bioessays* 28, 1091–1101. doi: 10.1002/bies.20493

González-Cabrero, N., Ruiz-Galea, M., Alegre, J., Toribio, M., and Celestino, C. (2018). Growth, morphology and maturation ability of *Pinus pinea* embryogenic suspension cultures. *Plant Cell Tiss. Org.* 135, 331–346. doi: 10.1007/s11240-018-1467-9

Grossmann, K. (2010). Auxin herbicides: current status of mechanism and mode of action. *Pest Manag. Sci.* 66, 113–120. doi: 10.1002/ps.1860

Gupta, P. K., and Timmis., R. (2005). "Mass propagation of conifer trees in liquid cultures—progress towards commercialization," in *Liquid Culture Systems for in vitro Plant Propagation*, eds. A. K. Hvoslef-Eide, and W. Preil (Dordrecht, Netherlands: Springer), 389–402.

Haapanen, M. (2020). Performance of genetically improved Norway spruce in one-third rotation-aged progeny trials in southern Finland. *Scand. J. Forest Res.* 35, 221–226. doi: 10.1080/02827581.2020.1776763

Hakman, I., Fowke, L. C., von Arnold, S., and Eriksson, T. (1985). The development of somatic embryos in tissue cultures initiated from immature embryos of *Picea abies* (Norway spruce). *Plant Sci.* 38, 53–59. doi: 10.1016/0168-9452(85)90079-2

Hazubska-Przybył, T., Ratajczak, E., Kalemba, E., and Bojarczuk, K. (2013). Growth regulators and guaiacol peroxidase activity during the induction phase of somatic embryogenesis in *Picea* species. *Dendrobiology* 69, 77–86. doi: 10.12657/denbio.069.009

Hazubska-Przybył, T., Ratajczak, E., Obarska, A., and Pers-Kamczyc, E. (2020). Different roles of auxins in somatic embryogenesis efficiency in two *Picea* species. *Int. J. Mol. Sci.* 21:3394. doi: 10.3390/ijms21093394

Högberg, K., and Varis, S. (2016). "Vegetative propagation of Norway spruce: experiences and present situation in Sweden and Finland," in *Vegetative Propagation of Forest Trees*, eds. Y.-S. Park, J. M. Bonga and H.-K. Moon (Seoul, Korea: National Institute of Forest Science), 538–550.

Kairong, C., Gengsheng, X., Xinmin, L., Gengmei, X., and Yafu, W. (1999). Effect of hydrogen peroxide on somatic embryogenesis of *Lycium barbarum* L. *Plant Sci.* 146, 9–16. doi: 10.1016/S0168-9452(99)00087-4

Klimaszewska, K., Lachance, D., Pelletier, G., Lelu, and, M., and Séguin, A. (2001). Regeneration of transgenic *Picea glauca*, P. *mariana, and P. abies* after cocultivation of embryogenic tissue with Agrobacterium tumefaciens. *In Vitro Cell. Dev.-Pl.* 37, 748–755. doi: 10.1007/s11627-001-0124-9

Klimaszewska, K., and Smith, D. R. (1997). Maturation of somatic embryos of *Pinus strobus* is promoted by a high concentration of gellan gum. *Physiol. Plantarum*. 100, 949–957. doi: 10.1111/j.1399-3054.1997.tb00022.x

Kormuták, A., Salaj, T., Matúšová, R., and Vooková, B. (2003). Biochemistry of zygotic and somatic embryogenesis in silver fir (*Abies alba* Mill.). *Acta Biol. Cracov. Bot*. 45, 59–62.

Kubeš, M., DráŽná, N., Konrádová, H., and Lipavská, H. (2014). Robust carbohydrate dynamics based on sucrose resynthesis in developing Norway spruce somatic embryos at variable sugar supply. *In Vitro Cell. Dev.-Pl.* 50, 45–57. doi: 10.1007/s11627-013-9589-6

Landis, T. D., Dumroese, R. K., and Haase, D. (2010). *The Container Tree nursery manual. Seedling Propagation. Agricultural handbook*. Washington, DC: US Department of Agriculture, Forest Service.

Lauri, P., Havlík, P., Kindermann, G., Forsell, N., Böttcher, H., and Obersteiner, M. (2014). Woody biomass energy potential in 2050. *Energy Policy*. 66, 19–31. doi: 10.1016/j.enpol.2013.11.033

Lelu-Walter, M., Bernier-Cardou, M., and Klimaszewska, K. (2008). Clonal plant production from self-and cross-pollinated seed families of *Pinus sylvestris* (L.) through somatic embryogenesis. *Plant Cell Tiss. Org.* 92, 31–45. doi: 10.1007/s11240-007-9300-x

Litvay, J. D., Verma, D. C., and Johnson, M. A. (1985). Influence of a loblolly pine (*Pinus taeda* L.). Culture medium and its components on growth and somatic embryogenesis of the wild carrot *(Daucus carota L.). Plant Cell Rep*. 4, 325–328. doi: 10.1007/BF00269890

Liu, H., Wang, J., Liu, J., Liu, T., and Xue, S. (2021). Hydrogen sulfide (H_2S) signaling in plant development and stress responses. *aBIOTECH* 2, 32–63. doi: 10.1007/s42994-021-00035-4

Mamun, N. H., Aidun, C. K., and Egertsdotter, U. (2018). Improved and synchronized maturation of Norway spruce (*Picea abies* (L.) H. Karst.) somatic embryos in temporary immersion bioreactors. *In Vitro Cell. Dev.-Pl.* 54, 612–620. doi: 10.1007/s11627-018-9911-4

Mignolet-Spruyt, L., Xu, E., Idänheimo, N., Hoeberichts, F. A., Mühlenbock, P., Brosché, M., et al. (2016). Spreading the news: Subcellular and organellar reactive oxygen species production and signalling. *J. Exp. Bot*. 67, 3831–3844. doi: 10.1093/jxb/erw080

Oulbi, S., Kohaich, K., Baaziz, M., Belkoura, I., and Loutfi, K. (2021). Peroxidase enzyme fractions as markers of somatic embryogenesis capacities in olive (*Olea europaea* L.). *Plants*. 10:901. doi: 10.3390/plants10050901

Park, Y. (2002). Implementation of conifer somatic embryogenesis in clonal forestry: technical requirements and deployment considerations. *Ann. For. Sci.* 59, 651–656. doi: 10.1051/forest:2002051

Peng, C., Gao, F., Wang, H., Shen, H., and Yang, L. (2020). Physiological and biochemical traits in Korean pine somatic embryogenesis. *Forests* 11:577. doi: 10.3390/f11050577

Rosvall, O., Bradshaw, R. H., Egertsdotter, U., Ingvarsson, P. K., Mullin, T. J., and Wu, H. (2019). Using Norway spruce clones in Swedish forestry: implications of clones for management. *Scand. J. Forest Res.* 5, 390–404. doi: 10.1080/02827581.2019.1590631

Saeed, T., and Shahzad, A. (2015). High frequency plant regeneration in Indian Siris via cyclic somatic embryogenesis with biochemical, histological and SEM investigations. *Ind. Crop. Prod*. 76, 623–637. doi: 10.1016/j.indcrop.2015.07.060

Sagisaka, S. (1976). The occurrence of peroxide in a perennial plant *Populus gelrica*. *Plant Physiol*. 57, 309–309. doi: 10.1104/pp.57.2.308

Serrano, I., Romero-Puertas, M. C., Sandalio, L. M., and Olmedilla, A. (2015). The role of reactive oxygen species and nitric oxide in programmed cell death associated with self-incompatibility. *J. Exp. Bot*. 66, 2869–2876. doi: 10.1093/jxb/erv083

Shohael, A. M., Ali, M. B., Hahn, E. J., and Paek, K. Y. (2007). Glutathione metabolism and antioxidant responses during *Eleutherococcus senticosus* somatic embryo development in a bioreactor. *Plant Cell Tiss. Org*. 89, 121–129. doi: 10.1007/s11240-007-9220-9

Singh, R., Singh, S., Parihar, P., Mishra, R. K., Tripathi, D. K., Singh, V. P., et al. (2016). Reactive Oxygen Species (ROS): Beneficial companions of plants' developmental processes. *Front. Plant Sci.* 7:1299. doi: 10.3389/fpls.2016.01299

Slesak, I., Libik, M., Karpinska, B., Karpinski, S., and Miszalski, Z. (2007). The role of hydrogen peroxide in regulation of plant metabolism and cellular

signaling in response to environmental stresses. *Acta Biochim. Pol*. 54, 39–50. doi: 10.18388/abp.2007_3267

Smirnoff, N., and Arnaud, D. (2018). Hydrogen peroxide metabolism and functions in plants. *New Phytol*. 221, 1197–1214 doi: 10.1111/nph.15488

Sun, H., Aidun, C. K., and Egertsdotter, U. (2010). Effects from shear stress on morphology and growth of early stages of Norway spruce somatic embryos. *Biotechnol. Bioeng*. 105, 588–599. doi: 10.1002/bit.22554

Taiz, L., Zeiger, E., Møller, I. M., and Murphy, A. (2015). *Plant Physiology and Development, 6th* ed. Sunderland, Massachusetts: Sinauer Associates, Inc.

Tikkinen, M., Varis, S., and Aronen, T. (2018a). Development of somatic embryo maturation and growing techniques of Norway spruce emblings towards large-scale field testing. *Forests* 9:325. doi: 10.3390/f9060325

Tikkinen, M., Varis, S., Peltola, H., and Aronen, T. (2018b). Improved germination conditions for Norway spruce somatic cotyledonary embryos increased survival and height growth of emblings. *Trees* 32, 1489–1504 doi: 10.1007/s00468-018-1728-6

Tikkinen, M., Varis, S., Välimäki, S., Nikkanen, T., and Aronen, T. (2019). "Somatic embryogenesis of Norway spruce in Finland – seven years from start to first commercial pilots," in *Proceedings of the 5th international Conference of the IUFRO Unit 2.09.02 on "Clonal Trees in the Bioeconomy Age: Opportunities and Challenges*", eds J. M. Bonga, Y. S. Park, and J. F. Trontin (Coimbra, Portugal: IUFRO), 166–172.

Välimäki, S., Paavilainen, L., Tikkinen, M., Salonen, F., Varis, S., and Aronen, T. (2020). Production of Norway spruce embryos in a temporary immersion system (TIS). In Vitro Cell. *Dev.-Pl.* 56, 430–439. doi: 10.1007/s11627-020-10068-x

Varis, S. (2018). "Norway Spruce *Picea abies* (L.) Karst," in *Step Wise Protocols for Somatic Embryogenesis of Important Woody Plants,* eds J. M. Jain and P. K. Gupta. (Dordrecht, Netherlands: Springer), 255–267. doi: 10.1007/978-3-319-89483-6_19

Varis, S., Ahola, S., Jaakola, L., and Aronen, T. (2017). Reliable and practical methods for cryopreservation of embryogenic cultures and cold storage of somatic embryos of Norway spruce. *Cryobiology* 76, 8–17. doi: 10.1016/j.cryobiol.2017.05.004

Verma, A., Malik, C. P., and Gupta, V. K. (2012). In Vitro effects of brassinosteroids on the growth and antioxidant enzyme activities in groundnut. *ISRN Agron.* 2012, 356485. doi: 10.5402/2012/356485

von Arnold, S., Bozhkov, P., Clapham, D., Dyachok, J., Filonova, L., Högberg, K., et al. (2005). Propagation of Norway spruce via somatic embryogenesis. *Plant Cell Tiss. Org*. 81, 323–329. doi: 10.1007/s11240-004-6662-1

von Arnold, S., and Hakman, I. (1988). Regulation of somatic embryo development in *Picea abies* by abscisic acid (ABA). *J. Plant Physiol*. 132, 164–169. doi: 10.1016/S0176-1617(88)80155-X

von Arnold, S., Sabala, I., Bozhkov, P., Dyachok, J., and Filonova, L. (2002). Developmental pathways of somatic embryogenesis. *Plant Cell Tiss. Org*. 69, 233–249. doi: 10.1023/A:1015673200621

Yang, L., Guo, H., Liu, Y., Zhang, D., Liu, H., and Shen, H. (2021). Relationship between H_2O_2 accumulation and NO synthesis during osmotic stress: promoted somatic embryogenesis of Fraxinus mandsurica. *J. Forestry Res*. 32, 917–925. doi: 10.1007/s11676-020-01115-9

Zhang, S. G., Han, S. Y., Yang, W. H., Wei, H. L., Zhang, M., and Qi, L. W. (2010). Changes in H_2O_2 content and antioxidant enzyme gene expression during the somatic embryogenesis of *Larix leptolepis*. *Plant Cell Tiss. Org*. 100, 21–29. doi: 10.1007/s11240-009-9612-0

Zhou, T., Yang, X., Guo, K., Deng, J., Xu, J., Gao, W., et al. (2016). ROS homeostasis regulates somatic embryogenesis via the regulation of auxin signaling in cotton. *Mol. Cell Proteomics*. 15, 2108–2124. doi: 10.1074/mcp.M115.049338

Zhu, T., Moschou, P. N., Alvarez, J. M., Sohlberg, J. J., and von Arnold, S. (2016). WUSCHEL-RELATED HOMEOBOX 2 is important for protoderm and suspensor development in the gymnosperm Norway spruce. *BMC Plant Biol*. 16:19. doi: 10.1186/s12870-016-0706-7

Conflict of Interest: The authors declare that the research was conducted in the absence of any commercial or financial relationships that could be construed as a potential conflict of interest.

Publisher's Note: All claims expressed in this article are solely those of the authors and do not necessarily represent those of their affiliated organizations, or those of the publisher, the editors and the reviewers. Any product that may be evaluated in this article, or claim that may be made by its manufacturer, is not guaranteed or endorsed by the publisher.

frontiers in Plant Science

METHODS
published: 08 February 2022
doi: 10.3389/fpls.2022.825340

An Improved and Simplified Propagation System for Pollen-Free Sugi (*Cryptomeria japonica*) *via* Somatic Embryogenesis

Tsuyoshi E. Maruyama[1], Momi Tsuruta[1], Saneyoshi Ueno[1], Kiyohisa Kawakami[2], Yukiko Bamba[3] and Yoshinari Moriguchi[4]*

[1]Department of Forest Molecular Genetics and Biotechnology, Forestry and Forest Products Research Institute, Tsukuba, Japan, [2]Verde Co., Ltd., Toyohashi, Japan, [3]Niigata Prefectural Forest Research Institute, Murakami, Japan, [4]Graduate School of Science and Technology, Niigata University, Niigata, Japan

OPEN ACCESS

Edited by:
Paloma Moncaleán, Neiker Tecnalia, Spain

Reviewed by:
Terezia Salaj, Institute of Plant Genetics and Biotechnology (SAS), Slovakia
Pingdong Zhang, Beijing Forestry University, China

***Correspondence:**
Tsuyoshi E. Maruyama
tsumaruy@ffpri.affrc.go.jp

Specialty section:
This article was submitted to Plant Development and EvoDevo, a section of the journal Frontiers in Plant Science

Received: *30 November 2021*
Accepted: *05 January 2022*
Published: *08 February 2022*

Citation:
Maruyama TE, Tsuruta M, Ueno S, Kawakami K, Bamba Y and Moriguchi Y (2022) An Improved and Simplified Propagation System for Pollen-Free Sugi (Cryptomeria japonica) via Somatic Embryogenesis. Front. Plant Sci. 13:825340. doi: 10.3389/fpls.2022.825340

Sugi (Japanese cedar, *Cryptomeria japonica*) is the most important forestry tree species in Japan, covering 44% of the total artificial forest area. Large amounts of pollen released from these forests each spring cause allergic reactions in approximately 40% of the population, which are a serious social and public health problem in Japan. As a countermeasure, there is an urgent need to reforest using male-sterile plants (MSPs; pollen-free plants); however, the production of MSPs *via* conventional methods is inefficient, time consuming, and requires considerable resources in terms of labor and space. In the present paper, we described an improved and simplified methodology for the efficient propagation of pollen-free Japanese cedar, combining the use of genetic markers (marker-assisted selection or marker-aided selection) for the early selection of male-sterile genotypes and the use of somatic embryogenesis (SE) for the clonal mass propagation of seedlings. We describe all the stages involved in the production process of somatic seedlings. Our results demonstrated that this methodology easily and efficiently produces MSPs with a discrimination rate of 100% in a short period of time. Production of 243.6 ± 163.6 cotyledonary embryos per plate, somatic embryo germination, and plantlet conversion frequencies of 87.1 ± 11.9% and 84.8 ± 12.6%, respectively, and a 77.6 ± 12.1% survival rate after *ex vitro* acclimatization was achieved. Moreover, we also describe an easy method for the collection of somatic embryos prior to germination, as well as an efficient and practical method for their storage at 5°C. Finally, a representative schedule for the propagation of pollen-free sugi somatic seedlings is presented as a reference for practical uses. This methodology will definitively help to accelerate the production of *C. japonica* MSPs across Japan.

Keywords: Cupressaceae, embryogenic cells, pollen-free plants, pollinosis, somatic embryogenesis, somatic seedlings, clonal propagation, marker-assisted selection

INTRODUCTION

Sugi (Japanese cedar, *Cryptomeria japonica* (Thunb. ex L.f.) D.Don, Cupressaceae) forests have been greatly exploited over the past 1,000 years; the artificial planting of sugi is estimated to have begun more than 500 years ago (Ohba, 1993), including clonal forestry *via* cuttings, which began in the beginning of the 15th century (Toda, 1974). Now, Japanese cedar is the most important forestry species in Japan, covering 44% of the total artificial forest and accounting for approximately 4.5 million ha (Forestry Agency, 2020). In contrast to its commercial importance, the large amounts of pollen released from sugi forests each spring cause allergic reactions, which are a serious social and public health problem in Japan; an estimated 40% of people living in Japan suffer from allergic rhinitis caused by sugi pollen (Matsubara et al., 2020), resulting in significant economic losses each year. In this context, the use of male-sterile plants (MSPs; pollen-free plants) in reforestation is one of the most effective countermeasures against pollinosis. However, the production of MSPs is associated with several problems that limit its practical implementation; one of these problems is the scarcity of material used for breeding. Since the probability of encountering male-sterile individuals in sugi forests is estimated to be one in several thousand (Igarashi et al., 2006), the discovery of new breeding material requires enormous effort. To date, only 23 male-sterile sugi individuals have been reported across the entire country (Saito, 2010); the majority of these male-sterile trees possess *MALE STERILITY 1* (*MS1*), a principal causative gene of male sterility in sugi (Moriguchi et al., 2020), which is associated with a developmental abnormality in the pollen tetrad period caused by one recessive allele *ms1* (Taira et al., 1999; Miura et al., 2011). At present, seeds for the propagation of *C. japonica* MSPs are produced by artificial crossing between a male-sterile tree (*ms1*/*ms1*), as a seed parent, and a pollen donor (an elite tree selected based on growth performance and morphological traits) with heterozygous sterile allele (*Ms1*/*ms1*; Maruyama et al., 2020; Tsuruta et al., 2021a).

Another challenge is the propagation and selection of pollen-free seedlings. Currently, MSPs are discriminated from the resulting seedlings after the application of gibberellin (GA_3), which induces early flowering in sugi (Shidei et al., 1959; Nagao, 1983). After the induction of flowering, approximately half of the propagated seedlings that are not pollen-free due to Mendelian inheritance are unusable fertile individuals that must be discarded, despite having been in the nursery for 2 to 3 years leading up to the selection test. In this conventional method, the seedling production efficiency is extremely low and requires many resources in terms of time, labor, and space. In this sense, our goal is to establish efficient and easy protocols to produce excellent Japanese cedar MSPs in a short period of time. Our strategy is based on a combination of the use of genetic markers (marker-assisted selection or marker-aided selection, MAS) for the early discrimination of male-sterile genotypes of embryogenic cell (EC) lines (ECLs) and the use of somatic embryogenesis (SE) for the clonal mass propagation of seedlings. The development of this novel technique for the efficient production of sugi MSPs was first reported by our research group (Maruyama et al., 2020). Then, we released improved methodologies for SE initiation (Maruyama et al., 2021a), somatic embryo production, and somatic plant regeneration (Maruyama et al., 2021b; Tsuruta et al., 2021b), as well as for the early effective selection of male-sterile ECLs (Hasegawa et al., 2021; Tsuruta et al., 2021a).

In the present report, we aim to further improve and simplify the methodology for the propagation of pollen-free Japanese cedar by describing a protocol for all the stages involved in the production process, including the preparation of SE initiation materials, the early discrimination of male-sterile genotype lines at the undifferentiated cell stage (EC) to produce MSPs at a rate of 100%, the production of somatic embryos, the germination and conversion of somatic plantlets, and the production of plug plants in greenhouse and containerized seedlings in the nursery. Moreover, we describe an easy method for collecting somatic embryos prior to germination, as well as an efficient and practical method for storage at 5°C without considerable loss of germination capacity. Finally, we present a representative schedule for the propagation of pollen-free sugi *via* SE (case study for the Niigata Prefecture, central region of Japan), as a reference for practical uses. We believe that this methodology provides basic and practical information that will accelerate the production of MSPs across the country and serve as a powerful tool to improve genetic molecular breeding technology for *C. japonica*.

MATERIALS AND METHODS

Plant Material Preparation

Plant materials for the propagation of pollen-free sugi were obtained by artificial crossings between a male-sterile tree (*ms1*/*ms1*) as a seed parent and a pollen donor with heterozygous sterile allele (*Ms1*/*ms1*; Maruyama et al., 2020; Tsuruta et al., 2021a). To ensure seed production, gibberellin (GA_3) treatments were applied to the branches to promote flowering before the artificial crossings. The female flowers of mother trees in the seed orchard were artificially pollinated from March to April with previously collected donor pollen from elite trees that were selected based on their growth performance and morphological traits. Subsequently, the produced seed cones were collected in mid-July and their seeds containing immature zygotic embryos, mostly represented by early embryo stages equivalent to stages 5–6 on the scale described by Pullman and Buchanan (2003), were used as plant material for the initiation of SE. Details of the seed preparation process are described in **Table 1** and **Figure 1**.

Culture Media and Conditions for SE

The culture media and conditions for the propagation of pollen-free sugi *via* SE are described in **Supplementary Table S1** and **Table 2**, respectively. After autoclaving for 15 min at 121°C, culture media containing basal salts at standard or modified concentrations from the original Embryo Maturation (EM) medium (Maruyama et al., 2000) were used, according to each step. In all steps, the plates were sealed with Parafilm®.

TABLE 1 | Equipment, procedure, and season for each step of plant material preparation for the initiation of somatic embryogenesis in pollen-free sugi (*C. japonica*).

Step	Equipment	Procedure	Season
Application of gibberellin (GA_3) to promote flowering	Gibberellin A_3[1] Sprayer Bucket Stepladder	Selected branches were sprayed or immersed into 100 mg L^{-1} GA_3 solution for approximately 3–5 s. A booster of GA_3 solution was applied approximately 1 week after the first treatment.	Late July and early August for male and female flowers, respectively
Harvest of branches with male flowers and pollen collection	Pruning shears Bottles Paper bags Stepladder Desiccator Silica gel	Harvested branches with male flowers were put in bottles with water and covered with paper bags. Branches were kept in a greenhouse (at about 25°C) until the male flowers opened and released pollen. Pollen collected in paper bags was kept in a desiccator with silica gel until use.	Late January to early February
Placement of pollination bags and artificial pollination	Pollination bags Selected pollen Pollen atomizer Stepladder Wire	Female flowers were covered with pollination bags (made with nonwoven material) before mid-February. Selected pollen was injected into the pollination bag using a pollen atomizer (about 0.2 g per bag) on sunny days from mid-March to early April (3 to 5 times).	Mid-February to early April
Collection of seed cones	Pruning shears Plastic trays Stepladder	Seed cones were separated from the harvested branches. Collected cones should be stored refrigerated (5°C) if not used immediately (up to about 4 to 8 weeks).	Mid-July
Extraction of seeds	Petri dishes Scalpels Paper tissue Ethanol	Seed cones were cleaned with tissue paper moistened with ethanol before they were opened with a scalpel. Seeds were removed from the cones and transferred to Petri dishes containing tissue paper moistened with water to avoid desiccation.	Mid-July

[1]*Gibberellin Kyowa Powder; Ministry of Agriculture, Forestry and Fisheries Registration No. 6007 (Kyowa Hakko Bio Co., Ltd., Tokyo, Japan).*

Embryogenic Culture Initiation

The whole megagametophyte, containing the immature zygotic embryo, was used as the initial explant for SE initiation. The seeds were surface sterilized with 1% (w/v) sodium hypochlorite solution (Wako Pure Chemical, Osaka, Japan) for 15 min, then rinsed three times for 5 min each with sterile distilled water. Then, the seed coat was removed with sterile scalpels and forceps to aseptically isolate the megagametophytes from the seeds under a dissecting microscope. Explants were placed horizontally into initiation EM-1 medium (**Supplementary Table S1**) and cultured under the conditions described in **Table 2**. The induction of ECs from the explants was monitored up to 12 weeks of culture. The ECLs were noted if initiated ECs proliferated after the first subculture.

Maintenance and Proliferation of ECLs

Proliferated ECs were collected with forceps from the initiation EM-1 medium and transferred to a maintenance/proliferation medium (EM-2, **Supplementary Table S1**). Subsequently, the tissues of established ECLs were regularly subcultured at 2-week intervals. EC masses of about 25–50 mg of fresh weight (FW) were cultured under the conditions described in **Table 2**.

Discrimination of Male-Sterile ECLs by MAS

Using 5 to 10 mg of the maintained ECs, DNA was extracted using InstaGene Matrix (Bio-Rad, Hercules, CA, United States). The *MS1* genotype of the ECL was determined using PCR amplification of the marker directly developed for the gene that causes male sterility (Tsuruta et al., 2021a), followed by electrophoresis on 1.5% agarose gel. Each reaction condition is described in **Table 3**.

Maturation of Somatic Embryos

For somatic embryo maturation, three to five proliferated EC masses (about 100 mg FW each) from the maintenance/proliferation medium (**Figure 2A**) were transferred and homogeneously dispersed by forceps into a plate containing maturation EM-3 medium (**Supplementary Table S1**). Each mass was dispersed on a surface equivalent to a circle with a diameter of approximately 2.5–3.0 cm (**Figure 2B**). Plates were sealed and cultured under the conditions described in **Table 2**.

Storage of Somatic Embryos

After the end of the maturation stage, culture plates containing both maturation medium and mature embryos (**Figure 2C**) were sealed with two more layers of Parafilm® then stored in Ziploc® freezer bags at 5°C (**Figure 2D**). The viability of stored somatic embryos was monitored at different storage periods (0, 6, 12, and 24 months) *via* germination tests on EM-4 medium (**Figure 2E**; **Supplementary Table S1**). Regenerated somatic plantlets were acclimatized in plant plugs (**Figure 2F**), as described in the following *ex vitro* Acclimatization section.

FIGURE 1 | Plant material preparation for the propagation of pollen-free sugi (*C. japonica*) *via* somatic embryogenesis. **(A)** Application of gibberellin (GA_3) to promote flowering. **(B)** Harvested branches with male flowers. **(C)** Branches with male flowers in bottles with water and covered with paper bags for pollen collection. **(D)** Covering of female flowers with pollination bags. **(E)** Injection of pollen into pollination bags with a pollen atomizer (yellow arrow; atomizer amplification is seen in the bottom right square). **(F)** Harvested branches with seed cones. **(G)** Collected seed cones. **(H)** Opened cone for seed extraction (cone size: 15 mm in diameter). **(I)** Seeds removed from cones (Petri dish size: 90 mm in diameter).

Somatic Embryo Germination and Plantlet Conversion

Somatic embryos were collected from the maturation medium with a spatula and transferred into a flask containing sterile distilled water. After several vigorous shaking episodes to separate the adhering proliferated ECs, the somatic embryos were collected on a tea strainer and then transferred into filter papers inside empty plates (**Figures 3A–F**). After dispersing the embryos into filter paper with forceps (**Figure 3G**), the plates were sealed and incubated at 25°C for approximately 2 weeks (**Figures 3H,I**) for remove the water remaining in filter papers before being transferred to the germination/conversion EM-4 medium (**Supplementary Table S1**) and cultured under the conditions described in **Table 2**. The emergence of roots (germination) and the emergence of both roots and epicotyl (plantlet conversion) were recorded after 8 weeks of culture.

Ex vitro Acclimatization and Growth of Acclimatized Somatic Plants

After 12 weeks of culture on the germination/conversion medium, regenerated somatic plantlets (**Figure 4A**) were gently transferred into plant plugs with forceps (**Figure 4B**), then kept in the greenhouse under mist watering control for *ex vitro* acclimatization (**Figure 4C**). During the acclimatization period, both mist and manual watering were applied. After the complete acclimatization of somatic plants (after approximately 3–4 weeks when roots had emerged; **Figure 4D**), mist watering was halted; irrigation continued with manual watering, usually once per day in the morning, and with the application of a plant-food solution once per week. Acclimatized plants were kept in the greenhouse for an additional 9–10 weeks before being transplanted into seedling containers (**Figures 4E,F**). The daylight intensity over the plug plants was regulated by a shade-net covering. Additional details of the *ex vitro* acclimatization conditions are described in **Table 2**.

Containerized Somatic Seedlings

Plug plants with heights greater than 5 cm (**Figure 4F**) were transplanted into seedling containers (**Figures 5A–C**) filled with a potting soil mixture fertilized with N-P-K and kept in the nursery under natural outdoor conditions (**Figures 5D,E**). Seedlings were irrigated daily for 15 min *via* sprinkler watering in the morning, and for 30 min in the summer season (15 min in the morning and 15 min in the evening). From July to September, once per week, additional fertilization with a plant-food solution was applied. To prevent pests and diseases, seedlings were fumigated with a Bordeaux mixture solution once every 2 weeks from June to September. Details of the containerized somatic seedling conditions are described in **Table 2**.

TABLE 2 | Medium, culture condition, and culture duration for each stage in the propagation of pollen-free sugi (*C. japonica*) plants *via* somatic embryogenesis.

Culture stage	Medium[1]	Culture conditions	Duration
Embryogenic culture initiation	EM-1[1]	Dark at 25°C; 90 × 15 mm Quad-plates (30–35 ml medium/plate); 3 megagametophytes/well (12/plate).	3–12 weeks
Embryogenic cell maintenance/ proliferation	EM-2[1]	Dark at 25°C; 90 × 15 mm Quad-plates (30–35 ml medium/plate); 3 embryogenic cell masses/well (12/plate).	2-week intervals
Maturation of somatic embryos	EM-3[1]	Dark at 25°C; 90 × 20 mm Mono-plates (30–40 ml medium/plate); 3–5 EC masses/plate.	6–10 weeks
Storage of somatic embryos	EM-3[1]	Dark at 5°C; Plates with cotyledonary embryos from the maturation stage were stored inside Ziploc® freezer bags.	up to 24 months
Somatic embryo germination and plantlet conversion	EM-4[1]	Light at 25°C; 16-h photoperiod (about 2,500–3,500 lx); 90 × 20 mm Mono-plates (30–40 ml medium/plate); about 50–150 coyledonary embryos/plate.	8–12 weeks
Ex vitro acclimatization of somatic plantlets	Plant plug[2]	Light: up to about 10,000 lx; Temperature: 15–35°C; Relative humidity: 30–70%; Mist watering: 20–30 s/every 20–30 min during the daytime; Manual watering: once per day, normally in the morning.	3–4 weeks
Growth of somatic plug plants after acclimatization	Plant plug[2]	Light: up to about 25,000 lx; Temperature: 15–35°C; Relative humidity: 30–70%; Manual watering: once per day, normally in the morning; Fertilization: 0.15% (w/v) plant-food solution[3] once per week.	9–10 weeks
Containerized somatic seedlings	Seedling container[4]	Natural nursery conditions; Potting soil: mixture of Cocopeat-old (80%) and Kanuma soil (20%) with a supplement of N-P-K (in mg L^{-1}: 500, 900, and 750, respectively)[5]; Sprinkler watering: 15 min once per day (15 min twice per day in the summer); Additional fertilization: 0.4% (v/v) plant-food solution[6] once per week from July to September; Seedling disinfection: application of a solution of Bordeaux mixture[7] once every 2 weeks from June to September.	9–16 months[8]

[1]*See* ***Supplementary Table S1***.
[2]*200 holes per tray Jiffy Preforma® plant plugs (Sakata Seed Co., Yokohama, Japan).*
[3]*Peter's 20-20-20 soluble fertilizer (The Hyponex Co., Inc., Hyponex Japan, Osaka, Japan).*
[4]*JFA-150 (150 ml; 8 × 5 cavities per tray) seedling containers (National Federation of Forest Seedling Cooperatives, Tokyo, Japan).*
[5]*Potting soil for container seedlings (Top Co., Ltd., Osaka, Japan).*
[6]*Hyponex 6-10-5 liquid fertilizer (The Hyponex Co., Inc., Hyponex Japan, Osaka, Japan).*
[7]*Bordeaux mixture IC-66D; Ministry of Agriculture, Forestry and Fisheries Registration No. 18645 (Inoue Calcium Co., Ltd., Kochi, Japan).*
[8]*Niigata Prefecture case study.*

Statistical Analysis

Cell line differences in terms of SE efficiencies (i.e., EC proliferation, somatic embryo maturation, germination, and plantlet conversion) and the growth of somatic seedlings (acclimatized somatic plants and containerized somatic seedlings) were tested using generalized linear models (GLMs) with cell line as the explanatory variable. For germination capacity after storage, we constructed a GLM with storage period as the explanatory variable; for these, Gaussian, Poisson, and binomial distributions were used for the error distributions of the proliferation and somatic seedling growth, maturation efficiency, and germination and conversion rates, respectively. For the analyses with cell line as the explanatory variable, the post-hoc analyses for pairwise comparisons of each cell line were conducted using the R package "multicomp" (Bretz et al., 2010) with BH adjustment.

RESULTS

Embryogenic Culture Initiation

Initiation frequencies from seed collection in mid-July varied from 0.9 to 49.9%, depending on the seed family and collection year; the average initiation frequency was 26.0% (SD ± 18.9) for the seven collections, including six different evaluated seed families (**Table 4**). Observations of the response of the initial explants to induce ECs, monitored for up to 12 weeks of culture, revealed that the extrusion of ECs from the explants started after approximately 2 weeks of culture, with evident proliferation at 3–4 weeks after extrusion. Although some explants responded after 9 weeks of culture, the majority did so between the 2nd and 8th week.

Maintenance and Proliferation of ECLs

After 2 weeks of culture on the maintenance/proliferation EM-2 medium, the 16 ECLs had an average proliferation rate of 5.3 ± 1.0 times the initial FW; this rate varied, depending on the ECL, from 3.5 to 7.5 times the initial FW of ECs (**Figure 6**). These differences in proliferation capacity between ECLs remained generally the same in subsequent routine subcultures.

Discrimination of Male-Sterile ECLs by MAS

Our simplified DNA extraction and DNA marker diagnosis methods allowed us to genotype *MS1* with only 15 min of extraction time per sample and a single PCR and electrophoresis (**Supplementary Figure S1**). Since the *MS1* gene itself was used as a DNA marker, based on the genotyping results, pollen-free ECLs could be selected with 100% accuracy.

TABLE 3 | Procedures and reaction conditions for a simplified method for the discrimination of pollen-free sugi (*C. japonica*) embryogenic cell lines.

Step	Equipment	Procedure	Reaction time
DNA extraction	Centrifuge Dry bath heater Vortex mixer Magnet stirrer	5 to 10 mg of ECs added to 200 µl of extraction solution with Chelex resin[1] and vortexed for 10 s. Following 8 min of incubation at 100°C and vortexing for 10 s, centrifugation was performed at 13,000 rpm for 1 min.	Within 15 min per sample
PCR amplification of the DNA marker designed on the *MS1* gene itself	Thermal cycler Ice bath	Ten microliters of PCR reaction mixture contained 1 µl of DNA extract, 3 µl of 2× QIAGEN Multiplex PCR Master Mix (Qiagen), and 0.2 µM each primer.[2] PCR cycling comprised of denaturation at 94°C for 15 min, followed by 35 cycles of 94°C for 15 s, 60°C for 30 s, and 72°C for 30 s, with a final extension for 5 min at 72°C.	Approx. 2 h
Electrophoresis and taking gel images	Gel electrophoresis system (such as Mupid) Gel imaging system	PCR products were separated by 1–1.5% agarose gel electrophoresis (30–40 min), then photographs of the stained gels were taken.	Approx. 1 h

[1]*InstaGene matrix (Bio-Rad, Hercules, CA, United States).*
[2]*Primer sequences described in Tsuruta et al. (2021a).*

Maturation and Storage of Somatic Embryos

Development of cotyledonary embryos was observed most frequently 6–8 weeks after the transfer of ECs to maturation medium (**Figures 2C, 3B**). As shown in **Supplementary Figure S2**, although the maturation efficiency differed among the ECLs, the induction of cotyledonary embryos was achieved in all lines tested. The average number of induced mature somatic embryos was 243.6 ± 163.7, with a range of 25.0 to 513.8 embryos per plate. We also investigated the effects of short- to medium-term cold storage (5°C) for the maintenance of the germination capacity of somatic embryos. Across the different tested storage periods, the average germination rate was 92.7 ± 7.5%, with a range of 78.8 to 100%. No significant decrease in the germination capacity of somatic embryos was observed after the different storage periods ($p > 0.05$, GLM, **Figure 7**).

Somatic Embryo Germination and Plantlet Conversion

The germination of mature somatic embryos began approximately 1–2 weeks after transfer to the germination/conversion EM-4 medium; in most cases, plantlet conversion was achieved after approximately 6 weeks of culture. As shown in **Supplementary Table S2**, embryo germination and plantlet conversion varied across the ECLs from 52.1 to 97.5% and 47.7 to 96.6%, respectively. The average germination and conversion rates for the 19 evaluated ECLs were 87.1 ± 11.9% and 84.8 ± 12.6%, respectively.

Ex vitro Acclimatization and Growth of Acclimatized Somatic Plants

Across somatic plant lines after acclimatization in plant plugs, the average survival rate was 77.6 ± 12.1%, ranging from 63.9 to 87.0%. Across the somatic plant lines 3 months after their transfer into plant plugs, the average growth in height was 5.8 ± 0.6 cm and the average range was 5.1–6.1 cm (**Figures 4F**, **8**).

Containerized Somatic Seedlings

After the transfer of the plug plants into seedling containers during the spring season, they were cultivated in the nursery until they reached a height of 30 cm or more (**Figures 5E,F**). The average survival rate was 91.7 ± 7.4%, ranging between 89.6 and 100.0% across somatic seedling lines. **Figure 9** shows the growth of containerized somatic seedlings in Niigata Prefecture before field planting. The average height/basal diameter for somatic seedling lines SSD-018 and SSD-112 was 38.1 cm/6.4 mm and 34.7 cm/6.1 mm, respectively.

DISCUSSION

Somatic Embryogenesis Initiation

Although SE from the vegetative material of selected adult trees is the ideal method for clonal propagation in all practical situations, like in other conifers, the initiation of SE in sugi remains limited to the use of seeds. Despite our considerable efforts to reproduce the successful SE initiation protocols for the adult trees of white spruce and some pines (Park et al., 2010; Klimaszewska et al., 2011; Malabadi et al., 2011; Teixeira da Silva and Malabadi, 2012), we have yet to achieve positive results in terms of inducing ECs from adult vegetative material in sugi and other Japanese conifers (Maruyama T.E., unpublished). Therefore, seeds remain the only starting material that can be used to initiate SE in sugi. Seed production in sugi is effectively promoted by stimulating flowering with the application of gibberellin (GA_3) during the summer season, mainly in late July and with a booster application in early August (**Table 1**; **Figure 1**). Similarly, although using different concentrations, forms of application, and types of gibberellin, this treatment is also reported to stimulate flowering in other conifers, including pines, cypresses, and Douglas firs (Hashizume, 1985; Kon and Koyama, 2000; Kato et al., 2015; Kong et al., 2021).

As detailed in our previous report (Maruyama et al., 2021a), sugi SE initiation from male-sterile seed families is influenced

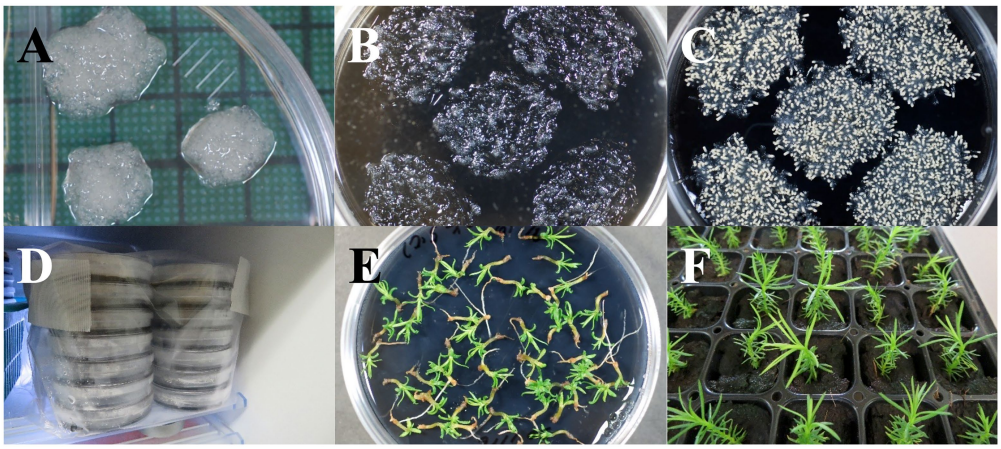

FIGURE 2 | Maturation and storage of somatic embryos of pollen-free sugi (*C. japonica*). **(A)** Embryogenic cell proliferation after 2 weeks of culture. **(B)** Proliferated embryogenic cells homogeneously dispersed into the maturation medium. **(C)** Somatic embryo maturation after approximately 6 weeks of culture. **(D)** Storage of somatic embryos at 5°C. **(E)** Germination of somatic embryos after 2 years of storage at 5°C. **(F)** Regenerated somatic plantlets from 2 year stored embryos transferred into plant plugs for *ex vitro* acclimatization. Diameter of plates: 90 mm; size of plant plugs: 23 × 23 × 38 mm.

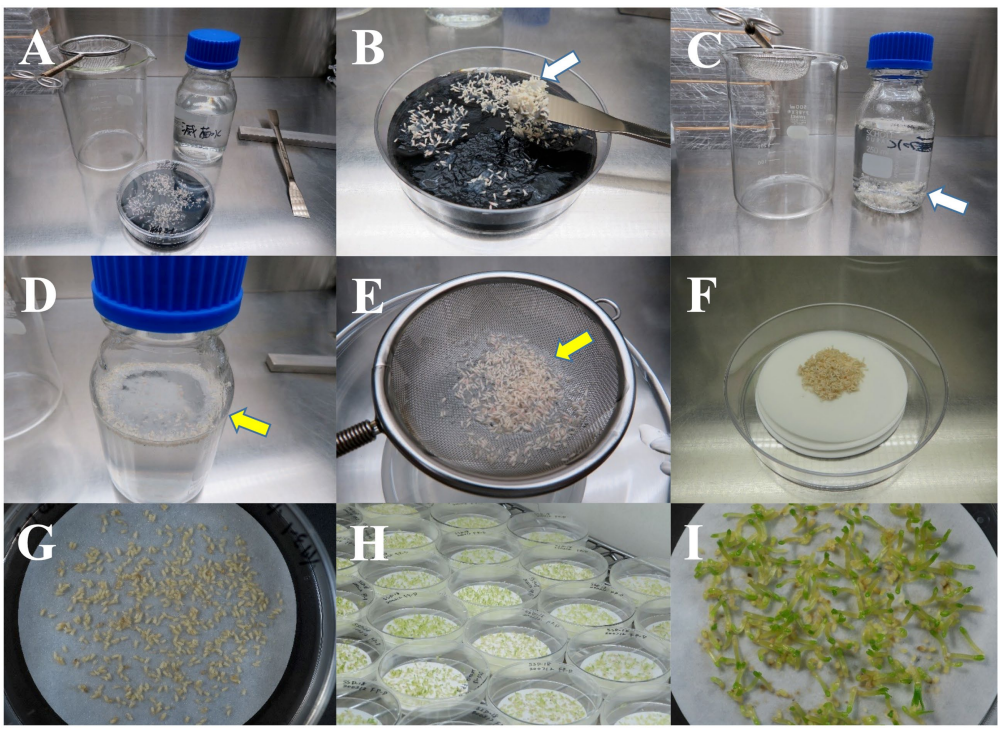

FIGURE 3 | Collection of pollen-free sugi (*C. japonica*) somatic embryos from the maturation medium. **(A)** Materials used for the collection of matured somatic embryos. **(B)** Clusters of somatic embryos and embryogenic cells (ECs; white arrow) collected using a spatula, then transferred into a flask with sterile distilled water **(C)**. **(D)** Embryos (yellow arrow) separated from the adhering proliferated ECs after vigorous shaking of the flask and then collected on a tea strainer **(E)**. **(F)** Collected embryos transferred into filter papers inside an empty plate. **(G)** Embryos placed into filter paper, then incubated inside empty plates for about 2 weeks before transfer to the germination/conversion medium **(H,I)**. Diameter of filter paper: 70 mm.

by several factors, mainly related to the initial explants, timing of collection, genotypes, and culture conditions for the induction of ECs. Although SE initiation is practically feasible from mid-June to late July (Maruyama et al., 2000, 2014), the highest initiation frequencies were achieved using whole megagametophytes as initial explant isolates from seeds collected in mid-July; this result is consistent with the reported initiation frequencies from open-pollinated (Ogita et al., 1999; Taniguchi and Kondo, 2000) and artificially pollinated (Taniguchi et al., 2020) male-fertile seed families. The results achieved throughout our experiments proved

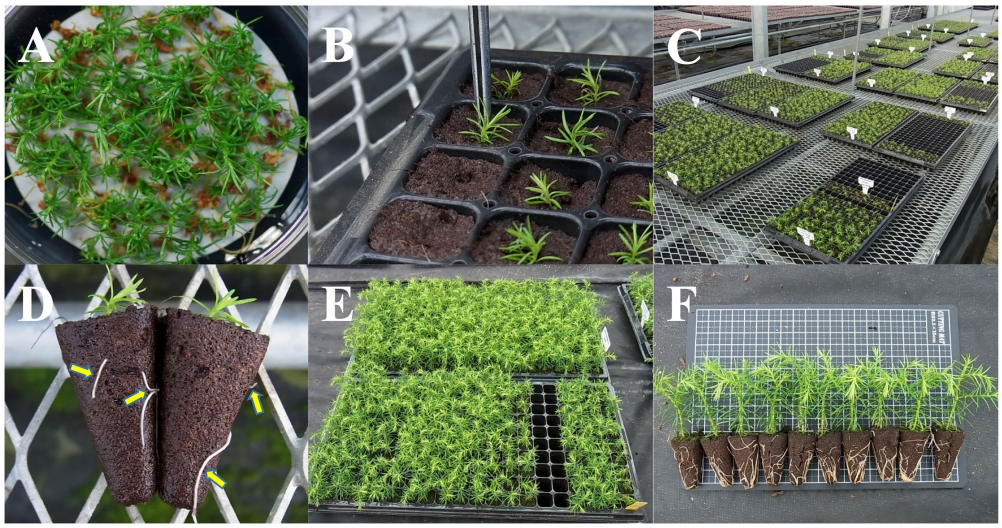

FIGURE 4 | *Ex vitro* acclimatization and growth of acclimatized pollen-free sugi (*C. japonica*) somatic plants. **(A)** *In vitro* regenerated somatic plantlets. **(B)** Transfer of somatic plantlets into plant plugs. **(C)** Plug plants kept inside the greenhouse under mist watering control. **(D)** Acclimatized somatic plants showing roots (yellow arrows) emerging from the plugs. **(E,F)** Growth and appearance of somatic plants approximately 3 months after their transfer into plant plugs. Size of plant plugs: 23 × 23 × 38 mm.

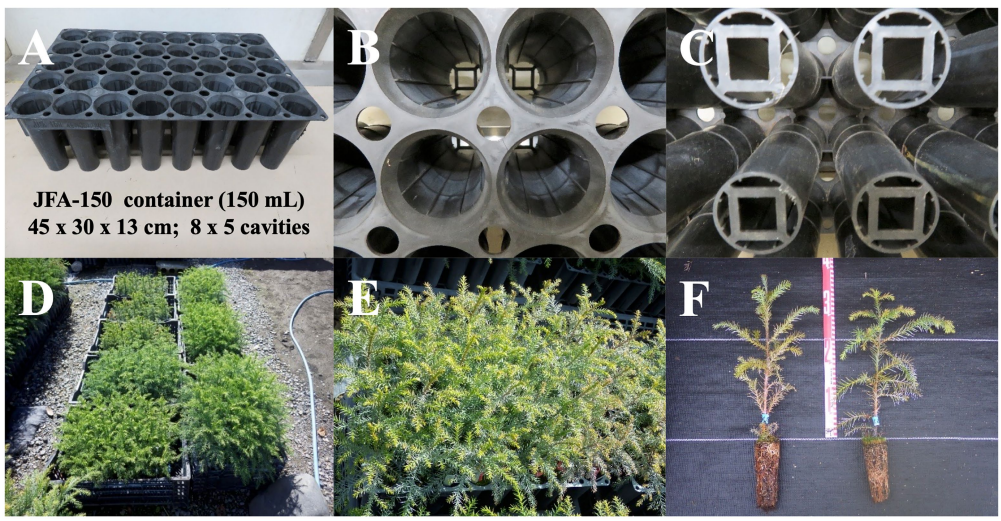

FIGURE 5 | Containerized somatic seedlings of pollen-free sugi (*C. japonica*). **(A)** JFA-150 container. **(B)** View of the ribs on the inner wall of the cavity. **(C)** Bottom of the container. **(D)** An example of the growth status of containerized somatic seedlings derived from different embryogenic cell lines. **(E,F)** Containerized seedlings with heights of more than 30 cm, suitable for planting in the field.

that, even though the initial explant, collection time, and culture conditions played an important role, the genotype of the plant material was the most influential factor for the initiation of SE. As shown in **Table 4**, the initiation rates varied considerably depending on the genotype of the initial explant. Similarly, in accordance with our results, the initiation of SE in several conifers is genetically controlled, perhaps independently of other traits (Klimaszewska et al., 2007). Since the most important role of conifer SE is the deployment of genetically tested tree varieties integrated in tree improvement programs (Park et al., 2006), improvement in SE initiation, with respect to capturing as many genotypes as possible to enhance the representation of families, is important for developing varietal lines and is also fundamental for the management of genetic diversity (Hargreaves et al., 2009). Therefore, the screening of responsive seed family genotypes *via* the multiyear selection of appropriate parents is necessary to increase the initiation rate of SE.

On the other hand, as reported for a number of species, extruded ECs did not always proliferate or result in the establishment of an ECL (Maruyama and Hosoi, 2019). Thus, initial extrusion from an explant should be distinguished from stable continuous growth, when assessing success rates (Klimaszewska et al., 2007). In our experiments, the induction of stable ECLs was used as the criterion for evaluating SE initiation capacity. Subsequently,

TABLE 4 | Embryogenic cell induction from different pollen-free sugi (*C. japonica*) seed families.

Seed family	Seed family code	Collection year	Number of explants tested	Explants with embryogenic cell induction	Induction rate (%)
♀ "Toyama-funen 1" × "Ohara 2" ♂ "Suzu 2"	TOS	2013	1,228	244	19.9
♀ "Shindai 3" ♂ "Suzu 2"	SSD	2016	420	59	14.0
♀ "Shindai 3" ♂ "Suzu 2"	S	2017	383	191	49.9
♀ "Toyama-funen 1" ♂ "Toyama-funen 1" × "Nakakubiki 4"	TON	2016	971	9	0.9
♀ "Fukushima-funen 1" ♂ "Shindai 3" × "Kamikiri 2"	FSKam	2017	516	62	12.0
♀ "Fukushima-funen 1" ♂ 'Ōi 7'	FO7	2017	636	259	40.7
♀ "Fukushima-funen 1" ♂ "Shindai 3" × "Kashiwazaki-shi 3"	FSKas	2017	429	191	44.5
				Mean (SD)	26.0 (18.9)

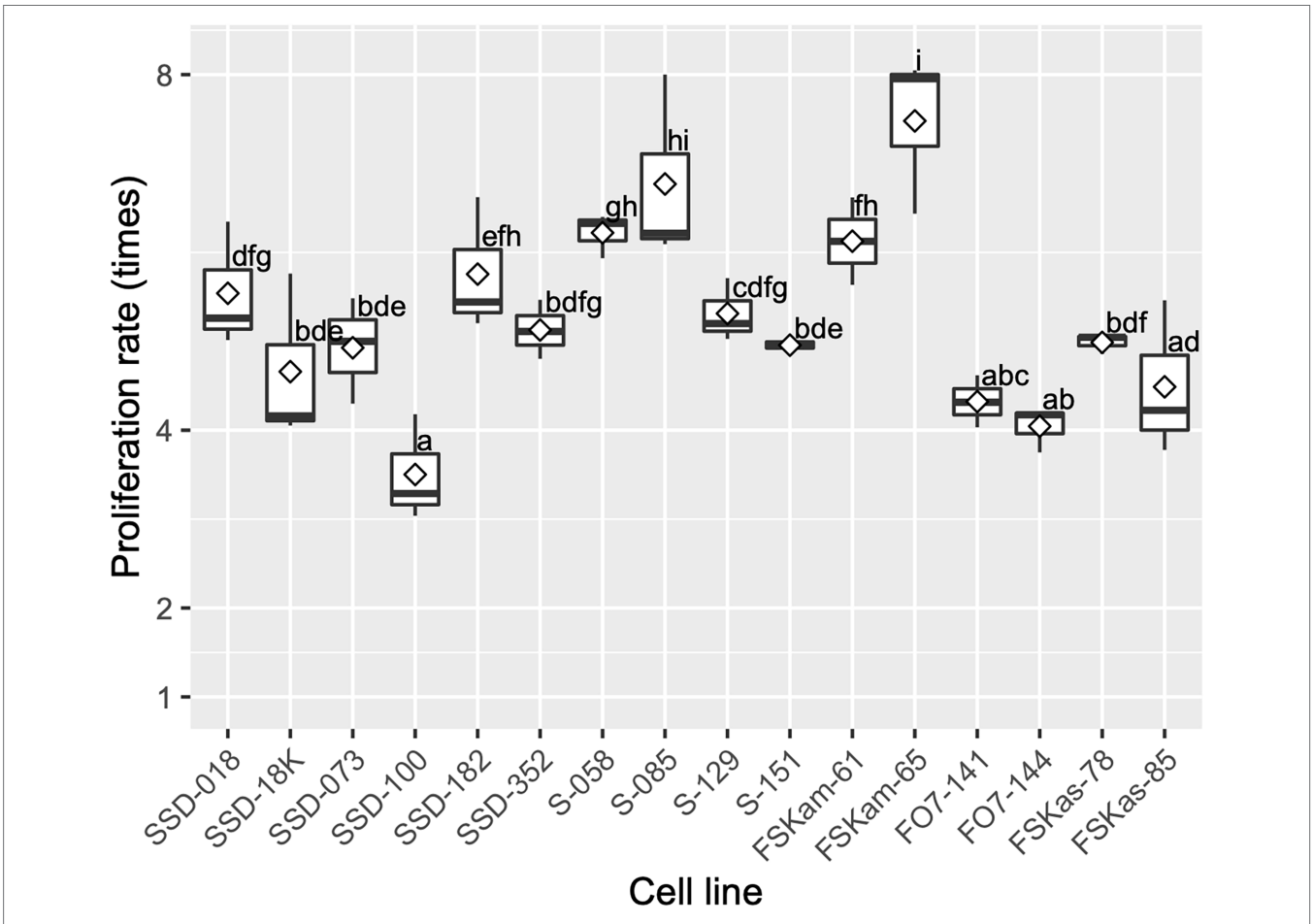

FIGURE 6 | Embryogenic cell proliferation efficiency for different cell lines of pollen-free sugi (*C. japonica*) derived from four seed families (proliferation rate average ± SD for each cell line). SSD: "Shindai 3" × "Suzu 2" (2016); S: "Shindai 3" × "Suzu 2" (2017); FSKam: "Fukushima-funen 1" × ("Shindai 3" × "Kamikiri 2"); FO7: "Fukushima-funen 1" × "Ōi 7"; and FSKas: "Fukushima-funen 1" × ("Shindai 3" × "Kashiwazaki-shi 3"). The open diamond in the boxplot represents the mean. The different letters indicate significant differences among the cell lines ($p < 0.05$, pairwise comparison with BH adjustment).

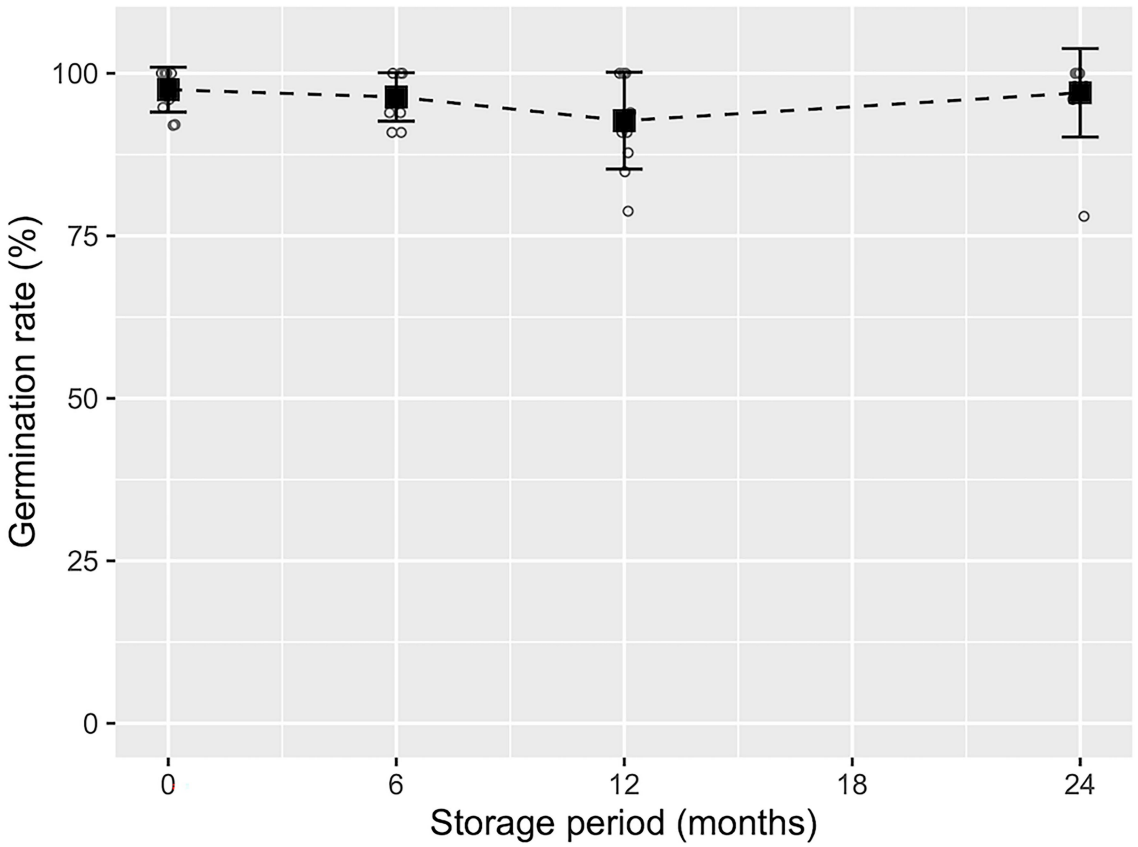

FIGURE 7 | Germination frequency of pollen-free sugi (*C. japonica*) somatic embryos derived from the SSD-018 embryogenic cell line after different storage periods. The average germination frequency (black square) with error bars (±SD) at each storage period is shown above the measurements (white circles).

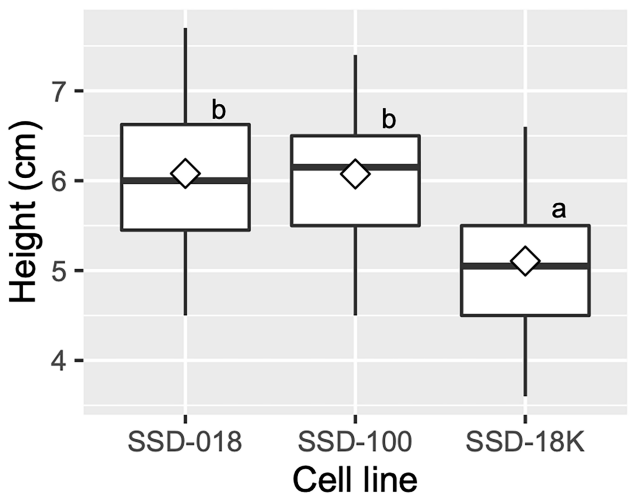

FIGURE 8 | Growth of acclimatized somatic plants of pollen-free sugi (*C. japonica*) 3 months after their transfer into plant plugs. The open diamond in the boxplot represents the mean. The different letters indicate significant differences among the cell lines ($p < 0.05$, pairwise comparison with BH adjustment).

the continuous proliferation of stable ECLs was promoted *via* culturing on medium supplemented with 2,4-dichlorophenoxyacetic acid and 6-benzylaminopurine; notwithstanding that the proliferation rate significantly varied across ECLs (**Figure 6**), the maintenance/proliferation EM-2 medium (**Supplementary Table S1**) described in this methodology was able to support the growth of ECs for several years using 2-week subculture routines. This medium has also been successfully used for the maintenance and proliferation of ECLs in other Japanese conifers (Maruyama et al., 2002, 2005a,b,c, 2007, 2011, 2012; Hosoi and Maruyama, 2012).

Discrimination of Male-Sterile ECLs by MAS

By combining simple DNA extraction with the InstaGene matrix and diagnosis with the marker developed in the *MS1* gene itself, the MAS of a pollen-free sugi line was achieved in the ECs of the early SE stage. This saved a significant amount of labor and space that is otherwise wasted on male-fertile samples, which must be maintained until a decision could be made based on gibberellin-induced flowering. Using the simple extraction method described here, DNA could be extracted from as little as 5 mg of ECs. The application of the InstaGene matrix to plants has been previously reported by HwangBo et al. (2010). We have also shown that this simple extraction method is very effective for coniferous ECs. Although the use of this extraction method can be extended to other materials like adult leaves, extraction is more difficult in later culture materials, such as cotyledonary embryos, than in ECs (Tsuruta et al., 2021a).

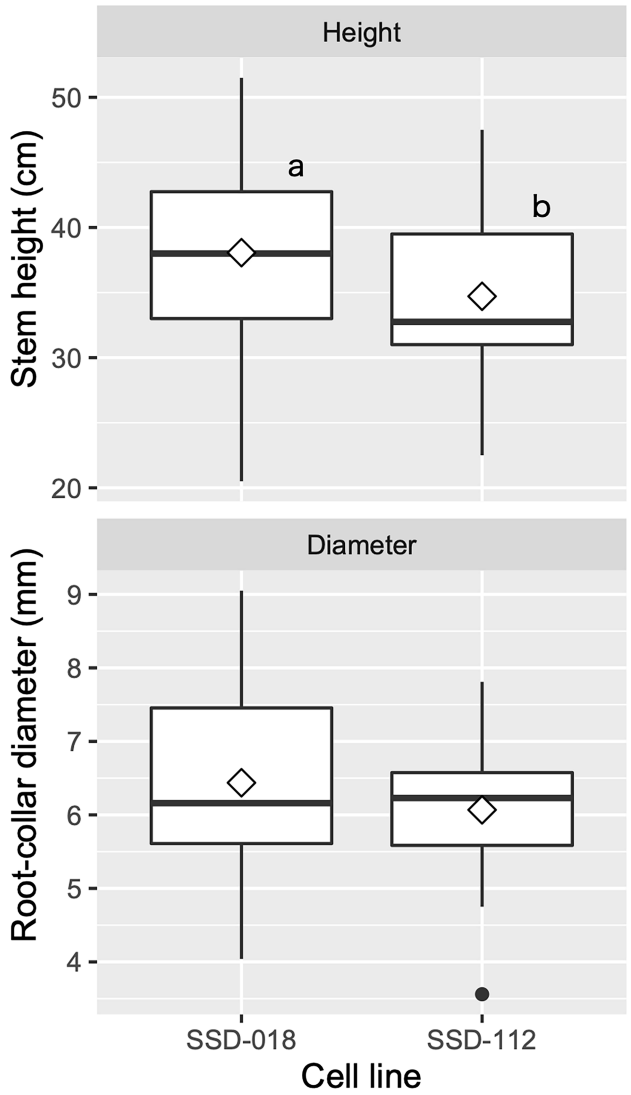

FIGURE 9 | Growth of containerized somatic seedlings of pollen-free sugi (*C. japonica*) in Niigata Prefecture (central region of Japan) before being planted in the field. The open diamond and the dot represent the mean and outlier, respectively. The different letters indicate significant differences among the cell lines ($p < 0.05$, pairwise comparison with BH adjustment).

DNA marker discrimination can also be made more stable. The previously used allele-specific PCR markers for genotype identification require a reaction for each allele, and sometimes show ambiguous bands (Hasegawa et al., 2020; Maruyama et al., 2020). In addition, recombination can be misidentified because previous MAS used markers linked to *MS1* (Ueno et al., 2019). Recent advances in genome sequencing technologies have made it possible to identify genes or mutations of objective traits, and gene-assisted selection (GAS) is also becoming possible for forest trees (Butcher and Southerton, 2007; Wilcox et al., 2007; Moriguchi et al., 2020). The determination of the *MS1* gene itself (Hasegawa et al., 2021) was a significant factor in achieving GAS in the MSP breeding of Japanese cedar.

Maturation and Storage of Somatic Embryos

The efficient maturation of many genotypes, as well as the production of somatic plants with a high field performance, is the most important criteria for using SE protocols; this is important for mass production and breeding programs in addition to being a powerful tool for basic studies of molecular, genetic and physiological processes, and for genetic engineering. The genotype of the ECLs, media formulations, and culture conditions are some of the principal factors that influence SE (Tautorus et al., 1991; Stasolla et al., 2002; Teixeira da Silva and Malabadi, 2012; Egertsdotter, 2019; Gulzar et al., 2020; Izuno et al., 2020; Maruyama et al., 2021a). The results of our experiment indicate that, although mature somatic embryos were achieved in all ECLs, there were significant differences in maturation efficiencies across the evaluated genotypes (**Supplementary Figure S2**). This result confirms that somatic embryo maturation in sugi is controlled by the genetic origin of the ECL and highlights the importance of selecting a highly responsive champion cell genotype (we named it the "Yokozuna" cell genotype, referring to a grand champion sumo wrestler) to optimize the efficiency of SE protocols. Our improved protocol demonstrates that, by selecting genotypes, more than 500 high-quality somatic embryos (more than 1,000 embryos per gram FW) can be produced per plate. The ultimate goal of successful maturation is based on the fact that large-scale production of high-quality somatic embryos requires a high frequency of germination and can become a vigorous planting stock (Klimaszewska et al., 2007).

The short- to medium-term cold storage (5°C) of somatic embryos (presented in **Figure 7**) demonstrated that sugi embryos can be stored for at least 2 years without a significant decrease in germination capacity. Although cryopreservation is the ideal method for preserving genetic materials, it requires expensive equipment and special procedures. Moreover, since the objective of the short- to medium-term storage of somatic embryos is to provide flexibility in the seedling production schedule, allowing easy regulation of the optimal period for the transfer of somatic seedlings to the field, maintaining an embryo germination capacity of approximately 90% for 6 to 24 months is adequate to allow it to be implemented into our methodology. In accordance with our results, Torres-Viñals et al. (2004) reported more than 90% germination from the fresh isolated somatic embryos of grapevines after 30 days of storage at 4°C. Similarly, for the same species but using desiccated somatic embryos, Jayasankar et al. (2005) reported 90% plant conversion after 42 months of storage at 4°C. In contrast, Bornman et al. (2003) reported that cold storage at 4°C had a deleterious effect on the naked or encapsulated somatic embryo germination of *Picea abies* (L.) H.Karst. when stored for 1 month or longer. The somatic embryo storage protocol described in our methodology is easy, simple and only requires a conventional refrigerator for storage at 5°C, which will facilitate its application to practical uses.

Somatic Embryo Germination and Plantlet Conversion

As shown in **Supplementary Table S2**, the high somatic embryo germination and conversion frequencies achieved in almost all of the evaluated ECLs demonstrated the high quality of the produced embryos. Even though the somatic embryo

production of sugi was promoted by increasing the osmotic pressure of the medium *via* the addition of a large amount of polyethylene glycol (175 g L^{-1}), the produced embryos germinated and converted into plantlets after transfer into a plant growth regulator-free medium, without the partial desiccation and/or cold postmaturation treatments that have been reported to be necessary in other conifers (Roberts et al., 1990; Lelu et al., 1995; Klimaszewska et al., 2007; Lara-Chavez et al., 2011; Liao and Juan, 2015; Pullman et al., 2016). In the present methodology, we also include a simple method for the collection of somatic embryos after maturation (**Figure 3**) and for their subsequent germination and plantlet conversion into the same medium (**Figure 4A**); we skip the growth step in culture flasks by transferring the regenerated plantlets directly from the germination plates to the plant plugs. This simplified procedure reduces labor and time compared to our previous protocols in which mature somatic embryos were collected individually with forceps to be transferred to the germination medium and then to another growth medium.

Ex vitro Acclimatization and Containerized Somatic Seedlings

Male-sterile somatic plantlets were successfully acclimatized in plant plugs according to the procedures described in **Table 2** and **Figure 4**. The plug plants grew well without signs of abnormal morphological appearance; although there were some differences in growth across the lines, most reached the appropriate height for transplantation into seedling containers after 9–10 weeks of cultivation. This result suggests that plant plugs of 200 holes per tray are appropriate to support the growth of sugi somatic plants. Although other larger-sized plant plugs (e.g., 128 and 72 holes per tray) also tested positively (data not shown), with a goal of reducing seedling production costs, we deemed it more appropriate to use smaller plant plugs (study in progress). After the transplantation of plug plants into containers, somatic seedlings were cultivated in the nursery. Currently, all over Japan, 150 ml (8 × 5 cavities per tray) and 300 ml (6 × 4 cavities per tray) type containers are the most popular containers used for seedlings and cuttings, respectively (FFPRI, 2021). However, this is the first report for Japanese cedar somatic seedlings. Therefore, due to the scarce information regarding tissue culture-derived plants and pollen-free sugi seedlings produced *via* SE, it is important to continue to accumulate information across many genotypes to support the development of propagation protocols for practical applications.

In the present case study in Niigata Prefecture, because field planting is restricted to the autumn season from September to November, the somatic plug plants that are transplanted into seedling containers in the spring, and reach the required size in the autumn of the same year, can be planted in the field as 1-year-old seedlings. The seedlings that did not reach the required height can be planted in the field in the following autumn as 2-year-old seedlings. Therefore, depending on seedling growth and conditioning, the cultivation period of the containerized seedlings in the nursery can vary from around 9 to 16 months.

Finally, summarized conditions and results for each stage of our methodology are shown in **Table 5**. Additionally, a

TABLE 5 | Summarized conditions and results for each stage in the propagation of pollen-free sugi (*C. japonica*) plants *via* somatic embryogenesis.

Stages	Summarized conditions	Summarized results	References
Embryogenic culture initiation	Culture of megagametophyte explants (isolated from seeds collected in mid-July and containing immature zygotic embryos) on EM-1 medium[1] for 1–3 months.	Initiation rate: 26.0% (SD ± 18.9); Initiation range: 0.9–49.9%	Maruyama et al., 2014, 2021a
Maintenance and proliferation of embryogenic cells	Subculture of induced embryogenic cells on EM-2 medium[1] every 2 weeks.	Proliferation rate: 5.3 times (SD ± 1.0); Proliferation range: 3.5–7.5 times	This report
Discrimination of male-sterile embryogenic cell lines	DNA extraction from embryogenic cells by InstaGene and DNA marker diagnosis of *MS1* genotype.	Discrimination probability of male-sterile embryogenic cell lines: 100%	Tsuruta et al., 2021a
Maturation of somatic embryos	Culture of proliferated embryogenic cells on EM-3 medium[1] for 6–10 weeks.	Average number of mature embryos per plate: 243.6 (SD ± 163.7); Range: 25.0–513.8	Tsuruta et al., 2021b
Storage of somatic embryos	Storage of developed somatic embryos on EM-3 medium[1] at 5°C for 0–2 years.	Germination rate: 92.7% (SD ± 7.5); Germination range: 78.8–100%	This report
Somatic embryo germination and plantlet conversion	Culture of mature somatic embryos on EM-4 medium[1] for 8–12 weeks.	Germination rate: 87.1% (SD ± 11.9); Germination range: 52.1–97.5%; Conversion rate: 84.8% (SD ± 12.6); Conversion range: 47.7–96.6%	Tsuruta et al., 2021b
Ex vitro acclimatization and growth of somatic plants	Acclimatization of somatic plantlets in plant plugs[2] inside greenhouse with 20–30 s mist watering every 20–30 min during the daytime for 3–4 weeks. Then, plants were irrigated by manual watering once per day and fertilized with a plant-food solution[3] once per week.	Survival rate: 77.6% (SD ± 12.1); Survival range: 63.9–87.0%. Plug plants with heights greater than 5 cm are ready to be transplanted into seedling containers in the spring season[4]	This report
Containerized somatic seedlings	Transfer of acclimatized plug plants into seedling containers[4] kept in the nursery with 15–30 min daily sprinkler watering and once per week additional fertilization[5] for 9–16 months.[6]	Survival rate: 91.7% (SD ± 7.4); Survival range: 89.6–100.0%. Containerized seedlings with heights greater than 30 cm are ready to be planted in the autumn season[4]	This report

[1] See ***Supplementary Table S1***.

[2] *200 holes per tray Jiffy Preforma® plant plugs (Sakata Seed Co., Yokohama, Japan).*

[3] *Peter's 20-20-20 soluble fertilizer (The Hyponex Co., Inc., Hyponex Japan, Osaka, Japan).*

[4] *JFA-150 (150 ml; 8 × 5 cavities per tray) seedling containers (National Federation of Forest Seedling Cooperatives, Tokyo, Japan).*

[5] *Hyponex 6-10-5 liquid fertilizer (The Hyponex Co., Inc., Hyponex Japan, Osaka, Japan).*

[6] *Niigata Prefecture case study.*

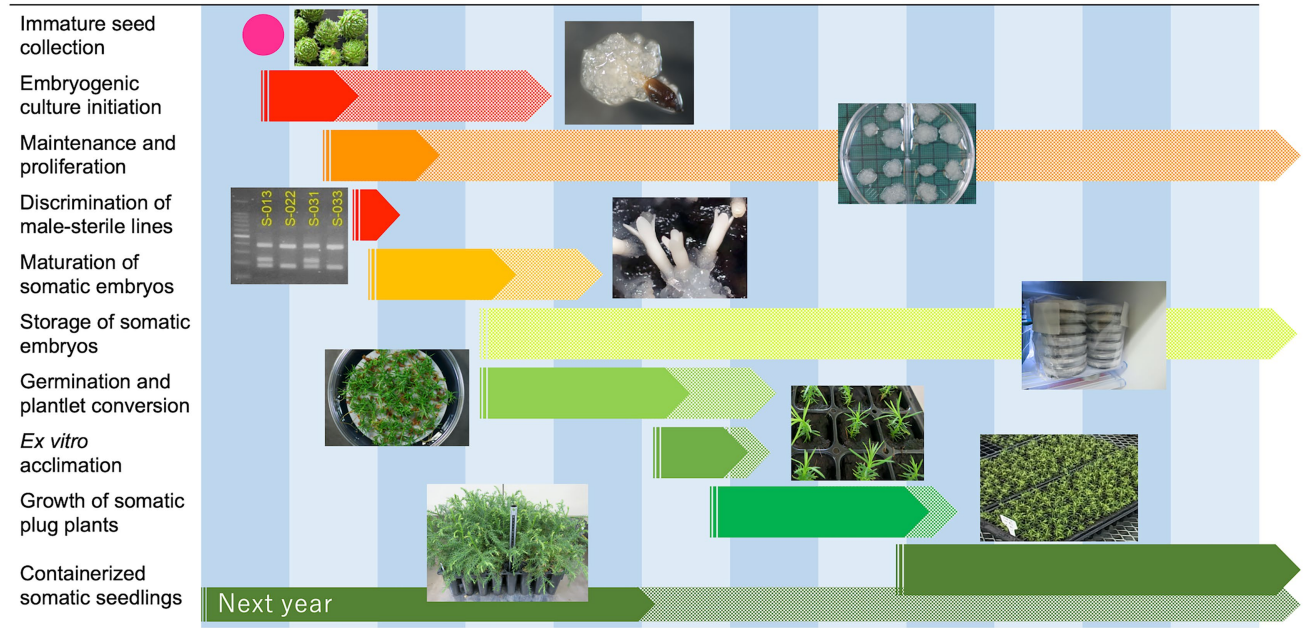

FIGURE 10 | A representative example schedule for the propagation of pollen-free sugi (*C. japonica*) *via* somatic embryogenesis.

representative schedule for the propagation of pollen-free sugi *via* SE (a case study for Niigata Prefecture, central region of Japan) is presented as a reference for practical uses (**Figure 10**). This schedule can be adapted to other regions of the country by adjusting the steps according to the respective planting season. The schedule is somewhat rigid during the first year due to the fact that the onset of SE is limited to a very short period of approximately 1 month, in which the explant is highly responsive (mainly July throughout Japan); however, after the first year, when embryogenic cultures have already been established, the schedule can be adjusted according to the objective and nursery practices. Flexibility can further increase if somatic embryo storage is used to regulate the production of seedlings at the required time.

CONCLUSION

In this paper, we presented an improved and simplified methodology for the propagation of pollen-free sugi (*C. japonica*) by combining the early selection of male-sterility lines by MAS and somatic seedling production through SE. This methodology uses simple DNA extraction with InstaGene (as first reported for conifers), a direct marker to discriminate male-sterile lines at the undifferentiated EC stage, and an efficient large-scale somatic embryo production system, which altogether allow for the production of 100% pollen-free somatic sugi plants under a considerably shorter timeframe than from seeds or cuttings. On the other hand, our methodology for the collection of somatic embryos from maturation medium, embryo germination and plantlet conversion, and the subsequent *ex vitro* acclimatization in plant plugs allowed us to further simplify our previously established protocols. Furthermore, in this study, we demonstrated that mature somatic embryos can be stored for at least 2 years without a considerable loss in germination capacity, which provides flexibility to manage the somatic seedling production schedule. This methodology provides basic and practical information that will help to accelerate the production of pollen-free Japanese cedar plants across Japan.

DATA AVAILABILITY STATEMENT

The original contributions presented in the study are included in the article/**Supplementary Material**, further inquiries can be directed to the corresponding author.

ETHICS STATEMENT

Written informed consent was obtained from the individual(s) for the publication of any potentially identifiable images or data included in this article.

AUTHOR CONTRIBUTIONS

TM, SU, MT, and YM: conceptualization and methodology. YM: funding acquisition and project administration. TM, MT, KK, and YB: plant material preparation. TM, MT, and SU: data curation. TM, MT, SU, KK, and YB: experiments and data analysis. TM and MT: writing – original draft. TM, MT,

SU, KK, YB, and YM: writing – review and editing. All authors have read and agreed to the published version of the manuscript.

FUNDING

This research was supported by grants from the Ministry of Agriculture, Forestry and Fisheries of Japan (MAFF) and Bio-oriented Technology Research Advancement Institution [BRAIN; The Science and Technology Research Promotion Program for Agriculture, Forestry, Fisheries and Food Industry (No. 28013B) and grants from BRAIN Research Program on Development of Innovative Technology (No. 28013BC)].

ACKNOWLEDGMENTS

The authors would like to thank Niigata Prefectural Forest Research Institute and Forestry Research Institute of Toyama Prefectural Agricultural, Forestry & Fisheries Research Center for their support in the preparation of plant materials.

SUPPLEMENTARY MATERIAL

The Supplementary Material for this article can be found online at: https://www.frontiersin.org/articles/10.3389/fpls.2022.825340/full#supplementary-material

REFERENCES

Bornman, C. H., Dickens, O. S. P., van der Merwe, C. F., Coetzee, J., and Botha, A.-M. (2003). Somatic embryos of *Picea abies* behave like isolated zygotic embryos *in vitro* with greatly reduced physiological vigour. *S. Afr. J. Bot.* 69, 176–185. doi: 10.1016/S0254-6299(15)30343-4

Bretz, F., Hothorn, T., and Westfall, P. (2010). *Multiple Comparisons Using R*. Boca Raton: CRC Press.

Butcher, P., and Southerton, S. (2007). "Marker-assisted selection in forestry species," in *Marker-Assisted Selection, Current Status and Future Perspectives in Crops, Livestock, Forestry and Fish*. eds. E. P. Guimarães, J. Ruane, B. D. Scherf, A. Sonnino and J. D. Dargie (Rome, Italy: FAO), 283–305.

Egertsdotter, U. (2019). Plant physiological and genetical aspects of the somatic embryogenesis process in conifers. *Scand. J. For. Res.* 34, 360–369. doi: 10.1080/02827581.2018.1441433

FFPRI (2021). *Conifer Container Seedlings for Forests –Results of a National Questionnaire on Seedling Cultivation Methods*. Tsukuba, Japan: Forestry and Forest Products Research Institute, 19.

Forestry Agency (2020). *Statistical Handbook of Forest and Forestry 2020*. Tokyo: Forestry Agency, Ministry of Agriculture, Forestry and Fisheries.

Gulzar, B., Mujib, A., Malik, M. Q., Sayeed, R., Mamgain, J., and Ejaz, B. (2020). Genes, proteins and other networks regulating somatic embryogenesis in plants. *J. Genet. Eng. Biotechnol.* 18:31. doi: 10.1186/s43141-020-00047-5

Hargreaves, C. L., Reeves, C. B., Find, J. I., Gough, K., Josekutty, P., Skudder, D. B., et al. (2009). Improving initiation, genotype capture, and family representation in somatic embryogenesis of *Pinus radiata* by a combination of zygotic embryo maturity, media, and explant preparation. *Can. J. For. Res.* 39, 1566–1574. doi: 10.1139/X09-082

Hasegawa, Y., Ueno, S., Wei, F. J., Matsumoto, A., Uchiyama, K., Ujino-Ihara, T., et al. (2021). Identification and genetic diversity analysis of a male-sterile gene (*MS1*) in Japanese cedar (*Cryptomeria japonica* D. Don). *Sci. Rep.* 11:1496. doi: 10.1038/s41598-020-80688-1

Hasegawa, Y., Ueno, S., Wei, F. J., Matsumoto, A., Ujino-Ihara, T., Uchiyama, K., et al. (2020). Development of diagnostic PCR and LAMP markers for *MALE STERILITY 1* (*MS1*) in *Cryptomeria japonica* D. Don. *BMC Res. Notes* 13:457. doi: 10.1186/s13104-020-05296-8

Hashizume, H. (1985). Effect of gibberellins on promotion of flowering in Pinaceae species. *Bull. Fac. Agric. Tottori Univ.* 37, 80–87.

Hosoi, Y., and Maruyama, T. E. (2012). Plant regeneration from embryogenic tissue of *Pinus luchuensis* Mayr, an endemic species in Ryukyu Island, Japan. *Plant Biotechnol.* 29, 401–406. doi: 10.5511/plantbiotechnology.12.0530a

HwangBo, K., Son, S. H., Lee, J. S., Min, S. R., Ko, S. M., Liu, J. R., et al. (2010). Rapid and simple method for DNA extraction from plant and algal species suitable for PCR amplification using a chelating resin Chelex 100. *Plant Biotechnol. Rep.* 4, 49–52. doi: 10.1007/s11816-009-0117-4

Igarashi, M., Watanabe, J., Saito, H., Ozawa, H., Saito, N., Furukawa, S., et al. (2006). Breeding of *Cryptomeria japonica* for the countermeasure of pollinosis. *Bull. Fukushima Prefect. For. Res. Cent.* 39, 1–9.

Izuno, A., Maruyama, T. E., Ueno, S., Ujino-Ihara, T., and Moriguchi, Y. (2020). Genotype and transcriptome effects on somatic embryogenesis in *Cryptomeria japonica*. *PLoS One* 15:e0244634. doi: 10.1371/journal.pone.0244634

Jayasankar, S., Van Aman, M., Cordts, J., Dhekney, S., Li, Z. T., and Gray, D. J. (2005). Low temperature storage of suspension culture-derived grapevine somatic embryos and regeneration of plants. *In Vitro Cell. Dev. Biol. Plant* 41:752. doi: 10.1079/IVP2005697

Kato, K., Hiraoka, Y., Iki, T., Ohira, M., Tsubomura, M., Ono, M., et al. (2015). Gibberellin treatment to *Chamaecyparis obtusa* –comparative study for the condition of male flower by the treatment using powdered or pasted gibberellin. *Kanto Shinrin Kenkyu* 62, 253–256.

Klimaszewska, K., Overton, C., Steward, D., and Rutledge, R. G. (2011). Initiation of somatic embryos and regeneration of plants from primordial shoots of 10-year-old somatic white spruce and expression profiles of 11 genes followed during the tissue culture process. *Planta* 233, 635–647. doi: 10.1007/s00425-010-1325-4

Klimaszewska, K., Trontin, J. F., Becwar, M. R., Devillard, C., Park, Y. S., and Lelu-Walter, M. A. (2007). Recent progress in somatic embryogenesis of four *Pinus* spp. *Tree For. Sci. Biotechol.* 1, 11–25.

Kon, H., and Koyama, H. (2000). Production of seeds in *Thujopsis dolabrata* Sieb. et Zucc. var. *hondai* Makino by gibberellin applied. *J. Jpn. For. Soc.* 82, 148–153. doi: 10.11519/jjfs1953.82.2_148

Kong, L., Jaquish, B., Zaharia, I., and von Aderkas, P. (2021). Phytohormone profiles of sterile Douglas-fir mutants and the responses to stem-injected gibberellins. *Trees* 35, 1961–1969. doi: 10.1007/s00468-021-02163-2

Lara-Chavez, A., Flinn, B. S., and Egertsdotter, U. (2011). Initiation of somatic embryogenesis from immature zygotic embryos of Oocarpa pine (*Pinus oocarpa* Schiede ex Schlectendal). *Tree Physiol.* 31, 539–554. doi: 10.1093/treephys/tpr040

Lelu, M.-A., Klimaszewska, K., Pflaum, G., and Bastien, C. (1995). Effect of maturation duration on desiccation tolerance in hybrid larch (*Larix* × *leptoeuropaea* Dengler) somatic embryos. *In Vitro Cell Dev. Biol.-Plant* 31, 15–20. doi: 10.1007/BF02632220

Liao, Y. K., and Juan, I.-P. (2015). Improving the germination of somatic embryos of *Picea morrisonicola* Hayata: effects of cold storage and partial drying. *J. For. Res.* 20, 114–124. doi: 10.1007/s10310-014-0445-2

Malabadi, R. B., Teixeira da Silva, J. A., Nataraja, K., Kumar, V., and Mulgund, G. S. (2011). Induction of somatic embryogenesis in mature coniferous forest trees. *Res. Biotechnol.* 2, 8–33.

Maruyama, T. E., and Hosoi, Y. (2019). Progress in somatic embryogenesis of Japanese pines. *Front. Plant Sci.* 10:31. doi: 10.3389/fpls.2019.00031

Maruyama, T. E., Hosoi, Y., Futamura, N., and Saito, M. (2014). Initiation of embryogenic cultures from immature seeds of pollen-free sugi (*Cryptomeria japonica*). *Kanto Shinrin Kenkyu* 65, 107–110.

Maruyama, T. E., Hosoi, Y., and Ishii, K. (2002). Somatic embryogenesis in Sawara cypress (*Chamaecyparis pisifera* Sieb. et Zucc.) for stable and efficient plant regeneration, propagation and protoplast culture. *J. For. Res.* 7, 23–34. doi: 10.1007/BF02762595

Maruyama, T. E., Hosoi, Y., and Ishii, K. (2005a). Somatic embryo production and plant regeneration of Japanese black pine (*Pinus thunbergii*). *J. For. Res.* 10, 403–407. doi: 10.1007/s10310-005-0159-6

Maruyama, T. E., Hosoi, Y., and Ishii, K. (2005b). Propagation of Japanese red pine (*Pinus densiflora* Zieb. et Zucc.). *Propag. Ornam. Plants* 5, 199–204.

Maruyama, T. E., Hosoi, Y., and Ishii, K. (2007). Somatic embryogenesis and plant regeneration in Yakutanegoyou, *Pinus armandii* Franch. var. *amamiana* (Koidz.) Hatusima, an endemic and endangered species in Japan. *In Vitro Cell Dev. Biol.-Plant* 43, 28–34. doi: 10.1007/s11627-006-9003-8

Maruyama, T. E., Hosoi, Y., and Katsuki, T. (2011). Plant regeneration of Yatsugataketouhi (*Picea koyamae*) through somatic embryogenesis. *Kanto Shinrin Kenkyu* 62, 127–130.

Maruyama, T. E., Hosoi, Y., and Katsuki, T. (2012). Somatic embryo induction from embryogenic cells of Himebaramomi (*Picea maximowiczii* Regel ex Mast.). *Kanto Shinrin Kenkyu* 63, 67–71.

Maruyama, T. E., Ishii, K., and Hosoi, Y. (2005c). Efficient plant regeneration of Hinoki cypress (*Chamaecyparis obtusa* Sieb. et Zucc.) via somatic embryogenesis. *J. For. Res.* 10, 73–77. doi: 10.1007/s10310-004-0105-z

Maruyama, T. E., Tanaka, T., Hosoi, Y., Ishii, K., and Morohoshi, N. (2000). Embryogenic cell culture, protoplast regeneration, cryopreservation, biolistic gene transfer and plant regeneration in Japanese cedar (*Cryptomeria japonica* D. Don). *Plant Biotechnol.* 17, 281–296. doi: 10.5511/plantbiotechnology.17.281

Maruyama, T. E., Ueno, S., Hirayama, S., Kaneeda, T., and Moriguchi, Y. (2020). Somatic embryogenesis and plant regeneration from sugi (Japanese cedar, *Cryptomeria japonica* D. Don, Cupressaceae) seed families by marker assisted selection for the male sterility allele *ms1*. *Plants* 9:1029. doi: 10.3390/plants9081029

Maruyama, T. E., Ueno, S., Hosoi, Y., Miyazawa, S.-I., Mori, H., Kaneeda, T., et al. (2021a). Somatic embryogenesis initiation in sugi (Japanese cedar, *Cryptomeria japonica* D. Don): responses from male-fertile, male-sterile, and polycoss-pollinated-derived seed explants. *Plants* 10:398. doi: 10.3390/plants10020398

Maruyama, T. E., Ueno, S., Mori, H., Kaneeda, T., and Moriguchi, Y. (2021b). Factors influencing somatic embryo maturation in sugi (Japanese cedar, *Cryptomeria japonica* (Thunb. ex L.f.) D. Don). *Plants* 10:874. doi: 10.3390/plants10050874

Matsubara, A., Sakashita, M., Gotoh, M., Kawashima, K., Matsuoka, T., Kondo, S., et al. (2020). Epidemiological survey of allergic rhinitis in Japan 2019. *Nippon Jibiinkoka Gakkai Kaiho* 123, 485–490. doi: 10.3950/jibiinkoka.123.485

Miura, S., Nameta, M., Yamamoto, T., Igarashi, M., and Taira, H. (2011). Mechanisms of male sterility in four *Cryptomeria japonica* individuals with obvious visible abnormality at the tetrad stage. *J. Jpn. For. Soc.* 93, 1–7. doi: 10.4005/jjfs.93.1

Moriguchi, Y., Ueno, S., Hasegawa, Y., Tadama, T., Watanabe, M., Saito, R., et al. (2020). Marker-assisted selection of trees with *MALE STERILITY 1* in *Cryptomeria japonica* D. Don. *Forests* 11:734. doi: 10.3390/f11070734

Nagao, A. (1983). Differences of flower initiation of *Cryptomeria japonica* under various alternating temperatures. *J. Jap. For. Soc.* 65, 335–338. doi: 10.11519/jjfs1953.65.9_335

Ogita, S., Ishikawa, H., Kubo, T., and Sasamoto, H. (1999). Somatic embryogenesis from immature and mature zygotic embryos of *Cryptomeria japonica* I: Embryogenic cell induction and its morphological characteristics. *J. Wood Sci.* 45, 87–91. doi: 10.1007/BF01192323

Ohba, K. (1993). "Clonal forestry with sugi (*Cryptomeria japonica*)," in *Clonal Forestry II, Conservation and Application*. eds. M. R. Ahuja and W. J. Libby (Berlin: Springer-Verlag), 66–90.

Park, S. Y., Klimaszewska, K., Park, J. Y., and Mansfield, S. D. (2010). Lodgepole pine: the first evidence of seed based somatic embryogenesis and the expression of embryogenesis marker genes in shoot bud cultures of adult trees. *Tree Physiol.* 30, 1469–1478. doi: 10.1093/treephys/tpq081

Park, Y. S., Lelu-Walter, M. A., Harvengt, L., Trontin, J. F., MacEacheron, I., Klimaszewska, K., et al. (2006). Initiation of somatic embryogenesis in *Pinus banksiana*, *P. strobus*, *P. pinaster*, and *P. sylvestris* at three laboratories in Canada and France. *Plant Cell Tissue Organ Cult.* 86, 87–101. doi: 10.1007/s11240-006-9101-7

Pullman, G. S., and Buchanan, M. (2003). Loblolly pine (*Pinus taeda* L.): stage-specific elemental analysis of zygotic embryo and female gametophyte tissue. *Plant Sci.* 164, 943–954. doi: 10.1016/S0168-9452(03)00080-3

Pullman, G. S., Olson, K., Fisher, T., Egertdotter, U., Frampton, J., and Bucalo, K. (2016). Fraser fir somatic embryogenesis: high frequency initiation, maintenance, embryo development, germination and cryopreservation. *New For.* 47, 453–480. doi: 10.1007/s11056-016-9525-9

Roberts, D. R., Sutton, B. C. S., and Flinn, B. S. (1990). Synchronous and high frequency germination of interior spruce somatic embryos following partial drying at high relative humidity. *Can. J. Bot.* 68, 1086–1090. doi: 10.1139/b90-136

Saito, M. (2010). Breeding strategy for the pollinosis preventive cultivars of *Cryptomeria japonica* D. Don. *J. Jpn. For. Soc.* 92, 316–323. doi: 10.4005/jjfs.92.316

Shidei, T., Akai, T., and Ichikawa, S. (1959). Flower bud formation on Sugi (*Cryptomeria japonica*) and Metasequoia (*Metasequoia glyptosytoboides*) by gibberellic acid treatment. *J. Jpn. For. Soc.* 41, 312–315.

Stasolla, C., Kong, L., Yeung, E. C., and Thorpe, T. E. (2002). Maturation of somatic embryos in conifers: morphogenesis, physiology, biochemistry, and molecular biology. *In Vitro Cell Dev. Biol.-Plant* 38, 93–105. doi: 10.1079/IVP2001262

Taira, H., Saito, M., and Furuta, Y. (1999). Inheritance of the trait of male sterility in *Cryptomeria japonica*. *J. For. Res.* 4, 271–273. doi: 10.1007/BF02762782

Taniguchi, T., Konagaya, K., and Nanasato, Y. (2020). Somatic embryogenesis in artificially pollinated seed families of 2nd generation plus trees and cryopreservation of embryogenic tissue in *Cryptomeria japonica* D. Don (sugi). *Plant Biotechnol.* 37, 239–245. doi: 10.5511/plantbiotechnology.20.0220a

Taniguchi, T., and Kondo, T. (2000). Difference in ability of initiation and maintenance of embryogenic cultures among sugi (*Cryptomeria japonica* D. Don) seed families. *Plant Biotechnol.* 17, 159–162. doi: 10.5511/plantbiotechnology.17.159

Tautorus, T. E., Fowke, L. C., and Dunstan, D. I. (1991). Somatic embryogenesis in conifers. *Can. J. Bot.* 69, 1873–1899. doi: 10.1139/b91-237

Teixeira da Silva, J. A., and Malabadi, R. B. (2012). Factors affecting somatic embryogenesis in conifers. *J. For. Res.* 23, 503–515. doi: 10.1007/s11676-012-0266-0

Toda, R. (1974). Vegetative propagation in relation to Japanese forest tree improvement. *N. Z. J. For. Sci.* 4, 410–417.

Torres-Viñals, M., Sabaté-Casaseca, S., Aktouche, N., Grenan, S., Lopez, G., Porta-Falguera, M., et al. (2004). Large-scale production of somatic embryos as a source of hypocotyl explants for *Vitis vinifera* micrografting. *Vitis* 43, 163–168. doi: 10.5073/vitis.2004.43.163-168

Tsuruta, M., Maruyama, T. E., Ueno, S., Hasegawa, Y., and Moriguchi, Y. (2021a). Marker-assisted selection for pollen-free somatic plants of sugi (Japanese cedar, *Cryptomeria japonica*): A simple and effective methodology for selecting male-sterile mutants with *ms1-1* and *ms1-2*. *Front. Plant Sci.* 12:748110. doi: 10.3389/fpls.2021.748110

Tsuruta, M., Maruyama, T. E., Ueno, S., Kaneeda, T., and Moriguchi, Y. (2021b). Plant regeneration and *in vitro* growth performance of male-sterile somatic plantlets of sugi (Japanese cedar, *Cryptomeria japonica*) derived from different embryogenic cell lines. *Forests* 12:1592. doi: 10.3390/f12111592

Ueno, S., Uchiyama, K., Moriguchi, Y., Ujino-Ihara, T., Matsumoto, A., Wei, F. J., et al. (2019). Scanning RNA-Seq and RAD-Seq approach to develop SNP markers closely linked to *MALE STERILITY 1* (*MS1*) in *Cryptomeria japonica* D. Don. *Breed. Sci.* 69, 19–29. doi: 10.1270/jsbbs.17149

Wilcox, P. L., Echt, C. E., and Burdon, R. D. (2007). "Gene-assisted selectiossn applications of association genetics for forest tree breeding," in *Association Mapping in Plants*. eds. N. C. Oraguzie, E. H. A. Rikkerink, S. E. Gardiner and H. N. de Silva (New York, NY: Springer), 211–247.

Conflict of Interest: KK was employed by the company Verde Co., Ltd.

The remaining authors declare that the research was conducted in the absence of any commercial or financial relationships that could be construed as a potential conflict of interest.

Publisher's Note: All claims expressed in this article are solely those of the authors and do not necessarily represent those of their affiliated organizations, or those of the publisher, the editors and the reviewers. Any product that may be evaluated in this article, or claim that may be made by its manufacturer, is not guaranteed or endorsed by the publisher.

frontiers in Plant Science

ORIGINAL RESEARCH
published: 14 February 2022
doi: 10.3389/fpls.2022.823617

Desiccation as a Post-maturation Treatment Helps Complete Maturation of Norway Spruce Somatic Embryos: Carbohydrates, Phytohormones and Proteomic Status

Kateřina Eliášová[1], Hana Konrádová[2], Petre I. Dobrev[1], Václav Motyka[1], Anne-Marie Lomenech[3], Lucie Fischerová[1], Marie-Anne Lelu-Walter[4], Zuzana Vondráková[1] and Caroline Teyssier[4]*

[1] Institute of Experimental Botany of the Czech Academy of Sciences, Prague, Czechia, [2] Department of Experimental Plant Biology, Faculty of Science, Charles University, Prague, Czechia, [3] Plateforme Proteome, University of Bordeaux, Bordeaux, France, [4] INRAE, ONF, BioForA, Orléans, France

OPEN ACCESS

Edited by:
Jorge M. Canhoto, University of Coimbra, Portugal

Reviewed by:
Célia M. Miguel, University of Lisbon, Portugal
Miguel Pedro Guerra, Federal University of Santa Catarina, Brazil

***Correspondence:**
Kateřina Eliášová
eliasova@ueb.cas.cz

Specialty section:
This article was submitted to Plant Development and EvoDevo, a section of the journal Frontiers in Plant Science

Received: *27 November 2021*
Accepted: *04 January 2022*
Published: *14 February 2022*

Citation:
Eliášová K, Konrádová H, Dobrev PI, Motyka V, Lomenech A-M, Fischerová L, Lelu-Walter M-A, Vondráková Z and Teyssier C (2022) Desiccation as a Post-maturation Treatment Helps Complete Maturation of Norway Spruce Somatic Embryos: Carbohydrates, Phytohormones and Proteomic Status. Front. Plant Sci. 13:823617. doi: 10.3389/fpls.2022.823617

Exposure of Norway spruce (*Picea abies*) somatic embryos and those of many other conifers to post-maturation desiccation treatment significantly improves their germination. An integration analysis was conducted to understand the underlying processes induced during the desiccation phase at the molecular level. Carbohydrate, protein and phytohormone assays associated with histological and proteomic studies were performed for the evaluation of markers and actors in this phase. Multivariate comparison of mature somatic embryos with mature desiccated somatic embryos and/or zygotic embryos provided new insights into the processes involved during the desiccation step of somatic embryogenesis. Desiccated embryos were characterized by reduced levels of starch and soluble carbohydrates but elevated levels of raffinose family oligosaccharides. Desiccation treatment decreased the content of abscisic acid and its derivatives but increased total auxins and cytokinins. The content of phytohormones in dry zygotic embryos was lower than in somatic embryos, but their profile was mostly analogous, apart from differences in cytokinin profiles. The biological processes "Acquisition of desiccation tolerance", "Response to stimulus", "Response to stress" and "Stored energy" were activated in both the desiccated somatic embryos and zygotic embryos when compared to the proteome of mature somatic embryos before desiccation. Based on the specific biochemical changes of important constituents (abscisic acid, raffinose, stachyose, LEA proteins and cruciferins) induced by the desiccation treatment and observed similarities between somatic and zygotic *P. abies* embryos, we concluded that the somatic embryos approximated to a state of desiccation tolerance. This physiological change could be responsible for the reorientation of Norway spruce somatic embryos toward a stage suitable for germination.

Keywords: desiccation tolerance, somatic embryogenesis, phytohormones, *Picea abies* (L.) Karst, proteomics, raffinose family oligosaccharides

INTRODUCTION

Somatic embryogenesis could play an important role in the commercial breeding of conifers, but many problems have to be solved before its widespread use in forest management, e.g., insufficient quality and yield of mature embryos and their low ability to germinate (Pullman and Bucalo, 2014). Eliminating these obstacles would enable enhanced embryogenic culture production, e.g., large-scale cultivation in bioreactors, which offers a promising method for conifer somatic embryogenesis owing to its increased efficiency and lower costs (Välimäki et al., 2020).

Desiccation of somatic embryos (SEs) prior to germination is a possible approach to enhance the amount and quality of germinated embryos. SEs of many conifer species are able to germinate without a prior desiccation phase as desiccation demand is species and/or genotype-specific (Klimaszewska et al., 2016). Nevertheless, mild or partial drying of SEs of *Picea* sp. has been suggested as a prerequisite for successful germination (e.g., Roberts, 1991; Find, 1997; Pond et al., 2002). Moreover, desiccation not only stimulates germination of SEs but also positively influences their conversion into plantlets. However, this effect depends strongly on the length and intensity of desiccation treatment. Slow long-term partial desiccation (up to 5 weeks) under high relative humidity may be more beneficial (Roberts et al., 1991) than 2-week desiccation under a lower relative humidity < 80% (Roberts et al., 1990b; Attree et al., 1991). Subjecting desiccation-sensitive cells to desiccation conditions of < 90% relative humidity can cause the loss of correct protein conformation, membrane phase transitions and RNA/DNA structural rearrangements and fragmentation (Leprince and Buitink, 2015).

The process of conifer embryogenesis is controlled by phytohormones. Their role in individual steps of somatic embryogenesis differs according to the developmental processes taking place in embryonic cultures or SEs. Endogenous levels of phytohormones in embryos are also affected by the hormonal composition of the cultivation medium. Auxins and cytokinins (CKs) are typical components of induction and proliferation media promoting cell division and growth, whereas abscisic acid (ABA) is added to culture media during the maturation step. ABA induces the maturation of conifer SEs, inhibits precocious germination during maturation, promotes the accumulation of storage proteins (Roberts et al., 1990a; Leal et al., 1995; von Aderkas et al., 2002) and contributes to the acquisition of desiccation tolerance (Hoekstra et al., 2001). High ABA levels have been shown to inhibit germination after maturation of hybrid larch SEs (Lelu and Label, 1994). However, the germination rate of hybrid larch SEs was improved by a period of partial drying in the cell under controlled relative humidity (Lelu et al., 1995). An extended desiccation phase was also shown to be required by Sitka spruce SEs when maturing on medium with high ABA content (Roberts et al., 1991). The positive effect of desiccation on the number and quality of germinated SEs has been attributed to decreased ABA levels (Dronne et al., 1997; Find, 1997) but also changes in carbohydrate and storage protein content (Bomal et al., 2002; Wang et al., 2014) and activation of antioxidant systems.

The development of conifer SEs encompasses key stages of zygotic embryogenesis in seeds (Attree and Fowke, 1993; Hakman, 1993; Nagmani et al., 1995; von Arnold et al., 2019). Mimicking conditions during seed development in an *in vitro* somatic embryogenesis system could enable optimization of cultivation procedures (Pullman and Bucalo, 2014). The late maturation phase in orthodox seeds is a period when seeds, after the accumulation of storage reserves, lose water and change to a quiescent dry state. Even though the term desiccation evokes the physical process of drying, this phase involves more than just water loss owing to physiological and biochemical changes taking place in seeds (Angelovici et al., 2010; Leprince et al., 2017). Acquisition of tolerance to certain stresses (low temperatures, water shortages and desiccation) during the final maturation phase is of special importance. This step must prepare seeds to not only withstand the loss of water but also to perform the synthesis of transcripts and proteins necessary for seed germination. These include proteins involved in protection against oxidative stress during dehydration and subsequent rehydration, meristematic growth, or provision of energy supply (Stasolla et al., 2004a; Lara-Chavez et al., 2012; Jing et al., 2017). Synthesis of protective substances, often starting during maturation, is amplified during the acquisition of tolerance to desiccation. Several families of proteins [e.g., LEA and small heat shock proteins (HSPs)] participate in this process by protecting the membrane structures of cells against oxidative species produced during desiccation (Huang et al., 2012; Amara et al., 2014). Their synthesis is also amplified in conifer SEs during late maturation or a desiccation phase (Stasolla et al., 2004b; Jing et al., 2017).

Proteins that provide enzymatic, structural or energetic functions are also important actors in the embryogenesis process. The energetic function is achieved by storage proteins, which also provide nitrogen during germination for *de novo* protein synthesis. Proteins that mainly accumulate during the end of maturation (Leprince and Buitink, 2010) are vicilin- and legumin-like proteins (Flinn et al., 1993; Klimaszewska et al., 2004), although albumin may also participate (Morel et al., 2014). In addition to these specific proteins, accumulation of raffinose family oligosaccharides (RFOs) and sucrose is considered a marker of the late maturation phase owing to their protective

Abbreviations: D2, D3 embryos, embryos desiccated for 2 or 3 weeks; HSP, heat shock protein; LEA, late embryogenesis abundant protein; M5 embryos, mature embryos after 5 weeks of maturation; M7, M8 embryos, embryos after 2 or 3 weeks of prolonged maturation; RFOs, raffinose family oligosaccharides; SE, somatic embryo; ZE, zygotic embryo; ZEf, fresh zygotic embryos; ZEd, dry zygotic embryos; ABA, abscisic acid; ABA-GE, ABA-glucose ester; *cis*Z9G, *cis*-zeatin 9-glucoside; *cis*ZOG, *cis*-zeatin *O*-glucoside; *cis*ZR, *cis*-zeatin 9-riboside; *cis*ZRMP, *cis*-zeatin 9-riboside-5′-monophosphate; *cis*ZROG, *cis*-zeatin 9-riboside *O*-glucoside; DHZ, dihydrozeatin; DHZR, dihydrozeatin 9-riboside; DHZRMP, dihydrozeatin 9-riboside-5′-monophosphate; DHZROG, dihydrozeatin 9-riboside *O*-glucoside; DHZ9G, dihydrozeatin 9-glucoside; DPA, dihydrophaseic acid; IAA, indole-3-acetic acid; IAA-Asp, IAA-aspartate; IAA-Glu, IAA-glutamate; iP, N^6-(Δ^2-isopentenyl) adenine; iPR, N^6-(Δ^2-isopentenyl) adenosine; iPRMP, N^6-(Δ^2-isopentenyl) adenosine-5′-monophosphate; NeoPA, neophaseic acid; 9OH-ABA, 9-hydroxy-ABA; OxIAA, oxo-IAA; PA, phaseic acid; PAA, phenylacetic acid; *trans*Z, *trans*-zeatin; *trans*ZOG, *trans*-zeatin *O*-glucoside; *trans*ZR, *trans*-zeatin 9-riboside; *trans*ZRMP, *trans*-zeatin 9-riboside-5′-monophosphate; *trans*ZROG, *trans*-zeatin 9-riboside *O*-glucoside.

functions and is related to the acquisition of desiccation tolerance (Hoekstra et al., 2001; Leprince et al., 2017). Non-structural carbohydrates in plants are multifunctional compounds that may offer a method for improving embryogenesis. Their widely accepted roles include a source of energy and carbon skeleton, osmotic agents, protection of the plant cell ultrastructure, direct signaling role and regulation of gene expression. A pattern of carbohydrate accumulation during the late maturation of zygotic embryos (ZEs) has been reported in conifer species such as *Picea abies* (Gösslová et al., 2001), *Pinus pinaster* (Morel et al., 2014) and *Pinus taeda* (Pullman and Buchanan, 2008). The prominent role of carbohydrates, including their exogenous supply, during conifer embryogenesis *in vitro*, is known (Lipavská and Konrádová, 2004). The distinct patterns of carbohydrate content and spectra during maturation, desiccation and germination have been suggested as indicators of regular Norway spruce SE development (Businge et al., 2013; Hudec et al., 2016). The importance of the RFO: sucrose (R/S) ratio for desiccation protection has also been reported (Sauter and van Cleve, 1991; Xiao and Koster, 2001). In maritime pine ZEs, the R/S ratio was shown to gradually increase during the late phase of maturation and the start of drying (Morel et al., 2014).

We have previously demonstrated (Vondráková et al., 2013) the positive effect of desiccation treatment on the germination capacity of mature Norway spruce SEs. To understand the molecular mechanisms involved in this process, in the present study, we investigated the histological and biochemical changes that occur in Norway spruce SEs after exposure to a post-maturation desiccation treatment. Phytohormone, carbohydrate and protein profiles were determined together with proteomic analysis of molecular functions and activated biological processes. Data were compared with that of ZEs.

MATERIALS AND METHODS

Plant Material

An embryogenic culture of *Picea abies* (L.) H. Karst, genotype AFO 541, was induced at AFOCEL (Nangis, France) from immature ZEs and received as a generous gift from Dr. Bercetche. The embryogenic culture was maintained on solid GD medium supplemented with 2,4-D, BAP and kinetin (Vondrakova et al., 2018). Maturation was performed in Magenta vessels with membrane rafts (Osmotek, Rehovot, Israel) on liquid GD medium (Gupta and Durzan, 1986) at 23 ± 1°C in the dark for five weeks and was subcultured weekly. The liquid GD medium was supplemented with 20 μM ABA (Sigma-Aldrich), 3.75% polyethylene glycol 4000 (PEG, Sigma-Aldrich) and 30 g L^{-1} of sucrose (Lachema, Brno, Czech Republic); the pH was adjusted to 5.8 before autoclaving. ABA and all organic components, except sucrose, were separately prepared and diluted, filter-sterilized and added to the cooled, autoclaved medium. The PEG solution was autoclaved separately and then added to the medium. After five weeks of maturation, clusters with SEs were grown on the maturation medium for an additional three weeks (subcultured weekly on fresh medium) or selected mature cotyledonary SEs were subjected to desiccation treatment during a three-week desiccation phase. Desiccation of SEs isolated from clusters was carried out under high relative humidity (near 100%) on dry filter paper in small Petri dishes (3 cm in diameter) that were left open and placed in large Petri dishes (18 cm in diameter) containing several layers of filter paper wetted with sterile water to maintain high relative humidity. The large Petri dishes were covered with lids, sealed with parafilm and then incubated in a cultivation room for three weeks under a 12 h photoperiod at 18 ± 1°C (Vondrakova et al., 2018). Throughout this study, we refer to this treatment as "desiccation" and the treated embryos as "desiccated", even though the water content (WC) in the SEs did not decrease significantly.

Phytohormones, carbohydrates and total protein content were measured in cotyledonary SEs collected after five weeks of maturation (M5) [i.e., in mature SEs according to the standard protocol (Vondrakova et al., 2018)], after seven (M7) and eight (M8) weeks of maturation (i.e., after additional two and three weeks of prolonged cultivation on the maturation medium) and after two (D2) and three weeks (D3) of desiccation. At the same time points, SEs were collected for morphological and histological observations. The maturation samples (M5, M7 and M8) were collected just before subculture. All samples for biochemical analyses were dried on cotton wool, then frozen in liquid nitrogen and stored at -80°C until analysis.

Zygotic embryos (ZEs) were collected from seeds of free-growing, open-pollinated Norway spruce [*Picea abies* (L.) H. Karst] trees in late summer, i.e., August (fresh ZEs; ZEf), and in winter, i.e., December/January (dry ZEs; ZEd). Samples were taken from the mid-part of the cones and processed immediately in the same way as SEs. Only ZEd were used for carbohydrate and phytohormone analyses.

All data were related to the dry weight of the collected material. The dry weight (DW) of all samples was obtained by reduction of the initial moisture content at 105°C to a constant weight (approx. 12 h).

Histological Analysis

Anatomical and histochemical observations were performed on the embryo sections. Ten embryos were processed for each embedding method and each histochemical staining for each type of sample. For a general overview, embryos were embedded in paraffin, whereas for more detailed cytological observations, embryos were embedded in glycol methacrylate. For embedding in paraffin, embryos were fixed in 50% FAA (5% (v/v) formalin, 5% (v/v) acetic acid, 50% (v/v) ethanol), dehydrated in an ethanol/butanol series, then infiltrated and embedded in paraffin, as described in Vondráková et al. (2015). Longitudinal sections (12 μm thick) were stained with 0.5% Ponceau xylidine in 2% acetic acid (Gutmann et al., 1996) to detect storage proteins (red coloration) or with Lugol's solution (Sass, 1958) for the detection of starch grains (blue-violet coloration). Both types of histochemical reactions were counterstained with azure II, which colored cellulose cell walls blue. For embedding in glycol methacrylate (Technovit 7100; Heraeus-Kulzer, Werheim, Germany), embryos were fixed in 2.5% glutaraldehyde in 100 mM phosphate buffer, dehydrated in an ethanol series, then infiltrated and embedded according to Eliášová et al. (2017). Longitudinal

sections were cut to a thickness of 4-5 μm, stained using the periodic acid-Schiff (PAS) procedure, and counterstained with a solution of 1% amido black 10B in 7% acetic acid (Kong and Yeung, 1992). With the PAS procedure, a pink-red coloration indicated the presence of insoluble carbohydrates (e.g., starch, cellulose), whereas, with the amido black stain, a blue coloration indicated proteins. Paraffin sections were observed under a Jenaval transmission light microscope (Zeiss, Jena, Germany). Images were captured using a Nikon DS-Fi3 camera (Tokyo, Japan) and processed using NIS-Elements AR 5.0 software (Laboratory Imaging, Prague, Czech Republic). Glycol methacrylate sections were observed using an Olympus BX63 light microscope (Tokyo, Japan) equipped with an Olympus DP74 CMOS camera. Images were captured and processed using the cellSens Olympus software.

Protein Analysis

Soluble proteins were extracted from three biological replicates of samples (about 20 to 50 mg FW (fresh weight) of frozen material, depending on the developmental stage) with 1 ml of buffer containing 2% v/w PVPP, 5% v/v β-mercaptoethanol, 2% v/v SDS, 0.1M DTT, 50 mM Tris HCl (pH 6.8) and 10% (v/v) glycerol. Protein content was determined using the Bradford assay with bovine serum albumin as a standard. Results (mean ± SE of 4 biological repetitions) were expressed as soluble protein content in μg mg^{-1} FW. The same quantities of extracted proteins (15 μg) were separated by sodium dodecyl sulfate-polyacrylamide gel electrophoresis (SDS-PAGE) on a 12% gel with stacking gel (4%) following standard protocols. The gel was stained for proteins with colloidal Coomassie brilliant blue G-250 (CBB-G).

Carbohydrate Analysis

A procedure described in Hudec et al. (2016) was used for soluble saccharide extraction and determination. Four to six biological replicates of samples of isolated embryos (ca. 70-100 mg FW) were freeze-dried and the dry weight was determined. The material was boiled with 80% (v/v) methanol (0.5 mL) at 75°C for 15 min, the solvent was vacuum evaporated and the residue was resuspended in an appropriate amount of Milli-Q ultrapure water (Millipore). After centrifugation at 14.000 g for 10 min, supernatants were filtered through 0.45 μm membrane filters (Millipore) and analyzed using high-performance liquid chromatography (HPLC) with refractometric detection and a Shodex Sugar SC1011 Pb^{2+} column (Shodex, Tokyo, Japan), mobile phase of Milli-Q water and a flow rate of 0.5 ml min^{-1}. The pellets remaining after the extraction of soluble carbohydrates were washed three times with ultrapure water, and then starch was hydrolyzed by α-amylase (Fluka Sigma-Aldrich, St. Louis, USA, 30 U) and amyloglucosidase (Fluka Sigma-Aldrich, St. Louis, USA, 60 U) in Na-acetate buffer (pH 4.5) at 37°C for 8 h. The released glucose was quantified by HPLC. The amount of starch was expressed as the glucose amount after enzymatic cleavage. The average values of all determined carbohydrates together with statistical data are given in **Supplementary Table 1**.

Phytohormone Analysis

Analysis of plant hormones at selected time points was conducted as described in Vondrakova et al. (2018). Homogenized samples (ca. 100 mg FW aliquots of three biological replicates for each type of sample) were incubated in cold extraction buffer (methanol/water/formic acid, 15/4/1, v/v/v, -20°C, 500 μL) containing a mixture of stable isotope-labeled internal standards [10 pmol; for details see Vondrakova et al. (2018)]. Two phytohormone fractions were obtained using reversed-phase and ion-exchange chromatography (Oasis-MCX, Waters, Milford, MA, USA): (1) fraction A (eluted with methanol) containing acidic and neutral compounds (auxins, ABA, and their derivatives), and (2) fraction B (eluted with 0.35 M NH_4OH in 70% methanol) containing hormones of basic character (CKs). Hormonal quantification was performed by a HPLC instrument (Ultimate 3000, Dionex, Sunnyvale, CA, USA) coupled to a hybrid triple quadrupole/linear ion trap mass spectrometer (3200 Q TRAP, Applied Biosystems, Foster City, CA, USA) as described previously (Djilianov et al., 2013), using the isotope dilution method with multilevel calibration curves. All data collected were processed with Analyst 1.5 software (Applied Biosystems), and hormonal concentrations were calculated as the amount per 1 g of dry weight of plant material considering that embryos have different WC at various stages of development. Average values of all determined phytohormones together with statistical data are given in **Supplementary Table 2**.

Proteomic Analysis

Total protein extracts were prepared from five replicates for each type of sample (approx. 100 mg FW) as previously described by Teyssier et al. (2014). Briefly, extraction was performed with phenol and precipitation was performed with ammonium acetate in ethanol. Protein pellets were resuspended in 8 M urea, 2 M thiourea, 4% CHAPS buffer adjusted to pH 8.5. Protein concentrations of the samples were determined by the Bradford method.

To limit gel-to-gel variations and to facilitate interpretation of the protein abundance in the two proteome comparisons, we opted for DIGE (differential gel electrophoresis) analysis. Three types of samples, each stained with a different fluorochrome, were loaded simultaneously onto the same gel, thus limiting spot location artifacts. The samples (125 μg each) were labeled with CyDyes^{TM} Fluor minimal dyes (GE Healthcare) Cy2, Cy3 or Cy5 according to the manufacturer's instructions. The labeled samples were then combined for 2D DIGE analytical gels to include the three different dyes and three different sample types, with a total amount of 300 μg, in each of the five repetition gels. Labeled samples were also used for picking gels of each type of sample, combining all biological repetitions with 100 μg of labeled proteins in the 600 μg total. Both types of mixture (for analytical and picking gels) were loaded onto 24 cm IPG strips, pH 4–7 (Protean IEF Cell system, BioRad, France) to perform the first-dimension separation, whereas 2D polyacrylamide gel electrophoresis (PAGE) was performed with 11% polyacrylamide gels. Low fluorescent glass plates were used for the second dimension to minimize

background fluorescence during scanning. Both types of gels were scanned using a Typhoon 9400 Trio variable mode imager (GE Healthcare) using optimal excitation/emission wavelengths for each DIGE fluorochrome (Cy2 498/524 nm; Cy3 554/575 nm; Cy5 648/663 nm) and a resolution of 200 μm. The picking gels were also stained with colloidal CBB-G. In addition to dye image analysis, relative quantification was carried out with PROGENESIS software (Non-linear Dynamics, UK) as described by Teyssier et al. (2014). The criteria for selection after statistical analysis were a threshold fold change of 2 and P value < 0.05. The corresponding spots were manually excised from the relevant picking gel and identified by mass spectrometry.

Protein Identifications by Mass Spectrometry

The destain, wash, proteolysis steps and sample preparation for MS are described elsewhere (Teyssier et al., 2014). Peptide mixtures were analyzed by online capillary nano HPLC (LC Packings, Amsterdam, The Netherlands) coupled to a nanospray LCQ Deca XP ion trap mass spectrometer (Thermo Finnigan, San Jose, CA, USA). Peptides were separated an analytical 75-mm id x 15-cm C18 Pep-Map column (LC Packings) with a 5–40% linear gradient of solvent B in 35 min (solvent A was 0.1% formic acid and solvent B was 0.1% formic acid in 80% ACN) and a 300 nL/min flow rate. MS data were acquired in a positive mode in a data-dependent mode. MS scans were recorded over a m/z range from 300 to 1700). Dynamic exclusion was set to 30 s and top 3 fragmentation in CID mode was performed with a normalized collision energy of 35% and an isolation width of 2 m/z.

Data were searched by SEQUEST through Proteome Discoverer 1.3 (Thermo Fisher Scientific Inc.) against the Whitebuilt36 protein database [67,034 entries (personnel communication by Mark Bohlmann; Lippert et al., 2009)] actualized with pab.aa.fasta realized in 2018 (71158 entries,[1]). Two missed enzyme cleavages were allowed. Mass tolerances in MS and MS/MS were set to 2 Da and 1 Da. Oxidation of methionine and carbamidomethylation on cysteine were searched as a dynamic modification. Peptide validation was performed using the Percolator algorithm (Käll et al., 2007) and only "high confidence" peptides were retained corresponding to a 1% false-positive rate at the peptide level.

Functional Characterization and Gene Ontology Analysis

Changes in expression relative to appropriate controls were calculated based on the cumulative intensity of each peptide (classifying proteins with ≥ 2-fold change ratios as up- or down-regulated). All sequences were mapped against gene ontology (GO) terms in the *Arabidopsis thaliana* TAIR database[2] for functional annotation. The proteins were then classified according to their biological functions using Web Gene Ontology Annotation Plot software for biological processes and molecular function (Panther,[3]).

[1]https://conekt.sbs.ntu.edu.sg/species/view/9

[2]https://www.arabidopsis.org/

[3]http://pantherdb.org/

Statistical Analysis

Statistical analysis of the carbohydrate and phytohormone data was conducted using the Sigma Plot statistical package (Systat Software, San Jose, CA, United States). The significance of differences in mean values was evaluated using a one-way analysis of variance (ANOVA). Mean values were compared using Tukey's test, and differences between means with $P < 0.05$ were considered significant. Data are shown in **Supplementary Tables 1, 2**.

For protein analysis, statistical analysis was carried out with R software (version 3.3.2; RStudio, 2021). Effects of the treatments on total protein content were evaluated using one-way ANOVA. Variations of this parameter during maturation were analyzed with multiple comparisons of means with Tukey contrasts ($P < 0.05$). For the 2-D PAGE analysis, the intensity change for each spot was analyzed with Student's t-test based on the normalized spot volume ($P < 0.05$).

To explore and visualize correlations between sample types and measured variables (stachyose, raffinose, sucrose, glucose, fructose, inositol, starch, protein, ABAs, IAAs, CKs, DW/FW), the data were subjected to multivariate analysis with FactoMineR (Lê et al., 2008). The phytohormone content was grouped by families: ABAs pooled ABA, DPA, PA, ABA-GE, NeoPA and 9OH-ABA content; IAAs pooled IAA, IAA-Asp, IAA-Glu, Ox-IAA and PAA content; CKs pooled tZ, tZR, tZROG, tZ9G, tZOG, tZRMP, DHZ, DHZR, DHZROG, DHZ9G, DHZRMP, cZR, cZOG, ZROG, cZ9G, cZRMP, iP, iPR and iPRMP content.

RESULTS

Mature SEs with well-developed cotyledons, and shoot and root apical meristems after five weeks of maturation (M5) were used as starting material for subsequent experiments (**Figure 1A**).

During maturation prolonged for 2 or 3 weeks, cotyledonary SEs (on the surface of clusters) enlarged. In most of them, disintegration and callogenesis appeared on the surface of the embryos. The isolated SEs grew slowly at the start of desiccation, the root pole turned red (**Figure 2A**) and later on the cotyledons became green. No morphological changes and no callogenesis occurred during the second and third weeks of desiccation (**Figure 2B**).

Fresh zygotic embryos collected in late summer were already well morphologically developed, similarly to M5 embryos, and almost filled the corrosion cavity inside the megagametophyte (**Figures 3A,B**). ZEd collected in winter filled the entire corrosion cavity; morphologically, they differed from ZEf only by more elongated cotyledons.

WC in M5 embryos was 4.5 ± 0.35 g H_2O g^{-1} DW. During prolonged maturation, WC decreased to 3.6 ± 0.19 g H_2O g^{-1} DW in M8 embryos. This value was significantly comparable to WC achieved after two weeks of desiccation treatment (3.78 ± 0.44 g H_2O g^{-1} DW in D2). During the third week of desiccation, WC increased (4.65. ± 0.13 g H_2O g^{-1} DW) and was not significantly different from the value in M5 embryos. WC in ZEf (0.55 ± 0.08 g H_2O g^{-1} DW) and ZEd

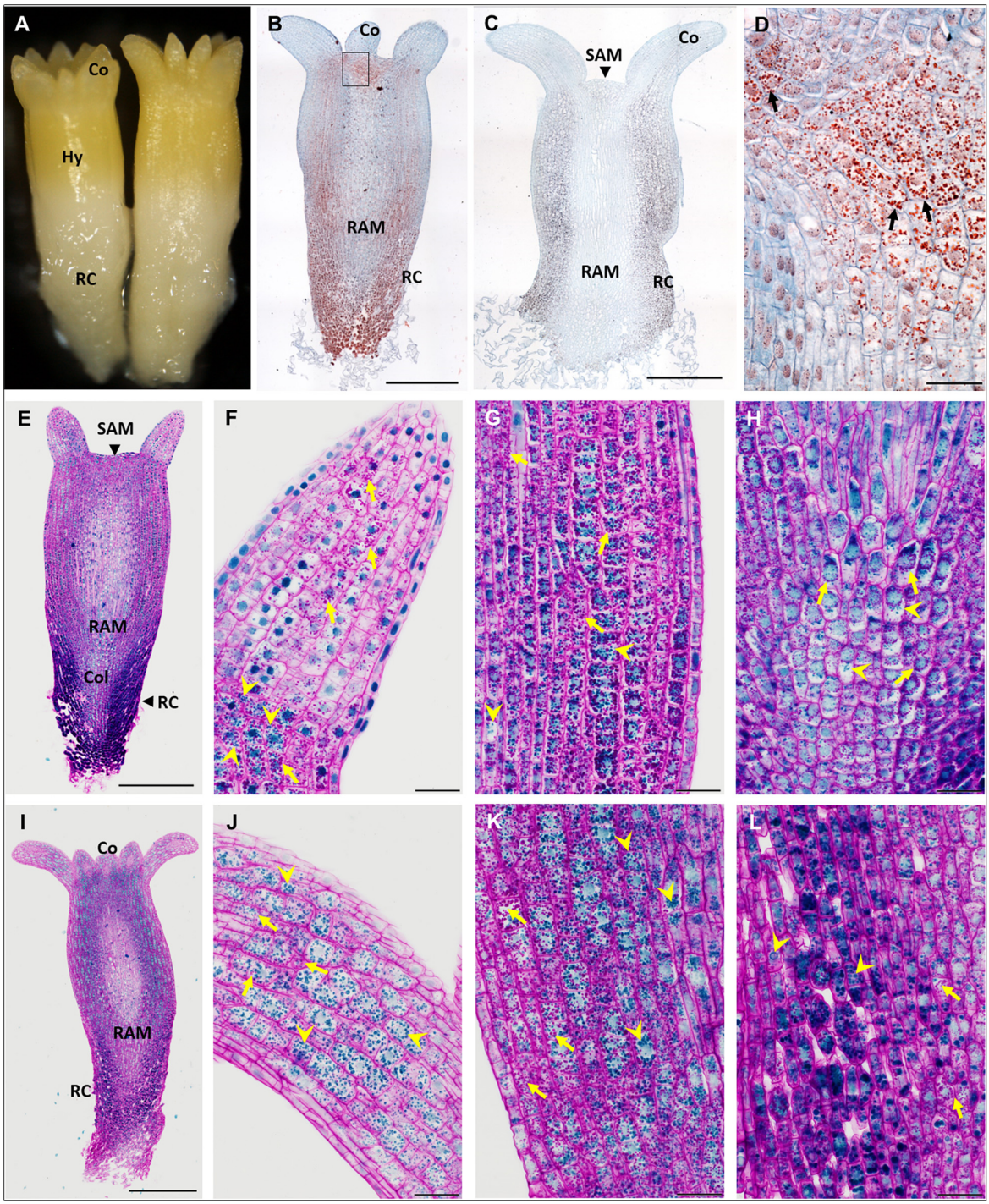

FIGURE 1 | Accumulation of storage compounds in somatic embryos (SEs) of *P. abies* after five and eight weeks of maturation. **(A–H)** Five weeks of maturation (M5); **(I–L)** eight weeks of maturation (M8). **(A)** Morphology of a M5 embryo. **(B)** Longitudinal section of a M5 embryo; storage proteins (in red) were detected in protein storage vacuoles (PSVs) using Ponceau xylidine stain, cell walls were counterstained with azure II (in blue); accumulation of PSVs was prominent below the cotyledons and shoot apical meristem and in the root cap. **(C)** Longitudinal section of a M5 embryo; starch grains were detected using Lugol's solution (dark points), cell walls were counterstained with azure II; accumulation of starch was prominent mainly in the hypocotyl cortex and root cap, and to a lesser extent under the shoot apical meristem and in the cotyledons. **(D)** Detail of the zone below the cotyledon, corresponding to the inset in panel **(B)**, with prominent PSVs (arrows). **(E)** Longitudinal section of a M5 embryo stained with PAS/amido black (polysaccharides stained magenta in cell walls and starch grains, proteins stained blue in nuclei and PSVs); accumulation of storage proteins was marked in the root cap cells. **(F)** Detail of a cotyledon in panel **(E)** with the predominant accumulation of starch grains (arrows); PSVs accumulated at the bottom of the cotyledon (arrowheads). **(G)** Detail of the hypocotyl cortex in panel **(E)**, where starch grains (arrows)

(Continued)

FIGURE 1 | predominated over PSVs (arrowheads). **(H)** Detail of the columella in panel **(E)**, where both storage compounds occurred to a lesser extent than in the root cap cells; starch grains usually surrounded nuclei (arrows); PSVs were more dispersed in the cytoplasm (arrowheads). **(I)** Longitudinal section of a M8 embryo stained with PAS/amido black; accumulation of storage proteins was less prominent in the M8 SE root cap than in M5. **(J)** Detail of the cotyledon in panel **(I)** with abundant PSVs (arrowheads) and starch grains (arrows). **(K)** Detail of the hypocotyl cortex in panel **(I)** with abundant PSVs (arrowheads) and starch grains (arrows). **(L)** Detail of the root cap cells (on the left side) and columella cells (on the right side) in panel **(I)**, both with abundant PSVs (arrowheads) and starch grains (arrows). Co, cotyledons; Col, columella; Hy, hypocotyl; RAM, root apical meristem; RC, root cap; SAM, shoot apical meristem. Scale bars represent: 500 μm in panels **(B,C,E,I)**; 50 μm in panels **(D–L)**.

(0.31 ± 0.07 g H_2O g^{-1} DW) differed significantly from WC values in all SE samples.

During subsequent steps of the investigation, differences between SEs in the development stages M5, M7, M8 and D2, D3 and ZEs were described on biochemical levels, i.e., in the content of non-structural carbohydrates, starch and proteins and in phytohormone profiles. For more precise determination of differences among somatic M5, M7, M8 and D2, D3 embryos and ZEs, histological and proteomic analyses were performed.

Histological Analysis

The accumulation of storage compounds (proteins and starch) and their localization within maturated (M5, M8) and desiccated (D2, D3) SEs, and within ZEf and ZEd were followed using histological analysis.

In M5 embryos (**Figure 1A**), storage proteins were deposited in protein storage vacuoles (PSVs) located in the cytoplasm (**Figures 1B,E**). PSVs accumulated predominantly below the shoot apical meristem (SAM) and at the base of cotyledons (**Figures 1B,D,F**), in the cortex of the hypocotyl (**Figure 1G**) and in the root cap (**Figures 1B,E**). A smaller number of PSVs occurred in the cotyledons (**Figure 1F**), in the central part of embryos, and in the columella below the root apical meristem (RAM) (**Figure 1H**). The size of the PSVs differed according to their localization. PSVs accumulated mainly in the upper parts of embryos (cotyledons, upper part of hypocotyl). Toward the root pole of the embryos, the size of PSVs enlarged; the largest ones occurred in cells of the root cap, usually in small numbers and often along with many tiny PSVs. Starch grains were distributed in a similar way as PSVs (**Figures 1C,E**); they accumulated mainly below the SAM and cotyledons, in the hypocotyl cortex (**Figure 1G**) and in cells of the root cap (**Figure 1C**). To a lesser extent, starch grains occurred in the cotyledons (**Figure 1F**), the central part of embryos, and in the columella (**Figure 1H**). Generally, the vacuolization of embryo cells was low and limited to cotyledons and/or the very upper region of the hypocotyl. No deposits were observed in the vacuoles. Cell divisions were observed in cells of the protoderm, cotyledons and procambium.

During prolonged maturation, the distribution of storage compounds in SEs did not change (**Figure 1I**). The accumulation of storage proteins increased greatly in cells of the cotyledons (**Figure 1J**). PSVs were abundant in both the hypocotyl cortex (**Figure 1K**) and the root cap (**Figure 1L**). Numerous starch grains persisted in all parts of the embryos (**Figures 1J–L**). Cell divisions were not observed.

In desiccated SEs, pronounced changes in the deposition of storage proteins and starch grains (**Figure 2B**) were found. The vacuolization of cells in the hypocotyl and cotyledons increased during the first two weeks (D2), and vacuoles enlarged further during the third week of desiccation (D3). Numerous PSVs were found inside these vacuoles in the cotyledons and hypocotyl. In the upper part of the hypocotyl below the cotyledons and below the apical meristem (SAM) (**Figure 2C**), mostly intact PSVs were located in the cytoplasm. In the lower parts of the hypocotyl (toward the root pole) of D2 embryos, mostly intact PSVs occurred in vacuoles (**Figure 2D**), whereas in D3 embryos, PSVs inside vacuoles exhibited different degrees of degradation (**Figures 2G,H**). This degradation of PSVs occurred in an ascending gradient toward the root pole. In the lower parts of the hypocotyl, intact PSVs were rare, but the vacuoles contained an amorphous substance that stained blue, which may have been the content of fused PSVs sequestered in the vacuoles (**Figures 2G,H**). Further toward the root meristem (RAM), PSVs showed a dispersed content (**Figure 2H**). Vacuolization or degradation/utilization of the PSV content was not observed in the cells of the root cap in D2 (**Figures 2E,F**), but in D3 root cap cells, almost no PSVs occurred (**Figure 2I**). Starch grains were found in all parts of the embryo bodies, where they accompanied storage proteins, e.g., below the SAM (**Figure 2C**), in the hypocotyl (**Figure 2D**), in the RAM and columella (**Figure 2E**), and in the root cap (**Figure 2F**). However, in comparison to M5, M7 and M8 embryos, the amount and size of starch grains decreased markedly during the first two weeks of desiccation. This trend continued during the third week of desiccation. Only rarely, starch grains were found in the hypocotyl (**Figures 2G,H**). In the root pole, starch grains occurred almost only in the central region of the columella and not in the pericolumn (**Figure 2I**). Cell divisions occurred in the protoderm, the procambium, below the SAM, in the RAM region (**Figure 2E**) and occasionally in the cotyledons in D2 embryos and more often in D3 embryos.

Fresh zygotic embryos had abundant PSVs throughout their cotyledons (**Figure 3C**) and hypocotyl (**Figures 3E,F**), but also in the SAM (**Figure 3C**), in the region of the RAM, procambium and columella (**Figure 3D**), and in cells of the root cap (**Figure 3G**). Numerous starch grains were found in all these tissues (**Figures 3C–G**). Numerous PSVs were also found in ZEd, e.g., in the SAM (**Figure 3H**) and cotyledons (**Figure 3I**), and tiny PSVs occurred in the columella (**Figure 3J**). In the hypocotyl, cells were highly vacuolated. PSVs merged in the upper part of the hypocotyl (toward the cotyledons) (**Figure 3K**) and were probably utilized. In the lower part of the hypocotyl, a higher extent of utilization of storage proteins was found (**Figure 3L**). Utilization of storage proteins also occurred in cells of the root cap (**Figure 3M**). Small starch grains were rarely found in the cotyledons (**Figure 3I**), hypocotyl (**Figures 3K,L**) and columella (**Figure 3J**).

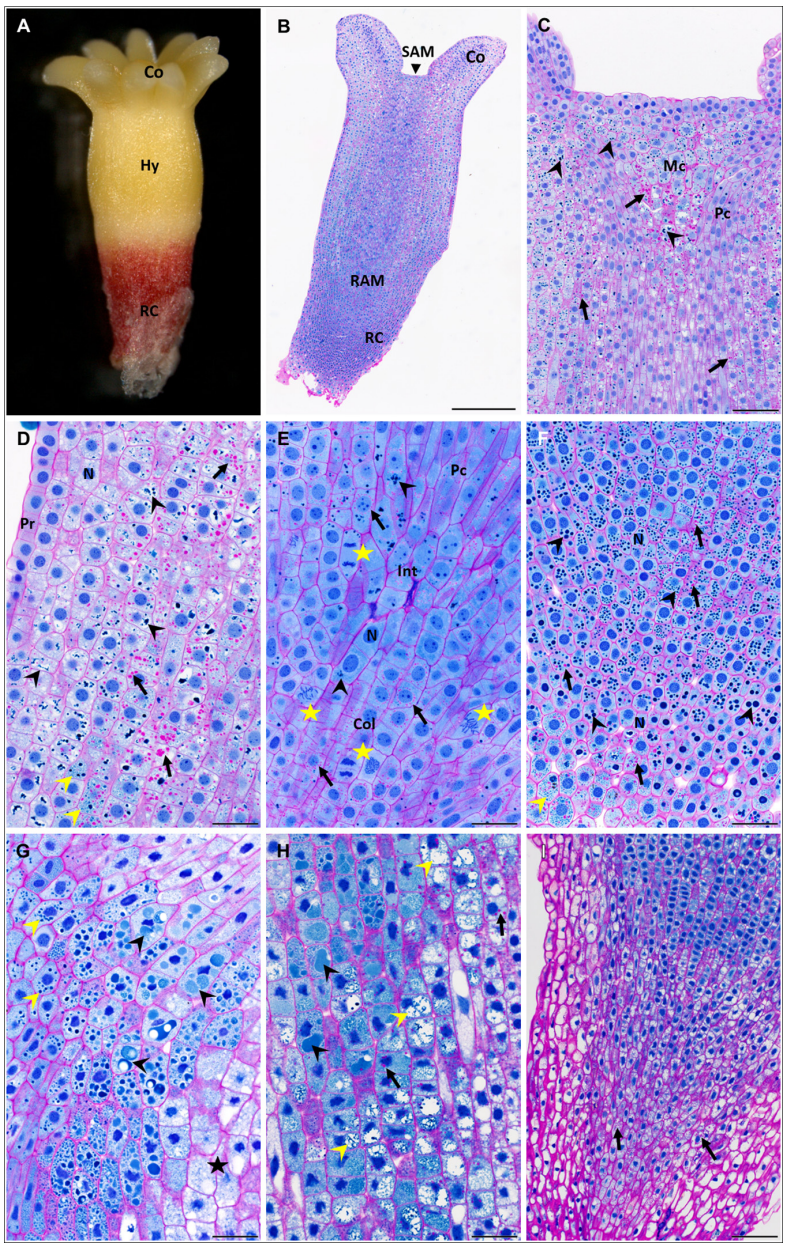

FIGURE 2 | Accumulation of storage compounds in somatic embryos (SEs) of *P. abies* after two and three weeks of desiccation. **(A–F)** Two weeks of desiccation (D2); **(G–I)** three weeks of desiccation (D3). **(A)** Morphology of a D2 embryo; note the red coloring of the root cap that was induced during desiccation in light. **(B)** Longitudinal section of a D2 embryo stained with PAS/amido black [polysaccharides in cell walls and starch grains stained magenta, proteins in nuclei and protein storage vacuoles (PSVs) stained blue]. **(C)** Detail of the shoot apex in panel **(B)**; starch grains (arrows) accumulated frequently in the region of central mother cells of the shoot meristem and in cortical cells but less in cells of the procambium; PSVs (arrowheads) were located similarly. **(D)** Detail of the hypocotyl cortex in panel **(B)**; starch grains occurred predominantly in deeper cortical cells than in sub-protodermal cells (arrows); individual PSVs occurred in the cytoplasm, but more often PSVs clustered and/or fused in vacuoles (black arrowheads); very tiny PSVs occurred in some cells (yellow arrowhead). **(E)** Detail of the root apical meristem in panel **(B)**; starch grains (arrows) often surrounded nuclei; PSVs were rare (arrowheads); note the frequent mitotic figures (stars) next to root initials and in the columella. **(F)** Detail of the root cap in panel **(B)**; starch grains were present in most root cap cells (arrows), but PSVs of different sizes predominated (black arrowheads); very tiny PSVs occurred in the distal region of the embryo (yellow arrowhead). **(G)** Detail of the hypocotyl cortex below the cotyledons of a D3 embryo; starch grains were very rare; intact individual PSVs were observed (yellow arrowheads) in cells located in the central pith of the embryo contrary to cells of the sub-protodermal region (star); in the cells in between, proteinaceous content occurred in large vacuoles as an amorphous material (black arrowheads). **(H)** Detail of the basal part of the hypocotyl cortex of a D3 embryo; starch grains were more abundant than below the cotyledons (arrows); individual PSVs disappeared, while the proteinaceous content occurred in large vacuoles as an amorphous (black arrowheads) or dispersed material (yellow arrowheads). **(I)** Root cap of a D3 embryo was free of PSVs, starch grains occurred only in the central part (arrows). Co, cotyledons; Col, columella; Hy, hypocotyl; Int, root initials; Mc, mother cells of the shoot meristem; N, nucleus; Pc, procambium; Pr, protoderm; RAM, root apical meristem; RC, root cap; SAM, shoot apical meristem. Scale bars represent: 500 μm in panel **(B)**; 100 μm in panels **(C,I)**; 50 μm in panels **(D–H)**.

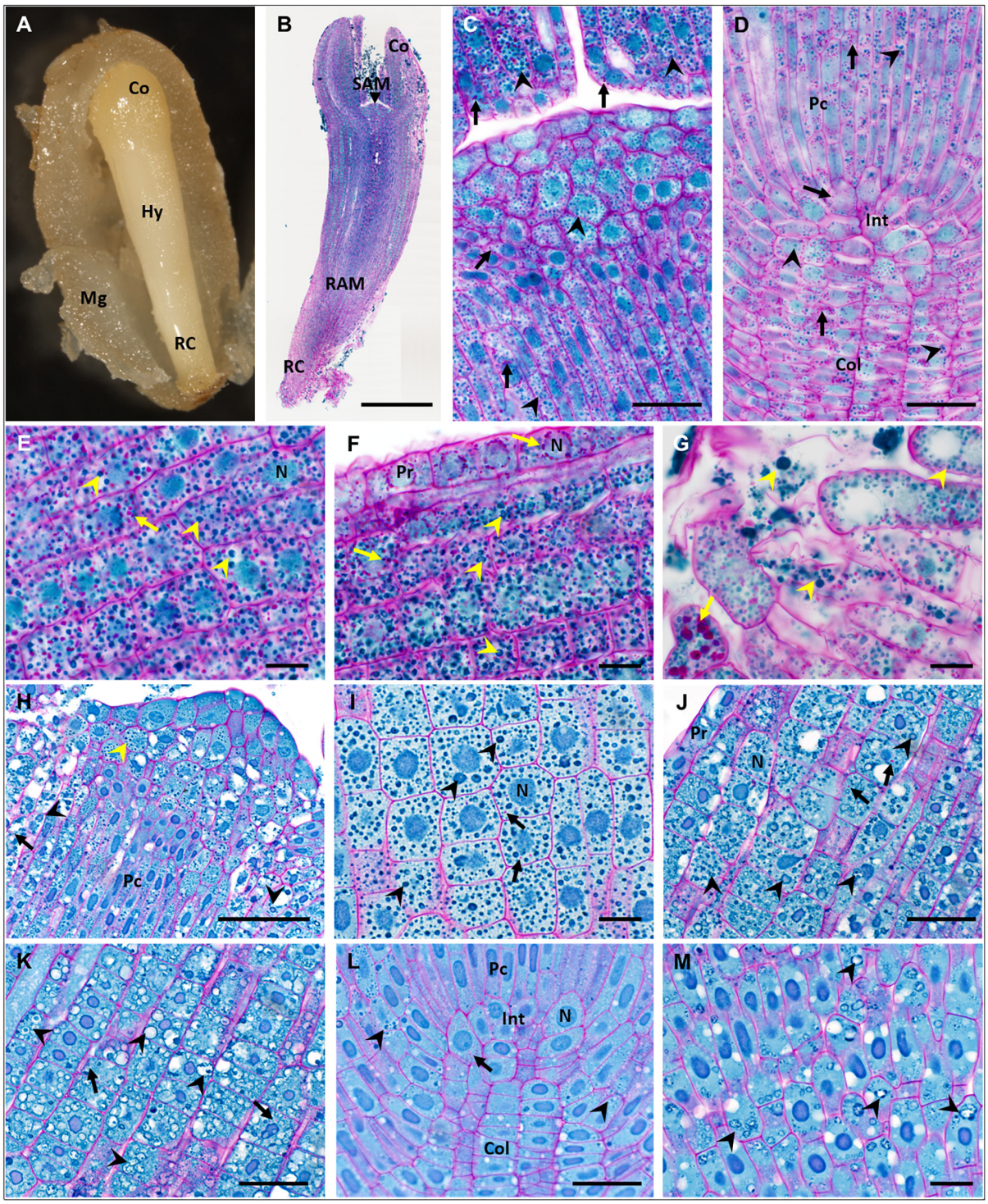

FIGURE 3 | Accumulation of storage compounds in fresh and dry zygotic embryos (ZEs) of *P. abies*. **(A–G)** fresh ZE (ZEf); **(H–M)** dry ZE (ZEd). **(A)** Morphology of a ZEf in a megagametophyte. **(B)** Longitudinal paraffin section of a ZEf stained with PAS/amido black (polysaccharides in cell walls and starch grains stained magenta, proteins in nuclei and protein storage vacuoles (PSVs) stained blue). **(C)** Detail of the shoot apical meristem and part of the cotyledons in panel **(B)**; starch grains (arrows) and PSVs (arrowheads) were abundant in all types of cells. **(D)** Detail of the root apical meristem in panel **(B)**; numerous starch grains (arrows) and PSVs (arrowheads) occurred in all cells of the procambium, root initials and columella. **(E)** Detail of the hypocotyl cortex in panel **(B)** proximal to cotyledons; numerous starch grains (arrows) and intact PSVs (arrowheads) occurred in all cells. **(F)** Detail of protodermal and cortical cells of the basal part of the hypocotyl in panel **(B)**; numerous starch grains (arrows) and PSVs (arrowheads) occurred in all cortical cells; starch grains surrounded nuclei in protoderm. **(G)** Detail of the most distal cells

(Continued)

FIGURE 3 | of the root cap in panel **(B)**; starch grains (arrows) and PSVs (arrowheads) of different sizes filled all cells. **(H)** Detail of the shoot apical meristem of a ZEd resin longitudinal section; compact PSVs (yellow arrowhead) occurred in apical and subapical vacuolated cells and in the procambium, whereas in vacuolated cells below cotyledons on both sides of the image, PSVs fused to larger vacuoles with amorphous proteinaceous content (black arrowheads). **(I)** Detail of cells in a ZEd cotyledon; PSVs (arrowheads) predominated over rare tiny starch grains (arrows). **(J)** Detail of protodermal and cortical cells in the apical part of the ZEd hypocotyl; numerous PSVs (arrowheads) of different sizes and proteinaceous content (amorphous or dispersed in fused PSVs) predominated over the rare, tiny starch grains (arrows). **(K)** Detail of cortical cells in the basal part of the ZEd hypocotyl; numerous swollen PSVs (arrowheads) almost free of proteinaceous content predominated over the rare, tiny starch grains (arrows). **(L)** Detail of the root apical meristem of ZEd; only very rare starch grains (arrow) and PSVs (arrowheads) occurred in the cells of the procambium, root initials and columella. **(M)** Detail of the root cap cells of ZEd; only PSVs with dispersed proteinaceous content (arrowheads) were observed. Co, cotyledons; Col, columella; Hy, hypocotyl; Int, root initials; Mg, megagametophyte; N, nucleus; Pc, procambium; Pr, protoderm; RAM, root apical meristem; RC, root cap; SAM, shoot apical meristem. Scale bars: **(B)** 500 μm; **(C,D,J–L)** 50 μm; **(H)** 100 μm; **(E–G,I,M)** 20 μm.

Protein Analysis

No change in protein content was found when SEs were kept on the maturation medium during prolonged maturation (M5 versus M7 and M8 embryos). Desiccation induced a decrease in protein content in D2 and D3 embryos in comparison to M5 embryos (**Table 1**). The protein content in the ZEs was higher than in all stages of SEs. The treatment effect was significant with a P value $< 2.05 \times 10^{-06}$. Electrophoresis profile analysis of total protein extracts was performed as a qualitative assay of SE protein content (**Figure 4**). Two or three weeks of desiccation did not induce any change in the protein profile in the detected bands and their intensity. In contrast, the intensities of some bands increased in ZEs as well as in M8 embryos. These bands corresponded to storage proteins identified by mass spectrometry as cruciferina (also called 7S-globulin), cruciferin (11S-globulin) and 2S albumin. They also corresponded to the major bands in the megagametophyte.

Non-structural Carbohydrate Analysis

During prolonged maturation, starch levels in SEs remained high. The starch content in M7 embryos was comparable to that in M5 embryos but increased significantly a week later (M8). However, the starch content differed significantly in desiccated embryos. Desiccation treatment led to a marked decrease (to about 1/3 of the value of M5 embryos) of starch content compared to that detected in D2 and D3. Similarly low content of starch was found in ZEd (**Figure 5A**).

M5 embryos contained high amounts of sucrose together with low content of hexoses (with fructose being more abundant than glucose). Prolonged maturation did not lead to significant changes in the carbohydrate spectrum, which exhibited only a slight increase in total soluble carbohydrates (M8). This was in sharp contrast to D2 and D3, where the total carbohydrate content was reduced. The proportion of monosaccharides was very low compared to the proportion of disaccharide sucrose. In D2 and D3, newly emerged RFOs, i.e., raffinose and stachyose, and galactinol (an intermediate of RFO synthesis) were detected. In D3 embryos, RFOs represented more than 23% of the total soluble carbohydrates and the proportion of RFOs to sucrose (R/S ratio) was 0.37. Sucrose contributed the main part of the spectrum in all SE samples under study. Embryos also contained inositol in their carbohydrate spectra (**Figure 5B**).

The corresponding characteristics were followed in fully developed isolated ZEd. The soluble saccharide spectrum comprised RFOs and sucrose as the prevailing constituents (together accounting for approx. 92% of total soluble saccharides, R/S ratio = 1.43), and hexoses (with glucose being more abundant than fructose) and inositol as minor constituents (**Figure 5B**). Traces of galactose were identified in the spectrum of ZEd (see **Supplementary Table 1**).

TABLE 1 | Quantitative analysis of total proteins in somatic embryos after five weeks of maturation (M5), two (M7) and three weeks (M8) of prolonged maturation, and after two (D2) and three (D3) weeks of desiccation compared to cotyledonary fresh ZEs.

Samples	Total protein content (μg.mg-1 FW)
M5	126.0 ± 4.9^{ab}
M7	114.2 ± 13.0^{a}
M8	111.4 ± 16^{a}
D2	96.8 ± 7.5^{a}
D3	94.0 ± 4.3^{a}
ZE	146.0 ± 7.0^{b}

Values are means of three biological repetitions ± SE.
Significant differences at $P < 0.05$ are indicated in different letters.

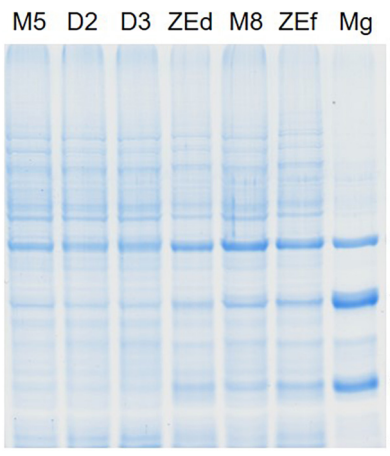

FIGURE 4 | Representative SDS-PAGE total protein profile comparison in somatic (SEs) and zygotic (ZEs) embryos of *P. abies*. The location of major storage proteins identified by mass spectrometry in SEs, dry ZEs and the megagametophyte (Mg) in the protein pattern is shown by arrows. Line M5 – SEs after 5 weeks of maturation, line M8 – SEs after 8 weeks of prolonged maturation, line D2 – SEs after 2 weeks of desiccation, line D3 – SEs after 3 weeks of desiccation, line ZEd – dry ZE, ZEf – fresh ZE, Mg – megagametophyte.

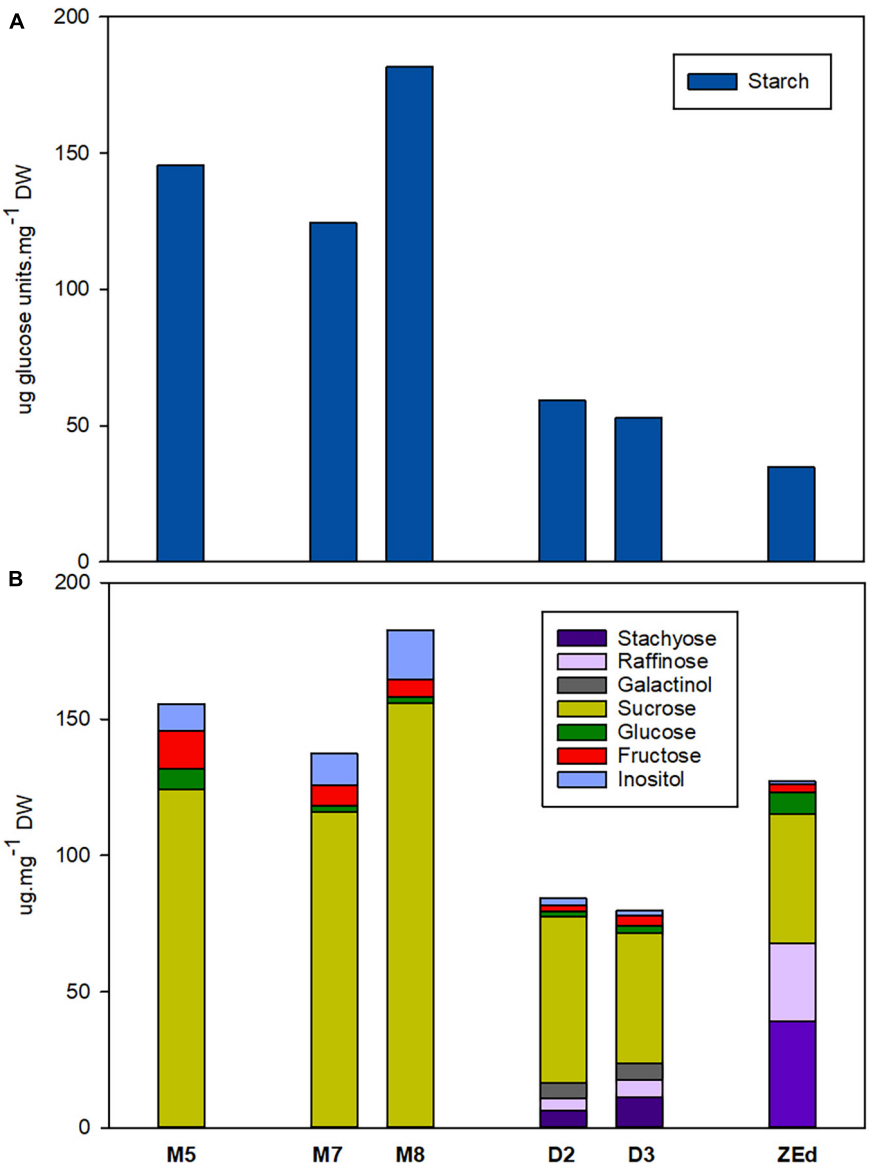

FIGURE 5 | Endogenous non-structural carbohydrates in *P. abies* somatic (SEs) and zygotic (ZEs) embryos. **(A)** Starch content (expressed as glucose amount after enzymatic starch cleavage); **(B)** Soluble carbohydrate content and spectrum. M5 – mature SEs after 5 weeks of maturation, M7 and M8 – SEs after 7 and 8 weeks of prolonged maturation, D2 and D3 – SEs after 2 and 3 weeks of desiccation, ZEd – dry ZEs; *n* = 4–6. Components of carbohydrate spectrum that accounted for less than 1% of the total carbohydrates are included only in **Supplementary Table 1**.

Phytohormone Analysis

Abscisic Acid and Its Derivatives

M5 embryos contained relatively high levels of ABA and its derivatives (approx. 630 000 pmol/g DW), which reflected the addition of exogenous ABA to the liquid maturation medium. Despite that, a significant reduction of endogenous ABA content in embryos occurred during prolonged maturation. After three weeks of prolonged maturation (M8), levels of ABA reached 51% of the concentration detected in M5 embryos. The content of ABA derivatives was relatively low (in comparison to the concentration of ABA itself). DPA, PA and ABA-GE detected in M5 embryos were also found after prolonged maturation. Compared to M5 embryos, DPA and PA levels decreased significantly during prolonged maturation (M8) to 66 and 58%, respectively. In contrast, a significant increase in ABA-GE content was recorded in M8. An even greater decrease in ABA levels was detected in desiccated embryos. At the end of desiccation (D3), levels of ABA had dropped significantly to 27% of its M5 concentration. PA, DPA and other ABA derivatives (NeoPA, 9OH-ABA) were present in minute amounts in desiccated embryos, not exceeding 4% of their respective values in M5. In contrast, the ABA-GE content in embryos at the end of desiccation was comparable to the values found in M5 embryos.

In ZEd, the content of ABA and its derivatives was significantly lower than in all analyzed SEs (approx. 1540 pmol/g of DW). Their spectrum was similar to that of M5 embryos, with a predominance of ABA (more than 80%) and lower abundances of DPA (8%), PA (5%) and ABA-GE (5%) (**Figure 6**).

Auxins

The total content of auxins in SEs was relatively low, reaching about 2,000 pmol/g DW in M5 embryos. During prolonged maturation, the total content of auxins in embryos did not change, but the ratio between particular auxin derivatives differed considerably. After three weeks of prolonged maturation (M8), levels of IAA in the embryos decreased significantly to 47% of the value detected in M5 embryos. In contrast, a substantial increase in the concentrations of IAA amino acid conjugates, such as IAA-Asp (262%) and IAA-Glu (237%), was observed in M8. Interestingly, the prolonged maturation did not cause any apparent changes in the levels of Ox-IAA, the major IAA catabolite, and the non-indole phenolic auxin PAA. In desiccated embryos, enhancement of the total auxin content was recorded from the second to the third week of desiccation. This enhancement in D3 was due to considerably higher concentrations of IAA-Asp (216%), Ox-IAA (321%) and PAA (162%) compared to M5 embryos. On the other hand, the IAA content significantly decreased in desiccated embryos (to 80%).

In ZEd, the concentration of auxins was significantly lower than in SEs (ca. 390 pmol/g DW). The most substantially decreased levels compared to those of M5 embryos were recorded for IAA (17-fold) and PAA (10-fold). In contrast, the decrease was only ca. 1.5 to 3-fold for IAA-Asp and Ox-IAA, respectively, representing the prevailing auxin derivatives in ZEd (**Figure 7**).

Cytokinins

The total content of CKs (**Figure 8**) was relatively low in M5 embryos, not exceeding 850 pmol/g DW. In total, 16 isoprenoid CK derivatives were detected in M5 embryos, including free bases (bioactive forms), ribosides (transport forms), *O*-glucosides (storage forms) and phosphates (immediate biosynthetic precursors). Whereas *O*-glucosides and phosphates represented the predominant forms of CKs (approx. 85% of total CK pool), interestingly, no *N*-glucosides were found in SEs. The content and composition of CKs remained conserved during prolonged maturation. In contrast, a significant increase in CK levels was observed during desiccation. The total CK content in embryos desiccated for 2 and 3 weeks was more than three times higher (approx. 2890 and 2560 pmol/g DW, respectively) compared to M5 embryos. This enhancement was especially caused by an increase (more than 4.5-fold) of *O*-glucoside concentration.

The total CK pool in SEs was composed of *trans*Z (5 forms), *cis*Z, DHZ (4 forms both) and iP (3 forms), and the proportion of each particular group was characterized separately (**Figure 9**). Generally, DHZ- and *cis*Z-type CKs prevailed in M5 embryos as well as during prolonged maturation, with concentrations ranging from 260-380 and 250-505 pmol/g DW, respectively. During desiccation, levels of DHZ- and *cis*Z-types increased substantially compared to those in M5 embryos, primarily due to the enhanced accumulation of DHZROG and *cis*ZROG. Similarly, increased concentrations in desiccated embryos (approx. 40 pmol/g of DW) compared to M5 embryos (approx. 25 pmol/g of DW) were found for *trans*Z-type CKs, representing the least abundant CK forms. In contrast, levels of iP and its derivatives were not much affected by the desiccation

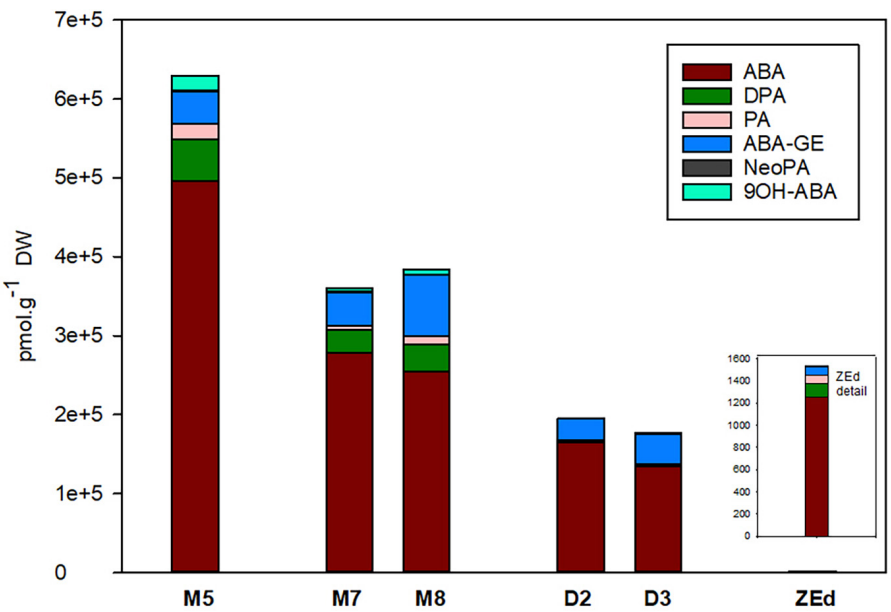

FIGURE 6 | Content of ABA and its derivatives in *P. abies* somatic (SEs) and zygotic (ZEs) embryos. M5 – mature SEs after 5 weeks of maturation, M7 and M8 – SEs after 7 and 8 weeks of prolonged maturation, D2 and D3 – SEs after 2 and 3 weeks of desiccation, ZEd – dry ZEs. ABA, abscisic acid; ABA-GE, ABA-glucosylester; PA, phaseic acid; DPA, dihydrophaseic acid; NeoPA, neophaseic acid; 9OH-ABA, 9-hydroxy-ABA.

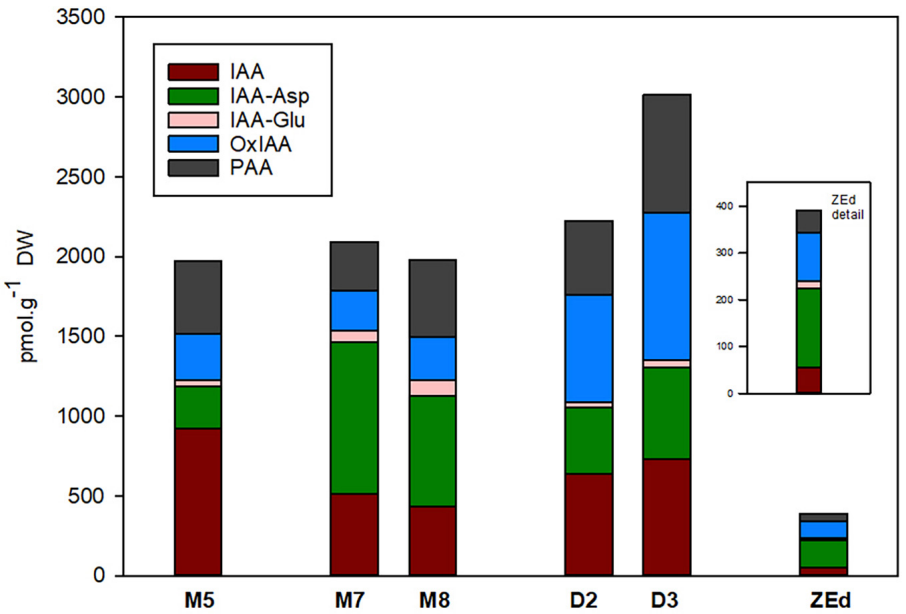

FIGURE 7 | Content of auxins and their derivatives in *P. abies* somatic (SEs) and zygotic (ZEs) embryos. M5 – mature SEs after 5 weeks of maturation, M7 and M8 – SEs after 7 and 8 weeks of prolonged maturation, D2 and D3 – SEs after 2 and 3 weeks of desiccation, ZEd – dry ZEs. IAA, indole-3-acetic acid; IAA-Asp, IAA-aspartate; IAA-Glu, IAA-glutamate; OxIAA, oxo-IAA; PAA, phenylacetic acid.

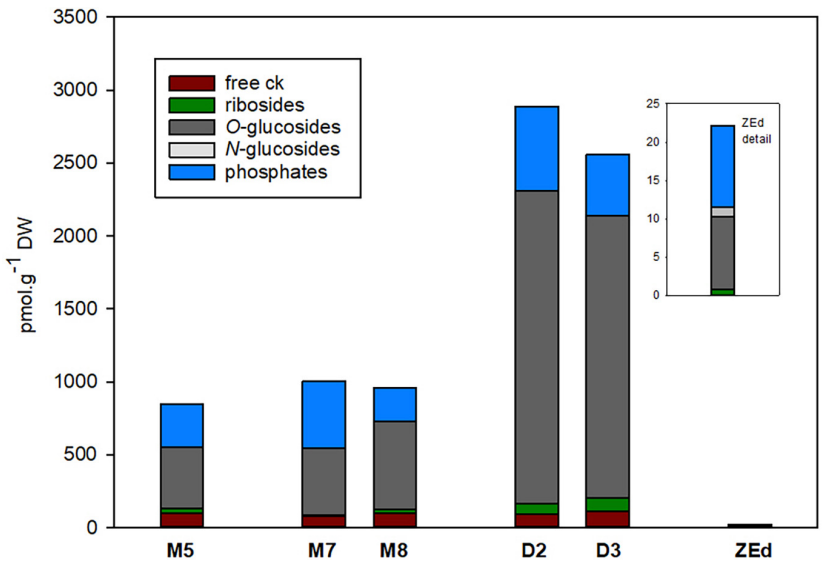

FIGURE 8 | Total content of cytokinin forms in *P. abies* somatic (SEs) and zygotic (ZEs) embryos. M5 – mature SEs after 5 weeks of maturation, M7 and M8 – SEs after 7 and 8 weeks of prolonged maturation, D2 and D3 – SEs after 2 and 3 weeks of desiccation, ZEd – dry ZEs.

step and fluctuated near 200 pmol/g DW in both M5 and desiccated embryos.

The total pool of CKs in ZEd was significantly lower than in SEs (e.g., approx. 38-fold compared to M5 embryos). The CK spectrum was analogous to M5 and desiccated embryos, with *O*-glucosides and phosphates representing the dominant CK forms (42% and 48% of the total CK pool, respectively). Interestingly, in contrast to SEs, *N*-glucosides were detected in ZEd, although in relatively low quantities not exceeding 6% of the total CK pool (**Figures 8**, **9**). Among *N*-glucosides, only those glycosylated at the *N9* but not the *N7* position were found.

Multivariate Analysis

To assess the variation between embryo samples, we performed principal component analysis (PCA) using available biochemical variables (levels of fructose, glucose, inositol, raffinose, stachyose,

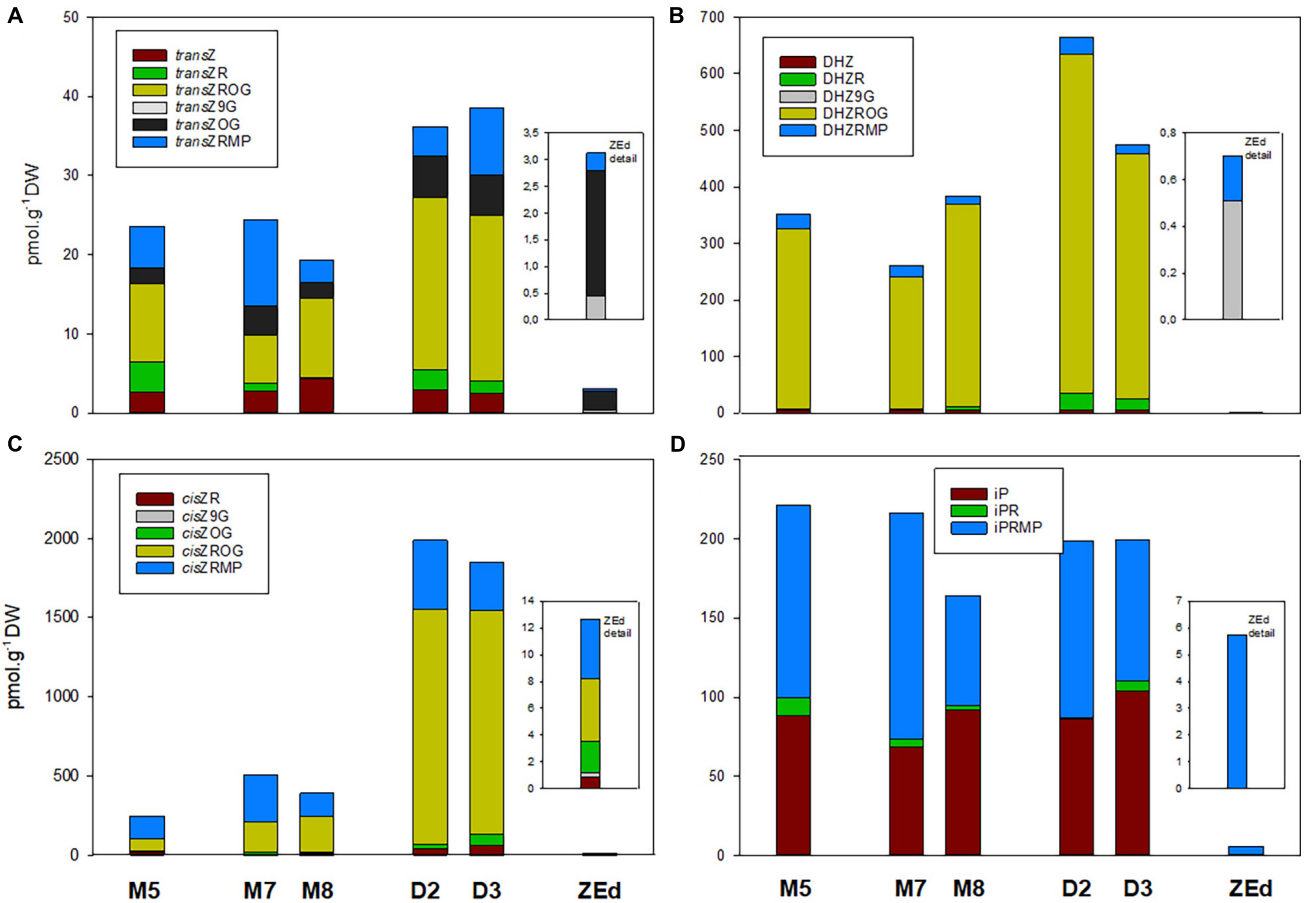

FIGURE 9 | Content of individual cytokinins and their derivatives in *P. abies* somatic (SEs) and zygotic (ZEs) embryos. **(A)** *Trans*-zeatin types: *trans*Z, *trans*-zeatin; *trans*ZR, *trans*-zeatin 9-riboside; *trans*ZOG, *trans*-zeatin *O*-glucoside; *trans*ZROG, *trans*-zeatin 9-riboside *O*-glucoside; *transZRMP*, *trans*-zeatin 9-riboside-5′-monophosphate. **(B)** Dihydrozeatin types: DHZ, dihydrozeatin; DHZR, dihydrozeatin 9-riboside; DHZ9G, dihydrozeatin-9-glucoside; DHZROG, dihydrozeatin 9-riboside *O*-glucoside; DHZRMP, dihydrozeatin 9-riboside-5′-monophosphate. **(C)** *Cis*-zeatin types: *cis*ZR, *cis*-zeatin 9-riboside; *cis*ZOG, *cis*-zeatin *O*-glucoside; *cis*Z9G, *cis*-zeatin 9-glucoside; *cis*ZROG, *cis*-zeatin 9-riboside *O*-glucoside; *cis*ZRMP, *cis*-zeatin 9-riboside-5′-monophosphate. **(D)** N^6-(Δ^2-isopentenyl) adenine types: iP, N^6-(Δ^2-isopentenyl) adenine**;** iPR, N^6-(Δ^2-isopentenyl) adenosine; iPRMP, N^6-(Δ^2-isopentenyl) adenosine-5′-monophosphate. M5 – mature SEs after 5 weeks of maturation, M7 and M8 – SEs after 7 and 8 weeks of prolonged maturation, D2 and D3 – SEs after 2 and 3 weeks of desiccation, ZEd – dry ZEs.

starch, sucrose, protein, ABAs, IAAs, CKs). The plane formed by the first two main components (Dim 1 and Dim 2, **Figure 10A**) showed good separation of the samples according to their type. Dim 1 explained almost 60% of the variance between samples. According to the correlation circle (**Figure 10B**), which represents the correlation between the first two main components and the biochemical characteristics of the samples, the content of ABAs and proteins was strongly correlated with Dim 1, whereas the content of raffinose and stachyose contributed negatively. Whether the correlation was positive or negative, the biochemical variables most involved in this sample type clustering were ABAs, raffinose, stachyose, then proteins. The proximity between the raffinose and stachyose vectors, of equivalent length, indicated a high degree of association between these two variables. CKs and IAAs did not participate in Dim 1 only in Dim 2, which explained 28.1% of the variance between samples. Dim 2 contributed to the separation of the ZE and desiccated SE stages (**Figure 10A**). The relative and absolute contributions of the biochemical variables to the main components are given in **Supplementary Table 3**.

Proteomic Studies

A proteomic study was carried out to (1) define the degree of similarity between M5 embryos and ZEf (comparison M5-ZEf), and (2) to understand the effect of desiccation treatment on protein profile comparing M5 embryos with D3 embryos (comparison M5-D3).

Approximately 970 individual protein spots on three replicate gels were detected for each M5, ZEf and D3 embryo. These proteins were present for each type of sample. Among them, only 224 were significantly different ($P < 0.05$, ratio between normalized spot abundances of ≥ 2), with 169 and 91 in the M5-ZEf and M5-D3 comparisons, respectively (**Table 2**). Some proteins had significantly different abundances in both comparisons. Almost all of them were more abundant (8

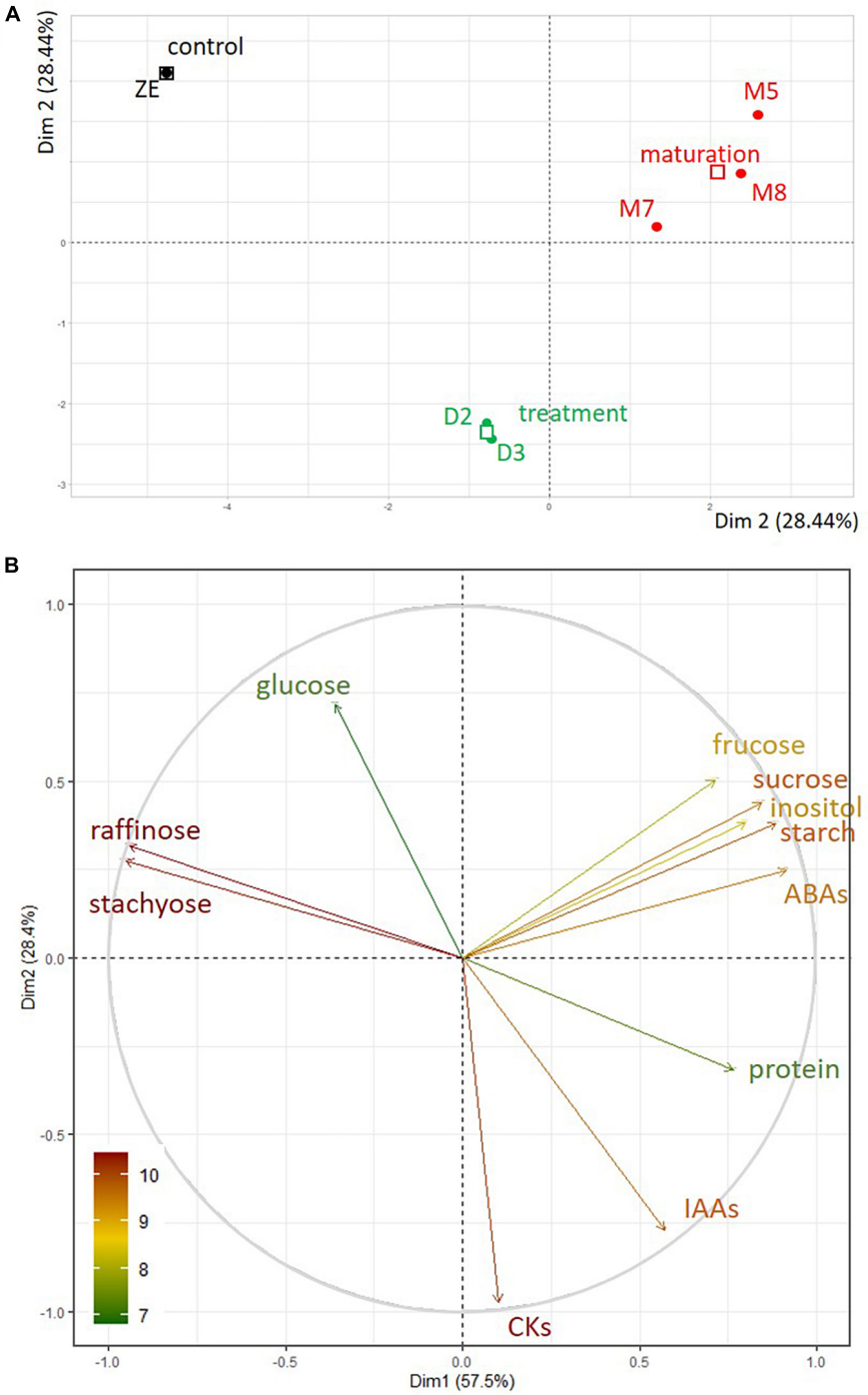

FIGURE 10 | (A) PCA of somatic embryos maturing during five (M5) or eight (M8) weeks or desiccated during two (D2) or three (D3) weeks, and dry zygotic embryos (ZE) according to their biochemical dataset (stachyose, raffinose, sucrose, glucose, fructose, inositol, starch, protein, ABAs, IAAs, CKs), in the factorial plan Dim 1 - Dim 2. **(B)** Correlation circle between the biochemical variables in the PCA of the samples in the factorial plan Dim 1 - Dim 2. The contribution of the biochemical variables is represented by the color of their respective vector.

proteins, **Table 2**) or less abundant (28 proteins, **Table 2**) in M5 embryos than in the other type of samples, indicating that M5 embryos were very different from ZEf and to a lesser extent from desiccated SEs. PCA, which clearly separated the samples according to the abundance of significant proteins (**Supplementary Figure 1**), indicated D3 had a medium composition between the M5 and ZEf proteomes in Dim 1 (64.5% of the explained variance). The proteins were identified by mass

TABLE 2 | Distribution of 224 significant proteins identified in the two proteomic comparisons between cotyledonary somatic embryos matured for five weeks (M5) and fresh cotyledonary zygotic embryos (M5-ZE) or between M5 embryos before and after three weeks of desiccation (M5-D3), in the function of the overexpression ways.

			Comparison M5-ZE(169 sign.[a] proteins)	
			M5 < ZE[b]	M5 > ZE[b]
Comparison M5-D3 (91 sign.[a]. proteins)		protein number[c]	116	53
	M5 < D3[b]	54	28	0
	M5 > D3[b]	37	1	8

[a]*sign.: significant;* [b]*x > y: proteins more abundant in x than in y and vice versa,* [c]*number of unique proteins identified in the two analyses.*

spectrometry. The level of abundance of each significant protein was compared according to the type of sample (**Supplementary Table 4**). It appeared that the most abundant proteins in M5 embryos in the comparison 'M5-D3' were also more abundant in the comparison 'M5-ZEf'. Similarly, the proteins which became more abundant during SE desiccation (in D3) were also more abundant in ZEf than in M5 embryos.

Functional annotation of the 224 proteins was performed according to the gene ontology classification system using homologous proteins in *Arabidopsis thaliana*. In this classification, a gene ontology (GO) term for molecular functions or biological processes is not attributed to every protein. In order to consider every protein, we manually adapted this classification by introducing two additional categories: "stored energy" and "desiccation protein", corresponding to the parent molecular functions of the concerned proteins. The fold changes of protein abundance and molecular functions and biological processes assigned to the significant proteins are indicated in **Supplementary Table 5**.

Molecular functions of the proteins over- or under-expressed in ZEf were the same as those found in D3 (**Figure 11A**). Stress or desiccation response proteins, proteins with catalytic or nutrient reservoir activities, and storage proteins were amplified in D3 embryos and ZEf. Almost no molecular function was amplified in M5 embryos compared to samples D3 and ZEf. Only the function of stabilization was reduced in D3 and ZEf compared to M5 embryos.

The same biological processes were found to be activated in ZEf as in D3 embryos when compared to M5 embryos, according to the pattern observed at the scale of the modified molecular functions (**Figure 11B**).

Thus, the proteomes of ZEf and D3 embryos were more involved than that of M5 embryos in the "acquisition of desiccation tolerance", "generation of precursor metabolites and energy", "metabolic process", "response to stress", "response to stimulus" and "stored energy" processes. This last category included the most abundant proteins, which were cupin family storage proteins cruciferina and cruciferin 3. Only the biological process "protein metabolic process" was more active in ZEf than M5 embryos, whereas it was equivalent in M5 and D3 embryos.

DISCUSSION

For several conifers, including Norway spruce, it has been reported that conversion of embryos to plantlets can be improved by applying a desiccation period to aid reaching "physiological maturity" and positively influence germination (Stasolla and Yeung, 2003; Maruyama and Hosoi, 2012; Hazubska-Przybyl et al., 2015; Liao and Juan, 2015). In our previous experiments, embryos of the line AFO 541 cultivated without desiccation treatment were not able to develop radicles. 60–80% of embryos germinated after three weeks of desiccation, in contrast to only 20% of embryos that germinated without desiccation treatment. Non-completed emblings could not be transferred to *ex vitro* systems (Vondráková et al., 2013).

Our new analyses in the present study, using the same line AFO 541, provide a set of structural and biochemical parameters before (M5), after (D2-D3) or without (M8) desiccation treatment and show unambiguous effects of the desiccation phase in comparison with prolonged maturation. We demonstrated that the desiccation phase induces molecular and biological shifts that are not triggered by prolonged maturation. These modifications seem to correspond to the usual late maturation events that occur in most seeds (Angelovici et al., 2010; Leprince et al., 2017), including conifer seeds (Carrier et al., 1999; Silveira et al., 2004; Balbuena et al., 2011). Prolonged maturation resulted in callus formation on the surface of most embryos. The onset of callogenesis was detected after only six weeks of maturation (Eliášová et al., 2018). Callus never formed on desiccated embryos. Our comparison of SEs and ZEs showed some similarities (to a certain extent) in storage proteins and non-structural carbohydrates changes. The proteomic analysis confirmed these similarities. Biological processes activated in D3 embryos were the same as those activated in ZEf when both were compared to M5 embryos. These changes were consistent with data from previous studies (e.g., Hazubska-Przybyl et al., 2015; Liao and Juan, 2015). In contrast, the results of the phytohormone analysis indicated quantitative differences between SEs and ZEd.

Modifications of Storage Compound Levels

Storage reserves may help an embryo to tolerate desiccation by increasing the dry weight (Attree et al., 1995; Pérez et al., 2020). They are used as sources of energy and amino acids during seedling germination and growth until autotrophy is acquired. Their quantity (Kong et al., 1999) and quality are important variables dictating the future vigor of the seedling. Storage reserves are gradually produced to varying degrees at different stages of development. Joy et al. (1991) reported

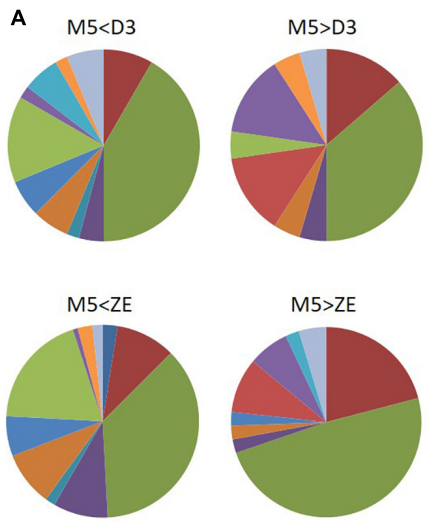

A	M5<D3	M5>D3	M5<ZE	M5>ZE
antioxidant activity	0	0	3	0
binding	4	3	12	9
catalytic activity	20	8	45	21
dessiccation protein	2	1	11	1
enzyme regulator activity	1	0	2	0
nutritient reservoir activity	3	1	11	1
response to stress	3	0	8	1
stabilisation	0	3	0	4
storage protein	7	1	23	0
structural molecule activity	1	3	1	3
translation regulator activity	3	0	0	1
transporter activity	1	1	3	0
undefined	3	1	2	2

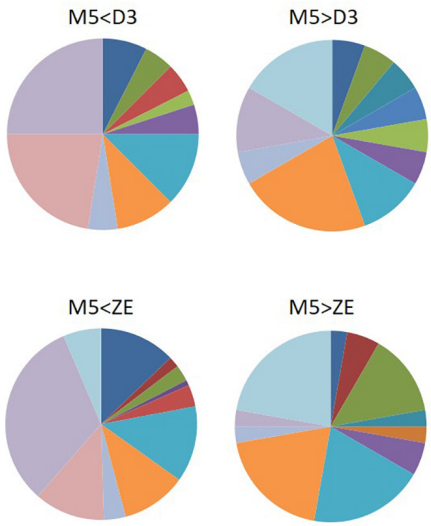

B	M5<D3	M5>D3	M5<ZE	M5>ZE
acquisition of desiccation tolerance	2	1	14	1
apoptotic process	0	0	2	2
carbohydrate metabolic process	2	1	3	5
catabolic process	0	0	1	0
cellular amino acid metabolic process	0	1	0	1
coenzyme metabolic process	0	0	0	1
cytokinesis = cellular process	0	1	0	0
generation of precursor metabolites & energy	2	0	4	0
intracellular transport	1	1	0	0
lipid metabolic process	2	1	0	2
metabolic process	5	2	14	7
protein metabolic process	4	4	12	7
response to stimulus	2	1	4	1
response to stress	9	0	13	0
seed maturation process	1	0	0	0
stored energy	10	2	35	1
undefined or others	0	3	7	8

FIGURE 11 | Gene ontology analysis of differentially expressed proteins. **(A)** Molecular function of the differentially abundant proteins between mature SEs (M5) and fresh ZEs or SEs after three weeks of desiccation (D3). **(B)** Biological processes modified by the differentially abundant proteins between the proteomes of M5 and fresh ZE, or of M5 and D3. On the left side of the figure, the colors represent the percentages of proteins involved in the indicated molecular function or biological process, whereas on the right side of the figure, the tables indicate the numbers of corresponding proteins. M5 > ZE and M5 > D3: proteins overexpressed in M5 in comparison to ZE or D3; M5 < ZE and M5 < D3: proteins overexpressed in ZE and D3, respectively.

that starch accumulated first, followed by lipids and proteins during later maturation stages of white spruce. Compared to mature ZEd of white spruce or ZEf of maritime pine (Tereso et al., 2007), SEs of both these species accumulated more starch. However, the cotyledonary ZEf of maritime pine showed numerous starch grains, in contrast to the ZEd of white spruce. In Norway spruce, we detected a high amount of starch grains in M5 embryos, which decreased during the first two weeks of prolonged maturation. The comparison we made with ZEf at the histological level (**Figure 3**) revealed an accumulation of starch grains comparable to that of M5 embryos. Longer cultivation of SEs on the maturation medium resulted in significantly higher starch accumulation, which could be ascribed to ectopic starch grain accumulation in M8 embryos that often suffered from morphological abnormalities and callogenesis. On the contrary, the desiccation treatment caused a substantial reduction in the starch content, which approached a very low level in ZEd. The biochemical determination generally confirmed our analysis based on histochemical evidence. These results indicate that starch represents a transient energy source in both SEs and ZEs. Most importantly, they imply the preparation of the embryos in a dry state, where the starch content is low after conversion into

sugars such as sucrose and RFOs, which helps to prevent lethal effects of water stress (Yathisha et al., 2020).

In conifers, proteins make an important contribution to the energy reserves of seeds and embryos. Our results showed that the protein content at the end of maturation was very similar to that already reported in *P. abies* by Businge et al. (2013). However, it was lower than in ZEf, indicating that the somatic embryogenesis protocol does not provide embryos with protein energy reserves equivalent to those present in ZEf. This phenomenon has been widely observed in the somatic embryogenesis of conifers (Klimaszewska et al., 2004; Businge et al., 2013). Desiccation, during which SEs are no longer provided with nutrients, causes a small drop in protein content in embryos, whose maintenance of respiration and minimum metabolism consume storage compounds, as shown by the degradation of PSVs in D3 embryos (**Figure 2**). Although a slight decrease in protein content was also observed in SEs whose maturation was extended to eight weeks (samples M8), this must indicate another phenomenon. We interpreted the decline as going beyond the late maturation stage, during which energy reserves accumulate (Leprince et al., 2017) and engaging in the germination process, as has already been described for *Pinus sylvestris* SEs (Lelu-Walter et al., 2008). Qualitatively, the same protein profiles were obtained for mature and desiccated SEs as for ZEs. More intense bands corresponding to reserve proteins have already been identified in *P. abies* (Hakman et al., 1990; Businge et al., 2013), although they were not localized on the gel, unlike in our study. These corresponded to ubiquitous storage proteins (vicilin- and legumin-like globulins) in plants that have already been identified for many conifers, e.g., maritime pine (Morel et al., 2014) and larch (Teyssier et al., 2014). Lara-Chavez et al. (2012) observed an increase in transcripts encoding the legumin- and vicilin-like proteins at the end of maturation, but these proteins may be expressed only later if the conditions are favorable (Leprince et al., 2017). This is consistent with our findings of the increased storage proteins production in D3 embryos compared to M5.

Soluble Carbohydrate Profile of Desiccated Somatic Embryos Resembles the Profile of Zygotic Embryos

M5 embryos have a typical carbohydrate spectrum with a high sucrose:hexose ratio. A very similar robust pattern was described earlier in the same line (Lipavska et al., 2000) and also in another highly embryogenic *P. abies* line (Hudec et al., 2016) or *P. glauca* and *P. mariana* lines (Iraqi and Tremblay, 2001). In contrast to prolonged maturation, during desiccation, remarkable changes in the amount and spectrum of soluble carbohydrates were induced in SEs. Most importantly, desiccation induced the synthesis of RFOs, which have been reported to be a substantial component of mature conifer ZEs (e.g., Downie and Bewley, 2000; Gösslová et al., 2001; Konradova et al., 2003; Pullman and Buchanan, 2008). During somatic embryogenesis, it has been shown in some species that RFOs accumulate as early as during maturation (Carpenter et al., 2000; Morel et al., 2014). In Norway spruce SEs, their accumulation is associated with the effect of post-maturation treatments, e.g., fast desiccation (Bomal et al., 2002), high humidity desiccation (Konradova et al., 2003; Kubes et al., 2014; Hudec et al., 2016) or cold treatment (Konradova et al., 2003). However, it remains controversial whether the presence of RFOs is responsible for improving embryo germination. Several reports have indicated that levels of RFOs are closely linked to the degree of tolerance to stress. Carpenter et al. (2000) suggested that an appropriate marker for the full maturity of SEs of the genus Pinus is the level of oligosaccharides of RFOs and dehydrins, with increased RFO levels resulting in improved germination. Businge et al. (2013) attributed improved germination of *P. abies* SEs to high levels of sucrose, raffinose and LEA proteins, which promoted the acquisition of desiccation tolerance. Bomal et al. (2002) stated that a high sucrose content and occurrence of raffinose were in agreement with the development of tolerance to fast desiccation in *P. mariana* SEs. The protective action of sucrose has been attributed to its capacity to stabilize proteins and membranes, probably by replacing their hydration coatings (Crowe et al., 1992). Raffinose increases the availability of sucrose by preventing its crystallization, and thus enhances the protective action of sucrose (Koster and Leopold, 1988; Oliver et al., 1998). For this reason, it is often suggested that the RFO:sucrose (R/S) ratio is more critical for desiccation protection than absolute carbohydrate levels (Sauter and van Cleve, 1991; Xiao and Koster, 2001). The optimal RFO:sucrose ratio reported to maintain the glassy state is 1:5.7 (approx. 0.18) (Koster, 1991; Koster and Bryant, 2005), but a much lower ratio of 1:20 (0.05) has been shown to be sufficient (Lin and Huang, 1994). Here, a functional complex of sucrose and RFOs appears to be used as well (0.18 for D2 and 0.37 for D3 embryos).

Another possible action of RFOs during desiccation is a reduction in the availability of monosaccharides due to the synthesis of RFOs, leading to the suppression of respiration, and thus metabolic activity of the seed (Leprince et al., 1992; Pammenter and Berjak, 1999). Finally, they may also play a role as quenchers of reactive oxygen species formed during dehydration (reviewed by Keunen et al., 2013).

Raffinose family oligosaccharide biosynthesis begins with the reversible transfer of a galactosyl residue from galactinol as the most common donor to a sucrose molecule to form raffinose (Keller and Pharr, 1996; Peterbauer and Richter, 2001). Thus, monitored levels of galactinol in SEs compared to those in ZEd might indicate a slightly different coordination/balance of carbon distribution into compounds closely related to RFO synthesis. Galactinol probably provides a similar protective function for embryos, and thus complements the protective function of this group of substances.

The carbohydrate status in desiccated SEs of Norway spruce corresponded better with that of ZEd, as the endogenous soluble carbohydrate spectrum of these dormant, winter-harvested ZEs was characterized by a comparable amount of sucrose, high proportion of RFOs and only low amounts of glucose, fructose and inositol. The total level of carbohydrates per unit DW was significantly lower in ZEs compared to SEs (in agreement with Konradova et al., 2003).

Although the level of RFOs in SEs after desiccation treatment did not reach that in ZEs, it was still enough to secure the multiple functions mentioned above. Similarly, lower R/S ratios found in SEs compared to their zygotic counterparts exceeded the R/S value considered sufficient for the protective function of RFOs.

Modifications of Phytohormone Content

Substantial differences were found in the content of analyzed phytohormones (ABA, auxins and CKs) in SEs during prolonged maturation and desiccation. Significantly lower levels of phytohormones were detected in ZEd, with profiles of particular derivatives mostly similar to those of SEs.

Abscisic acid determines conifer SE maturation and germination. Its application induces the start of SE maturation and is essential for successful embryo development (e.g., von Arnold and Hakman, 1988; von Arnold et al., 1996; Filonova et al., 2000; von Aderkas et al., 2002). Although the whole maturation process has been shown to continue on medium weekly supplemented with a high concentration of ABA, a reduction of endogenous ABA content (necessary for optimal germination) begins already during the second part of maturation (Vondrakova et al., 2018). Our present data show that ABA reduction further continues during prolonged maturation. However, no substantial influence was evident on the composition of ABA-type derivatives in M7 and M8 embryos.

A decrease in ABA levels is usually considered as the main effect of desiccation treatment (Kermode et al., 1989; Find, 1997). Lower levels of ABA are necessary for successful germination, e.g., in seeds and/or embryos of *Picea glauca* and *Picea morrisonicola* (Liu et al., 2015; Liao and Juan, 2015). We detected a larger decrease of free ABA concentration in D2 and D3 embryos when compared to M3 and M5 embryos (Vondrakova et al., 2018) as well as M7 and M8 embryos (as demonstrated here).

Moreover, desiccation treatment also induced a reduction in the content of ABA derivatives PA and DPA. The decrease in concentrations of ABA, PA, and DPA in desiccated embryos was mainly linked to the change of cultivation conditions, i.e., the absence of exogenous ABA. ABA-GE (ABA storage conjugate) was present in maturated as well as in desiccated embryos. Relatively constant levels of ABA-GE have been observed during seed development of Douglas-fir (Chiwocha and von Aderkas, 2002).

During maturation, comparable concentrations of total auxins were found in M5, M7 and M8 embryos. It was previously demonstrated that maximal auxin concentrations during maturation correlate with the polarization of SEs (Vondrakova et al., 2018). In this step, the IAA-amino acid conjugates IAA-Asp and IAA-Glu are the main auxin forms. Similarly, a high level of IAA-Asp has been detected during SE and ZE maturation in Douglas-fir and larch (von Aderkas et al., 2001; Chiwocha and von Aderkas, 2002). The content of auxins decreases from the third to the fifth week of maturation and the participation of IAA-Asp and IAA-Glu is minimal in M5 embryos (Vondrakova et al., 2018). As shown here, IAA was the main auxin in M5 embryos, followed by the non-indole weak auxin PAA. During prolonged maturation, the share of IAA decreased, whereas that of IAA-Asp increased. Despite these changes in the proportion of particular auxin derivatives, the total content of auxins remained at a low and relatively constant level. This may be the reason for the rooting inability of SEs because auxins regulate the root pole formation and rooting of embryos (Brunoni et al., 2019). In our experimental system, similar concentrations of auxins were found in M5, M7, M8 and D2 embryos, and an increase in auxin levels was detected just before germination (D3). The main difference between matured and desiccated embryos was in the proportion of different auxins. Although IAA-Asp was prevalent in M7 and M8 embryos, Ox-IAA was predominant in desiccated embryos. Oxidation of IAA is an important step to control auxin concentrations in angiosperms and, along with IAA conjugation, to respond to perturbation of IAA homeostasis (Brunoni et al., 2020). Our finding of Ox-IAA in desiccated SEs and ZEd is quite surprising as Brunoni et al. (2020) have shown that conjugation predominates over oxidation in maintaining IAA homeostasis in Norway spruce seedlings.

Endogenous levels of CKs have been shown to be rather low during maturation, but their diversity is high (Vondrakova et al., 2018). As shown here, the proportion and content of CKs remained unchanged throughout prolonged maturation (M7, M8) compared to M5 embryos. During prolonged maturation, the CK pool was represented mainly by *cis*Z- and DHZ-types, while iP- and *trans*Z-types occurred in significantly lower concentrations. This finding corresponds well with the results of Quesnelle and Emery (2007), who found that *cis*-zeatins were the primary CK forms during pea embryogenesis, whereas corresponding *trans*-isomers were only minor constituents.

A large increase in concentration was found in desiccated embryos for all CK forms except iP-types, mainly due to the enhanced accumulation of *O*-glucosides (predominantly DHZROG and *cis*ZROG). Involvement of these *O*-glucosides was demonstrated in our previous work during the desiccation and germination of Norway spruce SEs (Vondrakova et al., 2018). Cytokinin *O*-glucosides are generally regarded to accumulate in mature and senescing tissues (Letham and Palni, 1983), and the *O*-glucosylation is thought to be reversible since ß-glucosidases are capable of hydrolyzing them in plants (Brzobohatý et al., 1993). *O*-glucosylation represents a rapid and efficient mechanism of CK inactivation, but the role of *O*-glucosides in plant biology remains unclear (Záveská-Drábková et al., 2021). Unfortunately, no other studies have demonstrated a potential role of cytokinin *O*-glucosides in SE development, since only fundamental CKs (free bases and ribosides) and other basic auxins and ABA derivatives (ABA, ABA-GE, IAA, IAA-Asp) were analyzed in somatic embryogenesis until recently due to limitations in the available methodology (Jourdain et al., 1997; Vágner et al., 1998; von Aderkas et al., 2001; Zhou et al., 2017).

In all our analyses, extremely low concentrations of phytohormones were found in ZEd. Despite this, the hormonal spectra mostly corresponded with those in M5 embryos, especially in the case of ABA derivatives and auxins. However, in contrast to SEs, ZEd also contained cytokinin *N*-glucosides (*N*9- but not *N*7-glucosides), apparently irreversible forms widely

distributed throughout the plant kingdom (Pokorná et al., 2021). Very low concentrations of phytohormones in Norway spruce ZEd suggest a possible correlation between the minimum WC in these winter seeds and their low biochemical activity, which seems to be related to the deep dormancy of Norway spruce seeds during the winter season.

Modifications of the Proteome of Desiccated Somatic Embryos Make Them Closer to Zygotic Embryos

Comparative proteomic analyses revealed significantly differentially accumulated proteins between the compared proteomes. Biological processes modified by desiccation are discussed in the light of functional classes of GO. The processes most represented by the identified significant proteins were "Metabolic process" - "Stored energy", "Acquisition of desiccation tolerance", "Response to stimulus", and "Response to stress". They corresponded to those often amplified during the late maturation of various conifer seeds or SEs (Stasolla et al., 2003; Stasolla et al., 2004b; Silveira et al., 2008) or in comparison of late somatic and zygotic maturation (Balbuena et al., 2009; Lara-Chavez et al., 2012; Morel et al., 2014; Jing et al., 2017).

As in many studies, we did not observe overexpression of proteins involved in photosynthesis which are activated after germination. However, this has been investigated in a recent study analyzing the mechanisms taking place during partial desiccation of SEs of *Pinus asperata* (Jing et al., 2017). In our study, the changes in proteomic profile observed between D3 and M5 embryos were very similar to those between ZEf and M5 embryos, with most of the modified biological processes being amplified. This suggests that (1) desiccation causes protein reprogramming, resulting in a proteome approaching that of ZEf, as shown by the carbohydrate and auxin assays, and (2) desiccation treatment induces some biological processes without inhibiting any of those expressed in M5 embryos. Nevertheless, the number of significant proteins, as well as the abundance ratios modified by desiccation, were lower than those in ZEf. Therefore, even if desiccation induced reprogramming of the proteome of M5 embryos toward ZEf (Fait et al., 2006; Angelovici et al., 2010), D3 was not yet fully equivalent to ZEf (**Supplementary Figure 1**). This was confirmed by the multivariate analysis based on all biochemical variables measured (**Figure 10**).

The main protein functional classes amplified after desiccation, as well as RFO synthesis and modification of phytohormone profiles observed in this study, participate in the characteristic events of the late maturation phase of embryos, i.e., activation of storage metabolism of energy reserves, acquisition of desiccation tolerance and development of stress response systems.

Activation of Storage Metabolism of Energy Reserves

The accumulation of storage reserves before the quiescent state of embryos is necessary to support the germination and growth of the seedlings before their energy autonomy. In conifers, these reserves are stored mainly in protein and lipid forms. Both D3 embryos and ZEf showed overexpression of storage proteins but without abundance modification of the enzymes involved in their synthesis. Thus, we deduced that their syntheses took place earlier before stages D3 and ZEf. Storage proteins are major sources of nitrogen and carbon during subsequent seed germination and early seedling growth. The presence of these proteins in various isoforms is due to the multigenic character of these proteins grouped into families (Li et al., 2007). The identified cruciferin and cruciferina, members of the cupin superfamily, are respectively vicilin- and legumin-like protein globulins. Among the storage proteins of conifers, they represent the majority of storage forms (Hakman et al., 1990; Flinn et al., 1993; Lelu-Walter et al., 2008; Teyssier et al., 2011; Morel et al., 2014). We also detected an albumin 2S storage protein on the retard gel (**Figure 4**), the abundance of which was not modified by desiccation. However, the synthesis of energy reserves may begin before the acquisition of tolerance to desiccation (Marques et al., 2019); we deduced that the synthesis of 2S albumin occurred prior to the M5 stage.

Lipids are another source of energy reserve during the germination of conifer embryos but also for their respiratory activities during the late maturation phase (Leprince et al., 2017). However, we did not detect overexpression of the proteins involved in their synthesis. Although the sequence of storage deposition processes occurring at the end of embryogenesis is often species-specific, the synthesis of storage lipids often takes place prior to or simultaneously with the synthesis of storage proteins (Righetti et al., 2015; Leprince et al., 2017). This has been shown for *P. abies*, in which lipid synthesis is maximal after 4 weeks of maturation (Grigová et al., 2007).

In SEs (Vestman et al., 2011; Jing et al., 2017), as in orthodox seeds (Ntuli et al., 2011), the end of maturation is associated with higher activities of the systems involved in stress defense (stress-related proteins, RFOs, secondary metabolites) in prevision of the increased level of oxidation of cells during dehydration. Also, the correlation between the amplified presence of stress-related proteins and the acquisition of desiccation tolerance has been demonstrated in many studies and their synthesis directly contributes to this acquisition (Stasolla et al., 2004b; Finnie et al., 2006; Silveira et al., 2008; Sghaier et al., 2009; Shi et al., 2010).

Acquisition of Desiccation Tolerance

Desiccation tolerance is a multifactorial trait that involves the protection of macromolecules and membranes from the deleterious effects of water removal. The best-known proteins involved in this protection are late embryogenesis abundant proteins (LEA) and heat shock proteins (HSPs) (Stasolla et al., 2003; Personat et al., 2014). Only a few LEA proteins were identified among the proteins whose abundance was modulated by desiccation in our study. These were Em-like protein GEA6, belonging to LEA group 1, late embryogenesis abundant domain-containing protein and LEA 31. All of these proteins were more abundant in D3 than in M5 embryos. This also applied to all LEAs identified in the M5/ZEf analysis, which were then more numerous in ZEf. LEA proteins are sequentially synthesized during embryo development, probably related to their very diverse functions during late maturation and germination (Chatelain et al., 2012), with maximal abundance at the late

maturation stage (Leprince et al., 2017). In conifers, many studies have shown the presence of their transcripts from the middle of maturation (Stasolla et al., 2003; Vales et al., 2007; Silveira et al., 2008) or the presence of the proteins at the end of the maturation (Silveira et al., 2008; Businge et al., 2013; Morel et al., 2014). Furthermore, many LEAs may already be synthesized prior to the M5 stage, and therefore cannot be revealed by a comparative proteomic study.

Development of Stress Response Systems

Stress-related proteins, generally present in the late maturation stage, are classified as stress- or stimulus-response proteins. These proteins, which stabilize molecular structures (chaperones, HSPs), maintain homeostasis and neutralize deleterious reactive oxygen species (ROS) (e.g., catalase, superoxide dismutase), participate in different stages of embryo development (Fehér et al., 2003). Their expression has been shown to be amplified after a post-maturation treatment inducing desiccation tolerance and increased germination capacity in *Pinus asperata* SEs (Jing et al., 2017). This was not the case in D3 embryos, although the treatment did improve the germination ability, as seen in our previous study (Vondráková et al., 2013). It is important to dissociate the aptitudes of embryos for desiccation from the aptitudes for germination. Since HSPs are involved in the maintenance of membrane and molecular structures in cells in low WC, this protection is not essential for late-maturing embryos for which the water status remains normal.

Anticipation of the deleterious oxidative damage inherent in the desiccation of embryos involves the accumulation of antioxidant enzymes that can neutralize them. In this study, several such proteins were identified (glutathione peroxidase 6, glutathione transferase-29, glyoxalase, lipocalin-1, and oxidoreductase), which were all up-regulated in D3 and ZEf. In the latter, the panel of proteins was more extensive since it was complemented by superoxide dismutase, peroxiredoxin type 2 and 1-cysteine peroxiredoxin 1. Whereas only the latter has been shown to be expressed during the acquisition of dehydration tolerance (Leprince and Buitink, 2010), the others may be active during other periods of plant development characterized by a high content of hydrogen peroxide, such as germination or early embryogenesis (Huang et al., 2012; Jing et al., 2017).

To summarize, unlike prolonged maturation, the post-maturation desiccation treatment triggered (i) a significant decrease in ABA content and shift in ABA catabolism toward the accumulation of storage form ABA-GE, (ii) a decrease in the content of starch, (iii) accumulation of RFOs, storage proteins, LEA and stress-related proteins, and (iv) activation of antioxidative systems. These modifications could be markers of the acquisition of desiccation tolerance. Given their simultaneous occurrence at the late maturation stage, it is reasonable to assume the entry of mature SEs into this process.

CONCLUSION

The present work revealed that SEs were modified during desiccation, i.e., post-maturation treatment at high relative humidity, on all levels tested. The accumulation of compounds (RFOs, LEA) that are believed to protect cell structures from the consequences of desiccation strongly suggests that SEs approach a state of tolerance to drying without a marked decrease in water content. The control realized by prolonging the maturation for the same time as the desiccation treatment applied in parallel confirmed that the observed metabolic and physiological shifts were indeed the consequence of the applied treatment. The biological process changes observed in the treated SEs were very similar to those occurring in ZEs during the late phase of maturation of orthodox seeds before the winter season. We suggest that they may be important for further embryo development and contribute to successful germination.

DATA AVAILABILITY STATEMENT

The original contributions presented in the study are included in the article/**Supplementary Material**; further inquiries can be directed to the corresponding author.

AUTHOR CONTRIBUTIONS

KE, ZV, CT, and M-AL-W conceived and planned the experiments. ZV and LF prepared all the plant material. KE carried out the histological analyses. HK performed the carbohydrate content quantification. PD and VM performed phytohormone analyzes. CT and A-ML carried out the proteomic analysis. ZV and CT carried out the statistical analysis. KE, ZV, CT, HK, VM, and M-AL-W wrote and reviewed the manuscript. All authors discussed the results and contributed to the final manuscript.

FUNDING

We acknowledge the support of the Czech Ministry of Education, Youth and Sports (project no. 7AMB12FR017), the French Ministry of Foreign Affairs and the French Ministry of Higher Education and Research through the BARRANDE Programme for the Czech Republic/France Science Cooperation, and the support of the Czech Science Foundation (project no. 19-12262S).

ACKNOWLEDGMENTS

We would like to thank technicians Jana Kališová, Marie Korecká and Jaroslava Špačková for their excellent work. We would also like to thank the Sees-editing, Ltd., for proofreading of the manuscript.

SUPPLEMENTARY MATERIAL

The Supplementary Material for this article can be found online at: https://www.frontiersin.org/articles/10.3389/fpls.2022.823617/full#supplementary-material

REFERENCES

Amara, I., Zaidi, I., Masmoudi, K., Ludevid, M., Pagès, M., Goday, A., et al. (2014). Insights into late embryogenesis abundant (LEA) proteins in plants: from structure to the functions. *Am. J. Plant Sci.* 5, 3440–3455. doi: 10.4236/ajps.2014.522360

Angelovici, R., Galili, G., Fernie, A. R., and Fait, A. (2010). Seed desiccation: a bridge between maturation and germination. *Trends Plant Sci.* 15, 211–218. doi: 10.1016/j.tplants.2010.01.003

Attree, S. M., and Fowke, L. C. (1993). Embryogeny of gymnosperms: advances in synthetic seed technology of conifers. *Plant Cell Tissue Organ Cult.* 35, 1–35. doi: 10.1007/bf00043936

Attree, S. M., Moore, D., Sawhney, V. K., and Fowke, L. C. (1991). Enhanced maturation and desiccation tolerance of white spruce [*Picea glauca* (Moench) Voss] somatic embryos: effects of a non-plasmolysing water stress and abscisic acid. *Ann. Bot.* 68, 519–525.

Attree, S. M., Pomeroy, M. K., and Fowke, L. C. (1995). Development of white spruce (*Picea glauca* (Moench.) Voss) somatic embryos during culture with abscisic acid and osmoticum, and their tolerance to drying and frozen storage. *J. Exp. Bot.* 46, 433–439. doi: 10.1093/jxb/46.4.433

Balbuena, T. S., Jo, L., Pieruzzi, F. P., Dias, L. L. C., Silveira, V., Santa-Catarina, C., et al. (2011). Differential proteome analysis of mature and germinated embryos of *Araucaria angustifolia*. *Phytochemistry* 72, 302–311. doi: 10.1016/j.phytochem.2010.12.007

Balbuena, T. S., Silveira, V., Junqueira, M., Dias, L. L. C., Santa-Catarina, C., Shevchenko, A., et al. (2009). Changes in the 2-DE protein profile during zygotic embryogenesis in the Brazilian Pine (*Araucaria angustifolia*). *J. Proteomics* 72, 337–352. doi: 10.1016/j.jprot.2009.01.011

Bomal, C., Le, V. Q., and Tremblay, F. M. (2002). Induction of tolerance to fast desiccation in black spruce (*Picea mariana*) somatic embryos: relationship between partial water loss, sugars, and dehydrins. *Physiol. Plant.* 115, 523–530. doi: 10.1034/j.1399-3054.2002.1150406.x

Brunoni, F., Collani, S., Casanova-Sáez, R., Šimura, J., Karady, M., Schmid, M., et al. (2020). Conifers exhibit a characteristic inactivation of auxin to maintain tissue homeostasis. *New Phytol.* 226, 1753–1765. doi: 10.1111/nph.16463

Brunoni, F., Ljung, K., and Bellini, C. (2019). Control of root meristem establishment in conifers. *Physiol. Plant.* 165, 81–89. doi: 10.1111/ppl.12783

Brzobohatý, B., Moore, I., Kristoffersen, P., Bako, L., Campos, N., Schell, J., et al. (1993). Release of active cytokinin by a β-glucosidase localized to the maize root meristem. *Science* 262, 1051–1054. doi: 10.1126/science.8235622

Businge, E., Bygdell, J., Wingsle, G., Moritz, T., and Egertsdotter, U. (2013). The effect of carbohydrates and osmoticum on storage reserve accumulation and germination of Norway spruce somatic embryos. *Physiol. Plant.* 149, 273–285. doi: 10.1111/ppl.12039

Carpenter, C. V., Koester, M. K., and Gupta, P. K. (2000). *Method for Determining Maturity of Conifer Somatic Embryos. USA Patent Application US6117678A*. Mountain View, CA: Google.

Carrier, D. J., Kendall, E. J., Bock, C. A., Cunningham, J. E., and Dunstan, D. I. (1999). Water content, lipid deposition, and (+)-abscisic acid content in developing white spruce seeds. *J. Exp. Bot.* 50, 1359–1364. doi: 10.1093/jexbot/50.337.1359

Chatelain, E., Hundertmark, M., Leprince, O., Le Gall, S., Satour, P., Deligny-Penninck, S., et al. (2012). Temporal profiling of the heat-stable proteome during late maturation of *Medicago truncatula* seeds identifies a restricted subset of late embryogenesis abundant proteins associated with longevity. *Plant Cell Environ.* 35, 1440–1455. doi: 10.1111/j.1365-3040.2012.02501.x

Chiwocha, S., and von Aderkas, P. (2002). Endogenous levels of free and conjugated forms of auxin, cytokinins and abscisic acid during seed development in Douglas fir. *Plant Growth Regul.* 36, 191–200. doi: 10.1023/A:1016522422983

Crowe, J. H., Hoekstra, F. A., and Crowe, L. M. (1992). Anhydrobiosis. *Annu. Rev. Physiol.* 54, 579–599. doi: 10.1146/annurev.ph.54.030192.003051

Djilianov, D. L., Dobrev, P. I., Moyankova, D. P., Vankova, R., Georgieva, D. T., Gajdosova, S., et al. (2013). Dynamics of endogenous phytohormones during desiccation and recovery of the resurrection plant species *Haberlea rhodopensis*. *J. Plant Growth Regul.* 32, 564–574. doi: 10.1007/s00344-013-9323-y

Downie, B., and Bewley, J. D. (2000). Soluble sugar content of white spruce (*Picea glauca*) seeds during and after germination. *Physiol. Plant.* 110, 1–12. doi: 10.1034/j.1399-3054.2000.110101.x

Dronne, S., Label, P., and Lelu, M. A. (1997). Desiccation decreases abscisic acid content in hybrid larch (*Larix x leptoeuropaea*) somatic embryos. *Physiol. Plant.* 99, 433–438. doi: 10.1034/j.1399-3054.1997.990311.x

Eliášová, K., Vondráková, Z., Gemperlová, L., Nedìla, V., Runštuk, J., Fischerová, L., et al. (2018). The response of *Picea abies* somatic embryos to UV-B radiation depends on the phase of maturation. *Front. Plant Sci.* 9:1736. doi: 10.3389/fpls.2018.01736

Eliášová, K., Vondráková, Z., Malbeck, J., Trávníčková, A., Pešek, B., Vágner, M., et al. (2017). Histological and biochemical response of Norway spruce somatic embryos to UV-B irradiation. *Trees* 31, 1279–1293. doi: 10.1007/s00468-017-1547-1

Fait, A., Angelovici, R., Less, H., Ohad, I., Urbanczyk-Wochniak, E., Fernie, A. R., et al. (2006). Arabidopsis seed development and germination Is associated with temporally distinct metabolic switches. *Plant Physiol.* 142, 839–854. doi: 10.1104/pp.106.086694

Fehér, A., Pasternak, T. P., and Dudits, D. (2003). Transition of somatic plant cells to an embryogenic state. *Plant Cell Tissue Organ Cult.* 74, 201–228. doi: 10.1023/A:1024033216561

Filonova, L. H., Bozhkov, P. V., Brukhin, V. B., Daniel, G., Zhivotovsky, B., and von Arnold, S. (2000). Two waves of programmed cell death occur during formation and development of somatic embryos in the gymnosperm, Norway spruce. *J. Cell Sci.* 113, 4399–4411.

Find, J. I. (1997). Changes in endogenous ABA levels in developing somatic embryos of Norway spruce (*Picea abies* (L.) Karst.) in relation to maturation medium, desiccation and germination. *Plant Sci.* 128, 75–83. doi: 10.1016/S0168-9452(97)00141-6

Finnie, C., Bak-Jensen, K. S., Laugesen, S., Roepstorff, P., and Svensson, B. (2006). Differential appearance of isoforms and cultivar variation in protein temporal profiles revealed in the maturing barley grain proteome. *Plant Sci.* 170, 808–821. doi: 10.1016/j.plantsci.2005.11.012

Flinn, B. S., Roberts, D. R., Newton, C. H., Cyr, D. R., Webster, F. B., and Taylor, I. E. P. (1993). Storage protein gene expression in zygotic and somatic embryos of interior spruce. *Physiol. Plant.* 89, 719–730. doi: 10.1111/j.1399-3054.1993.tb05278.x

Gösslová, M., Svobodová, H., Lipavská, H., Albrechtová, J., and Vreugdenhil, D. (2001). Comparing carbohydrate status during Norway spruce seed development and somatic embryo formation. *In Vitro Cell. Dev. Biol.* 37, 24–28.

Grigová, M., Kubeš, M., Drážná, N., Řezanka, T., and Lipavská, H. (2007). Storage lipid dynamics in somatic embryos of Norway spruce (*Picea abies*): histochemical and quantitative analyses. *Tree Physiol.* 27, 1533–1540. doi: 10.1093/treephys/27.11.1533

Gupta, P., and Durzan, D. (1986). Plantlet regeneration via somatic embryogenesis from subcultured callus of mature embryos of *Picea abies* (Norway spruce). *In Vitro Cell. Dev. Biol.* 22, 685–688. doi: 10.1007/bf02623484

Gutmann, M., Charpentier, J. P., Doumas, P., and Jay-Allemand, C. (1996). Histological investigation of walnut cotyledon fragments for a better understanding of in vitro adventitious root initiation. *Plant Cell Rep.* 15, 345–349. doi: 10.1007/BF00232369

Hakman, I. (1993). Embryology in Norway spruce (*Picea abies*). An analysis of the composition of seed storage proteins and deposition of storage reserves during seed development and somatic embryogenesis. *Physiol. Plant.* 87, 148–159. doi: 10.1111/j.1399-3054.1993.tb00137.x

Hakman, I., Stabel, P., Engström, P., and Eriksson, T. (1990). Storage protein accumulation during zygotic and somatic embryo development in *Picea abies* (Norway spruce). *Physiol. Plant.* 80, 441–445. doi: 10.1111/j.1399-3054.1990.tb00065.x

Hazubska-Przybyl, T., Wawrzyniak, M., Obarska, A., and Bojarczuk, K. (2015). Effect of partial drying and desiccation on somatic seedling quality in Norway and Serbian spruce. *Acta Physiol. Plant.* 37:1735. doi: 10.1007/s11738-014-1735-1

Hoekstra, F. A., Golovina, E. A., Tetteroo, F. A. A., and Wolkers, W. F. (2001). Induction of desiccation tolerance in plant somatic embryos: how exclusive is the protective role of sugars? *Cryobiology* 43, 140–150. doi: 10.1006/cryo.2001.2358

Huang, H., Møller, I. M., and Song, S.-Q. (2012). Proteomics of desiccation tolerance during development and germination of maize embryos. *J. Proteomics* 75, 1247–1262. doi: 10.1016/j.jprot.2011.10.036

Hudec, L., Konrádová, H., Hašková, A., and Lipavská, H. (2016). Norway spruce embryogenesis: changes in carbohydrate profile, structural development and response to polyethylene glycol. *Tree Physiol.* 36, 548–561. doi: 10.1093/treephys/tpw016

Iraqi, D., and Tremblay, F. M. (2001). Analysis of carbohydrate metabolism enzymes and cellular contents of sugars and proteins during spruce somatic embryogenesis suggests a regulatory role of exogenous sucrose in embryo development. *J. Exp. Bot.* 52, 2301–2311. doi: 10.1093/jexbot/52.365.2301

Jing, D. L., Zhang, J. W., Xia, Y., Kong, L. S., OuYang, F. Q., Zhang, S. G., et al. (2017). Proteomic analysis of stress-related proteins and metabolic pathways in *Picea asperata* somatic embryos during partial desiccation. *Plant Biotechnol. J.* 15, 27–38. doi: 10.1111/pbi.12588

Jourdain, I., Lelu, M. A., and Label, P. (1997). Hormonal changes during growth of somatic embryogenic masses in hybrid larch. *Plant Physiol. Biochem.* 35, 741–749.

Joy, R. W. IV, Yeung, E. C., Kong, L., and Thorpe, T. A. (1991). Development of white spruce somatic embryos: I. Storage product deposition. *In Vitro Cell. Dev. Biol. Plant* 27, 32–41. doi: 10.1007/BF02632059

Käll, L., Canterbury, J., Weston, J., Noble, W. S., and MacCoss, M. J. (2007). Semi-supervised learning for peptide identification from shotgun proteomics datasets. *Nat. Methods* 4, 923–925. doi: 10.1038/nmeth1113

Keller, F., and Pharr, D. M. (1996). "Metabolism of carbohydrates in sinks and sources: galactosyl-sucrose oligosaccharides," in *Photoassimilate Distribution in Plants and Crops: Source–Sink Relationships*, eds E. Zamski and A. A. Schaffer (New York, NY: Marcel Dekker), 157–183. doi: 10.1071/ar9860157

Kermode, A. R., Dumbroff, E. B., and Bewley, J. D. (1989). The role of maturation drying in the transition from seed development to germination. 7. Effects of partial and complete desiccation on abscisic acid levels and sensitivity in *Ricinus communis* L. Seeds. *J. Exp. Bot.* 40, 303–313. doi: 10.1093/jxb/40.2.303

Keunen, E., Peshev, D., Vangronsveld, J., van den Ende, W., and Cuypers, A. (2013). Plant sugars are crucial players in the oxidative challenge during abiotic stress: extending the traditional concept. *Plant Cell Environ.* 36, 1242–1255. doi: 10.1111/pce.12061

Klimaszewska, K., Hargreaves, C., Lelu-Walter, M. A., and Trontin, J. F. (2016). "Advances in conifer somatic embryogenesis since year 2000," in *In vitro Embryogenesis in Higher Plants. Methods in Molecular Biology*, Vol. 1359, eds M. A. Germanà and M. Lambardi (New York, NY: Springer Science and Business Media), 131–166. doi: 10.1007/978-1-4939-3061-6_7

Klimaszewska, K., Morency, F., Jones-Overton, C., and Cooke, J. (2004). Accumulation pattern and identification of seed storage proteins in zygotic embryos of *Pinus strobus* and in somatic embryos from different maturation treatments. *Physiol. Plant.* 121, 682–690. doi: 10.1111/j.1399-3054.2004.00370.x

Kong, L., and Yeung, E. C. (1992). Development of white spruce somatic embryos: II. Continual shoot meristem development during germination. *In Vitro Cell. Dev. Biol. Plant* 28, 125–131. doi: 10.1007/BF02823060

Kong, L., Attree, S. M., Evans, D. E., Binarova, P., Yeung, E. C., and Fowke, L. C. (1999). "Somatic embryogenesis in white spruce: studies of embryo development and cell biology," in *Somatic Embryogenesis in Woody Plants. Forestry Sciences*, eds M. Jain, P. K. Gupta, and R. J. Newton (Dordrecht: Springer), 1–28. doi: 10.1007/978-94-017-3032-7_1

Konradova, H., Grigova, M., and Lipavska, H. (2003). Cold-induced accumulation of raffinose family oligosaccharides in somatic embryos of Norway spruce (*Picea abies*). *In Vitro Cell. Dev. Biol. Plant* 39, 425–427. doi: 10.1079/Ivp2003426

Koster, K. L. (1991). Glass formation and desiccation tolerance in seeds. *Plant Physiol.* 96, 302–304. doi: 10.1104/pp.96.1.302

Koster, K. L., and Bryant, G. (2005). "Dehydration in model membranes and protoplasts: contrasting effects at low, intermediate and high hydrations," in *Cold Hardiness in Plants: Molecular Genetics, Cell Biology and Physiology*, eds T. H. H. Chen, M. Uemura, and S. Fujikawa (Wallingford: CABI Publishing), 219–234. doi: 10.1079/9780851990590.0219

Koster, K. L., and Leopold, A. C. (1988). Sugars and desiccation tolerance in seeds. *Plant Physiol.* 88, 829–832. doi: 10.1104/pp.88.3.829

Kubes, M., Drazna, N., Konradova, H., and Lipavska, H. (2014). Robust carbohydrate dynamics based on sucrose resynthesis in developing Norway spruce somatic embryos at variable sugar supply. *In Vitro Cell. Dev. Biol. Plant* 50, 45–57. doi: 10.1007/s11627-013-9589-6

Lara-Chavez, A., Egertsdotter, U., and Flinn, B. S. (2012). Comparison of gene expression markers during zygotic and somatic embryogenesis in pine. *In Vitro Cell. Dev. Biol. Plant* 48, 341–354. doi: 10.1007/s11627-012-9440-5

Lê, S., Josse, J., and Husson, F. (2008). FactoMineR: an R package for multivariate analysis. *J. Stat. Softw.* 25, 1–18. doi: 10.18637/jss.v025.i01

Leal, I., Misra, S., Attree, S. M., and Fowke, L. C. (1995). Effect of abscisic acid, osmoticum and desiccation on 11s storage protein gene expression in somatic embryos of white spruce. *Plant Sci.* 106, 121–128. doi: 10.1016/0168-9452(95)04081-5

Lelu, M. A., and Label, P. (1994). Changes in the levels of abscisic acid and its glucose ester conjugate during maturation of hybrid larch (*Larix* × *leptoeuropaea*) somatic embryos, in relation to germination and plantlet recovery. *Physiol. Plant.* 92, 53–60. doi: 10.1111/j.1399-3054.1994.tb06654.x

Lelu, M. A., Klimaszewska, K., Pflaum, G., and Bastien, C. (1995). Effect of maturation duration on desiccation tolerance in hybrid larch (*Larix* × *leptoeuropaea dengler*) somatic embryos. *In Vitro Cell. Dev. Biol. Plant* 31, 15–20. doi: 10.1007/BF02632220

Lelu-Walter, M. A., Bernier-Cardou, M., and Klimaszewska, K. (2008). Clonal plant production from self- and cross-pollinated seed families of *Pinus sylvestris* (L.) through somatic embryogenesis. *Plant Cell Tissue Organ Cult.* 92, 31–45. doi: 10.1007/s11240-007-9300-x

Leprince, O., and Buitink, J. (2010). Desiccation tolerance: from genomics to the field. *Plant Science* 179, 554–564. doi: 10.1016/j.plantsci.2010.02.011

Leprince, O., and Buitink, J. (2015). Introduction to desiccation biology: from old borders to new frontiers. *Planta* 242, 369–378. doi: 10.1007/s00425-015-2357-6

Leprince, O., Pellizzaro, A., Berriri, S., and Buitink, J. (2017). Late seed maturation: drying without dying. *J. Exp. Bot.* 68, 827–841. doi: 10.1093/jxb/erw363

Leprince, O., Vanderwerf, A., Deltour, R., and Lambers, H. (1992). Respiratory pathways in germinating maize radicles correlated with desiccation tolerance and soluble sugars. *Physiol. Plant.* 85, 581–588. doi: 10.1111/j.1399-3054.1992.tb04758.x

Letham, D. S., and Palni, L. M. S. (1983). The biosynthesis and metabolism of cytokinins. *Annu. Rev. Plant Physiol.* 34, 163–197. doi: 10.1146/annurev.pp.34.060183.001115

Li, Q., Wang, B. C., Xu, Y., and Zhu, Y. X. (2007). Systematic studies of 12S seed storage protein accumulation and degradation patterns during Arabidopsis seed maturation and early seedling germination stages. *J. Biochem. Mol. Biol.* 40, 373–381. doi: 10.5483/bmbrep.2007.40.3.373

Liao, Y., and Juan, I. P. (2015). Improving the germination of somatic embryos of *Picea morrisonicola* Hayata: effects of cold storage and partial drying. *J. For. Res.* 20, 114–124. doi: 10.1007/s10310-014-0445-2

Lin, T.-P., and Huang, N.-H. (1994). The relationship between carbohydrate composition of some tree seeds and their longevity. *J. Exp. Bot.* 45, 1289–1294. doi: 10.1093/jxb/45.9.1289

Lipavská, H., and Konrádová, H. (2004). Invited review: somatic embryogenesis in conifers: The role of carbohydrate metabolism. *In Vitro Cell. Dev. Biol. Plant* 40, 23–30. doi: 10.1079/ivp2003482

Lipavska, H., Svobodova, H., Albrechtova, J., Kumstyrova, L., Vagner, M., and Vondrakova, Z. (2000). Carbohydrate status during somatic embryo maturation in Norway spruce. *In Vitro Cell. Dev. Biol. Plant* 36, 260–267. doi: 10.1007/s11627-000-0048-9

Lippert, D., Yuen, M., and Bohlmann, J. (2009). Spruce proteome DB: a resource for conifer proteomics research. *Tree Genet. Genomes* 5, 723–727. doi: 10.1007/s11295-009-0220-2

Liu, Y., Müller, K., El-Kassaby, Y. A., and Kermode, A. R. (2015). Changes in hormone flux and signaling in white spruce (*Picea glauca*) seeds during the transition from dormancy to germination in response to temperature cues. *BMC Plant Biol.* 15:292. doi: 10.1186/s12870-015-0638-7

Marques, A., Nijveen, H., Somi, C., Ligterink, W., and Hilhorst, H. (2019). Induction of desiccation tolerance in desiccation sensitive *Citrus limon* seeds. *J. Integr. Plant Biol.* 61, 624–638. doi: 10.1111/jipb.12788

Maruyama, T. E., and Hosoi, Y. (2012). Post-maturation treatment improves and synchronizes somatic embryo germination of three species of Japanese pines. *Plant Cell Tissue Organ Cult.* 110, 45–52. doi: 10.1007/s11240-012-0128-7

Morel, A., Trontin, J.-F., Corbineau, F., Lomenech, A.-M., Beaufour, M., Reymond, I., et al. (2014). Cotyledonary somatic embryos of *Pinus pinaster* Ait. most

closely resemble fresh, maturing cotyledonary zygotic embryos: biological, carbohydrate and proteomic analyses. *Planta* 240, 1075–1095. doi: 10.1007/s00425-014-2125-z

Nagmani, R., Diner, A., Garton, S., and Zipf, A. (1995). "Anatomical comparison of somatic and zygotic embryogeny in conifers," in *Somatic Embryogenesis in Woody Plants*, eds S. Jain, P. Gupta, and R. Newton (Dordrecht: Kluwer Academic), 23–48.

Ntuli, T. M., Finch-Savage, W. E., Berjak, P., and Pammenter, N. W. (2011). Increased drying rate lowers the critical water content for survival in embryonic axes of English oak (*Quercus robur* L.) Seeds F. *J. Integr. Plant Biol.* 53, 270–280. doi: 10.1111/j.1744-7909.2010.01016.x

Oliver, M. J., O'Mahony, P., and Wood, A. J. (1998). "To dryness and beyond" – Preparation for the dried state and rehydration in vegetative desiccation-tolerant plants. *Plant Growth Regul.* 24, 193–201. doi: 10.1023/A:1005863015130

Pammenter, N. W., and Berjak, P. (1999). A review of recalcitrant seed physiology in relation to desiccation-tolerance mechanisms. *Seed Sci. Res.* 9, 13–37. doi: 10.1017/S0960258599000033

Pérez, H., Hill, L. M., and Walters, C. (2020). "A protective role for accumulated dry matter reserves in seeds during desiccation: implications for conservation," in *Agricultural, Forestry and Bioindustry Biotechnology and Biodiscovery*, eds P. Chong, D. Newman, and D. Steinmacher (Cham: Springer), 133–142.

Personat, J.-M., Tejedor-Cano, J., Prieto-Dapena, P., Almoguera, C., and Jordano, J. (2014). Co-overexpression of two heat shock factors results in enhanced seed longevity and in synergistic effects on seedling tolerance to severe dehydration and oxidative stress. *BMC Plant Biol.* 14:56. doi: 10.1186/1471-2229-14-56

Peterbauer, T., and Richter, A. (2001). Biochemistry and physiology of raffinose family oligosaccharides and galactosyl cyclitols in seeds. *Seed Sci. Res.* 11, 185–197. doi: 10.1079/SSR200175

Pokorná, E., Hluska, T., Galuszka, P., Hallmark, H. T., Dobrev, P. I., Záveská Drábková, L., et al. (2021). Cytokinin N-glucosides: occurrence, metabolism and biological activities in plants. *Biomolecules* 11:24. doi: 10.3390/biom11010024

Pond, S. E., von Aderkas, P., and Bonga, J. M. (2002). Improving tolerance of somatic embryos of *Picea glauca* to flash desiccation with a cold treatment (desiccation after cold acclimation). *In Vitro Cell. Dev. Biol. Plant* 38, 334–341. doi: 10.1079/Ivp2002304

Pullman, G. S., and Bucalo, K. (2014). Pine somatic embryogenesis: analyses of seed tissue and medium to improve protocol development. *New For.* 45, 353–377. doi: 10.1007/s11056-014-9407-y

Pullman, G. S., and Buchanan, M. (2008). Identification and quantitative analysis of stage-specific carbohydrates in loblolly pine (*Pinus taeda*) zygotic embryo and female gametophyte tissues. *Tree Physiol.* 28, 985–996. doi: 10.1093/treephys/28.7.985

Quesnelle, P. E., and Emery, R. J. N. (2007). cis-Cytokinins that predominate in *Pisum sativum* during early embryogenesis will accelerate embryo growth in vitro. *Can. J. Bot.* 85, 91–103. doi: 10.1139/b06-149

Righetti, K., Vu, J. L., Pelletier, S., Vu, B. L., Glaab, E., Lalanne, D., et al. (2015). Inference of longevity-related genes from a robust coexpression network of seed maturation identifies regulators linking seed storability to biotic defense-related pathways. *Plant Cell* 27, 2692–2708. doi: 10.1105/tpc.15.00632

Roberts, D. R. (1991). Abscisic acid and mannitol promote early development, maturation and storage protein accumulation in somatic embryos of interior spruce. *Physiol. Plant.* 83, 247–254. doi: 10.1111/j.1399-3054.1991.tb02149.x

Roberts, D. R., Sutton, B. C. S., and Flinn, B. S. (1990b). Synchronous and high-frequency germination of interior spruce somatic embryos following partial drying at high relative humidity. *Can. J. Bot.* 68, 1086–1090. doi: 10.1139/b90-136

Roberts, D. R., Flinn, B. S., Webb, D. T., Webster, F. B., and Sutton, B. C. S. (1990a). Abscisic acid and indole-3-butyric acid regulation of maturation and accumulation of storage proteins in somatic embryos of interior spruce. *Physiol. Plant.* 78, 355–360. doi: 10.1111/j.1399-3054.1990.tb09048.x

Roberts, D. R., Lazaroff, W. R., and Webster, F. B. (1991). Interaction between maturation and high relative humidity treatments and their effects on germination of sitka spruce somatic embryos. *J. Plant Physiol.* 138, 1–6. doi: 10.1016/S0176-1617(11)80720-0

Sass, J. E. (1958). *Botanical Microtechnique*. Ames, IA: The Iowa State University Press.

Sauter, J. J., and van Cleve, B. (1991). Biochemical and ultrastructural results during starch-sugar-conversion in ray parenchyma cells of *Populus* during cold adaptation. *J. Plant Physiol.* 139, 19–26. doi: 10.1016/S0176-1617(11)80158-6

Sghaier, B., Kriaa, W., Bahloul, M., Novo, J. V. J., and Drira, N. (2009). Effect of ABA, arginine and sucrose on protein content of date palm somatic embryos. *Sci. Hortic.* 120, 379–385. doi: 10.1016/j.scienta.2008.11.035

Shi, J., Zhen, Y., and Zheng, R.-H. (2010). Proteome profiling of early seed development in *Cunninghamia lanceolata* (Lamb.) Hook. *J. Exp. Bot.* 61, 2367–2381. doi: 10.1093/jxb/erq066

Silveira, V., Balbuena, T. S., Santa-Catarina, C., Floh, E. I. S., Guerra, M. P., and Handro, W. (2004). Biochemical changes during seed development in *Pinus taeda* L. *Plant Growth Regul.* 44, 147–156. doi: 10.1007/s10725-004-2601-8

Silveira, V., Santa-Catarina, C., Balbuena, T. S., Moraes, F. M. S., Ricart, C. A. O., Sousa, M. V., et al. (2008). Endogenous abscisic acid and protein contents during seed development of *Araucaria angustifolia*. *Biol. Plant.* 52, 101–104. doi: 10.1007/s10535-008-0018-3

Stasolla, C., and Yeung, E. (2003). Recent advances in conifer somatic embryogenesis: improving somatic embryo quality. *Plant Cell Tissue Organ Cult.* 74, 15–35.

Stasolla, C., Belmonte, M. F., Van Zyl, L., Craig, D. L., Liu, W., Yeung, E. C., et al. (2004a). The effect of reduced glutathione on morphology and gene expression of white spruce (*Picea glauca*) somatic embryos. *J. Exp. Bot.* 55, 695–709. doi: 10.1093/jxb/erh074

Stasolla, C., Bozhkov, P. V., Chu, T. M., Van Zyl, L., Egertsdotter, U., Suarez, M. F., et al. (2004b). Variation in transcript abundance during somatic embryogenesis in gymnosperms. *Tree Physiol.* 24, 1073–1085. doi: 10.1093/treephys/24.10.1073

Stasolla, C., van Zyl, L., Egertsdotter, U., Craig, D., Liu, W. B., and Sederoff, R. R. (2003). The effects of polyethylene glycol on gene expression of developing white spruce somatic embryos. *Plant Physiol.* 131, 49–60. doi: 10.1104/pp.015214

RStudio (2021). *Integrated Development Environment for R*. Boston, MA: RStudio, PBC.

Tereso, S., Zoglauer, K., Milhinhos, A., Miguel, C., and Oliveira, M. M. (2007). Zygotic and somatic embryo morphogenesis in *Pinus pinaster*: comparative histological and histochemical study. *Tree Physiol.* 27, 661–669. doi: 10.1093/treephys/27.5.661

Teyssier, C., Grondin, C., Bonhomme, L., Lomenech, A. M., Vallance, M., Morabito, D., et al. (2011). Increased gelling agent concentration promotes somatic embryo maturation in hybrid larch (*Larix* × *eurolepsis*): a 2-DE proteomic analysis. *Physiol. Plant.* 141, 152–165. doi: 10.1111/j.1399-3054.2010.01423.x

Teyssier, C., Maury, S., Beaufour, M., Grondin, C., Delaunay, A., Le Metté, C., et al. (2014). In search of markers for somatic embryo maturation in hybrid larch (*Larix* × *eurolepis*): global DNA methylation and proteomic analyses. *Physiol. Plant.* 150, 271–291. doi: 10.1111/ppl.12081

Vágner, M., Vondráková, Z., Strnadová, Z., Eder, J., and Macháčková, I. (1998). Endogenous levels of plant growth hormones during early stages of somatic embryogenesis of *Picea abies*. *Adv. Hortic. Sci.* 12, 11–18.

Vales, T., Feng, X., Ge, L., Xu, N., Cairney, J., Pullman, G. S., et al. (2007). Improved somatic embryo maturation in loblolly pine by monitoring ABA-responsive gene expression. *Plant Cell Rep.* 26, 133–143. doi: 10.1007/s00299-006-0221-7

Välimäki, S., Paavilainen, L., Tikkinen, M., Salonen, F., Varis, S., and Aronen, T. (2020). Production of Norway spruce embryos in a temporary immersion system (TIS). *In Vitro Cell. Dev. Biol. Plant* 56, 430–439. doi: 10.1007/s11627-020-10068-x

Vestman, D., Larsson, E., Uddenberg, D., Cairney, J., Clapham, D., Sundberg, E., et al. (2011). Important processes during differentiation and early development of somatic embryos of Norway spruce as revealed by changes in global gene expression. *Tree Genet. Genomes* 7, 347–362.

von Aderkas, P., Lelu, M. A., and Label, P. (2001). Plant growth regulator levels during maturation of larch somatic embryos. *Plant Physiol. Biochem.* 39, 495–502.

von Aderkas, P., Rohr, R., Sundberg, B., Gutmann, M., Dumont-BéBoux, N., and Lelu, M. A. (2002). Abscisic acid and its influence on development of the embryonal root cap, storage product and secondary metabolite accumulation in hybrid larch somatic embryos. *Plant Cell Tissue Organ Cult.* 69, 111–120.

von Arnold, S., and Hakman, I. (1988). Regulation of somatic embryo development in *Picea abies* by abscisic acid (ABA). *J. Plant Physiol.* 132, 164–169. doi: 10.1016/S0176-1617(88)80155-X

von Arnold, S., Clapham, D., and Abrahamsson, M. (2019). Embryology in conifers. *Adv. Bot. Res.* 89, 157–184. doi: 10.1016/bs.abr.2018.11.005

von Arnold, S., Clapham, D., Egertsdotter, U., and Mo, L. H. (1996). Somatic embryogenesis in conifers - A case study of induction and development of somatic embryos in *Picea abies*. *Plant Growth Regul.* 20, 3–9.

Vondrakova, Z., Dobrev, P. I., Pesek, B., Fischerova, L., Vagner, M., and Motyka, V. (2018). Profiles of endogenous phytohormones over the course of Norway spruce somatic embryogenesis. *Front. Plant Sci.* 9:1283. doi: 10.3389/fpls.2018.01283

Vondráková, Z., Eliášová, K., Vágner, M., Martincová, O., and Cvikrová, M. (2015). Exogenous putrescine affects endogenous polyamine levels and the development of *Picea abies* somatic embryos. *Plant Growth Regul.* 75, 405–414. doi: 10.1007/s10725-014-0001-2

Vondráková, Z., Trávníčková, A., Malbeck, J., and Cvikrová, M. (2013). "The effect of different desiccation treatments on polyamine metabolism of spruce somatic embryos," in *Proceedings of the 13th Conference of the Experimental Plant Biology*, Košice, 160.

Wang, W.-Q., Ye, J.-Q., Rogowska-Wrzesinska, A., Wojdyla, K. I., Jensen, O. N., Møller, I. M., et al. (2014). Proteomic comparison between maturation drying and prematurely imposed drying of *Zea mays* seeds reveals a potential role of maturation drying in preparing proteins for seed germination, seedling vigor, and pathogen resistance. *J. Proteome Res.* 13, 606–626. doi: 10.1021/pr4007574

Xiao, L., and Koster, K. L. (2001). Desiccation tolerance of protoplasts isolated from pea embryos. *J. Exp. Bot.* 52, 2105–2114. doi: 10.1093/jexbot/52.364.2105

Yathisha, N. S., Barbara, P., Gügi, B., Yogendra, K., Jogaiah, S., Azeddine, D., et al. (2020). Vegetative desiccation tolerance in *Eragrostiella brachyphylla*: biochemical and physiological responses. *Heliyon* 6:e04948. doi: 10.1016/j.heliyon.2020.e04948

Záveská-Drábková, L., Honys, D., and Motyka, V. (2021). Evolutionary diversification of cytokinin-specific glucosyltransferases in angiosperms and enigma of missing *cis*-zeatin *O*-glucosyltransferase gene in Brassicaceae. *Sci. Rep.* 11:7885. doi: 10.1038/s41598-021-87047-8

Zhou, X., Zheng, R., Liu, G., Xu, Y., Zhou, Y., Laux, T., et al. (2017). Desiccation treatment and endogenous IAA levels are key factors influencing high frequency somatic embryogenesis in *Cunninghamia lanceolata* (Lamb.) hook. *Front. Plant Sci.* 8:2054. doi: 10.3389/fpls.2017.02054

Conflict of Interest: The authors declare that the research was conducted in the absence of any commercial or financial relationships that could be construed as a potential conflict of interest.

Publisher's Note: All claims expressed in this article are solely those of the authors and do not necessarily represent those of their affiliated organizations, or those of the publisher, the editors and the reviewers. Any product that may be evaluated in this article, or claim that may be made by its manufacturer, is not guaranteed or endorsed by the publisher.

frontiers in Plant Science

ORIGINAL RESEARCH
published: 09 March 2022
doi: 10.3389/fpls.2022.824781

Effect of Methyl Jasmonate in Gene Expression, and in Hormonal and Phenolic Profiles of Holm Oak Embryogenic Lines Before and After Infection With *Phytophthora cinnamomi*

Marian Morcillo[1†], *Ester Sales*[2†], *Elena Corredoira*[3], *María Teresa Martínez*[3], *Juan Segura*[1] *and Isabel Arrillaga*[1*]

[1] Departamento de Biología Vegetal, Facultad de Farmacia, Instituto de Biotecnología y Biomedicina (BiotecMed), Universidad de Valencia, Valencia, Spain, [2] Departamento de Ciencias Agrarias y del Medio Natural, Instituto Universitario de Investigación en Ciencias Ambientales (IUCA), Universidad de Zaragoza, Escuela Politécnica Superior, Huesca, Spain, [3] Unidad Técnica Biotecnología y Mejora Forestal, Misión Biológica de Galicia, CSIC, Santiago de Compostela, Spain

The dieback syndrome affecting *Quercus ilex* and other oak species impels the search for tolerant plant genotypes, as well as methods of plant immunization against such infections. Elicitation treatments can be an effective strategy to activate plant defense response and embryogenic lines represent a promising tool to generate new tolerant genotypes and also to study early markers involved in defense response. The aim of the presented work was to investigate changes in gene expression, and in hormonal and phenolic profiles induced in three holm oak embryogenic lines (ELs) elicited with methyl jasmonate (MeJA) before and after infection with the oomycete *Phytophthora cinnamomi*, which is the main biotic agent involved in this pathogenic process. The three ELs, derived from three genotypes, showed different basal profiles in all tested parameters, noting that the VA5 naïve genotype from a scape tree was characterized by a basal higher expression in *NADPH-dependent cinnamyl alcohol dehydrogenase (CAD)* and *chalcone synthase* (*CHS)* genes and also by higher caffeic acid content. Our work also identifies changes triggered by MeJA elicitation in holm oak embryogenic lines, such as increases in ABA and JA contents, as well as in levels of most of the determined phenolic compounds, especially in caffeic acid in Q8 and E00 ELs, but not in their biosynthesis genes. Irrespective of the EL, the response to oomycete infection in holm oak elicited plant material was characterized by a further increase in JA. Since JA and phenols have been described as a part of the *Q. ilex* defense response against *P. cinnamomi,* we propose that MeJA may act as an induced resistance (IR) stimulus and that in our embryogenic material induced both direct (detected prior to any challenge) and primed (detected after subsequent challenge) defense responses.

Keywords: biotic stress, dieback, elicitor, epigenetic memory, induced resistance, phenols, *Quercus ilex*, somatic embryogenesis

OPEN ACCESS

Edited by:
Sandra Isabel Correia, University of Coimbra, Portugal

Reviewed by:
Nuria Alburquerque, Center for Edaphology and Applied Biology of Segura, Spanish National Research Council (CSIC), Spain
Melissa Hamner Mageroy, Norwegian Institute of Bioeconomy Research (NIBIO), Norway

***Correspondence:**
Isabel Arrillaga
isabel.arrillaga@uv.es

[†]These authors have contributed equally to this work

Specialty section:
This article was submitted to Plant Development and EvoDevo, a section of the journal Frontiers in Plant Science

Received: *29 November 2021*
Accepted: *26 January 2022*
Published: *09 March 2022*

Citation:
Morcillo M, Sales E, Corredoira E, Martínez MT, Segura J and Arrillaga I (2022) Effect of Methyl Jasmonate in Gene Expression, and in Hormonal and Phenolic Profiles of Holm Oak Embryogenic Lines Before and After Infection With Phytophthora cinnamomi. Front. Plant Sci. 13:824781. doi: 10.3389/fpls.2022.824781

INTRODUCTION

Holm oak (*Quercus ilex* L.) is the most abundant and representative species of the Mediterranean forests, from Portugal and Morocco to Turkey. Holm oak, however, is particularly abundant in Spain, where it occupies around 3 million ha, usually in mixed forests with *Pinus* spp., *Quercus coccifera* or *Q. suber* (Martínez et al., 2019). Besides its common presence in the Southwest natural forests of the Iberian Peninsula, *Quercus ilex* appears in ecosystems with anthropic origin and maintenance, the so-called *dehesas* in Spain, and *montados* in Portugal. These agrosilvo-pastoral systems support a diversity of ecologic and economical services, such as acorn, honey, and black truffle production (Montero et al., 2017), therefore contributing to sustainable rural development. These ecosystems also have a great landscape, and historical and cultural value, being part of the Special Areas of Conservation defined in EU Council Directive 92/43/EEC (Council of Europe, UNEP and ECNC, 1996).

Despite their great ecological and economical value, these Mediterranean ecosystems are seriously threatened by holm oak decline, a disease also affecting cork oak (*Quercus suber),* and that is mainly caused by the oomycete *Phytophthora cinnamomi*. Abiotic stresses, such as drought, combined with biotic stresses and the low natural regeneration rates observed for these tree species (González-Rodríguez et al., 2011), result in a complex problem aggravated by climate change. The Mediterranean area has been reported to be the most prominent climate change hot-spot, along with Northeastern Europe, according to a Regional Climate Change Index (RCCI) that estimated a large decrease in mean precipitation and an increase in precipitation variability during the dry (warm) season (Giorgi, 2006). As these expected climatic conditions, as mentioned, would favor pathogen infections in holm oak roots, there is an urgent need in obtaining cork- and holm oak plant material more adapted to upcoming ecological restrictions, and with improved tolerance to *P. cinnamomi*.

With this aim, in Spain, during the past decades, coordinated projects have implemented prevention and restoration strategies to protect natural forests and dehesas, as well as the selection of tolerant individuals in infested areas. Recently, a national program for breeding and conservation of cork- and holm oak genetic resources against the decline syndrome has also been established. For exploiting all the genetic variability existing in natural populations, superior genotypes should be vegetatively propagated, but this task is hampered by the low rooting capability of oak cuttings, which is even reduced with the aging of the trees (Martínez et al., 2020, 2021). In this context, biotechnological tools such as somatic embryogenesis constitute an interesting alternative allowing clonal propagation of holm oak adult trees (Blasco et al., 2013; Barra-Jiménez et al., 2014; Martínez et al., 2017, 2020, 2021), although acclimatization of generated plants needs to be improved. Furthermore, combining somatic embryogenesis with chemical elicitors it is possible to induce resistance triggering natural plant defenses, as a complementary strategy to breeding programs developed to obtain resilient plant material (Morcillo et al., 2020). Induced resistance (IR) is a plant state associated with an enhanced ability to resist pests and pathogen attacks or abiotic stress after an inducing stimulus. The IR phenotype is mediated by direct and primed defense responses. Defense priming refers to earlier and faster or stronger activation of cellular defense responses when the plant is subsequently challenged with the biotic or abiotic stress, and it is associated with alterations that take place directly upon IR stimulation, such as epigenetic alterations, increased receptor presence, or accumulation of hormones, among others (De Kesel et al., 2021).

Phytohormones play vital roles in plant responses to biotic and abiotic stressors and elicitors (Wang et al., 2021). Among them, abscisic acid (ABA) has been described as a pivotal hormone in plant stress defense, and its interaction with other hormones, mainly jasmonic acid (JA), salicylic acid (SA) and ethylene (ET) have also been described (Ku et al., 2018; Yang et al., 2019; Deboever et al., 2020; Bharath et al., 2021). Plant induced systemic response (ISR) depends on responsiveness to JA and ethylene rather than to SA (Goellner and Conrath, 2008; Han and Kahmann, 2019; Yang et al., 2019). In recent years, exogenous application of methyl-jasmonate (MeJA) to plant *in vitro* cultures has emerged as a novel technique for inducing hyperaccumulation of secondary metabolites (Ho et al., 2018). In addition, it has been demonstrated that this elicitor activates antioxidant enzymes and upregulates the expression of defense-related genes (Ho et al., 2020). In a previous work (Morcillo et al., 2020), we tested several elicitation treatments and found that applying 50 μM MeJA in liquid medium for 3 days to holm oak embryogenic lines (ELs) increased H_2O_2 production after being challenged against active oomycete, without altering somatic embryos development. Since plant defense responses have been reported to be mediated by H_2O_2 production (Lin et al., 2005; Wang et al., 2015), and the role of reactive oxygen species (ROS) in plant resistance to fungal pathogens is well-established (Lehmann et al., 2015), the higher H_2O_2 content in these MeJA treated embryos indicates activation of defense mechanisms. Corroborating this, we observed lower mycelium growth rates toward control than toward MeJA-elicited holm oak somatic embryos in dual cultures confronted to *P. cinnamomi* (Morcillo et al., 2020), although the oomycete development was not inhibited.

Several studies reported on the importance of secondary metabolites, mainly phenol-derivates, for the susceptible and resistant interaction between woody species and *P. cinnamomi* (Cahill et al., 1992). Also, during pathogen attack the phenylpropanoid pathway genes were found to be overexpressed, resulting in increasing activities and accumulation of various phenolic compounds (Yadav et al., 2020). More recently, our group demonstrated that axillary shoots from tolerant holm oak genotypes established *in vitro* had higher total phenol content than other susceptible genotypes (Martínez et al., 2021).

The aim of this study was to determine whether priming holm oak embryogenic lines with MeJA modifies gene expression and hormone and phenolic profiles before and after infection with *P. cinnamomi*. For this purpose, three holm oak genotypes (E00, Q8,

and VA5), one of them (VA5) being a tolerant tree selected in our breeding program, were tested.

MATERIALS AND METHODS

Plant and Oomycete Material

The experiments were undertaken with three ELs established from the E00, Q8, and VA5 holm oak genotypes. Embryogenic lines E00 and Q8, generated as described in Barra-Jiménez et al. (2014), were kindly provided by Dr. M. Toribio from IMIDRA (Instituto Madrileño de Investigación y Desarrollo Rural, Agrario y Alimentario, Madrid, Spain), while the VA5 line was established in our lab from male catkins of an "escape" tree, following the protocols described in Blasco et al. (2013). The genotype VA5 is a 50–100-year-old holm oak located in Mount of Vallivana (Castellón, Spain, 40°31'60"N, 0°1'0"E) that grows in soil naturally infested with *Phytophthora cinnamomi* and does not present symptoms of decline. Genotypes Q8 (Quintos de Mora, Los Yémenes, Toledo, Spain, 39°24'23"N, 4°4'19"W) and E00 (El Encín, Alcalá de Henares, Madrid, Spain, 40°3'02"N, 3°17'11"W) have not been previously exposed to *P. cinnamomi*, since they grow in an area not affected by the oomycete. The three ELs were routinely maintained in MS (Murashige and Skoog, 1962) medium supplemented with 20 μM silver thiosulfate and 4 g/L activated charcoal (named after MS/STS/AC medium), conditions that induced secondary embryogenesis, as described by Martínez et al. (2015).

Phytophthora cinnamomi strain 1,630 was kindly provided by Dr. P. Abad (group Phytopathogenic fungi, Instituto Agroforestal Mediterráneo—Universidad Politécnica de Valencia, Spain) and was maintained in PDA medium (Potato Dextrose Agar, Pronadisa, Spain) by subculturing mycelium pieces of 0.5 cm^2 to fresh medium every 15 days.

Elicitation and Infection Treatments

For each holm oak embryogenic line, three aliquots of about 1 g of plant material containing somatic embryos at the globular stage were cultured for 3 days in 250 mL Erlenmeyer flasks containing 40 mL of Elicitin Secretion Medium (ESM, Horta et al., 2008) supplemented with 50 μM MeJA, as described in Morcillo et al. (2020). After this period, plant material was recovered by filtering and was transferred to MS/STS/AC medium.

Suspensions of *P. cinnamomi* strain 1,630 were prepared by inoculating in flasks with 40 mL of ESM, 5 sections of 0.5 cm^2 of mycelium, taken from 10-days-old PDA cultures. Flasks were then incubated under agitation (50 rpm) and in the dark, in a growth chamber at 23 ± 2°C for 4 days. Subsequently, oomycete cultures were filtered (Whatman® paper N2) and the liquid extract was diluted to 20% (v/v) with ESM. Samples (1 g) of control and elicited embryogenic material, cultivated in MS/STS/AC medium for 14 days, were immersed for 3 h in 40 mL of this oomycete suspension, and then recovered by filtering and transferred again to solid plates containing MS/STS/AC medium. After 24 h, plant material was either frozen in liquid nitrogen or lyophilized, and stored at −80°C until analysis. For each line and treatment, 3 replicates were prepared.

Gene Expression Analysis

We investigated by qPCR the expression of four genes coding for key enzymes involved in phenolic compounds synthesis: *chorismate synthase* (*CS*), *phenylalanine-ammonia-lyase* (*PAL*), *NADPH-dependent cinnamyl alcohol dehydrogenase* (*CAD1*), and *chalcone synthase* (*CHS*), using primers designed for *Quercus suber* by Chaves et al. (2011). An elongation factor (*EF*) was used as a reference gene, with primers designed by Soler et al. (2008). Total RNA isolation from 0.1 g of frozen aliquots of holm oak embryogenic cell lines was performed using the Plant and Fungi RNA isolation kit (Norgen Biotek, Thorold, Canada). After treatment with DNase (Takara Bio Inc., Japan), 1 μg of RNA from each sample was used to synthetize cDNA with a reverse transcriptase kit (Takara Bio Inc., Japan). Amplifications were performed as described in Martínez et al. (2021). Gene expression was estimated by the $2^{-\Delta CT}$ method described by Pfaffl (2001).

Hormone Content Determinations

The content in three hormones regulating biotic stress response (ABA, JA, and SA) was determined using lyophilized samples (25 ± 3 mg) of control and elicited and/or infected holm oak ELs. Homogenized material was extracted with 80% methanol acidified with 1% acetic acid. At this point, internal standards (deuterium-labeled hormones from OlChemim Ltd., Olomouc, Czeck Republic), were also added. Extracts were obtained in agitation at 4°C for 1 h, then were maintained overnight at −20°C, and then evaporated under vacuum. Dry residues were dissolved in 1% acetic acid aqueous solution and injected in a reverse phase column (HLB Oasis 30 mg, Waters Corporation, USA), as described by Seo et al. (2011). After that, samples were dried again and finally resuspended in 5% acetonitrile acidified with 1% acetic acid. These extracts were analyzed by LC/MS/MS (Instituto de Biología Molecular y Celular de Plantas, IBMCP, Valencia) using a Q-Exactive Orbitrap™ (Thermo Fisher Scientific, USA) that was equipped with a reverse phase column Accucore C18 (2.6 mm, 100 mm; Thermo Fisher Scientific, USA), and coupled to a mass spectrometer. Hormones were separated in a gradient of 2–55% acetonitrile acidified with 0.05% acetic acid, with a flow rate of 0.4 mL/min for 21 min. Analysis conditions were as follows: capillar temperature, 300°C; ionization spray voltage 3.0 kV; heater temperature, 150°C; gas flow 40 mL/min; auxiliary gas flow, 10 mL/min; negative mode. Contents in ABA, JA, and SA were determined using integrated calibration curves and software Xcalibur 4.0 and TraceFinder 4.1 SP1.

Phenolic Content Determinations

Samples (0.1 mg) of lyophilized material from control, elicited and infected E00, Q8, and VA5 ELs were extracted with 1 mL of 80% methanol for 30 min in an ultrasonic bath. Three replicated samples were prepared for each line and treatment. After being filtered (0.22 μm), extracts were analyzed by UPLC/QTOF. Analyses were performed in a UPLC-QTOF system (ABSciex TripleTOF™ 5600 LC/MS/MS, Servicio Central de Apoyo a la Investigación Experimental, SCSIE, Universidad de Valencia) with a Waters UPLC C18 column (50 mm x 2.1, 1.7 μm). The mobile phase was a gradient of methanol and water (**Table 1**),

TABLE 1 | Gradient of elution used for separating phenolic compounds by UPLC/QTOF.

Time (min)	H_2O 0.1% Formic acid	MeOH 0.1% Formic acid
0	90	10
2	90	10
13	0	100
15	0	100
15.1	90	10
22	90	10

both acidified with 0.1% formic acid, at a flow rate of 0.4 mL/min. Accumulating time was 100 ms, and ionization conditions were: ion source 50 psi, curtain gas 1:25 psi, temperature 400°C, voltage (ISVF)−4500, and collision energy−50. Acquisition data was performed in negative mode, in a mass range of 80–1,200 m/z.

Among the detected compounds, it was possible to quantify four phenolic acids (caffeic, ellagic, ferulic and sinapic), the flavanol quercetin, and a proanthocyanidin, prodelphinidin B3. We obtained calibration curves using 6 serial dilutions (25–1,000 mg/mL) of reference standards of the four acids (Sigma- Aldrich, USA), and a reference standard of quercetin-3-O-glucoside (Extrasynthese, Genay Cedex, France).

Statistical Analysis

Data were analyzed by analysis of variance (ANOVA), and are presented as mean ± standard error of three independent replications. When appropriate, treatment means were separated using *t*-test or Tukey's HSD. Data that not followed a normal distribution were analyzed by the Kruskal-Wallis non-parametric ANOVA and values distributions pairwise comparison. Correlation coefficients were also estimated among the determined parameters. All statistical analyses were performed using SPSS for Windows, version 26 (SPSS Inc., Chicago, IL, USA). A principal component analysis was performed using R software (R Core Team, 2020).

RESULTS

Gene Expression Patterns in Elicited and Infected Holm Oak Embryogenic Material

Our qPCR analysis of the transcription of four genes regulating phenols biosynthesis in holm oak ELs showed significant differences in the expression patterns that varied among lines and treatments, but results depended on the studied gene. When averaged among treatments, expression of the *CS* gene varied among genotypes ($p < 0.001$), and the response to infection and elicitation treatments also differed in each holm oak line. Basal expression of the *CS* gene depended on the line ($p = 0.002$), since control samples of ELs from genotype E00 showed significantly lower expression levels than those from Q8 and VA5 (**Table 2**). Furthermore, these low expression levels in E00 control plant material were not affected by elicitation with MeJA and/or infection with *P. cinnamomi,* while these treatments affected *CS* gene expression in the other two lines ($p = 0.046$ and $p = 0.011$ for Q8 and VA5, respectively). However, significant differences were observed only after infection of control or elicited Q8 embryogenic material, and after elicitation in the VA5 line, in which this treatment reduced *CS* gene expression but levels were recovered after infection (**Table 2**). Expression pattern of the *PAL* gene did not vary significantly among lines but was significantly affected by treatment ($p = 0.014$), since infection with *P. cinnamomi* induced higher levels of expression of this gene, particularly in elicited material (2-fold increase). In contrast, *CAD* gene expression (**Table 2**) significantly differed among lines ($p = 0.016$), since on average it was significantly lower in E00 ($2^{-\Delta CT} = 0.27 \pm 0.04$) than in VA5 ($2^{-\Delta CT} = 0.44 \pm 0.02$), the values of which did not differ from those determined in plant material from the Q8 line ($2^{-\Delta CT} = 0.36 \pm 0.02$). Elicitation and infection treatments did not affect *CAD* expression in the three analyzed holm oak ELs. Finally, *CHS* gene expression pattern varied among lines ($p = 0.049$), being on average significantly higher in E00 embryogenic material ($2^{-\Delta CT} = 0.014 \pm 0.002$) than in that from the Q8 line ($2^{-\Delta CT} = 0.009 \pm 0.002$), while VA5 material showed intermediate values ($2^{-\Delta CT} = 0.012 \pm 0.005$). Elicitation and infection treatments also differentially affected *CHS* gene expression in the three lines ($p = 0.007$), since it remained unchanged in E00 (**Table 2**), but was significantly repressed after infection in elicited material of Q8 and in control and elicited material of VA5. Specific comparations on gene expression between treatments are depiced in **Supplementary Figure 1** corroborating that gene expression patterns depended on the genotype.

Interestingly, we estimated significant correlations among expression levels of some genes, since samples with higher transcription abundance of the *CS* gene also showed higher expression levels of both *PAL* ($\rho = 0.681$, $p < 0.001$) and *CAD* ($\rho = 0.476$, $p = 0.003$) genes. Furthermore, expression rates of these two genes also showed significant positive correlation ($\rho = 0.388$, $p = 0.019$).

Hormone Profiles in Elicited and Infected Holm Oak Embryogenic Cultures

Levels of ABA determined in *Q. ilex* embryogenic lines were on average similar among lines, but elicitation with 50 μM MeJA and infection with *P. cinnamomi* affected differentially the production of this hormone in embryogenic material from the three analyzed genotypes (**Figure 1A**). Non- parametric analyses showed that basal levels of ABA were significantly higher in Q8 cells than in those from E00 and VA5 genotypes (40.10 ± 0.35 ng/g DW front to 11.15 ± 0.09 and 13.25 ± 0.26 ng/g DW, respectively; $p = 0.027$). This higher content determined in Q8 ELs was significantly reduced after elicitation (2-fold decrease) and also after infection (3-fold decrease), and when both treatments were combined (9-fold decrease). The low basal levels determined in control material from E00 and VA5 were also significantly altered after elicitation and infection treatments ($p = 0.015$ and $p = 0.024$, respectively), since they were slightly reduced after infection and increased after MeJA elicitation.

TABLE 2 | Expression of *chorismate synthase* (*CS*), *phenylalanine-ammonia-lyase* (*PAL*), *NADPH-dependent cinnamyl alcohol dehydrogenase* (*CAD*), and *chalcone synthase* (*CHS*) genes in embryogenic lines from E00, Q8, and VA5 *holm oak* genotypes.

	Treatment	E00	Q8	VA5	Mean
CS	Control	0.005 ± 0.002	0.036 ± 0.004	0.038 ± 0.005	0.026 ± 0.011
	Infected	0.009 ± 0.002	0.056 ± 0.008	0.032 ± 0.005	0.032 ± 0.014
	Elicited	0.004 ± 0.000	0.038 ± 0.004	0.011 ± 0.002[x]	0.017 ± 0.010
	Elicited + Infected	0.009 ± 0.001	0.032 ± 0.003	0.030 ± 0.005	0.024 ± 0.008
PAL	Control	0.056 ± 0.018	0.103 ± 0.018	0.120 ± 0.037	0.093 ± 0.019
	Infected	0.104 ± 0.024	0.155 ± 0.025	0.116 ± 0.035	0.125 ± 0.016
	Elicited	0.044 ± 0.008	0.110 ± 0.012	0.021 ± 0.002	0.058 ± 0.027
	Elicited + Infected	0.131 ± 0.023	0.086 ± 0.015	0.135 ± 0.046	0.117 ± 0.016[y]
CAD	Control	0.205 ± 0.072	0.306 ± 0.090	0.450 ± 0.027	0.320 ± 0.071
	Infected	0.284 ± 0.074	0.382 ± 0.051	0.424 ± 0.019	0.363 ± 0.042
	Elicited	0.212 ± 0.026	0.398 ± 0.039	0.467 ± 0.075	0.359 ± 0.076
	Elicited + Infected	0.360 ± 0.112	0.338 ± 0.005	0.400 ± 0.154	0.366 ± 0.018
CHS	Control	0.017 ± 0.004	0.007 ± 0.002	0.024 ± 0.008	0.016 ± 0.005
	Infected	0.013 ± 0.002	0.007 ± 0.002	0.005 ± 0.001[y]	0.008 ± 0.002
	Elicited	0.014 ± 0.002	0.015 ± 0.003	0.015 ± 0.002	0.015 ± 0.000
	Elicited + Infected	0.012 ± 0.002	0.006 ± 0.001[y]	0.003 ± 0.001[y]	0.007 ± 0.003

Samples were taken from control and elicited with 50 μM methyl-jasmonate embryogenic lines, before and after infection with a suspension of P. cinnamomi. Data are mean ± SE of triplicated amplifications performed with three biological replicates of each treatment and line.

[x] *Significantly affected by elicitation, $p < 0.05$ according to t-test.*

[y] *Significantly affected by infection, $p < 0.05$ according to t-test.*

We found very low basal levels of JA in holm oak ELs (on average 41.22 ± 32.59 ng/g DW), particularly in plant material from E00 and VA5 genotypes, and these levels were significantly affected by elicitation and infection treatments ($p < 0.001$). Jasmonic acid contents did not increase significantly after infection with *P. cinnamomi* (on average 70.08 ± 13.22 ng/g DW), while levels of this hormone increased significantly (about 9-fold) in embryogenic material from the three genotypes after the elicitation treatment (**Figure 1B**). Infection of this elicited material resulted in even higher contents of JA (3-fold increase). These changes were observed in embryogenic cells from the three analyzed genotypes, without significant differences among lines in their JA content ($p = 0.388$).

Levels of SA in holm oak ELs varied among lines ($p < 0.001$) and were also affected differentially by elicitation and infection treatments, which significantly altered SA contents of E00 ($p = 0.043$) and Q8 ($p = 0.024$) lines, but not those determined in VA5 plant material ($p = 0.578$). Basal SA levels in embryogenic material from the Q8 genotype were significantly higher than those found in material from E00 and VA5 genotypes ($p = 0.027$). Infection with *P. cinnamomi* significantly affected SA content in material from the E00 genotype, since it increased from 24.73 ± 1.64 ng/g DW determined in control samples to 54.67 ± 7.77 ng/g DW in the infected ELs, and SA levels were also significantly higher (53.27 ± 1.23 ng/g DW) in elicited and infected E00 material (**Figure 1C**). In contrast, after infection with *P. cinnamomi* we observed in embryogenic material from the Q8 genotype reduced SA contents, but this effect was significant only for elicited material (from 260.85 ± 0.14 to 65.40 ± 13.63 ng/g DW).

Phenolic Content Determinations

Non-parametric one-way analysis of variance found significant differences among lines for ellagic, ferulic, and sinapic acid contents ($p < 0.001$, $p < 0.001$, and $p = 0.009$, respectively). These differences were explained by the higher levels of ellagic acid determined in E00 plant material, in contrast to those found in ELs from Q8 and VA5 genotypes, and by the lower ferulic and sinapic acids contents determined in material from the VA5 line.

A Kruskal-Wallis test also revealed that caffeic acid contents of holm oak ELs were significantly affected by elicitation and infection treatments ($p < 0.001$), and the variation observed in pairwise comparisons depended on the genotype. Basal levels of caffeic acid determined in embryogenic material from the tolerant VA5 genotype were significantly higher than those found in control material from E00 and Q8 genotypes (1,6746 ± 2,364 front to 7,493 ± 2,609 and 5,194 ± 1,469 ppb, respectively, $p = 0.022$). After elicitation with 50 μM MeJA, caffeic acid content increased significantly in these two E00 and Q8 ELs (on average 2.7-fold), while decreasing in VA5 plant material in a similar rate (**Figure 2A**). Infection with *P. cinnamomi* reduced caffeic acid levels in both control and elicited plant material from the three genotypes (**Figure 2A**), but these differences were significant for control material of the VA5 genotype (11-fold decrease) and for elicited material from the E00 and Q8 lines (6-fold decrease on average).

Ellagic acid content depended on the genotype, as mentioned, and significant differences were also observed among treatments for the three ELs ($p = 0.033$, $p = 0.034$, and $p = 0.016$ for E00, Q8 and VA5 lines, respectively). Levels determined in control samples varied significantly among lines ($p = 0.039$), since those from the E00 genotype were higher than those determined in

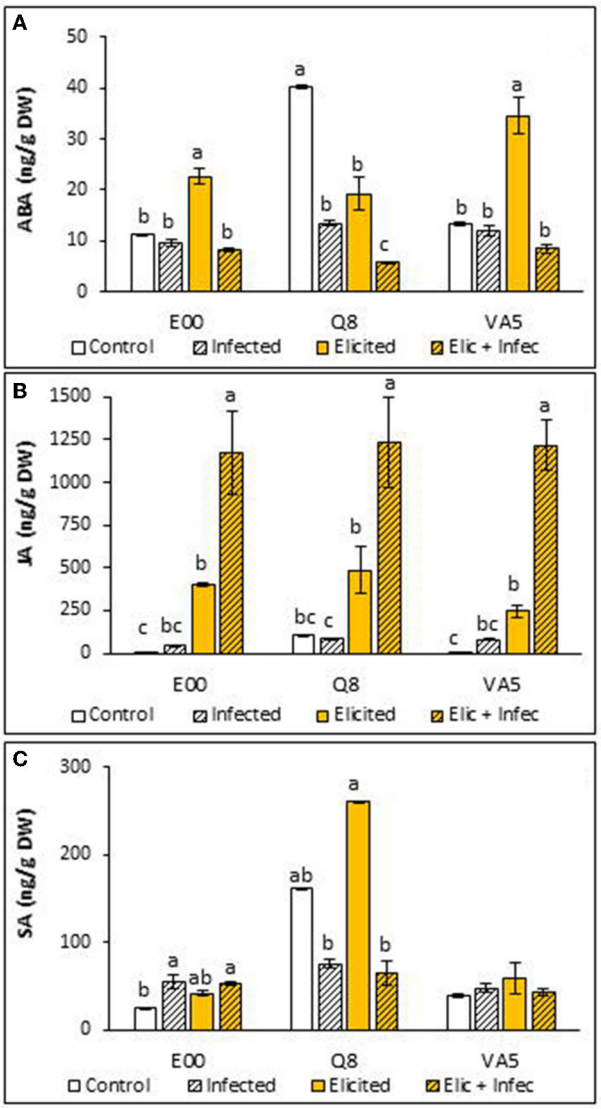

FIGURE 1 | Hormones content in control and elicited with 50 μM methyl-jasmonate embryogenic lines from three *Quercus ilex* genotypes (E00, Q8, and VA5), before and after infection with *P. cinnamomi*. For each line and treatment, data are mean ± SE of abscisic acid **(A)**, jasmonic acid **(B)** and salicylic acid **(C)** determinations, performed by triplicate. Within each line, values followed by the same letter did not differ significantly ($p < 0.05$) from one another, according to distribution pairwise comparisons in a Kruskal-Wallis test.

Q8 samples, while embryogenic material from the VA5 genotype showed intermediate values (**Figure 2B**). Irrespective of the genotype, these basal levels were not significantly affected by the elicitation treatment. The higher initial rates determined in E00 embryogenic material remained unchanged also after infection with *P. cinnamomi*. In contrast, infection increased ellagic acid content in samples (elicited or not) from Q8 and VA5 ELs, although this increase was not significant for elicited Q8 material, which contrasted with the drastic increase (3.7-fold) observed in elicited material from the E00 genotype.

Elicitation and infection treatments affected ferulic acid content of holm oak embryogenic lines, since significant differences were observed among E00 ($p = 0.016$), Q8 ($p = 0.025$) and VA5 ($p = 0.016$) samples. In E00 and Q8 ELs elicitation with 50 μM MeJA significantly increased ferulic acid contents, while the low basal levels observed in VA5 remained unaffected (**Figure 2C**). This differential response to the elicitation treatment was more evident in infected samples, since ferulic acid contents of control embryogenic material from the three genotypes did not change after exposure to *P. cinnamomi*, while were significantly reduced in elicited embryogenic cultures from E00 and Q8 genotypes and significantly increased in those from the VA5 genotype (**Figure 2C**).

Regarding sinapic acid contents, the responses of ELs to elicitation and infection treatments depended on the genotype but significant differences were also observed ($p = 0.041$, $p < 0.001$, and $p = 0.003$ for E00, Q8, and VA5 plant material, respectively). Basal sinapic acid levels were significantly different among the three analyzed lines ($p < 0.001$), since plant material from the Q8 line showed initially higher contents (8,244 ± 924 ppb) than those from E00 and VA5 genotypes (2,124 ± 53 and 504 ± 206 ppb, respectively). Elicited samples from E00 and Q8 lines showed increased levels of this acid as compared to controls (**Figure 2D**), but this difference was significant only for E00 plant material. The sinapic acid contents determined in embryogenic cells from the VA5 genotype were not affected by the MeJA priming treatment, while increasing significantly after infection with *P. cinnamomi*. Sinapic acid production slightly increased in infected material from the E00 genotype, while infection of elicited E00 material with *P. cinnamomi* induced a significant 25-fold decrease in this acid (**Figure 2D**). Finally, infection of Q8 control and elicited material slightly reduced sinapic acid levels in this line.

Quercetin contents of holm oak ELs were significantly affected by elicitation and infection treatments ($p = 0.001$), since on average levels of this flavanol decreased after infection as compared to control and elicited material, but the response depended on the genotype of the EL (**Figure 2E**). No significant differences were observed among samples from the Q8 line ($p = 0.090$), while elicitation and infection treatments affected quercetin contents of E00 and VA5 lines ($p = 0.024$ and $p = 0.019$).The lower levels determined in control E00 material drastically increased after elicitation with MeJA (about 18-fold), and decreased after infection with *P. cinnamomi* (about 8-fold). In contrast, infection with the oomycete significantly reduced the quercetin content of VA5 embryogenic material, that was not affected by the elicitation treatment.

Prodelphinidin B3 contents determined in holm oak ELs did not vary among lines ($p = 0.214$) and were on average not affected by elicitation and infection treatments ($p = 0.522$). However, when the ANOVA was performed separately for each genotype, we corroborated this result for the E00 genotype, but we found significant variation among treatments for the Q8 line ($p < 0.001$), since prodelphinidin B3 was not detected in infected

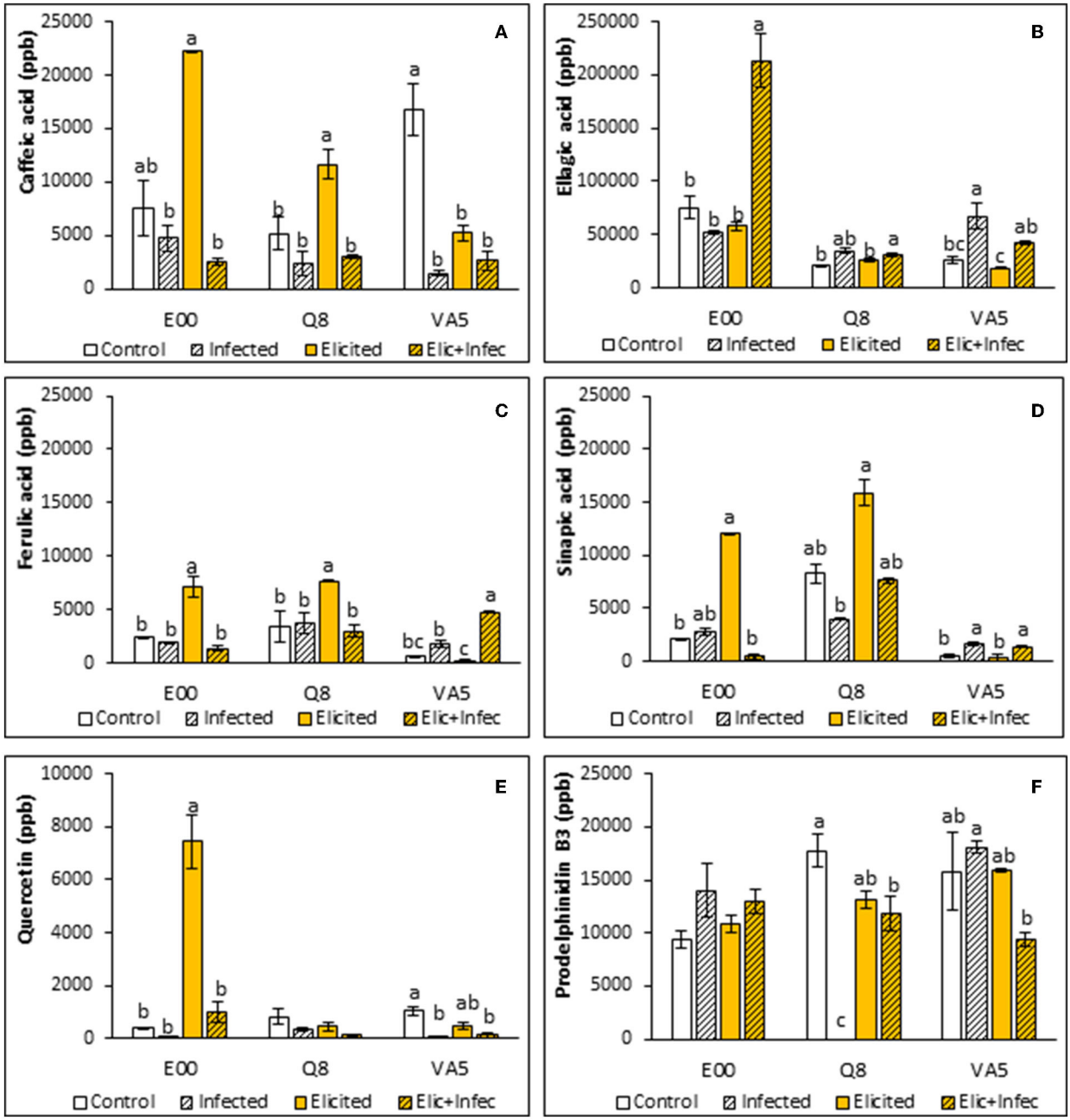

FIGURE 2 | Phenolic compounds content in control and elicited with 50 μM methyl-jasmonate embryogenic material from three *Quercus ilex* genotypes (E00, Q8, and VA5), before and after infection with *P. cinnamomi.* For each line and treatment, data are mean ± SE of caffeic acid **(A)**, ellagic acid **(B)**, ferulic acid **(C)**, sinapic acid **(D)**, quercetin **(E)**, and prodelphinidin B3 **(F)** determinations, performed by triplicate. Within each line, values followed by the same letter did not differ significantly ($p < 0.05$) from one another, according to distribution pairwise comparisons in a Kruskal-Wallis test.

material and decreased significantly in elicited and infected ELs from this genotype (**Figure 2F**). In contrast, infection with *P. cinnamomi* increased prodelphinidin B3 content in non-elicited material from the VA5 genotype, while levels of this anthocyanidin decreased after infection of MeJA treated samples.

When results from the three holm oak genotypes and four treatments were combined, we found that higher levels of ferulic acid significantly correlated with higher levels of sinapic acid ($\rho = 0.761$, $p < 0.001$ and with lower levels of prodelphinidin B3 ($\rho = -0.385$, $p = 0.020$). We also found a significant positive correlation between caffeic acid and quercetin contents ($\rho = 0.499$, $p = 0.002$). Phenolic compounds accumulation was also correlated to hormone contents, since higher levels of ABA were associated to higher contents in caffeic acid ($\rho = 0.467$, $p = 0.004$)

and quercetin ($\rho = 0.488$, $p = 0.003$), and with lower levels of ellagic acid ($\rho = -0.545$, $p = 0.001$). Increases in JA contents were positively correlated with increases in ferulic acid content ($\rho = 0.338$, $p = 0.044$), while levels of SA showed significant positive correlation with sinapic acid content ($\rho = 0.467$, $p = 0.004$) and negative correlation with ellagic acid content ($\rho = -0.431$, $p = 0.009$). Finally, we also estimated significant correlations between phenolic compounds contents and levels of expression of genes related to phenol metabolism, since ellagic acid content was inversely correlated to higher levels of expression of *CS* ($\rho = -0.476$, $p = 0.003$) and *CAD* ($\rho = -0.343$, $p = 0.040$) genes, while expression of the *PAL* gene was inversely correlated to caffeic acid content ($\rho = -0.351$, $p = 0.036$). In contrast, expression of the *CHS* gene was positively correlated to caffeic acid ($\rho = 0.636$, $p < 0.001$) and quercetin ($\rho = 0.512$, $p = 0.001$) contents. Expression of this gene was inversely correlated with JA levels ($\rho = -0.340$, $p = 0.042$), while higher contents in SA were significantly associated with higher expression rates of the *CS* gene ($\rho = 0.440$, $p = 0.007$).

These relationships among the determined variables can be observed in a principal component analysis (PCA) that resumes variability found in holm oak ELs after the elicitation and infection treatments (**Figure 3**). Higher variation was found in the response of ELs to the elicitation treatment, that was characterized by increases in *CHS* gene expression and in ABA and SA contents, as well as in levels of most of the determined phenolic compounds. Infection with *P. cinnamomi* of either control or elicited holm oak ELs was mainly characterized by overexpression of *CS*, *PAL,* and *CAD* genes, and by higher contents in JA and, in a less extent, in ellagic acid.

DISCUSSION

Holm oak decline in the Southwest of the Iberian Peninsula is caused by abiotic (climate and edaphic conditions, topography, and inter and intraspecific competence) and biotic factors such as xylophagous insects and pathogens, particularly the oomycete *Phytophthora cinnamomi* (González-Rodríguez et al., 2011; Duque-Lazo et al., 2018). In this scenario, it is necessary to generate new genotypes with an increased resilience to the pathogen, as well as to develop tools to identify tolerant genotypes. With this aim, we tested whether priming holm oak embryogenic lines with MeJA induces a primed phenotype associated to changes in gene expression and in hormones and phenolic profiles, and if these profiles are modified after challenging plant material to the oomycete.

The four genes of which expression was analyzed in this work *(CS, PAL, CAD,* and *CHS*) have been reported as candidate genes in cork oak response to the oomycete (Oßwald et al., 2014), and are related to the biosynthesis of phenylpropanoids (Martínez et al., 2021). The VA5 embryogenic line, generated from a tolerant tree, displayed a basal phenotype with high expression in *PAL*, *CAD,* and *CHS* genes, as compared to E00 and Q8 lines. Elicitation of VA5 line with MeJA decreased or did not alter the expression of these genes while increasing *CHS* gene expression in the other genotypes (**Supplementary Figure 1A**). Although differences were not significant, we observed a trend of increased expression of *CS, PAL,* and *CAD* genes after infection with oomycete in lines E00 and Q8, but not in the VA5 line (**Supplementary Figure 1B**). Besides, the expression of the *CHS* gene was significantly repressed in infected material from the tolerant genotype, while it remained unaffected in E00 and Q8 embryogenic cells. In contrast, *PAL* and *CHS* genes were upregulated when *in-vitro* derived shoots established from the VA5 genotype were confronted for 17 days with *P. cinnamomi* in dual cultures (Martínez et al., 2021) corroborating that the transcriptional level of genes coding for *PAL* and *CHS* enzymes is tissue-dependent (Rubio-Rodríguez et al., 2021). Both, *PAL* and *CS* genes were upregulated after infection of the elicited VA5 and E00 lines, respectively (**Supplementary Figure 1C**). Some studies show that the induction of an enhanced stress response by stimulation with pathogen virulent strains or elicitors such as SA or BTH is only evident after a subsequent infection with the active pathogen (Mur et al., 1996; Cameron et al., 1999; van Wees et al., 1999; Kohler et al., 2002). In our work, however, none of the genes studied was upregulated when the MeJA-primed lines were challenged with the oomycete as compared to infected controls (**Supplementary Figures 1B,C**). These results could be explained by a decline in the expression at the time that samples were collected (14 days after elicitation) as described in Milan et al. (2017) or by the suppression of gene expression induced by some metabolites which are produced by the phenylpropanoid pathway, as described in Rubio-Rodríguez et al. (2021). Uncorrelation between terpene metabolite production and the expression of their biosynthesis genes was reported in a MeJA-treated genotype of Norway spruce (Mageroy et al., 2020).

The degree of plant resistance to stress is influenced by systemic signals mediated by phytohormones; thus, SA-mediated signaling triggers resistance against biotrophic and hemi-biotrophic pathogens, while the signal mediated by the combination of JA and ET activates resistance to necrotrophic pathogens. Although JA and SA signaling pathways are currently described as antagonistic, other studies show that JA-mediated defenses are also effective against biotrophic or hemi-biotrophic pathogens (Han and Kahmann, 2019). In our study, ABA, JA, and SA contents were determined in embryogenic lines E00, Q8, and VA5. Elicitation caused a generalized increase in ABA concentration, except in the Q8 line, which basal levels were much higher than those from the other two lines; infection induced an ABA decrease, only significant in the samples that had been previously elicited. ABA is involved in the initiation of adaptative responses to various environmental conditions, although in relation to disease resistance its effect has been considered to be negative (Mauch-Mani and Mauch, 2005) which may be explained by the role of ABA in the inhibition of phytoalexin biosynthesis and *PAL* transcripts accumulation, in addition to being used by pathogens as an effector molecule (Lievens et al., 2017). There is also evidence that ABA interferes at different levels with the biotic stress response pathways mediated by SA and JA/ET (de Torres Zabala et al., 2009). However, several studies report a positive effect of ABA accumulation in terms of resistance to diseases caused by viruses, due to its

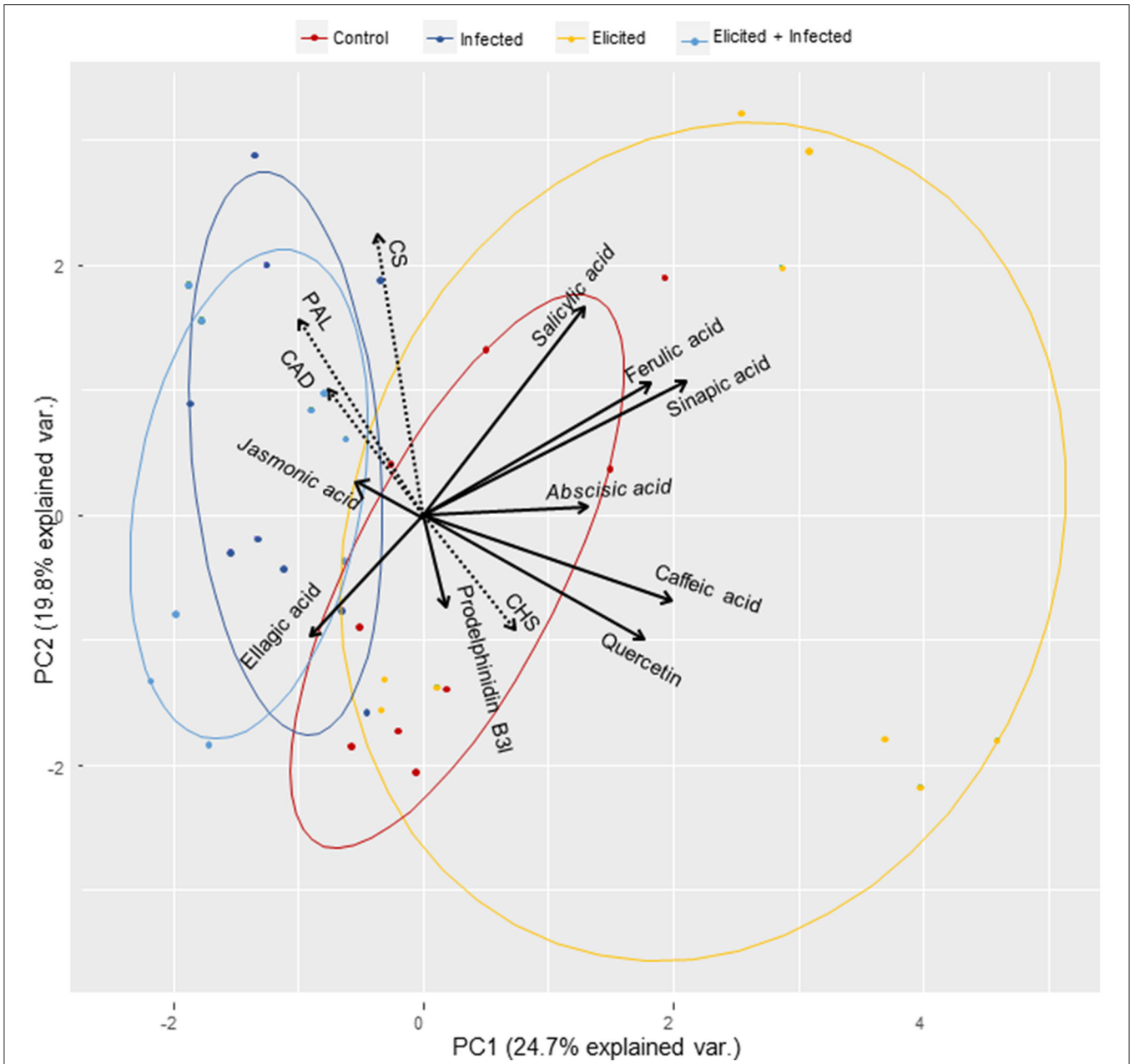

FIGURE 3 | Principal component analysis of the observed variation in the expression of four genes: *chorismate synthase (CS)*, *phenylalanine-ammonia-lyase (PAL)*, *NADPH-dependent cinnamyl alcohol dehydrogenase (CAD)* and *chalcone synthase (CHS),* and in the content of hormones (abscisic acid, jasmonic acid and salicylic acid) and phenolic compounds (caffeic acid, ellagic acid, ferulic acid, sinapic acid, quercetin and prodelphinidin B3) in *Quercus ilex* embryogenic lines after elicitation with 50 mM MeJA and/or infection with *P. cinnamomi*. For each treatment, ELs from 3 genotypes were analyzed in triplicate.

ability to inhibit the transcription of a β-1,3-glucanase, forming a physical barrier against the spread of the virus (Whenham et al., 1986; Beffa et al., 1996; Rezzonico et al., 1998), but in their interaction with pathogen fungi and oomycetes ABA accumulation compromises host resistance (Mauch-Mani and Mauch, 2005).

Elicitation with MeJA increased the JA content of holm oak Els, and infection induced a dramatic increase in the content of this hormone only in these samples that had been previously elicited (**Figure 1B**), while levels of JA of not elicited samples were similar to those of the uninfected control. It has been reported that the JA-mediated defense pathway is activated by infection with necrotrophic pathogens (Thomma et al., 1998; Glazebrook, 2005), which promote the biosynthesis of this hormone, triggering the stress response (Ramirez-Estrada et al., 2016). Corroborating this, Long et al.

(2021) reported the requirements of jasmonate signaling for defense responses against *Phytophthora nicotianae* in tobacco, which included the phenylpropanoid and the sesquiterpenoid biosynthesis pathways. In Norway, spruce accumulation of JA and not SA following wounding of MeJA-treated bark has also been reported (Mageroy et al., 2020) and authors suggest that MeJA primes JA-dependent defenses in the species although they found difficulties to link the response with expression pattern of PR proteins or JA biosynthesis enzymes. We also suggest that the observed increase in JA content could be considered as a marker of the activation of the defense response to the pathogen, since it is common in the three lines tested.

Holm oak ELs contents in SA varied among the different lines, and increased by elicitation but were not altered after infection (**Figure 1C**). This could indicate that elicitation might activate several defense pathways, while the response to the infection with this necrotrophic pathogen is mediated by the JA signaling pathway. However, a synergistic behavior between both hormones has been reported in the response to abiotic and biotic stresses (Yang et al., 2019). Also, some effectors from necrotrophic and biotrophic fungal pathogens have probed to alter the available pool of chorismate, the precursor of the SA, by different mechanisms such as the isochorismatases produced by *Phytophthora sojae* (Han and Kahmann, 2019). However, our results indicate that SA content was significantly associated to higher expression rates of the *CS* gene, therefore we did not observe this infection mechanism in the pathosystem *Quercus ilex-Phytophthora cinnamomi*.

Plants release a great diversity of phenolic compounds related to stress defense (Rashad et al., 2020), many of them are produced in the phenylpropanoid biosynthesis pathway. These secondary metabolites include flavonoids, monolignols, phenolic acids, stilbenes and coumarins, all of them playing an essential role in the vital development of plants as essential components of cell walls, and as phytoalexins against herbivores and pathogens, as well as protectors against intense light and UV radiation (Sharma and Gautam, 2019; Wallis and Galarneau, 2020). Our study analyzed the variation in the phenolic profile of E00, Q8, and VA5 lines, determining the content of phenolic acids (caffeic, ellagic, ferulic, and sinapic acids), the flavanol quercetin and the proanthocyanin prodelphinidin B3. The phenolic profile of the VA5 line, generated from a tolerant tree, differed from the other two lines. It is worth noting the high caffeic acid content detected in this line, which can be considered as a marker of defense that was also detected in susceptible lines after eliciting with MeJA (**Figure 2A**), along with increased levels of sinapic and ferulic acids and of quercetin in the E00 line. Caffeic acid and its derivatives are considered secondary metabolites of great importance for actively participating in the defense mechanism of plants against biotic stress (Riaz et al., 2018). This acid is involved in the synthesis of lignin, which allows a strengthening of the cell wall, and it also inhibits the synthesis of proteins in pathogenic cells, while increases in caffeic acid activate the production of enzymes that have a role in the inhibition of pathogens (Osbourn, 1996; Davidson, 1997; Riaz et al., 2018). We found that expression of the *PAL* gene was inversely correlated to caffeic acid content ($\mu = -0.351$, $p = 0.036$) probably due to a transcriptional inhibition of the *PAL* gene exerted by the metabolite (Zhang and Liu, 2015). Overall, elicitation with MeJA caused significant increases in sinapic, ferulic, and caffeic acids and in quercetin (**Figure 3**). This increased production of phenol derivates was also obtained when applying elicitors to roots of bitter melon (Chung et al., 2016) and stevia plants (González-Chavira et al., 2018). Finally, sterile filtrates of *Verticillum non-alfalfae* significantly increased *PAL* activity in hop cell lines (Kunej et al., 2020). In our assays, infection decreased caffeic acid content in control ELs, suggesting that the oomycete infection inhibits the expression of some genes related to tannin biosynthesis, as was described in holm oak (Gallardo et al., 2019). These authors reported that mechanical defoliation (considered an abiotic stress) increased the transcription of genes related to the synthesis of tannins, while infection with the oomycete would inhibit its expression, being partly responsible for the dieback symptoms. Therefore, the increased contents in these phenolic acids observed in elicited holm oak ELs could suppose a defense mechanism to subsequent infections. In other studies, infection with *Phytophthora parasitica* or *Xanthomonas campestris* of plant tissues treated with lipopolysaccharides from these pathogens resulted in significant increases in the production of phytoalexins, flavonoids, and phenolic conjugates (Newman et al., 2002). Therefore, the increase in ellagic acid after infection in elicited samples can be considered as a marker of stress response, being common in all three lines.

There are few reports on the effect of priming on forest tree species. Indeed, most of them are related just to one genotype (as an example see Mageroy et al., 2020). Here we report on work done with 3 holm oak genotypes (including one derived from a "scape" tree, VA5) and found phenotypic differences, therefore demonstrating that genotypes might display different strategies (gene expression, metabolite and hormonal profiles) after pathogen infection, which supports the complexity of the plant-pathogen interaction. Our work identifies changes triggered by MeJA elicitation in holm oak embryogenic lines, characterized by increases in ABA and JA contents, as well as in levels of most of the determined phenolic compounds, especially in caffeic acid, but not in their biosynthesis genes. The response to oomycete infection in holm oak elicited plant material is characterized by a further increase in JA. Since JA and phenols have been described as a part of the *Q. ilex* defense response against *P. cinnamomi,* we propose that MeJA may act as an IR stimulus. In our previous work (Morcillo et al., 2020), we performed dual cultures with MeJA-elicited ELs confronted to *P. cinnamomi* mycelium, and we referred increases in H_2O_2 content, therefore indicating an activation of defense responses. In conclusion, MeJA induced in our embryogenic material both direct (detected prior to any challenge) and primed (detected after subsequent challenge) defense responses. Further studies focused on the underlying mechanisms involved in this primed defense response need to be addressed.

DATA AVAILABILITY STATEMENT

The original contributions presented in the study are included in the article/**Supplementary Material**, further inquiries can be directed to the corresponding author/s.

AUTHOR CONTRIBUTIONS

IA, ES, and JS contributed to conception and design of the study. ES and MM performed the statistical analysis. MM, EC, MTM, and ES performed the experiments. MM, ES, and IA wrote the first draft of the manuscript. MM, MTM, EC, JS, IA, and ES wrote sections of the manuscript. All authors contributed to manuscript revision, read, and approved the submitted version.

FUNDING

This work was supported by the research project co-financed by MICINN and the EU (AGL2013-47400-C4-04-R, AGL2016-76143-C4-01-R, AGL2016-76143-C4-04-R, and PID2020112627RB) and by a predoctoral contract to MM (BES-2014-069171).

ACKNOWLEDGMENTS

Authors would like to thank Dr. Toribio and Dr. Abad and their research groups for providing the embryogenic lines and the oomycete strain used in this study, respectively, to Álex Alborch for the technical assistance, and to Vicent Arbona (Jaume I University) for help in preliminary hormone assays.

SUPPLEMENTARY MATERIAL

The Supplementary Material for this article can be found online at: https://www.frontiersin.org/articles/10.3389/fpls.2022.824781/full#supplementary-material

Supplementary Figure 1 | Relative gene expression ($2^{-\Delta\Delta Ct}$) of *Chorismate Synthase (CS), Phenylalanine-Ammonia-Lyase (PAL)*, *NADPH-dependent Cinnamyl Alcohol Dehydrogenase (CAD),* and *Chalcone Synthase (CHS)* genes in embryogenic lines from three holm oak genotypes (E00, Q8, and VA5) after elicitation with MeJA **(A)**, and after infection with *Phytophthora cinnamomi* of control **(B)**, or elicited plant material **(C)**. For each genotype and gene, data are mean ± SE of ratios of gene expression estimated from triplicated amplifications performed with three biological replicates. Values above or below 1 denote up- or downregulation of the gene, respectively; *Denotes significant effect of the treatment as compared to the reference sample, either control **(A,B)** or elicited **(C)** plant material.

REFERENCES

Barra-Jiménez, A., Blasco, M., Ruiz-Galea, M., Celestino, C., Alegre, J., Arrillaga, I., et al. (2014). Cloning mature holm oak trees by somatic embryogenesis. *Trees* 28, 657–667. doi: 10.1007/s00468-014-0979-0

Beffa, R. S., Hofer, R.-M., Thomas, M., and Meins, F. (1996). Decreased susceptibility to virus disease of β-1,3-glucanase-deficient plants generated by antisense transformation. *Plant Cell* 8, 1001–1011. doi: 10.2307/3870211

Bharath, P., Gahir, S., and Raghavendra, A. S. (2021). Abscisic acid-induced stomatal closure: an important component of plant defense against abiotic and biotic stress. *Front. Plant Sci.* 12, 615114. doi: 10.3389/fpls.2021.615114

Blasco, M., Barra, A., Brisa, C., Corredoira, E., Segura, J., Toribio, M., et al. (2013). Somatic embryogenesis in holm oak male catkins. *Plant Growth Regul.* 71, 261–270. doi: 10.1007/s10725-013-9826-3

Cahill, D., Bennett, I., and Mccomb, J. A. (1992). Resistance of micropropagated *Eucalyptus marginata* to *Phytophthora cinnamomi*. *Plant Dis.* 76, 630–632. doi: 10.1094/PD-76-0630

Cameron, R. K., Paiva, N. L., Lamb, J., and Dixon, R. A. (1999). Accumulation of salicylic acid and PR-1 gene transcripts in relation to the systemic acquired resistance (SAR) response induced by *Pseudomonas syringae* pv. *tomato in Arabidopsis*. *Physiol. Mol. Plant Pathol.* 55, 121–130. doi: 10.1006/pmpp.1999.0214

Chaves, I., Passarinho, J. A. P., Capitão, C., Chaves, M. M., Fevereiro, P., and Ricardo, C. (2011). Temperature stress effects in *Quercus suber* leaf metabolism. *J. Plant Physiol.* 168, 1729–1734. doi: 10.1016/j.jplph.2011.05.013

Chung, I.-M., Thiruvengadam, M., Rekha, K., and Rajakumar, G. (2016). Elicitation enhanced the production of phenolic compounds and biological activities in hairy root cultures of bitter melon (*Momordica charantia* L.). *Brazilian Arch. Biol. Technol.* 59, 1–10. doi: 10.1590/1678-4324-2016160393

Council of Europe, UNEP and ECNC (1996). *The Pan-European Biological and Landscape Diversity Strategy: A Vision for Europe's Natural Heritage*. Tilburg: European Centre for Nature Conservation.

Davidson, P. M. (1997). "Chemical preservatives and natural antimicrobial compounds" in *Food Microbiology-Fundamentals and Frontiers*, eds M. P. Doyle, L. R. Beuchat, and T. J. Montville (Washington DC: ASM Press).

De Kesel, J., Conrath, U., Flors, V., Luna, E., Mageroy, M. H., Mauch-Mani, B., et al. (2021). The induced resistance lexicon: do's and don'ts, *Trends Plant Sci.* 26, 685–691. doi: 10.1016/j.tplants.2021.01.001

de Torres Zabala, M., Bennett, M. H., Truman, W. H., and Grant, M. R. (2009). Antagonism between salicylic and abscisic acid reflects early host-pathogen conflict and moulds plant defense responses. *Plant J.* 59, 375–386. doi: 10.1111/j.1365-313X.2009.03875.x

Deboever, E., Deleu, M., Mongrand, S., Lins, L., and Fauconnier, M. L. (2020). Plant-pathogen interactions: underestimated roles of phyto-oxylipins. *Trends Plant Sci.* 25, 22–34. doi: 10.1016/j.tplants.2019.09.009

Duque-Lazo, J., Navarro-Cerrillo, R. M., van Gils, H., and Groen, T. A. (2018). Forecasting oak decline caused by *Phytophthora cinnamomi* in Andalusia: Identification of priority areas for intervention. *For. Ecol. Manage.* 417, 122–136. doi: 10.1016/j.foreco.2018.02.045

Gallardo, A., Morcuende, D., Solla, A., Moreno, G., Pulido, F., and Quesada, A. (2019). Regulation by biotic stress of tannins biosynthesis in *Quercus ilex*: Crosstalk between defoliation and *Phytophthora cinnamomi* infection. *Physiol. Plant.* 165, 319–329. doi: 10.1111/ppl.12848

Giorgi, F. (2006). Climate change hot-spots. *Geophys. Res. Lett.* 33, 1–4. doi: 10.1029/2006GL025734

Glazebrook, J. (2005). Contrasting mechanisms of defense against biotrophic and necrotrophic pathogens. *Annu. Rev. Phytopathol.* 43, 205–227. doi: 10.1146/annurev.phyto.43.040204.135923

Goellner, K., and Conrath, U. (2008). Priming: It's all the world to induced disease resistance. *Eur. J. Plant Pathol.* 121, 233–242. doi: 10.1007/s10658-007-9251-4

González-Chavira, M. M., Estefania-Ojeda, S., Pons-Hernández, J. L., Guevara-González, R. G., and Guzmán Maldonado, S. H. (2018). Cambios en el contenido de compuestos fenólicos, esteviosidos y nivel de metilación en *Stevia rebaudiana* elicitada. *Rev. Mex. Ciencias Agrícolas* 9, 1435–1446. doi: 10.29312/remexca.v9i7.1314

González-Rodríguez, V., Navarro-Cerrillo, R. M., and Villar, R. (2011). Artificial regeneration with *Quercus ilex* L. and *Quercus suber L.* by direct

seeding and planting in southern Spain. *Ann. For. Sci.* 68, 637–646. doi: 10.1007/s13595-011-0057-3

Han, X., and Kahmann, R. (2019). Manipulation of phytohormone pathways by effectors of filamentous plant pathogens. *Front. Plant Sci.* 10, 822. doi: 10.3389/fpls.2019.00822

Ho, T. T., Lee, J. D., Jeong, C. S., Paek, K. Y., and Park, S. Y. (2018). Improvement of biosynthesis and accumulation of bioactive compounds by elicitation in adventitious root cultures of *Polygonum multiflorum*. *Appl. Microbiol. Biotechnol.* 102, 199–209. doi: 10.1007/s00253-017-8629-2

Ho, T. T., Murthy, H. N., and Park, S.-Y. (2020). Methyl jasmonate induced oxidative stress and accumulation of secondary metabolites in plant cell and organ cultures. *Int. J. Mol. Sci.* 21:716. doi: 10.3390/ijms21030716

Horta, M., Sousa, N., Coelho, A. C., Neves, D., and Cravador, A. (2008). *In vitro* and *in vivo* quantification of elicitin expression in *Phytophthora cinnamomi*. *Physiol. Mol. Plant. Pathol.* 73, 48–57. doi: 10.1016/j.pmpp.2009.02.003

Kohler, A., Schwindling, S., and Conrath, U. (2002). Benzothiadiazole-induced priming for potentiated responses to pathogen infection, wounding, and infiltration of water into leaves requires the NPR1/NIM1 gene in *Arabidopsis*. *Plant Physiol.* 128, 1046–1056. doi: 10.1104/pp.010744

Ku, Y.-S., Sintaha, M., Cheung, M.-Y., and Lam, H.-M. (2018). Plant Hormone Signaling Crosstalks between Biotic and Abiotic Stress Responses. *Int. J. Mol. Sci.* 19:3206. doi: 10.3390/ijms19103206

Kunej, U., Mikulič-Petkovšek, M., Radišek, S., and Štajner, N. (2020). Changes in the phenolic compounds of hop (*Humulus lupulus* L.) induced by infection with *Verticillium nonalfalfae*, the causal agent of hop verticillium wilt. *Plants* 9, 1–16. doi: 10.3390/plants9070841

Lehmann, S., Serrano, M., L'Haridon, F., Tjamos, S. E., and Metraux, J. P. (2015). Reactive oxygen species and plant resistance to fungal pathogens. *Phytochemistry* 112, 54–62. doi: 10.1016/j.phytochem.2014.08.027

Lievens, L., Pollier, J., Goossens, A., Beyaert, R., and Staal, J. (2017). Abscisic acid as pathogen effector and immune regulator. *Front. Plant Sci.* 8, 1–15. doi: 10.3389/fpls.2017.00587

Lin, W., Hu, X., Zhang, W., Rogers, W. J., and Cai, W. (2005). Hydrogen peroxide mediates defence responses induced by chitosans of different molecular weights in rice. *J. Plant Physiol.* 162, 937–944. doi: 10.1016/j.jplph.2004.10.003

Long, J., Yang, M., Zuo, C., Song, N., He, J.-M., Zeng, J., et al. (2021). Requirement of Jasmonate signaling for defense responses against *Alternaria alternata* and *Phytophthora nicotianae* in tobacco. *Crop Sci.* 61, 4273–4283. doi: 10.1002/csc2.20625

Mageroy, M. H., Wilkinson, S. W., Tengs, T., Cross, H., Almvik, M., Pétriacq, P., et al. (2020). Molecular underpinnings of methyl jasmonate-induced resistance in Norway spruce. *Plant Cell Environ.* 43, 1827–1843. doi: 10.1111/pce.13774

Martínez, M. T., Arrillaga, I., Sales, E., Pérez-Oliver, M. A., González-Mas, M., C., et al. (2021). Micropropagation, characterization, and conservation of *Phytophthora cinnamomi*-tolerant holm oak mature trees. *Forests* 12:1634. doi: 10.3390/f12121634

Martínez, M. T., San José, M. C., Vieitez, A. M., Cernadas, M. J., Ballester, A., and Corredoira, E. (2017). Propagation of mature *Quercus ilex* L. (holm oak) trees by somatic embryogenesis. *Plant Cell Tissue Organ Cult.* 131, 321–333. doi: 10.1007/s11240-017-1286-4

Martínez, M. T., San-José, M. C., Arrillaga, I., Cano, V., Morcillo, M., Cernadas, M. J., et al. (2019). Holm oak somatic embryogenesis: Current status and future perspectives. *Front. Plant Sci.* 10, 239. doi: 10.3389/fpls.2019.00239

Martínez, M. T., Vieitez, A. M., and Corredoira, E. (2015). Improved secondary embryo production in Quercus alba and Q. *rubra* by activated charcoal, silver thiosulphate and sucrose: Influence of embryogenic explant used for subculture. *Plant Cell Tissue Organ Cult.* 121, 531–546. doi: 10.1007/s11240-015-0722-6

Martínez, M. T., Vieitez, F. J., Solla, A., Tapias, R., Ramírez-Martín, N., and Corredoira,. E. (2020). Vegetative propagation of *Phytophthora cinnamomi*-tolerant holm oak genotypes by axillary budding and somatic embryogenesis. *Forest* 11:841. doi: 10.3390/f11080841

Mauch-Mani, B., and Mauch, F. (2005). The role of abscisic acid in plant-pathogen interactions. *Curr. Opin. Plant Biol.* 8, 409–414. doi: 10.1016/j.pbi.2005.05.015

Milan, E. B., Mandoulakani, B. A., and Kheradmand, F. (2017). The effect of methyl jasmonate on the expression of phenylalanine ammonia lyase and eugenol-o-methyl transferase genes in basil. *Philipp Agric Sci* 100, 163–167. doi: 10.1021/jf060568c

Montero, G., Ruiz-Peinado, R., and Pasalodos, M. (2017). La dehesa: estructura, producciones arbóreas y tendencias de su gestión silvopascícola. *Foresta* 68, 44–63.

Morcillo, M., Sales, E., Ponce, L., Guillén, A., Peris, J. B., Segura, J., et al. (2020). Effects of elicitors on holm oak somatic embryos development and efficacy inducing tolerance to *Phytophthora cinnamomi*. *Sci. Rep.* 10:15166. doi: 10.1038/s41598-020-71985-w

Mur, L. A. J., Naylor, G., Warner, S. A. J., Sugars, J. M., White, R. F., and Draper, J. (1996). Salicylic acid potentiates defense gene expression in tissue exhibiting acquired resistance to pathogen attack. *Plant J.* 9, 559–571. doi: 10.1046/j.1365-313X.1996.09040559.x

Murashige, T., and Skoog, F. (1962). A revised medium for rapid growth and bio assays with tobacco tissue cultures. *Physiol. Plant.* 15, 473–497. doi: 10.1111/j.1399-3054.1962.tb08052.x

Newman, M. A., Von Roepenack-Lahaye, E., Parr, A., Daniels, M. J., and Dow, J. M. (2002). Prior exposure to lipopolysaccharide potentiates expression of plant defenses in response to bacteria. *Plant J.* 29, 487–495. doi: 10.1046/j.0960-7412.2001.00233.x

Osbourn, A. E. (1996). Preformed antimicrobial compounds and plant defense against fungal attack. *Plant Cell* 8, 1821–1831. doi: 10.2307/3870232

Oßwald, W., Fleischmann, F., Rigling, D., Coelho, A. C., Cravador, A., Diez, J., et al. (2014). Strategies of attack and defence in woody plant-*Phytophthora* interactions. *For. Pathol.* 44, 169–190. doi: 10.1111/efp.12096

Pfaffl, M. W. (2001). A new mathematical model for relative quantification in real-time RT-PCR. *Nucleic Acids Res.* 29:e45. doi: 10.1093/nar/29.9.e45

R Core Team (2020). *R: A Language and Environment for Statistical Computing*. Vienna: R Foundation for Statistical Computing.

Ramirez-Estrada, K., Vidal-Limon, H., Hidalgo, D., Moyano, E., Golenioswki, M., Cusid,ó, R. M., et al. (2016). Elicitation, an effective strategy for the biotechnological production of bioactive high-added value compounds in plant cell factories. *Molecules* 21:182. doi: 10.3390/molecules21020182

Rashad, Y., Aseel, D., and Hammad, S. (2020). "Phenolic compounds against fungal and viral plant diseases" in *Plant Phenolics in Sustainable Agriculture*, eds R. Lone, R. Shuab, and A. Kamili (Singapore: Springer). doi: 10.1007/978-981-15-4890-1_9

Rezzonico, E., Flury, N., Meins, F., and Beffa, R. (1998). Transcriptional down-regulation by abscisic acid of pathogenesis-related β-1,3-glucanase genes in tobacco cell cultures. *Plant Physiol.* 117, 585–592. doi: 10.1104/pp.117.2.585

Riaz, U., Kharal, M. A., Murtaza, G., Zaman, Q., uz, Javaid, S., Malik, H. A., et al. (2018). Prospective roles and mechanisms of caffeic acid in counter plant stress: a mini review. *Pakistan J. Agric. Res.* 32, 8–19. doi: 10.17582/journal.pjar/2019/32.1.8.19

Rubio-Rodríguez, E., Vera-Reyes, I., Sepúlveda-García, E. B., Ramos-Valdivia, A. C., and Trejo-Tapia, G. (2021). Secondary metabolite production and related biosynthetic genes expression in response to methyl jasmonate in *Castilleja tenuiflora* Benth *in vitro* plants. *Plant Cell Tissue Organ Cult.* 144, 519–532. doi: 10.1007/s11240-020-01975-3

Seo, M., Jikumaru, Y., and Kamiya, Y. (2011). "Profiling of hormones and related metabolites in seed dormancy and germination studies" in *Seed Dormancy*, ed A. R. Kermode (Nueva Jersey: Methods Mol. Biol. Humana Press). doi: 10.1007/978-1-61779-231-1_7

Sharma, N., and Gautam, A. K. (2019). Early pathogenicity events in plant pathogenic fungi: a comprehensive review. *Biol. Forum AIJ* 11, 24–34.

Soler, M., Serra, O., Molinas, M., García-Berthou, E., Caritat, A., and Figueras, M. (2008). Seasonal variation in transcript abundance in cork tissue analyzed by real time RT-PCR. *Tree Physiol.* 28, 743–751. doi: 10.1093/treephys/28.5.743

Thomma, B. P. H. J., Eggermont, K., Penninckx, I. A. M. A., Mauch-Mani, B., Vogelsang, R., Cammue, B. P. A., et al. (1998). Separate jasmonate-dependent and salicylate-dependent defense-response pathways in *Arabidopsis* are essential for resistance to distinct microbial pathogens. *Proc. Natl. Acad. Sci. U.S.A.* 95, 15107–15111. doi: 10.1073/pnas.95.25.15107

van Wees, S. C., Luijendijk, M., Smoorenburg, I., van Loon, L. C., and Pieterse, C. M. J. (1999). Rhizobacteria-mediated induced systemic resistance (ISR) in *Arabidopsis* is not associated with a direct effect on expression of known defense-related genes but stimulates the expression of the jasmonate-inducible gene *Atvsp* upon challenge. *Plant Mol. Biol.* 41, 537–549. doi: 10.1023/A:1006319216982

Wallis, C. M., and Galarneau, E. R.-A. (2020). Phenolic Compound Induction in Plant-Microbe and Plant-Insect Interactions: A Meta-Analysis. *Front. Plant Sci.* 11, 2034. doi: 10.3389/fpls.2020.580753

Wang, K., Liao, Y., Kan, J., Han, L., and Zheng, Y. (2015). Response of direct or priming defense against *Botrytis cinerea* to methyl jasmonate treatment at different concentrations in grape berries. *Int. J. Food Microbiol.* 194, 32–39. doi: 10.1016/j.ijfoodmicro.2014.11.006

Wang, Y., Mostafa, S., Zeng, W., and Jin, B. (2021). Function and mechanism of Jasmonic Acid in plant responses to Abiotic and Biotic Stresses. *Int. J. Mol. Sci.* 22:8568. doi: 10.3390/ijms22168568

Whenham, R. J., Fraser, R. S. S., Brown, L. P., and Payne, J. A. (1986). Tobacco-mosaic-virus-induced increase in abscisic-acid concentration in tobacco leaves: Intracellular location in light and dark-green areas, and relationship to symptom development. *Planta* 168, 592–598. doi: 10.1007/BF00392281

Yadav, V., Wang, Z., Wei, C., Amo, A., Ahmed, B., Yang, X., et al. (2020). Phenylpropanoid pathway engineering: an emerging approach towards plant defense. *Pathogens* 9:312. doi: 10.3390/pathogens9040312

Yang, J., Duan, G., Li, C., Liu, L., Han, G., Zhang, Y., et al. (2019). The crosstalks between jasmonic acid and other plant hormone signaling highlight the involvement of jasmonic acid as a core component in plant response to biotic and abiotic stresses. *Front. Plant Sci.* 10, 1349. doi: 10.3389/fpls.2019.01349

Zhang, X., and Liu, C. (2015). Multifaceted regulations of gateway enzyme phenylalanine ammonia-lyase in the biosynthesis of phenylpropanoids. *Mol. Plant J.* 8, 17–27. doi: 10.1016/j.molp.2014.11.001

Conflict of Interest: The authors declare that the research was conducted in the absence of any commercial or financial relationships that could be construed as a potential conflict of interest.

Publisher's Note: All claims expressed in this article are solely those of the authors and do not necessarily represent those of their affiliated organizations, or those of the publisher, the editors and the reviewers. Any product that may be evaluated in this article, or claim that may be made by its manufacturer, is not guaranteed or endorsed by the publisher.

frontiers in Plant Science

ORIGINAL RESEARCH
published: 10 March 2022
doi: 10.3389/fpls.2022.838421

Constitutive Overexpression of a Conifer *WOX2* Homolog Affects Somatic Embryo Development in *Pinus pinaster* and Promotes Somatic Embryogenesis and Organogenesis in *Arabidopsis* Seedlings

*Seyedeh Batool Hassani[1†], Jean-François Trontin[2], Juliane Raschke[1], Kurt Zoglauer[1] and Andrea Rupps[1]**

[1] Department of Plant Systematics and Evolution, Institute of Biology, Humboldt-Universität zu Berlin, Berlin, Germany, [2] BioForBois, Wood & Construction Industry Department, FCBA, Cestas, France

OPEN ACCESS

Edited by:
Víctor M. Loyola-Vargas, Scientific Research Center of Yucatán (CICY), Mexico

Reviewed by:
Neftali Ochoa-Alejo, Centro de Investigación y de Estudios Avanzados del Instituto Politécnico Nacional, Mexico
An Yan, Howard Hughes Medical Institute (HHMI), United States

***Correspondence:**
Andrea Rupps
andrea.rupps@biologie.hu-berlin.de

†Present address:
Seyedeh Batool Hassani, Faculty of Life Sciences and Biotechnology, Shahid Beheshti University, Tehran, Iran

Specialty section:
This article was submitted to Plant Development and EvoDevo, a section of the journal Frontiers in Plant Science

Received: *17 December 2021*
Accepted: *24 January 2022*
Published: *10 March 2022*

Citation:
Hassani SB, Trontin J-F, Raschke J, Zoglauer K and Rupps A (2022) Constitutive Overexpression of a Conifer WOX2 Homolog Affects Somatic Embryo Development in Pinus pinaster and Promotes Somatic Embryogenesis and Organogenesis in Arabidopsis Seedlings. Front. Plant Sci. 13:838421. doi: 10.3389/fpls.2022.838421

Although full sequence data of several embryogenesis-related genes are available in conifers, their functions are still poorly understood. In this study, we focused on the transcription factor *WUSCHEL-related HOMEOBOX 2 (WOX2)*, which is involved in determination of the apical domain during early embryogenesis, and is required for initiation of the stem cell program in the embryogenic shoot meristem of *Arabidopsis*. We studied the effects of constitutive overexpression of *Pinus pinaster WOX2* (*PpWOX2*) by *Agrobacterium*-mediated transformation of *P. pinaster* somatic embryos and *Arabidopsis* seedlings. Overexpression of *PpWOX2* during proliferation and maturation of somatic embryos of *P. pinaster* led to alterations in the quantity and quality of cotyledonary embryos. In addition, transgenic somatic seedlings of *P. pinaster* showed non-embryogenic callus formation in the region of roots and subsequently inhibited root growth. Overexpression of *PpWOX2* in *Arabidopsis* promoted somatic embryogenesis and organogenesis in a part of the transgenic seedlings of the first and second generations. A concomitant increased expression of endogenous embryogenesis-related genes such as *AtLEC1* was detected in transgenic plants of the first generation. Various plant phenotypes observed from single overexpressing transgenic lines of the second generation suggest some significant interactions between *PpWOX2* and *AtWOX2*. As an explanation, functional redundancy in the WOX family is suggested for seed plants. Our results demonstrate that the constitutive high expression of *PpWOX2* in *Arabidopsis* and *P. pinaster* affected embryogenesis-related traits. These findings further support some evolutionary conserved roles of this gene in embryo development of seed plants and have practical implications toward somatic embryogenesis induction in conifers.

Keywords: homologous genes, homologous and heterologous overexpression, genetic transformation, *WOX2*, WUSCHEL, LEC1

INTRODUCTION

With respect to the divergence of angiosperms and gymnosperms, many morphological differences of embryogenesis and embryo development have to be considered (Bowe and Coat, 2000; Cairney et al., 2006; Cairney and Pullman, 2007). Many studies using *Arabidopsis* as a model plant have increased our knowledge of the function of embryogenesis-related genes in angiosperms (Laux et al., 1996; Lotan et al., 1998; Boutilier et al., 2002; Haecker et al., 2004; Breuninger et al., 2008; Jeong et al., 2011; Chung et al., 2016; Horstman et al., 2017). In contrast, little is known about the function of genes that regulate embryogenesis in conifers (Cairney and Pullman, 2007; De Silva et al., 2008; Trontin et al., 2016a). This is because of particular challenges of conifers. These species have long breeding cycles, large physical size, and slow growth. As a result, a number of powerful genetic approaches used in model plants, such as identification of zygotic embryo-defective mutants and T-DNA insertional mutagenesis, are impracticable. Moreover, recalcitrance to vegetative propagation through conventional or tissue culture methods (mostly aging/phase-change effects) often results in lack of an efficient system for direct plant regeneration from selected superior trees. Available methods are, therefore, mostly "retroactive" and based on somatic embryogenesis initiation from immature seeds coupled with cryopreservation to preserve the juvenility of embryogenic tissue. Selected genotypes after field evaluation of somatic seedlings in clonal tests can be propagated from a cryopreserved juvenile stock. This is currently the preferred and powerful strategy in conifers to overcome recalcitrance of mature trees (Klimaszewska and Cyr, 2002; Bonga et al., 2010) to achieve clonal propagation of superior genotypes and for gene functional studies by genetic transformation of embryogenic cultures (Klimaszewska et al., 2007, 2009, 2016).

The first step for assignment of gene functions in conifers is usually based on sequence similarities between conifers and model angiosperms. Most embryogenesis-related genes identified in *Arabidopsis* (a global network of ca. 300–450 genes) (Tzafrir et al., 2004; De Smet et al., 2010) have homologous candidate sequences in conifers (Cairney and Pullman, 2007; Zhang et al., 2012). The second one is analysis of transgenic plants following overexpression and/or knock-down of the candidate genes. Such reverse genetics approach for functional gene studies remains challenging in most conifers, because significant genomic resources are needed (genome sequence, expressed sequence tags, etc.), as well as efficient genetic transformation and plant regeneration systems (Trontin et al., 2007). Significant progress has been achieved in several conifer species of high economical interest (*Pinus*, *Picea*, and *Larix*) based on *Agrobacterium*-mediated genetic transformation of embryogenic cultures and plant regeneration by somatic embryogenesis (Trontin et al., 2007; Klimaszewska et al., 2009, 2016; Bonga et al., 2010). Such a system has been developed for reverse genetics in maritime pine (*Pinus pinaster* Ait.) during the past 15 years (Trontin et al., 2002, 2007, 2016b; Lelu-Walter et al., 2016) and was implemented by multinational EU consortia (e.g., Sustainpine, 2010–2013[1]; ProCoGen, 2012–2015[2]) for functional gene studies (Trontin et al., 2013; El-Azaz et al., 2020).

An embryogenesis-related gene that is crucial for early embryo development in angiosperms is *WUSCHEL-related HOMEOBOX 2* (*WOX2*). In *Arabidopsis*, *WOX2* is required for cell fate decisions and domain delineation in the apical domain during embryo development, including initiation of shoot meristem stem cells (Haecker et al., 2004; Xiao et al., 2006; Breuninger et al., 2008; Zhang et al., 2017). In post-embryonic development, *WOX2* seems to be involved in lateral organ formation and separation (Chung et al., 2016). The *WOX2* gene encodes a member of the *WOX* family of homeodomain transcription factors. WOX proteins share a homeobox that encodes a WUS-type homeodomain. In addition to the homeodomain, many WUS/WOX proteins contain a conserved WUS-box (TLPLFPMH) located downstream of the homeodomain in both angiosperms and gymnosperms (Haecker et al., 2004; Nardmann and Werr, 2006; see also **Figure 1**). Dolzblasz et al. (2016) reported that the canonical WUS-box is essential for stem cell maintenance within shoot apical meristem in *Arabidopsis*. Moreover, several overexpression studies indicate that WOX family members containing the conserved WUS-box are involved in plant growth and development. For example, induced overexpression of *WOX5* in *Arabidopsis* produces extra layers of stem cells in columella root cap (Zhang et al., 2010). Overexpression of *WOX1* in *Arabidopsis* leads to defects in meristem development (Zhang et al., 2011). Transgenic plants overexpressing *WUSCHEL* (*WUS*, founding member of the *WOX* family) in *Arabidopsis* led to high frequency of somatic embryo (SE) formation in all tissues without any need for exogenous plant hormone supply (Laux et al., 1996; Zuo et al., 2002). Furthermore, in angiosperms other than *Arabidopsis*, the overexpression of *AtWUS* induced somatic embryogenesis and callus formation (Arroyo-Herrera et al., 2008; Solís-Ramos et al., 2009; Bouchabke-Coussa et al., 2013).

In conifers, the transcription factor *WOX2* is considered as an important developmental regulator during early somatic embryogenesis (Klimaszewska et al., 2010; Trontin et al., 2016a) and has been proposed as a putative marker for effective initiation of somatic embryogenesis and to predict embryogenic potential (Palovaara and Hakman, 2008; Klimaszewska et al., 2010, 2011; Miguel et al., 2016; Alvarez et al., 2018). Zhu et al. (2016) revealed that the *WOX2* from *Picea abies* (*PaWOX2*) plays more crucial roles during early embryogenesis (i.e., protoderm formation and suspensor expansion) than during late embryogenesis.

Genomic resources are now accumulating in model conifers, especially for *Picea* and *Pinus* species (Birol et al., 2013; Nystedt et al., 2013; Neale et al., 2014; Plomion et al., 2016). For this study, we focused on *P. pinaster,* as the production of similar genomic sequence data was initiated during the European ProCoGen project (2011–2015[2]). Moreover, a reference transcriptome has

[1]https://www.scbi.uma.es/sustainpinedb

[2]http://www.procogen.eu

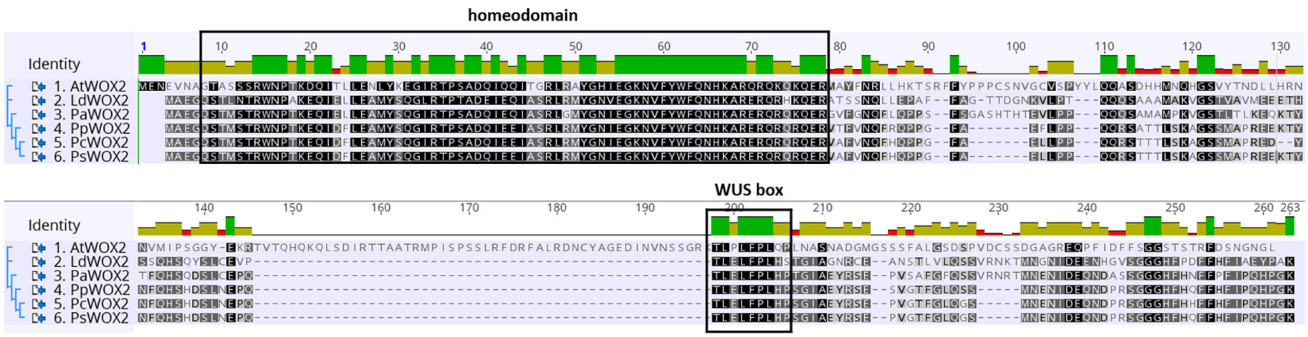

FIGURE 1 | Comparative WOX2 amino acid sequences in the angiosperm *Arabidopsis thaliana* (AtWOX2) and in 5 conifers, namely, *Larix decidua* (LdWOX2), *Picea abies* (PaWOX2), *Pinus pinaster* (PpWOX2), *Pinus contorta* (PcWOX2), and *Pinus sylvestris* (PsWOX2). Introduced gaps in the amino acid sequences are indicated by dashes. Boxes show the putative WOX homeodomain and WUS box. Amino acid identity is shown by a color code.

been made available for this species (SustainpineDB database[1]) (Canales et al., 2014).

To our knowledge, there has been no report up to now on the overexpression of *WOX2* isolated from conifers in both gymnosperms and, more specifically, angiosperms. The genetic transformation of *Pinus* is a long and difficult process typically achieved in about 12 months. Deregulating *WOX2* with same binary vector in both *P. pinaster* and *Arabidopsis* would provide additional insights into evolutionary conserved roles of this gene in gymnosperms and angiosperms, particularly during somatic embryogenesis. In this study, we analyzed the constitutive overexpression of *WOX2* isolated from *P. pinaster* (*PpWOX2*) in both *P. pinaster* SE and *Arabidopsis* seedlings. Our results showed that the endogenous expression of *PpWOX2* is enhanced in early proliferating embryos and significantly decreased during SE development in *P. pinaster*. Constitutive overexpression of *PpWOX2* in *P. pinaster* embryogenic cultures affected SE development and promoted callus formation in the root region of regenerated somatic seedling. In *Arabidopsis* seedlings, *PpWOX2* overexpression led to increased propensity to somatic embryogenesis and organogenesis, likely by alteration of expression patterns of embryogenesis-related genes.

MATERIALS AND METHODS

Plant Materials and Growth Conditions

P. pinaster

Somatic embryos (SEs) of a *P. pinaster* embryogenic line (PN519) were used for genetic transformation and transgenic plant production. PN519 was initiated at FCBA in 1999 from an immature zygotic embryo (full-sib progeny, Breton et al., 2006) according to the method of Bercetche and Pâques (1995). This line has good abilities for both genetic transformation and plant regeneration by somatic embryogenesis and has been, therefore, extensively characterized for the past 15 years (Trontin et al., 2002, 2007, 2013, 2016b; Breton et al., 2006; Lelu-Walter et al., 2016).

A. thaliana

Seeds of *Arabidopsis thaliana* (L.) Heynh. (ecotype Columbia-0) were obtained from the Nottingham *Arabidopsis* Stock Center[3]. For germination, the *Arabidopsis* seeds were soaked first in tap water at 4°C for 2 days and thereafter transferred to potting soil (Stender, Schermbeck, Germany) and grown for 4–6 weeks at 21–23°C under short day conditions (10-h light/14-h dark cycle) with illumination at ∼120 μE m^{-2} s^{-1} provided by HQI Powerstar 400W/D (Osram Licht AG, Munich, Germany). For flower induction, plants were cultivated under the same but longer day conditions (16-h light).

Both SEs and non-embryogenic calluses were obtained from wild-type (WT) *Arabidopsis* plant seedlings after induction following the method reported by Gaj (2001). WT SE and non-embryogenic WT calluses were used as positive (embryogenic) and negative (non-embryogenic) controls, respectively.

Characterization of WOX2 in P. pinaster (PpWOX2) and Cloning

In silico search for *WOX2* sequences in the *P. pinaster* expressional database (see Canales et al., 2014) was performed by Philippe Label (INRAE, France). The cDNA sequence of a putative *P. pinaster* homolog to *WOX2* (*PpWOX2*) was identified in SustainpineDB (nine unigenes assigned to conifer *WOX2*) and submitted under accession number (Acc.) KY773924.1 at the National Center for Biotechnology Information (NCBI) GenBank, and its cloning was performed. *PpWOX2* was concurrently sequenced by Alvarez et al. (2018) and deposited in GenBank under accession number KU962991. The two published sequences are identical (570 bp).

Alignment of the deduced amino acid sequence of *PpWOX2* [Acc. ARS01278 in this study; concurrently deposited by Alvarez et al. (2018), Acc. ANC94872] with homologous WOX2 protein sequences from *Pinus sylvestris* (PsWOX2, Acc. CAT02937.2; Nardmann et al., unpublished), *Pinus contorta* (PcWOX2, Acc. ADR10436.1; Park et al., 2010), *Picea abies* (PaWOX2, Acc. CAL18267.1; Palovaara and Hakman, 2008), *Larix decidua* (LdWOX2, Acc. AEF56564.2; Rupps et al., 2016), and *A. thaliana*

[3]http://www.nasc.co.uk

(AtWOX2, Acc. NP_200742.2; Tabata et al., 2000) was carried out using the Geneious R10.2.3 software (Biomatters Ltd., Auckland, New Zealand). Gaps were included in the sequences to optimize the alignment.

Binary Vector Construction for Constitutive Overexpression of PpWOX2

To generate the *35S::PpWOX2* vector, the *GUSPlus* gene of the *35S::GUSPlus* cassette from the binary vector *pCAMBIA1305.2* (GenBank Acc. AF354046)[4] was replaced with the *PpWOX2* gene isolated from *P. pinaster* (Acc. KY773924). The *GUSPlus* gene was excised from *pCAMBIA1305.2* by restriction with *Nco*I and *Pml*I. The entire open reading frame of *PpWOX2* was amplified from cDNA (obtained from total RNA extract) using specific primers (**Table 1**). The PCR fragment (570 bp) was then ligated into the *Nco*I and *Pml*I sites of the digested *pCAMBIA1305.2*. The resulting *35S::PpWOX2* binary vector was checked by sequencing and introduced into the disarmed *Agrobacterium tumefaciens* strain *C58/C1* using the freeze-thaw method (Nishiguchi et al., 1987). The *pCAMBIA1305.2* vector harbors a constitutive expression cassette (*35S::HPTII*) for selection of transgenic events with hygromycin. This antibiotic is effective in maritime pine (Trontin et al., 2002, 2007).

[4]www.cambia.org

TABLE 1 | List of gene-specific primers used for transgene analyses and reverse transcription quantitative (RT-q) PCR in *Pinus pinaster* and *Arabidopsis*.

Gene	Oligonucleotide name	Oligonucleotide sequence (5′ – 3′)
Primers for transgene analyses		
HPTII	HPTII-fw	AAC ATC GCC TCG CTC CAG TCA ATG A
	HPTII-rev	AAT AGC TGC GCC GAT GGT TTC TAC A
NPTII	NPTII-fw	CTA TGG CTG GAA GGA AAG CTG
	NPTII-rev	TCA GGC TTG ATC CCC AGT AAG
PpWOX2	PpWOX2-fw	TGG AGG CCA TGT ACA GTC AA
	PpWOX2-rev	GCC AGG TGG TTG ATG AAA CT
CaMV35S	CaMV35S	CTA TCC TTC GCA AGA CCC TTC
	T35S_rev	GGT CAC TGG ATT TTG GTT TTA GG
Primers for RT-qPCR in *P. pinaster* (reference genes)		
Helicase	PpHELI_fw	GGA GCT CTT GAT GAG ATG GAG
	PpHELI_rev	GGA AGG ACA AAT GGA TCA CG
Expressed protein At2g32170	Pp32170_fw	TCT TTA CTC CCA TGG CGT TC
	Pp32170_rev	TGT TTG GGA GAT TGC TGA AAG
Mitosis Protein YLS8	PpYLS8_fw	GTG GAT CAG GCC ATT CTA GC
	PpYLS8_rev	ACC TCC GTT ATG TCC ACC AG
Primers for RT-qPCR in *Arabidopsis* (reference genes)		
SAND	SAND-fw	AAC TCT ATG CAG CAT TTG ATC CAC T
	SAND-rev	TGA TTG CAT ATC TTT ATC GCC ATC
PP2A	PP2A-fw	AAG GTA AAG AAG ACA GCA ACG A
	PP2A-rev	GCC AAC ATT AAC ATT AGT AGC AGA G
PEX4	PEX4-fw	CCT CTT AAC TGC GAC TCA GG
	PEX4-rev	TTT GTG CCA TTG AAT TGA ACC C
Primers for RT-qPCR in *P. pinaster* and/or *Arabidopsis* (genes of interest)		
PpWOX2	3Pinpi_WOX2_ORF_fw	ATC CGG CAT CGC TGA ATA C
	3Pinpi_WOX2_ORF_rev	TAC TTG CCA GGA TGC TGA GG
AtLEC1	At-LEC-ORF-B-fw	CAT GGT TAT GGG AGG TGG TC
	At-LEC-ORF-B-rev	AGA GCC ACC ACC AAC ACT G
AtWUS	At-WUS-ORF-fw	ACC CAA CTC GGT TAT GAT GG
	At-WUS-ORF-rev	GCT GGG ATA TGG CTT GTT ATG
AtWOX2	At-WOX2-ORF-fw	TCA AAC GTG GGT TGT GTC AG
	At-WOX2-ORF-rev	AGC CAC CAC TTG GAA TCA TC

Agrobacterium-Mediated Transformation of P. pinaster

Agrobacterium-mediated genetic transformation of *P. pinaster* proliferating SE was performed with proliferating SE, 7 days after sub-culture, i.e., during the phase of active SE growth on proliferation medium.

The transformation procedure was a combination of a reference FCBA/INRAE protocol designed during the Sustainpine project for *P. pinaster* [Trontin and Lelu-Walter, 2010; partially published in Trontin et al. (2002, 2007)] and the "droplet method" adapted for *Larix decidua* (Taryono, 2000). The co-cultivation procedure was performed according to the "droplet method". One colony of *Agrobacterium C58/C1* was inoculated in a liquid YEB medium with appropriate antibiotics at 28°C for approximately 16 h while shaking (200 rpm). The optical density at 600 nm (OD_{600}) of *Agrobacterium* suspension was adjusted to about 0.5. Each clump of immature proliferating SEs was inoculated with one droplet (30 μl) of the *Agrobacterium* suspension. The SEs and agrobacteria were co-cultivated for 2 days in an MSG medium (Klimaszewska, 1989) with 0.1 M acetosyringone in darkness at 21–23°C. For elimination of agrobacteria, the co-cultivated SEs were washed with a 200-ml liquid MSG medium supplemented with 300 mg l^{-1} timentin (MSG-T) for 30 min. Afterward, the SEs were collected on filter paper in a Büchner funnel using a vacuum pump and a short low-pressure pulse. The filter paper was subsequently placed into a solidified MSG-T medium for 10 days. Selection for transgenic embryo clumps (transgenic lines) was performed on an MSG-T medium supplemented with 10 mg l^{-1} hygromycin for 2 weeks. The SEs were then sub-cultured every 2 weeks into the MSG-T medium plus 15 mg l^{-1} hygromycin for 6 weeks. After the selection procedure, transformation efficiency was calculated as the number of hygromycin-resistant lines confirmed by PCR analysis (PCR+ lines) per gram fresh mass (FM) of co-cultivated proliferating SEs.

All transformation experiments were performed twice, and up to 10 PCR+ lines were cryopreserved.

After preliminary SE maturation experiments, we selected two independent PCR+ lines that showed quite stable *PpWOX2* overexpression during SE proliferation (lines OE_#11 and OE_#15). The maturation experiments were performed at the same time for both *35S::PpWOX2* lines, as well as for one empty vector transgenic control line, *pCAMBIA 1305.2* (EV-pC05), and the non-transgenic WT PN519 control line. All transgenic and control lines were managed simultaneously and at the same subculture frequency to avoid any differences related with aging effect.

Culture of Embryogenic Line, Somatic Embryos, and Seedlings of *P. pinaster*

The whole process of SE development since reactivation from the cryopreserved stock involved three developmental stages:

proliferation, maturation, and conversion (Ramarosandratana et al., 2001). In proliferating embryogenic tissues, an immature SE consists of an embryonic region of small, densely cytoplasmic cells subtended by long, highly vacuolated suspensor cells (**Figures 2A,B**). During maturation, the embryonic region became more prominent and opaque. Finally, a cotyledonary SE shows a shoot apex and a root pole containing primary meristems, a well-defined cotyledon ring, and a hypocotyl (**Figure 2C**). Cotyledonary SEs have a potential to germinate and develop into rooted somatic seedlings (**Figure 2D**).

Maintenance and Cryopreservation of Proliferating Immature Somatic Embryos

The PN519 embryogenic line was initially reactivated from the FCBA cryopreserved stock following the method described by Harvengt (2005) but using a modified Litvay et al. (1985) basal formulation (mLV) as reported in Klimaszewska et al. (2001, 2007). Proliferating immature SEs were sub-cultured every 10–14 days on Petri dishes in an mLV basal medium (Klimaszewska et al., 2001, 2007) supplemented with 2 μM 2,4-D (2,4-dichlorophenoxyacetic) acid (Sigma-Aldrich, Germany) and 1 μM BAP (6-benzylaminopurine; Sigma-Aldrich, Germany). Embryogenic cultures were maintained in darkness at 22 ± 2°C. Re-cryopreservation of PN519 transgenic and non-transgenic control WT lines was performed using a protocol previously established for *Abies* and *Larix* species (Zoglauer et al., 2003). Any thawed SE culture batch was reactivated within 1–2 months prior to maturation.

Somatic Embryo Maturation, Yield in Cotyledonary Somatic Embryos, and Morphological Analysis

Development of SEs to reach the cotyledonary stage was performed on mLV-based maturation medium as the best option reported for maritime pine (Lelu-Walter et al., 2016; Trontin et al., 2016b). The method described by Morel et al. (2014) was used with slight modifications. Briefly, 1 g of proliferating SEs (3–5 days after sub-culture in mLV proliferation medium) was washed first and then suspended in 10 ml of the mLV liquid medium without plant growth regulators (PGRs). An aliquot of a suspension (1 ml containing ∼100 mg proliferating SEs) was spread on a sterile filter paper (Whatman No. 2, diameter 11 cm), air-dried at ambient temperature, and placed on a Petri dish in an mLV medium supplemented with 80 μM abscisic acid (ABA; Duchefa, Haarlem, The Netherlands) and 0.2 M sucrose, and solidified with 1% (w/v) gellan gum (Gelrite; Duchefa, Haarlem, The Netherlands). All maturation cultures were maintained in darkness and at 22 ± 2°C. Each maturation experiment was performed on 10 Petri dishes and repeated 2–3 times.

After 12–14 weeks, SE development reached the cotyledonary stage (Morel et al., 2014). Embryogenic potential was estimated as the number of cotyledonary SEs per g FM of embryogenic tissue. Cotyledonary SEs of *PpWOX2* transgenic lines and controls (transgenic EV-pC05 line and non-transgenic WT) were classified according to their morphological characteristics as "normal" (cotyledons with symmetrical radial development, **Figure 2E**), "deformed" (cotyledons with asymmetric development, e.g., one cotyledon, two cotyledons, etc., **Figures 2F,G**), or "not separated," fused embryos (two embryos not clearly separated from each other, **Figure 2H**; Marum et al., 2009).

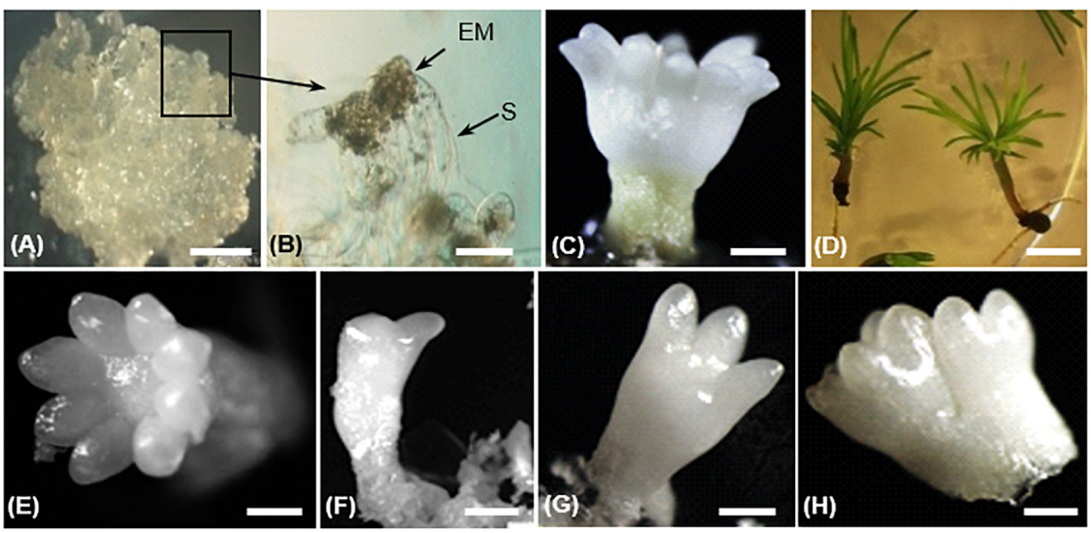

FIGURE 2 | Different steps of somatic embryo (SE) development in *Pinus pinaster* **(A–D)** and morphology of harvested cotyledonary SEs **(E–H)** in transgenic *35S::PpWOX2* lines and control lines (transgenic EV-pC05 line and the non-transgenic WT).**(A)** Embryogenic culture containing proliferating immature SE; **(B)** proliferating SEs showing embryo proper (EP) and suspensor cells (S); **(C)** cotyledonary SE after 14 weeks in maturation medium; **(D)** somatic seedlings after 8 weeks in conversion medium. Cotyledonary SEs from *PpWOX2* and control lines were classified according to different categories such as **(E)** normal (cotyledons with symmetrical radial development), **(F,G)** deformed (cotyledons with asymmetrical development), and **(H)** not separated, fused embryos. Scale bars: **(A)** 3 mm, **(B)** 0.1 mm, **(B,C,E–H)** 2 mm, and **(D)** 5 mm.

Conversion of Cotyledonary Somatic Embryos Into Somatic Seedlings, and Acclimatization

To convert cotyledonary SEs into plantlets, fully developed embryos with well-shaped cotyledons (normal SEs) were placed horizontally onto Petri dishes on the surface of an mLV medium supplemented with 3% sucrose (w/v) and solidified with 0.4% (w/v) Gelrite and 0.06% (w/v) plant agar (Duchefa, Haarlem, The Netherlands). The cultures were maintained in darkness at 22 ± 2°C for 10 days. Afterward, the seedlings were transferred to a long day photoperiod (14-h light, 120 μE m^{-2} s^{-1}, OSRAM Lumilux Cool White light) at 22 ± 2°C for 6–8 more weeks. Seven embryos were placed in each plate. Three replicates were used for each treatment, and experiments for SE conversion were repeated three times. After 6 weeks, the SEs were scored as converted into viable somatic seedlings if an elongated epicotyl, green cotyledons, and primary needles as well as an elongating root apex were observed. The percentage of somatic seedlings with root elongation was determined after 8 weeks of culture.

Callus Induction From Transgenic *PpWOX2* Somatic Seedlings in *P. pinaster*

The ability of different explants from *P. pinaster* somatic seedlings to initiate embryogenic tissue and/or non-embryogenic callus was tested for *PpWOX2* transgenic lines, the empty vector (EV-pC05), and non-transgenic WT control lines. Needle/hypocotyl and root explants of somatic seedlings were collected 6–8 weeks after germination of cotyledonary SEs and cultivated in a conversion medium, i.e., mLV basal medium (Klimaszewska et al., 2001, 2007) without PGRs. The cultures were incubated in darkness for 8 weeks at 21–23°C.

Agrobacterium-Mediated Transformation of *A. thaliana*

Agrobacterium-mediated transformation of *Arabidopsis* seedling plants using the 35S::*PpWOX2* vector was performed with a modified floral-dip method to obtain T_0 seeds (Weigel and Glazebrook, 2002). To select transgenic lines and for regeneration of first-generation (T_1) plants, water-soaked and cold-treated (2 days at 4°C) T_0 seeds were surface-sterilized by immersion in 1.5% NaOCl (active chlorine) for 15 min, followed by three rinses in autoclaved *Aqua purificata* (aqua pur.). Then, the T_0 seeds were cultured *in vitro* in an MS medium (Murashige and Skoog, 1962) supplemented with 20 mg l^{-1} hygromycin and incubated for 4–6 weeks under short day conditions (10-h light, 120 μE m^{-2} s^{-1}). Hygromycin-resistant transgenic T_1 plants obtained from treated T0 seeds were transferred to potting soil for 3–4 weeks under long day conditions to promote flowering. Plants from two independent T_1 transgenic lines (PpWOX2-line #1 and PpWOX2-line #2) were self-pollinated. Resulting seeds of the T_1 generation were harvested and subsequently cultured in an MS medium supplemented with 20 mg l^{-1} hygromycin to regenerate T_2 transgenic plants. The two selected T_1 transgenic lines were shown to be homozygotes for the *PpWOX2* transgene based on both hygromycin-resistance assay and PCR analysis of their T_2 progenies (data not shown).

Histological Studies on *Arabidopsis* Tissues

For preparation of histological sections, *Arabidopsis* tissues (green callus containing embryo-like or leaf-like structures) were fixed in 3% (v/v) glutaraldehyde for 24 h at 4°C. Samples were rinsed in 1 × PBS and dehydrated in an ethanol series (30, 50, 70, 90, and 100%) at 4°C. The samples were then infiltrated in an ethanol:historesin solution (glycol methacrylate, GMA-Leica) ratio series (4:1, 4:2, 4:3, 4:4, 3:4, 2:4, 1:4, and finally 100% historesin) and embedded in historesin (15 ml infiltration solution + 1 ml hardener; Leica, Wetzlar, Germany). Five-μm thick slices were obtained with a rotary microtome (HM 355S; Microm, Walldorf, Germany). The sections were floated on aqua pur. at room temperature, picked up in clean glass slides, and air-dried at 42°C. The sections were stained with 0.5% (w/v) ponceau S for 6 min, rinsed in aqua pur., and stained again with 0.5% (w/v) methylene blue for 15 s followed by rapid rinse in aqua pur. The stained sections were examined using an Olympus SZ X12 microscope.

Molecular Analyses

Confirmation of Transgene Integration

Plant genomic DNA from both *P. pinaster* and *Arabidopsis* materials (transgenic line, embryo, and seedlings) was isolated from a 100-mg FM tissue according to a modified Doyle (1990) protocol (Dumolin et al., 1995).

To confirm genetic transformation, putative independent transgenic events (hygromycin-resistant lines) were tested by PCR using specific primers (**Table 1**) targeting *PpWOX2* (*PpWOX2*-fw and T35S_rev, 592-bp fragment; *PpWOX2*-rev and CaMV35S, 315-bp fragment*)* and *HPTII (HPTII-fw, HPTII-rev,* 412-bp fragment).

For detection of persistent *Agrobacterium* in the putative transgenic events (false positive amplification), PCR was also performed with *NPTII*-specific primers (**Table 1**, **557**-bp fragment).

Gene Expression Analysis by Reverse Transcription-Quantitative PCR

Total RNA from proliferating SEs and cotyledonary SEs of *P. pinaster* was isolated with RNeasy® Plant Mini Kit (Qiagen, Venlo, The Netherlands) using an RLC lysis buffer containing guanidine hydrochloride according to manufacturer's instructions. Total RNA from somatic seedlings of *P. pinaster* (germinated for 6–8 weeks) was isolated according to Chang et al. (1993). Total RNA from *Arabidopsis* seedlings was extracted using TRIzol (Invitrogen) following manufacturer's instructions. cDNA was synthesized from 1 μg total RNA using QuantiTect® Reverse Transcription Kit (Qiagen, Venlo, The Netherlands) as described in the manufacturer's instructions.

Reverse transcription-quantitative (RT-q) PCR reactions were performed with a CFX96™ Real-Time PCR detection system (Bio-Rad, Hercules, CA, United States). Reactions were performed with 1 μl template (10 ng cDNA), 5 μl 2 × SYBR Green Master mix (SensiMix™ SYBR No-ROX Kit; Bioline,

Memphis, TN, USA), 0.3 μl forward and reverse primers (10 μmol μl^{-1}), and aqua pur. to a final volume of 10 μl.

Measurements were carried out on three reactions per cDNA sample (technical replicates) and three cDNA samples that were synthesized from independent RNA samples (biological replicates). Negative controls, i.e., either autoclaved aqua pur. or RNA without reverse transcriptase as template, were included in each run. Three reference genes encoding Helicase (TC151784 from *P. pinaster),* expressed protein At2g32170 (TC125990 from *Pinus taeda*), and mitosis protein YLS8 (TC136697 from *P. pinaster*) were used in combination for normalization of the relative expression of *PpWOX2* in *P. pinaster* (**Table 1**). The expression of these genes was shown to be constant during SE development (Arndt, 2013). The relative expression of *PpWOX2* (both transgene and endogenous genes), *AtWOX2*, *AtWUSCHEL* (*AtWUS*), and *AtLEC1* in *Arabidopsis* was normalized to the expression levels of three reference genes from *Arabidopsis* (*SAND:* At2g28390, *PP2A:* At1g13320, and *PEX4:* At5g25760, **Table 1**) validated by Czechowski et al. (2005).

Real-time RT-qPCR data were analyzed using Bio-Rad CFX Manager Version 1.6.541.1028 and qbase PLUS. Accurate normalization based on multiple internal control genes was achieved following the method of Vandesompele et al. (2002).

RESULTS

Identification of *PpWOX2* and Expression During Somatic Embryo Development in *P. pinaster*

The cDNA sequence (570 bp) of a putative *P. pinaster* homolog to *WOX2* (*PpWOX2*) was independently identified in SustainpineDB [(Acc. KY773924); in this study: Acc. KU962991, Alvarez et al., 2018].

The deduced PpWOX2 protein sequence (Acc. ARS01278; in this work: Acc. ANC94872, Alvarez et al., 2018) shares conserved characteristic features of the plant WOX family (Alvarez et al., 2018). In addition to the conserved homeodomain, many plant WUS/WOX proteins contain a conserved WUS-box (TLPLFP) located downstream of the homeodomain (**Figure 1**, Haecker et al., 2004; Nardmann and Werr, 2006), including in *Pinus pinaster* (Alvarez et al., 2018). Such a putative WUS-box was identified in the PpWOX2 protein sequence and shows the same differences in amino acid sequence compared to *Arabidopsis* (TLPLFPLQP) as other conifers from genera *Pinus*, *Picea* and *Larix* (TLELFPLHP).

Pinus pinaster WOX2 expression (both transgene and endogenous genes) was investigated during normal development of *P. pinaster* SE by RT-qPCR (wild-type samples). Significant variation was detected by ANOVA [$F(8,18) = 23.479$, $P < 0.05$; **Figure 3A**]. Relative expression was highest in proliferating immature SEs and then significantly decreased in cotyledonary SEs. A very low level of *PpWOX2* expression was detected in 6–8-week–old somatic seedlings although not significantly different from that of cotyledonary SEs.

Transformation Efficiency of *P. pinaster* PN519 Line and *PpWOX2* Expression in Transgenic Lines

The transformation efficiency of proliferating SEs with the *35S::PpWOX2* construct or the control empty vector *pCAMBIA1305.2* was 11.9 and 26.0 PCR+ lines g^{-1} FM, respectively. The presence of T-DNA (*HPTII* and *PpWOX2* PCR detection) was confirmed in hygromycin-resistant *35S::PpWOX2* lines in different developmental steps (proliferating SEs, cotyledonary SEs, and somatic seedlings; **Figure 4**). The *NPTII* bacterial selectable marker was not detected in these PCR+ lines during SE development (**Figure 4**), supporting that PCR+ lines are free from contaminating agrobacteria. Ten 35S::*PpWOX2* PCR+ lines and five transgenic control lines (EV-pC05) could be cryopreserved.

Following RT-qPCR, two independent *35S::PpWOX2* lines (#11 and #15) showed higher *PpWOX2* relative expression compared to the wild type (WT) in the three analyzed developmental steps [$F(8,23) = 7.27$, $P < 0.05$; **Figure 3A**]. Observed differences were only significant for line #15 in the proliferating and mature stages but highly significant for both transgenic lines (#11 and #15) in the seedling stage. Similar results were obtained for any of the eight additional *35S::PpWOX2* lines that were generated and cryopreserved (data not shown). Similar to WT, relative expression was decreased in cotyledonary SEs compared to proliferating SEs (although only significant for line #15), suggesting some phase change effect on transition between early and late embryogenesis. Although some differences may exist, in our experiments, *PpWOX2* expression was similar between proliferating SEs and somatic seedlings (no significant differences) in both lines #11 and #15.

Development of *P. pinaster* Somatic Embryos Overexpressing *PpWOX2*

The effect of high constitutive overexpression of *PpWOX2* on SE development in *P. pinaster* was analyzed by evaluating SE maturation and conversion into plantlets for the *35S::PpWOX2* lines (#11 and #15) and controls (WT and EV-pC05).

PpWOX2 over-expressing lines #11 and #15 produced similar and significantly reduced yields in cotyledonary SEs compared to WT (**Figure 3B**). However, embryos of the control transgenic line EV-pC05 showed a similar significant trend [$F(4,84) = 17.046$, $P < 0.05$; **Figure 3B**], suggesting some technical issue related to the genetic transformation procedure (see Discussion and **Supplementary Table 1**). In maritime pine, it has been reported that hygromycin selection could result in reduced yields in cotyledonary SEs (Trontin et al., 2007).

No significant morphological differences were observed between WT and transgenic control line EV-pC05. In contrast, the ANOVA revealed significant variation in normal and deformed embryos among *PpWOX2* transgenic and control lines [$F(11,213) = 30.16$, $P < 0.05$; **Figure 3C**]. The transgenic lines showed significantly reduced yields in normal embryos. Accordingly, a significant, higher percentage of proliferating SEs from lines #11 (47%) and #15 (39%) developed into deformed embryos, mostly with asymmetric development of

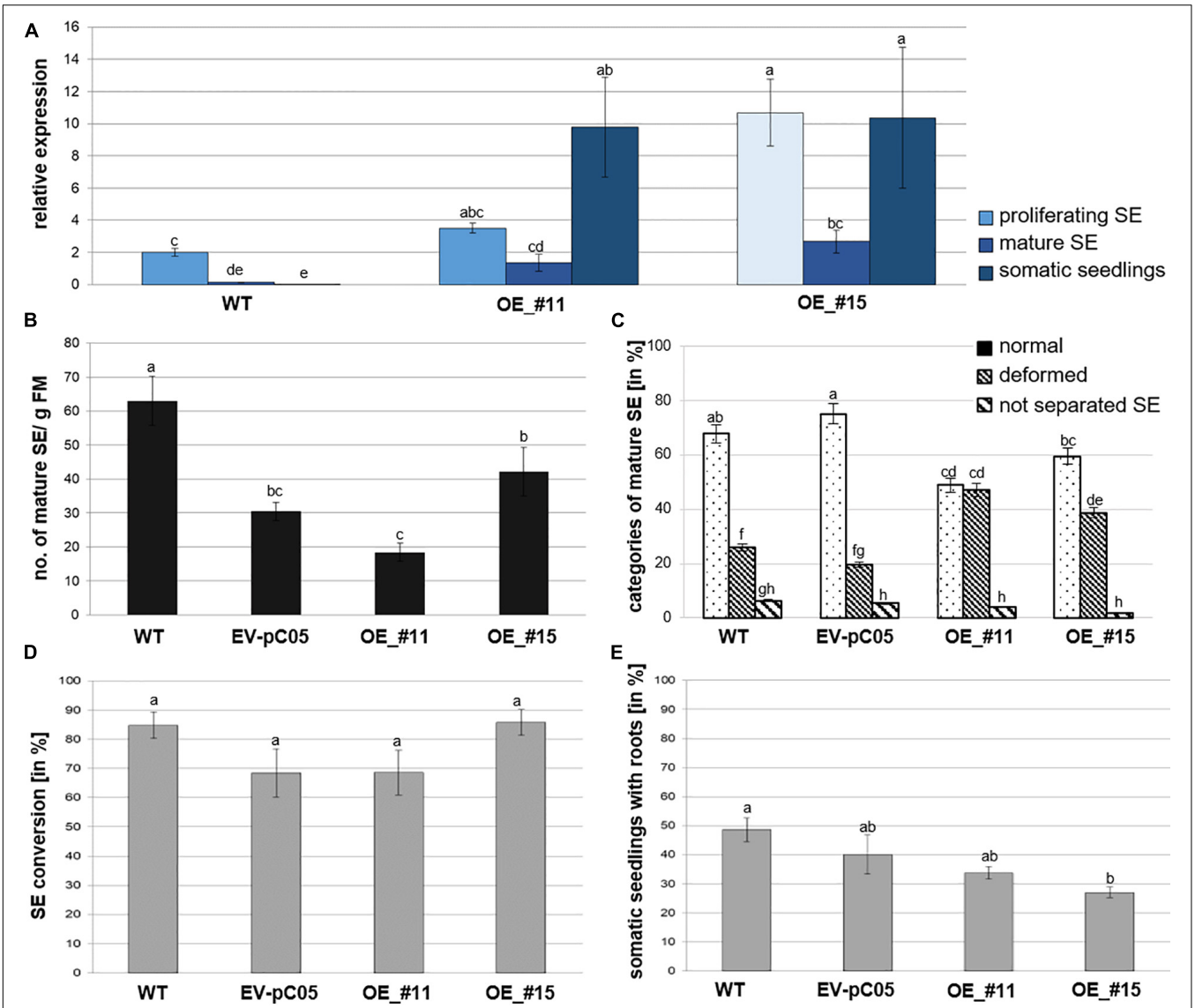

FIGURE 3 | Analysis of *35S::PpWOX2* overexpressing *P. pinaster* lines #11 and #15 (OE_#11 and OE_#15) and controls (WT, EV-pC05) with regard to *PpWOX2* transgene expression following **(A)** RT-qPCR analysis, **(B)** SE maturation, **(C)** cotyledonary SE morphology, and **(D)** conversion **(D)** as well as **(E)** root development. **(A)** Relative expression of *PpWOX2* in proliferating SEs, cotyledonary SEs, and somatic seedlings by RT-qPCR. **(B)** Number of cotyledonary SEs per g FM after 12–14 weeks in maturation medium. **(C)** Percentage of cotyledonary SEs (n = 70) with different morphological phenotypes classified as normal, deformed, or not separated (fused) after 12–14 weeks in maturation medium. **(D)** Percentage of SEs (n = 21) converted into somatic seedlings after 6 weeks in germination medium. **(E)** Percentage of somatic seedlings (n = 21) with active root growth after 8 weeks in conversion medium. Embryos of control transgenic line EV-pC05 were transformed with *pCAMBIA1305.2* (empty vector). WT line was the original PN519 line used for transformation experiment. Each value represents mean ± standard error obtained from three biological replicates and **(A)** 3, **(D,E)** 4, or **(B,C)** 7–10 technical replicates. Bars with different letters are significantly different (ANOVA, $P < 0.05$).

cotyledons when compared to the WT (25%) and control line EV-pC05 (18%).

The overexpression of *PpWOX2* had no detectable early effect on conversion of cotyledonary SEs into somatic seedlings for both *35S::PpWOX2* lines #11 and #15 as compared with the WT and EV-pC05 (**Figure 3D**). High conversion rates were observed for all lines (68–85%). Accordingly, no significant difference in the frequency of somatic seedlings showing active root growth could be detected between *35S::PpWOX2* lines and the EV-pC05 control (**Figure 3E**). As some reduced frequency is observed for all transgenic lines compared to the WT, especially in the case of line #15 $F(4,19) = 5.002$, $P = 0.006$; **Figure 3E**, (as for SE yield), some adverse effects of the genetic transformation procedure have again been suggested.

Somatic embryo (SE) viability was significantly reduced compared to controls after 8–10 weeks of culture in a conversion medium (**Figure 5**). Interestingly, line #15, which had the lowest ability for rooting, showed callus formation in the root region,

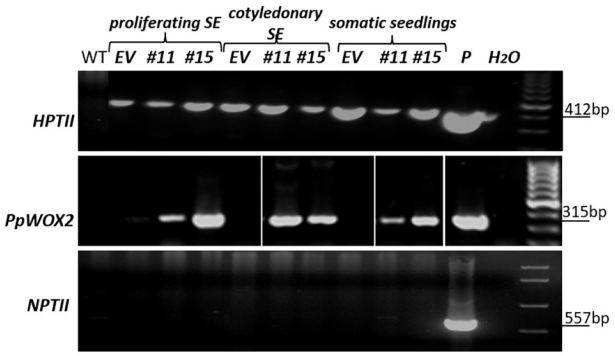

FIGURE 4 | PCR analyses to confirm the presence and stability of the transgene in *35S::PpWOX2 P. pinaster* lines in various developmental steps from proliferating immature SEs to cotyledonary SEs and somatic seedlings. Lines #11 and #15 are PCR-positive (PCR+) throughout SE development. PCR amplification of *HPTII* (412 bp), *PpWOX2* (315 bp), and *NPTII* (557 bp). Empty vector (EV): embryos of control line EV-pC05 transformed with *pCAMBIA1305.2*, *P* = *35S::PpWOX2*-isolated plasmid (positive PCR control). WT, wild-type, non-transgenic PN519 control line. H_2O, negative PCR control (water as template).

and further root development was prevented in 73% of the somatic seedlings (**Figures 3E**, **5D,E**).

To further examine the ability of transgenic plants overexpressing *PpWOX2* to initiate callus production, primary needle/hypocotyls and root explants from the *35S::PpWOX2*, EV-pC05, and WT somatic seedlings were cultured in an mLV medium without PGRs for 8 weeks. No direct somatic embryogenesis initiation could be detected under such experimental conditions. The calli obtained from the different types of explants from all lines were compact and white yellow, and did not differentiate into proliferating SEs (non-embryogenic calli).

The percentage of non-embryogenic callus formation from root explants was significantly higher in line #15 (100%) than in the WT (16%) and EV-pC05 (48%) controls [$F(7,16) = 6.407$, $P = 0$; **Figure 6**]. The observed increase in EV-pC05 compared to the WT explants was also significant and could indicate some habituation phenomenon of transgenic lines (following repeated subculture) to auxin supplemented in the proliferation medium. Nevertheless, this result shows that constitutive overexpression of *PpWOX2* in line #15 resulted in increased propensity to callus formation in the root pole, which, in turn, could be detrimental to root growth and subsequent plant viability (**Figures 3E**, **5**). In the case of line #11, non-embryogenic callus formation (45%) was significantly increased compared to WT, but was not when compared to EV-pC05 [$F(4,84) = 17.046$, $P = 0$; **Figure 6**].

Nearly 65% of the needle/hypocotyl explants of both *35S::PpWOX2* lines #11 and #15 showed callus formation (**Figure 6**), and this was a significantly higher rate than that of the EV-pC05 (24%) and WT controls (0%). Similar to the root explants, EV-pC05 produced significantly more callus from needle/hypocotyl explants than the WT, suggesting, as mentioned earlier, some impact of the genetic transformation procedure.

Overall, the data showed that somatic seedlings of the *35S::PpWOX2* lines have an increased ability to initiate non-embryogenic callus on needle/hypocotyl only (line #11) or both needle/hypocotyl and root explants (line #15) compared to the non-transgenic WT and transgenic EV-pC05 controls.

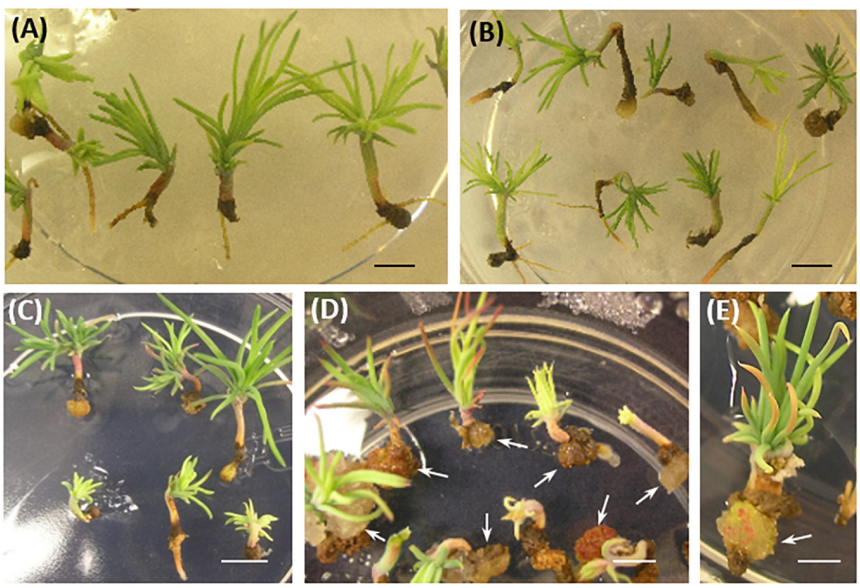

FIGURE 5 | *P. pinaster* somatic seedlings from *35S::PpWOX2* transgenic lines and controls (EV-pC05, WT) after 8–10 weeks in conversion medium. **(A)** WT and **(B)** EV-pC05 somatic seedlings with similar and normal phenotype. The root growth of somatic seedlings from the *35S::PpWOX2* lines was reduced **(C,D)** and ultimately affected SE viability and behavior. Note the formation of callus in the root region of line #15 [**(D,E)**, arrows] compared to the WT and EV-pC05 controls **(A,B)**. Scale bars: **(A)** 2 mm, **(B–D)** 3 mm, and **(E)** 1 mm.

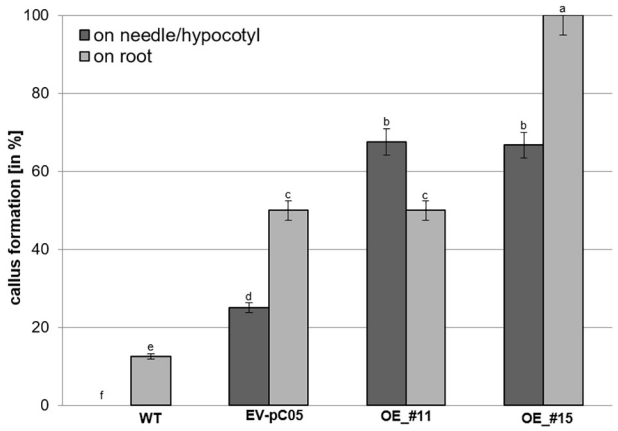

FIGURE 6 | Percentage of non-embryogenic callus formation from *P. pinaster* primary needle/hypocotyl or root explants ($N \approx 20$) of the *35S::PpWOX2* lines #11 and #15, transgenic EV-pC05, and non-transgenic WT controls in mLV medium without PGR (conversion medium). Each value represents mean ± standard error from three biological replicates and five Petri dishes as technical replicates. Bars with different letters indicate significant differences (ANOVA, $P < 0.05$).

Phenotypic Response in Arabidopsis Plants Overexpressing PpWOX2

The overexpression of *PpWOX2* in *Arabidopsis* had different effects on the phenotype of transgenic (PCR+) seedlings from the T_1 and T_2 generations.

Considering *PpWOX2*-expressing plants from the T_1 generation, significant variation in the frequency of four classes of phenotypes were detected [$F(3,8) = 9.74$, $P = 0.005$, **Figure 7A**]. Only 16% of the *PpWOX2*-T_1 transgenic seedlings showed the WT normal phenotype (**Figures 8A,F**), and the remaining 84% of the plants showed alterations such as stunted growth (34%, **Figure 8G**), embryo-like structures (35%, **Figure 8H**), and leaf-like structures (14%, **Figure 8J**). Histological examinations of the embryo-like structures (**Figure 8H**) revealed the presence of globular SEs with actively dividing cells (**Figure 8I**). Histochemical observation of the leaf-like structures (**Figure 8J**) only showed leaf anatomical characteristics without any evidence for embryo formation (**Figure 8K**).

In contrast to the T_1 generation, a high percentage of the *PpWOX2*-expressing T_2 plants showed normal (WT) growth with significant differences between the two investigated lines, *PpWOX2*_At#1 (85%) and *PpWOX2*_At#2 [60%, $F(7,24) = 21.635$, $P = 0$; **Figure 7B**]. Stunted growth was observed in only 9–15% of the plants without significant difference between the lines (**Figure 7B**). In addition, two new phenotypes were observed that did not appear previously in the T_1 generation. First, a number of T_2 seedlings (5–22%) were arrested in the two-cotyledon stage (**Figure 7B**), and no further leaf formation was observed (**Figure 8L**). This phenotype was found more frequently in *PpWOX2*_At#2 (22%) than in *PpWOX2*_At#1 (5%) lines [$F(7,24) = 21.63$, $P = 0$, **Figure 7B**]. Second, embryo-like structures suggesting direct somatic embryogenesis was observed at root tips of some plants from both *PpWOX2* transgenic lines (**Figure 8M**) but in quite low frequency (≤1.7%, **Figure 7B**).

The morphology and regeneration ability of embryo-like structures obtained from *PpWOX2* T_1 plants (**Figure 8H**) were compared with that of SEs (**Figure 8C**) and non-embryogenic calluses (**Figure 8B**) initiated from the WT seedlings. Embryo-like structures and SEs were similar in their germination and regeneration abilities and phenotypes, as illustrated in **Figure 8D** (WT SEs) and 8N (*PpWOX2* plants derived from embryo-like

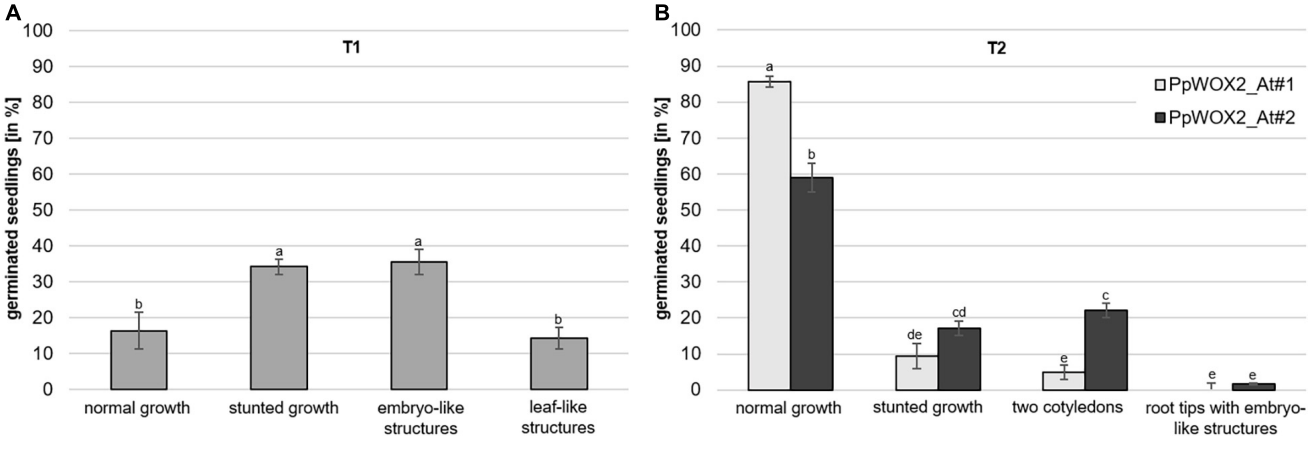

FIGURE 7 | Frequency of different phenotypes among *PpWOX2* overexpressing *Arabidopsis* plants from the T_1 or T_2 generation. **(A)** T_0 seeds transformed with the *35S::PpWOX2* gene cassette were germinated and resulting T_1 plants (N = 70–80) developed different phenotypes (normal or stunted growth, embryo-like and leaf-like structures) in various frequencies. **(B)** T_1 seeds transformed with the *35S::PpWOX2* gene cassette (N = 70–80) were germinated and resulting T_2 plants from 2 independent transgenic lines (*PpWOX2*_At#1 and *PpWOX2*_At#2) developed either some phenotypes similar to those of T_1 plants (normal growth and stunted growth) or new phenotypes not previously detected in the T_1 plants (only two cotyledons and plants with root tips that formed embryo-like structures). Error bars indicate standard error for means of three biological replicates and 7–8 technical replicates. Bars with different letters show significant statistical differences ($P < 0.05$).

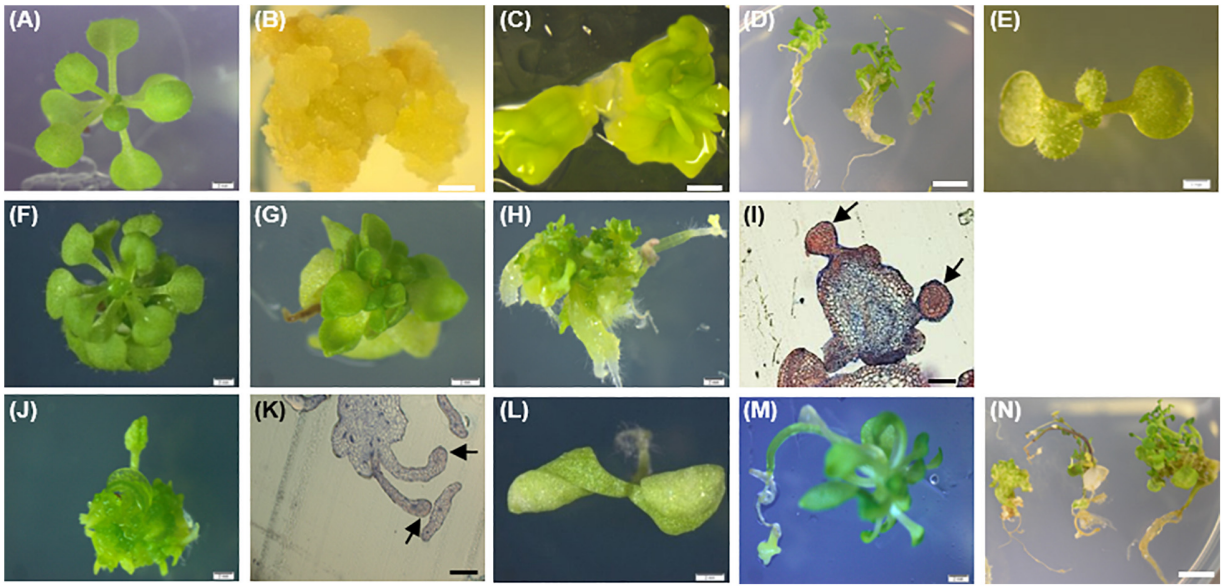

FIGURE 8 | Phenotypes of the *35S::PpWOX2* transgenic plants, transgenic EV-pC05, and non-transgenic WT control plants of *Arabidopsis*. **(A)** WT seedling from first (T_1) or second (T_2) generation grown in MS medium without PGRs for 7 weeks. **(B)** WT non-embryogenic callus. **(C)** WT SEs obtained from explants of immature zygotic embryos cultivated in an induction medium (B5 medium supplemented with 5 μM 2,4-D) after 4 weeks. **(D)** WT SEs germinated and developed into somatic plants in MSR medium after 2 weeks. **(E)** EV-pC05 transgenic plant (transformed with the *pCAMBIA1305.2* empty vector) grown in MS medium supplemented with 20 mg l^{-1} hygromycin. These control plants exhibited a normal phenotype similar to that of WT seedlings **(A)** in both T_1 and T_2 generations. *PpWOX2*-transformed seeds of the T_1 generation germinated in MS medium supplemented with 20 mg l^{-1} hygromycin and exhibiting **(F)** normal growth, **(G)** stunted growth, **(H)** embryo-like structures, or **(J)** leaf-like structures. Histological aspects of **(I)** embryo-like structures and **(K)** leaf-like structures (arrows) were analyzed after staining with Ponceau-methylene blue. The T_2 generation of *PpWOX2* transgenic seeds developed into plants with **(F)** normal growth, **(G)** stunted growth, **(L)** two cotyledons, or **(M)** root tips forming embryo-like structures. **(N)** Embryo-like structure from the *PpWOX2* T_1 plant generation converted into somatic plants in MSR medium. Scale bars: **(B,C,H,J)**, and **(L)** 0.5 mm; **(A,E,F,G)** 1 mm; **(D,N)** 1.2 mm; and **(I,K)** 0.2 mm.

structures), respectively. No plant regeneration could be obtained from non-embryogenic calluses.

The *PpWOX2* transgenic plants initiated flower formation earlier (12–15 days after germination) than the WT and EV-pC05 control plants (22–28 days). Control transgenic line EV-pC05 exhibited normal growth (a phenotype similar to that of WT-plants) in both the T_1 and T_2 generations (**Figure 8E**).

Expression of Endogenous Embryogenesis-Related Genes in Arabidopsis Plants Overexpressing PpWOX2

In order to investigate whether the constitutive overexpression of *PpWOX2* in *Arabidopsis* affects the expression of selected embryogenesis-related endogenous genes, the expression of *AtWOX2*, *AtWUS*, and *AtLEC1* was estimated by RT-qPCR in *35S::PpWOX2* T_1 and T_2 transgenic lines exhibiting different phenotypes (**Figure 9**). Controls were the empty vector transgenic line (EV-pC05_At) and various non-transgenic lines with unknown (WT seedlings), demonstrated (WT SE), or no (non-embryogenic callus) embryogenic ability. All analyzed tissues (excluding non-embryogenic callus) were sampled from plants of the same age and developmental stage.

The relative expression of *PpWOX2* was confirmed to be significantly higher in transgenic *Arabidopsis* plants of both T_1 and T_2 generations than in transgenic (EV-pC05_At) and non-transgenic (WT) controls [$F(7,16) = 3.882$, $P = 0.012$; **Figure 9A**]. Among the different phenotypes observed for the T_1 and T_2 plants, expression was similar and lowest for plants showing normal and stunted growth as illustrated for the *PpWOX2*_At#2 line (**Figure 9A**, right graph). *PpWOX2* expression was much higher in T_1 plants showing embryo- or leaf-like structures than in transgenic plants with normal growth (10- to 35-fold ratio, data not shown). Similarly, *PpWOX2* expression was significantly higher in T_2 plants with the "two-cotyledon" phenotype for both lines *PpWOX2*_At#1 (data not shown) and *PpWOX2*_At#2 (128-fold ratio, **Figure 9A**, right graph). The reduced behavior of T_2 transgenic plants with root tips showing an embryo-like structure did not allow for gene expression analysis.

In contrast to *PpWOX2*, the expression of *AtWOX2* (**Figure 9B**) was mostly similar in the T_1 plants and controls (**Figure 9B**). Only plants with the "leaf-like structure" phenotype showed significantly reduced *AtWOX2* expression compared to the non-transgenic SE control. Considering the T_2 plants, some significant differences were observed for the *PpWOX2*_At#1 line, which showed higher *AtWOX2* expression than the EV-pC05_At and non-embryogenic callus controls. However, the expression was similar to that of control non-transgenic seedlings and SE (WT). Similarly, no significant difference compared to controls could be detected in the case of line *PpWOX2*_At#2 when all plant phenotypes were considered together as a mixture. Analyzing

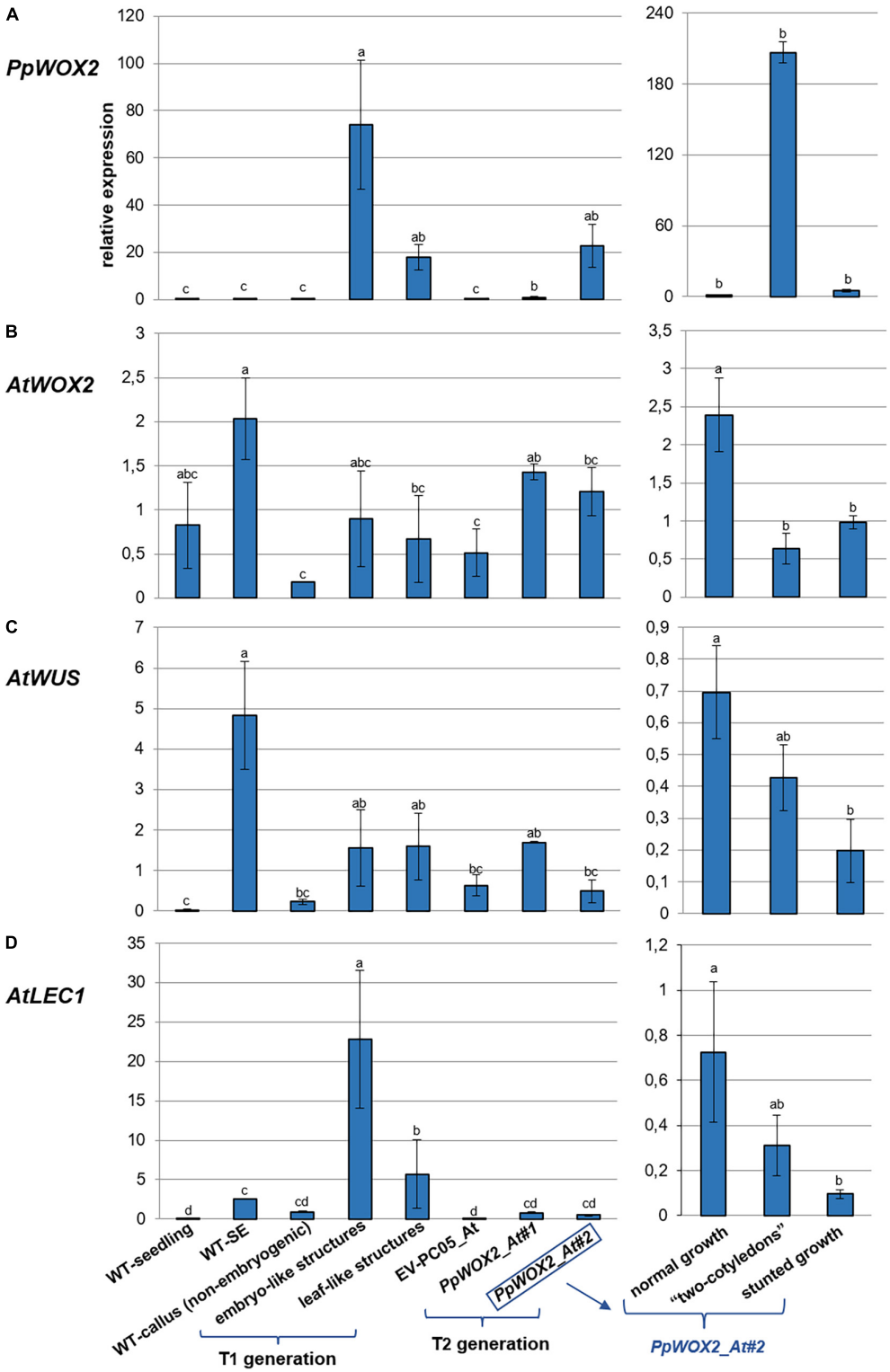

FIGURE 9 | Relative expression of **(A)** *PpWOX2*, **(B)** *AtWOX2*, **(C)** *AtWUS*, and **(D)** *AtLEC1* in *Arabidopsis* plants obtained from *PpWOX2* overexpressing lines (T_1 and T_2 generations), transgenic EV-pC05_At, and non-transgenic WT controls (seedlings and somatic embryos/SE) at the same age and developmental stage by RT-qPCR. Each value represents mean ± standard error of three biological replicates and three technical replicates. Bars with different letters indicate significant differences (ANOVA, $P < 0.05$). The different phenotypes are illustrated in **Figure 8**. Samples *PpWOX2*_At#1 and *PpWOX2*_At#2 from the T_2 generation are a mixture of plants with the "normal," "two-cotyledon," and "stunted growth" phenotypes. Gene expression is presented separately for these three phenotypes for line *PpWOX2_At#2* (right part of the figure).

separately the different plant phenotypes for this line revealed that *AtWOX2* expression is similarly and significantly reduced in plants with two cotyledons or stunted growth compared to plants with normal growth (**Figure 9B**, right graph). We concluded that *PpWOX2* overexpression had apparently little effect on the expression of endogenous *WOX2*. The *PpWOX2*_At#2 data for plants with normal, stunted, or two-cotyledon phenotypes, however, suggest some inverse relationship between *PpWOX2* (**Figure 9A**) and *AtWOX2* expressions (**Figure 9B**).

In the case of *AtWUS* expression (**Figure 9C**), some significant differences with non-transgenic control seedlings were detected for T_1 plants and T_2 plants from the *PpWOX2*_At#1 line (higher expression than in WT seedlings). *AtWUS* expression in T_2 plants from the *PpWOX2*_At#2 line was also significantly lower than in non-transgenic control SEs. However, *AtWUS* expression was found to be similar in both T_1 and T_2 *PpWOX2* transgenic plants and EV-pC05_At transgenic control, suggesting that *PpWOX2* overexpression had no drastic effect on the expression of this gene. *AtWUS* expression was found to be higher in T_2 plants from line *PpWOX2*_At#2 exhibiting normal growth (significant) and "2 cotyledon" phenotype (non-significant) compared to plants with "stunted" phenotype (**Figure 9C**, right graph). However, there is no clear correlation with *PpWOX2* transgene expression.

Expression of *AtLEC1* is significantly higher in T_1 plants with embryo-like and leaf-like structures than in all the controls (**Figure 9D**). In contrast, no significant difference could be detected in the case of T_2 plants. However, considering line *PpWOX2*_At#2, *AtLEC1* expression (**Figure 9D**, right graph) showed a pattern similar to that for *AtWUS* (**Figure 9C**, right graph), i.e., higher expression in plants with normal growth (significant) and "two-cotyledon" phenotype (non-significant) compared to plants with stunted growth.

In brief, high *PpWOX2* expression in T_1 transgenic plants with embryo-like or leaf-like structures is correlated with increased expression of *AtLEC1* but not *AtWOX2* or *AtWUS*. High *PpWOX2* expression in T_2 transgenic plants with the "2-cotyledon" phenotype is correlated with decreased expression of *AtWOX2*.

DISCUSSION

In angiosperms, the transcription factor *WOX2* is necessary for cell fate and delineation of the apical embryo domain during embryogenesis (Haecker et al., 2004; Xiao et al., 2006). Zhang et al. (2017) demonstrated that *WOX2* contributes to the initiation of shoot meristem stem cells in the embryo of *Arabidopsis*. Several reverse genetic studies have been reported on knockout and overexpression of *WOX2* in angiosperms, mainly in *Arabidopsis* (Haecker et al., 2004; Jeong et al., 2011; Elhiti et al., 2013; Chung et al., 2016; Zhang et al., 2017). For example, loss of *AtWOX2* function in zygotic embryos of *Arabidopsis* has only relatively mild consequences and results in aberrant divisions at the apex of the globular pro-embryo and, occasionally, seedlings with a single cotyledon (Haecker et al., 2004; Jeong et al., 2011). In contrast, overexpression of *AtWOX2* in *Arabidopsis* causes severe growth defects and further morphological phenotypes by impairing plant organ formation (Chung et al., 2016).

In conifers, much attention has been paid to identify genes that are important during embryogenesis [Park et al., 2010; Rupps et al., 2016; reviewed in Cairney and Pullman (2007), Miguel et al. (2016), Trontin et al. (2016a)] but a considerable number of studies are still needed to unravel the precise spatiotemporal function of each gene. Zhu et al. (2016) reported that downregulation of *WOX2* of *Picea abies* (*PaWOX2*) during early embryogenesis resulted in significant decrease in the yield of mature embryos. In contrast, downregulation of *PaWOX2* after late embryo formation had no effect on further embryo development and maturation. In this study, we focused on the functional study on a *WOX2* gene isolated from *P. pinaster* (*PpWOX2*) by constitutive overexpression of *PpWOX2* in both *P. pinaster* SEs and *Arabidopsis* seedlings.

The deduced WOX2 protein shares the WUS-type homeodomain and the conserved WUS-box of the WOX family proteins (**Figure 1**). Based on phylogenetic analyses, the 15 members of the WOX family are divided into three clades: the ancient clade, the intermediate clade, and the WUS clade (modern clade) (van der Graaff et al., 2009; Hedman et al., 2013; Lian et al., 2014; Alvarez et al., 2018). The modern clade contains *WUS* and *WOX1-7* members that are found in seed plants, confirming an evolutionary relationship among *WOX* genes of this group (Lian et al., 2014; Alvarez et al., 2018). *PpWOX2* shares high identity to its homolog in *Pinus sylvestris* (97%) and *Pinus contorta* (95%), low global identity to the *WOX2* of *Picea abies* (76%) and *Larix decidua* (63%), and very low identity to the *WOX2* of *Arabidopsis* (35%) (Hedman et al., 2013; Zhu et al., 2016).

The expression of endogenous *PpWOX2* in *P. pinaster* is high in the SE proliferation step but significantly decreases after SE maturation. No *PpWOX2* expression could be detected later in somatic seedlings. These data confirmed (SE development) and extend (somatic plant development) previous results obtained by Alvarez et al. (2018) from a different *P. pinaster* embryogenic line and following a different protocol for somatic embryogenesis. A similar *WOX2* expression pattern has been found in other conifers such as *Larix decidua* (Rupps et al., 2016), *Picea abies* (Palovaara et al., 2010a; Hedman et al., 2013), and *Picea glauca* (Klimaszewska et al., 2011). These differences in *WOX2* expression during SE development may be explained by an internal control of *PpWOX2* by other genes that are differentially expressed during development, such as polar auxin transport-related genes (PIN genes) (Palovaara and Hakman, 2009). Considering these expression data, it would be interesting to confirm that *PpWOX2* can be used in *P. pinaster* to distinguish in the proliferation stage embryogenic from non-embryogenic tissues. In conifers, the expression of *WOX2* is indeed known as a putative marker for effective initiation of somatic embryogenesis and to predict the embryogenic potential (embryogenecity) of a culture (Palovaara and Hakman, 2008; Park et al., 2010; Klimaszewska et al., 2011; Miguel et al., 2016).

Over-expression of *PpWOX2* in proliferating SEs of *P. pinaster* had, apparently, a negative effect on maturation (**Figure 3B**). Both lines, OE_#11 and OE_#15, were found to have a

significant lower maturation ability than the non-transgenic WT control. These results are consistent with those reported by Klimaszewska et al. (2010). In this report, it was shown that induced overexpression of *AtWUS* in SEs of *Picea glauca* had a striking effect on SE maturation by disrupting embryo development. According to this result, it may be postulated that *WOX* genes of (at least) the modern clade influence embryo development in conifers. However, embryos of the empty vector control line (EV-pC05) also showed significant decrease in maturation yield in our experiments compared to non-transgenic WT embryos, suggesting that reduced yield could also result from transgene positional effects and/or technical issues such as differences in physiological aging between transgenic lines and WT controls (discussed in **Supplementary Table 1**). In maritime pine, physiological aging of embryogenic lines results in reduced maturation yield (Breton et al., 2006; Lelu-Walter et al., 2016; Trontin et al., 2016b). Aging effects could, therefore, result from unperceived differences in management of transgenic and WTs during the long process of genetic transformation. The development of a simplified, rapid, and improved genetic transformation protocol of embryogenic tissues would be profitable to reduce possible protocol-related effects on maturation yield. Furthermore, the choice of a selective agent may influence maturation results. Hygromycin is known to affect negatively maturation yield in *P. pinaster* when used at 20 mg l^{-1} (Trontin et al., 2007). Although hygromycin concentration was reduced to 10–15 mg l^{-1} in our experiments, hygromycin could have affected the regeneration of transgenic embryos of the *PpWOX2* and control EV-pC05 lines.

The overexpression of *PpWOX2* in *P. pinaster* negatively affected SE development with i) significantly increased frequency of deformed SE, especially asymmetrical cotyledon development (lines OE_#11 and OE_#15, **Figure 3C**) and ii) non-embryogenic callus formation in the root pole of germinating somatic seedlings, with subsequent inhibition of root growth (especially in the highly overexpressing line OE_#15, **Figures 3E**, **5D,E**). Similarly, Klimaszewska et al. (2010) reported the inhibition of root growth in somatic seedlings of *Picea glauca* after induced overexpression of *AtWUS* during SE conversion. Following downregulation of *WOX2* during early embryogenesis in *Picea abies*, a unique function of *WOX2* was suggested in conifers during protoderm development and suspensor expansion, which are important steps for proper early embryo development (Zhu et al., 2016).

To further investigate the propensity of young *P. pinaster* somatic seedlings transformed with *PpWOX2* by callus formation, needle/hypocotyl and root explants from two transgenic lines were cultured in the mLV medium (Litvay et al., 1985) without PGRs. No formation of embryogenic tissue could be detected from both transgenic lines and controls, suggesting that *PpWOX2* constitutive overexpression had no major and direct effect that could stimulate embryogenic potential in young somatic seedlings without PGRs. mLV is the currently preferred basal medium for *P. pinaster* to initiate somatic embryogenesis from immature zygotic embryos (with or without PGRs, Trontin et al., 2016b) and secondary embryogenesis from cotyledonary SEs and somatic seedlings (with PGRs, Klimaszewska et al., 2009). Furthermore, mLV is useful to induce non-embryogenic callus formation from young to more mature materials with or without PGRs (Trontin et al., 2016b,c). Therefore, we initially considered that the overexpression of *PpWOX2* could be sufficient to stimulate the formation of embryogenic tissues from somatic seedling explants. However, as in most conifer species (see Bonga et al., 2010), initiation of somatic embryogenesis in *P. pinaster* materials older than immature zygotic embryos (Trontin et al., 2016c) or cotyledonary or young germinating SEs (Klimaszewska et al., 2009) is still difficult to achieve and may require the additional use of PGRs such as auxin and/or cytokinins. Recently, it was shown that abscisic acid (ABA) supplementation can also lead to initiation of somatic embryogenesis in the Douglas fir (*Pseudotsuga menziesii*) (Walther et al., 2021) and has to be taken into consideration as a signal for SE activation. Induction of secondary somatic embryogenesis from germinated SEs could be obtained but at low rate with a combination of 2,4-D (9.5 μM) and BA (4.5 μM) in *P. pinaster* (Klimaszewska et al., 2009). In *Capsicum annuum*, ectopic *BABY BOOM* expression is not sufficient to induce embryogenesis, and exogenous cytokinin is required for SE formation (Heidmann et al., 2011). However, ectopic expression of *BABY BOOM* in *Arabidopsis* and *Brassica* led to spontaneous formation of SEs and cotyledon-like structures in seedlings without the use of exogenous PGRs (Boutilier et al., 2002). The enhanced embryogenic potential of young somatic seedlings in *P. pinaster* may require a combination of ectopic expression of embryogenesis-related gene(s) and adequate PGR treatment and/or other environmental conditions.

Instead of embryogenic callus, non-embryogenic callus formation was determined with high frequency in needle/hypocotyl (significant in both lines #11 and #15) and/or root explants (significant in line #15) of *PpWOX2* somatic seedlings (**Figure 6**) cultivated in mLV deprived of PGRs. Non-embryogenic callus formation was similarly significantly enhanced in the transgenic control EV-pC05 line compared to the WT, suggesting some technical issues related with genetic transformation. However, this increase was lower than that observed for the *35S::PpWOX2* lines except in the case of line #11 for the root explants. These results may be explained by alteration in levels of endogenous hormones, particularly auxin, in response to *PpWOX2* overexpression in somatic seedlings. Recent studies showed that at the time of stem cell initiation, *WOX2* affects the auxin pathway by increase in expression of the auxin transporter *PIN1* gene (Zhang et al., 2017). In conifers, Palovaara and Hakman (2009) suggested that polar auxin transport is involved in regulation of the expression of both the auxin efflux carrier (encoded by *PIN1*) and *WOX2*. N-1-naphthylphthalamic acid (NPA) treatment of embryos before cotyledon initiation, indeed, disrupted the endogenous auxin pattern and expression of both *PIN1-like* and *WOX2* (Hakman et al., 2009). Interestingly, the expression of *PIN* homologs was associated with the auxin immunolocalization pattern during cotyledon formation in *Picea abies* (Palovaara et al., 2010b). It was suggested that correct auxin transport is crucial during transition from early to pre-cotyledonary embryos and that it is involved in the coordinated regulation of *WOX2* and *PIN1* (Trontin et al., 2016a), which,

in turn, could affect both cotyledonary embryo development (especially cotyledon formation) and normal root formation. Further analysis is needed to consider the interplay of *PpWOX2* and auxin in *P. pinaster* and other conifers.

Furthermore, the heterologous overexpression of *PpWOX2* in *Arabidopsis* resulted in transgenic seedlings (T_1 and T_2 generations) with different phenotypes such as normal growth, stunted growth, and embryo-like and leaf-like structures. One-third (35%) of the first generation of *PpWOX2*-At plants showed embryo-like structures. In addition, a similarly high number of T_1 plants exhibited stunted growth (35%) and leaf-like structures (15%). *PpWOX2* expression was comparatively low in T_1 plants exhibiting a normal growth phenotype (similar data to "normal growth"-type of T_2 plants, **Figure 9A**, right graph). In different phenotypes of T_2 plants, reduced *PpWOX2* expression in the normal phenotype compared to stunted- and even more (significant) two-cotyledon phenotypes (**Figure 9A**) apparently resulted in increase in frequency of the normal phenotype in T_2 plants compared to the other phenotypes (**Figure 7B**), while a positive link between the expression of *PpWOX2* and the frequency of abnormal phenotypes was observed in the T_2 plants. Similarly, the overexpression of *PpWOX2* in immature SEs of *P. pinaster* (**Figure 3A**) is correlated to decrease in the frequency of normal, well-developed, cotyledonary embryos compared to the WT (**Figure 3B**), although not significant in our experiments when compared to the EV-PC05 transgenic control. Overall, these results suggest that the high, constitutive expression of *PpWOX2* negatively affects the frequency of the normal phenotype in both *Arabidopsis* and *P. pinaster*.

PpWOX2 expression is higher in the transgenic T1 and T2 plants than in the WT control material (seedlings, SEs, non-embryogenic callus) and transgenic control EV-pC05 (**Figure 9A** and **Supplementary Table 1**). However, the different phenotypes observed in transgenic T1 and T2 plants (**Figures 7**, **8**) are only weakly supported by gene expression data (e.g., lower *PpWOX2* expression in the T2 plants with normal and stunted growth than in the "two-cotyledon" plants, **Figure 9**). Some post-transformation silencing effects related to 35S promoter inactivation (a well-known effect during transgenesis) may be partially responsible for such discrepancy. It can be suspected that transgene inactivation (and associated phenotype reversion) could be high in the T2 generation as the frequency of plants with normal phenotype is significantly higher (60–85%) than in T1 (15–20% only). Different *PpWOX2* expression levels revealed by RT-qPCR may, therefore, not reflect the actual levels of PpWOX2 protein production. Our data do not allow for a study on whether transcriptional or post-transcriptional silencing mechanisms could be involved. However, considering the high levels of *PpWOX2* expression observed in some plants with abnormal phenotypes, such as the two-cotyledon T2 plants (At#2), and embryo-like and leaf-like T1 structures (**Figure 9A**), it could largely be an effect of post-transcriptional or even translational regulation of *PpWOX2* expression. There is generally low support in our experiments for an effect of *PpWOX2* overexpression (**Figure 9A**) on the germination rate of T1 and T2 plants (**Figure 7**). Observed data may be more related with various degrees of silencing, as only T2 plants with normal phenotype germinated with excellent rates (similar to those of WT seedlings).

Moreover, in *Arabidopsis*, the embryo-like and leaf-like phenotypes in T_1 plants, persistence of the stunted growth phenotype in T_1 (35%) and T_2 plants (up to 15%), and production of T_2 plants with two cotyledons (5–20%) or formation of embryo-like structures on the root tip (1.7%) directed us to analyze the endogenous expression of several major embryogenesis-related genes (*AtWOX2*, *AtLEC1,* and *AtWUS*) to investigate a putative association with observed phenotypes. As hundreds of genes are probably involved in *Arabidopsis* embryogenesis, an extension of this expression study and additional transcriptomic and/or proteomic approaches are required to gain further insight into intrinsic processes (Tzafrir et al., 2004; De Smet et al., 2010; Elhiti et al., 2013).

PpWOX2 constitutive over-expression in *Arabidopsis* had a globally low effect on endogenous *AtWOX2* and *AtWUS* expressions, which are roughly similar in transgenic lines and controls from the T_1 and T_2 generations.

The expression of *AtLEC1* was much more affected, especially in the T_1 generation (significant overexpression). Indeed, transgenic *PpWOX2* plants from the T_1 generation with embryo-like and leaf-like structures showed very high expression of *AtLEC1* compared to the WT non-transgenic (seedlings, SEs, and non-embryogenic callus) and transgenic (EV-pC05_At) controls. These strong results suggest that overexpression of *PpWOX2* in *Arabidopsis* may stimulate embryogenesis and organogenesis through coordinated overexpression of *AtLEC1*. Consistent with this outcome, previous reports support that the over-expression of *AtLEC1* in *Arabidopsis* induced somatic embryogenesis in vegetative cells (Lotan et al., 1998).

In addition, the expression of *PpWOX2* in transgenic plants with embryo-like and leaf-like structures was much higher (10 − 35-fold) than in transgenic plants with normal growth. Therefore, a plausible explanation is that ectopic expression of *PpWOX2* in *Arabidopsis* might act redundant with *AtWOX*2 in inducing embryogenesis and/or organogenesis. Another possible explanation is that the overexpression of *PpWOX2* in *Arabidopsis* might result in the over-expression of *AtWUS,* which activates the expression of *LEC1* and promotes somatic embryogenesis. It was reported that *AtWUS* promoted somatic embryogenesis and activated the expression of *LEC1*, *LEC2,* and *FUS3* in cotton (Zheng et al., 2014). The authors suggested that *AtWUS* may alter *PIN* expression, which could lead to establishment of new auxin gradients. Subsequently, a new auxin response was formed and stimulated the expression of *LEC1*, *LEC2,* and *FUS3*. In addition, the overexpression of *GgWUS* from *Gnetum gnemon* (Coniferopsida) in *Arabidopsis* was observed to induce somatic embryogenesis and organogenesis (Nardmann et al., 2009). In fact, *WUS* is involved in regulation of both meristematic stem cells (pluripotent) and embryogenic stem cells (totipotent) (Elhiti et al., 2013). Moreover, *WUS* is known as an embryogenesis marker in embryonic cells, and its overexpression in *Arabidopsis* resulted in somatic embryogenesis and repeated formation of adventitious shoots in the absence of auxin (Zuo et al., 2002; Elhiti, 2010). We did not obtain clear results of

AtWUS expression during our experiments. The data showed some high expression of *AtWUS* compared to the non-transgenic WT seedling control, but the differences were not significant compared with the other non-transgenic (WT-SE, WT-callus) and transgenic (EV-pC05_At) controls. The heterologous expression of *PpWOX2* in *Arabidopsis* (which only has 35% similarity with *AtWOX2,* **Figure 1**) cannot apparently direct increased expression of either *AtWUS* (**Figure 9C**) or *AtWOX2* (**Figure 9B**), which, in turn, could affect the expression of *AtWUS* and/or *AtLEC1*. Specific experiments are, therefore, needed to confirm this hypothesis.

Considering the emergence of various phenotypes in the T_2 generation following *PpWOX2* overexpression, our data showed that the normal/abnormal plant phenotype is associated with altered *AtWOX2*, *AtWUS,* and *AtLEC1* expression (*PpWOX2_At#2*). It is suggested that variable levels of ectopic overexpression of *PpWOX2* could affect the expression of these three embryogenesis-related genes.

One possible further explanation on how overexpression of *PpWOX2* in *Arabidopsis* can stimulate somatic embryogenesis and organogenesis is the high similarity of the *WUS* family-specific homeodomain and the WUS-box from PpWOX2 and AtWOX2 proteins. In plants, the *WOX* homeobox is assigned to a subfamily of homeobox transcription factors that are involved in plant embryonic patterning. However, the function of the *WOX* homeobox has not yet been analyzed in plants. In animals, it is confirmed that a homeobox gene family (HOX), which is expressed in specific embryo domains, has a major regulatory role during early pattern formation, similar to that of the WOX homeobox family (Haecker et al., 2004). In this study, the complete protein sequences of PpWOX2, AtWOX2, and AtWUS show low similarity (35%), but they share high similarity (78%) in the WUS-type homeodomain and WUS-box. Wu et al. (2007) suggested that functional redundancy in the WOX family was not solely determined by overall protein sequence similarity but by high similarities of the homeodomains.

Thus, it can be concluded that high similarities of the WUS-type homeodomain and WUS-box among *PpWOX2*, *AtWOX2,* and *AtWUS* might be sufficient for functional redundancy in these *WOX* proteins. This speculation is supported by several lines of evidence:

First, the homology of *WOX* homeodomains among the *WOX* genes supports three major clades: the ancient, intermediate, and modern clades. According to phylogenetic analysis, the *WOX1-7* and *WUS* genes are grouped in the modern clade. Some subgroups from the modern clade have been lost in several species (e.g., lack of WOX1/6 subgroup in rice). These studies imply that *WOX* members in the modern clade may have a conserved and redundant function (Hedman et al., 2013; Lian et al., 2014; Alvarez et al., 2018).

Second, in angiosperms, the expression of *WUS* and *WOX5* is specific to the shoot and root regions, respectively. Furthermore, Sarkar et al. (2007) demonstrated that *WOX5* and *WUS* are interchangeable for stem cell control in *Arabidopsis*. In contrast, Nardmann et al. (2009) reported that *Ginkgo biloba WUS* (*GbWUS*) and *Pinus sylvestris WUS* (*PsWUS*) are expressed in both the shoots and the roots, and suggested that the *WUS* and *WOX5* genes are the result of an angiosperm-specific gene duplication.

CONCLUSION

Our results suggest that constitutive overexpression of *PpWOX2* in *Arabidopsis* seedlings alters the expression of embryogenesis-related genes (*AtLEC1* and/or *AtWUS*), which, in turn, could promote the formation of SEs and organs. Further reverse genetics studies through inducible overexpression of combinations of embryogenesis-related genes and possibly an additional (hormonal) stimulus might be helpful to overcome recalcitrance to somatic embryogenesis of already differentiated tissues in *Pinus pinaster*. These findings might be helpful to gain insights into conifer embryogenesis and, in best case, to develop strategies for induction of somatic embryogenesis from adult conifer trees (Lelu-Walter et al., 2016; Trontin et al., 2016c).

DATA AVAILABILITY STATEMENT

The datasets presented in this study can be found in online repositories. The names of the repository/repositories and accession number(s) can be found below: https://www.ncbi.nlm.nih.gov/, KY773924.1.

AUTHOR CONTRIBUTIONS

AR, KZ, JR, and SH conceived and designed the research project with expert guidance from J-FT for the maritime pine work. J-FT provided PN519 as starting material for maritime pine. J-FT and AR provided the plasmids and methods for the plant transformation experiments. SH and AR conducted the experiments, analysed the data and wrote the manuscript. KZ and AR supervised the lab work. All authors reviewed and approved the final version of the manuscript.

FUNDING

This study was supported by a Yousef Jameel Scholarship Fund. This study also received specific financial support from Bundes Ministerium für Bildung und Forschung (Germany, BMBF-FKZ-AZ0315706B) and French National Research Agency (ANR-09-KBBE-0007) through a transnational KBBE project (SUSTAINPINE 2010-2013, PLE2009-0016, Coord. F. Cánovas/University of Málaga) as well as a MULTIFOREVER transnational project (since 2019, Coord. J-FT/FCBA, Pierroton, and/or AR/HUB, Berlin) supported within the framework of the European Research Area Network Cofund "ForestValue – Innovating forest-based bioeconomy" (773324) jointly funded by national organizations (in France: ANR-19-SUM2-0002-01); in Germany: Fachagentur Nachwachsende Rohstoffe e.V. (FKZ 22040218). Handling of the PN519 embryogenic line at FCBA (cryopreservation, reactivation, and multiplication) benefited from the technical support of the XYLOBIOTECH facility (XYLOFOREST platform, ANR-10-EQPX-16).

ACKNOWLEDGMENTS

We thank Dr. Philippe Label (INRAE, France) for the identification of the *PpWOX2* sequence in *Pinus pinaster* databases.

SUPPLEMENTARY MATERIAL

The Supplementary Material for this article can be found online at: https://www.frontiersin.org/articles/10.3389/fpls.2022.838421/full#supplementary-material

REFERENCES

Alvarez, J. M., Bueno, N., Cañas, R. A., Avila, C., Cánovas, F. M., and Ordás, R. J. (2018). Analysis of the WUSCHEL-RELATED HOMEOBOX gene family in *Pinus pinaster*: new insights into the gene family evolution. *Plant Physiol. Biochem.* 123, 304–318. doi: 10.1016/j.plaphy.2017.12.031

Arndt, N. (2013). *Establishing of New Reference Genes and Quantitative PCR Analysis During Somatic Embryogenesis of P. pinaster Ait.* M.Sc. thesis. Berlin: Humboldt-Universität zu Berlin.

Arroyo-Herrera, A., Gonzalez, A. K., Moo, R. C., Quiroz-Figueroa, F. R., Loyola-Vargas, V. M., Rodriguez-Zapata, L. C., et al. (2008). Expression of WUSCHEL in Coffeacanephoracauses ectopic morphogenesis and increases somatic embryogenesis. *Plant Cell Tissue Organ Cult.* 94, 171–180. doi: 10.1007/s11240-008-9401-1

Bercetche, J., and Pâques, M. (1995). "Somatic embryogenesis in maritime pine (*Pinus pinaster*)," in *Protocol for Somatic Embryogenesis in Woody Plants*, eds S. Jain, P. Gupta, and R. Newton (Dordrecht: Springer), 221–242.

Birol, I., Raymond, A., Jackman, S. D., Pleasance, S., Coope, R., Taylor, G. A., et al. (2013). Assembling the 20 Gb white spruce (*Picea glauca*) genome from whole-genome shotgun sequencing data. *Bioinformatics* 29, 1492–1497. doi: 10.1093/bioinformatics/btt178

Bonga, J. M., Klimaszewska, K. K., and Aderkas, P. (2010). Recalcitrance in clonal propagation, in particular of conifers. *Plant Cell Tissue Organ Cult.* 100, 241–254. doi: 10.1007/s11240-009-9647-2

Bouchabke-Coussa, O., Obellianne, M., Linderme, D., Montes, E., Maia-Grondard, A., Vilaine, F., et al. (2013). WUSCHEL over-expression promotes somatic embryogenesis and induces organogenesis in cotton (*Gossypium hirsutum* L.) tissues cultured in vitro. *Plant Cell Rep.* 32, 675–686. doi: 10.1007/s00299-013-1402-9

Boutilier, K., Offringa, R., Sharma, V. K., Kieft, H., Ouellet, T., Zhang, L., et al. (2002). Ectopic expression of BABY BOOM triggers a conversion from vegetative to embryonic growth. *Plant Cell* 14, 1737–1749. doi: 10.1105/tpc.001941

Bowe, L. M., and Coat, G. (2000). Phylogeny of seed plants based on all three genomic compartments: extant gymnosperms are monophyletic and Gnetales' closet relatives are conifers. *Proc. Natl. Acad. Sci. U.S.A.* 97, 4092–4097. doi: 10.1073/pnas.97.8.4092

Breton, D., Harvengt, L., Trontin, J.-F., Bouvet, A., and Favre, J.-M. (2006). Long-term sub-culture randomly affects morphology and subsequent maturation of early somatic embryos in maritime pine. *Plant Cell Tissue Organ Cult.* 87, 95–108. doi: 10.1007/s11240-006-9144-9

Breuninger, H., Rikirsch, E., Hermann, M., Ueda, M., and Laux, T. (2008). Differential expression of WOX genes mediates apical-basal axis formation in the *Arabidopsis* embryo. *Dev. Cell* 14, 867–876. doi: 10.1016/j.devcel.2008.03.008

Cairney, J., and Pullman, G. S. (2007). The cellular and molecular biology of conifer embryogenesis. *New Phytol.* 176, 511–536. doi: 10.1111/j.1469-8137.2007.02239.x

Cairney, J., Zheng, L., Cowels, A., Hsioa, J., Zismann, V., Liu, J., et al. (2006). Expressed sequence tags from loblolly pine embryos reveal similarities with angiosperm embryogenesis. *Plant Mol. Biol.* 62, 485–501. doi: 10.1007/s11103-006-9035-9

Canales, J., Bautista, R., Label, P., Gómez-Maldonado, J., Lesur, I., Fernández-Pozo, N., et al. (2014). De novo assembly of maritime pine transcriptome: implications for forest breeding and biotechnology. *Plant Biotechnol. J.* 12, 286–299. doi: 10.1111/pbi.12136

Chang, S., Puryear, J., and Cairney, J. (1993). A simple and efficient method for isolating RNA from pine trees. *Plant Mol. Biol. Rep.* 11, 113–116. doi: 10.1385/MB:19:2:201

Chung, K., Sakamoto, S., Mitsuda, N., Suzuki, K., Ohme-Takagi, M., and Fujiwara, S. (2016). WUSCHEL-RELATED HOMEOBOX 2 is a transcriptional repressor involved in lateral organ formation and separation in *Arabidopsis*. *Plant Biotechnol.* 33, 245–253. doi: 10.5511/plantbiotechnology.16.0202a

Czechowski, T., Stitt, M., Altmann, T., Udvardi, M. K., and Scheible, W. R. (2005). Genome-wide identification and testing of superior reference genes for transcript normalization in *Arabidopsis*. *Plant Physiol.* 139, 5–17. doi: 10.1104/pp.105.063743

De Silva, V., Bostwick, D., Burns, K. L., Oldham, C. D., Skryabina, A., Sullards, M. C., et al. (2008). Isolation and characterization of a molecule stimulatory to growth of somatic embryos from early stage female gametophyte tissue of loblolly pine. *Plant Cell Rep.* 27, 633–646. doi: 10.1007/s00299-007-0484-7

De Smet, I., Lau, S., Mayer, U., and Jürgen, G. (2010). Embryogenesis – the humble beginnings of plant life. *Plant J.* 61, 959–970. doi: 10.1111/j.1365-313X.2010.04143.x

Dolzblasz, A., Nardmann, J., Clerici, E., Causier, B., van der Graaff, E., Chen, J., et al. (2016). Stem cell regulation by *Arabidopsis* WOX genes. *Mol. Plant* 9, 1028–1039. doi: 10.1016/j.molp.2016.04.007

Doyle, J. J. (1990). Isolation of plant DNA from fresh tissue. *Focus* 12, 13–15.

Dumolin, S., Demesure, B., and Petit, R. J. (1995). Inheritance of chloroplast and mitochondrial genomes in pedunculate oak investigated with an efficient PCR method. *Theor. Appl. Genet.* 91, 1253–1256. doi: 10.1007/BF00220937

El-Azaz, J., de la Torre, F., Pascual, M. B., Debille, S., Canlet, F., Harvengt, L., et al. (2020). Transcriptional analysis of arogenate dehydratase genes identifies a link between phenylalanine biosynthesis and lignin biosynthesis. *J. Exp. Bot.* 71, 3080–3093. doi: 10.1093/jxb/eraa099

Elhiti, M. A. (2010). *Molecular Characterization of Several Brassica Shoot Apical Meristem Genes and the Effect of Their Altered Expression During in Vitro Morphogenesis*. Dissertation. Winnipeg, MB: University of Manitoba.

Elhiti, M., Stasolla, C., and Wang, A. (2013). Molecular regulation of plant somatic embryogenesis. *In Vitro Cell. Dev. Biol. Plant* 49, 631-642. doi: 10.1007/s11627-013-9547-3

Gaj, M. D. (2001). Direct somatic embryogenesis as a rapid and efficient system for in vitro regeneration of *Arabidopsis thaliana*. *Plant Cell Tissue Organ Cult.* 64, 39–46. doi: 10.1023/A:1010679614721

Haecker, A., Gross-Hardt, R., Geiges, B., Sarkar, A., Breuninger, H., Herrmann, M., et al. (2004). Expression dynamics of WOX genes mark cell fate decisions during early embryonic patterning in *Arabidopsis thaliana*. *Development* 131, 657–668. doi: 10.1242/dev.00963

Hakman, I., Hallberg, H., and Palovaara, J. (2009). The polar auxin transport inhibitor NPA impairs embryo morphology and increases the expression of an auxin efflux facilitator protein PIN during Piceaabies somatic embryo development. *Tree Physiol.* 29, 483–496. doi: 10.1093/treephys/tpn048

Harvengt, L. (2005). "Somatic embryogenesis in Maritime pine (*Pinus pinaster*Ait.)," in *Protocols of Somatic Embryogenesis in Woody Plants, Forestry Sciences*, Vol. 77, eds S. M. Jain and P. K. Gupta (Berlin: Springer Verlag), 107–120. doi: 10.1007/1-4020-2985-3_10

Hedman, H., Zhu, T., von Arnold, S., and Sohlberg, J. J. (2013). Analysis of the WUSCHEL RELATED HOMEOBOX gene family in the conifer Piceaabies reveals extensive conservation as well as dynamic patterns. *BMC Plant Biol.* 13:89. doi: 10.1186/1471-2229-13-89

Heidmann, I., De Lange, B., Lambalk, J., Angenent, G. C., and Boutilier, K. (2011). Efficient sweet pepper transformation mediated by the BABY BOOM transcription factor. *Plant Cell Rep.* 30, 1107–1115. doi: 10.1007/s00299-011-1018-x

Horstman, A., Li, M., Heidmann, I., Weemen, M., Chen, B., Muino, J. M., et al. (2017). The BABY BOOM transcription factor activates the LEC1-ABI3-FUS3-LEC2 network to induce somatic embryogenesis. *Plant Physiol.* 175, 848–857. doi: 10.1104/pp.17.00232

Jeong, S., Bayer, M., and Lukowitz, W. (2011). Taking the very first steps: from polarity to axial domains in the early *Arabidopsis* embryo. *J. Exp. Bot.* 62, 1687–1697. doi: 10.1093/jxb/erq398

Klimaszewska, K. (1989). Plantlet development from immature zygotic embryos of hybrid larch through somatic embryogenesis. *Plant Sci.* 63, 95–103. doi: 10.1016/0168-9452(89)90105-2

Klimaszewska, K., and Cyr, D. R. (2002). Conifer somatic embryogenesis: I. Development. *Dendrobiologia* 48, 31–39.

Klimaszewska, K., Hargreaves, C., Lelu-Walter, M.-A., and Trontin, J.-F. (2016). "Advances in conifer somatic embryogenesis since year 2000," in *In Vitro Embryogenesis in Higher Plants*, eds M. A. Germanà and M. Lambardi (New York, NY: Springer), 131–166. doi: 10.1007/978-1-4939-3061-6_7

Klimaszewska, K., Noceda, C., Pelletier, G., Label, P., Rodriguez, R., and Lelu-Walter, M. (2009). Biological characterization of young and aged embryogenic cultures of *Pinus pinaster* (Ait.). *In Vitro Cell. Dev. Biol. Plant* 45, 20–33. doi: 10.1007/s11627-008-9158-6

Klimaszewska, K., Overton, C., Stewart, D., and Rutledge, R. G. (2011). Initiation of somatic embryos and regeneration of plants from primordial shoots of 10-year-old somatic white spruce and expression profiles of 11 genes followed during the tissue culture process. *Planta* 233, 635–647. doi: 10.1007/s00425-010-1325-4

Klimaszewska, K., Park, Y. S., Overton, C., MacEacheron, I., and Bonga, J. M. (2001). Optimized somatic embryogenesis in *Pinus strobus* L. *In Vitro Cell. Dev. Biol. Plant* 37, 392–399. doi: 10.1007/s11627-001-0069-z

Klimaszewska, K., Pelletier, G., Overton, C., Stewart, D., and Rutledge, R. G. (2010). Hormonally regulated overexpression of *Arabidopsis* WUS and conifer LEC1 (CHAP3A) in transgenic white spruce: implications for somatic embryo development and somatic seedling growth. *Plant Cell Rep.* 29, 723–734. doi: 10.1007/s00299-010-0859-z

Klimaszewska, K., Trontin, J.-F., Becwar, M. R., Devillard, C., Park, Y. S., and Lelu-Walter, M. A. (2007). Recent progress in somatic embryogenesis of four *Pinus* spp. *Tree For. Sci. Biotechnol.* 1, 11–25.

Laux, T., Mayer, K. F., Berger, J., and Jurgens, G. (1996). The WUSCHEL gene is required for shoot and floral meristem integrity in *Arabidopsis*. *Development* 122, 87–96. doi: 10.1242/dev.122.1.87

Lelu-Walter, M.-A., Klimaszewska, K., Miguel, C., Aronen, T., Hargreaves, C., Teyssier, C., et al. (2016). "Somatic embryogenesis for more effective breeding and deployment of improved varieties in *Pinus* sp.: bottlenecks and recent advances," in *Somatic Embryogenesis – Fundamental Aspects and Applications*, eds V. M. Loyola-Vargas and N. Ochoa-Alejo (Cham: Springer Verlag), 319–365. doi: 10.1007/978-3-319-33705-0_19

Lian, G., Ding, Z., Wang, Q., Zhang, D., and Xu, J. (2014). Origins and evolution of WUSCHELRELATEDHOMEOBOX protein family in plant kingdom. *Sci. World J.* 2014:534140. doi: 10.1155/2014/534140

Litvay, J. D., Verma, D. C., and Johnson, M. A. (1985). Influence of a loblolly pine (*Pinus taeda* L.). Culture medium and its components on growth and somatic embryogenesis of the wild carrot (*Daucus carota* L.). *Plant Cell Rep.* 4, 325–328. doi: 10.1007/BF00269890

Lotan, T., Ohto, M. A., Yee, K. M., West, M. A., Lo, R., Kwong, R. W., et al. (1998). *Arabidopsis* LEAFY COTYLEDON1 is sufficient to induce embryo development in vegetative cells. *Cell* 93, 1195-1205. doi: 10.1016/s0092-8674(00)81463-4

Marum, L., Loureiro, J., Rodriguez, E., Santos, C., Oliveira, M. M., and Miguel, C. (2009). Flow cytometric and morphological analyses of *Pinus pinaster* somatic embryogenesis. *J. Biotechnol.* 143, 288–295. doi: 10.1016/j.jbiotec.2009.08.001

Miguel, C. M., Rupps, A., Raschke, J., Rodrigues, A. S., and Trontin, J.-F. (2016). "Impact of molecular studies on somatic embryogenesis development for implementation in conifer multi-varietal forestry," in *Vegetative Propagation of Forest trees*, eds Y.-S. Park, J. M. Bonga, and H.-K. Moon (Seoul: Korea Forest Research Institute), 373–421.

Morel, A., Trontin, J.-F., Corbineau, F., Lomenech, A.-M., Beaufour, M., Reymond, I., et al. (2014). Cotyledonary somatic embryos of *Pinus pinaster*Ait. most closely resemble fresh, maturing cotyledonary zygotic embryos: biological, carbohydrate and proteomic analyses. *Planta* 240, 1075–1095. doi: 10.1007/s00425-014-2125-z

Murashige, T., and Skoog, F. (1962). A revised medium for rapid growth and bio assays with tobacco tissue cultures. *Physiol. Plant.* 15, 473–497.

Nardmann, J., and Werr, W. (2006). The shoot stem cell niche in angiosperms: expression patterns of WUS orthologues in rice and maize imply major modifications in the course of mono-and dicot evolution. *Mol. Biol. Evol.* 23, 2492–2504. doi: 10.1093/molbev/msl125

Nardmann, J., Reisewitz, P., and Werr, W. (2009). Discrete shoot and root stem cell-promoting WUS/WOX5 functions are an evolutionary innovation of angiosperms. *Mol. Biol. Evol.* 26, 1745–1755. doi: 10.1093/molbev/msp084

Neale, D., Wegrzyn, J., Stevens, K., Zimin, A. V., Puiu, D., Crepeau, M. W., et al. (2014). Decoding the massive genome of loblolly pine using haploid DNA and novel assembly strategies. *Genome Biol.* 15:R59. doi: 10.1186/gb-2014-15-3-r59

Nishiguchi, R., Takanami, M., and Oka, A. (1987). Characterization and sequence determination of the replicator region in the hairy-root-inducing plasmid pRiA 4b. *Mol. Gen. Genet.* 206, 1–8. doi: 10.1007/BF00326529

Nystedt, B., Street, N. R., Wetterbom, A., Zuccolo, A., Lin, Y. C., Scofield, D. G., et al. (2013). The Norway spruce genome sequence and conifer genome evolution. *Nature* 497, 579–584. doi: 10.1038/nature12211

Palovaara, J., and Hakman, I. (2008). Conifer WOX-related homeodomain transcription factors, developmental consideration and expression dynamic of WOX2 during Piceaabies somatic embryogenesis. *Plant Mol. Biol.* 66, 533–549. doi: 10.1007/s11103-008-9289-5

Palovaara, J., and Hakman, I. (2009). WOX2 and polar auxin transport during spruce embryo pattern formation. *Plant Signal. Behav.* 4, 153–155. doi: 10.4161/psb.4.2.7684

Palovaara, J., Hallberg, H., Stasolla, C., and Hakman, I. (2010a). Comparative expression pattern analysis of WUSCHEL-RELATEDHOMEOBOX 2 (WOX2) and WOX8/9 in developing seeds and somatic embryos of the gymnosperm Piceaabies. *New Phytol.* 188, 122–135. doi: 10.1111/j.1469-8137.2010.03336.x

Palovaara, J., Hallberg, H., Stasolla, C., Luit, B., and Hakman, I. (2010b). Expression of a gymnosperm PIN homologous gene correlates with auxin immunolocalization pattern at cotyledon formation and in demarcation of the procambium during Piceaabies somatic embryo development and in seedling tissues. *Tree Physiol.* 30, 479–489. doi: 10.1093/treephys/tpp126

Park, S. Y., Klimaszewska, K., Park, J. Y., and Mansfield, S. D. (2010). Lodgepole pine: the first evidence of seed-based somatic embryogenesis and the expression of embryogenesis marker genes in shoot bud cultures of adult trees. *Tree Physiol.* 30, 1469–1478. doi: 10.1093/treephys/tpq081

Plomion, C., Bastien, C., Bogeat-Triboulot, M.-B., Bouffier, L., Déjardin, A., Duplessis, S., et al. (2016). Forest tree genomics: 10 achievements from the past 10 years and future prospects. *Ann. For. Sci.* 73, 77–103. doi: 10.1007/s13595-015-0488-3

Ramarosandratana, A., Harvengt, L., Bouvet, A., Calvayrac, R., and Pâques, M. (2001). Influence of the embryonal-suspensor mass (ESM) sampling on development and proliferation of maritime pine somatic embryos. *Plant Sci.* 160, 473–479. doi: 10.1016/s0168-9452(00)00410-6

Rupps, A., Raschke, J., Rümmler, M., Linke, B., and Zoglauer, K. (2016). Identification of putative homologs of *Larix decidua* to BABYBOOM (BBM), LEAFY COTYLEDON1 (LEC1), WUSCHEL-related HOMEOBOX2 (WOX2) and SOMATIC EMBRYOGENESIS RECEPTOR-like KINASE (SERK) during somatic embryogenesis. *Planta* 243, 473–488. doi: 10.1007/s00425-015-2409-y

Sarkar, A. K., Luijten, M., Miyashima, S., Lenhard, M., Hashimoto, T., Nakajima, K., et al. (2007). Conserved factors regulate signalling in *Arabidopsis thaliana* shoot and root stem cell organizers. *Nature* 446, 811–814. doi: 10.1038/nature05703

Solís-Ramos, L. Y., González-Estrada, T., Nahuath-Dzib, S., Zapata-Rodriguez, L. C., and Castano, E. (2009). Over-expression of WUSCHEL in C. Chinense causes ectopic morphogenesis. *Plant Cell Tissue Organ Cult.* 96, 279–287. doi: 10.1007/s11240-008-9485-7

Tabata, S., Kaneko, T., Nakamura, Y., Kotani, H., Kato, T., Asamizu, E., et al. (2000). Sequence and analysis of chromosome 5 of the plant *Arabidopsis thaliana*. *Nature* 408, 823–826. doi: 10.1038/35048507

Taryono, M. (2000). *Somatische Embryogenese and Transformation bei der Europäischen Lärche (Larix decidua Mill.).* Dissertation. Berlin: Humboldt-Universität zu Berlin.

Trontin, J.-F., and Lelu-Walter, M. A. (2010). Agrobacterium-Mediated Genetic Transformation of Maritime Pine (Embryogenic Line PN519) Using pCbar as Standard, Reference Binary Vector. Sustainpine WP3 Common Protocol. N°1/V01(10/06/2010). Protocol Disseminated to Sustainpine WP3 Partners. SUSTAINPINE Multinational Project. Plant KBBE, PL2-2009-0016.

Trontin, J.-F., Debille, S., Canlet, F., Harvengt, L., Lelu-Walter, M. A., Label, P., et al. (2013). "Somatic embryogenesis as an effective regeneration support for reverse genetics in maritime pine: the Sustainpine collaborative project as a case study," in *Proceeding of the IUFRO Working Party 2.09.02 Conference on "Integrating Vegetative Propagation, Biotechnology and Genetic Improvement for Tree Production and Sustainable Forest Management", 25-28/06/2012, Brno*, eds Y. S. Park and J. M. Bonga, 184–187. Available online at: http://www.iufro.org/science/divisions/division-2/20000/20900/20902/publications (accessed March 20, 2013).

Trontin, J.-F., Harvengt, L., Garin, E., Lopez-Vernaza, M. A., Arancio, L., Hoebeke, J., et al. (2002). Towards genetic engineering of maritime pine (*Pinus pinaster* Ait.). *Ann. For. Sci.* 59, 687-697. doi: 10.1051/forest:2002057

Trontin, J.-F., Klimaszewska, K., Morel, A., Hargreaves, C., and Lelu-Walter, M. A. (2016a). "Molecular aspects of conifer zygotic and somatic embryo development: a review of genome-wide approaches and recent insights," in *In Vitro Embryogenesis in Higher Plants*, eds M. A. Germanà and M. Lambardi (New York, NY: Springer Science+Business Media), 167–207. doi: 10.1007/978-1-4939-3061-6_8

Trontin, J.-F., Teyssier, C., Morel, A., Harvengt, L., and Lelu-Walter, M. A. (2016b). "Prospects for new variety deployment through somatic embryogenesis in maritime pine," in *Vegetative Propagation of Forest Trees*, eds Y.-S. Park, J. M. Bonga, and H.-K. Moon (Seoul: Korea Forest Research Institute), 572–606.

Trontin, J.-F., Aronen, T., Hargreaves, C., Montalbán, I. A., Moncaleán, P., Reeves, C., et al. (2016c). "International effort to induce somatic embryogenesis in adult pine trees," in *Vegetative Propagation of Forest Trees*, eds Y.-S. Park, J. M. Bonga, and H.-K. Moon (Seoul: Korea Forest Research Institute), 211–260.

Trontin, J.-F., Walter, C., Klimaszewska, K., Park, Y. S., and Lelu-Walter, M. A. (2007). Recent progress in genetic transformation of four *Pinus* spp. *Transgenic Plant J.* 1, 314–329.

Tzafrir, I., Pena-Muralla, R., Dickerman, A., Berg, M., Rogers, R., Hutchens, S., et al. (2004). Identification of genes required for embryo development in *Arabidopsis*. *Plant Physiol.* 135, 1206–1220. doi: 10.1104/pp.104.045179

van der Graaff, E., Laux, T., and Rensing, S. A. (2009). The WUS homeobox-containing (WOX) protein family. *Genome Biol.* 10:248. doi: 10.1186/gb-2009-10-12-248

Vandesompele, J., De Preter, K., Pattyn, F., Poppe, B., Van Roy, N., De Paepe, A., et al. (2002). Accurate normalization of real-time quantitative RT-PCR data by geometric averaging of multiple internal control genes. *Genome Biol.* 3:research34.1. doi: 10.1186/gb-2002-3-7-research0034

Walther, M., Wagner, I., Raschke, J., Zoglauer, K., and Rupps, A. (2021). Abscisic acid induces somatic embryogenesis and enables the capture of high-value genotypes in Douglas fir (*Pseudotsuga menziesii* [MIRB.] Franco). *Plant Cell Tissue Organ Cult.* 148, 45–59. doi: 10.1007/s11240-021-02159-3

Weigel, D., and Glazebrook, J. (2002). *Arabidopsis. A Laboratory Manual*. New York, NY: Cold Spring Harbor Laboratory Press, 165.

Wu, X., Chory, J., and Weigel, D. (2007). Combinations of WOX activities regulate tissue proliferation during *Arabidopsis* embryonic development. *Dev. Biol.* 309, 306–316. doi: 10.1016/j.ydbio.2007.07.019

Xiao, W., Custard, K. D., Brown, R. C., Lemmon, B. E., Harada, J. J., Goldberg, R. B., et al. (2006). DNA methylation is critical for *Arabidopsis* embryogenesis and seed viability. *Plant Cell* 18, 805–814. doi: 10.1105/tpc.105.038836

Zhang, H., Han, W., De Smet, I., Talboys, P., Loya, R., Hassan, A., et al. (2010). ABA promotes quiescence of the quiescent centre and suppresses stem cell differentiation in the *Arabidopsis* primary root meristem. *Plant J.* 64, 764–774. doi: 10.1111/j.1365-313X.2010.04367.x

Zhang, Y., Wu, R., Qin, G., Chen, Z., Gu, H., and Qu, L. J. (2011). Over-expression of WOX1leads to defects in meristem development and polyamine homeostasis in *Arabidopsis*. *J. Integr. Plant Biol.* 53, 493–506. doi: 10.1111/j.1744-7909.2011.01054.x

Zhang, Y., Zhang, S., Han, S., Li, X., and Qi, L. (2012). Transcriptome profiling and in silico analysis of somatic embryos in Japanese larch (*Larix leptolepis*). *Plant Cell Rep.* 31, 1637–1657. doi: 10.1007/s00299-012-1277-1

Zhang, Z., Tucker, E., Hermann, M., and Laux, T. (2017). A molecular framework for the embryonic initiation of shoot meristem stem cells. *Dev. Cell* 40, 264–277. doi: 10.1016/j.devcel.2017.01.002

Zheng, W., Zhang, X., Yang, Z., Wu, J., Li, F., Duan, L., et al. (2014). AtWUSCHEL promotes formation of the embryogenic callus in *Gossypium hirsutum*. *PLoS One* 9:e87502. doi: 10.1371/journal.pone.0087502

Zhu, T., Moschou, P. N., Alvarez, J. M., Sohlberg, J. J., and Arnold, S. (2016). WUSCHEL-RELATED HOMEOBOX 2 is important for protoderm and suspensor development in the gymnosperm Norway spruce. *BMC Plant Biol.* 16:19. doi: 10.1186/s12870-016-0706-7

Zoglauer, K., Behrendt, U., Rahmat, A., and Ross, H. (2003). *Somatic Embryogenesis—the Gate to Biotechnology in Conifers*. Vienna: Springer, 175–202. doi: 10.1007/978-3-7091-6040-4_11

Zuo, J., Niu, Q. W., Frugis, G., and Chua, N. H. (2002). The WUSCHEL gene promotes vegetative-to-embryonic transition in *Arabidopsis*. *Plant J.* 30, 349–359. doi: 10.1046/j.1365-313x.2002.01289.x

Conflict of Interest: The authors declare that the research was conducted in the absence of any commercial or financial relationships that could be construed as a potential conflict of interest.

Publisher's Note: All claims expressed in this article are solely those of the authors and do not necessarily represent those of their affiliated organizations, or those of the publisher, the editors and the reviewers. Any product that may be evaluated in this article, or claim that may be made by its manufacturer, is not guaranteed or endorsed by the publisher.

frontiers in Plant Science

ORIGINAL RESEARCH
published: 15 March 2022
doi: 10.3389/fpls.2022.857611

miR160 Interacts *in vivo* With *Pinus pinaster AUXIN RESPONSE FACTOR 18* Target Site and Negatively Regulates Its Expression During Conifer Somatic Embryo Development

*Ana Alves[1], Ana Confraria[2,3], Susana Lopes[1,3], Bruno Costa[1,4], Pedro Perdiguero[5], Ana Milhinhos[1,3], Elena Baena-González[2,3], Sandra Correia[6] and Célia M. Miguel[1,7]**

[1]Faculty of Sciences, BioISI—Biosystems and Integrative Sciences Institute, University of Lisbon, Lisbon, Portugal, [2]Instituto Gulbenkian de Ciência, Oeiras, Portugal, [3]GREEN-IT Bioresources for Sustainability, ITQB NOVA, Oeiras, Portugal, [4]INESC-ID, Instituto Superior Técnico, Universidade de Lisboa, Lisbon, Portugal, [5]Department of Genetics, Physiology and Microbiology, Faculty of Biological Sciences, Complutense University of Madrid (UCM), Madrid, Spain, [6]Department of Life Sciences, Centre for Functional Ecology, University of Coimbra, Coimbra, Portugal, [7]Instituto de Biologia Experimental e Tecnológica, Oeiras, Portugal

OPEN ACCESS

Edited by:
Elena Corredoira,
Institute of Agrobiological Research of Galicia (CSIC), Spain

Reviewed by:
Lisheng Kong,
University of Victoria, Canada
Tzvetanka D. Dinkova,
National Autonomous University of Mexico, Mexico

***Correspondence:**
Célia M. Miguel
cmmiguel@fc.ul.pt

Specialty section:
This article was submitted to Plant Development and EvoDevo, a section of the journal Frontiers in Plant Science

Received: 18 January 2022
Accepted: 21 February 2022
Published: 15 March 2022

Citation:
Alves A, Confraria A, Lopes S, Costa B, Perdiguero P, Milhinhos A, Baena-González E, Correia S and Miguel CM (2022) miR160 Interacts in vivo With Pinus pinaster AUXIN RESPONSE FACTOR 18 Target Site and Negatively Regulates Its Expression During Conifer Somatic Embryo Development. Front. Plant Sci. 13:857611. doi: 10.3389/fpls.2022.857611

MicroRNAs (miRNAs) are key regulators of several plant developmental processes including embryogenesis. Most miRNA families are conserved across major groups of plant species, but their regulatory roles have been studied mainly in model species like *Arabidopsis* and other angiosperms. In gymnosperms, miRNA-dependent regulation has been less studied since functional approaches in these species are often difficult to establish. Given the fundamental roles of auxin signaling in somatic embryogenesis (SE) induction and embryo development, we investigated a previously predicted interaction between miR160 and a putative target encoding *AUXIN RESPONSE FACTOR 18* in *Pinus pinaster* (*PpARF18*) embryonic tissues. Phylogenetic analysis of *AUXIN RESPONSE FACTOR 18* (*ARF18*) from *Pinus pinaster* and *Picea abies*, used here as a model system of conifer embryogenesis, showed their close relatedness to *AUXIN RESPONSE FACTOR* (*ARF*) genes known to be targeted by miR160 in other species, including Arabidopsis *ARF10* and *ARF16*. By using a luciferase (LUC) reporter system for miRNA activity in *Arabidopsis* protoplasts, we have confirmed that *P. pinaster* miR160 (ppi-miR160) interacts *in vivo* with *PpARF18* target site. When the primary miR160 from *P. pinaster* was overexpressed in protoplasts under non-limiting levels of ARGONAUTE1, a significant increase of miR160 target cleavage activity was observed. In contrast, co-expression of the primary miRNA and the target mimic *MIM160* led to a decrease of miR160 activity. Our results further support that this interaction is functional during consecutive stages of SE in the conifer model *P. abies*. Expression analyses conducted in five stages of development, from proembryogenic masses (PEMs) to the mature embryo, show that conifer *ARF18* is negatively regulated by miR160 toward the fully developed mature embryo when miR160 reached its highest

expression level. This study reports the first *in vivo* validation of a predicted target site of a conifer miRNA supporting the conservation of miR160 interaction with *ARF* targets in gymnosperms. The approach used here should be useful for future characterization of miRNA functions in conifer embryogenesis.

Keywords: microRNA, *ARF*, pine, *Pinus pinaster*, gymnosperm, embryogenesis

INTRODUCTION

MicroRNAs (miRNAs) are small non-coding RNA molecules (20–24 nucleotides) involved in the regulation of gene expression in all domains of life, including in plants, mammals, and even in bacteria and viruses. In plants, *MIR* genes are transcribed by RNA polymerase II into primary miRNAs (pri-miRNAs). Due to the presence of complementary regions within the transcribed sequences, hairpin structures are formed and processed by the RNase III-type endonuclease DICER-LIKE 1 to form precursor miRNAs (pre-miRNAs). The pre-miRNAs undergo additional processing by DCL1 and its partners HYPONASTIC LEAVES 1 and SERRATE, producing miRNA/miRNA* duplexes, which are then loaded into ARGONAUTE1 (AGO1). AGO1 is the effector protein within the RNA-Induced Silencing Complex (RISC), directing translational inhibition or cleavage of the target mRNA transcripts by sequence complementarity of the loaded miRNA (reviewed by Achkar et al., 2016; Yu et al., 2017).

MicroRNAs regulate a broad range of biological processes, such as apoptosis, metabolism, development, and cell proliferation (Ambros, 2004; Bartel, 2004). Since plant miRNAs and their involvement in developmental processes were first reported in *Arabidopsis* (Reinhart et al., 2002), several studies over the last years have uncovered fundamental functions of miRNAs in plant embryo patterning and maturation (Schwartz et al., 1994; Nodine and Bartel, 2010; Willmann et al., 2011; Seefried et al., 2014; Plotnikova et al., 2019). In fact, miRNAs and their associated machinery are so essential that disrupting the miRNA multiprotein regulatory system or effector proteins in higher plants leads to embryo development arrestment at the early globular stage (Schwartz et al., 1994). The functions of plant miRNAs during embryogenesis; however, remain poorly characterized mainly due to the small size of early zygotic embryos embedded in maternal seed coat tissues, making their isolation and subsequent characterization of the RNA populations a difficult task (Vashisht and Nodine, 2014; Schon and Nodine, 2017). Therefore, somatic embryogenesis (SE), in which somatic cells are induced to undergo embryogenic transition, further progressing to the development of embryos that mirror their zygotic counterparts, is widely used as an experimental model to study zygotic embryogenesis (ZE).

Transcriptomic analysis in *Arabidopsis* revealed that about 98% of *MIR* genes, from 114 families, are active during SE induction (Szyrajew et al., 2017). In addition, miRNAs control of transcription factors and phytohormone metabolic pathways is key during different steps of the SE process (reviewed in Siddiqui et al., 2019). As in *Arabidopsis*, other angiosperms like *Oryza sativa*, *Zea mays*, *Gossypium hirsutum*, *Solanum lycopersicum*, and *Dimocarpus longan*, show differential expression of miRNAs at several developmental stages of SE (reviewed by Alves et al., 2021). In gymnosperms, on the other hand, not many miRNA studies are reported. A genome-wide transcriptomic study conducted in *Pinus pinaster* provided data suggesting a relevant role of miRNAs during zygotic embryo development (de Vega-Bartol et al., 2013). In *Larix laptolerix* (Zhang et al., 2012, 2013), *Picea balfouriana* (Li et al., 2017), and *P. pinaster* (Rodrigues et al., 2019), miRNA expression profiles also point to important miRNA regulatory functions during SE. Particularly in *P. pinaster*, 36 conserved miRNAs from 17 miRNA families were found differentially expressed during zygotic embryo development (Rodrigues et al., 2019). Among these, several miR160 isoforms were upregulated in late zygotic and late somatic embryos (Rodrigues et al., 2019). MiR160 is also known to be involved in *Arabidopsis* embryogenesis, being associated to the regulation of auxin signaling by targeting several *AUXIN RESPONSE FACTORS* (*ARFs*), namely *ARF10*, *ARF16*, and *ARF17* (Rhoades et al., 2002; Liu et al., 2007, 2020; Wójcik et al., 2017). Repression of *ARF17* by miR160 during *Arabidopsis* ZE was shown to be required for proper subprotodermal cell division patterns (Liu et al., 2007; Plotnikova et al., 2019). The opposite expression profiles of *ARF10/ARF16/ARF17* and miR160 in *Arabidopsis* embryogenic cultures suggested that miR160 might also contribute to the acquisition of embryogenic capacity in *Arabidopsis* somatic cells (Szyrajew et al., 2017; Wójcik et al., 2017). Direct repression of both *ARF10* and *ARF17* by miR160 regulates the development of the root cap, the activity of the root apical meristem (RAM; Wang et al., 2005), hypocotyl elongation (Dai et al., 2021), root architecture, and seed germination (Liu et al., 2007). Also in *Arabidopsis*, miR160-*ARF10* were linked to the control of cellular reprogramming and callus formation (Liu et al., 2016). In *P. pinaster*, one of the miR160 isoforms was upregulated in late zygotic and mature somatic embryos (Rodrigues et al., 2019) and it putatively targets a transcript annotated as *ARF18* (*AUXIN RESPONSE FACTOR 18* in *Pinus pinaster*, *PpARF18*; Cañas et al., 2017).

Despite the apparent conservation between most miRNA families in angiosperms and gymnosperms (Zhang et al., 2006), the regulatory interaction between miRNAs and target genes has been barely explored in gymnosperms because functional approaches are more difficult to establish in these plants. In this work, we addressed the functional conservation of miR160 in the regulation of auxin signaling during conifer embryogenesis. Firstly, we validated *PpARF18* as a target of *P. pinaster* miR160 (ppi-miR160) using a reporter system for miRNA activity in

Arabidopsis protoplasts. Secondly, we analyzed the expression patterns of miR160 and its validated target in consecutive stages of embryo development as a first step toward their functional characterization. As a model system for conifer embryogenesis, we used Norway spruce (*Picea abies*; Filonova et al., 2000; von Arnold and Clapham, 2008) due to its well-established and highly synchronized system of embryo development.

MATERIALS AND METHODS

Plant Material and Growth Conditions

Arabidopsis thaliana (L.) Heynh. plants in Columbia (Col-*0*) background were used to validate the miRNA-target interaction. Sterilized and stratified seeds of wild-type (WT) and the transgenic lines *mir160b* and *mir160c* (Wójcik et al., 2017) were sowed in pots with a 1:3 vermiculite/soil mixture. Plants were grown under a photoperiod of 12 h light (100 μE; 22°C)/12 h dark (18°C). Leaves of 5-week-old plants were harvested 2 h after the onset of the light period, both for protoplasts isolation and for RNA extraction.

The embryogenic cell line 61:21 of Norway spruce (*P. abies* L. Karst) was used as a model system for conifer somatic embryogenesis. The terminology used to describe somatic embryogenesis at different SE developmenral stages in this report was based on the referenced articles (Filonova et al., 2000; von Arnold and Clapham, 2008). The cultures were treated as described previously (von Arnold and Clapham, 2008). Briefly, proembryogenic masses (PEMs) were maintained every 2–3 weeks under proliferation on half-strength LP medium (von Arnold and Eriksson, 1981) supplemented with 9 μM 2,4-D, 4.4 μM BA, and 1% sucrose. To stimulate differentiation of early somatic embryos (EEs), cultures were washed by transferring 4–5 embryogenic clusters to tubes containing 50 ml half-strength liquid LP medium (prematuration medium). After washing by slowly inverting the tube for 1 min, settled cell aggregates (approx. 5 ml) were transferred to 250 ml Erlenmeyer flasks with 100 ml of prematuration medium. The cultures were grown on a gyratory shaker at 100 rpm, in darkness at 22°C. After 1 week, 2 ml of suspension cells were plated on top of two filter papers (Whatman no. 2) placed on maturation medium BMI-SI (Krogstrup, 1986) supplemented with 30 μM abscisic acid (ABA) and 3% sucrose, for the development of late embryos (LEs) and mature embryos (MEs). The filter papers were transferred to fresh maturation medium every 2 weeks and kept in the dark at 22°C. The media were solidified with 0.35% (w/v) Gelrite and the pH was adjusted to 5.8 before autoclaving. For the maturation medium, L-Glutamine (3 mM) and ABA were filter-sterilized and added to the autoclaved and cooled medium prior to pouring into sterile Petri dishes. To study the expression profiles of miR160 and *ARF18* during *P. abies* embryo development, 70–100 mg of PEMs, EEs, LEs, and MEs samples were collected for RNA extraction. PEMI and PEMIII were collected as cell aggregates from the proliferation medium. EEs and LEs were collected as cell aggregates after 1 week on prematuration medium and after 2–3 weeks on maturation medium, respectively. ME developed after 5–8 weeks on maturation medium. After 5 weeks ME1 were collected as maturing embryos characterized by the initiation of cotyledons. After 6–7 and 8 weeks, incompletely mature (ME2) and fully mature (ME3) embryos with at least four cotyledons were collected, respectively. The samples were frozen in liquid nitrogen and stored at −80°C.

In silico Analysis of miR160: *ARF* Interaction

The interaction between ppi-miR160 and an *ARF* encoding gene (sp_v3.0_unigene806) had been previously predicted in *Pinus pinaster* (Rodrigues et al., 2019; Perdiguero et al., 2021). To identify the homologous sequences in *P. abies* different searches were performed using nucleotide Basic Local Alignment Search Tool (BLASTN). Firstly, the precursor sequence of ppi-miR160 was used as query in miRBase database (Kozomara et al., 2019)[1] against precursor sequences from *P. abies*. The pre-miRNA sequence in *P. abies* containing exactly the same mature miRNA sequence than *P. pinaster* was selected. Secondly, the *P. pinaster* transcript sequence encoding the *ARF* identified as target was used as query in ConGenie database against high confidence gene models from *P. abies*. Homologous sequences to the conifer mature miR160 were also searched in well-documented model species, including *Arabidopsis thaliana*, *Oryza sativa*, and *Solanum lycopersicum*. For this, data from miRBase was retrieved and sequence alignment was performed using Clustal software implemented in Jalview. To analyze the homology of conifer *ARF*s and those previously described in model species, all proteins annotated as ARFs identified in *Arabidopsis*, *O. sativa*, and *S. lycopersicum* genomes were retrieved from RefSeq database (O'Leary et al., 2016)[2] and aligned with deduced amino acid sequences from conifer *ARF*s using ClustalW implemented in MEGA software. The phylogenetic tree was generated using the maximum-likelihood ratio method and tested by using bootstrap with 1,000 replications.

Cloning and Preparation of Constructs for *Arabidopsis* Protoplasts Transfection

The pUC18-based pHBT95 (accession no. EF090408; Yoo et al., 2007) was used as backbone for the constructs used in protoplast transfection. This included reporter constructs (**Supplementary Figure S1A**) expressing the firefly luciferase (*fLUC*) gene and constructs (**Supplementary Figure S1B**), where effectors were expressed under the *35S* promoter and *NOS* terminator (Luehrsen et al., 1992).

Reporter Constructs

Reporters for miRNA activity were built according to the system described by Martinho et al. (2015). Specifically, the selected cleavable and noncleavable *P. pinaster* ppi-miR160 target sites were inserted in the 3′UTR of *fLUC* by site-directed mutagenesis.

[1]https://www.mirbase.org
[2]https://www.ncbi.nlm.nih.gov/refseq/

Unigene806 was identified as the putative target of *P. pinaster* ppi-miR160 (mature sequence TGCCTGGCTCCCTGTATGCCA) by Rodrigues et al. (2019) when using psRNAtarget (Dai and Zhao, 2011; Dai et al., 2018) against the reference *P. pinaster* transcriptome (Canales et al., 2014). In the latest version of the *P. pinaster* transcriptome, *Unigene806* is annotated as *ARF18* (*PpARF18*; Cañas et al., 2017).

To build a specific luciferase (LUC)-based reporter for ppi-miR160 activity, we introduced the putative target site from *Unigene806* in the 3′UTR of luciferase by site-directed mutagenesis, similarly to what was described by Martinho et al. (2015)—primer pair LUC_C_ARF18 (**Supplementary Table S1**). In parallel to this cleavable version (C), we generated a non-cleavable construct (NC) as control—primer pair LUC_NC_ARF18 (**Supplementary Table S1**). Primers for NC reporter carried two mutations in the complementary position 10 and 11 of the ppi-miR160. The PCR reaction for mutagenesis consisted of 2.5 µl *Pfu* buffer, 2.5 µl 2.5 mM dNTPs, 1.5 µl of 1 µM of each primer (**Supplementary Table S1**), 50 ng of plasmid DNA pHBT95, 0.5 µl *Pfu* DNA Polymerase (Promega), and sterile water up to 25 µl. The reaction mix was split into two 12.5 µl aliquots: one used for PCR amplification and a second one kept as a negative control. The mutagenesis PCR was carried under the following conditions: 1 cycle to 95°C for 3 min followed by 18 cycles of 30 s at 95°C, 60 s at 55 and 68°C for 10 min. Around 0.5 µl of *DpnI* was added to both PCR reaction and the negative control and then incubated at 37°C overnight. About 4 µl of each reaction was used to transform 50 µl of MC1061 competent cells. The constructs were verified by sequencing.

For growing cultures for plasmid DNA maxipreps, *Escherichia coli* MC1061 were used to achieve a consistently high DNA yield and quality. Bacteria transformation, growth and plasmid isolation, and purification were performed as described (Confraria and Baena-González, 2016).

Effector Constructs

Primers were designed containing the appropriate restriction sites (BamHI and PstI) to amplify and clone the miR160 precursor downstream of the constitutive *35S* promoter. For amplification of pri-miR160 (pri160) primers were designed based on *Pinus taeda* genomic sequences, scaffold C32559718, position 66,547–66,567 (Rodrigues et al., 2019) encompassing 200 bp upstream and downstream of the 5′ and 3′ of the mature miRNA (Cuperus et al., 2010; **Supplementary Table S1**, primiR160_BamHI_F and primiR160_PstI_R) and amplification was performed from *P. pinaster* genomic DNA isolated from root tissues with the CTAB method (Doyle and Doyle, 1990). The pri160 sequence was PCR amplified with 0.2 mM of dNTPs, 0.5 µM of each primer, 0.02 U/µl of Phusion™ HF DNA Polymerase (Thermo Scientic™), 1x Phusion HF Buffer, and 50–250 ng of gDNA. The cycling conditions consisted of 30 s at 98°C, followed by 35 cycles of 10 s at 98°C, 20 s at 55°C as T annealing and 2 min at 72°C, and the last cycle of 5 min at 72°C. The PCR products were separated by electrophoresis in 0.8% agarose gel stained with RedSafe™ Nucleic Acid Staining Solution (iNtRON Biotechnology) and visualized under UV light. PCR products were purified using High Pure PCR Product Purification Kit (Roche), cloned into pGEM®-T Easy (Promega) which was then transformed into JM109 High-Efficiency Competent Cells, following manufacturer's instructions. The transformants with confirmed insert by colony PCR were grown overnight at 37°C in liquid LB supplemented with 100 µg/ml ampicillin and then the plasmid DNA was extracted using the QIAprep Spin Miniprep Kit (QIAGEN), according to the manufacturer's instructions. After sequence confirmation by Sanger sequencing, double digestion with BamHI (MB09201, NZYTECH) and PstI (MB10301, NZYTECH) of the plasmid with the insert (pri160) and the vector pHBT95 was performed. Both insert and vector digestion products were separated by electrophoresis in agarose gel and purified using the High Pure PCR Product Purification Kit (Roche). The purified insert was ligated to pHBT95 using T4 Ligase (MB000703, NZYTECH), and then transformed into MC1061 competent cells.

To generate *MIM160*, site-specific mutagenesis was performed using a *MIM319* construct (Martinho et al., 2015) as template. The PCR reaction conditions for site-directed mutagenesis were the same as described above, using the primers IPS1_MIM160 (**Supplementary Table S1**).

Arabidopsis Protoplast Isolation and Transfection

Fully expanded leaves of 5-week-old non-flowering plants were used for protoplast isolation as already described (Confraria and Baena-González, 2016).

For miRNA activity assays, 8–10 µg of luciferase-based reporters were used in combination with 12–10 µg of effector/control constructs and 1 µg of *35S::GUS* (Martinho et al., 2015) as transfection control. All the constructs used, including the controls, are listed in **Table 1**. About 2×10^4 protoplasts were transfected using a ratio of 1 µg CsCl-purified maxiprep plasmid DNA per 1×10^3 transfected protoplasts. The mER7 plasmid was used as control DNA (Kovtun et al., 1998). After PEG-Ca^{2+} transfection (Confraria and Baena-González, 2016) protoplasts were incubated overnight under light (15 µE, 25°C). On the following day, protoplasts were harvested by centrifugation at 100 *g* for 3 min, flash-frozen on dry ice, and used for luciferase and β-glucuronidase analysis (Confraria and Baena-González, 2016). To calculate normalized relative light units (nRLU), LUC activity values were divided by GUS activity values. Four biological replicates, corresponding to four independent protoplast batches, and each replicate consisting of two independent transfections were used to calculate the mean and SE for each sample.

RNA Extraction

Total RNA was extracted from Norway spruce embryonic tissues using the Plant/Fungi Total RNA Purification Kit (NORGEN BIOTEK CORP.), according to kit instructions. To eliminate DNA contamination, the rigorous protocol of DNase TURBO-*free*™ Kit (Invitrogen) was used. RNA samples were quantified using the fluorometer Qubit 3.0 using RNA BR Assay Kit (Thermo Fisher Scientific).

TABLE 1 | List of the plasmids used in protoplast transfection.

Vector	Insert	Resistance	Description
pHBT95	mER7	Ampicillin	Control DNA
pHBT95	GUS	Ampicillin	Transfection control
p35S-HA-GW	AGO1	Ampicillin	WT AGO1, HA-tagged
pHBT95	pri160	Ampicillin	Genomic sequence for primary ppi-miR160
pHBT95	*MIM160*	Ampicillin	*IPS1* containing target mimic for ppi-miR160
pHBT95	C-*fLUC*$_{ARF18}$	Ampicillin	Target site for ppi-miR160 (from *PpARF18*) introduced into 3′UTR of firefly luciferase
pHBT95	NC-*fLUC*$_{ARF18}$	Ampicillin	Non-cleavable target site for ppi-miR160 (mutated from *PpARF18*) introduced in 3′UTR of firefly luciferase

Quantitative RT-qPCR

For quantifying miR160 expression an absolute quantification was performed using ready to order TaqMan® MicroRNA Assay ID 000341 for ath-miR160a (Applied Biosystems® by Thermo Fisher Scientific) using total RNA from seven different stages of Norway spruce embryo development (PEMI, PEMIII, EE, LE, ME1, ME2, and ME3). Oligonucleotides identical to the conserved mature miR160 were ordered[3] and used to prepare a standard curve. The complementary DNA (cDNA) synthesis was performed from 10 ng of DNase treated total RNA using TaqMan® MicroRNA Reverse Transcription Kit (Applied Biosystems® by Thermo Fisher Scientific) and the miRNA-specific 5x RT primer provided. Each 20 µl qPCR reaction mixture included 1x TaqMan® Universal PCR Master Mix II, No UNG (Applied Biosystems®), 1x TaqMan® MicroRNA Assay primer 20x and the cDNA, prepared according to manufacturer's recommendations.

Relative quantification of *ARF18* in *P. abies* (MA_98506g0010)[4] was performed in the same stages of Norway spruce embryo development mentioned above. Primers (RT_pabARF18) were designed using Primer3web (**Supplementary Table S1**).[5] cDNA synthesis was performed using SuperScript® IV First-Strand Synthesis System (Invitrogen™) and oligo(dT)$_{20}$ primer using 1 µg of total RNA per 13 µl reaction, according to manufacturer's instructions. Each 20 µl qPCR reaction mix included 1x SYBR Green I Master (Roche Diagnostics), 500 nM of each primer and 1,5 µl of 1:5 diluted cDNA. The amplification program was the same for all genes: 95°C for 5 min, 40 cycles of 10 s at 95°C, 15 s at 62°C, and 12 s at 72°C. Primer specificity was monitored by analyzing the melting curves. Negative controls were prepared using total RNA as template in qPCR amplification. As additional controls, positive and non-template controls (NTC) were included in all plates. *Picea abies ARF18* transcript profiles were normalized using three reference genes *CDC2* (Wadenbäck et al., 2008), *EF-α*, and *PHOS* (Vestman et al., 2011). Relative expression levels were calculated using the Pfaffl (2001) method.

All qPCR experiments were performed in a LightCycler 480 (Roche Diagnostics) with white 96-well plates (Roche Diagnostics). The experiments included three biological replicates with at least two technical replicates, except for EEs for which two biological replicates were used.

Statistical Analysis

The statistical analyses were performed with Prism 9 program using either the unpaired Student *t*-test or a two-way ANOVA ($p < 0.05$), followed by Tukey's honestly significant difference test (Tukey HSD-test; $p < 0.05$) or Sidak's multiple comparison test. The figures show the average from biological replicates with the SE or SD.

RESULTS

Conifer *ARF18* Is Closely Related to *Arabidopsis ARF10/ARF16*

To investigate the interaction of ppi-miR160 with its predicted target, we started by confirming the genomic sequence of the precursor (pre-miR160) through PCR amplification and sequencing (**Figure 1A**). Since *P. abies* SE was used in this work as a model for analysis of miR160-*ARF18* expression during embryo development, a BLASTN search was performed against *P. abies* precursor sequences available in miRBase resulting in the identification of pab-*MIR160*a (accession MI0016116). The mature sequence within pab-*MIR160*a is identical to ppi-*MIR*160 and only two mismatches were found between the precursor sequences (**Figure 1B**), which have no influence in the secondary structure (**Figure 1A**). The alignment performed with *Arabidopsis* miR160 precursor sequences revealed that ath-*MIR160*a is the closest to ppi-*MIR160* and pab-*MIR160*a (**Figure 1B**). As to the mature miR160, alignment of *P. pinaster* and *P. abies* sequences with those from *Arabidopsis*, *O. sativa*, and *S. lycopersicum* available from miRbase (Kozomara et al., 2019) showed that they are identical, with the exception of *Osa-miR160e* and *Osa-miR160f* (**Figure 1C**).

In previous reports of *P. pinaster* miRNA analyses, *Unigene806* was identified as a potential target of ppi-miR160 in developing

[3]Biomers.net
[4]Congenie.org
[5]https://primer3.ut.ee

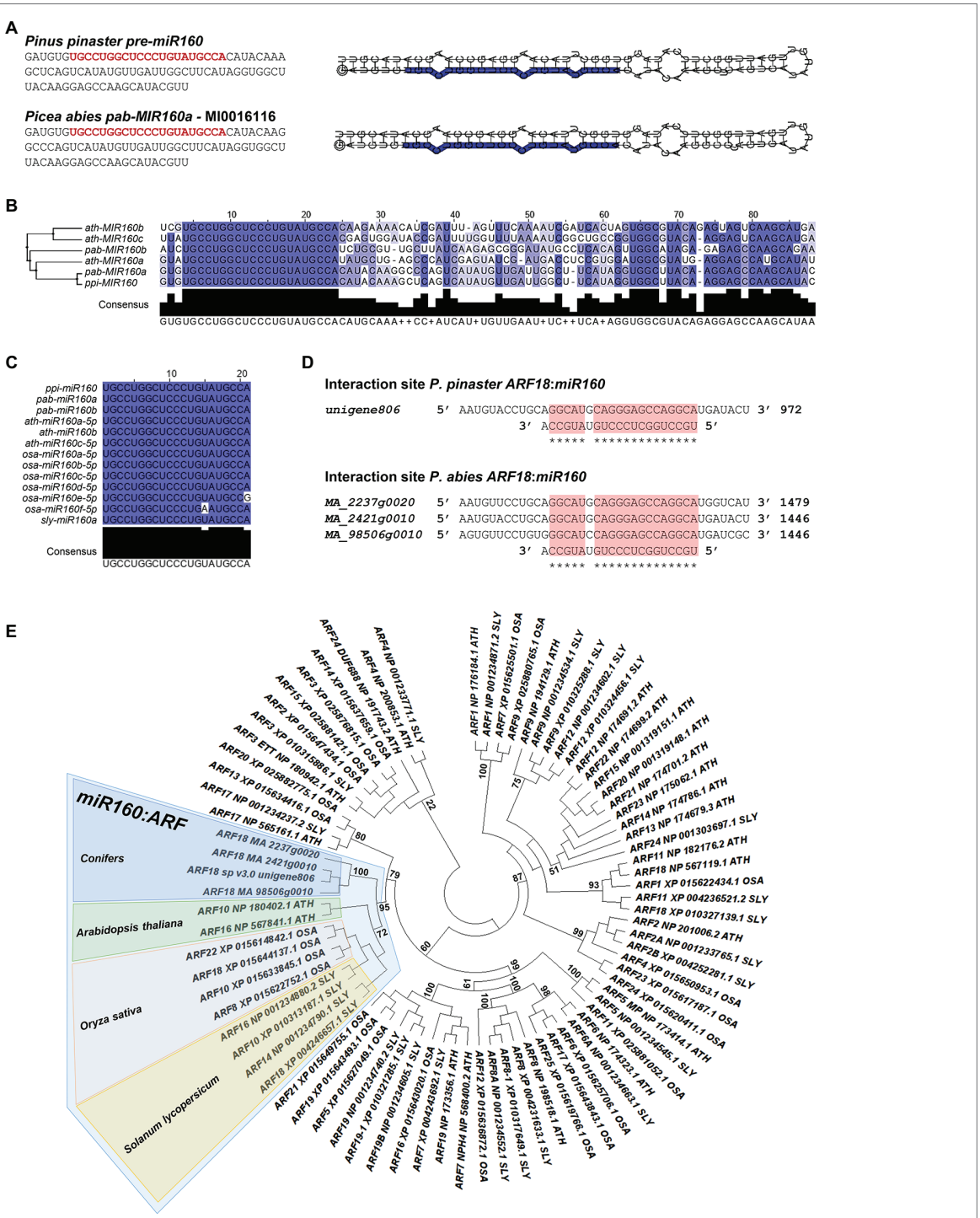

FIGURE 1 | *In silico* analysis of miR160: *AUXIN RESPONSE FACTOR* (*ARF*) interaction. **(A)** *Pinus pinaster* and *Picea abies* precursor-miR160 (pre-miR160) sequences. The sequence from *P. pinaster* was obtained in this work, whereas the *P. abies* sequence corresponds to MI0016116, annotated as pab-MIR160a in miRBase database. The miR160 mature sequence is highlighted in red. The shown secondary structures for both precursors were predicted and visualized using RNA Folding annotation tool implemented in the UEA sRNA workbench (Stocks et al., 2012). **(B)** Sequence alignment and phylogenetic tree constructed by the Maximum-Likelihood method of miR160 precursor sequences from *Arabidopsis thaliana* (*ath*), *P. abies* (*pab*) and *P. pinaster* (*ppi*). **(C)** Alignment of mature miR160 sequences from *A. thaliana* (*ath*), *Oryza sativa* (*osa*), *Solanum lycopersicum* (*sly*), *P. abies* (*pab*), and *P. pinaster* (*ppi*). High sequence conservation is represented in dark blue; white positions indicate no sequence conservation. **(D)** Target sites for miR160 in *P. pinaster* and *P. abies* transcripts annotated as *AUXIN RESPONSE FACTOR 18* (*ARF18*). The target site is indicated with a red box. **(E)** Phylogenetic tree of ARF protein sequences from *A. thaliana*, *O. sativa*, and *S. lycopersicum* and deduced amino acid sequences of *ARF18* identified in conifers as potential target for miR160. The highlighted branch shows the more correlated proteins between the different species. The maximum-likelihood method was used with 1,000 bootstrap replicates.

embryos (Rodrigues et al., 2019) and in roots from adult plants by degradome analysis (Perdiguero et al., 2021). A BLASTN search using *P. pinaster Unigene806* as query against Congenie database (v1.0; Nystedt, et al., 2013; Sundell et al., 2015) resulted in the identification of three high confidence gene models in *P. abies* (*MA_2237g0020*, *MA_2421g0010* and *MA_98506g0010*) showing high coverage of the *P. pinaster* sequence. All these transcripts are annotated as *AUXIN RESPONSE FACTOR* 18 (*ARF18*) both in the last version of *P. pinaster* transcriptome (Cañas et al., 2017; de Maria et al., 2020; Modesto et al., 2021) and in Congenie database (accessed data December 2021), and all the sequences show a potential target site for miR160 (**Figure 1D**). The phylogenetic analysis performed with *P. pinaster* and *P. abies ARF18* sequences to determine their relationship with the *ARF*s from other selected species highlighted a global branch that grouped them with *Arabidopsis* (*Ath*) *ARF10* and *ARF16*, *O. sativa* (*Osa*) *ARF8*, *ARF10*, *ARF18*, and *ARF22*, and also *ARF10*, *ARF14*, *ARF16*, and *ARF18* from *S. lycopersicum* (*Sly*; **Figure 1E**).

PpARF18 Cleavable Reporter Is Recognized by ath-miR160a

By combining miRNA gain- and loss-of-function through miRNA and target mimics overexpression, we probed the *in vivo* interaction of *P. pinaster* miR160 with its predicted *PpARF18* target site (Rodrigues et al., 2019). To this aim, *fLUC*-based miRNA activity sensors were generated for transient expression assays using *Arabidopsis* mesophyll protoplasts. We started by constructing a reporter with the putative target cleavage site sequence in the 3′UTR of *fLUC* ("cleavable" C-$fLUC_{ARF18}$—**Figure 2A**). In parallel, we used site-directed mutagenesis to engineer a noncleavable version carrying a target site with mutations in positions complementary to positions 10 and 11 of ppi-miR160 to prevent slicing ("noncleavable" NC-$fLUC_{ARF18}$; **Figure 2B**; Li et al., 2013; Martinho et al., 2015). As a first test, the $fLUC_{ARF18}$ reporters were transiently expressed in *Arabidopsis* protoplasts. Given that mature miR160 sequences in both *Arabidopsis* and *P. pinaster* were found identical (**Figure 1C**), we expected the miRNA target site in the C-$fLUC_{ARF18}$ would be recognized by the endogenous miRNA (ath-miR160), thus modulating target expression through mRNA cleavage. After determining the normalized luciferase activity, considered as an inverse quantitative readout of miRNA activity, a significantly lower activity was obtained for the C-$fLUC_{ARF18}$ when compared to its noncleavable variant (Control, **Figure 2C**). These results are consistent with a high ath-miR160 activity, confirming the susceptibility of the cleavable $fLUC_{ARF18}$ reporter to endogenous ath-miR160 post-transcriptional regulation.

To further test the specificity of the miRNA reporters, a target mimic was overexpressed (*MIM160*) to downregulate miR160. When using target mimicry, the plant miRNA is sequestered by an RNA molecule that is only partially complementary to the miRNA, producing a bulge in the region where cleavage of the true miRNA target occurs (**Figure 2D**; Franco-Zorrilla et al., 2007; Todesco et al., 2010), and thus preventing miRNA function (Todesco et al., 2010). When *MIM160* was overexpressed, no significant differences were observed between the luciferase activities of the C-$fLUC_{ARF18}$ and NC-$fLUC_{ARF18}$ reporters (**Figure 2C**). Based on these results, we can conclude that ath-miR160 was sequestered by *MIM160*, resulting in reduced miRNA levels.

To investigate if *PpARF18* was preferentially targeted by the ath-miR160a isoform, having the most similar precursor to ppi-*MIR160* (**Figure 1C**), C-$fLUC_{ARF18}$ was expressed in *miR160b* and *miR160c Arabidopsis* loss-of-function mutants, which accumulate reduced levels of the respective isoforms (Wójcik et al., 2017). In this way, we expected any decrease in target cleavage to be the result of a lower abundance of ath-miR160, including all the isoforms. In *miR160b Arabidopsis* mutants no significant differences could be detected in the measured luciferase activity when compared to the wild-type (WT) plants (**Figure 3A**). Surprisingly, in *miR160c Arabidopsis* mutants a significant increase in miRNA activity was observed, as shown by the decrease in the luciferase activity between WT and the mutant (**Figure 3A**). Quantification of ath-miR160 in the *mir160b* and *mir160c* mutants confirmed its increased expression in *mir160c* plants (**Figure 3B**), possibly compensating for the *miR160c* mutation. These results further suggest that the C-$fLUC_{ARF18}$ reporter is preferentially targeted by the miR160a isoform.

Pinus pinaster miR160 Interacts *in vivo* With Its Predicted *PpARF18* Target Site

Overexpressing primary miRNA sequences was shown to be sufficient for the correct processing and accumulation of the respective mature miRNAs (Martinho et al., 2015). To test the interaction of ppi-miR160 with its predicted target *PpARF18* (Rodrigues et al., 2019), the primary miR160 from *P. pinaster* (pri-miR160, or in short "pri160") and the C-$fLUC_{ARF18}$ and NC-$fLUC_{ARF18}$ reporters were co-expressed in the presence or absence of AGO1, the effector protein in miRNA target cleavage (Achkar et al., 2016; Yu et al., 2017; **Figure 4**). Luciferase activity of the reporter C-$fLUC_{ARF18}$ was affected by endogenous ath-miR160 (Control) and showed no significant variation when pri160 and AGO1 were overexpressed alone. However, the co-expression of pri160 and AGO1 led to a decrease of 62% in luciferase activity when compared to pri160 expression, supporting the occurrence of high ppi-miR160 activity in *Arabidopsis* protoplasts when AGO1 levels are not limiting (**Figure 4**). Furthermore, when *MIM160* was expressed alone or in combination with other elements, the luciferase activity of the C-$fLUC_{ARF18}$ significantly increased, indicating a lower miR160 activity when compared to the endogenous ath-miR160 or the ppi-miR160 generated by pri160 overexpression (**Figure 4**). The NC-$fLUC_{ARF18}$ reporter was not affected by the overexpression of any other factor, remaining higher than C-$fLUC_{ARF18}$ in all situations. Luciferase levels of NC-$fLUC_{ARF18}$ reporter were identical to those obtained when *MIM160* was co-expressed with C-$fLUC_{ARF18}$ reporter, both indicating miR160 loss-of-function (**Figure 4**). These results experimentally validate the interaction between ppi-miR160 and *P. pinaster ARF18* target site, supporting *PpARF18* as a true ppi-miR160 target as predicted earlier by Rodrigues et al. (2019).

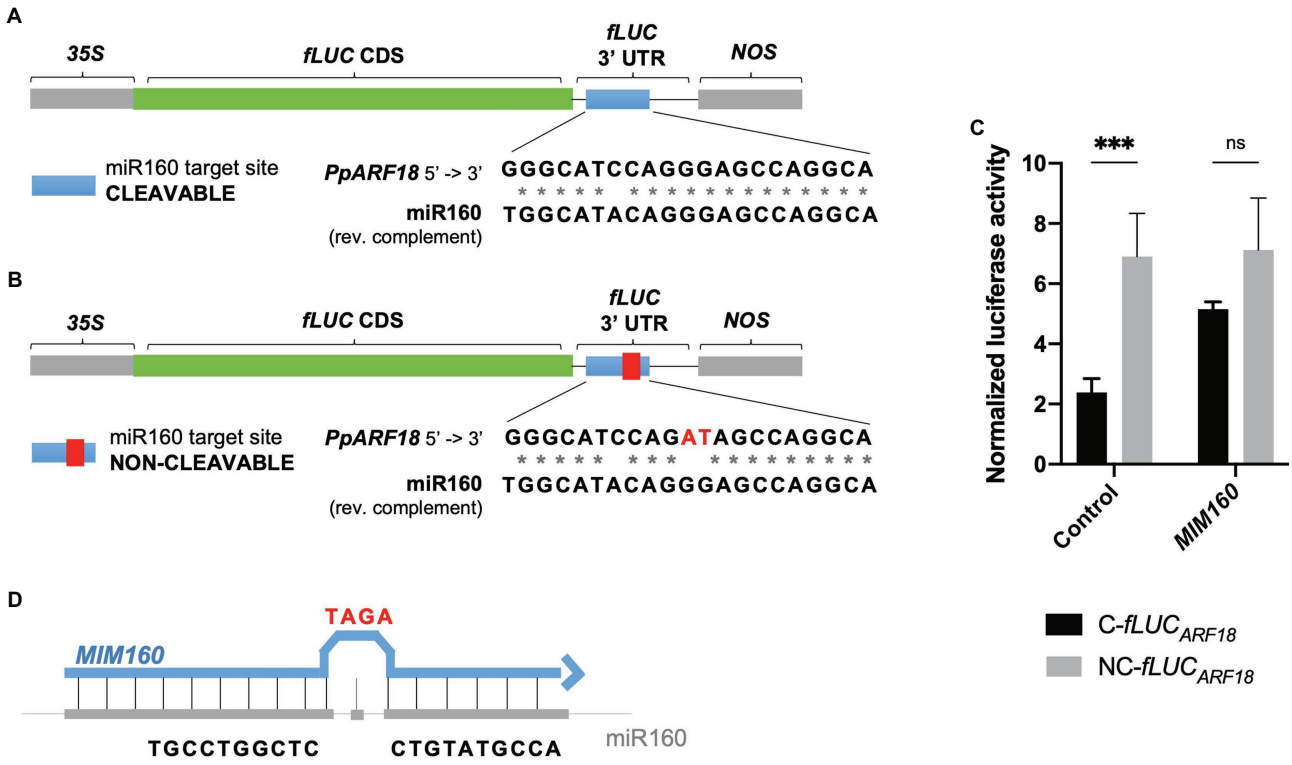

FIGURE 2 | Firefly Luciferase (*fLUC*) microRNA (miRNA) reporters used to monitor miR160 activity in *Arabidopsis* protoplasts. **(A)** The *P. pinaster* miR160 (ppi-miR160) *AUXIN RESPONSE FACTOR 18* in *Pinus pinaster* (Pp*ARF18*) target site was introduced in the 3′UTR region of *fLUC*, generating the cleavable reporter. **(B)** The non-cleavable reporter was produced harboring mutations in positions corresponding to the 10th and 11th nucleotides of the mature miR160 sequence (showed in red). **(C)** Normalized luciferase activity of cleavable (C-*fLUC*) and noncleavable (NC-*fLUC*) reporters as a measure of miR160a activity. Asterisks (*) represent significant differences ($p < 0.001$) obtained by two-way ANOVA and Sidak's multiple comparison test. **(D)** Target mimic with a modification of the central sequence by addition of three extra nucleotides (C to TAGA), resulting in a bulge formation.

Expression of *Picea abies ARF18* Decreases Toward More Advanced Stages of SE and Negatively Correlates With miR160 Expression

After validating the interaction of *PpARF18* with ppi-miR160 *in vivo*, this interaction was explored during the different stages of conifer somatic embryo development. For this, we favored using *P. abies* over *P. pinaster* due to its well-established and highly synchronized system of embryo development, which makes it an excellent model of SE in conifers (Filonova et al., 2000; von Arnold and Clapham, 2008). Also, both the ppi-miR160 isoform and the *ARF18* target sequences are conserved (**Figures 1C,D**) between *P. pinaster* (*Unigene806*) and *P. abies* (*MA_98506g0010*). Expression of *P. abies* miR160 and *ARF18* were evaluated in five stages of development including proembryogenic masses in proliferation (PEMs), EE, LE, and mature embryos (ME1, ME2, and ME3; **Figure 5A**).

The results showed that *P. abies* miR160 was strongly downregulated in the PEMI stage (**Figure 5B**), while the *ARF18* steady-state mRNA levels were strongly upregulated (**Figure 5C**). In addition, there was a progressive accumulation of miR160 in consecutive developmental stages toward *P. abies* embryo maturation, reaching its highest level in the fully developed mature embryo (ME3; **Figure 5B**). On the other hand, *P. abies ARF18* steady-state mRNA levels showed a clear inverse tendency, decreasing towards embryo maturation with the mature embryos presenting the lowest expression levels (**Figure 5C**). A negative correlation ($r = -0.3847$; $p = 0.115$) between the expression of *ARF18* and miR160 in *P. abies* SE (**Figure 5D**) was confirmed.

DISCUSSION

In this work, we showed that the miR160 of *Pinus pinaster* interacts *in vivo* with the *PpARF18* target site (**Figure 4**) and that this interaction is functional during somatic embryogenesis in a conifer model (**Figure 5**). Previous work investigating miRNAs involved in pine embryogenesis had predicted a highly probable functional miR160 binding site within *P. pinaster ARF18* target mRNA (Rodrigues et al., 2019). Computational algorithms, such as the one used, may predict numerous possible mRNA targets for a specific miRNA (Kuhn et al., 2008) but only a few will be true functional targets. In fact, *PpARF18* was among the 82 putative targets of ppi-miR160 predicted by Rodrigues et al. (2019). More recent work provided further support to the functionality of this interaction by degradome analysis in roots of *P. pinaster* (Perdiguero et al., 2021). In

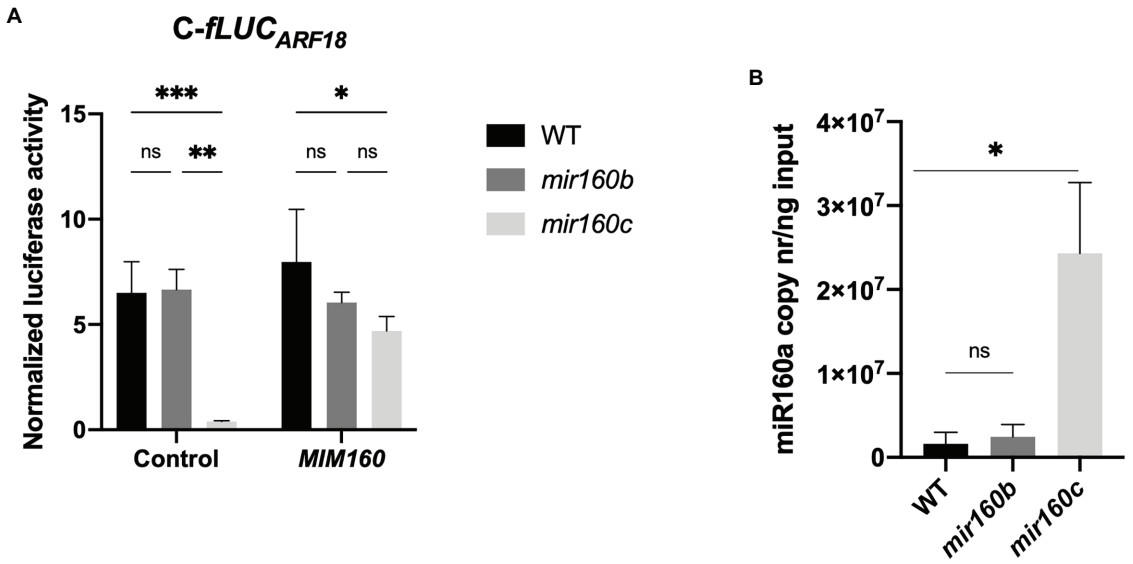

FIGURE 3 | Different levels of ath-miR160a activity in *mir160b* and *mir160c Arabidopsis* protoplasts. **(A)** Normalized luciferase activity of cleavable (C-*fLUC*$_{ARF18}$) reporter for ath-miR160a activity in wild-type (WT), *mir160b* and *mir160c Arabidopsis* protoplasts in the presence of the indicated elements. Bars represent mean ± SE of at least two independent experiments with two technical replicates each. Asterisks (*) represent significant differences according to *p* value classification ($p < 0.05$) obtained by two-way ANOVA and Tukey's multiple comparison test. **(B)** Absolute quantification of miR160a copy number in WT vs. *mir160b* and *mir160c Arabidopsis*. Bars represent mean ± SD of three biological replicates. Asterisks (*) represent significant differences ($p < 0.05$) obtained by an unpaired *t*-test comparing each mutant to WT. ns, non-significant.

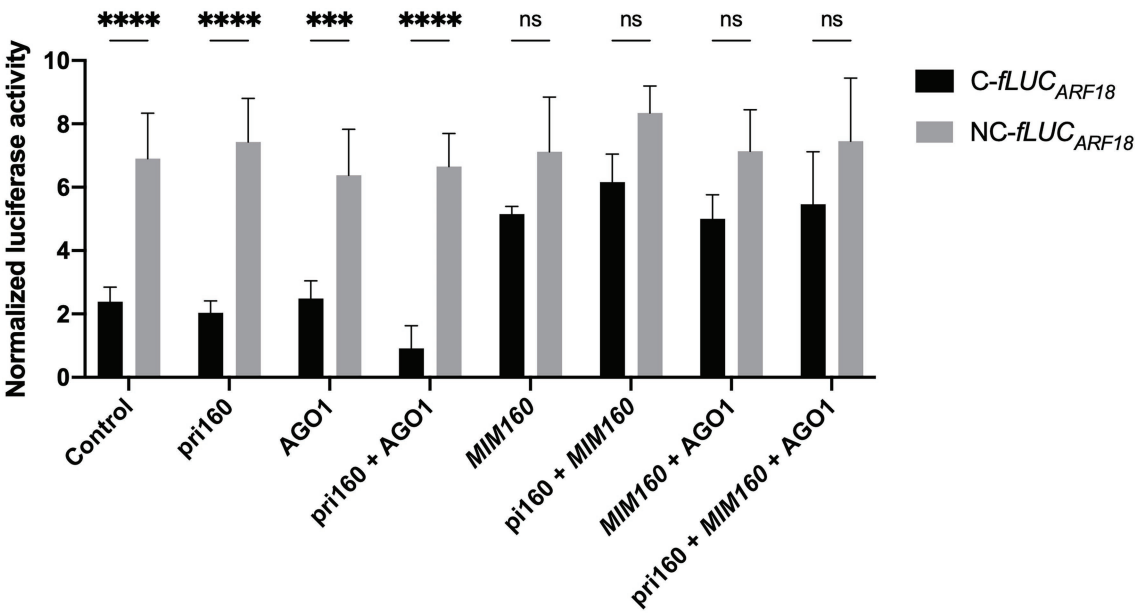

FIGURE 4 | Normalized luciferase activity from reporter constructs as a measure of miR160 activity in *Arabidopsis* protoplasts transfected for overexpression of the indicated elements. Asterisks (*) represent significant differences according to *p* value classification ($p < 0.001$) obtained by two-way ANOVA and Sidak's multiple comparison test. Bars of all graphics represent mean ± SE of four independent experiments with two technical replicates each.

Arabidopsis, miR160 is known to target *ARF10/16/17* (Wójcik et al., 2017; Das et al., 2018; Lin et al., 2018; Dai et al., 2021) and in *P. abies*, used here as model for SE, no information is available regarding miR160 target interaction. Given that methods for *in vivo* validation of miRNA/mRNA pairs and their expression analyses during embryo development have been established in *Arabidopsis* (reporter assays in protoplasts) and *P. abies* (SE), respectively, the similarity between miR160

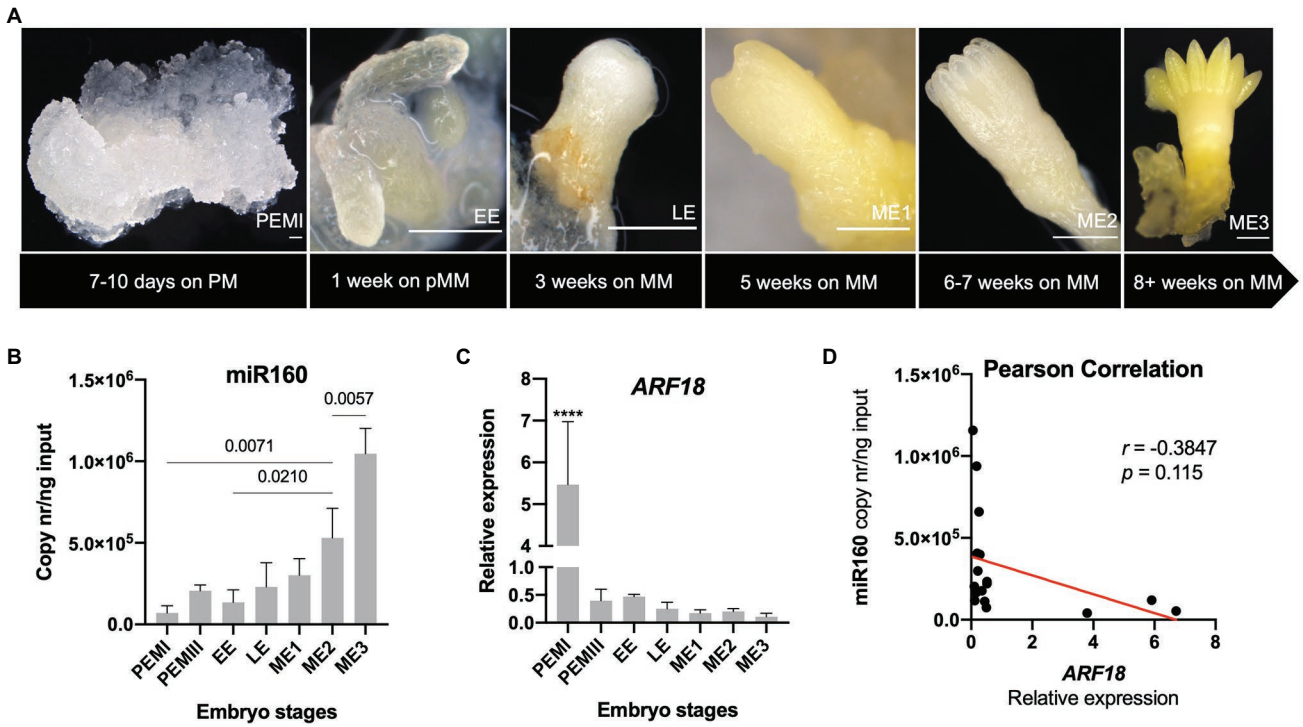

FIGURE 5 | Expression profiles of *Picea abies* miR160 and *ARF18* during somatic embryogenesis. **(A)** Different developmental stages of somatic embryogenesis, from proembryogenic masses (PEMI) on proliferation medium (PM) to fully mature embryo (ME3) on maturation medium (MM). Bars correspond to 500 µm. **(B)** Absolute quantification of miR160 (copy nr/ng input) across the selected embryo developmental stages. Significant differences of pairs of bars are marked with the *p* value, obtained by one-way ANOVA and Tukey's multiple comparison test. **(C)** Relative expression levels of *ARF18* during the selected stages of *P. abies* somatic embryo development. *CDC2*, *EF1-α*, and *PHOS* were used as reference genes. **(D)** Pearson correlation of expression levels between miR160 and *ARF18*. Error bars correspond to the SD for the RT-qPCR values of three biological replicates, except for early embryos (EEs) for which two biological replicates were used.

sequences and their respective targets in these species were analyzed and compared to the equivalent sequences in selected conifer models. Being a conserved miRNA, it was not surprising to verify that miR160 mature sequences were identical in all the analyzed species, with the exception of *Osa-miR160e* and *Osa-miR160f*. However, the precursor sequences were less similar in most cases except in *P. abies* and *P. pinaster*, where only two mismatches were detected; such mismatches did not affect the precursor secondary structure. In *Arabidopsis*, the most similar precursor corresponded to isoform ath-mirR160a, which is consistent with our transient expression results in *miR160b* and *miR160c* protoplasts (**Figure 3**).

As to the target sequences, our phylogenetic analysis showed that *P. pinaster* and *P. abies ARF18* grouped with *Arabidopsis AthARF10/16*, *O. sativa OsaARF8/10/18/22*, and *S. lycopersicum SlyARF10/14/16/18* (**Figure 1D**). From these, it is known that *AthARF10/16* (Wójcik et al., 2017; Das et al., 2018; Lin et al., 2018; Dai et al., 2021), *OsaARF8/10/18/22* (Huang et al., 2016), and *SlyARF10* (Hendelman et al., 2012) are targeted by miR160. A recent phylogenomic synteny network analysis with more than 3,500 ARFs from major streptophyte lineages proposed a classification of angiosperm *ARF* genes in six groups (Gao et al., 2020) and revealed which gymnosperms *ARF* genes were the closest sister lineage to each one of these six groups. Based on the length of the phylogeny tree branches, the authors further suggested lower amino acid substitution rates and higher levels of sequence conservation in the gymnosperm *ARFs*, possibly due to the usually longer generation times in the gymnosperms. From the three major subfamilies or clades of *ARFs* (Finet et al., 2013) encompassing the six groups, the clade C subfamily comprises genes from every major plant lineage, including the *Arabidopsis ARF10/16/17* within the group IV of angiosperms *ARF* genes (Gao et al., 2020). The split that generated angiosperms clade C *ARF10/16/17* is suggested to have occurred early in angiosperm evolution, and no duplications have been found in the ancestors of non-angiosperm species (Mutte et al., 2018; Gao et al., 2020). Our phylogenetic analysis suggests that *P. pinaster* and *P. abies ARF18*, targeted by miR160, are functionally related to the sequence that originated *ARF10* and *ARF16* in angiosperms. Thus, conifer *ARF18* might act as a putative orthologue of *AthARF10* and/or *AthARF16*.

As a first step toward the functional characterization of the miRNA-mRNA interaction during embryo development in conifers, we validated this interaction *in vivo* using a reporter system in *Arabidopsis* mesophyll protoplasts. By repressing the production of the firefly luciferase reporter

protein (fLUC), we show that ppi-miR160 specifically binds to and drives the cleavage of the C-*fLUC*$_{ARF18}$ reporter, harboring the *PpARF18* target site (**Figures 2**, **4**). While testing the sensitivity of our system to varying ath-miR160 endogenous levels using protoplasts from *miR160b* and *miR160c* mutants, we found that the ath-miR160a isoform is the most active one against the C-*fLUC*$_{ARF18}$ reporter (**Figure 3**). We also detected a strong increase in ath-miR160 activity in *miR160c* (**Figure 3**), that we attribute to the overaccumulation of ath-miR160a, as a compensatory mechanism for the *miR160c* mutation. This system for *in vivo* quantification of miRNA activity in *Arabidopsis* protoplasts (Martinho et al., 2015) revealed extremely useful to study miR160 in *P. pinaster*, which like many other gymnosperm species, are not amenable to stable transformation with miRNA reporter systems or these procedures are extremely difficult and time-consuming (Schwab et al., 2009; Nodine and Bartel, 2010; Wójcik et al., 2017). Assuming the miRNA biogenesis machinery processing the miR160 precursor sequence is conserved across both plant groups (**Figure 1**), and the confirmed identity of the mature miRNA160 sequences of *Arabidopsis* and *P. pinaster*/*P. abies*, it was expected that the observations in *Arabidopsis* protoplasts accurately reflect the post-transcriptional interaction occurring in the conifer's cells.

Our results in the somatic embryogenesis of *P. abies*, where the expression of miR160 gradually increased showing the highest expression in the mature embryo stages, are in agreement with previous work in conifers (Rodrigues et al., 2019), in which the same miR160 isoform showed a higher expression in late stages of *P. pinaster* zygotic and somatic embryo development. Furthermore, and as expected by the miR160-*PpARF18* target site validated interaction, an opposite expression pattern was observed between miR160 and its target during the same developmental period (**Figure 5**). However, miRNA160-mediated regulation of conifer *ARF18* does not exclude its regulation by additional mechanisms at the transcriptional and post-transcriptional levels, possibly modulated by the hormone environment used during somatic embryogenesis. Nonetheless, the (i) negatively correlated expression of miR160 and *ARF18* in *P. abies* somatic embryogenesis, (ii) the phylogenetic data showing the identity or close relatedness of the miR160 and the target sequences in *Arabidopsis* and conifers, and (iii) the previously gathered degradome data from *P. pinaster* tissues highlighting miR160-*PpARF18* as a high confidence interaction, strongly support the functional interaction during conifer embryo development.

AUXIN RESPONSE FACTOR proteins are key to the transcriptional response to auxin and in *Arabidopsis* they are encoded by a large gene family that acts either as activators or repressors of auxin response genes (Remington et al., 2004; Okushima et al., 2005; Liu et al., 2015). Their biological functions are complex to dissect because different gene family members often show overlapping expression patterns converging on the regulation of specific biological processes (Rademacher et al., 2011). The involvement of different ARFs in several developmental processes controlled by auxins, namely zygotic and somatic embryogenesis regulation is evident in *Arabidopsis* (Rademacher et al., 2011; Wójcikowska and Gaj, 2017). However, their roles in developmental processes in gymnosperms have been less explored. In *Arabidopsis*, at least 14 *ARF* genes are transcribed during SE, including *ARF10*, *ARF16*, and *ARF17* (Wójcikowska and Gaj, 2017) which were described as significantly upregulated during SE induction. In the analyzed *P. abies* SE cultures, the closest stage to SE induction corresponds to proembryogenic masses (PEMI). In this stage, the miR160 target *ARF18* is also highly expressed compared to the subsequent developmental stages. Conifer *ARF18* seems to be actively involved in the early stages of SE, being repressed as the embryo develops to reach maturation. As conifer *ARF18* is closely related to *Arabidopsis ARF16*, as suggested by our phylogenetic analysis (**Figure 1D**), it likely exhibits auxin response repressor activity which may be important to regulate genes required for active cell proliferation during the induction of SE and early embryo development. A significant accumulation of miR160 in *Arabidopsis* has been reported in somatic embryos (Wójcikowska et al., 2018), but its role has been studied mostly in the induction of SE, where miR160 interaction with the LEC2-mediated pathway was investigated. The authors proposed a model in which the targets of miR160 (*ARF10*/*ARF16*) and of miR165/166 (*PHB*/*PHV*) control SE induction by positively regulating LEC2. This results in the upregulation of *YUC* genes and consequent activation of auxin biosynthesis and accumulation, thus triggering auxin-response genes involved in SE induction (Wójcikowska et al., 2018). LEC2 is also considered a major regulator of seed maturation by controlling the synthesis and the accumulation of protein and lipid reserves (Stone et al., 2008; Wójcik et al., 2017). However, surprisingly, it has been recently reported that *LEC2* is absent from the genomes of *P. abies* and *Pinus taeda* and it is possibly lacking in conifers in general (Ranade and Egertsdotter, 2021), but the availability of additional genomic data from gymnosperm species in the near future, including the genome sequences of *P. pinaster* and other gymnosperms, will help to further clarify this issue. Although the miRNA-mRNA regulatory nodes are thought to have undergone parallel evolution in different plant groups (Cui et al., 2017), the angiosperms and gymnosperm groups diverged approximately 300 million years ago (Magallón et al., 2013). Therefore, alternative or specific regulatory networks may be active where miR160 functions might be involved.

Further molecular studies are also needed to uncover crosstalk of conifer miR160-*ARF18* with other hormone pathways. Indeed, as suggested by Wójcikowska et al. (2018), *ARF10*/*ARF16* may impact the signaling pathways of ABA and/or cytokinins, thereby contributing to SE induction. Dai et al. (2021) also described that the transcript levels of auxin and brassinosteroid signaling-related genes are possibly modulated by miR160-*ARF10*/16/*17* during hypocotyl elongation in *Arabidopsis*.

As far as we know, our study reports the first *in vivo* validation of a gymnosperm miRNA with its predicted target, and the use of this approach as a first step in the functional characterization of miRNAs will be of great utility for future studies of miRNA functions in conifer embryogenesis.

DATA AVAILABILITY STATEMENT

The original contributions presented in the study are included in the article/**Supplementary Material**, further inquiries can be directed to the corresponding author.

AUTHOR CONTRIBUTIONS

AA, AC, and CM designed the research. AA prepared the constructs, performed the protoplast transfection experiments, and all the expression analyses. PP and BC performed the *in silico* analyses. SL and AM participated in the protoplasts isolation and transfection experiments and RT-PCR analysis, respectively. EB-G, AC, and SC provided guidance during the protoplast transfection experiments and interpretation of results. AA and CM wrote the manuscript. All authors contributed to the article and approved the submitted version.

FUNDING

This research was supported by Fundação para a Ciência e Tecnologia, I.P. (FCT), through PhD grants SFRH/BD/128827/2017 to AA, SFRH/BD/143771/2019 to BC, and PD/BD/114359/2016 to SL, CEEC/IND/00175/2017 contract to AM and R&D Unit grants to "GREEN-IT – Bioresources for Sustainability" (UIDB/04551/2020 and UIDP/04551/2020), BioISI (UIDB/04046/2020 and UIDP/04046/2020), and CFE – Center for Functional Ecology – Science for People and the Planet (UIDB/04004/2020). The People Programme (Marie Curie Actions) of the EU Seventh Framework Programme (FP7/2007-2013) is acknowledged for REA grant agreement n° PIEF-GA-2013-627761.

ACKNOWLEDGMENTS

The authors wish to thank Sara von Arnold who kindly provided Norway spruce embryogenic cell line 61:21, Gaj Malgorzata for providing the seeds of *Arabidopsis* mutants *mir160b* and *mir160c*, Vera Nunes (IGC Plant Facility) for excellent plant care, and Inês Modesto for the help in bioinformatic analysis.

SUPPLEMENTARY MATERIAL

The Supplementary Material for this article can be found online at: https://www.frontiersin.org/articles/10.3389/fpls.2022.857611/full#supplementary-material

REFERENCES

Achkar, N. P., Cambiagno, D. A., and Manavella, P. A. (2016). MiRNA biogenesis: a dynamic pathway. *Trends Plant Sci.* 21, 1034–1044. doi: 10.1016/j.tplants.2016.09.003

Alves, A., Cordeiro, D., Correia, S., and Miguel, C. (2021). Small non-coding RNAs at the crossroads of regulatory pathways controlling somatic embryogenesis in seed plants. *Plants* 10:504. doi: 10.3390/plants10030504

Ambros, V. (2004). The functions of animal microRNAs. *Nature* 431, 350–355. doi: 10.1038/nature02871

Bartel, D. P. (2004). MicroRNAs: genomics, biogenesis, mechanism, and function. *Cell* 116, 281–297. doi: 10.1016/S0092-8674(04)00045-5

Canales, J., Bautista, R., Label, P., Gómez-Maldonado, J., Lesur, I., Fernández-Pozo, N., et al. (2014). De novo assembly of maritime pine transcriptome: implications for forest breeding and biotechnology. *Plant Biotechnol. J.* 12, 286–299. doi: 10.1111/pbi.12136

Cañas, R. A., Li, Z., Pascual, M. B., Castro-Rodríguez, V., Ávila, C., Sterck, L., et al. (2017). The gene expression landscape of pine seedling tissues. *Plant J.* 91, 1064–1087. doi: 10.1111/tpj.13617

Confraria, A., and Baena-González, E. (2016). "Using *Arabidopsis* protoplasts to study cellular responses to environmental stress" in *Environmental Responses in Plants. Methods in Molecular Biology*. ed. P. Duque, *Vol.* 1398 (New York, NY: Humana Press), 247–269.

Cui, J., You, C., and Chen, X. (2017). The evolution of MicroRNAs in plants. *Curr. Opin. Plant Biol.* 35, 61–67. doi: 10.1016/j.pbi.2016.11.006

Cuperus, J. T., Montgomery, T. A., Fahlgren, N., Burke, R. T., Townsend, T., Sullivan, C. M., et al. (2010). Identification of MIR390a precursor processing-defective mutants in *Arabidopsis* by direct genome sequencing. *Proc. Natl. Acad. Sci. U. S. A.* 107, 466–471. doi: 10.1073/pnas.0913203107

Dai, X., Lu, Q., Wang, J., Xiang, F., and Liu, Z. (2021). MiR160 and its target genes *ARF10*, *ARF16* and *ARF17* modulate hypocotyl elongation in a light, BRZ, or PAC-dependent manner in *Arabidopsis*: MiR160 promotes hypocotyl elongation. *Plant Sci.* 303:110686. doi: 10.1016/j.plantsci.2020.110686

Dai, X., and Zhao, P. X. (2011). PsRNATarget: a plant small RNA target analysis server. *Nucleic Acids Res.* 39, W155–W159. doi: 10.1093/nar/gkr319

Dai, X., Zhuang, Z., and Zhao, P. X. (2018). PsRNATarget: a plant small RNA target analysis server (2017 release). *Nucleic Acids Res.* 46, W49–W54. doi: 10.1093/nar/gky316

Das, S. S., Yadav, S., Singh, A., Gautam, V., Sarkar, A. K., Nandi, A. K., et al. (2018). Expression dynamics of MiRNAs and their targets in seed germination conditions reveals MiRNA-ta-SiRNA crosstalk as regulator of seed germination. *Sci. Rep.* 8:1233. doi: 10.1038/s41598-017-18823-8

de Maria, N., Guevara, M. A., Perdiguero, P., Vélez, M. D., Cabezas, J. A., López-Hinojosa, M., et al. (2020). Molecular study of drought response in the Mediterranean conifer *Pinus pinaster* Ait.: differential transcriptomic profiling reveals constitutive water deficit-independent drought tolerance mechanisms. *Ecol. Evol.* 10, 9788–9807. doi: 10.1002/ece3.6613

de Vega-Bartol, J. J., Simões, M., Lorenz, W. W., Rodrigues, A. S., Alba, R., and Dean, J. F. D., et al. (2013). Transcriptomic analysis highlights epigenetic and transcriptional regulation during zygotic embryo development of *Pinus pinaster*. *BMC Plant Biol.* 13: 123. doi: 10.1186/1471-2229-13-123

Doyle, J. J., and Doyle, J. L. (1990). Isolation of plant DNA from fresh tissue. *Focus* 12, 13–15.

Filonova, L. H., Bozhkov, P. V., and von Arnold, S. (2000). Developmental pathway of somatic embryogenesis in *Picea abies* as revealed by time-lapse tracking. *J. Exp. Bot.* 51, 249–264. doi: 10.1093/jexbot/51.343.249

Finet, C., Berne-Dedieu, A., Scutt, A. P., and Marlétaz, F. (2013). Evolution of the ARF gene family in land plants: old domains, new tricks. *Mol. Biol. Evol.* 30, 45–56. doi: 10.1093/molbev/mss220

Franco-Zorrilla, J. M., Valli, A., Todesco, M., Mateos, I., Puga, M. I., Rubio-Somoza, I., et al. (2007). Target mimicry provides a new mechanism for regulation of microRNA activity. *Nat. Genet.* 39, 1033–1037. doi: 10.1038/ng2079

Gao, B., Wang, L., Oliver, M., Chen, M., and Zhang, J. (2020). Phylogenetic synteny network analyses reveal ancestral transpositions of auxin response factor genes in plants. *Plant Methods* 16:70. doi: 10.1186/s13007-020-00609-1

Hendelman, A., Buxdorf, K., Stav, R., Kravchik, T., and Arazi, T. (2012). Inhibition of lamina outgrowth following *Solanum lycopersicum* AUXIN RESPONSE FACTOR 10 (*Sl*ARF10) derepression. *Plant Mol. Biol.* 78, 561–576. doi: 10.1007/s11103-012-9883-4

Huang, J., Li, Z., and Zhao, D. (2016). Deregulation of the OsmiR160 target gene Os*ARF18* causes growth and developmental defects with an alteration of auxin signaling in rice. *Sci. Rep.* 6:29938. doi: 10.1038/srep29938

Kovtun, Y., Chiu, W. L., Zeng, W., and Sheen, J. (1998). Suppression of auxin signal transduction by a MAPK cascade in higher plants. *Nature* 395, 716–720. doi: 10.1038/27240

Kozomara, A., Birgaoanu, M., and Griffithd-Jones, S. (2019). miRbase: from microRNA sequences to function. *Nucleic Acids Res.* 47, D155–D162. doi: 10.1093/nar/gky1141

Krogstrup, P. (1986). Embryolike structures from cotyledons and ripe embryos of Norway spruce (*Picea abies*). *Can. J. For. Res.* 16, 664–668. doi: 10.1139/x86-116

Kuhn, D. E., Martin, M. M., Feldman, D. S., Terry, A. V., Nuovo, G. J., and Elton, T. S. (2008). Experimental validation of miRNA targets. *Methods* 44, 47–54. doi: 10.1016/j.ymeth.2007.09.005

Li, J. -F., Chung, H. S., Niu, Y., Bush, J., McCormack, M., and Sheen, J. (2013). Comprehensive protein-based artificial microRNA screens for effective gene silencing in plants. *Plant Cell* 25, 1507–1522. doi: 10.1105/tpc.113.112235

Li, Q., Deng, C., Xia, Y., Kong, L., Zhang, H., Zhang, S., et al. (2017). Identification of novel miRNAs and miRNA expression profiling in embryogenic tissues of *Picea balfouriana* treated by 6-benzylaminopurine. *PLoS One* 12:e0176112. doi: 10.1371/journal.pone.0176112

Lin, J. S., Kuo, C.C., Yang, I.C., Tsai, W.A., Shen, Y.H., and Lin, C.C., et al. (2018). MicroRNA160 modulates plant development and heat shock protein gene expression to mediate heat tolerance in *Arabidopsis*. *Front. Plant Sci.* 9: 68. doi: 10.3389/fpls.2018.00068

Liu, J., Hua, W., Hu, Z., Yang, H., Zhang, L., Li, R., et al. (2015). Natural variation in ARF18 gene simultaneously affects seed weight and silique length in polyploid rapeseed. *Proc. Natl. Acad. Sci. U. S. A.* 112, E5123–E5132. doi: 10.1073/pnas.1502160112

Liu, Z., Li, J., Wang, L., Li, Q., Lu, Q., Yu, Y., et al. (2016). Repression of callus initiation by the miRNA-directed interaction of auxin–cytokinin in *Arabidopsis thaliana*. *Plant J.* 87, 391–402. doi: 10.1111/tpj.13211

Liu, P. P., Montgomery, T. A., Fahlgren, N., Kasschau, K. D., Nonogaki, H., and Carrington, J. C. (2007). Repression of AUXIN RESPONSE FACTOR10 by microRNA160 is critical for seed germination and post-germination stages. *Plant J.* 52, 133–146. doi: 10.1111/j.1365-313X.2007.03218.x

Liu, N., Wu, S., Li, Z., Khan, A. Q., Hu, H., Zhang, X., et al. (2020). Repression of microRNA 160 results in retarded seed integument growth and smaller final seed size in cotton. *Crop J.* 8, 602–612. doi: 10.1016/j.cj.2019.12.004

Luehrsen, K. R., de Wet, J. R., and Walbot, V. (1992). Transient expression analysis in plants using firefly luciferase reporter gene. *Methods Enzymol.* 216, 397–414. doi: 10.1016/0076-6879(92)16037-k

Magallón, S., Hilu, K. W., and Quandt, D. (2013). Land plant evolutionary timeline: gene effects are secondary to fossil constraints in relaxed clock estimation of age and substitution rates. *Am. J. Bot.* 100, 556–573. doi: 10.3732/ajb.1200416

Martinho, C., Confraria, A., Elias, C. A., Crozet, P., Rubio-Somoza, I., Weigel, D., et al. (2015). Dissection of miRNA pathways using *Arabidopsis* mesophyll protoplasts. *Mol. Plant* 8, 261–275. doi: 10.1016/j.molp.2014.10.003

Modesto, I., Sterck, L., Arbona, V., Gómez-Cadenas, A., Carrasquinho, I., van de Peer, Y., et al. (2021). Insights into the mechanisms implicated in *Pinus pinaster* resistance to pinewood nematode. *Front. Plant Sci.* 12:690857. doi: 10.3389/fpls.2021.690857

Mutte, S. K., Kato, H., Rothfels, C., Melkonian, M., Wong, G. K.-S., and Weijers, D. (2018). Origin and evolution of the nuclear auxin response system. *elife* 7:e33399. doi: 10.7554/eLife.33399

Nodine, M. D., and Bartel, D. P. (2010). MicroRNAs prevent precocious gene expression and enable pattern formation during plant embryogenesis. *Genes Dev.* 24, 2678–2692. doi: 10.1101/gad.1986710

Nystedt, B., Street, N. R., Wetterbom, A., Zuccolo, A., Lin, Y. C., Scofield, D. G., et al. (2013). The Norway spruce genome sequence and conifer genome evolution. *Nature* 497, 579–584. doi: 10.1038/nature12211

O'Leary, N. A., Wright, M. W., Brister, J. R., Ciufo, S., Haddad, D., McVeigh, R., et al. (2016). Reference sequence (RefSeq) database at NCBI: current status, taxonomic expansion, and functional. *Nucleic Acids Res.* 44, D733–D745. doi: 10.1093/nar/gkv1189

Okushima, Y., Overvoorde, P. J., Arima, K., Alonso, J. M., Chan, A., Chang, C., et al. (2005). Functional genomic analysis of the AUXIN RESPONSE FACTOR gene family members in *Arabidopsis thaliana*: unique and overlapping functions of *ARF7* and *ARF19*. *Plant Cell* 17, 444–463. doi: 10.1105/tpc.104.028316

Perdiguero, P., Rodrigues, A. S., Chaves, I., Costa, B., Alves, A., María, N., et al. (2021). Comprehensive analysis of the IsomiRome in the vegetative organs of the conifer *Pinus pinaster* under contrasting water availability. *Plant Cell Environ.* 44, 706–728. doi: 10.1111/pce.13976

Pfaffl, M. W. (2001). A new mathematical model for relative quantification in real-time RT-PCR. *Nucleic Acids Res.* 29:e45. doi: 10.1093/nar/29.9.e45

Plotnikova, A., Kellner, M. J., Schon, M. A., Mosiolek, M., and Nodine, M. D. (2019). MicroRNA dynamics and functions during *Arabidopsis* embryogenesis. *Plant Cell* 31, 2929–2946. doi: 10.1105/tpc.19.00395

Rademacher, E. H., Moller, B., Lokerse, A. S., Llavata-Peris, C. I., van den Berg, W., and Weijers, D. (2011). A cellular expression map of the *Arabidopsis AUXIN RESPONSE FACTOR* gene family. *Plant J.* 68, 597–606. doi: 10.1111/j.1365-313X.2011.04710.x

Ranade, S. S., and Egertsdotter, U. (2021). In silico characterization of putative gene homologues involved in somatic embryogenesis suggests that some conifer species may lack *LEC2*, one of the key regulators of initiation of the process. *BMC Genomics* 22:392. doi: 10.1186/s12864-021-07718-8

Reinhart, B. J., Weinstein, E. G., Rhoades, M. W., Bartel, B., and Bartel, D. P. (2002). MicroRNAs in plants. *Genes Dev.* 16, 1616–1626. doi: 10.1101/gad.1004402

Remington, D. L., Vision, T. J., Guilfoyle, T. J., and Reed, J. W. (2004). Contrasting modes of diversification in the *aux/IAA* and *ARF* gene families. *Plant Physiol.* 135, 1738–1752. doi: 10.1104/pp.104.039669

Rhoades, M. W., Reinhart, B. J., Lim, L. P., Burge, C. B., Bartel, B., and Bartel, D. P. (2002). Prediction of plant microRNA targets. *Cell* 110, 513–520. doi: 10.1016/s0092-8674(02)00863-2

Rodrigues, A. S., Chaves, I., Costa, B. V., Lin, Y. C., Lopes, S., Milhinhos, A., et al. (2019). Small RNA profiling in *Pinus pinaster* reveals the transcriptome of developing seeds and highlights differences between zygotic and somatic embryos. *Sci. Rep.* 9:11327. doi: 10.1038/s41598-019-47789-y

Schon, M. A., and Nodine, D. M. (2017). Widespread contamination of *Arabidopsis* embryo and endosperm transcriptome data sets. *Plant Cell* 29, 608–617. doi: 10.1105/tpc.16.00845

Schwab, R., Maizel, A., Ruiz-Ferrer, V., Garcia, D., Bayer, M., Crespi, M., et al. (2009). Endogenous TasiRNAs mediate non-cell autonomous effects on gene regulation in *Arabidopsis thaliana*. *PLoS One* 4:e5980. doi: 10.1371/journal.pone.0005980

Schwartz, B., Yeung, E., and Meinke, D. (1994). Disruption of morphogenesis and transformation of the suspensor in abnormal suspensor mutants of *Arabidopsis*. *Development* 120, 3235–3245. doi: 10.1242/dev.120.11.3235

Seefried, W. F., Willmann, M. F., Clausen, R. L., and Jenik, P. D. (2014). Global regulation of embryonic patterning in *Arabidopsis* by microRNAs. *Plant Physiol.* 165, 670–687. doi: 10.1104/pp.114.240846

Siddiqui, Z. H., Abbas, Z. K., Ansari, M. W., and Khan, M. N. (2019). The role of miRNA in somatic embryogenesis. *Genomics* 111, 1026–1033. doi: 10.1016/j.ygeno.2018.11.022

Stocks, M. B., Moxon, S., Mapleson, D., Woolfenden, H. C., Mohorianu, I., Folkes, L., et al. (2012). The UEA sRNA workbench: a suite of tools for analysing and visualizing next generation sequencing microRNA and small RNA datasets. *Bioinformatics* 28, 2059–2061. doi: 10.1093/bioinformatics/bts311

Stone, S. L., Braybrook, S. A., Paula, S. L., Kwong, L. W., Meuser, J., Pelletier, J., et al. (2008). *Arabidopsis LEAFY COTYLEDON2* induces maturation traits and auxin activity: implications for somatic embryogenesis. *Proc. Natl. Acad. Sci. U. S. A.* 105, 3151–3156. doi: 10.1073/pnas.0712364105

Sundell, D., Mannapperuma, C., Netotea, S., Delhomme, N., Lin, Y. C., Sjödin, A., et al. (2015). The plant genome integrative explorer resource: PlantGenIE.org. *New Phytol.* 208, 1149–1156. doi: 10.1111/nph.13557

Szyrajew, K., Bielewicz, D., Dolata, J., Wójcik, A. M., Nowak, K., Szczygieł-Sommer, A., et al. (2017). MicroRNAs are intensively regulated during induction of somatic embryogenesis in *Arabidopsis*. *Front. Plant Sci.* 8:18. doi: 10.3389/fpls.2017.00018

Todesco, M., Rubio-Somoza, I., Paz-Ares, J., and Weigel, D. (2010). A collection of target mimics for comprehensive analysis of microRNA function in *Arabidopsis thaliana*. *PLoS Genet.* 6:e1001031. doi: 10.1371/journal.pgen.1001031

Vashisht, D., and Nodine, M. D. (2014). MicroRNA functions in plant embryos. *Biochem. Soc. Trans.* 42, 352–357. doi: 10.1042/BST20130252

Vestman, D., Larsson, E., Uddenberg, D., Cairney, J., Clapham, D., Sundberg, E., et al. (2011). Important processes during differentiation and early development of somatic embryos of Norway spruce as revealed by changes in global gene expression. *BCM Proceedings* 5, 1–362. doi: 10.1186/1753-6561-5-S7-P78

von Arnold, S., and Clapham, D. (2008). "Spruce embryogenesis," in *Plant Embryogenesis*. eds. M. F. Suárez and P. V. Bozhkov (Totowa, NJ: Humana Press), 31–47.

von Arnold, S., and Eriksson, T. (1981). In vitro studies of adventitious shoot formation in *Pinus contorta*. *Can. J. Bot.* 59, 870–874. doi: 10.1139/b81-121

Wadenbäck, J., von Arnold, S., Egertsdotter, U., Walter, M. H., Grima-Pettenati, J., Goffner, D., et al. (2008). Lignin biosynthesis in transgenic Norway spruce plants harboring an antisense construct for cinnamoyl CoA reductase (CCR). *Transgenic Res.* 17, 379–392. doi: 10.1007/s11248-007-9113-z

Wang, J. W., Wang, L. J., Mao, Y. B., Cai, W. J., Xue, H. W., and Chen, X. Y. (2005). Control of root cap formation by microRNA-targeted auxin response factors in *Arabidopsis*. *Plant Cell* 17, 2204–2216. doi: 10.1105/tpc.105.033076

Willmann, M. R., Mehalick, A. J., Packer, R. L., and Jenik, P. D. (2011). MicroRNAs regulate the timing of embryo maturation in *Arabidopsis*. *Plant Physiol.* 155, 1871–1884. doi: 10.1104/pp.110.171355

Wójcik, A. M., Nodine, M. D., and Gaj, M. D. (2017). MiR160 and MiR166/165 contribute to the *LEC2*-mediated auxin response involved in the somatic embryogenesis induction in *Arabidopsis*. *Front. Plant Sci.* 8, 2024. doi: 10.3389/fpls.2017.02024

Wójcikowska, B., Botor, M., Morończyk, J., Wójcik, A. M., Nodzyński, T., Karcz, J., et al. (2018). Trichostatin a triggers an embryogenic transition in *Arabidopsis* explants via an auxin-related pathway. *Front. Plant Sci.* 9:1353. doi: 10.3389/fpls.2018.01353

Wójcikowska, B., and Gaj, M. D. (2017). Expression profiling of *AUXIN RESPONSE FACTOR* genes during somatic embryogenesis induction in *Arabidopsis*. *Plant Cell Rep.* 36, 843–858. doi: 10.1007/s00299-017-2114-3

Yoo, S. D., Cho, Y. H., and Sheen, J. (2007). Arabidopsis mesophyll protoplasts: a versatile cell system for transient gene expression analysis. *Nat. Protoc.* 2, 1565–1572. doi: 10.1038/nprot.2007.199

Yu, Y., Jia, T., and Chen, X. (2017). The 'how' and 'where' of plant microRNAs. *New Phytol.* 216, 1002–1017. doi: 10.1111/nph.14834

Zhang, B., Pan, X., Cannon, C. H., Cobb, G. P., and Anderson, T. A. (2006). Conservation and divergence of plant microRNA genes. *Plant J.* 46, 243–259. doi: 10.1111/j.1365-313X.2006.02697.x

Zhang, J., Zhang, S., Han, S., Li, X., Tong, Z., and Qi, L. (2013). Deciphering small noncoding RNAs during the transition from dormant embryo to germinated embryo in larches (*Larix leptolepis*). *PLoS One* 8:e81452. doi: 10.1371/journal.pone.0081452

Zhang, J., Zhang, S., Han, S., Wu, T., Li, X., Li, W., et al. (2012). Genome-wide identification of microRNAs in larch and stage-specific modulation of 11 conserved microRNAs and their targets during somatic embryogenesis. *Planta* 236, 647–657. doi: 10.1007/s00425-012-1643-9

Conflict of Interest: The authors declare that the research was conducted in the absence of any commercial or financial relationships that could be construed as a potential conflict of interest.

Publisher's Note: All claims expressed in this article are solely those of the authors and do not necessarily represent those of their affiliated organizations, or those of the publisher, the editors and the reviewers. Any product that may be evaluated in this article, or claim that may be made by its manufacturer, is not guaranteed or endorsed by the publisher.

frontiers | Frontiers in Plant Science

ORIGINAL RESEARCH
published: 10 May 2022
doi: 10.3389/fpls.2022.887980

Rice LEAFY COTYLEDON1 Hinders Embryo Greening During the Seed Development

Fu Guo[1,2†], Peijing Zhang[1,3†], Yan Wu[1†], Guiwei Lian[1], Zhengfei Yang[4,5], Wu Liu[4], B. Buerte[1], Chun Zhou[1], Wenqian Zhang[1], Dandan Li[2], Ning Han[1], Zaikang Tong[6], Muyuan Zhu[1], Lin Xu[4], Ming Chen[1*] and Hongwu Bian[1*]*

[1] College of Life Sciences, Zhejiang University, Hangzhou, China, [2] Hainan Institute, Zhejiang University, Yazhou Bay Science and Technology City, Sanya, China, [3] Liangzhu Laboratory, Zhejiang University Medical Centre, Hangzhou, China, [4] National Key Laboratory of Plant Molecular Genetics, CAS Centre for Excellence in Molecular Plant Sciences, Institute of Plant Physiology and Ecology, Chinese Academy of Sciences, Shanghai, China, [5] College of Life Sciences, Shanghai Normal University, Shanghai, China, [6] State Key Laboratory of Subtropical Silviculture, Zhejiang A&F University, Lin'an, China

OPEN ACCESS

Edited by:
Jonny E. Scherwinski-Pereira, Brazilian Agricultural Research Corporation (EMBRAPA), Brazil

Reviewed by:
Yilong Hu, South China Botanical Garden (CAS), China
Tao Guo, South China Agricultural University, China

***Correspondence:**
Hongwu Bian
hwbian@zju.edu.cn
Ming Chen
mchen@zju.edu.cn
Lin Xu
xulin@cemps.ac.cn

[†] These authors have contributed equally to this work

Specialty section:
This article was submitted to Plant Development and EvoDevo, a section of the journal Frontiers in Plant Science

Received: 02 March 2022
Accepted: 14 April 2022
Published: 10 May 2022

Citation:
Guo F, Zhang P, Wu Y, Lian G, Yang Z, Liu W, Buerte B, Zhou C, Zhang W, Li D, Han N, Tong Z, Zhu M, Xu L, Chen M and Bian H (2022) Rice LEAFY COTYLEDON1 Hinders Embryo Greening During the Seed Development. Front. Plant Sci. 13:887980. doi: 10.3389/fpls.2022.887980

LEAFY COTYLEDON1 (LEC1) is the central regulator of seed development in Arabidopsis, while its function in monocots is largely elusive. We generated *Oslec1* mutants using CRISPR/Cas9 technology. *Oslec1* mutant seeds lost desiccation tolerance and triggered embryo greening at the early development stage. Transcriptome analysis demonstrated that *Oslec1* mutation altered diverse hormonal pathways and stress response in seed maturation, and promoted a series of photosynthesis-related genes. Further, genome-wide identification of OsLEC1-binding sites demonstrated that OsLEC1 bound to genes involved in photosynthesis, photomorphogenesis, as well as abscisic acid (ABA) and gibberellin (GA) pathways, involved in seed maturation. We illustrated an OsLEC1-regulating gene network during seed development, including the interconnection between photosynthesis and ABA/GA biosynthesis/signaling. Our findings suggested that OsLEC1 acts as not only a central regulator of seed maturation but also an inhibitor of embryo greening during rice seed development. This study would provide new understanding for the OsLEC1 regulatory mechanisms on photosynthesis in the monocot seed development.

Keywords: seed development, seed maturation, OsLEC1, photosynthesis, CRISPR/Cas9

INTRODUCTION

Seeds store the genetic hardware within the embryo, which guarantees the orderly unfolding of the plant's next life cycle in interaction with the environment (Sreenivasulu and Wobus, 2013). During seed development, the major tissue types and stem-cell niches of plants are established. Thus, knowledge of seed development is essential for a full understanding of plant development (Gillmor et al., 2020). Plant seed development is divided into two phases: morphogenesis phase and maturation phase. During the morphogenesis phase, the basic body plan of the embryo and endosperm are established (Lau et al., 2012; Li and Berger, 2012); chloroplast biogenesis and photosynthesis are also initiated during this period in many angiosperm taxa (Puthur et al., 2013). During the maturation phase, photosynthesis, the accumulation of storage compounds, and the induction of desiccation tolerance and preparation for seed dormancy are the main processes (Jo et al., 2019).

Seed development is genetically controlled by at least four regulators, LEAFY COTYLEDON 1 (LEC1), LEC2, FUSCA 3 (FUS3), and ABSCISIC ACID INSENSITIVE 3 (ABI3) (Giraudat et al., 1992; Meinke, 1992; Luerssen et al., 1998; Stone et al., 2001). Generally, *lec1*, *lec2*, *fus3,* and *abi3* mutants represent reduction of desiccation tolerance and seed dormancy (Meinke, 1992; Keith et al., 1994; Meinke et al., 1994; West et al., 1994; Parcy et al., 1997; Lotan et al., 1998; Nambara et al., 2000; Stone et al., 2001; Pelletier et al., 2017). LEC1 acts as a central regulator of seed development through combinatorial binding with ABA-RESPONSIVE ELEMENT-BINDING PROTEIN 3 (AREB3), BASIC LEUCINE ZIPPER 67 (bZIP67), and ABI3 (Jo et al., 2019).

In Arabidopsis, loss-of-function mutations of *LEC1* cause defects in storage proteins and lipid accumulation, acquisition of desiccation tolerance, and suppression of germination and leaf primordia initiation (Meinke, 1992; Meinke et al., 1994; West et al., 1994; Santos-Mendoza et al., 2008). Moreover, ectopic expression of *LEC1* induces embryonic development and the activation of genes involved in maturation and storage, as well as lipid accumulation in vegetative organs (Lotan et al., 1998; Kagaya et al., 2005; Mu et al., 2008). A few of studies have explored the effects of the overexpression of *LEC1* in carrot, maize, and rice. Expressing carrot *C-LEC1* driven by the Arabidopsis *LEC1* promoter could complement the viviparous and desiccation intolerant defects of Arabidopsis *lec1-1* mutant (Yazawa et al., 2004). Overexpression of maize (*Zea mays*) *LEAFY COTYLEDON 1* (*ZmLEC1)* increases seed oil production by up to 48% but reduces seed germination and leaf growth (Shen et al., 2010). In rice, *OsLEC1* overexpression results in abnormalities in the development of leaves, panicles, and spikelets (Zhang and Xue, 2013). Heterologous expression of *OsNF-YB7* (*OsLEC1*) in Arabidopsis *lec1-1* complements the *lec1-1* defects. OsNF-YB7 defect causes lethality (Niu et al., 2021). However, how LEC1 regulates rice seed development is not clear.

In the present study, we generated *Oslec1* mutants using a gene-editing technique. Phenotype analysis revealed that dry seeds of *Oslec1* mutants could not germinate but fresh seeds of the mutants germinated normally, suggesting lack of desiccation tolerance. Notably, embryos of mutants turned green during early seed development. Subsequently, RNA-seq transcriptional profiling and ChIP-seq were used to identify the underlying mechanisms via which *OsLEC1* regulates photosynthesis-related genes and seed-maturation related genes. Our studies provide new insights that OsLEC1 is an inhibitor of embryo greening during rice seed development, in addition to being a central regulator of seed maturation.

RESULTS

OsLEC1 Deficiency Disrupts Seed Desiccation Tolerance and Germination

We first established that LEC1 was largely conserved while typically different in a few sites between monocots and dicots by performing multiple alignments (**Supplementary Figures 1A,B**). To determine the physiological functions of OsLEC1 in rice, we used the CRISPR/Cas9 technology to knock out *OsLEC1*. We generated more than 30 transformant plants in the T0 generation, in which seven homozygous deletion mutants were screened using PCR and DNA sequencing (data not shown). DNA sequencing analysis showed that *Oslec1-1* and *Oslec1-2* contained a 1 bp deletion (G) at the gRNA1 site, and a 1 bp insertion (A or T) at the gRNA2 site (**Figure 1A**), leading to frameshift mutations and generating premature stop codons at aa157 (**Supplementary Figure 1C**). Thus, *Oslec1-1* and *Oslec1-2* mutations disrupted the original protein structure from 254 to 157 aa. Except for the shorter height of the mutants compared to the wild type plants, we did not observe obviously abnormal morphological phenotypes, including the tillering or grain number (**Supplementary Figure 2**). While >90% of the wild type seeds germinated after drying at 37°C for 3 days, none of the mutant seeds germinated (**Figures 1B,D**). Surprisingly, freshly harvested mutant seeds germinated and even rooted at 24 h after imbibition, when the wild type plant had not germinated yet (**Figure 1E**, **Supplementary Figure 3**). Finally, >90% of *Oslec1-1* and *Oslec1-2* fresh seeds germinated, similar to the wild type (**Figure 1C**). Further, 2,3,5-Triphenyltetrazolium chloride (TTC) staining revealed that the dry seeds of *Oslec1* mutants displayed green primordium without any red tissues, indicating completely lethal embryos in the dry mutant seeds (**Figure 1D**). Interestingly, green leaf primordia were observed in *Oslec1-1* and *Oslec1-2* embryos but not in wild type ones, suggesting chlorophyll accumulation in the *Oslec1* embryos. Meanwhile, we tested the embryo vitality of freshly harvested seeds (about 25 days after pollination [DAP]) using TTC staining. The embryo vitality of *Oslec1* fresh seeds was similar to that of the wild type seeds (**Figure 1E**).

Our results revealed that the *Oslec1* mutation disrupted desiccation tolerance but initiated chlorophyll accumulation in seed development, suggesting that *OsLEC1* acts as a key regulator of seed maturation in rice.

OsLEC1 Deficiency Leads to a Green Embryo During Seed Development

Further, we examined the embryo phenotypes of the *Oslec1* mutants and wild type plants at different stages of rice seed development. Wild type embryos remain white during the whole process of rice seed development. In contrast to the wild type embryos, *Oslec1* mutant embryos displayed green apical shoots at 7 DAP (**Figure 2A**, **Supplementary Figure 4**). Subsequently, the apical shoot remained green in *Oslec1* mutant embryos at 25 DAP (**Figure 2B**, **Supplementary Figure 4**). Surprisingly, after imbibing water for only 3 h at 37°C, the epiblasts covering the embryos were split by the sprouting shoots in the *Oslec1* mutants, indicating more rapid germination in comparison to the wild type plants (**Figure 2C**, **Supplementary Figure 4**).

Scanning electron microscopy (SEM) showed that at 7 DAP, the shoot apical meristems in wild type embryos were embedded in the covering epiblast (**Figure 2D**), while those in the mutants were exposed (**Figure 2E**). Semi-thin longitudinal sections of embryos exhibited an ordered three-layer leaf primordium in the intact coleoptile of wild type embryos (**Figure 2F**), whereas in

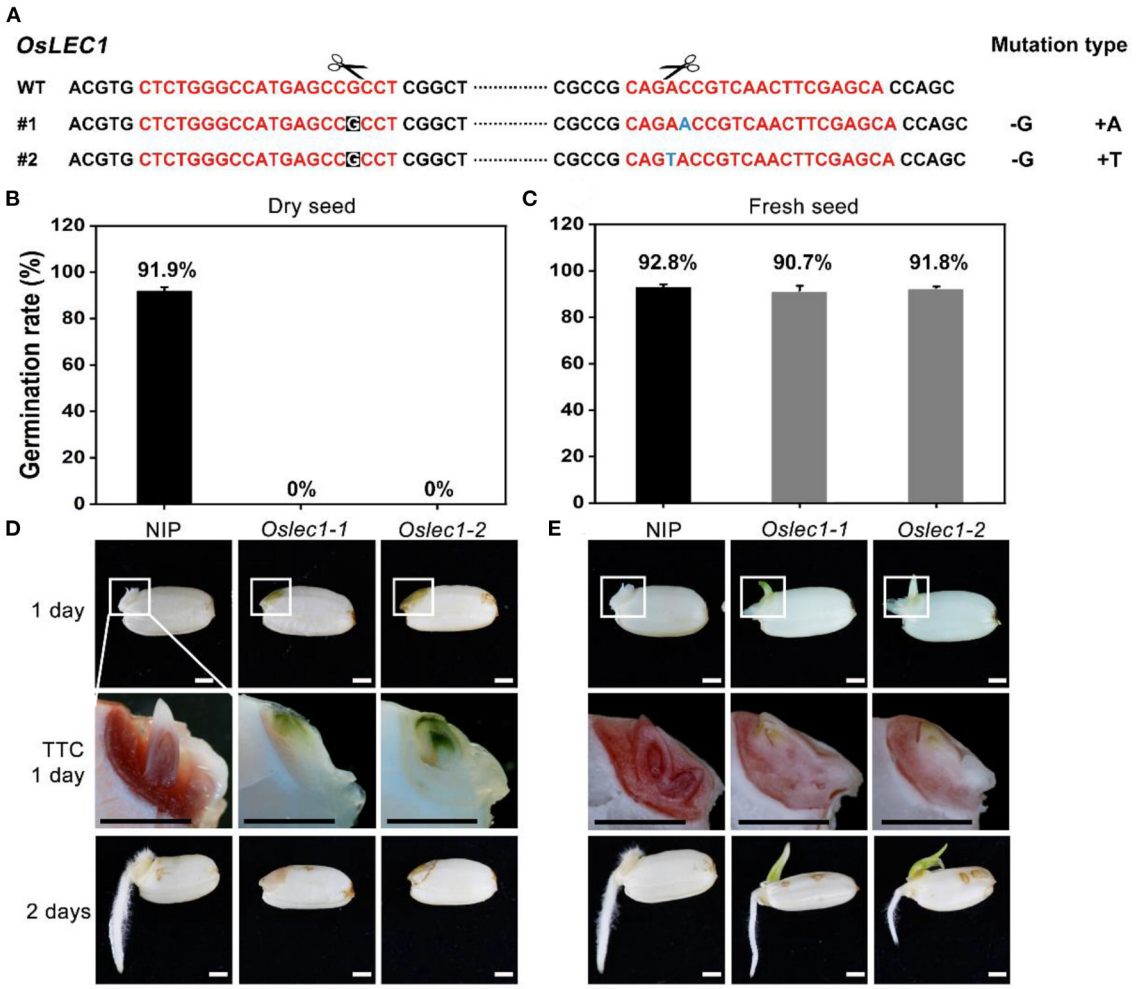

FIGURE 1 | Germination phenotypes of *Oslec1* mutants. **(A)** Mutation sites in the *Oslec1* mutant DNA. The red sequence represents the designed guide RNA (gRNA) for the wild type rice and the scissors represent the predicted knockout sites. The letters with a black background represent the deleted bases, and the blue letter represents the inserted base. **(B,C)** Germination rates of dry seeds and the fresh seeds of the wild type and *Oslec1* mutants after 1 day of imbibition at 37°C. **(D,E)** Photos of the wild type and *Oslec1* mutant seeds after 1 day of imbibition at 37°C (1 day) and 1 day on wet filter paper at 28°C (2 days). Photos of group "TTC 1 day" were the amplification of the regions in white boxes in group "1 day," indicating the embryos stained by TTC for 3 h at 37°C. Scale bars = 1 mm.

Oslec1 mutant embryos at 7 DAP, the primary leaves were spread out (**Figure 2G**). Furthermore, the wild type embryos were bent while *Oslec1* mutant embryos were straight (**Figures 2F,G**). Thus, the green embryos of *Oslec1* mutants showed that leaf primordia initiation were triggered in the embryo. Moreover, the scutella parenchyma of *Oslec1* mutants was abnormal compared with those of the wild type plants (**Figures 2H,J**). Transmission electron microscopy (TEM) revealed many lipid bodies and large starch grains in wild type embryos at 7 DAP, while major storage products were almost absent in *Oslec1* mutant embryos (**Figures 2J,K**). The above data suggested that *OsLEC1* might play a crucial role in the regulation of germination inhibition, and accumulation of storage compounds in rice seed development.

OsLEC1 Is Expressed Predominantly in Immature Embryos During Early Seed Development

We analyzed the expression pattern of *OsLEC1* based on an expression database (http://expression.ic4r.org/) (Xia et al., 2017) (**Supplementary Figure 5A**). The results showed that *OsLEC1* was highly expressed in the callus and immature seeds. Results of qRT-PCR further indicated that mRNA of OsLEC1 accumulated in the embryos but not in endosperm or glume of 20-DAP seeds (**Supplementary Figure 5B**). Subcellular localization showed that OsLEC1-GFP was enriched in the nucleus, which

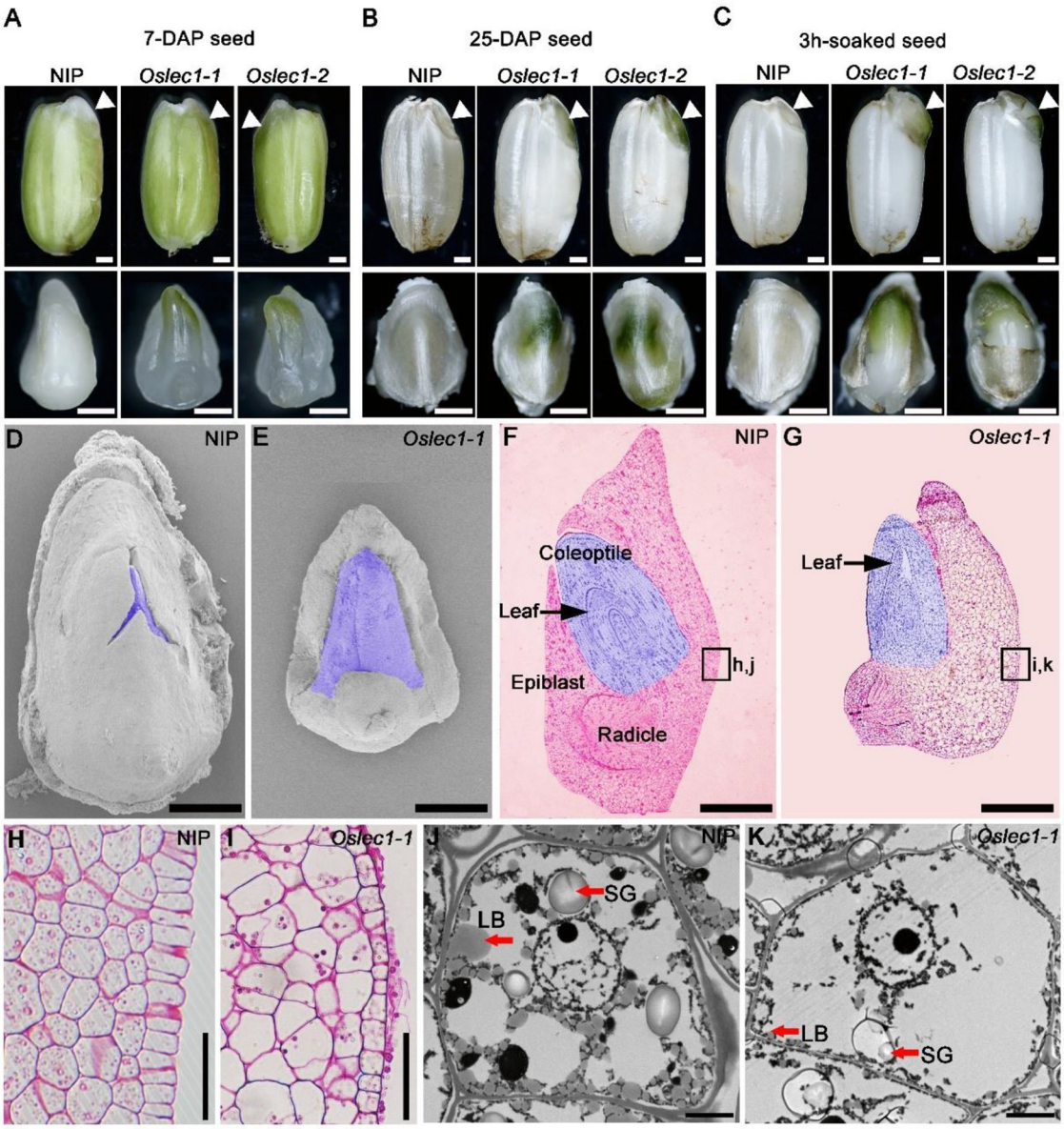

FIGURE 2 | Phenotypes of the developing seeds of *Oslec1* mutants. **(A)** Seeds and embryos (7-DAG) of wild type plants and *Oslec1* mutants. **(B)** Seeds and embryos (25-DAP) of wild type plants and *Oslec1* mutants. **(C)** Seeds and embryos of wild type plants and *Oslec1* mutants soaked in water for 3 h at 37°C. Scale bars = 500 μm. White triangles indicate the embryonic regions in complete seeds. **(D,E)** Scanning electron micrographs of embryos (7-DAP) of wild type plants and *Oslec1* mutants. The purple-colored regions indicate the germs of wild type plants and *Oslec1* mutants. Bars = 500 μm. **(F,G)** Longitudinal resin sections of embryos (7-DAP) of wild type plants and *Oslec1* mutants. The purple-colored regions indicate the germs of wild type plants and *Oslec1* mutants. Black arrows indicate the leaves in the coleoptiles. The leaves of *Oslec1* mutants are stretched out, and the epiblast wrapping the coleoptile is missing. Scale bars = 500 μm. **(H,I)** Amplification of the regions in black boxes in F and G, showing the difference in scutella parenchyma between the wild type and *Oslec1-1* mutant. Scale bars = 50 μm. **(J,K)** Electron micrographs of wild type and *Oslec1-1* embryos. Wild type **(J)** and *Oslec1-1* **(K)** scutellum sections from 7-DAP embryos. Scale bars = 2 μm.

was indicated by OsIAA1-mCherry in rice protoplasts (**Supplementary Figure 5C**).

pOsLEC1:GUS was expressed strongly in the dorsal section of immature embryos within 4-7 DAP (**Figures 3A,B**) and then declined to a relatively low level at 25 DAP (**Figures 3C–F**). Further, semi-thin sections of resin-embedded embryos showed that *OsLEC1* was predominantly expressed in the cells of scutella parenchyma, especially in the apical and basal part of the embryo at 8 DAP (**Figures 3G–I**). GUS activity could be detected at the scutellum of germinating mature seeds and in callus-induced from scutellum, but not in leaves and roots of seedlings within 14 DAG (**Supplementary Figure 6**). Expression patterns of *OsLEC1* indicated its possible function in the early stage of rice embryo development.

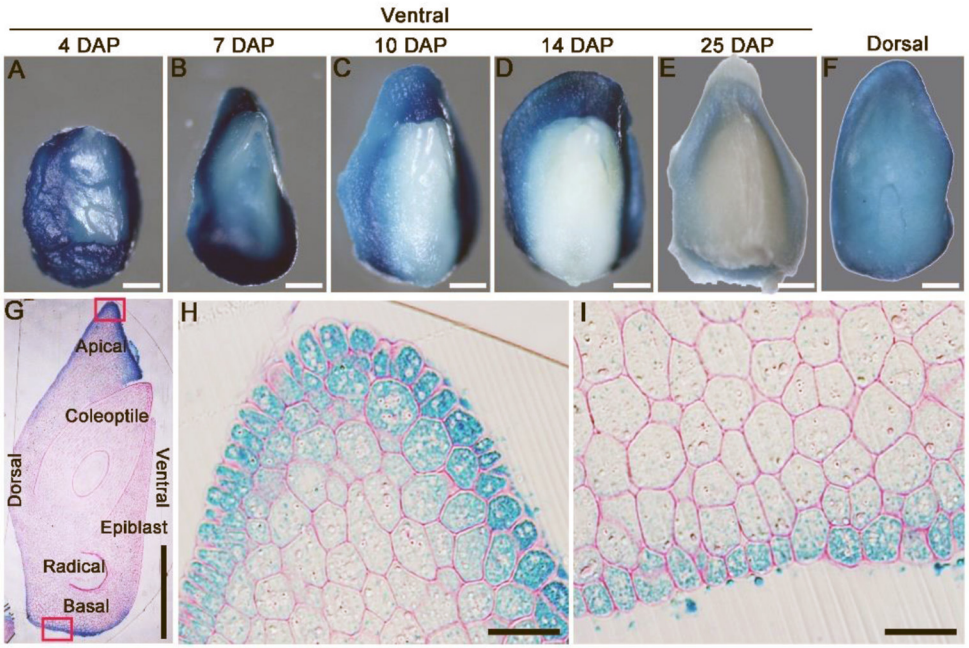

FIGURE 3 | Expression pattern of *OsLEC1*. **(A–E)** Ventral side of *pOsLEC1:GUS* embryos (4–25 DAP) stained in X-Gluc solution for 3 h at 37°C. Scale bars = 200 μm. **(F)** Dorsal side of *pOsLEC1:GUS* embryos (14 DAP) stained in X-Gluc solution for 3 h at 37°C. Scale bars = 200 μm. **(G)** Longitudinal resin section of embryos (7 DAP) of *pOsLEC1:GUS* embryo stained in X-Gluc solution overnight at 37°C. Scale bars = 200 μm. **(H,I)** Amplification of the regions in black boxes in G, showing the apical **(H)** and basal **(I)** parts of the scutella parenchyma, respectively. Scale bars = 50 μm.

Oslec1 Mutation Influences Multiple Developmental Processes in Rice Seeds

To identify the genes that were regulated by *OsLEC1*, we performed RNA-seq in *Oslec1-1* mutant and wild type embryos at two different stages of seed development: the early-stage (EE) embryos at 7 DAP and late-stage (LE) embryos at 25 DAP, representing the morphogenesis and maturation phases, respectively (**Figure 4**).

Spearman correlation of 12 samples in the two stages showed good repeatability with a coefficient (R^2) of above 0.99, and good heterogeneity with an R^2 below 0.75 (**Supplementary Figure 7**). The number of genes detected in wild type and *Oslec1* mutant embryos at the two stages are shown in **Figure 4A**. Compared with the wild type, there were 3,092 and 2,459 upregulated genes [$p < 0.05$, $\log_2$ (Fold change)$\geq$2] in *Oslec1-20* mutants at the two stages (EE and LE embryos), while there were only 1,062 and 402 downregulated genes [$p < 0.05$, $\log_2$ (Fold change) ≤ -2], respectively (**Figure 4B** and **Supplementary Tables 1–4**). The percentage of *Oslec1*-upregulated genes among the total number of differentially expressed genes (DEGs) (74.4 and 85.9%) was more than that of downregulated genes (25.6 and 14.1%), suggesting that *OsLEC1* mutation activated more genes than it suppressed. Thus, OsLEC1 might function mainly as a repressor in rice seed development.

Kyoto Encyclopedia of Genes and Genomes (KEGG) analysis showed that top pathways ($p < 0.05$) of differentially expressed genes detected in wild type and *Oslec1-1* embryos were similar at EE and LE stages (**Figure 4C**), including metabolic pathways, photosynthesis-antenna proteins, phenylpropanoid biosynthesis, biosynthesis of secondary metabolites, photosynthesis, and carbon fixation in photosynthetic organisms. KEGG terms related to amino sugar and nucleotide sugar metabolism, starch and sucrose metabolism, and plant hormone signal transduction were selectively enriched at the EE stage, while diterpenoid biosynthesis was preferentially enriched at the LE stage, as shown in **Figure 4C** and **Supplementary Table 5**. The results suggested that *Oslec1* mutation affects many biological pathways involved in photosynthesis, biomacromolecule biosynthesis and metabolism, and hormone signal transduction in seed development.

To further explore the transcriptional regulation of *OsLEC1* in the seed development, we identified all the GO terms significantly enriched (p value <0.01) in the biological progress of the two stages (**Figure 4D**, **Supplementary Tables 6–9**). The network showed that *Oslec1*-upregulated genes were mainly enriched in GO terms involved in photosynthesis, cellular oxidant detoxification, response to stimulus, metabolic process and regulation activity, while *Oslec1*-downregulated genes were mainly enriched in GO terms involved in response to stimulus biological process at EE and LE stages (**Figure 4D**, **Supplementary Figure 8**). The GO terms for *Oslec1*-upregulated mRNAs related to photosynthesis include photosynthesis, light

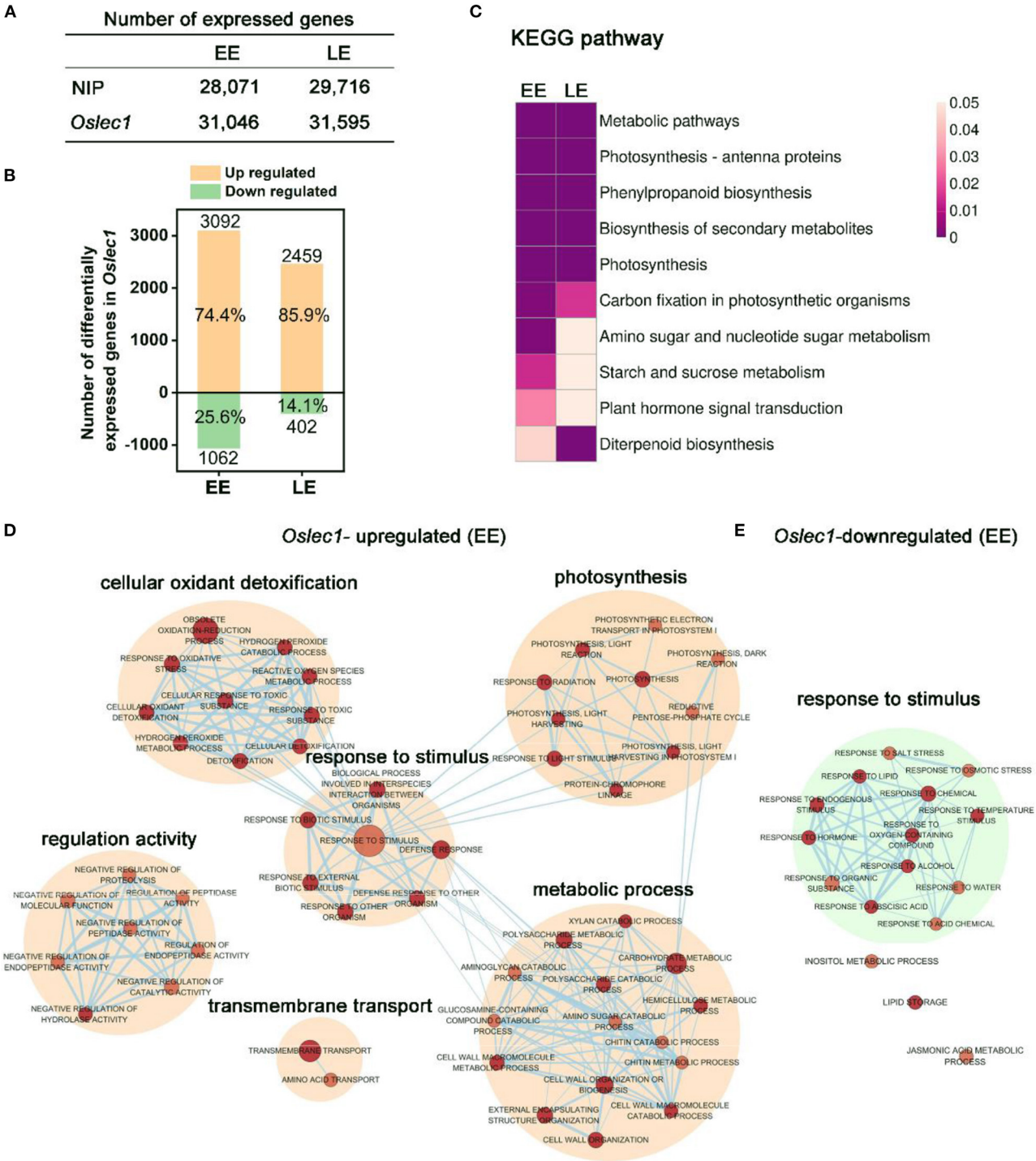

FIGURE 4 | mRNA profiling of *Oslec1* mutant embryos at early (EE) and late (LE) development stages. **(A)** The number of differentially expressed genes detected in wild type and *Oslec1-1* embryos at EE (7 DAP) and LE (25 DAP) stages. **(B)** The number of upregulated and downregulated genes in *Oslec1-1* embryos compared with that in wild type plants. **(C)** KEGG pathway analysis of differentially expressed genes detected in wild type and *Oslec1-1* embryos at EE and LE stages. **(D,E)** GO term analysis of upregulated **(D)** and downregulated **(E)** genes in *Oslec1-1* embryos compared with those in the wild type ones.

harvesting, and light reactions, consistent with the embryo greening phenotype of *Oslec1* mutants (**Figures 2**, **4D**). The GO terms for *Oslec1*-downregulated mRNAs involved in response to stimulus include response to water, ABA, hormones, and temperature stimulus (**Figure 4E**), consistent with the desiccation intolerant and rapid germination phenotypes related

to seed dormancy (**Figures 1**, **2**). Together, RNA-seq analysis suggested that *Oslec1* mutation affects two aspects in rice seed development: promoting photosynthesis-related pathways and interrupting seed maturation process.

Oslec1 Mutation Upregulates a Series of Genes Involved in Photosynthesis and Photomorphogenesis

We designated genes regulated by *OsLEC1* as those whose expression was at least four-fold higher or lower [log2(Foldchange)≥2 or < −2] in *Oslec1* mutants than that in wild type seeds at the same stage at a statistically significant level ($p < 0.05$). Compared with wild type embryos, most genes involved in photosystem I (*OsPSA*s), photosystem II (*OsPSB*s), and light-harvesting complex (*OsLHCAs* and *OsLHCBs*) (Ben-Shem et al., 2003; Gao et al., 2018) were synergistically upregulated in *Oslec1-1* embryos (**Figure 5A**). In addition, several DEGs involved in chloroplast development, as well as chlorophyll biosynthesis and degradation (Bollivar, 2006; Hu et al., 2021) were also upregulated, such as *OsSGRL*, *OsPORA*, *OsPORB,* and *OsNYC4* (**Figure 5A**). Chloroplast biosynthesis genes are in the majority, and the *OsPORA* with the largest increase is chloroplast biosynthesis related. The results suggested that *OsLEC1* repressed the transcription of many genes related to photosynthesis during rice embryo development.

In addition, DEGs involved in photomorphogenesis, and light response were analyzed (**Figure 5B**). The results showed that *OsCRY2*, *OsHY5*, *OsBBX (4*, *7*, *10*, *11*, *12*, *27*, *30)*, *OsEXPA (1*, *2*, *4*, *6, 7, 8, 12*, *13*, *15*, *21*, *24*, *25*, *29*, *32),* and *OsEXPB (2*, *3*, *4*, *5*, *6*, *9*,*11)* were significantly upregulated at least in one stage in the *Oslec1* embryos (**Figure 5B**, **Supplementary Table 10**). Ten members of the sulfurtransferase (Str) family (Bartels et al., 2007), were upregulated in the *Oslec1* mutant at least in one stage, including *OsStr (1*, *3*, 4, *5*, 7-*12)*. In addition, *OsGLK1* (*GOLDEN2-LIKE1*) (Waters et al., 2009), was upregulated significantly at the EE and LE stages.

The above results demonstrated that *Oslec1* mutation upregulated a series of genes involved in photosynthesis and photomorphogenesis in the developing embryos.

Oslec1 Mutation Regulates Genes Involved in Diverse Hormonal Pathways and Stress Response

We identified the transcription of genes involved in hormone biosynthesis, signaling, and accumulation of six main hormones: abscisic acid (ABA), gibberellin (GA), brassinosteroid (BR), zeatin, ethylene, and auxin (De Paepe and Van der Straeten, 2005; Yamaguchi, 2008; Dong et al., 2015; Keshishian and Rashotte, 2015; Kim and Russinova, 2020; Tan et al., 2021) (**Figure 5C**, **Supplementary Figure 10**). *OsPP2C (1, 08, 22, 30, 37, 59, 63), OsNCED1*, *OsSDR4,* and *OsABA45* (involved in ABA biosynthesis), as well as *OsABI3*, *OsABI4*, and *OsABI5* (involved in ABA signaling) were significantly downregulated in the *Oslec1-1* mutant. Conversely, *OsKO (1*, *4*, *5)*, *OsGA2OX (2*, *3*, *4*, *5*, *6*, *7*, *9)*, *OsGA3OX2*, *OsGA20OX (1*, *4*, *7),* and *OsGID1* (involved in GA biosynthesis) were significantly upregulated in the mutant (**Figure 5C**). In other hormonal pathways, several genes were differentially regulated. *OsCYP735A3* in zeatin biosynthesis and *OsHK2* in zeatin signaling, *OsBU1*, *OsSEPK1,* and *OsLAC15* in BR response, *OsACO (1, 2, 5)* in ethylene biosynthesis and *OsETR4* in ethylene signaling, *OsYUCCA (2*, *6)* in auxin biosynthesis, *OsGH3-13* in auxin accumulation, *OsIAA (2*, *12*, *16)* and many *OsSAURs* in the auxin signaling pathway were significantly upregulated (**Supplementary Figure 9**). Overall, the majority of the genes related to GA, zeatin, BR, ethylene, and auxin pathways were activated in the *Oslec1-1* embryos. In contrast, *Oslec1* mutation suppressed ABA biosynthesis and signaling in the developing seeds.

Stress response-related genes including *OsLEA*s, *OsHSP*s, and *OsHSF*s were also significantly dysregulated in the *Oslec1-1* mutant (**Figure 5D**, **Supplementary Table 11**). Results showed that 21 *OsLEA*s were significantly downregulated, while only three were upregulated, such as *OsLEA9, OsLEA11,* and *OsLEA24*. Similarly, most *OsHSP* and *OsHSF* genes were downregulated in the *Oslec1-1* mutant. It is noteworthy that the expression levels of *OsLEA* genes were more significantly downregulated at the EE stage than the LE stage (**Figure 5D**), suggesting that *Oslec1* mutation affected expression of *OsLEA*s predominantly in the early stage of seed development.

Expression levels of nine representative genes were detected in EE and LE stage embryos using qRT-PCR. The results showed that *OsPSAN*, *OsPSAW*, *OsLHCA3*, *OsPORB*, *OsGA2ox3,* and *OsGA2ox9* were significantly upregulated in the *Oslec1* mutant, while *OsABI3*, *OsLEA1* and *OsLEA17* were significantly downregulated in early and late stages of seed development, consistent with the RNA-seq results (**Supplementary Figure 10**).

Overall, the transcriptome analysis of the *Oslec1* mutant suggested that OsLEC1 regulated diverse sets of genes involved in photosynthesis, photomorphogenesis, stress response, and diverse hormones pathways in seed development.

Genome-Wide Identification of OsLEC1-Binding Sites

To determine which processes are directly regulated by OsLEC1, we performed chromatin immunoprecipitation followed by high-throughput sequencing (ChIP-seq) using the embryonic callus of *35S:3xFLAG-OsLEC1 2#* and wild type plants. We could not harvest enough young embryos from the *35S:3XFLAG-OsLEC1* transgenic plants to perform ChIP-seq experiment. According to the expression data of *OsLEC1* by GUS staining, embryonic callus seems to be the best alternative tissue besides of the embryo. Expression level of tagged protein and callus formation phenotype of *35S:3xFLAG-OsLEC1* lines are shown in **Supplementary Figure 11**. The peaks of *35S:3xFLAG-OsLEC1* were distributed mainly at the 5'-UTR sites, in a region within 2 kb upstream of the genes, while the peaks of the wild type did not show a significantly enriched sites and the normalized signal was significantly weaker than that of the *35S:3xFLAG-OsLEC1* (**Supplementary Figure 12**). In the *35S:3xFLAG-OsLEC1* group, 60.25% of the 27452 peaks were localized in the promoter region, including 51.96% within 1 kb of and 8.29% between 1 and 2 kb of the

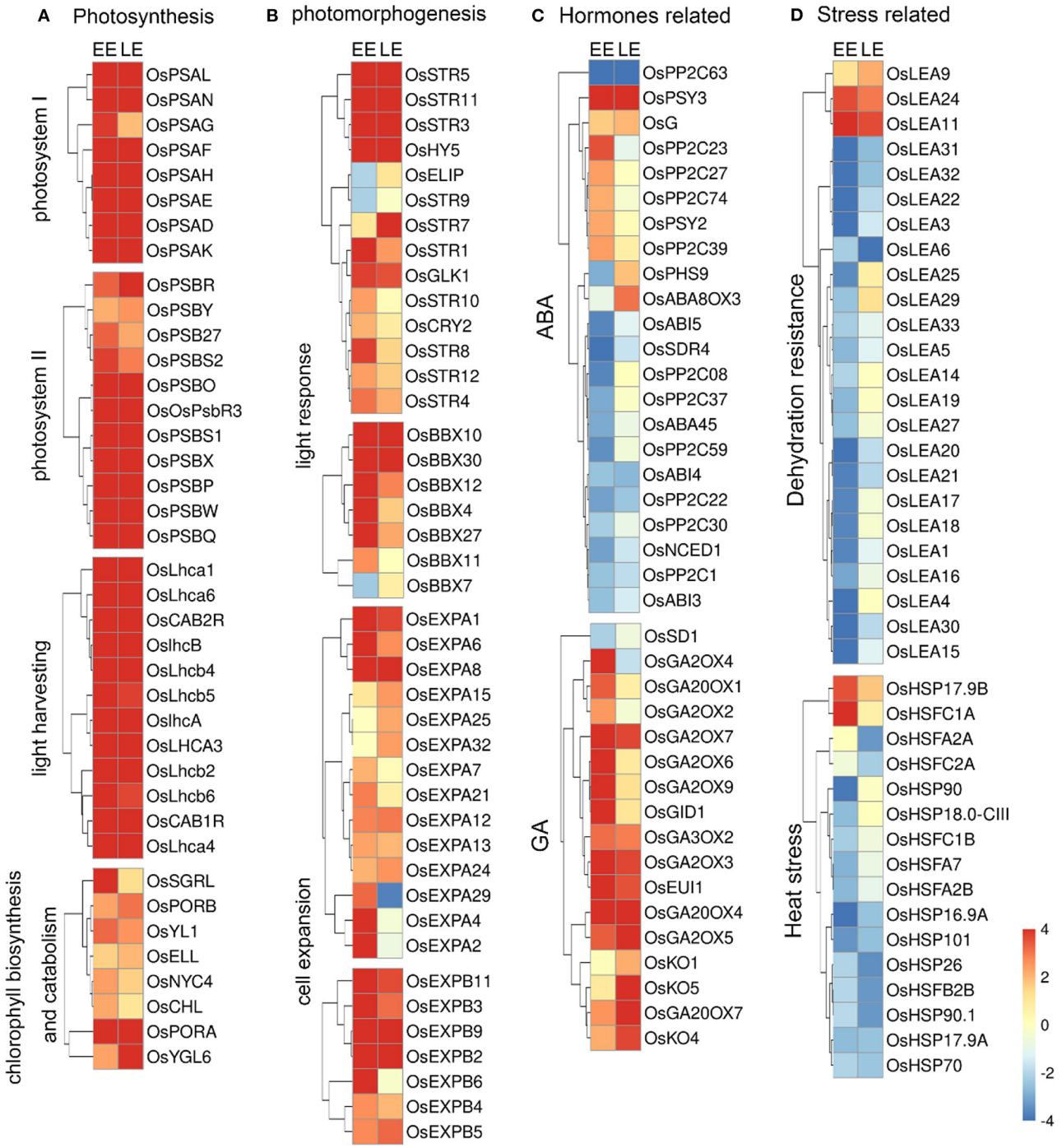

FIGURE 5 | Heat maps of differentially expressed genes in *Oslec1* embryos. **(A)** Heat maps of genes involved in photosynthesis, **(B)** photomorphogenesis, **(C)** hormone pathways, and **(D)** stress responses, including dehydration resistance and heat stress response.

promoter (**Figure 6A**). The top enriched KEGG pathways ($p < 0.05$) for these peak targets include amino sugar and nucleotide sugar metabolism (ko00520), butanoate metabolism (ko00650), N-glycan biosynthesis (ko00510), carotenoid biosynthesis (ko00906), and ribosome (ko03010) (**Figure 6B**, **Supplementary Table 12**).

DNA sequence motifs that were enriched in LEC1-binding genomic regions of 1 kb upstream of target genes were

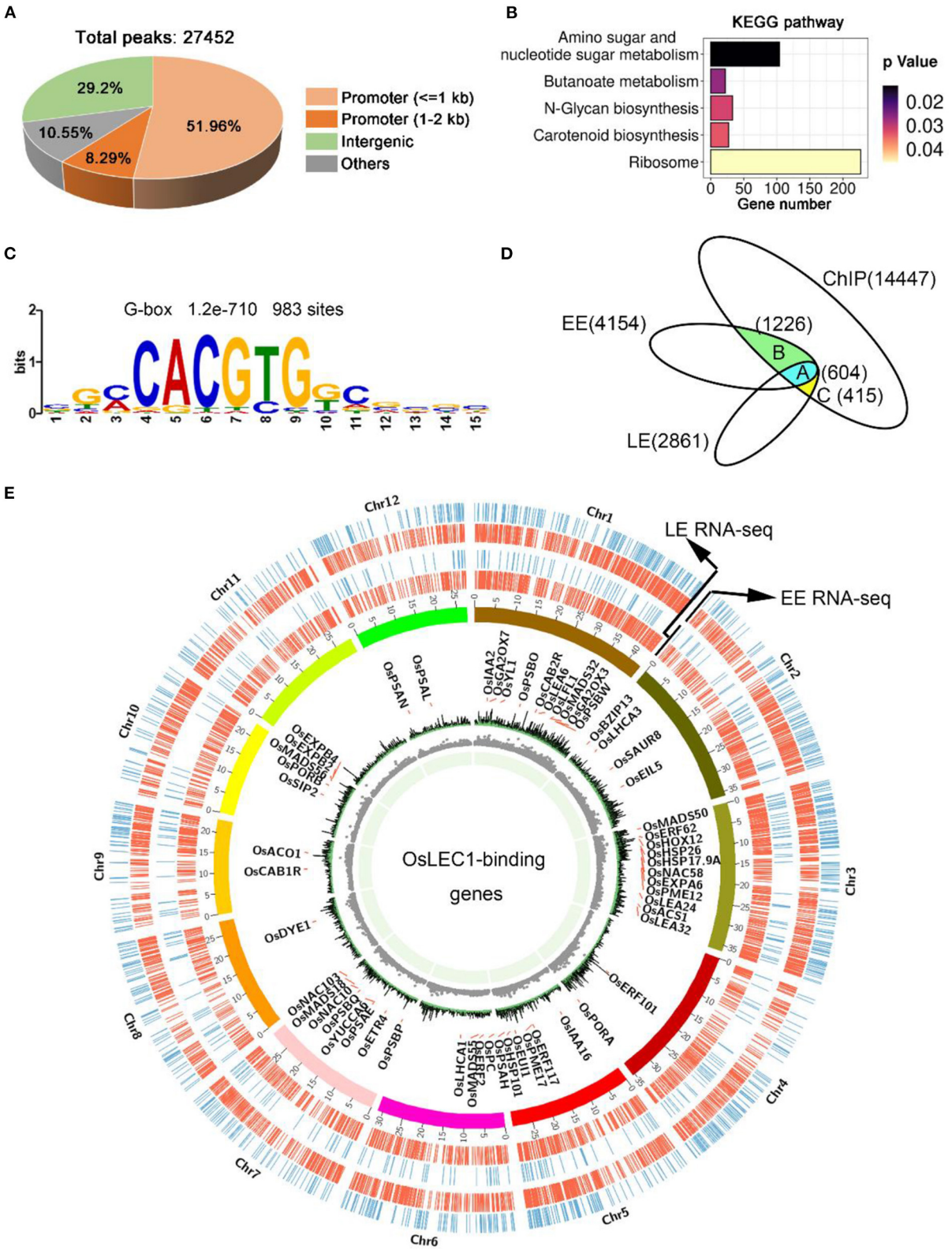

FIGURE 6 | OsLEC1-binding genes detected using ChIP-seq. **(A)** The distribution of peaks on the rice genome according to ChIP-seq results. **(B)** KEGG pathway analysis of OsLEC1-binding genes. **(C)** DNA sequence motif G-box that enriched in LEC1-bound genomic regions 1 kb upstream of target genes, which were identified via de novo motif-discovery analyses. **(D)** Venn diagrams show the overlap between genes bound by OsLEC1 and differentially expressed genes in *Oslec1-1*

(Continued)

FIGURE 6 | embryos. Group A indicates 604 genes detected using ChIP-seq and RNA-seq at EE and LE stages; group B indicates 1,226 genes detected using ChIP-seq and RNA-seq at the EE stage; group C indicates 415 genes detected using ChIP-seq and RNA-seq at the LE stage. **(E)** Genome browser view of the chromosomal region showing enrichment of genomic regions bound by OsLEC1 and genes regulated by OsLEC1. The name of the OsLEC1-binding genes are written within the cycle of chromosomes, and genes up-regulated or down-regulated by OsLEC1 are represented by red or blue lines respectively, outside the cycle of chromosomes.

identified via *de novo* motif-discovery analyses (**Figure 6C**). These motifs most closely corresponded with several cis-regulatory elements including the G-box (CACGTG) or ABRE-like (C/G/T) ACGTG(G/T) (A/C), which were significantly overrepresented in OsLEC1 target genes with 983 binding sites. We did not detect a CCAAT DNA motif. To determine the genes directly regulated by OsLEC1 in rice seed development, we analyzed the overlapping OsLEC1-binding genes via ChIP-seq, using the DEGs detected in *Oslec1* embryos at EE and LE stages. There were 14,447 unique target genes binding with OsLEC1, as well as 4,154 and 2,861 DEGs at EE and LE stage embryos of *Oslec1* mutants, respectively. Venn diagram showed that OsLEC1 bound to 604 DEGs at EE and LE stages (**Figure 6D**), which were mainly involved in photosynthesis, chlorophyll biosynthesis, flowering, dehydration resistance, cell wall, heat stress, and hormonal pathways (GA, auxin, ethylene) (**Supplementary Tables 13**, **14**). There were more target genes bound by OsLEC1 specifically at the EE stage (1226) than those at the LE stage (415) (**Figure 6D**), suggesting that OsLEC1 might control more gene expression pathways in the early stage of seed development. At the EE stage, OsLEC1-binding genes were involved in the ABA pathway, dehydration resistance, lipid metabolic processes, heat stress, cell wall, and other hormonal pathways (auxin, cytokinin, ethylene). At the LE stage, OsLEC1-binding genes were involved in response to stress, seed development, Jasmonate acid (JA), auxin-related and other transcriptional factors (**Supplementary Tables 13**, **14**).

A CIRCOS plot was constructed to identify and analyse similarities and differences between the OsLEC1 target genes according to ChIP-seq results with DEGs at EE and LE stages at the genome scale (**Figure 6E**). The gene density and number were larger at the EE stage compared with those at the LE stage. According to the annotation and the chromosomal distribution, target genes of OsLEC1 were mapped for all 12 rice chromosomes with similar densities (**Figure 6E**).

OsLEC1 Bound to DEGs in Photosynthesis and Seed Maturation Processes

According to the results above, we illustrated an OsLEC1-binding/regulating gene network using a combination of RNA-seq and ChIP-seq data. DEGs involved in photosystem I (*OsPSA*s), photosystem II (*OsPSB*s), light-harvesting complex (*OsLHCA*s), electron carrier (*OsPC*), and two genes encoding key enzymes in chlorophyll biosynthesis (*OsPORA* and *OsPORB*), were identified as OsLEC1-binding genes. These genes were upregulated (at least four folds compared with wild type) in *Oslec1* mutant embryos (**Figure 7A**), possibly contributing to embryo greening (**Figure 7C**).

In the ABA pathway, we identified *OsNCED1*, *OsSDR4*, *OsPP2C1*, and *OsABI3* as OsLEC1-binding genes, which were significantly downregulated in *Oslec1* embryos (**Figure 7B**). In the downstream of *OsABI3*, 13 *OsLEA*s and 12 *OsHSF*s/*OsHSP90.1* were identified as OsLEC1-binding genes and were significantly downregulated in *Oslec1* embryos (**Figure 7B**). We also found that *OsGA20ox1* and *OsGA2ox (3, 6, 7, 9),* which are involved in GA biosynthesis and deactivation, were identified as OsLEC1-binding genes and significantly upregulated in the EE- and LE-stage *Oslec1* embryos (**Figure 7B**). Cell expansion/cell wall-related genes *OsEXPAs*, *OsEXPBs,* and *OsPMEs,* downstream of the GA signaling pathway, were also identified as OsLEC1-binding and upregulated genes (**Figure 7B**). These results suggested that *Oslec1* mutation inhibited the seed maturation processes via inhibiting ABA signaling pathway and promoting GA signaling pathway (**Figure 7C**).

Integrative genomics viewer (IGV) was used for the straightforward visualization of OsLEC1-binding sites on nine target genes (**Figures 7A,B**). OsLEC1-binding sites of *OsPSAN*, *OsPSBW*, *OsLHCA3*, *OsPORB*, *OsLEA1,* and *OsLEA17* were found on the promoter regions, and those of *OsGA2ox3* and *OsABI3* were on the promoters and coding regions, while the binding site of *OsGA2ox9* was mainly on the coding region (**Figures 7D,F**, **Supplementary Figure 13**). Among them, *OsLHCA3*, *OsABI3*, and *OsLEA17* were verified by CHIP-qPCR in both embryos and callus of *35S:3xFLAG-OsLEC1*. The CHIP-qPCR results were consistent with IGV screenshot from the ChIP-seq (**Figures 7D–F**).

DISCUSSION

LEC1 is an essential regulator of seed maturation (Meinke et al., 1994; West et al., 1994; Lotan et al., 1998; To et al., 2006; Braybrook and Harada, 2008; Pelletier et al., 2017; Lepiniec et al., 2018; Jo et al., 2019). The studies on LEC1 function are summarized in **Supplementary Figure 14**. In the present study, we described the resulting seed development phenotypes of the rice *Oslec1* mutant and illustrated an OsLEC1-binding/regulating gene network using a combination of RNA-seq and ChIP-seq data. We found that *Oslec1* mutation did not cause embryo lethality but caused disrupted desiccation tolerance, which caused death due to drying after seed harvesting (**Figure 1**). Chlorophyll accumulation in *Oslec1* embryos was triggered at a very early stage of seed development (**Figure 2**). OsLEC1 could directly bind and regulate many genes involved in ABA/GA biosynthesis and signaling pathway, contributing to dormancy (**Figure 7**). It is widely recognized that phytohormones ABA and GA are the primary hormones regulating seed dormancy and

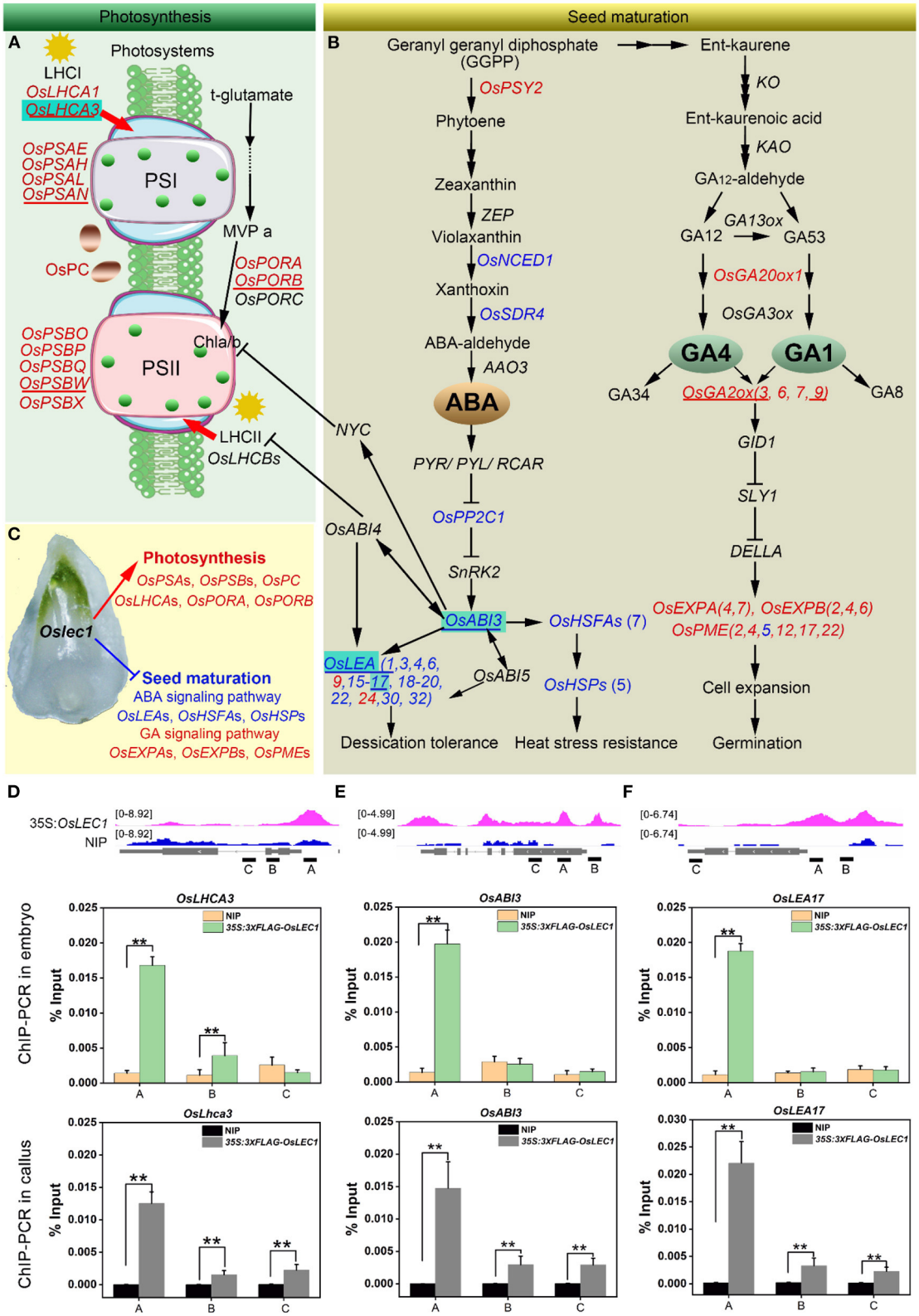

FIGURE 7 | A proposed model of the mutated *Oslec1* action. **(A)** Photosynthesis-related genes were up-regulated in the *Oslec1* mutant, including genes encoding key enzymes PSI, PSII, LHCI, LHCII and OsPC, etc. **(B)** *Oslec1* mutation regulated genes involved in seed maturation, including genes in ABA/GA biosynthesis and signaling pathways. **(C)** *Oslec1* mutation results in the activation of photosynthesis and the inhibition of seed maturation. Genes underlined indicate that they are verified by qRT-PCR. Genes in red indicate that they are upregulated in *Oslec1* embryos, and directly bound by OsLEC1; genes in blue indicate that they are

(Continued)

FIGURE 7 | downregulated in *Oslec1* embryos and directly bound by OsLEC1. **(D–F)** IGV screenshot of peak sites on genome sequences of OsLEC1-binding genes and ChIP-qPCR analysis of the binding genes in embryos and callus of *35S:3×FLAG-OsLEC1 2#* and the wild type. These three genes are all marked with cyan background in the model above. The asterisks show significant differences (*t*-test; $^{**}P < 0.01$) between 35S:3 × FLAG-OsLEC1 and the wild type.

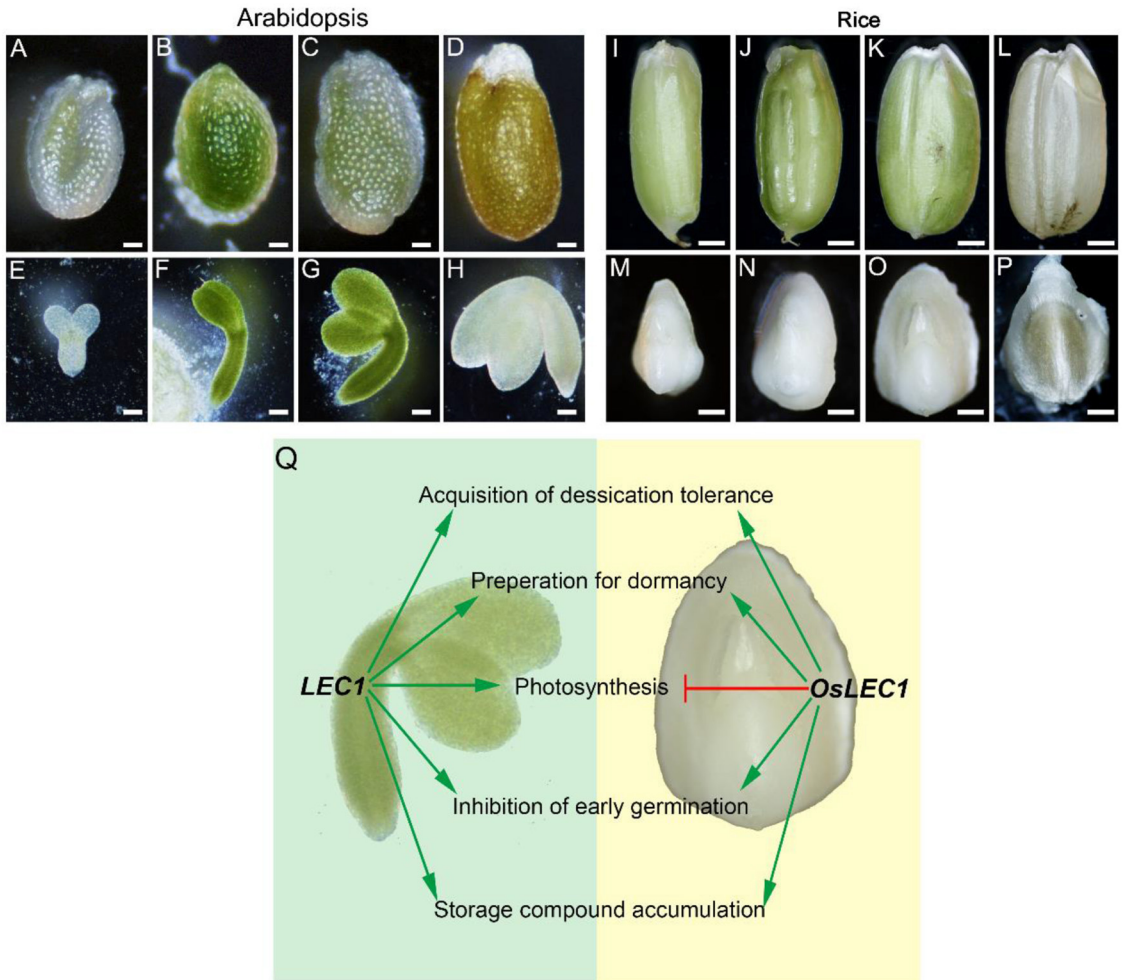

FIGURE 8 | Comparisons of LEC1 functions during seed development in rice and Arabidopsis. **(A–D)** Complete Arabidopsis seeds in different developmental stages. Scale bars = 200 μm. **(E–H)** Arabidopsis embryos in different developmental stages. Scale bars = 50 μm. **(I–L)** Complete rice seeds in different developmental stages. Scale bars = 500 μm. **(M–P)** Rice embryos in different developmental stages. Scale bars = 50 μm. **(Q)** Comparison of LEC1 functions during seed development in rice and Arabidopsis. Arrowed green lines represent promotional effects, and a flat red line show inhibitory effects.

germination, respectively (Finkelstein et al., 2002, 2008; Graeber et al., 2012; Lee et al., 2015). Levels of major storage molecules were dramatically reduced in *Oslec1* mutant embryos (**Figure 2**). Notably, the shoot apices of *Oslec1* embryos were activated and possessed leaf primordia, whereas wild type embryonic shoot apices were inactive and did not initiate leaf development (**Figure 2**). Similar phenotypes were reported in Arabidopsis (Meinke, 1992; Meinke et al., 1994; West et al., 1994). A recent study showed that OsNF-YB7 (OsLEC1) complements the developmental defects of *lec1-1* in Arabidopsis when driven by the *LEC1* native promoter (Niu et al., 2021). Therefore, OsLEC1 has a conservative function in seed maturation among dicots and monocots, which is required for the acquisition of desiccation tolerance and seed dormancy, storage compound accumulation, and inhibition of early germination (**Figure 8Q**).

ABA and GA are major players in seed dormancy and germination regulation (Cutler et al., 2010; Shu et al., 2016). Some clues indicate the interaction of LEC1 and ABA/GA pathways. LEC1-induced embryonic differentiation in vegetative seedlings is strictly dependent on an elevated level of ABA (Junker et al., 2012). LEC1/L1L-(NF-YC2) activation depends on ABA-response elements (ABRE) present in the promoter of Cruciferin C (CRC), which encodes a seed storage protein (Yamamoto et al., 2009), and the ABRE-like motif (C/G/T)ACGTG(G/T)(A/C)

was significantly overrepresented in LEC1 target genes (Pelletier et al., 2017). In addition, LEC1 interacts with DELLA proteins, which are GA signaling repressors. GA triggers the degradation of DELLAs to reverse LEC1 repression, thus promoting auxin accumulation to facilitate embryonic development (Hu et al., 2018). Furthermore, LEC1 interacts with different combinations of AREB3, bZIP67, and ABI3 to control diverse biological pathways during soybean seed development (Jo et al., 2020). LUC assay results showed that *NCED1*, *AREB3*, *GA3ox1,* and *GA20ox2* are bound and directly regulated by LEC1 (Jo et al., 2020). We showed that OsLEC1 bound to and positively regulated *OsNCED1*, *OsSDR4*, *OsPP2C*s, and *OsABI3* in ABA biosynthesis and signaling but negatively regulated *GA2ox3* and *GA2ox9* in the GA pathway (**Figure 7B**), consistent with previous studies. Taken together, OsLEC1 plays a conservative role in controlling seed maturation through the regulation of ABA and GA pathways.

Owing to the non-photosynthetic nature of the rice seed, the rice embryo remains white during seed development and maturation (**Figures 8I–P**), in contrast to the Arabidopsis seed which undergoes embryo greening (**Figures 8A–H**). Notably, *Oslec1* embryos turned green at 7 DAP (**Figure 2**), showing that photosynthesis had been activated in the very early stages of seed development. Compared with wild type plants, a series of photosynthesis-related genes were significantly upregulated in *Oslec1* embryos (**Figures 5A,B**), and some of them were also OsLEC1-binding targets (**Figure 6E**), indicating a suppressive effect of OsLEC1 on photosynthesis (**Figure 8Q**). The results revealed that OsLEC1 is a key inhibitor of photosynthesis-related genes in rice embryo development.

In Arabidopsis, LEC1 interacts with PHYTOCHROME INTERACTING FACTORs (PIF4) to coactivate genes involved in dark-induced hypocotyl elongation (Huang et al., 2015) and regulate *LHCB* genes through interaction with pirin, a protein that enhances TF binding in mammals (Warpeha et al., 2007). However, the role of LEC1 on photosynthesis was largely unknown. It was reported that maturing embryos of the *lec1* mutant display a paler green than wild type embryos, and most DEGs involved in photosynthesis and chloroplast biogenesis are downregulated in Arabidopsis *lec1* mutant (Pelletier et al., 2017). LUC assay showed that *PSBW* and *PSBP-1*, involved in photosynthesis system II, are activated by LEC1 in soybean embryo cotyledon cells, and LEC1 may interact with different TFs to activate distinct gene sets (Jo et al., 2020). Thus, LEC1 could promote but is not essential for photosynthesis and chloroplast biogenesis in Arabidopsis and soybean seed development (Pelletier et al., 2017; Jo et al., 2020). In contrast, our results show that OsLEC1 blocks photosynthesis in rice seed maturation. An explanation of the differences in the effect of LEC1 on photosynthesis in seed maturation between rice and Arabidopsis possibly lies in the different seed developing processes. Photosynthesis is activated sequentially during Arabidopsis embryo development (Allorent et al., 2013; Hu et al., 2018). Rice seed is non-photosynthetic, and has an endosperm for nutrient supply in the early stage of plant growth, and photosynthesis is completely absent in the embryo during seed development. Thus, the activation of photosynthesis in *Oslec1* mutants was easily observed in rice seed maturation in the present study. *OsLEC1*, a monocot homolog of *LEC1*, blocks photosynthesis in rice embryos. Evidence showed that *OsNF-YB7* (*OsLEC1*) expression could complement the developmental defects of Arabidopsis *lec1-1*, such as the morphology of cotyledons and the desiccation tolerance, but the cotyledons were green, suggesting that *OsLEC1* did not block photosynthesis in Arabidopsis embryos (Niu et al., 2021). This implies that, other genes, which controlling photosynthesis together with *LEC1,* also control Arabidopsis embryo maturation and greening. It is noteworthy that the mutations of OsLEC1 are present downstream of the DNA-binding domain, which could still be expected to generate a truncated protein (about 157 aa) including the DNA-binding domain (**Supplementary Figure 1**). Thus, we could not exclude the possibility that the mutations of OsLEC1 may have some residual or even additional functions. Further experiments are necessary to confirm the function of OsLEC1, for example, to construct a transgenic line with the *OsLEC1* driven by its endogenous promoter in the *Oslec1* mutant, or reconstruct the knockout lines of *OsLEC1* (by designing the gRNA in the upstream of the DNA binding domain). In addition, differences in the conserved region of the LEC1 protein sequence also suggested possible functional differences between LEC1 in dicots and monocots (**Supplementary Figure 1**). Therefore, we speculate that the role of OsLEC1 in rice is not identical to that of LEC1 Arabidopsis in photosynthesis (**Figure 8Q**).

In our ChIP-seq results, the G-box motif (CACGTG), was significantly overrepresented in all OsLEC1-target gene sets identified (**Figure 6C**), similar with the results in Arabidopsis (Pelletier et al., 2017). However, CCAAT motif, a known binding site of the LEC1 NF-Y complex, was not found in ChIP-seq binding results from callus. It was reported that the CCAAT-binding sequence motif bound by LEC1 was significantly overrepresented only in the Arabidopsis BCOT-stage seeds, but not in early and late-stage seeds (Pelletier et al., 2017). Binding sequences of LEC1 vary in different tissues and developmental stages. Thus, we verified that *OsLHCA3*, *OsABI3*, and *OsLEA17* bound by OsLEC1 in embryos, consistent with data from callus (**Figures 7D–F**). Therefore, the sequence motifs bound by LEC1 in embryos were, at least in part, similar to those in the callus. It is necessary to further study the role of OsLEC1-binding targets in rice embryos during the seed development.

In conclusion, our findings suggest that OsLEC1 is an inhibitor of embryo greening during seed development and a central regulator of seed maturation. Revealing the underlying mechanism of how OsLEC1 regulates seed maturation would help to generate strategies to enhance grain dormancy levels and prevent PHS (pre-harvest sprouting) of crop species. Breakthroughs regarding OsLEC1 regulatory mechanisms on photosynthesis would expand our understanding of the molecular network underlying photosynthesis, thus contributing to improving photosynthesis in agriculture.

METHODS

Plant Materials and Growth Conditions

Wild type "Nipponbare" rice (*Oryza sativa* L. ssp. *japonica*) and Columbia-0 (Col-0), as the wild type Arabidopsis, were used.

Oslec1, *pOsLEC1:GUS*, *35S:OsLEC1* mutants were all generated in the "Nipponbare" background. Plants were grown in a greenhouse under a 16 h light, 30°C/8 h dark, 24°C cycle.

For callus induction, sterile seeds were placed in callus induction medium (N6 basal medium supplemented with 10 μM 2,4-D, pH 5.8) and incubated in the growth chamber under a 16 h light, 28°C/8 h dark, 24°C cycle (Guo et al., 2018).

For the germination assay, rice seeds (dry or wet) were unshelled and soaked in distilled water at 30°C in the dark until they germinated. Protruded seeds were considered germinated seeds. Then, uniformly germinated seeds were placed in Petri dishes (12 cm) covered by filter paper soaked with distilled water and grown at 28°C and 90% relative humidity under 16 h light/8 h dark conditions.

Plasmid Construction and Rice Transformation

Oslec1 transgenic plants were generated using CRISPR-Cas9 technology, according to a previously described method (Xie et al., 2015). We designed two single gRNAs that specifically targeted the protein-coding regions of *OsLEC1*. The two gRNAs were assembled into a single vector using the polycistronic-tRNA-gRNA (PTG) strategy. Two gRNAs 5′-CTCTGGGCCATGAGCCGCCT-3′ and 5′-CAGACCGTCAACTTCGAGCA-3′ were assembled into a single vector *pRGEB32* using the polycistronic-tRNA-gRNA (PTG) strategy to construct *OsLEC1-PRGEB32*.

To generate the *pOsLEC1:GUS*, a 2841 bp genomic sequence upstream the ATG start codon of *OsLEC1* (*LOC_Os02g49370*) was cloned from the rice genome, and inserted into the *pENTR/D-TOPO* vector (Invitrogen, Carlsbad, CA, USA), and subsequently into the destination vector *pHGWFS7*, which contained a β-glucuronidase (GUS) gene fusion created via LR Clonase (Thermo Fisher Scientific, Waltham, MA, USA) reactions.

For the ChIP assay, *35S:3*FLAG-OsLEC1* was constructed first by fusing a sequence encoding the 3*FLAG peptide sequence with the *OsLEC1* cDNA, and the fusion was then inserted into pCAMBIA 1300 using infusion cloning according to the manufacturer's instructions.

The vectors *OsLEC1-PRGEB32*, *pOsLEC1:GUS,* and *35S:3*FLAG-OsLEC1* were introduced into rice callus using the *Agrobacterium tumefaciens*-mediated co-cultivation approach through the EHA105 strain. Homozygous T3 seeds were used for further experiments.

For subcellular co-localization of proteins, the coding sequence, not including the stop codon of OsLEC1, was cloned into the pUGW5 vector to generate the *35S:OsLEC1-GFP* via LR Clonase reactions according to the manufacturer's instructions. The *35S:OsIAA1-mcherry* vector has been described previously (Guo et al., 2021). The primers used are listed in **Supplementary Table 15**.

SEM, TEM, and Light Microscopy

For SEM analysis, 5-DAP and 25-DAP embryos of NIP and *Oslec1* were fixed overnight at 4°C in 2.5% glutaraldehyde in phosphate buffer (0.1 M, pH 7.0), washed three times in the phosphate buffer (0.1 M, pH 7.0) for 15 min at each step, then, postfixed with 1% OsO_4 in phosphate buffer for 2 h and washed three times in phosphate buffer. The samples were dehydrated through an ethanol gradient (30, 50, 70, 80, 90, 95, and 100% ethanol, 15 min each), then transferred to absolute ethanol, and dehydrated in Hitachi Model HCP-2 critical point dryer (Hitachi, Tokyo, Japan). The dehydrated sample was coated with gold-palladium in Hitachi Model E-1010 ion sputter for 4–5 min and observed using the Hitachi Model SU-8010 SEM (Hitachi, Tokyo, Japan).

For TEM, the samples were fixed in 2.5% glutaraldehyde and postfixed with 1% OsO4, then, dehydrated through an ethanol gradient, similar to the pre-treatment of SEM samples. After dehydration, samples were immersed in absolute acetone for 20 min, then, into 1:1 and 1:3 mixtures of absolute acetone and the final Spurr resin mixture for 1–3 h, respectively. Then, to the final Spurr resin mixture overnight.

Samples were placed in an Eppendorf containing Spurr resin and heated to 70°C for more than 9 h, then, sectioned in a LEICA EM UC7 ultratome. Sections were stained with uranyl acetate and alkaline lead citrate for 5 and 10 min, respectively, and observed using the Hitachi Model H-7650 TEM.

For light microscopy, the embedded samples were sectioned at 2–5 μm thickness using a rotary microtome (Leica, Wetzlar, Germany) and stained with basic fuchsin and observed using a Nikon C-C phase turret condenser (Nikon, Tokyo, Japan).

Histochemical Analysis of GUS Activity and TTC Staining

For GUS staining, *pOsLEC1:GUS* embryos were incubated in the X-Gluc solution overnight at 37°C, as described previously (Guo et al., 2016) and then fixed in 2.5% glutaraldehyde overnight to prepare them for imaging or semi-thin sectioning.

For TTC staining, the seeds were split longitudinally and soaked in 1% (w/v) TTC solution at 37°C for 3 h, as described previously (Zhang et al., 2020).

Subcellular Localization of OsLEC1

Rice protoplasts were prepared and transformed as previously described (Bai et al., 2014). Approximately 8 μg of the expression vector *35S:OsLEC1-GFP* was transferred into rice protoplasts, then, the protoplasts were cultured at room temperature in the dark for 16 h. Fluorescence signals were detected and photographed using an LSM710 NLO confocal laser scanning microscope (Zeiss, Mannheim, Germany). Excitation/emission wavelengths were 488 nm for GFP and 561/575–630 nm for mCherry. Fluorescence signals were analyzed using the Zen2009 (Carl Zeiss) software.

RNA Extraction and qRT-PCR Analysis

Total RNA was extracted from *Oslec1* and wild type embryos using the TRIZOL reagent (Invitrogen, Carlsbad, CA, USA) and cDNA was synthesized from 1 μg of total RNA using ReverTra Ace^{TM} qPCR RT Master Mix with gDNA Remover (TOYOBO, Osaka, Japan). qRT-PCR analysis was performed on a Mastercycler ep realplex system (Eppendorf, Hamburg, Germany) using LightCycler 480 SYBR Green Master Mix

(Roche, Indianapolis, USA). *OsUBQ5* was amplified and used as an internal standard to normalize the expression of tested genes. Experiments were performed in triplicate. The primers of the examined genes are listed in **Supplementary Table 15**.

RNA-Seq Analysis

We collected about 30 embryos of *Oslec1* and wild type (7 and 25 DAP) and extracted mRNAs to perform Illumina sequencing. Three biological replicates were conducted. Library construction and deep sequencing were carried out using the Illumina Hiseq 2500 (Biomarker Technologies, Beijing, China). The adapters and low-quality reads were removed using Trimmomatic (version 0.36) (Bolger et al., 2014). Afterwards, the clean reads were mapped to the rice reference genome (Oryza_sativa. IRGSP-1.0.45) using Hisat2 (version 2.1.0) (Kim et al., 2015). Transcripts were assembled and merged using StringTie (version 1.3.4d) (Pertea et al., 2015). DEGs were identified using DESeq2 (version 1.26.0) (Love et al., 2014), with a false discovery rate of < 0.05 and an absolute value of log2 (fold change) > 2.

The GO terms and KEGG enrichment analyses were performed using the online platform g:Profiler (https://biit.cs.ut.ee/gprofiler/gost) (Raudvere et al., 2019). The directed acyclic graphs of GO terms were constructed using the online platform AgriGO v2.0 (http://systemsbiology.cau.edu.cn/agriGOv2/) (Tian et al., 2017). The heat-map of the DEGs were drawn using the online platform Omicstudio (https://www.omicstudio.cn/login). Construction of the GO term network was performed using Cytoscape (Shannon et al., 2003). The RNA-seq data have been deposited in the Gene Expression Omnibus (GEO) database, www.ncbi.nlm.nih.gov/geo (Accession No: GSE179838).

ChIP, ChIP-QPCR, and ChIP-Seq Analysis

ChIP was performed as previously described (Xu et al., 2008). About 3 g of the wild type and *35S:3*FLAG-OsLEC1* callus were collected and treated with 1% formaldehyde for protein-DNA cross-linking. After fixation, chromatin was sonicated with Diagenode Bioraptor to generate 200–1,000 bp fragments. Chromatin was immunoprecipitated with anti-DDDDK monoclonal antibody (MBL, Beijing, China). Then, chromatin-antibody complexes were precipitated with anti-IgG paramagnetic beads (GE Healthcare, Uppsala, Sweden). After six washing steps, complexes were eluted and reverse-crosslinked. ChIP-qPCR was performed with three biological replicates, and each replicate was tested with three technical repeats. Three pairs of specific primers were designed for each target gene, based on different genomic sites. The primer sequences for ChIP-qPCR are listed in **Supplementary Table 15**. The results were normalized to the input control as previously reported (Asp, 2018).

DNA fragments from ChIP experiment were sent to Genergy Biotechnology (Shanghai, China) for ChIP-seq. ChIP-seq libraries were prepared using Ovation Ultralow Library Systems (Nugen) according to the manufacturer's instructions. Sequencing reads of the ChIP-seq were aligned using Bowtie2 (Langmead and Salzberg, 2012) against the Oryza sativa IRGSP-1.0 genome assembly, and only uniquely mapped sequencing reads were retained. MACS2 (Zhang et al., 2008) was used to call peaks compared to the input using q_value_thresholds=0.01. The aligned reads with biological replicates were processed based on the irreproducibility discovery rate (IDR) (Li et al., 2011). Peaks were then annotated using ChIPseeker (Yu et al., 2015). MEME-ChIP (Machanick and Bailey, 2011) suite was used to identify the DNA binding motif. Visualization of peaks on genomic regions was achieved with IGV 2 (Thorvaldsdóttir et al., 2013). OsLEC1-binding peak positions according to the ChIP-seq results and the DEGs at EE and LE stages between the *Oslec1* mutant and the wild type plants were visualized using CIRCOS (Wyatt et al., 2013). The ChIP-seq data have been deposited in the Gene Expression Omnibus (GEO) database, www.ncbi.nlm.nih.gov/geo (Accession No: GSE179596).

Western Blot Analysis

About 0.1 g callus from *35S:3XFLAG-OsLEC1* seeds cultured on CIM for 30 days were ground in liquid nitrogen and resuspended in the extraction buffer as previously reported (Zhang et al., 2020). Then the protein samples were resolved by 4–20% gradient SDS-PAGE and transferred to a 0.2-μm polyvinylidenefluoride membrane (Millipore). Proteins were detected with a primary anti-FLAG antibody and incubated with a secondary antibody as previously reported (Guo et al., 2021).

Protein Sequences Analysis

Protein sequences of the *LEC1* homologous genes in dicots and monocots were obtained from the National Center for Biotechnology Information database (https://www.ncbi.nlm.nih.gov/). The phylogenetic tree of the protein sequences was constructed with MEGA (https://www.megasoftware.net/) using the NJ method with the following parameters: Poisson correction, complete deletion, and bootstrap (1,000 replicates, random seed). Multiple sequence alignments of proteins were performed using the ALIGNMENT software (https://www.genome.jp/tools-bin/clustalw).

DATA AVAILABILITY STATEMENT

The datasets presented in this study can be found in online repositories. The names of the repository/repositories and accession number(s) can be found below: National Center for Biotechnology Information (NCBI) BioProject database under accession number GSE179596.

AUTHOR CONTRIBUTIONS

FG, HB, MC, and LX designed the research. PZ and YW performed the data analyses. GL, WL, BB, CZ, DL, ZY, and WZ performed the experiments. FG and HB wrote the manuscript. NH, ZT, MZ, MC, and LX revised the manuscript. All authors contributed to the article and approved the submitted version.

FUNDING

This research was supported by the grants from the National Natural Science Foundation of China (Grant Nos. 31971932 and 31771477), Science Foundation of Zhejiang Province

(Grant No. LGN21C130006), Sponsed by Research Startup Funding from Hainan Institute of Zhejiang University (NO. 0201-6602-A12202), the State Key Laboratory of Subtropical Silviculture (No. KF2017-09), and China Agriculture Research System (CARS-05-05A).

ACKNOWLEDGMENTS

We thank Yunrong Wu, Zhejiang University, for the management of the greenhouse, and appreciate the kind help from Weilan Wang, Junying Li, Nianhang Rong, and Li Xie in the Bio-ultrastructure analysis Laboratory of the Analysis Centre of Agrobiology and Environmental Sciences, Zhejiang University. Moreover, we thank Hua Wang and Zijuan Li, CAS Centre for Excellence in Molecular Plant Sciences, for their help in the study.

SUPPLEMENTARY MATERIAL

The Supplementary Material for this article can be found online at: https://www.frontiersin.org/articles/10.3389/fpls.2022.887980/full#supplementary-material

REFERENCES

Allorent, G., Courtois, F., Chevalier, F., and Lerbs-Mache, S. (2013). Plastid gene expression during chloroplast differentiation and dedifferentiation into non-photosynthetic plastids during seed formation. *Plant Mol. Biol.* 82, 59–70. doi: 10.1007/s11103-013-0037-0

Asp, P. (2018). How to Combine ChIP with qPCR. *Chromatin Immunoprecipitation: Methods and Protoc*. 1689, 29–42.

Bai, Y., Han, N., Wu, J., Yang, Y., Wang, J., Zhu, M., et al. (2014). A transient gene expression system using barley protoplasts to evaluate microRNAs for post-transcriptional regulation of their target genes. *Plant Cell Tissue Organ Culture (PCTOC)* 119, 211–219. doi: 10.1007/s11240-014-0527-z

Bartels, A., Mock, H.-P., and Papenbrock, J. (2007). Differential expression of Arabidopsis sulfurtransferases under various growth conditions. *Plant Physiol. Biochem.* 45, 178–187. doi: 10.1016/j.plaphy.2007.02.005

Ben-Shem, A., Frolow, F., and Nelson, N. (2003). Crystal structure of plant photosystem I. *Nature* 426, 630–635. doi: 10.1038/nature02200

Bolger, A. M., Lohse, M., and Usadel, B. (2014). Trimmomatic: a flexible trimmer for Illumina sequence data. *Bioinformatics* 30, 2114–2120. doi: 10.1093/bioinformatics/btu170

Bollivar, D. W. (2006). Recent advances in chlorophyll biosynthesis. *Photosyn. Res.* 90, 173–194. doi: 10.1007/s11120-006-9076-6

Braybrook, S. A., and Harada, J. J. (2008). LECs go crazy in embryo development. *Trends Plant Sci.* 13, 624–630. doi: 10.1016/j.tplants.2008.09.008

Cutler, S. R., Rodriguez, P. L., Finkelstein, R. R., and Abrams, S. R. (2010). Abscisic acid: emergence of a core signaling network. *Annu. Rev. Plant Biol.* 61, 651–679. doi: 10.1146/annurev-arplant-042809-112122

De Paepe, A., and Van der Straeten, D. (2005). Ethylene biosynthesis and signaling: an overview. *Vitam. Horm.* 72, 399–430. doi: 10.1016/S0083-6729(05)72011-2

Dong, T., Park, Y., and Hwang, I. (2015). Abscisic acid: biosynthesis, inactivation, homoeostasis and signalling. *Essays Biochem.* 58, 29–48. doi: 10.1042/bse0580029

Finkelstein, R., Reeves, W., Ariizumi, T., and Steber, C. (2008). Molecular aspects of seed dormancy. *Annu. Rev. Plant Biol.* 59, 387–415. doi: 10.1146/annurev.arplant.59.032607.092740

Finkelstein, R. R., Gampala, S. S., and Rock, C. D. (2002). Abscisic acid signaling in seeds and seedlings. *Plant Cell* 14, S15–45. doi: 10.1105/tpc.010441

Gao, J., Wang, H., Yuan, Q., and Feng, Y. (2018). Structure and function of the photosystem supercomplexes. *Front. Plant Sci.* 9:357. doi: 10.3389/fpls.2018.00357

Gillmor, C. S., Settles, A. M., and Lukowitz, W. (2020). Genetic screens to target embryo and endosperm pathways in arabidopsis and maize. *Methods in Mol. Biol.* 2122, 3–14.

Giraudat, J., Hauge, B. M., Valon, C., Smalle, J., Parcy, F., and Goodman, H. M. (1992). Isolation of the Arabidopsis-Abi3 gene by positional cloning. *Plant Cell* 4, 1251–1261. doi: 10.1105/tpc.4.10.1251

Graeber, K., Nakabayashi, K., Miatton, E., Leubner-Metzger, G., and Soppe, W. J. J. (2012). Molecular mechanisms of seed dormancy. *Plant Cell Environ.* 35, 1769–1786. doi: 10.1111/j.1365-3040.2012.02542.x

Guo, F., Han, N., Xie, Y., Fang, K., Yang, Y., Zhu, M., et al. (2016). The miR393a/target module regulates seed germination and seedling establishment under submergence in rice (Oryza sativa L.). *Plant Cell Environ.* 39, 2288–2302. doi: 10.1111/pce.12781

Guo, F., Huang, Y., Qi, P., Lian, G., Hu, X., Han, N., et al. (2021). Functional analysis of auxin receptor OsTIR1/OsAFB family members in rice grain yield, tillering, plant height, root system, germination, and auxinic herbicide resistance. *New Phytol.* 229, 2676–2692. doi: 10.1111/nph.17061

Guo, F., Zhang, H. D., Liu, W., Hu, X. M., Han, N., Qian, Q., et al. (2018). Callus initiation from root explants employs different strategies in rice and arabidopsis. *Plant Cell Physiol.* 59, 1782–1789. doi: 10.1093/pcp/pcy095

Hu, X., Gu, T., Khan, I., Zada, A., and Jia, T. (2021). Research progress in the interconversion, turnover and degradation of chlorophyll. *Cells* 10:3134. doi: 10.3390/cells10113134

Hu, Y., Zhou, L., Huang, M., He, X., Yang, Y., Liu, X., et al. (2018). Gibberellins play an essential role in late embryogenesis of Arabidopsis. *Nature plants* 4, 289–298. doi: 10.1038/s41477-018-0143-8

Huang, M., Hu, Y., Liu, X., Li, Y., and Hou, X. (2015). Arabidopsis LEAFY COTYLEDON1 mediates postembryonic development via interacting with PHYTOCHROME-INTERACTING FACTOR4. *Plant Cell* 27, 3099–3111. doi: 10.1105/tpc.15.00750

Jo, L., Pelletier, J. M., and Harada, J. J. (2019). Central role of the LEAFY COTYLEDON1 transcription factor in seed development. *J. Integr. Plant Biol.* 61, 564–580. doi: 10.1111/jipb.12806

Jo, L., Pelletier, J. M., Hsu, S. W., Baden, R., Goldberg, R. B., and Harada, J. J. (2020). Combinatorial interactions of the LEC1 transcription factor specify diverse developmental programs during soybean seed development. *Proc. Natl. Acad. Sci. U.S.A.* 117, 1223–1232. doi: 10.1073/pnas.1918441117

Junker, A., Monke, G., Rutten, T., Keilwagen, J., Seifert, M., Thi, T. M., et al. (2012). Elongation-related functions of LEAFY COTYLEDON1 during the development of *Arabidopsis thaliana*. *Plant J. Cell Mol. Biol.* 71, 427–442. doi: 10.1111/j.1365-313X.2012.04999.x

Kagaya, Y., Toyoshima, R., Okuda, R., Usui, H., Yamamoto, A., and Hattori, T. (2005). LEAFY COTYLEDON1 controls seed storage protein genes through its regulation of FUSCA3 and ABSCISIC ACID INSENSITIVE3. *Plant Cell Physiol.* 46, 399–406. doi: 10.1093/pcp/pci048

Keith, K., Kraml, M., Dengler, N. G., and Mccourt, P. (1994). fusca3: A heterochronic mutation affecting late embryo development in arabidopsis. *Plant Cell* 6, 589–600. doi: 10.2307/3869865

Keshishian, E. A., and Rashotte, A. M. (2015). Plant cytokinin signalling. *Essays Biochem.* 58, 13–27. doi: 10.1042/bse0580013

Kim, D., Langmead, B., and Salzberg, S. L. (2015). HISAT: a fast spliced aligner with low memory requirements. *Nat. Methods* 12, 357–360. doi: 10.1038/nmeth.3317

Kim, E. J., and Russinova, E. (2020). Brassinosteroid signalling. *Curr. Biol.* 30, R294–r298. doi: 10.1016/j.cub.2020.02.011

Langmead, B., and Salzberg, S. L. (2012). Fast gapped-read alignment with Bowtie 2. *Nat. Methods* 9, 357–359. doi: 10.1038/nmeth.1923

Lau, S., Slane, D., Herud, O., Kong, J., and Jürgens, G. (2012). Early embryogenesis in flowering plants: setting up the basic body pattern. *Annu. Rev. Plant Biol.* 63, 483–506. doi: 10.1146/annurev-arplant-042811-105507

Lee, H. G., Lee, K., and Seo, P. J. (2015). The Arabidopsis MYB96 transcription factor plays a role in seed dormancy. *Plant Mol. Biol.* 87, 371–381. doi: 10.1007/s11103-015-0283-4

Lepiniec, L., Devic, M., Roscoe, T. J., Bouyer, D., Zhou, D. X., Boulard, C., et al. (2018). Molecular and epigenetic regulations and functions of the LAFL transcriptional regulators that control seed development. *Plant Reprod.* 31, 291–307. doi: 10.1007/s00497-018-0337-2

Li, J., and Berger, F. (2012). Endosperm: food for humankind and fodder for scientific discoveries. *New Phytol.* 195, 290–305. doi: 10.1111/j.1469-8137.2012.04182.x

Li, Q., Brown, J. B., Huang, H., and Bickel, P. J. (2011). Measuring reproducibility of high-throughput experiments. *Ann. Appl. Stat.* 5:1752–1779. doi: 10.1214/11-AOAS466

Lotan, T., Ohto, M., Yee, K. M., West, M. A., Lo, R., Kwong, R. W., et al. (1998). Arabidopsis LEAFY COTYLEDON1 is sufficient to induce embryo development in vegetative cells. *Cell* 93, 1195–1205. doi: 10.1016/S0092-8674(00)81463-4

Love, M. I., Huber, W., and Anders, S. (2014). Moderated estimation of fold change and dispersion for RNA-seq data with DESeq2. *Genome Biol.* 15:550. doi: 10.1186/s13059-014-0550-8

Luerssen, K., Kirik, V., Herrmann, P., and Misera, S. (1998). FUSCA3 encodes a protein with a conserved VP1/ABI3-like B3 domain which is of functional importance for the regulation of seed maturation in *Arabidopsis thaliana*. *Plant J.* 15, 755–764. doi: 10.1046/j.1365-313X.1998.00259.x

Machanick, P., and Bailey, T. L. (2011). MEME-ChIP: motif analysis of large DNA datasets. *Bioinformatics* 27, 1696–1697. doi: 10.1093/bioinformatics/btr189

Meinke, D. W. (1992). A Homeotic Mutant of Arabidopsis-Thaliana with Leafy Cotyledons. *Science* 258, 1647–1650. doi: 10.1126/science.258.5088.1647

Meinke, D. W., Franzmann, L. H., Nickle, T. C., and Yeung, E. C. (1994). Leafy Cotyledon Mutants of Arabidopsis. *Plant Cell* 6, 1049–1064. doi: 10.2307/3869884

Mu, J., Tan, H., Zheng, Q., Fu, F., Liang, Y., Zhang, J., et al. (2008). LEAFY COTYLEDON1 is a key regulator of fatty acid biosynthesis in Arabidopsis. *Plant Physiol.* 148, 1042–1054. doi: 10.1104/pp.108.126342

Nambara, E., Hayama, R., Tsuchiya, Y., Nishimura, M., Kawaide, H., Kamiya, Y., et al. (2000). The role of ABI3 and FUS3 loci in *Arabidopsis thaliana* on phase transition from late embryo development to germination. *Dev. Biol.* 220, 412–423. doi: 10.1006/dbio.2000.9632

Niu, B., Zhang, Z., Zhang, J., Zhou, Y., and Chen, C. (2021). The rice LEC1-like transcription factor OsNF-YB9 interacts with SPK, an endosperm-specific sucrose synthase protein kinase, and functions in seed development. *Plant J. Cell Mol. Biol.* 106, 1233–1246. doi: 10.1111/tpj.15230

Parcy, F., Valon, C., Kohara, A., Misera, S., and Giraudat, J. (1997). The ABSCISIC ACID-INSENSITIVE3, FUSCA3, and LEAFY COTYLEDON1 loci act in concert to control multiple aspects of Arabidopsis seed development. *Plant Cell* 9, 1265–1277. doi: 10.1105/tpc.9.8.1265

Pelletier, J. M., Kwong, R. W., Park, S., Le, B. H., Baden, R., Cagliari, A., et al. (2017). LEC1 sequentially regulates the transcription of genes involved in diverse developmental processes during seed development. *Proc. Natl. Acad. Sci. U.S.A.* 114, E6710–E6719. doi: 10.1073/pnas.1707957114

Pertea, M., Pertea, G. M., Antonescu, C. M., Chang, T. C., Mendell, J. T., and Salzberg, S. L. (2015). StringTie enables improved reconstruction of a transcriptome from RNA-seq reads. *Nat. Biotechnol.* 33, 290–295. doi: 10.1038/nbt.3122

Puthur, J. T., Shackira, A. M., Saradhi, P. P., and Bartels, D. (2013). Chloroembryos: a unique photosynthesis system. *J. Plant Physiol.* 170, 1131–1138. doi: 10.1016/j.jplph.2013.04.011

Raudvere, U., Kolberg, L., Kuzmin, I., Arak, T., Adler, P., Peterson, H., et al. (2019). g:Profiler: a web server for functional enrichment analysis and conversions of gene lists (2019 update). *Nucleic Acids Res.* 47, W191–W198. doi: 10.1093/nar/gkz369

Santos-Mendoza, M., Dubreucq, B., Baud, S., Parcy, F., Caboche, M., and Lepiniec, L. (2008). Deciphering gene regulatory networks that control seed development and maturation in Arabidopsis. *Plant J.* 54, 608–620. doi: 10.1111/j.1365-313X.2008.03461.x

Shannon, P., Markiel, A., Ozier, O., Baliga, N. S., Wang, J. T., Ramage, D., et al. (2003). Cytoscape: a software environment for integrated models of biomolecular interaction networks. *Genome Res.* 13, 2498–2504. doi: 10.1101/gr.1239303

Shen, B., Allen, W. B., Zheng, P. Z., Li, C. J., Glassman, K., Ranch, J., et al. (2010). Expression of ZmLEC1 and ZmWRI1 Increases Seed Oil Production in Maize. *Plant Physiol.* 153, 980–987. doi: 10.1104/pp.110.157537

Shu, K., Liu, X. D., Xie, Q., and He, Z. H. (2016). Two faces of one seed: hormonal regulation of dormancy and germination. *Mol. Plant* 9, 34–45. doi: 10.1016/j.molp.2015.08.010

Sreenivasulu, N., and Wobus, U. (2013). Seed-development programs: a systems biology-based comparison between dicots and monocots. *Annu. Rev. Plant Biol.* 64, 189–217.

Stone, S. L., Kwong, L. W., Yee, K. M., Pelletier, J., Lepiniec, L., Fischer, R. L., et al. (2001). LEAFY COTYLEDON2 encodes a B3 domain transcription factor that induces embryo development. *Proc. Natl. Acad. Sci. U.S.A.* 98, 11806–11811. doi: 10.1073/pnas.201413498

Tan, S., Luschnig, C., and Friml, J. (2021). Pho-view of auxin: reversible protein phosphorylation in auxin biosynthesis, transport and signaling. *Mol. Plant* 14, 151–165. doi: 10.1016/j.molp.2020.11.004

Thorvaldsdóttir, H., Robinson, J. T., and Mesirov, J. P. (2013). Integrative Genomics Viewer (IGV): high-performance genomics data visualization and exploration. *Brief. Bioinformat.* 14, 178–192. doi: 10.1093/bib/bbs017

Tian, T., Liu, Y., Yan, H., You, Q., Yi, X., Du, Z., et al. (2017). agriGO v2.0: a GO analysis toolkit for the agricultural community, 2017 update. *Nucleic Acids Res.* 45, W122–W129. doi: 10.1093/nar/gkx382

To, A., Valon, C., Savino, G., Guilleminot, J., Devic, M., Giraudat, J., et al. (2006). A network of local and redundant gene regulation governs Arabidopsis seed maturation. *Plant Cell* 18, 1642–1651. doi: 10.1105/tpc.105.039925

Warpeha, K. M., Upadhyay, S., Yeh, J., Adamiak, J., Hawkins, S. I., Lapik, Y. R., et al. (2007). The GCR1, GPA1, PRN1, NF-Y signal chain mediates both blue light and abscisic acid responses in Arabidopsis. *Plant Physiol.* 143, 1590–1600. doi: 10.1104/pp.106.089904

Waters, M. T., Wang, P., Korkaric, M., Capper, R. G., Saunders, N. J., and Langdale, J. A. (2009). GLK transcription factors coordinate expression of the photosynthetic apparatus in Arabidopsis. *Plant Cell* 21, 1109–1128. doi: 10.1105/tpc.108.065250

West, M. A. L., Yee, K. M., Danao, J., Zimmerman, J. L., Fischer, R. L., Goldberg, R. B., et al. (1994). Leafy cotyledon1 is an essential regulator of late Embryogenesis and Cotyledon identity in Arabidopsis. *Plant Cell* 6, 1731–1745. doi: 10.2307/3869904

Wyatt, A. W., Mo, F., Wang, Y., and Collins, C. C. (2013). The diverse heterogeneity of molecular alterations in prostate cancer identified through next-generation sequencing. *Asian J. Androl.* 15, 301–308. doi: 10.1038/aja.2013.13

Xia, L., Zou, D., Sang, J., Xu, X. J., Yin, H. Y., Li, M. W., et al. (2017). Rice Expression Database (RED): an integrated RNA-Seq-derived gene expression database for rice. *J. Genet. Genomics* 44, 235–241. doi: 10.1016/j.jgg.2017.05.003

Xie, K. B., Minkenberg, B., and Yang, Y. N. (2015). Boosting CRISPR/Cas9 multiplex editing capability with the endogenous tRNA-processing system. *Proc. Natl. Acad. Sci. U.S.A.* 112, 3570–3575. doi: 10.1073/pnas.1420294112

Xu, L., Zhao, Z., Dong, A., Soubigou-Taconnat, L., Renou, J. P., Steinmetz, A., et al. (2008). Di- and tri- but not monomethylation on histone H3 lysine 36 marks active transcription of genes involved in flowering time regulation and other processes in *Arabidopsis thaliana*. *Mol. Cell. Biol.* 28, 1348–1360. doi: 10.1128/MCB.01607-07

Yamaguchi, S. (2008). Gibberellin metabolism and its regulation. *Annu. Rev. Plant Biol.* 59, 225–251. doi: 10.1146/annurev.arplant.59.032607.092804

Yamamoto, A., Kagaya, Y., Toyoshima, R., Kagaya, M., Takeda, S., and Hattori, T. (2009). Arabidopsis NF-YB subunits LEC1 and LEC1-LIKE activate transcription by interacting with seed-specific ABRE-binding factors. *Plant J.* 58, 843–856. doi: 10.1111/j.1365-313X.2009.03817.x

Yazawa, K., Takahata, K., and Kamada, H. (2004). Isolation of the gene encoding Carrot leafy cotyledon1 and expression analysis during somatic and zygotic embryogenesis. *Plant Physiol. Biochem.* 42, 215–223. doi: 10.1016/j.plaphy.2003.12.003

Yu, G., Wang, L. G., and He, Q. Y. (2015). ChIPseeker: an R/Bioconductor package for ChIP peak annotation, comparison and visualization. *Bioinformatics* 31, 2382–2383. doi: 10.1093/bioinformatics/btv145

Zhang, H., Guo, F., Qi, P., Huang, Y., Xie, Y., Xu, L., et al. (2020). OsHDA710-mediated histone deacetylation regulates callus formation of rice mature embryo. *Plant Cell Physiol.* 61, 1646–1660. doi: 10.1093/pcp/pcaa086

Zhang, J. J., and Xue, H. W. (2013). OsLEC1/OsHAP3E participates in the determination of meristem identity in both vegetative and reproductive developments of rice. *J. Integr. Plant Biol.* 55, 232–249. doi: 10.1111/jipb.12025

Zhang, Y., Liu, T., Meyer, C. A., Eeckhoute, J., Johnson, D. S., Bernstein, B. E., et al. (2008). Model-based analysis of ChIP-Seq (MACS). *Genome Biol.* 9:R137. doi: 10.1186/gb-2008-9-9-r137

Conflict of Interest: The authors declare that the research was conducted in the absence of any commercial or financial relationships that could be construed as a potential conflict of interest.

Publisher's Note: All claims expressed in this article are solely those of the authors and do not necessarily represent those of their affiliated organizations, or those of the publisher, the editors and the reviewers. Any product that may be evaluated in this article, or claim that may be made by its manufacturer, is not guaranteed or endorsed by the publisher.

Advantages of publishing in Frontiers

OPEN ACCESS
Articles are free to read for greatest visibility and readership

FAST PUBLICATION
Around 90 days from submission to decision

HIGH QUALITY PEER-REVIEW
Rigorous, collaborative, and constructive peer-review

TRANSPARENT PEER-REVIEW
Editors and reviewers acknowledged by name on published articles

Frontiers
Avenue du Tribunal-Fédéral 34
1005 Lausanne | Switzerland

Visit us: www.frontiersin.org
Contact us: frontiersin.org/about/contact

REPRODUCIBILITY OF RESEARCH
Support open data and methods to enhance research reproducibility

DIGITAL PUBLISHING
Articles designed for optimal readership across devices

FOLLOW US
@frontiersin

IMPACT METRICS
Advanced article metrics track visibility across digital media

EXTENSIVE PROMOTION
Marketing and promotion of impactful research

LOOP RESEARCH NETWORK
Our network increases your article's readership